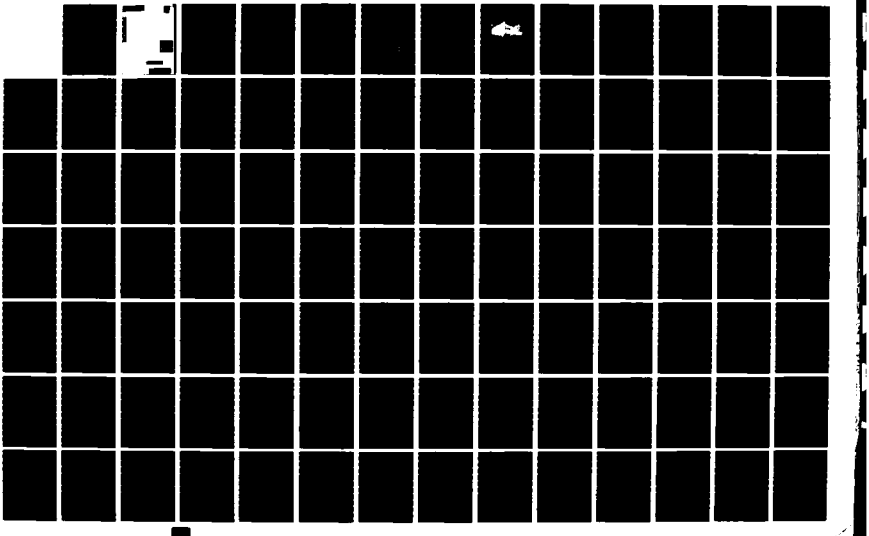
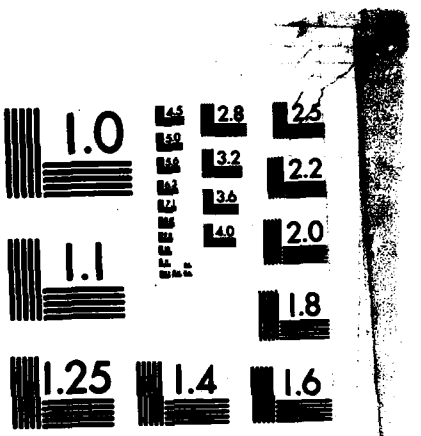
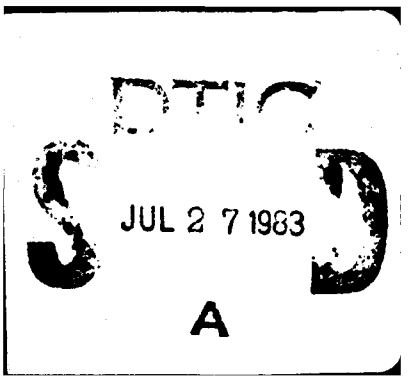
AD-A130 769 USAF/SCEEE SUMMER FACULTY RESEARCH PROGRAM RESEARCH 1/11
REPORTS VOLUME 1. (U) SOUTHEASTERN CENTER FOR
ELECTRICAL ENGINEERING EDUCATION INC S.
UNCLASSIFIED W D PEELE ET AL. OCT 82 AFOSR-TR-83-0613 F/G 5/1 NL





MICROCOPY RESOLUTION TEST CHART
NATIONAL BUREAU OF STANDARDS-1963-A


DTIC
JUL 2 7 1983
A

UNCLASSIFIED

SECURITY CLASSIFICATION OF THIS PAGE (When Data Entered)

REPORT DOCUMENTATION PAGE		READ INSTRUCTIONS BEFORE COMPLETING FORM
1. REPORT NUMBER AFOSR-TR- 83-0613	2. GOVT ACCESSION NO.	3. RECIPIENT'S CATALOG NUMBER
4. TITLE (and Subtitle) UNITED STATES AIR FORCE SUMMER FACULTY RESEARCH PROGRAM RESEARCH REPORT, VOLUME I		5. TYPE OF REPORT & PERIOD COVERED FINAL 6. PERFORMING ORG. REPORT NUMBER
7. AUTHOR(s) Warren D. Peele Earl L. Steele		8. CONTRACT OR GRANT NUMBER(s) F49620-82-C-0035
9. PERFORMING ORGANIZATION NAME AND ADDRESS Southeastern Center for Electrical Engineering Education 11th and Massachusetts Ave. St. Cloud, Florida 32769		10. PROGRAM ELEMENT, PROJECT, TASK AREA & WORK UNIT NUMBERS 61102F 2301/D5
11. CONTROLLING OFFICE NAME AND ADDRESS AFOSR/XOT Building 410 Bolling AFB, DC 20332		12. REPORT DATE October 1982 13. NUMBER OF PAGES
14. MONITORING AGENCY NAME & ADDRESS(if different from Controlling Office)		15. SECURITY CLASS. (of this report) UNCLASSIFIED 15a. DECLASSIFICATION/DOWNGRADING SCHEDULE

16. DISTRIBUTION STATEMENT (of this Report)

APPROVED FOR PUBLIC RELEASE; DISTRIBUTION UNLIMITED

17. DISTRIBUTION STATEMENT (of the abstract entered in Block 20, if different from Report)

18. SUPPLEMENTARY NOTES

19. KEY WORDS (Continue on reverse side if necessary and identify by block number)

20. ABSTRACT (Continue on reverse side if necessary and identify by block number)

The United States Air Force Summer Faculty Research Program (USAF-SFRP) is a program designed to introduce university, college, and technical institute faculty members to Air Force research. This is accomplished by faculty competition on a nationally advertised competitive basis for a ten-week assignment during the summer intersession to perform research at Air Force laboratories/centers. Each assignment is in a subject area and at an Air Force facility mutually agreed upon by the faculty member and the Air Force. In addition to compensation and travel expenses, a cost of living

DD FORM 1 JAN 73 1473 EDITION OF 1 NOV 65 IS OBSOLETE

UNCLASSIFIED

(over)

SECURITY CLASSIFICATION OF THIS PAGE (When Data Entered)

20. (cont)

allowance is also paid. The USAF-SFRP is sponsored by the Air Force Office of Scientific Research/Air Force Systems Command, United States Air Force, and is conducted by the Southeastern Center for Electrical Engineering Education(SCEEE).

AFOSR-TR- 83-0613

AIR FORCE OFFICE OF SCIENTIFIC RESEARCH (AFSC)
NOTICE OF TRANSMITTAL TO DTIC
This technical report has been reviewed and is approved for public release IAW AFR 190-12.
Distribution is unlimited.
MATTHEW J. KERPER
Chief, Technical Information Division

Approved for public release;
distribution unlimited.

1982 USAF/SCEEE SUMMER FACULTY RESEARCH PROGRAM

Conducted by

Southeastern Center for

Electrical Engineering Education

under

USAF Contract Number F49620-82-C-0035

RESEARCH REPORTS

Volume I of II

Submitted to

Air Force Office of Scientific Research

Bolling Air Force Base

Washington D.C.

by

Southeastern Center for
Electrical Engineering Education

October 1982

DTIC
ELECTE
JUL 2 7 1983
A

Accession For
NTIS GRA&I
DTIC TAB
Unannounced
Justification
By
Distribution/
Availability Codes
Dist Avail and/or Special
A

DTIC COPY INSPECTED 2

This document has been approved for public release and sale; its distribution is unlimited.

PREFACE

The United States Air Force Summer Faculty Research Program (USAF-SFRP) is a program designed to introduce university, college, and technical institute faculty members to Air Force research. This is accomplished by faculty competition on a nationally advertised competitive basis for a ten-week assignment during the summer intersession to perform research at Air Force laboratories/centers. Each assignment is in a subject area and at an Air Force facility mutually agreed upon by the faculty member and the Air Force. In addition to compensation and travel expenses, a cost of living allowance is also paid. The USAF-SFRP is sponsored by the Air Force Office of Scientific Research/Air Force Systems Command, United States Air Force, and is conducted by the Southeastern Center for Electrical Engineering Education (SCEEE).

The specific objectives of the 1982 USAF-SFRP are:

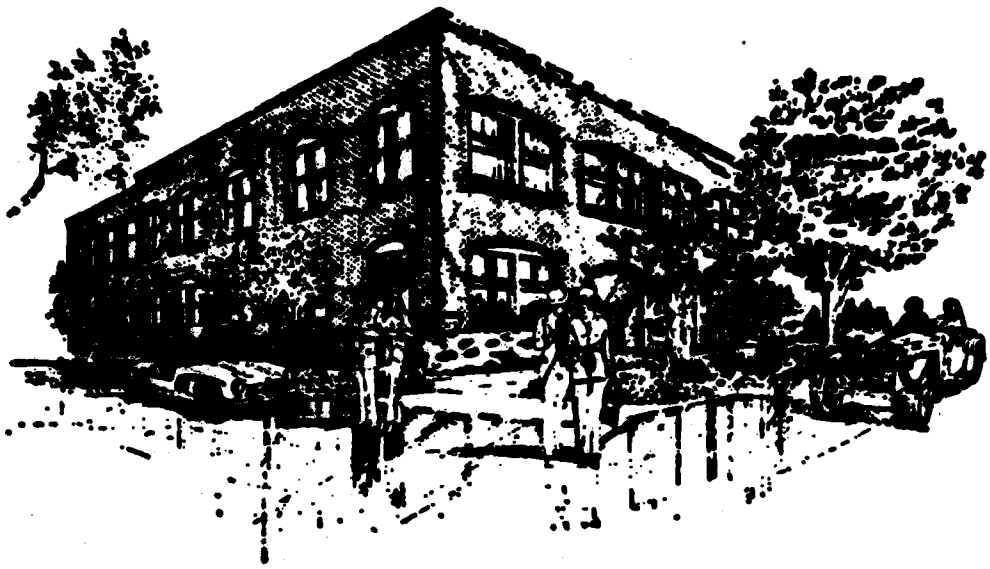
(1) To develop the basis for continuing research of interest to the Air Force at the faculty member's institution.

(2) To further the research objectives of the Air Force.

(3) To stimulate continuing relations among faculty members and their professional peers in the Air Force.

(4) To enhance the research interests and capabilities of scientific and engineering educators.

In the 1979 summer program, 70 faculty members participated, and in the 1980 and 1981 programs, 87 faculty members participated. In 1982, 91 faculty and 17 students participated. These researchers were assigned to 25 USAF laboratories/centers across the country. This two volume document is a compilation of the final reports written by the assigned faculty members about their summer research efforts.



SCREE
©
1981

NAME/ADDRESS	DEGREE, SPECIALTY, LABORATORY ASSIGNED
Prof. Richard G. Absher Professor University of Vermont Electrical Engineering Department Burlington, VT 05405 (802) 658-3330	Degree: Ph.D., Electrical Engineering, 1967 Specialty: Digital Systems, Modern Control Theory, Biomedical Engineering Assigned: RADC/Griffiss
Dr. Milton J. Alexander Professor Auburn University Management Department Auburn, AL 36830 (205) 826-4730	Degree: D.B.A., Management, 1968 Specialty: Management Information Systems, Operational Research Assigned: LMC
Dr. Gary L. Allen Assistant Professor Old Dominion University Psychology Department Norfolk, VA 23508 (804) 440-4444	Degree: Ph.D., Psychology, 1979 Specialty: Cognitive Psychology, Perception, Developmental Psychology Assigned: HRL/B
Dr. Silverio P. Almeida Professor Virginia Tech. Physics Department Blacksburg, VA 24061 (703) 961-5473	Degree: Ph.D., Physics Specialty: Laser Applications to Biophysics and Pattern Recognitions Problems Assigned: SAM
Dr. Muluneh Azene Assistant Professor Southern University Civil Engineering Department Baton Rouge, LA 70813 (504) 771-5871	Degree: Ph.D., Structural Mechanics, 1979 Specialty: Finite Element Analysis Assigned: ESC
Dr. Francesco L. Bacchialoni Associate Professor University of Lowell Electrical Engineering Dept. Lowell, MA 01854 (617) 452-5000	Degree: Ph.D., Engineering, 1946 Specialty: Control Systems, Signal Processing Assigned: GL
Dr. A. Terry Bahill Associate Professor Carnegie-Mellon University Electrical Engineering Dept. Pittsburg, PA 15213 (412) 578-2536	Degree: Ph.D., Electrical Engineering, 1975 Specialty: Biological Control Systems Assigned: AMRL

NAME/ADDRESS	DEGREE, SPECIALTY, LABORATORY ASSIGNED
Dr. Mason G. Bailey Associate Professor Western Carolina University Accounting/Information Systems Dept. Cullowhee, NC 28723 (704) 227-7401	Degree: Ph.D., Computer Science, 1978 Specialty: Computer Science, Operations Research Assigned: HRL/WP
Dr. Pradip M. Bakshi Professor Boston College Physics Department Chestnut Hill, MA 02167 (617) 969-0100	Degree: Ph.D., Theoretical Physics, 1962 Specialty: Theoretical Plasma Physics Assigned: GL
Dr. Gust Bambakidis Assistant Professor Wright State University Physics Department Dayton, OH 45435 (513) 873-2954	Degree: Ph.D., Physics, 1966 Specialty: Theoretical Physics Assigned: ML
Prof. Albert W. Biggs Professor University of Kansas Electrical Engineering Department Lawrence, KS 66045 (913) 864-4615	Degree: Ph.D., Electrical Engineering, 1965 Specialty: Microwaves, Antennas, and Wave Propagation Assigned: RADC/Hanscom
Dr. Jack J. Bourquin Associate Professor University of Missouri Electrical Engineering Department Rolla, MO 65401 (314) 341-4548	Degree: Ph.D., Electrical Engineering, 1968 Specialty: Circuits and Systems Assigned: AL
Dr. Willie A. Bragg Assistant Professor University of Cincinnati Early Childhood & Special Education Dept. Cincinnati, OH 45221 (513) 475-4542	Degree: Ph.D., Special Education, 1979 Specialty: Mental Retardation, Early Childhood Education Assigned: SAM
Dr. Eugene F. Brown Associate Professor VPI & SU Mechanical Engineering Department Blacksburg, VA 24061 (703) 961-7199	Degree: Ph.D., Mechanical Engineering, 1968 Specialty: Fluid Mechanics, Computational Fluid Dynamics Assigned: APL

NAME/ADDRESS	DEGREE, SPECIALTY, LABORATORY ASSIGNED
Dr. Sherman D. Brown Professor University of Illinois Ceramic Engineering Department Urbana, IL 61801 (217) 333-4766	Degree: Ph.D., Chemical Engineering, 1957 Specialty: Brittle Fracture, Ceramic Coatings, Glasses, High Temperature Materials Assigned: ML
Dr. Louis W. Buckalew Assistant Professor Alabama A&M University Psychology Department Normal, AL 35762 (205) 859-7451	Degree: M.S. & (ABD), Physiological Psychology, 1969 & (1979) Specialty: Physiological Psychology, Psychopharm, Human Engineering Assigned: AMRL
Dr. Donald L. Byrkett Associate Professor Miami University Systems Analysis Department Oxford, OH 45046 (513) 523-2325	Degree: Ph.D., Industrial Engineering, 1974 Specialty: Mathematical Modeling, Management Science Assigned: LC
Dr. Jimmie J. Cathey Associate Professor University of Kentucky Electrical Engineering Department Lexington, KY 40506 (606) 258-4684	Degree: Ph.D., Electrical Engineering, 1972 Specialty: Analysis, Design, and Control of Electrical Machinery Assigned: APL
Dr. Roger E. Cavallo Associate Professor State University of New York Computer & Information Science Dept. Utica, NY 13502 (315) 792-3315	Degree: Ph.D., Systems Science, 1978 Specialty: Systems Methodology Assigned: RADC/G
Dr. Junho Choi Assistant Professor Florida Institute of Technology Dept. of Electrical Engineering & CP Melbourne, FL 32901 (305) 723-3701	Degree: Ph.D., Electrical Engineering, 1978 Specialty: Digital Signal Processing, Control Systems Assigned: ESMC
Dr. David L. Cleeton Assistant Professor Oberling College Economics Department Oberlin, OH 44074 (216) 775-8482	Degree: Ph.D., Economics, 1980 Specialty: Microeconomics, Labor Economics, Public Finance Assigned: BRMC

NAME/ADDRESS	DEGREE, SPECIALTY, LABORATORY ASSIGNED
Dr. Gregory M. Corso Assistant Professor Georgia Institute of Technology Psychology Department Atlanta, GA 30332 (404) 894-4260	Degree: Ph.D., Engineering Psychology, 1978 Specialty: Human Performance Theory, Engineering Psychology Assigned: AMRL
Dr. Robert A. Douglas Professor North Carolina State University Civil Engineering Department Raleigh, NC 27650 (919) 737-2331	Degree: Ph.D., Engineering, 1956 Specialty: Mechanics of Solids, Impact and Stress Wave Propagation Assigned: ESC
Dr. Hamed K. Eldin Professor Oklahoma State University Industrial Engineering & Management Dept. Stillwater, OK 74078 (405) 624-6055	Degree: Ph.D., Industrial Engineering, 1951 Specialty: Project Management, Economic Analysis Inventory Theory Assigned: BRMC
Dr. John D. Enderle Assistant Professor North Dakota State University Electrical Engineering Department Fargo, ND 58105 (701) 237-7689	Degree: Ph.D., Biomedical Engineering, 1980 Specialty: Epidemiology, Signal Processing, Statistical Methods & Modeling Assigned: SAM
Dr. Fernando E. Fagundo Assistant Professor University of Florida Civil Engineering Department Gainesville, FL 32611 (904) 392-0851	Degree: Ph.D., Structural Engineering, 1980 Specialty: Analysis and Design of Reinforced Concrete Structural Systems, Assigned: ESC
Dr. Hubert S. Feild Associate Professor Auburn University Management Department Auburn, AL 36830 (205) 826-4039	Degree: Ph.D., Psychology, 1973 Specialty: Industrial Psychology Assigned: LMDC
Dr. Mack Felton, Jr. Chairman Southern University Biology Department New Orleans, LA 70126 (504) 282-4401	Degree: Ph.D., Microbiology, 1973 Specialty: Microbiology Assigned: SAM

NAME/ADDRESS	DEGREE, SPECIALTY, LABORATORY ASSIGNED
Dr. William L. Filippone Associate Professor University of Arizona Nuclear & Energy Engineering Dept. Tucson, AZ 85721 (602) 626-2514	Degree: Ph.D., Nuclear Engineering, 1970 Specialty: Charged and Neutral Particle Transport Theory Assigned: RADC/Hanscom
Dr. Dennis R. Flentge Assistant Professor Cedarville College Math & Science Department Cedarville, OH 45314 (513) 766-2211	Degree: Ph.D., Physical Chemisry, 1974 Specialty: Surface Chemistry, Catalysis and IR Spectroscopy Assigned: APL
Dr. Wilfred A. Fordon Associate Professor Michigan Technogical University Electrical Engineering Department Houghton, MI 49931 (906) 487-2550	Degree: Ph.D., Electrical Engineering, 1976 Specialty: Electromagnetic Theory, Pattern Recognition Assigned: ESD
Dr. Larry J. Forney Associate Professor Georgia Institute of Technology Chemical Engineering Department Atlanta, GA 30332 (404) 894-2825	Degree: Ph.D., Engineering Science, 1974 Specialty: Dynamics and Chemistry of Turbulent Jets and Plumes Assigned: AEDC
Dr. Albert J. Frasca Associate Professor Wittenberg University Physics Department Springfield, OH 45501 (513) 327-7821	Degree: Ph.D., Physics, 1966 Specialty: Low Energy Nuclear Physics, Solid State Physics Assigned: AL
Dr. Andris Freivalds Assistant Professor Penn State University Industrial & Mgmt. Systems Eng. Dept. University Park, PA 16802 (814) 863-2361	Degree: Ph.D., Bioengineering, 1979 Specialty: Human Factors, Biomechanics, Work Physiology Assigned: AMRL
Dr. Mark A. Fugelso Assistant Professor Penn State University Industrial Engineering Department University Park, PA 16802 (814) 863-2360	Degree: Ph.D., Microprocessor Controlled Twist Drill Grinding Machine, 1978 Specialty: Digital Computer Control of Special Machine Tools & Robots Assigned: ML

NAME/ADDRESS	DEGREE, SPECIALTY, LABORATORY ASSIGNED
Prof. Eugene H. Galluscio Professor Northwest Missouri State University Psychology Department Maryville, MO 64468 (816) 582-7141	Degree: Ph.D., Physiological Psychology,1970 Specialty: Neuropsychology, Brain Function, Visual Information Processing Assigned: HRL/Williams
Dr. Ronald L. Greene Assistant Professor University of New Orleans Physics Department New Orleans, LA 70148 (504) 286-6714	Degree: Ph.D., Physics, 1974 Specialty: Plasma Spectroscopy Assigned: AL
Dr. Keith C. Hanson Professor Lamar University Chemistry Department Beaumont, TX 77710 (713) 838-8267	Degree: Ph.D., Chemistry, 1967 Specialty: Organic Chemistry, Measurement of Physical Properties Assigned: FJSRL
Dr. Donald J. Healy Assistant Professor Georgia Institute of Technology Electrical Engineering Department Atlanta, GA 30332 (404) 894-2923	Degree: Ph.D., Electrical Engineering, 1981 Specialty: Image Processing (Communications) Assigned: AD
Prof. Ervin Hindin Professor Washington State University Civil & Environmental Engineering Dept. Pullman, WA 99164 (509) 335-7028	Degree: M.S., Environmental Chemistry, 1956 Specialty: Aquatic Chemistry, Water Supply Systems Assigned: ESC
Dr. Manuel A. Huerta Associate Professor University of Miami Physics Department Coral Gables, FL 33124 (305) 284-2323	Degree: Ph.D., Physics, 1970 Specialty: Plasma Physics, Fluid Mechanics, Electromagnetic Theory Assigned: AD
Dr. Francis J. Jankowski Professor Wright State University Engineering Department Dayton, OH 45435 (513) 873-2097	Degree: Sc.D., Physics, 1949 Specialty: Systems Engineering, Nuclear Engineering. Mechanical Engineering, Human Factors Engineering Assigned: WL

NAME/ADDRESS	DEGREE, SPECIALTY, LABORATORY ASSIGNED
Dr. Eric R. Johnson Assistant Professor Virginia Tech. Aerospace & Ocean Engineering Dept. Blacksburg, VA 24061 (703) 961-6699	Degree: Ph.D., Applied Mechanics, 1976 Specialty: Structural Stability & Composite Structures Assigned: FDL
Dr. James J. Kane Associate Professor Wright State University Chemistry Department Dayton, OH 45435 (513) 873-2352	Degree: Ph.D., Organic Chemistry, 1960 Specialty: Organic Chemistry Polymer Chemistry Assigned: ML
Dr. Samuel G. Kelly Assistant Professor University of Notre Dame Aerospace & Mechanical Engineering Dept. Notre Dame, IN 46556 (219) 239-7678	Degree: Ph.D., Engineering Mechanics, 1979 Specialty: Nonlinear Mechanics Assigned: FDL
Dr. Dennis M. Kern Assistant Professor University of Georgia Statistics & Computer Science Dept. Athens, GA 30602 (404) 542-2911	Degree: Ph.D., Statistics, 1976 Specialty: Microprocessors Assigned: SAM
Dr. Stuart T. Klapp Professor California State University Psychology Department Hayward, CA 94542 (415) 881-3484	Degree: Ph.D., Experimental Psychology, 1969 Specialty: Cognition and Human Performance Assigned: HRL/WP
Dr. Jerome Knopp Assistant Professor University of Missouri-Rolla Electrical Engineering Department Rolla, MO 65401 (314) 341-45439	Degree: Ph.D., Electrical Engineering Specialty: Electro-Optics Assigned: RADC/Griffiss
Dr. Keith Koenig Assistant Professor Mississippi State University Aerospace Engineering Department Mississippi State, MS 39762 (601) 323-3623	Degree: Ph.D., Aeronautics, 1978 Specialty: Laser Velocimetry, Separated Flow Assigned: AD

NAME/ADDRESS	DEGREE, SPECIALTY, LABORATORY ASSIGNED
Dr. Letitia J. Korbly Assistant Professor University of Alabama Mathematics Department Birmingham, AL 35294 (205) 934-2154	Degree: Ph.D., Mathematics, 1976 Specialty: Applied Math, Partial Differential Equations Assigned: WL
Dr. Philip Langer Associate Professor University of Colorado Ed. Psychology Department Boulder, CO 80309 (303) 492-8748	Degree: Ph.D., Education/Psychology, 1957 Specialty: Instructional Systems Assigned: HRL/L
Dr. Stephen F. Lin Associate Professor North Carolina Central University Chemistry Department Durham, NC 27707 (919) 683-6463	Degree: Ph.D., Physical Chemistry, 1970 Specialty: Physical Chemistry Assigned: RPL
Dr. Michael L. Lobb Assistant Professor University of Texas Graduate School of Social Work Arlington, TX 76019-0129 (817) 273-2707	Degree: Ph.D., Psychology, 1978 Specialty: Statistics and Experimental Design Assigned: SAM
Dr. D. J. Medeiros Assistant Professor Penn State University Industrial Engineering Department University Park, PA 16802 (814) 863-2364	Degree: Ph.D., Industrial Engineering, 1981 Specialty: Scheduling, Computer Simulation of Production/ Manufacturing Systems Assigned: ML
Dr. Thomas M. Miller Associate Professor University of Oklahoma Physics and Astronomy Department Norman, OK 70319 (405) 325-3961	Degree: Ph.D., Physics, 1968 Specialty: Experimental Atomic Collisions Assigned: GL
Dr. Michael J. Moloney Professor Rose-Hulman Institute of Technology. Physics Department Terre Haute, IN 47803 (812) 877-1511	Degree: Ph.D., Physics, 1966 Specialty: Solid State Electronic Devices, Modern Physics Assigned: AL

NAME/ADDRESS	DEGREE, SPECIALTY, LABORATORY ASSIGNED
Dr. Luigi Morino Professor Boston University Aerospace & Mechanical Engineering Dept. Boston, MA 02215 (617) 353-3069	Degree: Ph.D., Aerospace Engineering, 1966, Ph.D., Mechanical Engineering, 1963 Specialty: Unsteady Aerodymanics and Structural Dynamics Assigned: AD
Dr. David S. Moroi Professor Kent State University Physics Department Kent, OH 44242 (216) 672-2596	Degree: Ph.D., Atomic Physics, 1959 Specialty: Atomic Physics, Transport Phenomena in Liquid Crystals Assigned: ML
Dr. H. Troy Nagle, Jr. Professor Auburn University Electrical Engineering Department Auburn, AL 36849 (205) 826-4330	Degree: Ph.D., Electrical Engineering, 1968 Specialty: Computer Engineering Assigned: SAM
Dr. Eugene M. Norris Associate Professor George Mason University Mathematical Science Department Fairfax, VA 22030 (703) 323-2262	Degree: Ph.D., Mathematics, 1969 Specialty: Theoretical Computer Science Assigned: AL
Dr. Thomas H. Ortmeyer Assistant Professor Clarkson College Electrical Engineering Department Potsdam, NY 13676 (315) 268-6536	Degree: Ph.D., Electrical Engineering, 1980 Specialty: Electric Machinery and Power Systems Assigned: APL
Dr. Dean H. Owen Associate Professor Ohio State University Psychology Department Columbus, OH 43210 (614) 422-7641	Degree: Ph.D., Experimental Psychology, 1965 Specialty: Perception, Psychophysics, Flight Simulation Assigned: HRL/Williams
Dr. Charles K. Parsons Assistant Professor Georgia Institute of Technology College of Management Atlanta, GA 30332 (404) 894-2619	Degree: Ph.D., Psychology, 1980 Specialty: Item Response Theory Assigned: HRL/Brooks

NAME/ADDRESS	DEGREE, SPECIALTY, LABORATORY ASSIGNED
Dr. Surgounda A. Patil Professor Tennessee Technical University Math & Computer Science Department Cookville, TN 38501 (615) 528-3593	Degree: Ph.D., Statistics, 1966 Specialty: Statistical Problems Applicable to Engineering and Environment Assigned: WL
Dr. Lakhpat R. Pujara Associate Professor Wilberforce University Engineering/Mathematics Department Wilberforce, OH 45384 (513) 376-2911	Degree: Ph.D., Mathematics, 1971 M.S., Systems Engineering, 1981 Specialty: Control Systems Assigned: FDL
Dr. Zahir Qureshi Assistant Professor Rust College Biology Department Holly Springs, MS 36835 (601) 252-4661	Degree: Ed.D., Biochemistry, 1975 Specialty: Biochemistry Education Assigned: AMRL
Dr. Ronald L. Remke Assistant Professor University of South Floirda Electrical Engineering Department Tampa, FL 33620 (813) 974-2581	Degree: Ph.D., Electrical Engineering, 1977 Specialty: Electronic Devices, Materials, and Processes/ Thin Films Assigned: RADC/Griffiss
Dr. Richard W. Rice Assistant Professor Clemson University Chemical Engineering Department Clemson, SC 29631 (803) 656-3055	Degree: Ph.D., Chemical Engineering, 1972 Specialty: Catalysis, Chemical Kinetics Assigned: ESC
Dr. Gerhard X. Ritter Associate Professor University of Florida Math & Computer Science Department Gainesville, FL 32611 (904) 392-4988	Degree: Ph.D., Mathematics, 1971 Specialty: Pattern Recognition, Applied Mathematics Assigned: AD
Dr. John M. Russell Assistant Professor University of Oklahoma School of Aero. Mech. and Nuclear Eng. Norman, OK 70319 (405) 325-5011	Degree: Ph.D., Fluid Mechanics, 1981 Specialty: Incompressible Flows, Boundry Layers, Stability, Turbulence Assigned: FDL

NAME/ADDRESS	DEGREE, SPECIALTY, LABORATORY ASSIGNED
Dr. Sarwan S. Sandhu Assistant Professor University of Dayton Chemical Engineering Department Dayton, OH 45469 (513) 229-2627	Degree: Ph.D., Combustion, 1973 Specialty: Combustion Assigned: APL
Dr. Robert E. Schlegel Assistant Professor University of Oklahoma Industrial Engineering Department Norman, OK 70319 (405) 325-3721	Degree: Industrial Engineering,1980 Specialty: Human Factors Assigned: SAM
Dr. Eugene P. Schram Associate Professor Ohio State University Chemistry Department Columbus, OH 43210 (614) 222-1487	Degree: Ph.D. Inorganic Chemistry Specialty: Organometallic Chemistry Assigned: AL
Dr. K. Sam. Shanmugan Associate Professor University of Kansas Electrical Engineering Department Lawrence, KS 66045 (913) 864-4832	Degree: Ph.D. Specialty: Communication Systems Engineering Assigned: RADC/Griffiss
Dr. Trilochan Singh Associate Professor Wayne State University Mechanical Engineering Department Detroit, MI 48202 (313) 577-3845	Degree: Ph.D. Mechanical Engineering, 1970 Specialty: Combustion, Heat Transfer, Energy Conservation Assigned: APL
Dr. Boghos D. Sivazlian Professor University of Florida Industrial & Systems Engineering Dept. Gainesville, FL 32611 (904) 392-1464	Degree: Ph.D., Operations Research, 1966 Specialty: Operations Research, Math. Modeling, Military Problems Assigned: AD
Dr. Stanley L. Spiegel Assistant Professor University of Lowell Mathematics Department Lowell, MA 01854 (617) 738-5000	Degree: Ph.D., Physics, 1966 Specialty: Numerical Modeling and Computer Simulation of Geophysical Problems Assigned: GL

NAME/ADDRESS	DEGREE, SPECIALTY, LABORATORY ASSIGNED
Dr. Alexander P. Stone Professor University of New Mexico Mathematics Department Albuquerque, NM 87131 (505) 277-4643	Degree: Ph.D., Mathematics, 1965 Specialty: Differential Equations, Differential Geometry Assigned: WL
Dr. Alfred G. Striz Assistant Professor University of Oklahoma Aero Mechanical Nuclear Eng. Dept. Norman, OK 70319 (405) 325-5011	Degree: Ph.D., Aeronautics and Astronautics, 1981 Specialty: Aeroelasticity, Finite Elements, Aerospace Structure Assigned: AD
Dr. Patrick J. Sweeney Associate Professor University of Dayton Engineering Management Department Dayton, OH 45469 (513) 229-2238	Degree: Ph.D., Mechanical Engineering, 1977 Specialty: Simulation, O.R., Management Assigned: AMRL
Dr. Richard H. Tipping Professor University of Nebraska Physics Department Omaha, NE 68182 (402) 554-2510	Degree: Ph.D., Physics, 1969 Specialty: Molecular Spectroscopy, Atmospheric Physics Assigned: GL
Dr. Edward A. Walters Associate Professor University of New Mexico Chemistry Department Albuquerque, NM 87131 (505) 277-5239	Degree: Ph.D., Chemistry, 1966 Specialty: Physical Chemistry Assigned: WL
Dr. Kai Wang Associate Professor Wayne State University Mathematics Department Detroit, MI 48202 (313) 577-3193	Degree: Ph.D., Mathematics, 1972 Specialty: Spectral of graphs, Group Matrices Assigned: APL
Dr. Edward R. Ward, Jr. Associate Professor Alabama A & M University Biology Department Normal, AL 35762 (205) 859-7268	Degree: Ph.D., Microbiology, 1975 Specialty: Pathogenic Microbiology, Immunology Assigned: SAM

NAME/ADDRESS	DEGREE, SPECIALTY, LABORATORY ASSIGNED
Dr. Thomas E. Webb Professor Ohio State University Physiological Chemistry Department Columbus, OH 43210 (614) 422-0103	Degree: Ph.D., Biochemistry, 1961 Specialty: Biochemistry, Molecular Bioology, Carcinogenesis Assigned: AMRL
Prof. David Weimer Associate Professor Ohio Northern University Physics Department Ada, OH 45810 (419) 634-9921	Degree: M.S., Physics, 1946 Specialty: Gas dynamics, Shock Wave Phenomena, Electrooptical Effects and Instrumentation Assigned: APL
Dr. Thomas A. Wiggins Professor Penn State University Physics Department University Park, PA 16802 (814) 865-5233	Degree: Ph.D., Physics, 1980 Specialty: Physical Optics, Molecular Spectra Assigned: FJSRL
Dr. David H. Williams Assistant Professor University of Texas Electrical Engineering Department El Paso, TX 79968 (915) 747-5470	Degree: Ph.D., Electrical Engineeing, 1977 Specialty: Computer Graphics Assigned: WL
Dr. Robert E. Willis Assistant Professor Mercer University Physics Department Macon, GA 31207 (912) 744-2704	Degree: Ph.D., Physics, 1979 Specialty: Microwave Spectroscopy Assigned: AEDC
Dr. David C. Wilson Associate Professor University of Florida Mathematics Department Gainesville, FL 32611 (904) 392-6035	Degree: Ph.D., Mathematics, 1969 Specialty: Dimension Theory Assigned: FDL
Dr. Rama K. Yedavalli Assistant Professor Stevens Institute of Technology Mechanical Engineering Department Hoboken, NJ 07030 (201) 420-5574	Degree: Ph.D., Aerospace Engineering, 1981 Specialty: Sensitivity Theory for Linear Multivariable Optimal Control Systems Assigned: FDL

PARTICIPANT LABORATORY ASSIGNMENT

1982 USAF/SCEEE SUMMER FACULTY RESEARCH PROGRAM

AERO PROPULSION LABORATORY
(Wright-Patterson Air Force Base)

1. Dr. Eugene Brown - Virginia Polytechnic Institute & State University
2. Dr. Jimmie Cathey - University of Kentucky
3. Dr. Dennis Flentge - Cedarville College
4. Dr. Thomas Ortmeyer - Clarkson College
5. Dr. Sarwan Sandhu - University of Dayton
6. Dr. Kai Wang - Wayne State University
7. Prof. David Weimer - Ohio Northern University

AEROSPACE MEDICAL RESEARCH LABORATORY
(Wright-Patterson Air Force Base)

1. Dr. Terry Bahill - Carnegie-Mellon University
2. Dr. Louis Buckalew - Alabama A&M University
3. Dr. Gregory Corso - Georgia Institute of Technology
4. Dr. Andris Freivalds - Pennsylvania State University
5. Dr. Zahir Quershi - Rust College
6. Dr. Patrick Sweeney - University of Dayton
7. Dr. Thomas Webb - Ohio State University

ARMAMENT DIVISION
(Eglin Air Force Base)

1. Dr. Donald Healy - Georgia Institute of Technology
2. Dr. Manuel Huerta - University of Miami
3. Dr. Keith Koenig - Mississippi State University
4. Dr. Luigi Morino - Boston University
5. Dr. Gerhard Ritter - University of Florida
6. Dr. Boghos Sivazlian - University of Florida
7. Dr. Alfred Striz - University of Oklahoma

ARNOLD ENGINEERING DEVELOPMENT CENTER
(Arnold Air Force Station)

1. Dr. Larry Forney - Georgia Institute of Technology
2. Dr. Robert Willis - Mercer University

AVIONICS LABORATORY
(Wright-Patterson Air Force Base)

1. Dr. Jack Bourquin - University of Missouri
2. Dr. Albert Frasca - Wittenberg University
3. Dr. Ronald Greene - University of New Orleans
4. Dr. Michael Moloney - Rose-Hulman Institute of Technology
5. Dr. Eugene Norris - George Mason University
6. Dr. Eugene Schram - Ohio State University

BUSINESS RESEARCH MANAGEMENT CENTER
(Wright-Patterson Air Force Base)

1. Dr. David Cleeton - Oberlin College
2. Dr. Hamed Eldin - Oklahoma State University

EASTERN SPACE & MISSILE CENTER
(Patrick Air Force Base)
1. Dr. Junho Choi - Florida Institute of Technology

ELECTRONICS SYSTEMS DIVISION
(Hanscom Air Force Base)
1. Dr. Wilford Fordon - Michigan Technological University

ENGINEERING & SERVICES CENTER
(Tyndall Air Force Base)
1. Dr. Muluneh Azene - Southern University
2. Dr. Robert Douglas - North Carolina State University
3. Dr. Fernando Fagundo - University of Florida
4. Prof. Ervin Hindin - Washington State University
5. Dr. Richard Rice - Clemson University

FLIGHT DYNAMICS LABORATORY
(Wright-Patterson Air Force Base)
1. Dr. Eric Johnson - Virginia Polytechnic Institute & State University
2. Dr. Samuel Kelly - University of Notre Dame
3. Dr. Lakhpat Pujara - Wilberforce University
4. Dr. John Russell - University of Oklahoma
5. Dr. David Wilson - University of Florida
6. Dr. Rama Yedavalli - Stevens Institute of Technology

FRANK J. SEILER RESEARCH LABORATORY
(USAF Academy)
1. Dr. Keith Hanson - Lamar University
2. Dr. Thomas Wiggins - Pennsylvania State University

GEOPHYSICS LABORATORY
(Hanscom Air Force Base)
1. Dr. Francesco Bacchialoni - University of Lowell
2. Dr. Pradip Bakshi - Boston College
3. Dr. Thomas Miller - University of Oklahoma
4. Dr. Stanley Spiegel - University of Lowell
5. Dr. Richard Tipping - University of Nebraska

HUMAN RESOURCES LABORATORY/ADVANCED SYSTEMS DIVISION
(Wright-Patterson Air Force Base)
1. Dr. Mason Bailey - Western Carolina University
2. Dr. Stewart Klapp - California State Universilty

HUMAN RESOURCES LABORATORY/FLYING TRAINING DIVISION
(Williams Air Force Base)
1. Dr. Eugene Galluscio - Northwest Missouri State University
2. Dr. Dean Owen - Ohio State University

PARTICIPANT LABORATORY ASSIGNMENTS (Continued)

HUMAN RESOURCES LABORATORY/PERSONAL RESEARCH DIVISION
(Brooks Air Force Base)
1. Dr. Gary Allen - Old Dominion University
2. Dr. Charles Parsons - Georgia Institute of Technology

HUMAN RESOURCES LABORATORY/TECHNICAL TRAINING DIVISION
(Lowry Air Force Base)
1. Dr. Philip Langer - University of Colorado

LEADERSHIP & MANAGEMENT DEVELOPMENT CENTER
(Maxwell Air Force Base)
1. Dr. Hubert Feild - Auburn University

LOGISTICS COMMAND
(Wright-Patterson Air Force Base)
1. Dr. Donald Byrkett - Miami University

LOGISTICS MANAGEMENT CENTER
(Gunter Air Force Base)
1. Dr. Milton Alexander - Auburn Univerity

MATERIALS LABORATORY
(Wright-Patterson Air Force Base)
1. Dr. Gust Bambakidis - Wright State University
2. Dr. Sherman Brown - University of Illinois
3. Dr. Mark Fugelso - Pennsylvania State University
4. Dr. James Kane - Wright State University
5. Dr. Deborah Medeiros - Pennsylvania State University
6. Dr. David Moroi - Kent State University

ROCKET PROPULSION LABORATORY
(Edwards Air Force Base)
1. Dr. Stephen Lin - North Carolina Central University
2. Dr. Trilochan Singh - Wayne State University

ROME AIR DEVELOPMENT CENTER
(Griffiss Air Force Base)
1. Dr. Richard Absher - University of Vermont
2. Dr. Roger Cavallo - State University of New York
3. Dr. Jerome Knopp - University of Missouri/Rolla
4. Dr. Ronald Remke - University of South Florida
5. Dr. Sam Shanmugan - University of Kansas

ROME AIR DEVELOPMENT CENTER/ELECTRONICS TECHNOLOGY
(Hanscom Air Force Base)
1. Dr. Albert Biggs - University of Kansas
2. Dr. William Filippone - University of Arizona

PARTICIPANT LABORATORY ASSIGNMENT (Continued)

SCHOOL OF AEROSPACE MEDICINE
(Brooks Air Force Base)

1. Dr. Silverio Almeida - Virginia Polytechnic Institute and State University
2. Dr. Willie Bragg - University of Cincinnati
3. Dr. John Enderle - North Dakota State University
4. Dr. Mack Felton - Southern University
5. Dr. Dennis Kern - University of Georgia
6. Dr. Michael Lobb - University of Texas
7. Dr. Troy Nagle - Auburn University
8. Dr. Robert Schlegel - University of Oklahoma
9. Dr. Edward Ward - Alabama A&M University

WEAPONS LABORATORY
(Kirtland Air Force Base)

1. Dr. Francis Jankowski - Wright State University
2. Dr. Letitia Korbly - University of Alabama
3. Dr. Surgounda Patil - Tennessee Technological University
4. Dr. Alexander Stone - University of New Mexico
5. Dr. Edward Walters - University of New Mexico
6. Dr. David Williams - University of Texas

RESEARCH REPORTS
1982 USAF-SCEEE SUMMER FACULTY RESEARCH PROGRAM

Volume I Report Number	Title	Research Associate
1	Sensitivity Based Segmentation And Identification In Automatic Speech Recognition	Prof. Richard G. Absher
2	A Methodology For The Determination Of Input Date Accuracy In The Maintenance Data Collection System	Dr. Milton J. Alexander
3	Assessment of Visuospatial Abilities Using Complex Cognitive Tasks	Dr. Gary L. Allen
4	The Effect Of Modulation Transfer Functions On Flashblindness	Dr. Silverio P. Almeida
5	A Theoretical Evaluation Of The Airfield Pavement Analysis (AFPAV) Finite Element Model	Dr. M. Azene
6	Orbiting Geophysics Laboratory Experiment	Dr. Francesco L. Bacchial
7	Trials And Tribulations At The Helmet Mounted Oculomotor Facility	Dr. A. Terry Bahill
8	Feasibility Of Computer Graphics As An Aid To Aircraft Battle Damage Assessment	Dr. M. Gene Bailey
9	Effects Of Magnetic Shear On Lower Hybrid Waves In The Suprauroral Region	Dr. Pradip M. Bakshi
10	A Simple Model For Impurity Photo-Absorption In Silicon	Dr. Gust Bambakidis
11	Feasibility And Implementation Of A Near Field Antenna Range	Prof. Albert W. Biggs
12	Computer Simulation Of Channelized Receivers	Dr. Jack J. Bourquin
13	From Petite Aviatrix To USAF Aircrew: Historical Review And Current Status Of Female Fliers	Dr. Willie A. Bragg

Report Number	Title	Research Associate
14	Navier-Stokes Solvers For Ramjet Applications	Dr. Eugene F. Brown
15	Development Of Measurment Technique For Fiber-Matrix Adherence In Brittle-Brittle Composites	Dr. S. D. Brown
16	Force Tracking Proficiency In Operating Aircraft Controls	Dr. L. W. Buckalew
17	Spares Support Using Cannibalization	Dr. Donald L. Byrkett
18	Electrically Compensated Constant Speed Drive	Dr. Jimmie J. Cathey
19	An Expert System For Systems Research In Command And Control	Dr. Roger E. Cavallo
20	Adaptive Kalman Tracking Filter for ARIS System	Dr. Junho Choi
21	Incentive Contracting In Multi-Year Procurement	Dr. David Cleeton
22	Binary Classification And The Subtractive Approach	Dr. Gregory M. Corso
23	Evaluation Of The Non-Destructive Testing Of Airfield Pavements: Wave Propagation Aspects	Dr. Robert A. Douglas
24	AMIS - Acquisition Management Information System Problems And Promises	Dr. Hamed Kamal Eldin
25	Modeling And Tracking Saccadic Eye Movements	Dr. John D. Enderle
26	Dynamic Response Of Doubly Curved Cylindrical Shelter	Dr. Fernando E. Fagundo, J
27	Using Hard Criteria To Evaluate Leadership And Management Development Center Consultations	Dr. Hubert S. Feild

Report Number	Title	Research Associate
28	An Evaluation Of Indices Of Coronary Heart Disease (CHD) In A Diseased Free Population	Dr. Mack Felton, Jr.
29	Electron Transport Calculations Using The Method Of Streaming Rays	Dr. W. L. Filippone
30	Voltammetric Studies Of The Lithium/Vanadium Oxide Electrochemical Cell	Dr. Dennis R. Flentge
31	Integral Principles As Applied To Electromagnetic Propagation	Dr. Wilfred A. Fordon
32	Scaling Laws For Particle Breakup In Nozzle Generated Shocks	Dr. L. J. Forney
33	Oxygen-18 Implantation In GaAs	Dr. Albert J. Frasca
34	Modeling Of Active Neuromusculature Response To Mechanical Stress	Dr. Andris Freivalds
35	The Manufacturing Control Language For Robotic Work Cell	Dr. Mark A. Fugelso
36	Parafoveal Visual Information Processing As A Secondary Task Load	Prof. Eugene H. Galluscio
37	Three-Dimensional Visual Information Processing With Binocular Helmet-Mounted Displays	Prof. Eugene H. Galluscio
38	Shallow Donor And Exciton Binding Energies in Quantum Wells	Dr. Ronald L. Greene
39	Nitro Organic Compounds: A Synthetic Study	Dr. Keith Hansen
40	The Effect Of Certain Image Data Reduction Techniques On Edge Quality	Dr. Donald J. Healy
41	Evaluation Of Gas Chromatographic Methods For Determining Trace Levels Of Trichloroethylene In Water	Prof. Ervin Hindin

Report Number	Title	Research Associate
42	Basic Research Issues In Electromagnetic Rail Launchers With Plasma Driven Projectiles	Dr. Manuel A. Huerta
43	Operational Safety Review Methodology	Dr. Francis J. Jankowski
44	Modeling Localized Stress Fields In Composite Laminates	Dr. Eric R. Johnson
45	Synthesis Of Acetylene Terminated Sulfone (ATS) Candidates	Dr. James J. Kane
46	Mathematical Formulation Of The Shear Layer Over An Open Cavity	Dr. Samuel G. Kelly, III
47	Automating The Numerical Stereo Camera	Dr. Dennis M. Kern
48	Memory And Processing Limits In Decision Making	Dr. Stuart T. Klapp
49	Analysis And Modeling Of A Real-Time Holography System	Dr. Jerome Knopp
Volume II		
50	Numerical Solution Of The Three-Dimensional, Unsteady Euler Equation	Dr. Keith Koenig
51	Displaying Results From Numerical Calculations Using Computer Graphics	Dr. Letitia Korbly
52	Modification Of Current Feedback Strategies: A Text Synthesis Approach	Dr. Philip Langer
53	The Detection Of Hazardous Materials From Spills	Dr. Stephen F. Lin
54	Tentative Identification Awareness Stages Leading To Failure Of Vigilance	Dr. Michael L. Lobb
55	Order Release In An MRP Environment	Dr. D. J. Medeiros

Report Number	Title	Research Associate
56	The Measurement Of Ion-Molecule Reaction Rate Coefficients	Dr. Thomas M. Miller
57	A GaAs FET Computer Model With Applicaions To Magnetic Field Effects	Dr. Michael J. Moloney
58	Flutter Taming By Nonlinear Active Control	Dr. Luigi Morino
59	A Theory Of Photoluminescence For Excitons Bound To Two Types Of Neutral Acceptors In Silicon- A Study Of The Systems Si: (In, Al) and Si: (In, B)	Dr. David S. Moroi
60	Error Analysis Of The Karhunen-Loeve Transform In VCG Signal Processing	Dr. H. Troy Nagle, Jr.
61	Simulation Of Adaptive Networks Based On Rest Principle And Heterostatic Models	Dr. Eugene M. Norris
62	Aircraft Electric Power Generation Using Cascaded Symmetrically Wound Machines	Dr. Thomas H. Ortmeyer
63	Adaptation To Optical Flow Rates During Low Altitude, High Speed Flight	Dr. Dean H. Owen
64	The Robustness Of Unidimensional Item Response Theory Models	Dr. Charles K. Parsons
65	R-Reliable Intervals For The Sum Of Two Independent Normal Or Random Variables	Dr. S. A. Patil
66	Model Reduction Of Control Systems	Dr. L. R. Pujara
67	Measurement Of Levels Of Prostaglandin-E And Prostaglandin-F2α In Various Tissues, Urine, and Plasma Of Rats Given Nonadecafluorodecanoic Acid	Dr. Zahir Qureshi

Report Number	Title	Research Associate
68	A Preliminary Study Of Electromigration In Aluminum And Aluminum-Silicon Films	Dr. R. L. Remke
69	A Study Of Factors Affecting Soot Formation In A Swirl - Stabilized Combustor	Dr. Richard W. Rice
70	Development Of A Mathematical Foundation For Cellular Image Processing	Dr. Gerhard X. Ritter
71	Turbulent Boundary Layers Over Rough Surfaces In Hypersonic Flow	Dr. John M. Russell
72	Conceptualization Of The Dynamic Bahavior Of The Flow-Field In The APL Combustor	Dr. Sarwan S. Sandhu
73	Performance Demand And CNS Depressant Stressor Effects On Spatial Orientation Information Processing	Dr. Robert E. Schlegel
74	Metal Organic Chemical Vapor Deposition-Evaluation Of Current And Possible Future Chemical Systems As Related To The Formation Of Gallium Arsenide	Dr. Eugene P. Schram
75	Software Simulation Requirements For The CVA Program And Other Applications	Dr. K. Sam Shanmugan
76	Afterburning Suppression Kinetics In Rocket Exhaust	Dr. Trilochan Singh
77	On Estimating Probability Of Kill In Weapon Evaluation	Dr. B. D. Sivazlian
78	Methods For Computation Of Certain Diagnostics For The AFGL General Circulation Model	Dr. Stanley L. Spiegel
79	A Differential Geometric Approach To Electromagnetic Lens Design	Dr. Alexander P. Stone
80	The Use Of Experimental Input In Transonic Aerodynamics	Dr. Alfred G. Striz

Report Number	Title	Research Associate
81	A Dynamic Model Of Acceleration Stress Protection IN The Human Aircrew Member	Dr. Patrick J. Sweeney
82	Collision-Induced Absorption In The Far Infrared Spectrum of N_2	Dr. Richard H. Tipping
83	Photoionization Of Iodine Molecules And Clusters In A Supersonic Molecular Beam	Dr. Edward A. Walters
84	Data Communications Between CDC Cyber 750 and HP 1000	Dr. Kai Wang
85	Isolation Of Pyrogenic Exotoxin C From Staphylococcus Aureus Strains Associated Wtih Toxic-Shock Syndrome	Dr. Edward R. Ward, Jr.
86	Effect Of NDFDA On Fatty Acid Synthesis In Rat Liver	Dr. Thomas E. Webb
87	Hook Interferometry Using A Pulsed Dye Laser	Prof. David Weimer
88	Laser Damage In Films And Plastics	Dr. T. A. Wiggins
89	An Algorithm And Associated Data Structures For Hidden Surface Elimination	Dr. David H. Williams
90	Effort To Produce Metaboric Acid Vapor And Water Vapor Broadening Of Carbon Monoxide Absorption Lines	Dr. Robert E. Willis
91	3-Dimensional Grid Generation With Applications To High Performance Aircraft	Dr. David C. Wilson
92	Time Domain Analysis And Synthesis Of Robust Controllers For Large Scale LQG Regulators	Dr. Rama K. Yedavalli

1982 USAF-SCEEE SUMMER FACULTY RESEARCH PROGRAM

Sponsored by the

AIR FORCE OFFICE OF SCIENTIFIC RESEARCH

Conducted by the

SOUTHEASTERN CENTER FOR ELECTRICAL ENGINEERING EDUCATION

FINAL REPORT

SENSITIVITY BASED SEGMENTATION AND IDENTIFICATION IN AUTOMATIC SPEECH RECOGNITION

Prepared by:	Dr. Richard G. Absher
Academic Rank:	Professor
Department and University:	Computer Science and Electrical Engineering, University of Vermont
Research Location:	Rome Air Development Center, Intelligence and Reconnaissance Division
USAF Research Colleague:	Mr. Edward Cupples, IRAA
Date:	September 6, 1982
Contract No:	F49620-82-C-0035

SENSITIVITY BASED SEGMENTATION AND IDENTIFICATION IN AUTOMATIC SPEECH RECOGNITION

by

Dr. Richard G. Absher

ABSTRACT

A sensitivity analysis for the segmentation and identification of the phonetic units of speech was investigated. Elements of the sensitivity matrix, which express the relative change in each pole of the speech model to a relative change in each coefficient of the characteristic equation, was evaluated for each of the fifteen vowels for a single male speaker. It was found that the sensitivity matrix provides (1) a measure of the degree to which a vowel is "on target", (2) a categorical indicator for the group of front vowels, (3) a categorical indicator for the group of back vowels, and (4) may provide sufficient information to identify each particular vowel. Suggestions for further research in this area are offered.

Acknowledgement

The author would like to thank the Air Force Systems Command, the Air Force Office of Scientific Research and the Southeastern Center for Electrical Engineering Education for providing him with the opportunity to spend a very worthwhile and interesting summer at the Rome Air Development Center, Griffiss AFB, N.Y. He would like to acknowlege the Center, in particular the Intelligence and Reconnaissance Division, for its hospitality and excellent working conditions.

Finally, he would like to thank Mr. Edward Cupples and the entire IRAA staff for their collaboration, guidance, and helpful discussions.

I. INTRODUCTION:

Automatic Speech Recognition (ASR) has potential application to various USAF operational problems. Examples include voice control of devices and systems, intelligence data handling, and language identification. A practical ASR system "must operate on the continuous utterance of any number of speakers in moderate or even poor noise environments".[1] Major sources of difficulty include acoustic-phonetic variance and segmentation of the acoustic signal. The following discussion reviews the reasons for this difficulty and expresses the research problem.

Connected-speech-recognition systems have utilized techniques that represent sound patterns in smaller linguistic units than words; one being in terms of phonemes. However, the location and specification of the acoustic characteristics of phonemes has been a central problem to speech recognition. The problem is not attributable to mechanical limitations. Instead, it is considered to be the result of the very nature of human speech production and perception, for phonemes are not individual sounds, but rather classes of acoustically different sounds which speakers of a language have learned to call equivalent.

In contrast to the discrete units of linguistic analysis, (i.e., sentences, phrases, words, morphemes, phonemes) the acoustic representation of an utterance is semi-continuous. The problem for those studying speech recognition is to map semi-continuous acoustic waveforms into discrete linguistic units. Attempts to accomplish this task have revealed a number of sources of variation that make this mapping difficult. Lack of a one-to-one correspondence between acoustic segments and the linguistic units they represent can be attributable to (1) coarticulation, (2) allophonic variation, (3) stress and rate of speech production, and (4) individual speaker differences.

Coarticulation can be defined as the influence of one phoneme upon another. Logically, the mismatch between phoneme and acoustic representation caused by coarticulation can be divided into cases in which (1) a phoneme has more than one acoustic representation,

and (2) an acoustic segment can represent more than one phoneme. An example of the first case are vowels that have nasal cavity resonances and antiresonance when produced in nasal consonant contexts (e.g., m<u>a</u>n) but not in others (e.g., p<u>a</u>t). Speakers of a language group these different acoustic events into the same phoneme class, and so must speech recognition systems.

An example of the second kind of mismatch, where a unique acoustic signal can correspond to one of several phonemes, involves the noise burst frequency due to place of articulation of stop consonants in CV (consonant-vowel syllables). It has been demonstrated that a noise burst of a particular frequency is perceived by a listener as /p/ when followed by /i/. The same noise burst is perceived by a listener as /k/ when the following vowel was /ae/. As a consequence of multiple linguistic interpretations of the same acoustic segment, it is imperative that speech recognition systems be able to defer decisions about the phonemic identity of an acoustic event until context can be considered.

Allophonic variation refers to the language-specific systematic use of different sound segments (phones) to represent a particular phoneme. For example, the voiceless stop consonants /p/, /t/, /k/ have three allophones in English which occur in contexts specified by definable rules. Aspirated voiceless stops (produced with an audible puff of air at release) are used at the beginning of stressed syllables (e.g., pea). Unaspirated stops (produced without the audible release of air) are used (a) at the beginning of unstressed syllables (e.g., appear), (b) in clusters with /s/ (e.g., speak) and (c) at the ends of words (e.g., keep). Unreleased stops (produced without opening the vocal tract after closure) are used (a) when the stop consonant precedes a homorganic (same place) consonant (e.g., kee<u>p</u> me), and (b) optionally at the end of a phrase (e.g., keep).

Stress and rate of production affect the way in which speech sounds are articulated and, as a consequence, affect their acoustic representations. Under conditions of increased speech rate, the

duration of some speech segments is decreased and the articulatory targets achieved typically "fall short". Stressed segments, on the other hand, are known to be longer and to more closely approximate articulatory targets.

Inter-speaker differences in physical structure or dialect are another source of acoustic-linguistic mismatch. Inter-speaker differences in acoustic output that arise from differences in the physical structures themselves are predictable from the acoustic theory of production. In this widely accepted view, the vocal tract is considered a kind of resonating tube where movement of the vocal structures alter the shape of the tube and result in the production of different sounds. Important considerations are age and sex of the speaker, since both of these parameters influence the size of the larynx and the size of the vocal tract, causing differences in fundamental frequency and formant frequencies.

II. OBJECTIVES:

Most current computer based speech-recognition systems employ a three-step procedure. In the first step, a word or phrase is divided into time segments or frames. For each frame, a "best fit" is determined for a particular parametric representation (speech model). Next, a statistical decision rule is used to tentatively determine (or estimate) the phoneme corresponding to each frame. Third, a set of phonological decision rules is used to combine the phonemic decisions of the several frames and access lexical candidates.

The objective of the present research is to investigate a novel 2-level scheme for more accurate segmentation of the speech signal into phonetic units. Such a scheme may allow for a more accurate application of decision rules, and may provide a practicable framework for incorporation of acoustic-phonetic variance.

In the proposed system, the initial parametric representation of each frame consists of the linear prediction coefficients which can be used to express the coefficients of the following characteristic equation:

$$q(s) = s^n + a_2 s^{n-1} + \ldots + a_n s + a_{n+1} \qquad (1)$$

The second level of the segmentation depends on a sensitivity matrix with elements defined as:

$$S(k,i) = \frac{a_k}{r_i} \frac{dr_i}{da_k} \qquad (2)$$

This definition easily leads to the following closed-form expression:

$$S(k,i) = \frac{1}{k-1-n + \sum_{j=1}^{n} \frac{r_i}{r_i + P_{jk}}} \qquad \begin{matrix} i = 1, \ldots, n \\ k = 2, \ldots, n+1 \end{matrix} \qquad (3)$$

where r_i is a root of the characteristic equation and P_{jk} is the j-th root of the characteristic equation when its k-th coefficient is assigned the value zero. Thus S(k,i) expresses the relative change in the location of filter pole i to the relative change in coefficient a_k.

The short ten week research period required that the set of phonemes be limited to the initial and final representations of the fifteen vowels of a single male speaker. The specific objectives were (1) to evaluate the sensitivity matrix for each vowel, (2) to determine if the sensitivity matrix provides a measure of the degree to which a sound is "on target" and (3) to determine if the sensitivity matrix can be used to identify the individual phonemes.

III. PROGRESS REPORT:

The acoustic theory of speech production considers the vocal tract as a resonating tube that filters the source of sound. An approximate representation of the filter is:

$$T(s) = \prod_{i=1}^{3} \frac{r_i r_i^*}{(s + r_i)(s + r_i^*)} \qquad (4)$$

where the constant r_i and its complex conjugate r_i^* are determined by the values of the i-th formant frequency f_i and its bandwidth bw_i. That is,

$$r_i = \pi \cdot bw_j + j\, 2\pi f_i \qquad (5)$$

Expanding the denominator of T(s) gives the characteristic equation:

$$q(s) = s^6 + a_2 s^5 + \ldots + a_6 s + a_7 \qquad (6)$$

If any coefficient a_i is varied, then each constant r_j must also change. The sensitivity matrix, defined in equation (2), is a relative measure for the extent of these changes. As illustrated in Figure 1, it is possible to vary each coefficient, one at a time, from zero to infinity and make a sketch of the corresponding roots (root-locus) of the characteristic equation. These root changes reflect, as described by equation (5), the changes in formant frequency and formant bandwidth.

Note that the elements S(i,j) of the sensitivity matrix are proportional to the slopes of root-locus branches at the points corresponding to the particular coefficient values. Thus the elements of the sensitivity matrix are complex quantities which express the magnitude and direction of root changes due to coefficient changes. Because S(i,j) is normalized, a direction or phase of 0 means that the root is moving in the direction of the vector from the s-plane origin to the root.

For example, at the points labeled 1 on the curves for a_2 shown in Figure 1, increasing a_2 results in small changes in the three formant frequencies, but significantly changes the bandwidths. Expressed in terms of sensitivity elements, S(2,1) and S(2,3) have a phase of essentially 90 degrees, whereas S(2,2) has a phase of essentially 270 degrees. By contrast, at the points labeled 1 on the curves for a_3 shown in Figure 1, increasing a_3 results in small changes in bandwidth, but significant changes in formant frequencies. Expressed in terms of sensitivity elements, S(3,1) and S(3,3) have a phase of essentially 0 degrees, whereas S(2,2) has a phase of essentially 180 degrees.

Investigations to date have utilized vowel data reported by Dennis Klatt[2] and shown in Figure 2. These data are for his voice and were obtained from the analysis of many consonant-vowel productions. The parameters listed are the initial and final values of the first three formants and their bandwidths.

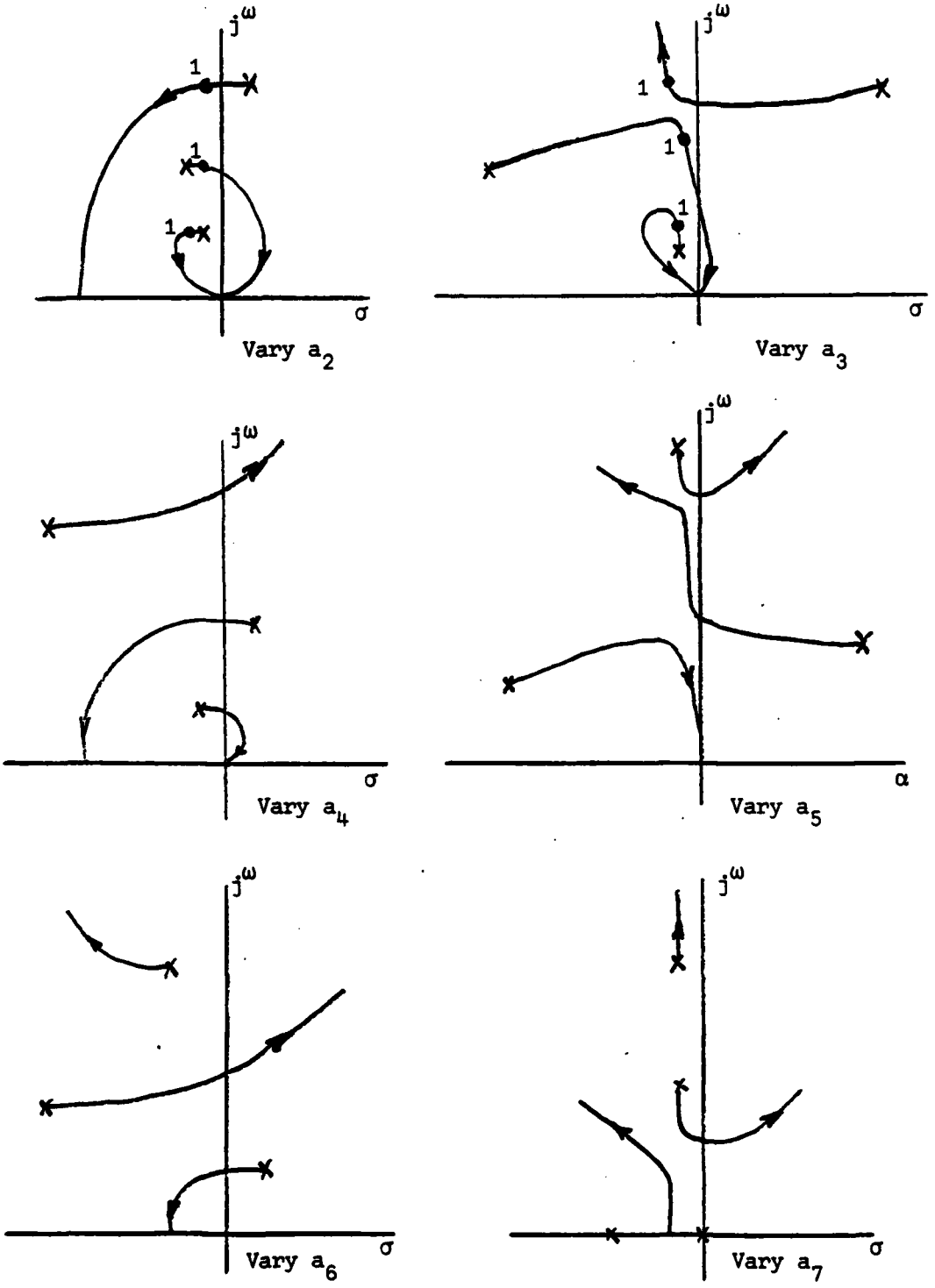


FIGURE 1 - ROOT-LOCUS SKETCHES

Table 2. Parameter values for the synthesis of selected vowels. If two values are given, the vowel is diphthongized or has a schwa-like offglide in the speech of the author. The amplitude of voicing, AV, and fundamental frequency, F0, must also be given contours appropriate for an isolated vowel.

Vowel	F1	F2	F3	B1	B2	B3
IY i	310	2020	2960	45	200	400
	290	2070	2960	60	200	400
IH ɪ	400	1800	2570	50	100	140
	470	1600	2600	50	100	140
EY e	480	1720	2520	70	100	200
	330	2020	2600	55	100	200
EH ɛ	530	1680	2500	60	90	200
	620	1530	2530	60	90	200
AE æ	620	1660	2430	70	150	320
	650	1490	2470	70	100	320
AA ɑ	700	1220	2600	130	70	160
AO ɔ	600	990	2570	90	100	80
	630	1040	2600	90	100	80
AH ʌ	620	1220	2550	80	50	140
OW o	540	1100	2300	80	70	70
	450	900	2300	80	70	70
UH ʊ	450	1100	2350	80	100	80
	500	1180	2390	80	100	80
UW u	350	1250	2200	65	110	140
	320	900	2200	65	110	140
ER ɝ	470	1270	1540	100	60	110
	420	1310	1540	100	60	110
AY ə^{y}	660	1200	2550	100	70	200
	400	1880	2500	70	100	200
AW ə^{w}	640	1230	2550	80	70	140
	420	940	2350	80	70	80
OY ə^{y}	550	960	2400	80	50	130
	360	1820	2450	60	50	160

FIGURE 2 - FORMANT FREQUENCIES AND BANDWIDTHS OF SELECTED VOWELS (reproduced from reference 2, page 291)

A computer program was written to

(1) calculate, from the formant frequencies and bandwidths, the coefficients of the characteristic equation,

(2) vary each coefficient a_i by $\pm$ 25% or $\pm$ 50% from its initial or nominal value,

(3) calculate the corresponding elements of the sensitivity matrix, and,

(4) make plots for the magnitude and phase of each sensitivity element as each coefficient a_i is varied.

All the vowel data of Figure 2 has been processed and is summarized in the following discussion.

Figures 3 and 4 show the magnitude and phase plots for S(2,*) for the high front vowel /IY/ as coefficient a(2) is varied $\pm$ 25% from its nominal value. In all plots, formants 1, 2, and 3 correspond to plotting symbols *, Δ , and □ . Thus, Figure 3 shows that formant 3 is the most sensitive and formant 1 is the least sensitive to changes in coefficient a(2). But even a sensitivity of .2 is small. Referring to Figure 4, the phase curves of formants 1 and 3 are essentially 90 degrees and the phase of formant 2 is essentially 270 degrees. Thus, an increase in coefficient a(2) increases the bandwidths of formants 1 and 3, decreases the bandwidth of formant 2, and essentially does not change any of the formant frequencies. This type of influence was found to hold for all vowels and also for coefficients a(4) and a(6).

For the same phoneme /IY/, Figures 5 through 8 show the magnitude and phase plots for sensitivity elements S(3,*) and S(5,*) as coefficients a(3) and a(5) are varied. Figures 6 and 8 show that under the nominal conditions of 1.0 a(3) and 1.0 a(5), the phase associated with each formant is essentially 0 or 180 degrees. A phase of 0 means that the root is moving in the direction of the vector from the s-plane origin to the root.

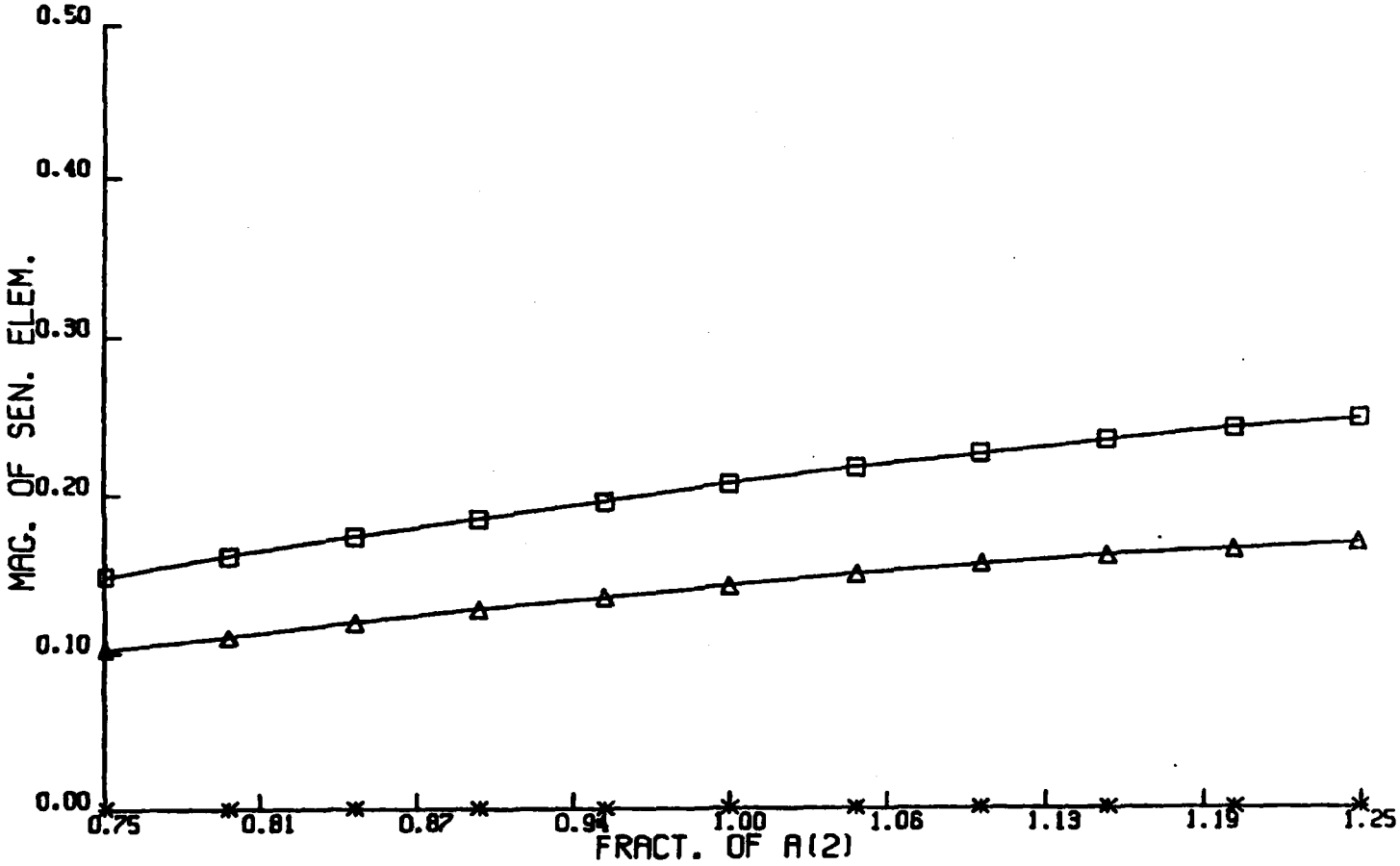


FIGURE 3 - PHONENE IY (1) S(2,*)

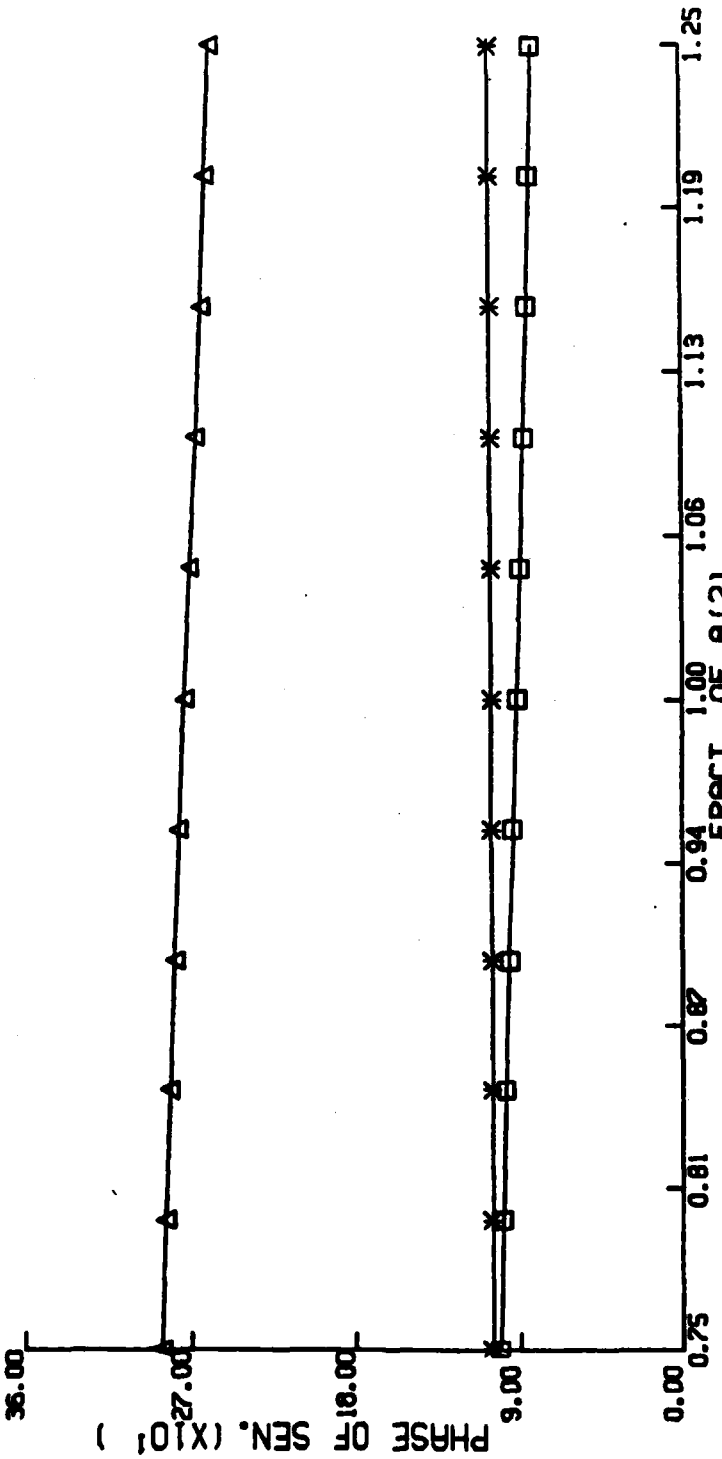


FIGURE 4 - PHONEME IY (1) S(2,*)

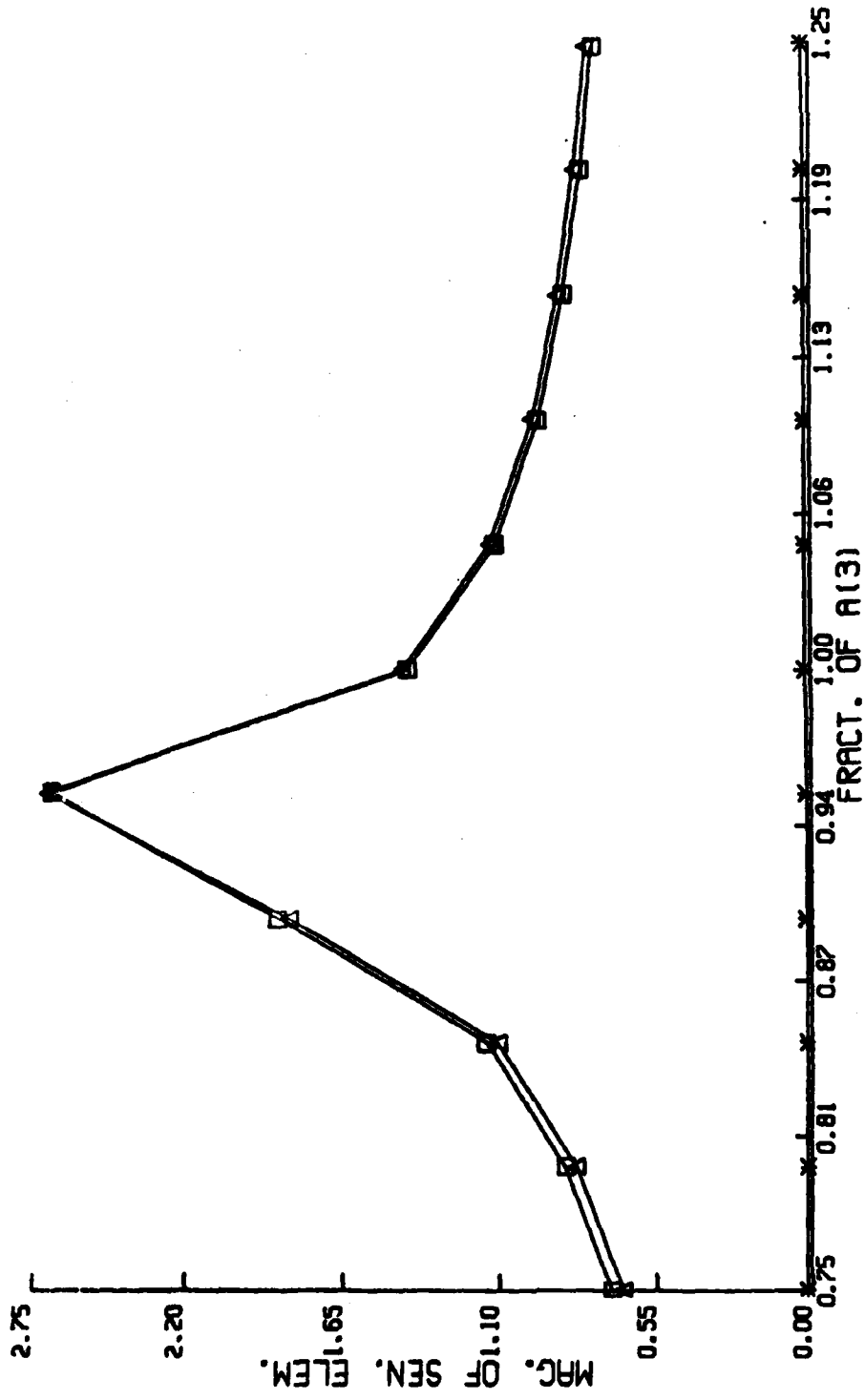


FIGURE 5 - PHONEME IY (1) S(3,*)

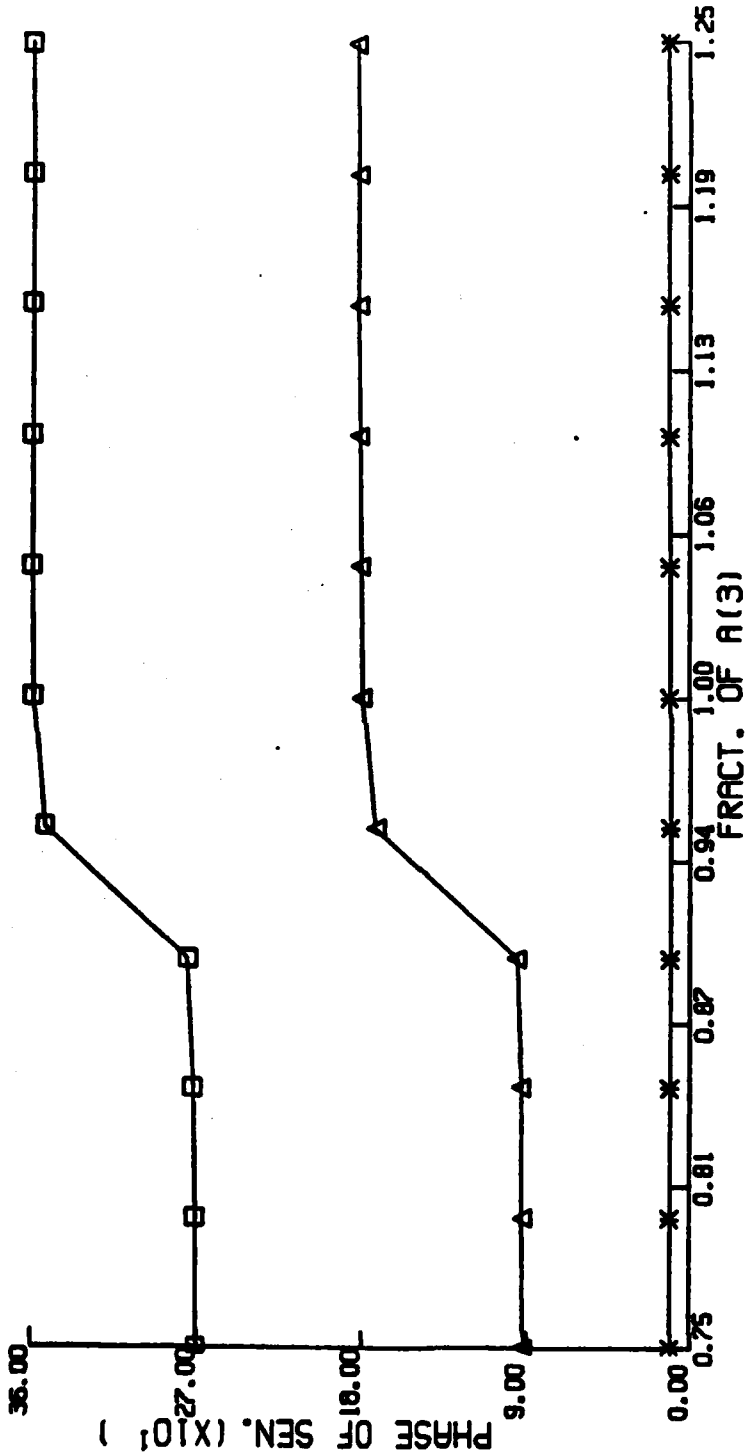


FIGURE 6 - PHONEME IY (1) S(3,*)

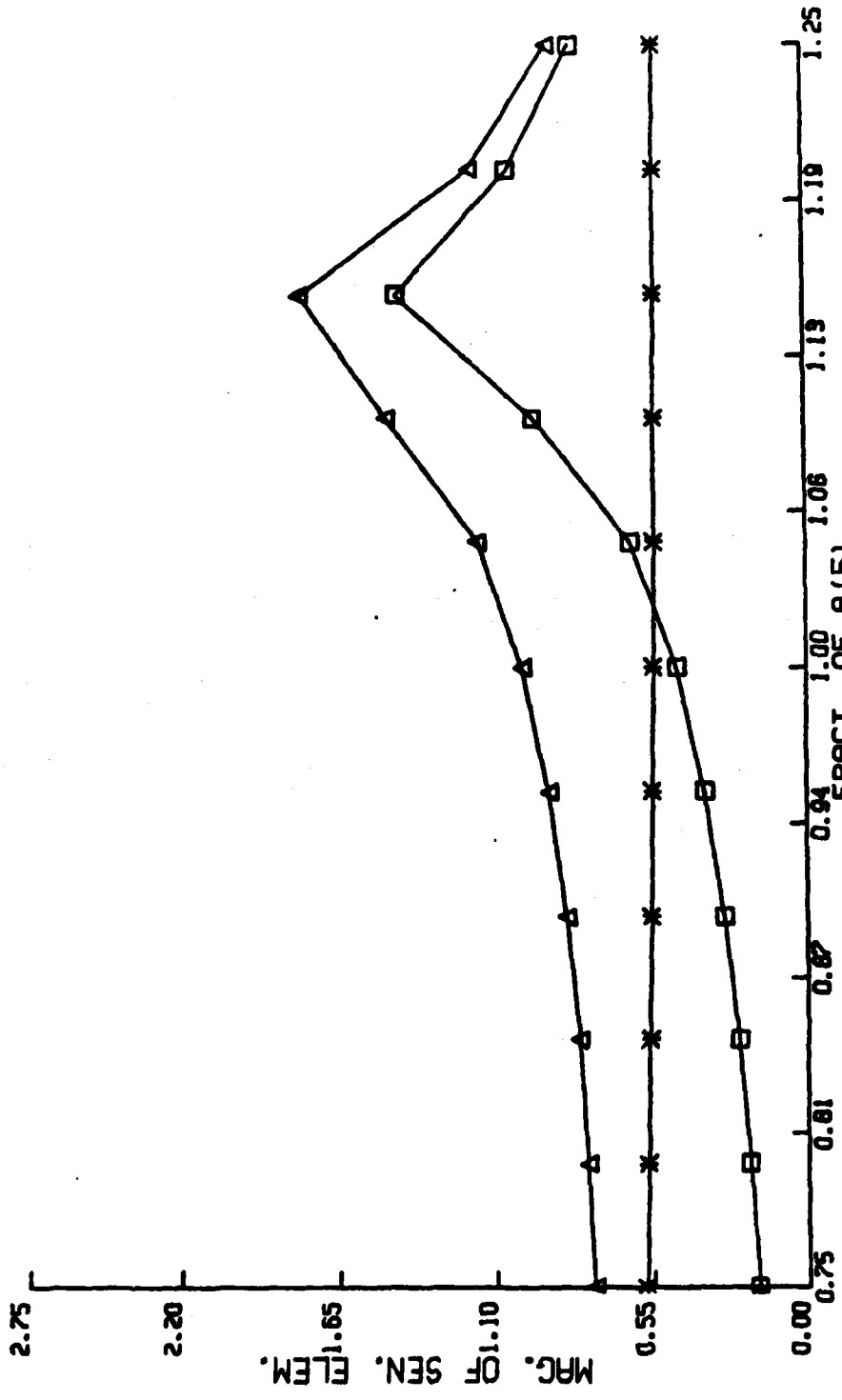


FIGURE 7 - PHONEME IY (1) S(5,*)

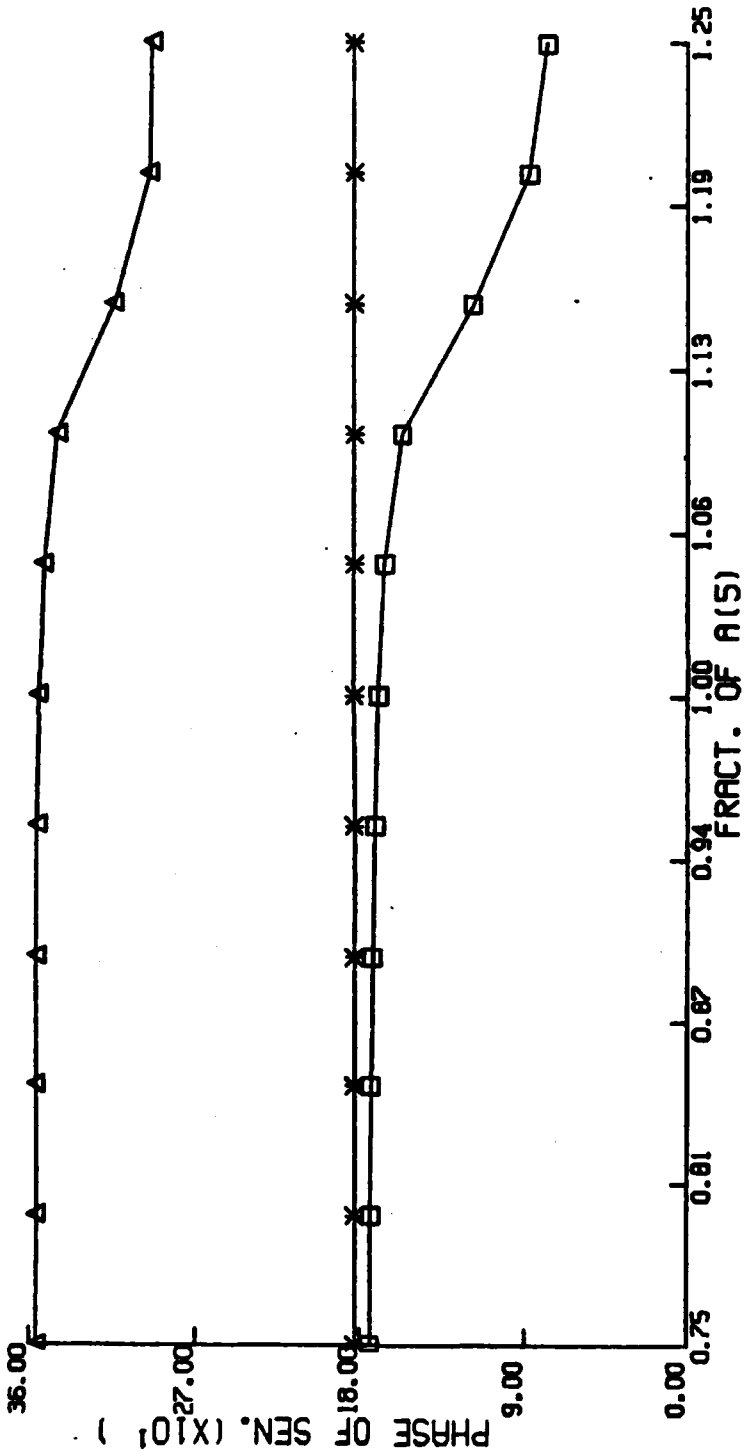


FIGURE 8 - PHONEME IY (1) S(5,*)

Referring to Figure 6, formant frequencies 1 and 3 are essentially increasing, formant frequency 2 essentially decreasing, and only small changes are occurring in the formant bandwidths as coefficient a(3) increases. As shown in Figure 8, the same kind of changes occur with a decrease in coefficient a(5). This kind of influence was also found to hold for coefficient a(7) and for all the vowels.

The observation that the phase relations described for odd and even numbered coefficients holds for all vowels suggests a categorical indicator for non-vowel waveforms.

Further examination of the phase curves of Figures 6 and 8 show that coefficient a(3) is essentially as low, and coefficient a(5) is essentially as high, as possible without formants 2 and 3 moving "around the corners" in their associated root-locus branches. That is, with nominal coefficient values, formants 2 and 3 are essentially as close together as possible without major changes in their bandwidths. This type of relationship between formants 2 and 3 was found to hold for the mid-vowel /ER/ and all the front vowels /IY, IH, EY, EH, AE/. Thus there is a clear categorical indicator for this group of vowels.

In contrast, the low back vowel /AH/ is described by Figures 9 through 14 which contain the magnitude and phase curves for S(3,*) and S(5,*) as either coefficient a(3) or a(5) is varied. The nominal value of coefficient a(3), as shown by Figures 9 and 10, is intermediate between the root-locus corners of formants 2 and 3 and the root-locus corners of formants 2 and 1. Figures 11 and 12 show that S(5,*) is now quite different in that the nominal value of coefficient a(5) is essentially as low as possible without formants 1 and 2 moving around their root-locus corners. This relationship between coefficient a(5) and formants 1 and 2 is also shown in Figures 13 and 14. Again, these kinds of relationships hold for all the back vowels /AA, AO, AH, OW, UH, UW, AY, AW, OY/ and serve as a clear categorical indicator.

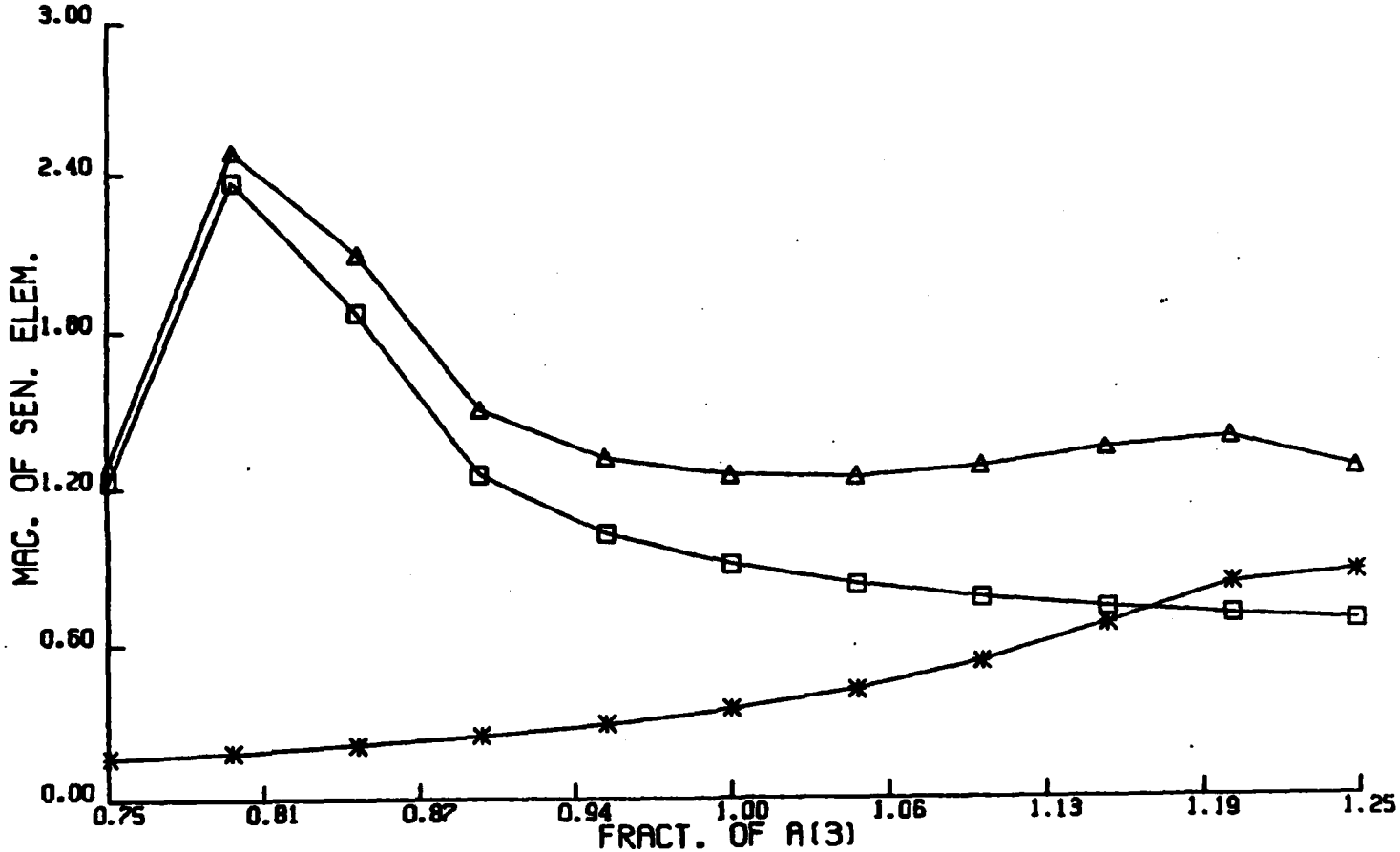


FIGURE 9 - PHONEME AA (6) S(3,*)

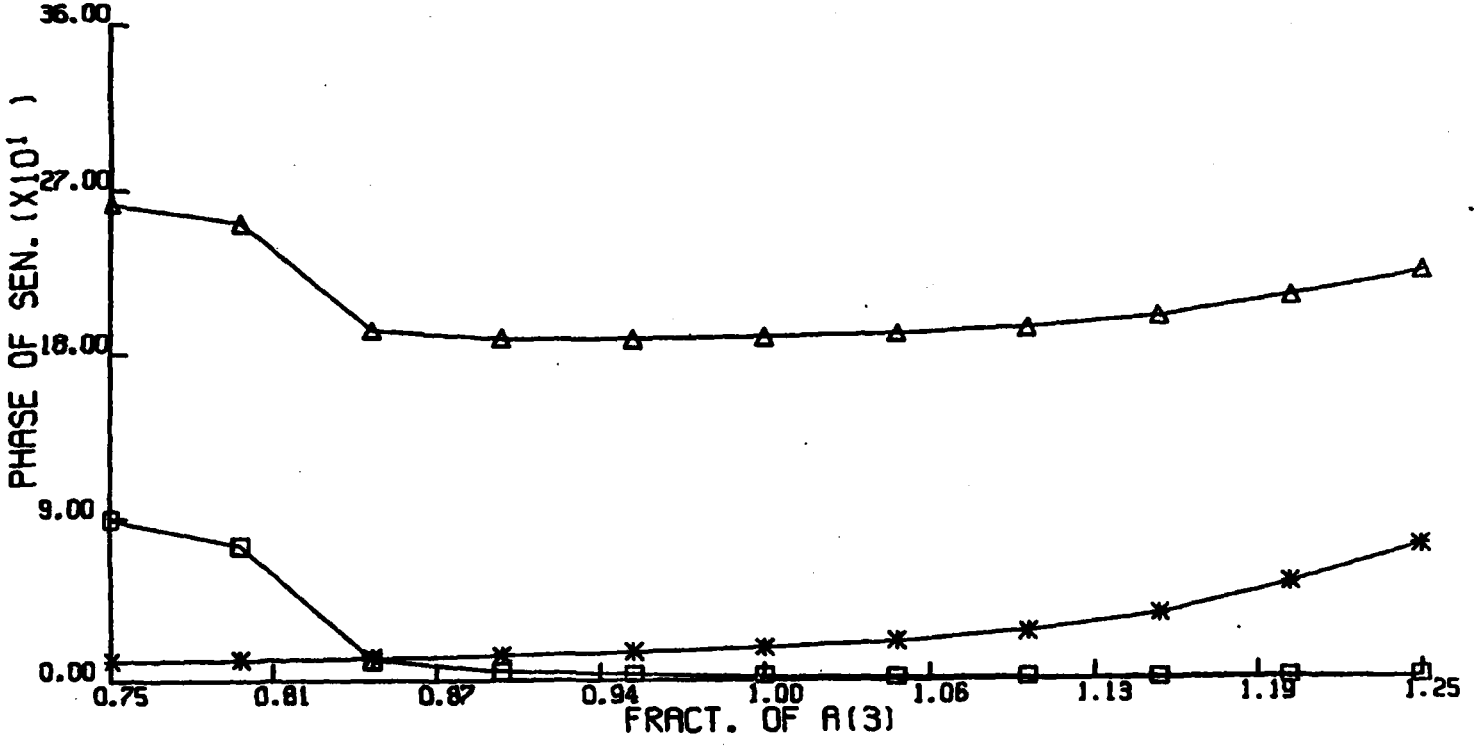


FIGURE 10 - PHONEME AA (6) S(3,*)

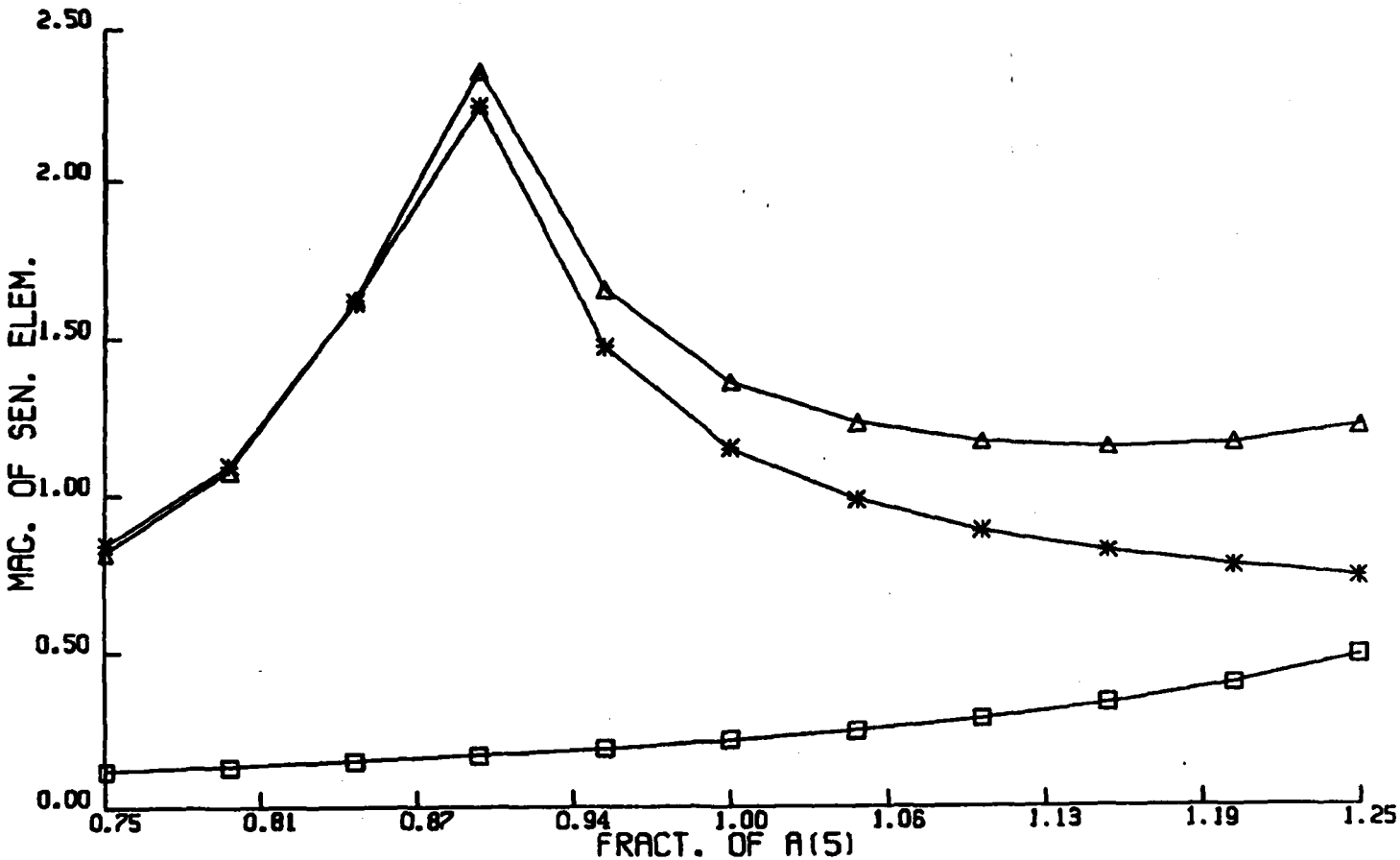


FIGURE 11 - PHONEME AA (6) S(5,*)

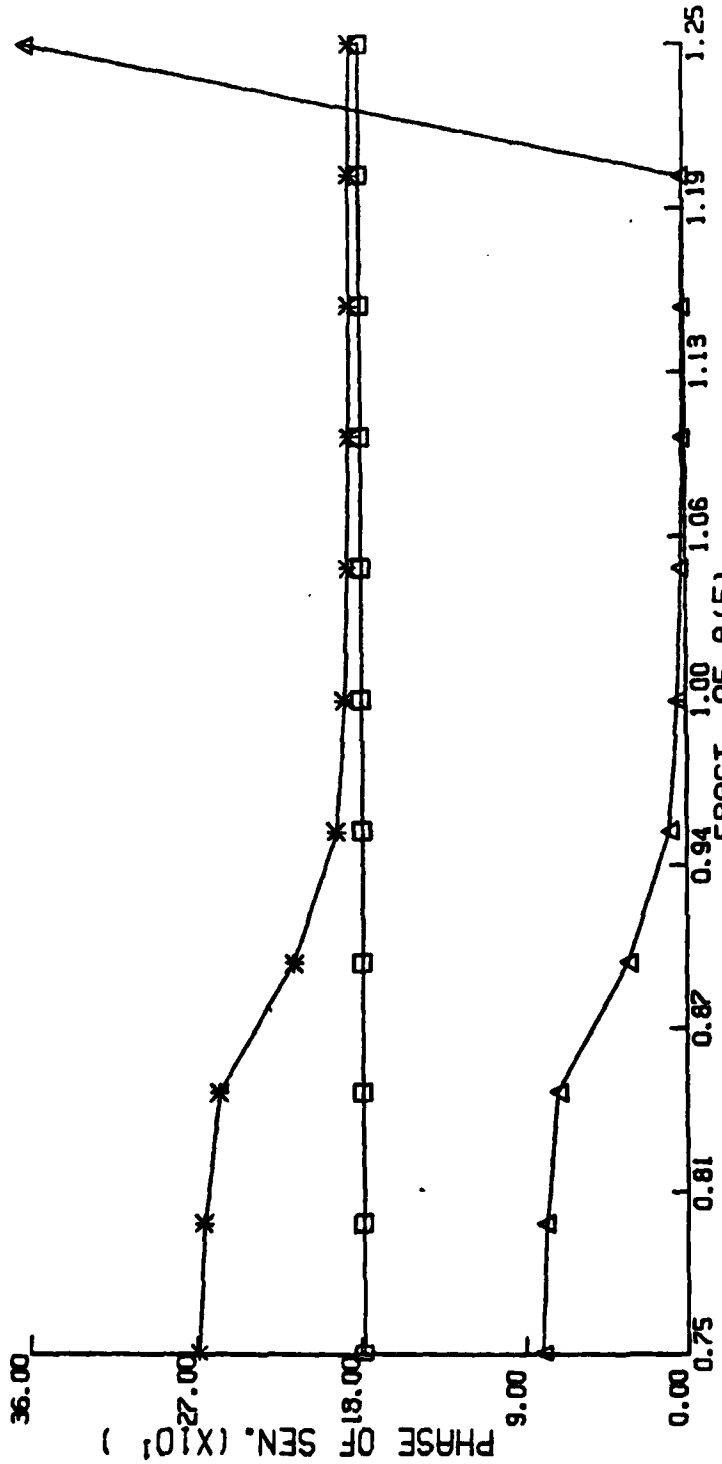


FIGURE 12 - PHONEME AA (6) S(5,*)

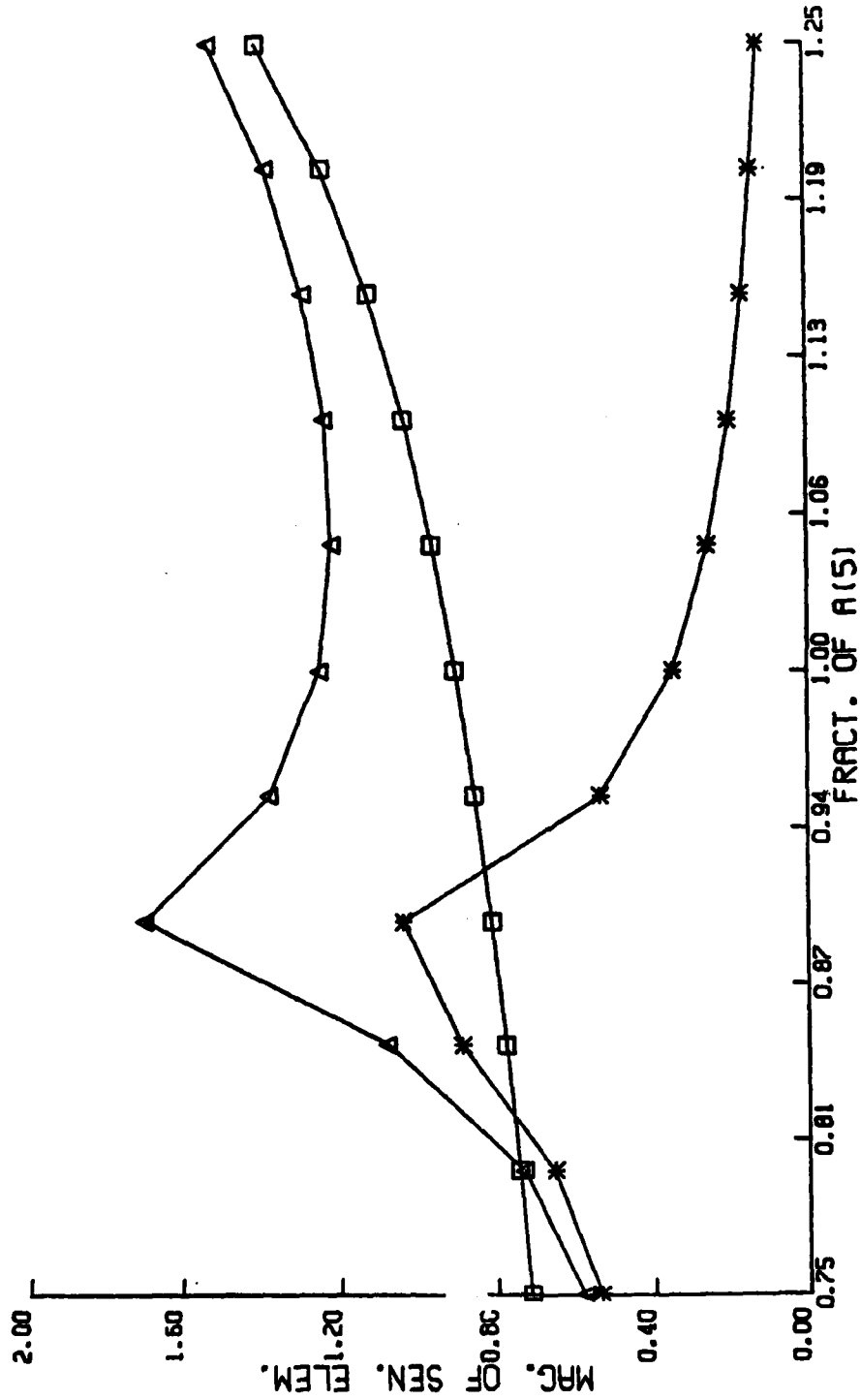


FIGURE 13 - PHONEME AA (6) S(3,*)

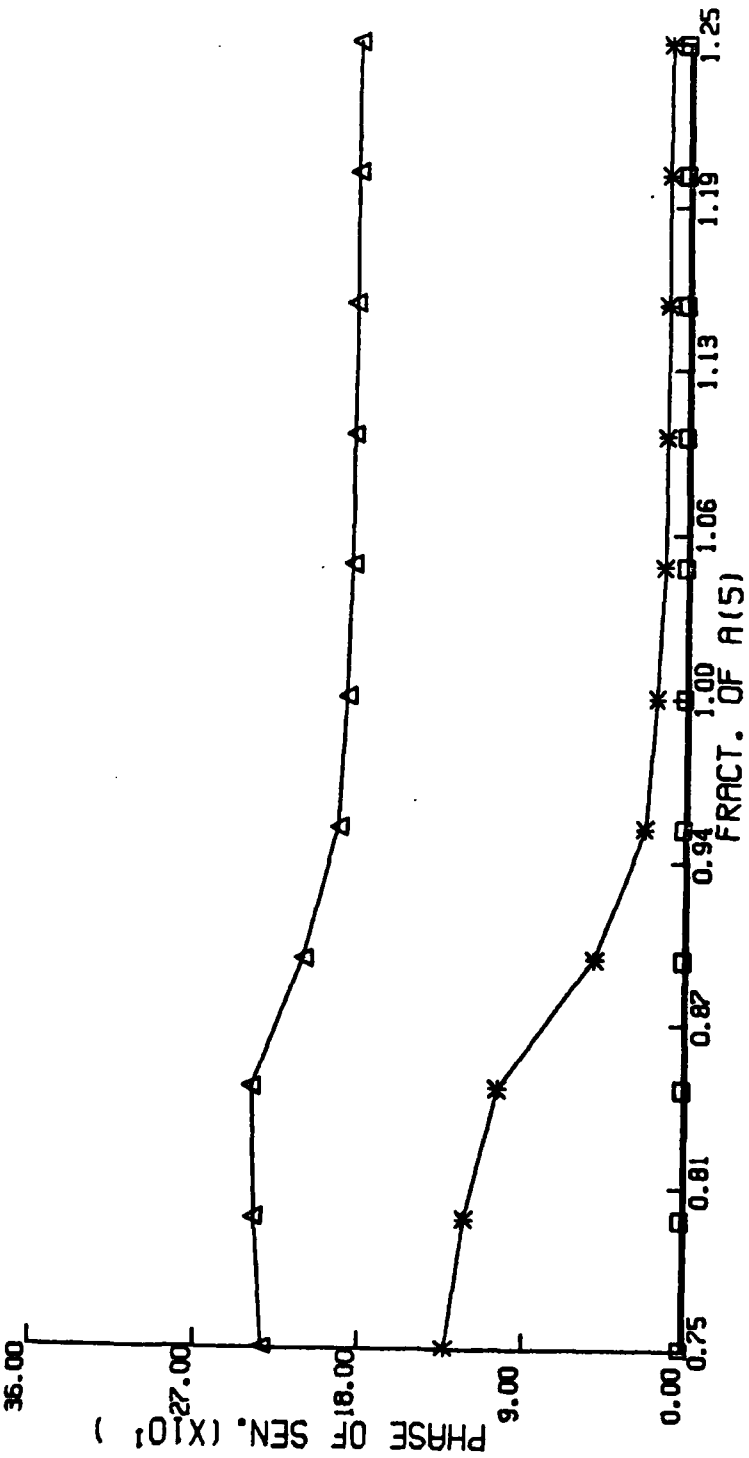


FIGURE 14 - PHONEME AA (6) S(3,*)

The changes that occur in moving from a high front vowel like /IY/ to a low front vowel like /AE/ are seen by comparing Figures 5 through 8 with Figures 15 through 18. Sensitivity elements S(3,1) and S(5,1) are larger for vowel /AE/ and reflect the property that root-locus corners for formants 2 and 3 are closer to the root-locus corners for formants 1 and 2. The changes in sensitivity element S(3,1) in moving from the highest to the lowest front vowel is shown in Figure 19. To mimic the effect of noise, also shown on the figure is how the sensitivity element S(3,1) changes due to a $\pm$ 5% change in coefficient a(5).

These results suggest that the sensitivity elements may be sufficient to identify the particular front vowel. If the starting conditions of some front vowels is similar, such as in /EY, EH/, further specificity may be obtained by observing the subsequent changes in the sensitivity elements. For example, the Klatt data is somewhat diphthongized and S(3,1) for phoneme /EY/ decreases from .067 to .023, whereas for phoneme /EH/ it increases from .087 to .150.

Another observation was made concerning the changes that occur in moving from a high to a low front vowel. Coefficients a(3) and a(5) must change in a compensatory way in order to maintain a fixed position, for all front vowels, relative to the root-locus corners of formants 2 and 3. For the Klatt data, the relative decrease in a(3) is .613 times the relative decrease in a(5). Figure 20 compares the actual formant frequency changes (*, Δ , $\square$) with the changes that would occur ($\bigstar$, $\bigcirc$, #) if coefficient a(7) was held fixed at the value for /IY/ and coefficients a(3) and a(5) vary as described above. Thus, the formant frequency changes between the vowels / IH, EY, EH, AE/ is primarily due to changes in coefficient a(7).

The changes that occur among the group of back vowels is reflected by the relative location of the root-locus corners for formants 2 and 3 and the root-locus corners for formants 1 and 2. Values of the sensitivity matrix are a measure of these locations and may be sufficient to identify sub-groups as well as the

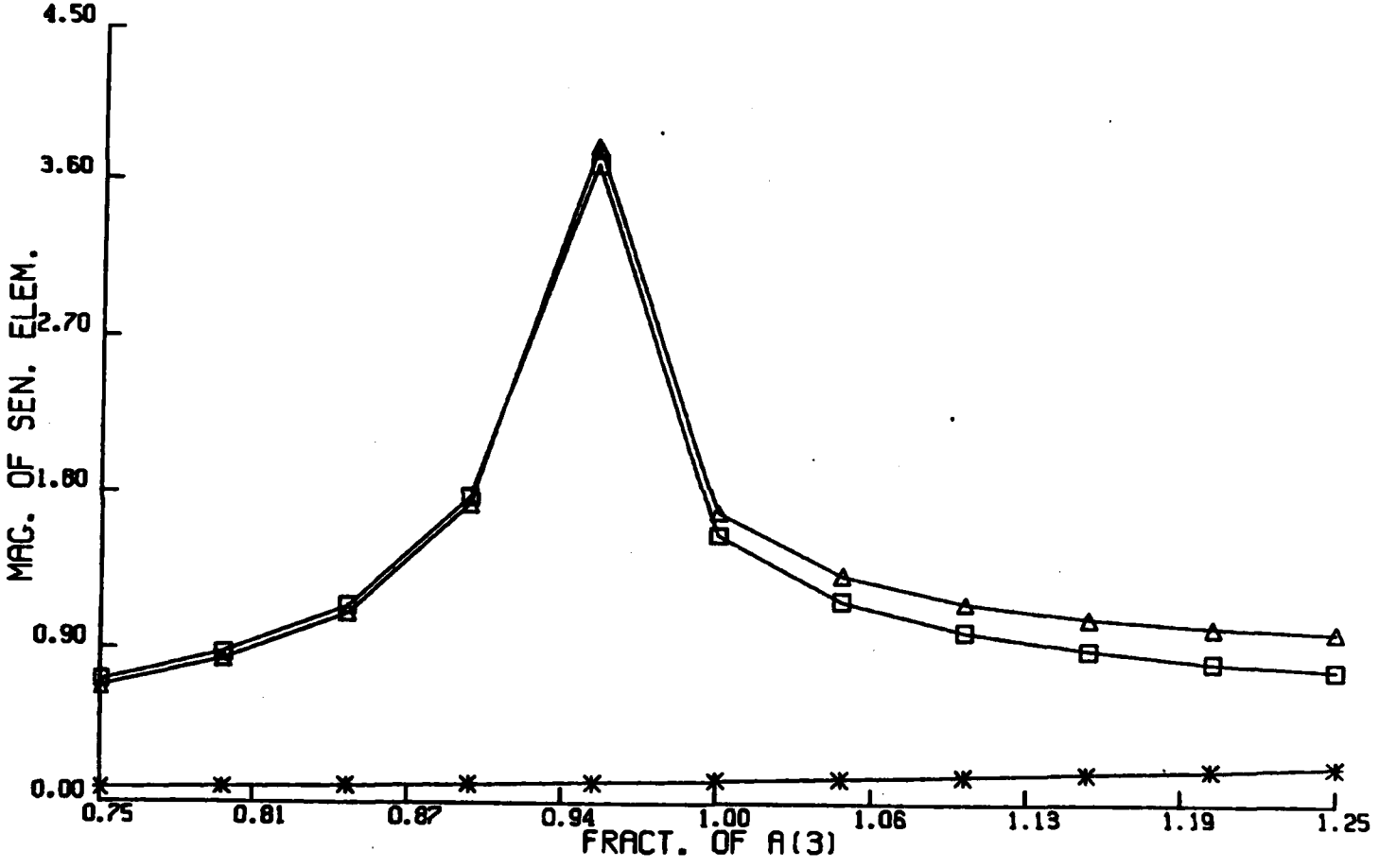


FIGURE 15 - PHONEME AE (5) S(3,*)

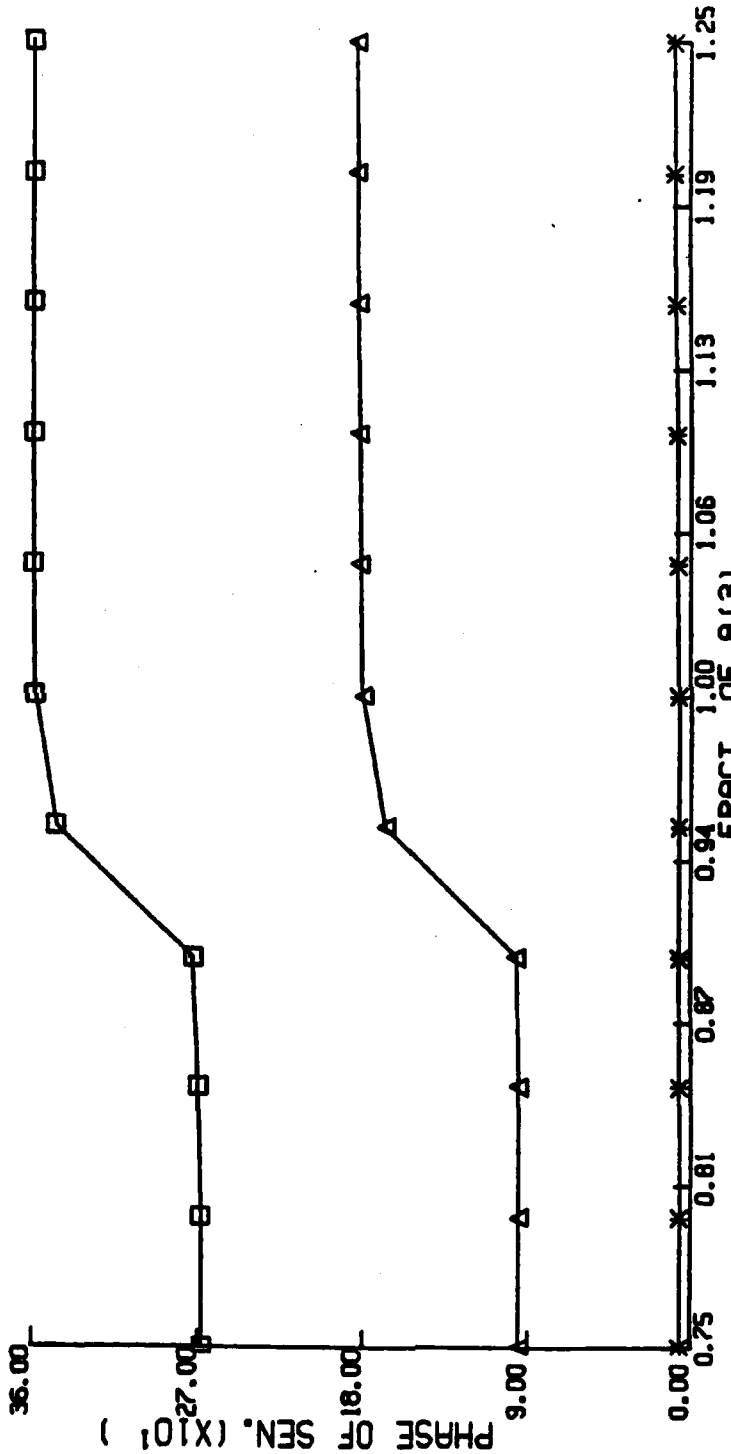


FIGURE 16 - PHONEME AE (5) S(3,*)

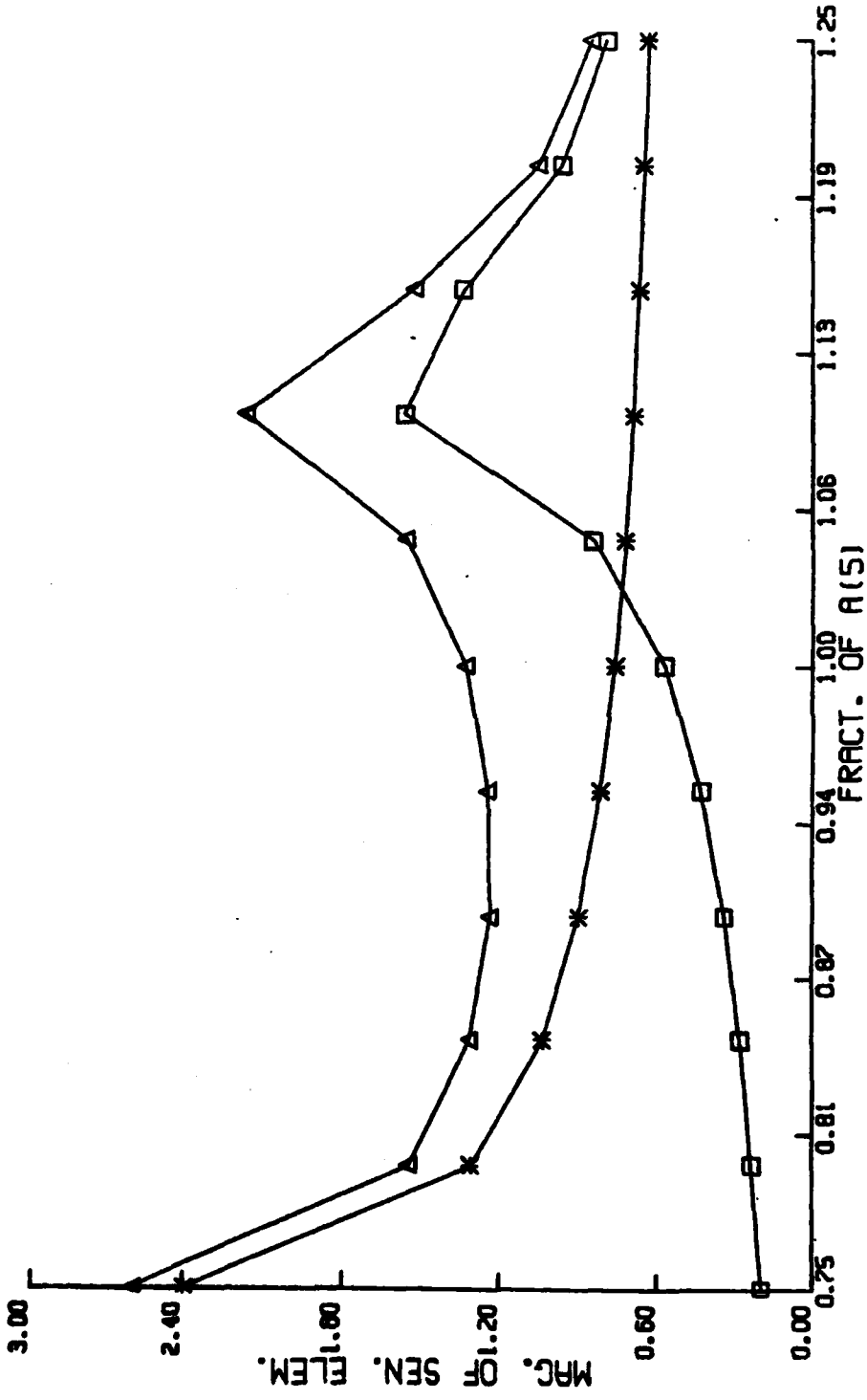


FIGURE 17 - PHONEME AE (5) S(5,*)

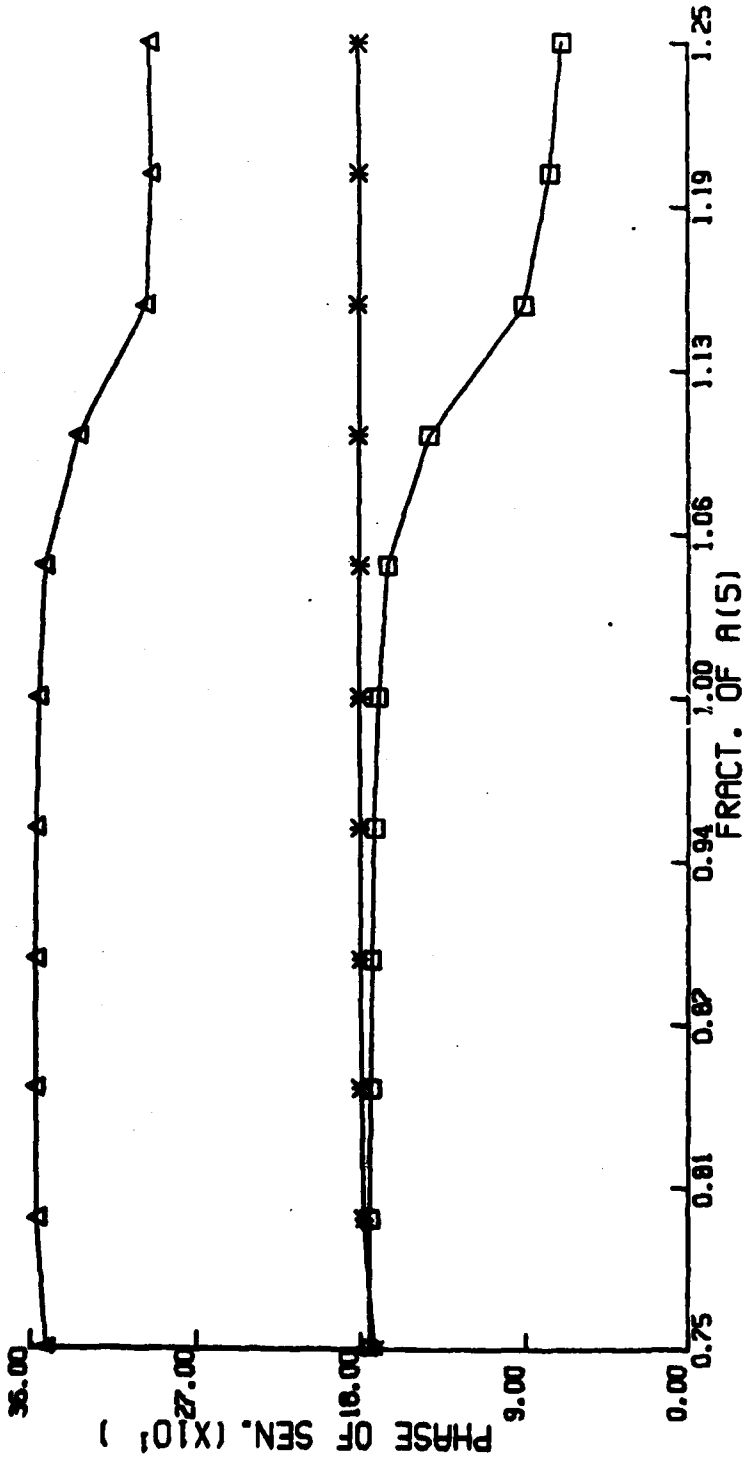


FIGURE 18 - PHONEME AE (5) S(5,*)

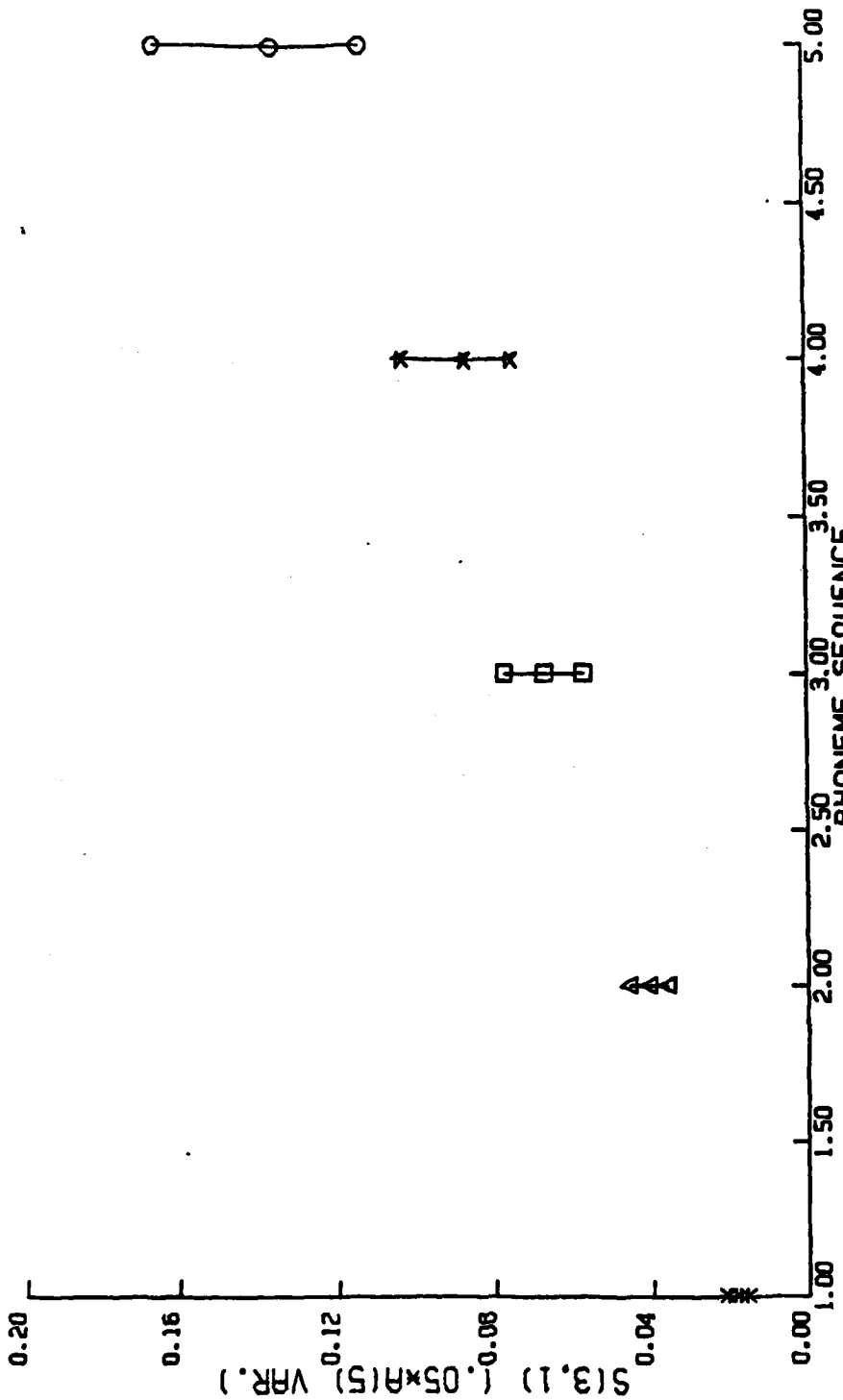


FIGURE 19 - KLATT DATA /IY,IH,EY,EH,AE/

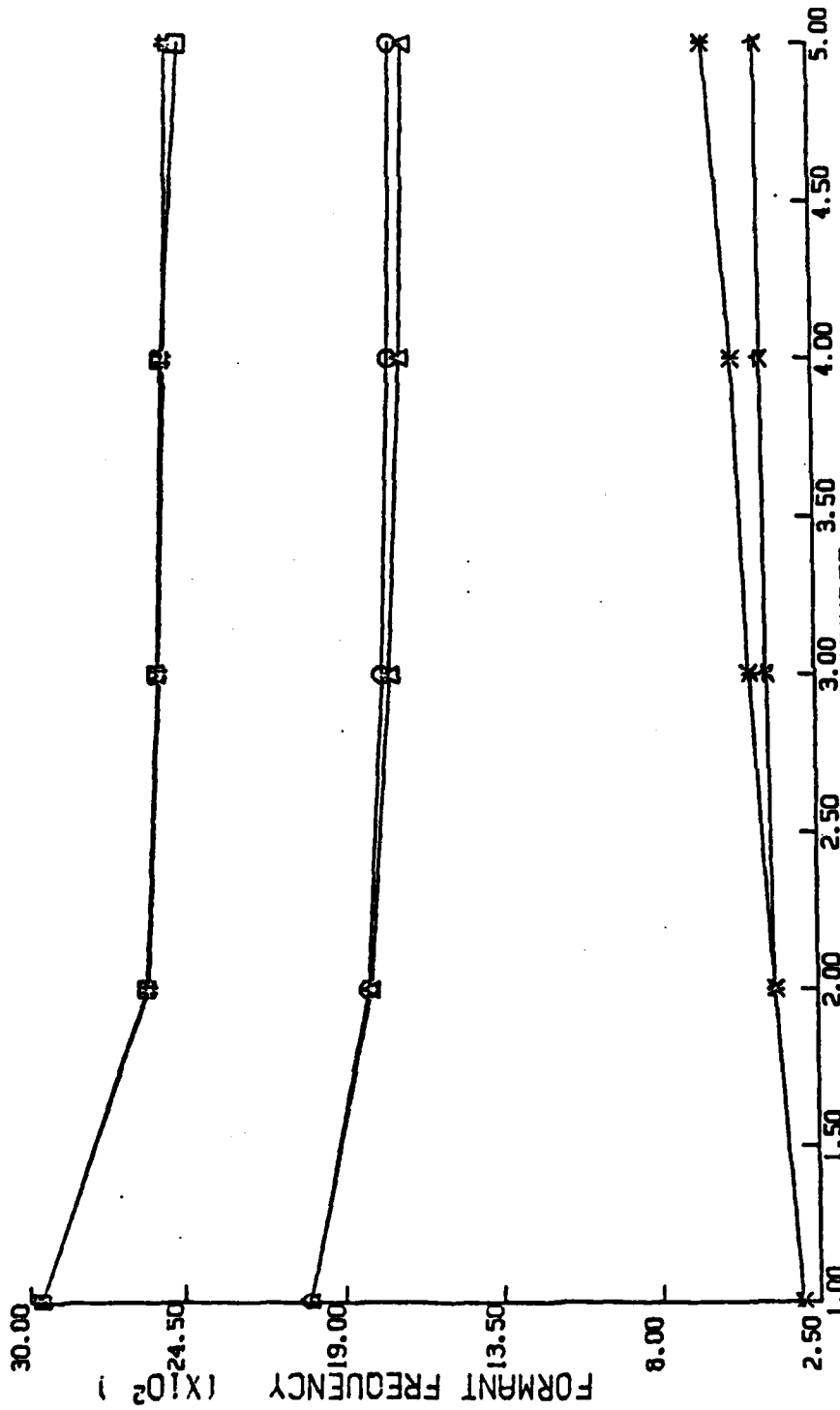


FIGURE 20 - KLATT AND MOD KLATT /IY, IH, EY, EH, AE/

particular back vowels. Illustrated by Figure 21 is the low back vowel sub-group /AA, AY, AW, AH/. Subsequent changes in the diphthongs /AY, AW/, (Δ , □), may again provide a greater specificity among the elements of this sub-group. The remaining back vowels are shown in Figure 22 where /OY/,(Δ), is another diphthong.

IV. DISCUSSION:

Changes in the shape of the vocal tract due to movement of vocal structures lead to various formant frequency and bandwidth changes. Kenneth Stevens has used simple acoustic tube models to investigate these interrelationships and has proposed that there is a quantal nature to speech. That is, "there are certain articulatory conditions for which a small change in some parameter describing the articulation gives rise to an apparently large change in the acoustic characteristics of the output; there are other conditions for which substantial perturbations of certain aspects of the articulation produce negligible changes in the characteristics of the acoustic signal".[3]

For the high front vowel /IY/, Stevens' acoustic analysis predicts a low first formant and that formants 2 and 3 should be close together. The sensitivity analysis of Klatt's data corroborates and extends Stevens' results by showing that this condition holds for all front vowels and for the mid-vowel /ER/. Stevens also considered the low and high back vowels /AA, UW/ and in each case concluded that formants 1 and 2 should be close. Again, the sensitivity analysis of Klatt's data corroborates and extends Stevens' results by showing that this condition holds for all back vowels.

In summary, the specific objectives have been met. The sensitivity matrix has been evaluated for the initial and final representations of the fifteen vowels in Klatt's data set. It was found that (1) the sensitivity matrix does provide a measure of the degree to which a sound is "on target" by locating the sound relative to the root-locus corners of formants 2 and 3 and those for formants 2 and 1; (2) that formants 2 and 3 being close to their root-locus corners provides a categorical indicator for the group of front vowels; (3) that formants 2 and 1 being close

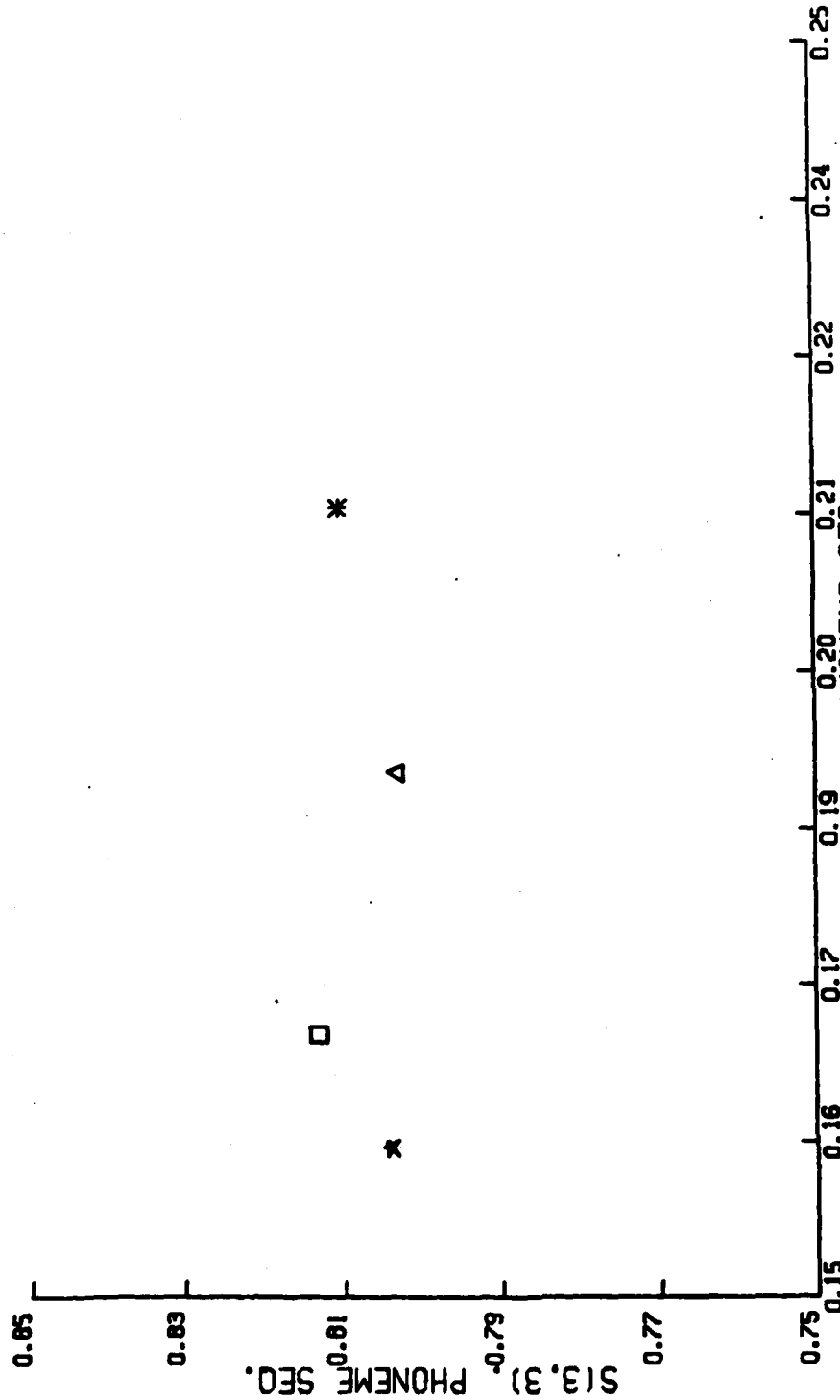


FIGURE 21 - KLATT DATA /AA,AY,AW,AH/

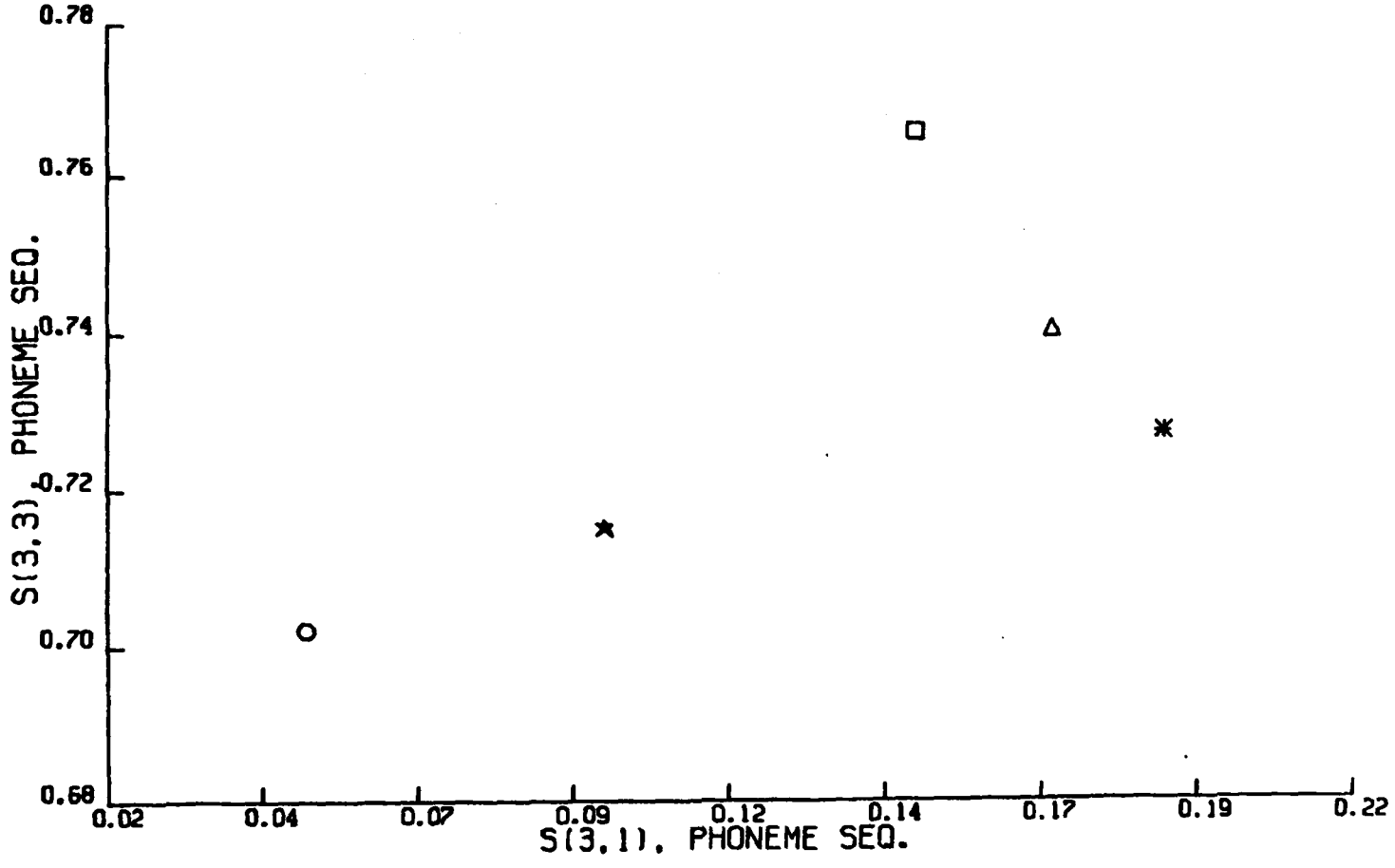


FIGURE 22 - KLATT DATA /AO, OY, OW, UH, UW/

to their root-locus corners provides a categorical indicator for the group of back vowels; and (4) that particular elements of the sensitivity matrix may provide sufficient information to identify the particular vowel.

V. RECOMMENDATIONS:

The positive results obtained with the Klatt data demonstrate that further investigations with the sensitivity matrix are warranted. A sequence of studies involving speech data obtained from several male and female speakers should clarify its usefulness. These data should consist of consonant-vowel-consonant (CVC) syllables containing the vowels, stop consonants, and the glide consonants. Task I should evaluate the changes in the sensitivity matrix that occur during the production of the vowels in the CVC syllables, test the conclusions reached in this report, and evaluate inter-speaker variations. Task II should evaluate and interpret changes in the sensitivity matrix for the vowels due to coarticulation. Task III should evaluate and interpret the sensitivity matrix for the initial and final consonants. Finally, Task IV should use the above results to build a reference library, and should evaluate the efficacy of the sensitivity matrix in terms of the accuracy of the resulting phonetic representation of unknown speech.

REFERENCES

1. Air Force Systems Command Research Planning Guide (Research Objectives), HQ AFSC TR 82-01, page 7-24.

2. Klatt, Dennis H., "Software for a Cascade/Parallel Formant Synthesizer", Unpublished course notes from Speech Communication, Massachusetts Institute of Technology, June 18-23, 1979, page 291.

3. Stevens, Kenneth N., "The Quantal Nature of Speech: Evidence from Articulatory-Acoustic Data", Ch. 3 in P. B. Denes and E. E. David, Jr., Human Communication, A Unified View, (1972) New York, McGraw-Hill, 51-66.

1982 USAF - SCEEE SUMMER FACULTY RESEARCH PROGRAM

Sponsored by the

AIR FORCE OFFICE OF SCIENTIFIC RESEARCH

Conducted by the

SOUTHEASTERN CENTER FOR ELECTRICAL ENGINEERING EDUCATION

FINAL REPORT

A METHODOLOGY FOR THE DETERMINATION OF INPUT DATA ACCURACY IN THE MAINTENANCE DATA COLLECTION SYSTEM

Prepared by:	Dr. Milton J. Alexander
Academic Rank:	Professor
Department and University:	Management Department Auburn University
Research Location:	Air Force Logistics Management Center Directorate of Maintenance
USAF Research Colleagues:	Lt Col David A. Dietsch Capt Lindel R. Thompson
Date:	September 8, 1982
Contract No:	F49620-82-C-0035

A METHODOLOGY FOR THE DETERMINATION OF INPUT DATA ACCURACY IN THE MAINTENANCE DATA COLLECTION SYSTEM

by

Milton J. Alexander

ABSTRACT

A methodology for the determination of input data accuracy in the maintenance data collection system is developed. The level of input data accuracy is subject to two different types of errors - data which should have been entered into the MDCS but was not (Class A errors) and erroneous data which was entered into the MDCS (Class B errors). The survey instrument which was developed provides a measure of Class A errors and three different types of Class B errors. A sampling plan was developed which will produce a random sample having a confidence level of 95 percent with minimal bias. A Statistical Package for the Social Sciences (SPSS) subprogram was prepared for the tabulation and analysis of the raw survey data. A recommendation for further study is also included.

ACKNOWLEDGEMENTS

The author would like to thank the Air Force Logistics Management Center (AFLMC) and the Southeastern Center for Electrical Engineering Education (SCEEE) for providing him with the opportunity to spend a very worthwhile and interesting summer at the AFLMC, Gunter AFS, Alabama. He would like to acknowledge, in particular, Capt Lindel Thompson for his assistance and collaboration on this project. Finally, he would like to thank Lt Colonel David A. Dietsch, Major David M. Crippen, and other members of the AFLMC staff for their patient assistance on this project.

I. INTRODUCTION

The Maintenance Data Collection System (also known as MDCS or the MDC System) was one of the first large-scale computerized information systems developed by government or industry. The MDCS was designed to collect the daily individual transaction data for all maintenance activities performed on all aircraft and ground support equipment in the USAF. The MDCS still functions today in much the same fashion as originally designed. MDCS utilization, however, has expanded and MDCS output is now a primary input to five other major AFLC management information systems.

The inadequacies and deficiencies of the MDCS have long been recognized. Sporadic attempts have been made to improve operational efficiency by redesigning the input data forms and the institution of maintenance data sampling plans (Alexander, p. 3). Notwithstanding these efforts, the accuracy of MDCS input data is still questionable. While the collected data may still be sufficiently valid for use in certain higher order information systems without major qualification, improvement in input data accuracy would reduce the uncertainty and anxiety associated with the information utilization of all dependent systems.

A project was undertaken in 1981 to develop method(s) for the measurement and evaluation of MDCS input data accuracy (Alexander, 1981). The proposed method for input data accuracy measurement was based on the computation of the joint probability for errors caused by not submitting any data for particular maintenance activities (Class A or Type 1 errors) and erroneous data on submitted input data records (Class B or Type 2 errors).

The two different accuracy determinations may be combined as a joint

probability function:

$[1 - P_{(\text{Class A error})}] \times [1 - P_{(\text{Class B error})}]$ = MDCS composite input data accuracy value.

The substitution in this equation of numerical values derived from a limited field study suggested that only 1 - 2 percent of all unscheduled maintenance activities were actually being reported into the MDCS correctly (Alexander, p. 10).

II. OBJECTIVES

The initial investigation of this problem defined the parameters and provided a general method for the measurement and evaluation of MDCS input data accuracy (Alexander, 1981). The subject study, however, did not provide a definitive method for the measurement of input data accuracy to the MDCS.

The principal purpose of this study is to develop a specific methodology for the accuracy measurement of MDCS input data. The accomplishment of this objective will provide a base for the evaluation of alternative MDCS data collection methods and techniques. By using before and after surveys, improvements in input data accuracy levels may be compared to data collection costs and the cost effectiveness of the improved data collection method determined.

The specific objectives of this study may be summarized as follows:

(1) To develop a survey instrument which will provide a measure of the MDCS input data accuracy level for a particular organization,

(2) To develop respondent sampling plan(s) which will produce survey results with various confidence levels, and

(3) To develop the SPSS subprogram for the tabulation and analysis of the survey data.

The research activities and findings associated with each of the objectives are discussed in the following sections of this report.

III. QUESTIONNAIRE CONSTRUCTION AND DESIGN

The following major questionnaire interest areas were determined from a close examination of the initial MDCS data accuracy questionnaire and the analysis of the information requirements for successful input data accuracy determination:

(1) Demographic data

(2) AFTO Form 349 record completion activity

(3) Work unit code activity

(4) How/mal code activity

(5) Action taken code activity

(6) Time spent on job

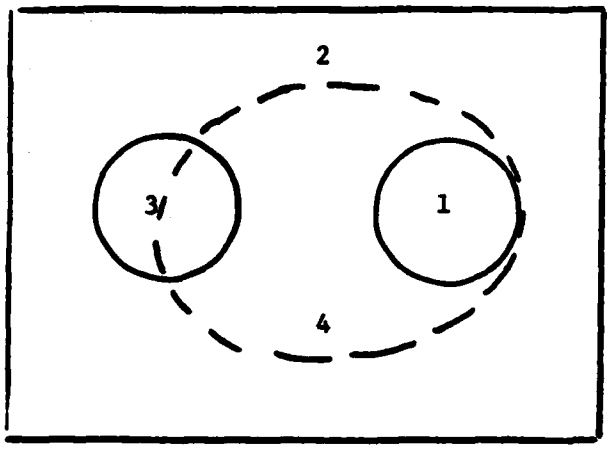
The required demographic data include age, sex, grade (both primary and duty Air Force Specialty Classification code), and work group code. Having these data items available will permit their later correlation with selected activity data to determine whether any peculiar or unusual activity patterns are present. Man number or social security number has been specifically omitted to prevent direct linkage of individuals with questionnaires. Response anonymity must be guaranteed to generate candid responses by the interview subjects.

Questions 2 through 6 were designed to elicit data relating to AFTO Form 349 record completion activity. In particular, this section of the

questionnaire seeks to establish a basis for the subsequent determination of Class A errors (data which should have been entered into the MDCS but was not). For TAC units independent verification of AFTO Form 349 record inputs is available by reconciling MMICS records with MDCS and noting the discrepancies. The only expedient way to obtain Class A error data for all other types of Air Force organizational units is the direct, questionnaire approach.

Questions relating to work unit code activity, how/mal code activity, and action taken code activity are similar in structure and were designed to produce two different types of data. The first type of data concerns utilization of the -06 code books. The response area has been divided into three mutually exclusive segments: (1) careful research of the -06 code book to determine the most descriptive and accurate response; (2) a quick examination of the -06 code book to locate a code for AFTO Form 349 entry; and (3) reliance on memory for the AFTO Form 349 code entry. The three different methods of code determination may be illustrated with a Venn diagram as shown in Figure 1.

The second type of code activity data sought is simply the careful, subjective estimate of the input accuracy of that particular type of data. The area enclosed by the dashed line in Figure 1 represents the correct AFTO Form 349 responses.



Key

1. Careful code book examination
2. Quick code book examination
3. Reliance on memory
4. Accurate input data

Venn Diagram of Code Activity

Figure 1

The two different approaches to code measurement were used to provide a rough cross check on each other. The data accuracy estimate, for example, should always be larger than the proportion of careful -06 code book references. Further, the -06 code book reference questions will provide insights on -06 code book utilization and the need for its revision.

The final questionnaire interest area, time spent on job, was included to determine whether particular organizational units were prone to over- or under-report the elapsed job times. There is some evidence that certain organizational units will use this data as a measure of manpower utilization which can seriously subvert data accuracy.

The questionnaire in final form is shown in Appendix 1.

IV. QUESTIONNAIRE SAMPLING PLANS

There is no need to require everyone in the maintenance function to complete a questionnaire when a random sample of sufficient size will provide

an excellent assessment of input data accuracy. The pertinent questions in the determination of the sampling plan concern two particular points: (1) the determination of sample size and (2) the selection method for the survey respondents.

The following mathematical formula for determining the sample size for research activities was developed by the research division of the National Education Association (NEA Research Bulletin, p. 99):

$$s = X^2NP(1 - P) \div d^2(N - 1) + X^2P(1 - P)$$

where

s = required sample size,

X^2 = the table value of chi-square for 1 degree of freedom at the desired confidence level,

N = the population size

P = the population proportion (assumed to be .50 since this would provide the maximum sample size), and

d = the degree of accuracy expressed as a proportion (.05).

Assuming that the total number of airmen who might complete AFTO Forms 349 in a major organizational unit would be 1500 (N = 1500) and substituting different chi-square table values for various confidence levels yields the following sample sizes for various confidence levels:

90% Confidence level - 230

95% Confidence level - 306

98% Confidence level - 403

99% Confidence level - 460

The most widely used confidence level by survey takers is 95 percent (Krejcie

and Morgan, p. 607) and this confidence level should be quite appropriate for these studies.

The second point which merits discussion is the process for the selection of questionnaire respondents. The ideal selection process is the random selection process in which each member of the population has the same probability of being selected. Inasmuch as the principal objective of this investigation is to determine the input data accuracy level for AFTO Form 349 records, and individual respondents may submit one or many AFTO Forms 349 during a given time period, the questionnaire respondent's probability for selection has been weighted by the frequency of AFTO Form 349 record input. That is, those individuals who turn in many AFTO Forms 349 will have correspondingly higher probabilities of being selected than will individuals who seldom turn in completed AFTO Forms 349.

The net effect of this selection process will be twofold. First, the selected respondents may take more care in the completion of the AFTO Forms 349 because they may be somewhat more responsible than the average respondent. Thus, there could be some bias toward higher reported accuracy levels than actually exists. Second, the respondent sample selected in this manner would also have a higher report submission rate than the average respondent. This bias would be toward the understatement of AFTO Form 349 submission rates. The direction of both biases is in the conservative direction and, if significant, will produce results with somewhat higher reliabilities.

The random selection of the respondent sample under the conditions discussed above will be dependent on the collection of AFTO Form 349 input data activity by man number for a particular time period; e.g., one month. If

man number data is not currently being collected, special efforts will have to be initiated to collect this data for the specified time period. This method of respondent sample selection will necessarily require advance warning to the organizational unit being evaluated which might conceivably introduce a bias in the results in an unknown direction.

An alternate method of respondent selection following the general guidelines above could be used if the preferred method is not feasible. The alternate method would require the summation of AFTO Form 349 activity by work group center and labor code 100. Proportionate numbers of respondents could be randomly selected from these organizational units to develop a stratified sample with approximately the same characteristics as the preferred sampling method. This method of respondent determination would be, of course, much more difficult to perform and might lead to some representative sampling rather than the preferred random sampling.

The sampling procedure should be made on a without replacement basis. That is, once a respondent has been selected through the sampling procedure, that individual will no longer be considered a part of the population. This will eliminate the need to double or triple count the responses of a particular individual merely because he happened to be selected by the draw more than once.

V. QUESTIONNAIRE SCORING AND ANALYSIS

The questionnaire responses should be collected on LMDC Form 46 for subsequent processing with an optical scanner for conversion into computer processable form.

The tabulation and presentation of results is a relatively straightforward

affair. The SPSS program listed in Appendix 2 will tabulate the responses for each question and prepare easily comprehendable bar charts. Further analysis of the data, such as cross-tabulation (chi square), analysis of variance and regression analysis may also be performed by adding additional program instructions as specified in the SPSS manual.

The composite input data accuracy value for an organization may be computed by the following formula (Alexander, 1981):

$$[1 - P_{(\text{Class A error})}] \times [1 - P_{(\text{Class B1 error})}] \times [1 - P_{(\text{Class B2 error})}] \times [1 - P_{(\text{Class B3 error})}] = \text{MDCS composite input data accuracy.}$$

The first value in the equation is the mean probability of the valid response means in question 4 of the questionnaire, $P_{(\text{Class A error})}$, subtracted from 1. The second value in the equation is the mean probability of the valid response means in question 9, $P_{(\text{Class B1 error})}$, subtracted from 1. The third and fourth values in the equation are the mean probabilities of the valid response means in questions 12 and 16 on the questionnaire.

In addition to the MDCS composite input data accuracy value, other insights may be gleaned from an analysis of the data. The reasons for not completing the required AFTO Forms 349, for example, is covered in question 6. The utilization of the -06 code book for various types of information is covered in questions 7, 8, 10, 11, 14 and 15. Finally, the questionnaire results may be combined with other organizational observations and inferences drawn about the quality of organizational leadership and management.

VI. RECOMMENDATIONS

The survey instrument which has been developed appears to be satisfactory for its intended purpose. There is, however, no way to ascertain its adequacy until it has been tested in the field. The following steps are recommended to bring this project to a successful conclusion:

(1) Approval of the survey instrument so that it may be administered to several different organizational units.

(2) Administration of the questionnaire to four or more maintenance organizations.

(3) Tabulation and analysis of the results.

(4) Preparation of a final report covering the entire investigation, together with the major conclusions from the investigation.

APPENDIX 1

QUESTIONNAIRE

1. My total time in my present duty AFSC is:

   0. Less than 6 months
   1. At least 6 months but less than 1 year
   2. At least 1 year but less than 2 years
   3. At least 2 years but less than 3 years
   4. At least 3 years but less than 5 years
   5. At least 5 years but less than 8 years
   6 At least 8 years but less than 12 years
   7. 12 years or more

2. During a typical work day I usually work on _____ unscheduled maintenance jobs:

   0. 0 - 2
   1. 3 - 4
   2. 5 - 6
   3. 7 - 8
   4. 9 - 10
   5. 11 - 12
   6. 13 - 15
   7. More than 15

3. I am responsible for completing the AFTO Form 349 for _____ of the unscheduled maintenance jobs I work on during a typical work day.

   0. None to 10%
   1. More than 10% but less than 20%
   2. More than 20% but less than 40%
   3. More than 40% but less than 60%
   4. More than 60% but less than 80%
   5. More than 80% but less than 90%
   6. More than 90%
   7. Unable to answer

4. I turn in the completed AFTO Forms 349 for which I am responsible about _____ of the time.

0. None to 10%
1. More than 10% but less than 20%
2. More than 20% but less than 40%
3. More than 40% but less than 60%
4. More than 60% but less than 80%
5. More than 80% but less than 90%
6. More than 90%
7. Unable to answer

5. I usually complete my AFTO Forms 349:

0. Immediately after I finish the job.
1. As soon as I get some free time.
2. During lunch break.
3. At the end of my shift.
4. First thing on the following work day.
5. When reminded by my supervisor.
6. At some other time.
7. Never.

6. The most important reason why I do not complete all of the AFTO Forms 349 for which I am responsible is:

0. No AFTO Form 349 was received.
1. It is too hot, cold, noisy and/or dirty.
2. I don't happen to have a pen or pencil handy.
3. Not enough time.
4. No one asks for all of the completed AFTO Forms 349.
5. I forget to fill them out later.
6. I do my best to fill out all of my AFTO Forms 349.
7. Some other reason.

7. I <u>carefully</u> <u>research</u> the -06 code book to determine the most accurate and descriptive work unit code on _____ of the AFTO Forms 349 I complete.

0. Less than 10%
1. More than 10% but less than 20%
2. More than 20% but less than 40%
3. More than 40% but less than 60%
4. More than 60% but less than 80%
5. More than 80% but less than 90%
6. More than 90%
7. Unable to answer

8. I enter from memory a work unit code without checking the -06 code book on _____ of the AFTO Forms 349 I complete.

0. Less than 10%
1. More than 10% but less than 20%
2. More than 20% but less than 40%
3. More than 40% but less than 60%
4. More than 60% but less than 80%
5. More than 80% but less than 90%
6. More than 90%
7. Unable to answer

9. I would estimate that _____ of the work unit codes I enter on the AFTO Forms 349 are good, accurate and reliable work unit codes.

0. Less than 10%
1. More than 10% but less than 20%
2. More than 20% but less than 40%
3. More than 40% but less than 60%
4. More than 60% but less than 80%
5. More than 80% but less than 90%
6. More than 90%
7. Unable to answer

10. I carefully research the -06 code book to determine the most accurate and descriptive how/mal code on _____ of the AFTO Forms 349 I complete.

0. Less than 10%
1. More than 10% but less than 20%
2. More than 20% but less than 40%
3. More than 40% but less than 60%
4. More than 60% but less than 80%
5. More than 80% but less than 90%
6. More than 90%
7. Unable to answer

11. I enter from memory the how/mal code without checking the -06 code book on _____ of the AFTO Forms 349 I complete.

0. Less than 10%
1. More than 10% but less than 20%
2. More than 20% but less than 40%
3. More than 40% but less than 60%
4. More than 60% but less than 80%
5. More than 80% but less than 90%
6. More than 90%
7. Unable to answer

12. I would estimate that _____ of the how/mal codes I enter on the AFTO Forms 349 are good, accurate and reliable how/mal codes.

0. Less than 10%
1. More than 10% but less than 20%
2. More than 20% but less than 40%
3. More than 40% but less than 60%
4. More than 60% but less than 80%
5. More than 80% but less than 90%
6. More than 90%
7. Unable to answer

13. On the average for all jobs, the time I report on the AFTO Form 349 compared to actual time spent is:

0. About 50% of actual time spent
1. About 75% of actual time spent
2. A little less (90%) than actual time spent
3. The same as actual time spent
4. A little more (110%) than actual time spent
5. About 150% of actual time spent
6. About double the actual time spent
7. Enough time to make me look good

14. I carefully research the -06 code book to determine the most accurate and descriptive action taken code on _____ of the AFTO Forms 349 I complete.

0. Less than 10%
1. More than 10% but less than 20%
2. More than 20% but less than 40%
3. More than 40% but less than 60%
4. More than 60% but less than 80%
5. More than 80% but less than 90%
6. More than 90%
7. Unable to answer

15. I enter from memory the action taken code without checking the -06 code book on _____ of the AFTO Forms 349 I complete.

0. Less than 10%
1. More than 10% but less than 20%
2. More than 20% but less than 40%
3. More than 40% but less than 60%
4. More than 60% but less than 80%
5. More than 80% but less than 90%
6. More than 90%
7. Unable to answer

16. I would estimate that _____ of the action taken codes I enter on the AFTO Forms 349 are good, accurate and reliable action taken codes.

0. Less than 10%
1. More than 10% but less than 20%
2. More than 20% but less than 40%
3. More than 40% but less than 60%
4. More than 60% but less than 80%
5. More than 80% but less than 90%
6. More than 90%
7. Unable to answer

APPENDIX 2

```
 1   RUN NAME              MDC SURVEY
 2   VARIABLE LIST         GRADE,AGE,SEX,WGCODE,DAFSC,Q1 TO Q23
 3   INPUT MEDIUM          DISK
 4   N OF CASES            UNKNOWN
 5   INPUT FORMAT          FIXED (T2,F1.0,T4,F2.0,F1.0,T8,A4,T13,
 6                         F5.0,T26,23F1.0)
 7   PRINT FORMATS         WGCODE (A)
 8   RECODE                GRADE,AGE,SEX,Q1 TO Q23 (BLANK=10)
 9   MISSING VALUES        GRADE,AGE,SEX,Q1 TO Q23 (10)
10   FREQUENCIES           GENERAL=WGCODE,DAFSC
11   OPTIONS               3,6,8
12   READ INPUT DATA
13   FREQUENCIES           INTEGER=GRADE,AGE,SEX,Q1 TO Q23
14   OPTIONS               3,6,8,9
15   STATISTICS            ALL
```

REFERENCES

1. Alexander, M. J., The Determination of Input Data Accuracy in the Maintenance Data Collection System, Gunter Air Force Station, AL: Logistics Management Center, 1981.

2. Krejcie, R. V. and Morgan, D. W., Determining Sample Size for Research Activities, Journal of Educational and Psychological Measurement, 1970, 30, pp. 607-610.

3. Small Sample Techniques, The NEA Research Bulletin, Vol. 38 (December, 1960), p. 99.

1982 USAF-SCEEE SUMMER FACULTY RESEARCH PROGRAM

Sponsored by the

AIR FORCE OFFICE OF SCIENTIFIC RESEARCH

Conducted by the

SOUTHEASTERN CENTER FOR ELECTRICAL ENGINEERING EDUCATION

FINAL REPORT

ASSESSMENT OF VISUOSPATIAL ABILITIES USING COMPLEX COGNITIVE TASKS

Prepared by:	Dr. Gary L. Allen
Academic Rank:	Assistant Professor
Department and University:	Department of Psychology Old Dominion University
Research Location:	Air Force Human Resources Laboratory, Manpower and Personnel Division, Test and Training Research Branch
USAF Research Colleague:	Dr. Raymond E. Christal
Date:	September 20, 1982
Contract No.:	F49620-82-C-0035

ASSESSMENT OF VISUOSPATIAL ABILITIES USING COMPLEX COGNITIVE TASKS

by

Gary L. Allen

ABSTRACT

The focus of this research effort was on the identification of visuospatial cognitive abilities and the incorporation of these abilities into complex cognitive tasks for application in a testing context. The initial study involved determining the relationship between a battery of psychometric visuospatial tests and performance on a complex, visually presented macrospatial task. In the second study the relationship between psychometric memory tests and performance on a specially designed Maze Learning Task was examined. Results from these studies suggested the value of additional basic research concerned with the role of visuospatial abilities in human information processing and the acquisition of procedural knowledge.

Acknowledgement

Appreciation is expressed to the Air Force Systems Command, the Air Force Office of Scientific Research, and the Southeastern Center for Electrical Engineering Education for providing this research opportunity at the Air Force Human Resources Laboratory, Manpower and Personnel Division, Brooks AFB, Texas. The cooperation of AFHRL personnel at all levels is gratefully acknowledged.

The research in this report was developed and carried out in consultation with Dr. Raymond Christal, Col. David Payne, Dr. Patrick Kyllonen, Mr. Johnny Weismuller, and visiting scientist Dr. Nancy Anderson of the Test and Training Research Branch, AFHRL's Manpower and Personnel Division.

I. INTRODUCTION:

In an effort to meet the demands of personnel testing in the era of the all-volunteer force, military research organizations such as the Air Force Office of Scientific Research have mandated research aimed at advancing the state of the art in assessing cognitive abilities and in utilizing improved assessment techniques for increasing the efficiency of decisions regarding personnel classification and training. Two major innovations, one involving instrumentation and the other involving cognitive theory, have stimulated the development of new cognitive testing technology. The combination of computerized testing and the information processing perspective on cognitive abilities have opened up a new realm of assessment possibilities that are currently being explored in basic research. In an effort to exploit these new possibilities, a new computerized testing facility was developed under the auspices of AFOSR at the Air Force Human Resources Laboratory, Manpower and Personnel Division.[1,2] The research described in this report was designed to lay the groundwork necessary for the development and implementation of innovative, complex cognitive tasks in the visuospatial domain that would be compatable with this computerized testing facility.

The substantive area selected for study concerned visuospatial cognitive abilities. This area of inquiry is significant for both theoretical reasons. Visuospatial abilities represent a unique facet of human cognition that has recently received considerable attention from cognitive psychologists.[3,4] Cognitive tests involving these abilities have been shown to have predictive validity with regard to mechanical aptitude and artistic skills.[4,5,6] Also, numerous occupations have been described as

involving spatial abilities and skills.[7] In addition, there remains the relatively unexplored possibility that visuospatial abilities could be exploited in the service of education and training, enterprises which currently rely heavily upon verbal/linguistic abilities.

The prospect of assessing visuospatial abilities by means of computerized testing provides the opportunity to devise new assessment instruments that are less abstract than traditional pencil-and-paper tests in this domain and more similar to actual complex real-world tasks involving these abilities. Computer testing technology also permits an examination of improvement in task performance with continued effort. Information about these rates of information acquisition, which may prove to be a new source of predictive power in ability testing[1], also provide a means of examining the role of visuospatial information processing in the acquisition of procedural knowledge.

II. OBJECTIVES:

The objectives for this project included the development and administration of two experimental visuospatial cognitive tasks that could conceivably be adapted in the future to be predictive instruments in a testing context. The first task, referred to as the Scrambled Route Task,[8] presented a problem in visuospatial reasoning. During the task, individuals were presented with a randomly ordered sequence of slides comprising a route. Subsequently, they made a series of distance estimates involving locations along the route, disregarding the random nature of the original presentation. The purpose of the first study was to specify the relationship of the Scrambled Route Task to a number of other

cognitive tests in the visuospatial domain. To meet this objective, the Scrambled Route Task was administered with a battery of nine psychometric tests, each of which involved some type of visuospatial information processing. The statistical and conceptual relationship between the Scrambled Route Task and the psychometric tests was determined in a correlational analysis.

The second task in the project was a computerized Maze Learning Task, developed at Old Dominion University. This task was designed to provide insight into the relative benefit of visuospatial versus verbal instructions for different individuals in learning a series of commands to navigate a maze. As with the previous task, the Maze Learning Task was accompanied by a battery of factor-referenced cognitive tests. Consequently, it was possible to view the study as an investigation of aptitude-treatment interaction. The scores from the psychometric tests represented the aptitude portion of this interaction; the different sets of maze instructions, i.e., visual versus linguistic, represented the treatment portion. The modes of instruction were compared statistically by means of an analysis of variance. The relationship between the Maze Learning Task under both instructional conditions and the psychometric tests was determined in a correlational analysis.

III. STUDY 1:

A. Approach. Participants in this study were tested on the Scrambled Route Task and on a battery of nine paper-and-pencil tests of visuospatial abilities. The Scrambled Route Task required subjects to first view a randomly sequenced presentation of scenes portraying a one km walk

through an urban landscape, and then to make estimates of distance in reference to a set of test scenes from the presentation. The scrambled route was portrayed by a series of color slides projected automatically at a rate of 5 sec/slide. Had the slides been sequentially ordered, successive slides would have depicted standpoints 20 m apart (except when corners were negotiated). After the randomized presentation, a single slide was designated as a standard reference point, and a succession of 28 slides were shown. Subjects estimated the distance from the standard reference point to each of the 28 test scenes using a magnitude estimation procedure. Subjects' performance on the task was assessed by computing log estimated distance as a function of log actual distance in a simple linear regression analysis. The resulting power function and correlation coefficient reflected the accuracy and quality of each subject's performance. The exponent (slope) and correlation of this function were included in the subsequent correlational analysis with scores from the battery of psychometric tests.

The battery, which consisted of nine different visuospatial tests selected from the files of the test library at AFHRL, included Estimation of Length, Shapes of Objects, Rotated Blocks, Viewing Position, Form Board, Pattern Completion, Letter Matching, Position Recall, and Object Memory. The source of these tests and the cognitive factors that they involve are shown in Table 1. Subjects' performance on each test was scored by the standard formulation: number of items correct - number of items incorrect/number of options - 1.

Data were collected from 237 basic trainees at the AFHRL experimental testing facility at Lackland AFB, Texas. Males and females were tested in

approximately a 2:1 ratio. Four testing sessions were required to complete data collection.

Table 1. Battery of Visuospatial Ability Tests

Test	Source	Major Factor
Estimation of Length	Technical School Spatial Battery[9]	Undetermined
Shapes of Objects	" "	Visualization[10]
Rotated Blocks	" "	Spatial Orientation[10]
Viewing Position	" "	" "
Form Board	" "	Visualization
Pattern Completion	Nonverbal Aptitude Battery[11]	Logical Reasoning[10]
Letter Matching	" "	Perceptual Speed[10]
Position Recall	Individual test	Visual Memory[10]
Object Memory	Individual test	Visual Memory

B. Results. The results of the correlational analysis involving performance scores from the Scrambled Route Task and scores from the nine psychometric visuospatial abilities tests are shown in Table 2. The pattern of scores among psychometric tests conformed to expectations in the sense that tests believed to involve the same cognitive factor produced the highest correlation coefficients. The Shapes of Objects Test and Form Board Test, both of which involve the visualization factor, correlated more highly with each other than either did with any other test. The same can be said of the Position Recall Test and Object Memory Test, both of which tap the visual memory factor. The Rotated Blocks Test and Viewing Position Test, both of which involve the spatial orien-

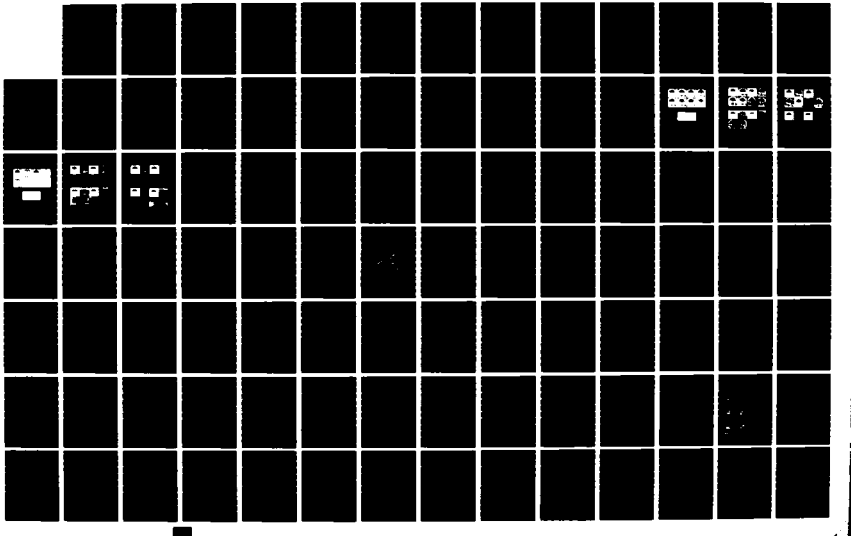
tation (relations) factor, were highly related, but they were both highly correlated with the tests of visualization. This finding supports the contention that these factors are very closely related.[3]

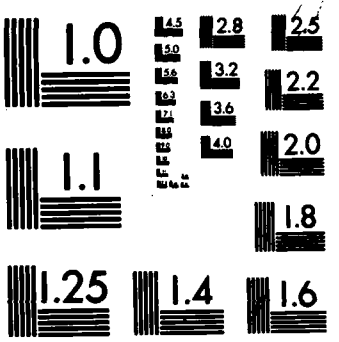
The Estimation of Length Test, which required subjects to match line lengths to a set of standards, correlated positively to all other test scores, suggesting that it involes a simple visuospatial component that plays a role in most psychometric test in this ability domain. Much the same can be said of the Letter Matching Test, which assessed perceptual speed. Further, the fact that these two tests correlated most highly with each other indicates that they both may involve rapid coding of simple visual input. The Pattern Completion Test, which was expected to assess spatial reasoning, correlated very highly with the tests of visualization and spatial orientation (relations). These correlations imply the test involved a spatial relations factor as well as rule induction ability.

The two measures from the Scrambled Route Task, i.e., slopes and correlations, produced that highest correlation in the study. The magnitude of this correlation indicates that either of these scores alone could be used to represent task performance. The most striking finding of the study was the lack of high correlations between the psychometric test scores from the pencil-and-paper battery and the measures from the Scrambled Route Task. The highest correlations with the former measures were with the Pattern Completion Test, a result which was consistent with the proposition that the Scrambled Route Task involves visuospatial reasoning to some extent. However, the major implication ot the relatively low correlations is that macrospatial cognitive tasks may involve cognitive

AD-A130 769 USAF/SCEEE SUMMER FACULTY RESEARCH PROGRAM RESEARCH REPORTS VOLUME 1.. (U) SOUTHEASTERN CENTER FOR ELECTRICAL ENGINEERING EDUCATION INC S.. 2/11

UNCLASSIFIED W D PEELE ET AL. OCT 82 AFOSR-TR-83-0613 F/G 5/1 NL





MICROCOPY RESOLUTION TEST CHART
NATIONAL BUREAU OF STANDARDS-1963-A

Table 2. Pearson Correlation Coefficients for Study 1

	Est Length	Shapes Obj	Rotated Bl	View Posit	Form Board	Pat Compl	Let Match	Posit Rec	Obj Memory	SR-slope	SR-correl
Est Length	----										
Shapes Obj	+.21	----									
Rotated Bl	+.35	+.51	----								
View Posit	+.29	+.53	+.49	----							
Form Board	+.31	+.64	+.55	+.52	----						
Pat Compl	+.30	+.41	+.54	+.52	+.51	----					
Let Match	+.38	+.12	+.21	+.26	+.20	+.29	----				
Posit Rec	+.25	+.17	+.27	+.31	+.19	+.30	+.34	----			
Obj Memory	+.31	+.20	+.29	+.34	+.22	+.32	+.26	+.43	----		
SR-slope	+.01	+.14	+.18	+.14	+.14	+.19	-.01	+.14	-.02	----	
SR-correl	+.05	+.17	+.23	+.18	+.20	+.27	+.07	+.17	+.05	+.85	----

Note: Underscoring denotes $p < .05$; double underscoring denotes $p < .01$.

abilities that are not assessed by current psychometric tests of visuo-spatial aptitudes. The accuracy of this implication must be verified through additional research. As noted later, such research will be facilitated through recent technological advances.

IV. STUDY 2:

A. Approach. Participants in this study were tested on a computerized Maze Learning Task and on a battery of six psychometric tests from the Kit of Factor Referenced Cognitive Tests.[10] The Maze Learning Task consisted of a study phase and a test phase. In the study phase, participants studied instructions concerning the correct path through a 6 x 6 block maze on the microprocessor monitor screen. Each participant was tested on two mazes. A set of verbal instructions (i.e., 21 commands of the variety "Left-2 blocks","Right-1 block") was provided for one maze; graphic instructions (i.e., a map of the correct path) was provided for the other. The first maze was learned perfectly before the second was presented. Each subject in the study went through alternating study and test phases until he or she completed two consecutive errorless trials through the maze. Feedback regarding response accuracy was provided after each move was entered into the computer.

The battery of pencil-and-paper cognitive tests, which consisted primarily of memory tests, included Digit Span, Object-Number, First and Last Names, Copying, Shape Memory, and Building Memory. These are shown in Table 3. Subjects' performance on each test was scored according to the manual accompanying the Kit of Factor Referenced Cognitive Tests.[12]

Data were collected from 28 males and 28 female basic trainees at the AFHRL Manpower and Personnel Division's experimental automated testing facility at Lackland AFB, Texas. Two testing sessions were required to complete data collection. At the Lackland facility are 28 Terak 8510A microprocessors, with dual disk drive and UCSD-Pascal Operating

Systems.

Table 3. Battery of Memory Ability Tests

Test	Source	Major Factor
Visual Digit Span	Kit of Factor Referenced Cognitive Tests	Memory Span
Object-Name	"	Associative Memory
First & Last Names	"	" "
Copying	"	Flexibility of Closure
Shape Memory	"	Visual Memory
Building Memory	"	" "

B. Results. A preliminary analysis revealed no differences in the difficulty of the two mazes used in the Maze Learning Task. A 2 (sex) x 2 (order of presentation) x 2 (instructional condition) mixed Analysis of Variance with 12 subjects/cell performed on the number of trials required to achieve the criterion of two consecutive errorless test trials yielded a significant main effect for instructional condition, F (1, 44) = 15.31, $p < .001$. Criterion was achieved after an average of 4.8 trials with graphic instructions as compared to an average of 6.5 trials with verbal instructions. No other main effects and no interactions achieved statistical significance. A similar ANOVA performed on the total number of errors made prior to criterion revealed significant effects of order of instructional conditions, F (1, 44) = 4.99, $p < .05$, and instructional condition, F (1, 44) = 27.40, $p < .001$, and a significant interaction involving these two factors, F (1, 44) = 4.55, $p < .05$. The interaction simply signified the fact that the relative advantage of learning with

graphic instructions was exaggerated following a learning experience with verbal instructions, primarily because of the increased errors when verbal instructions were provided initially. The mean number of errors to criterion with verbal instructions was 41.4 when received with the first maze to be learned and 23.5 when received with the second maze to be learned. The comparable means with graphic instructions were 16.5 and 13.0, respectively. No other main effects and no interactions in addition to this one were statistically significant. The findings from both ANOVAs indicate clearly that spatial knowledge of a procedural nature was transmitted and learned more effectively through graphic instructions than through verbal instructions.

The number of trials to criterion and the number of errors to criterion were included with scores from the six psychometric tests in a correlational analysis, the results of which are shown in Table 4. For the most part, the pattern of correlations among test scores was to be expected. The correlation coefficient for the two measures of associate memory, i.e., the Object-Number Test and First and Last Name Test, was highly significant, as was the coefficient for the two measures of visual memory, i.e., the Shape Memory Test and the Building Memory Test. Unexpected were significant correlations between performance on the Shape Memory Test and performance on both tests of associative memory. Also unanticipated was the significant correlations involving performance on the Shape Memory Test and the Visual Digit Span Test. The measures of trials to criterion and errors to criterion were highly correlated within and between instructional conditions, as would be expected.

Table 4. Pearson Correlation Coefficients for Study 2

Span	----									
Obj-No	+.03	----								
Names	+.04	+.72	----							
Copy	-.15	+.06	-.03	----						
Shape	+.26	+.36	+.47	+.06	----					
Bldg	+.17	+.22	+.19	+.22	+.47	----				
TTC-g	-.21	+.21	+.20	-.25	-.09	-.33	----			
E-g	-.13	+.16	+.16	-.28	-.06	-.33	+.90	----		
TTC-v	+.01	+.25	+.12	-.11	-.14	-.32	+.44	+.43	----	
E-v	+.24	+.03	+.01	-.09	-.05	-.27	+.27	+.37	+.68	----
	Span	Obj-No	Names	Copy	Shape	Bldg	TTC-g	E-g	TTC-v	E-v

Note: Underscoring denotes $p < .05$; double underscoring denotes $p < .01$.

Eight significant correlations were found between psychometric test scores and performance measures from the Maze Learning Task. Signiciant negative correlations were found between scores on the Building Memory Test on the one hand and both trials to criterion and errors to criterion measures for both instructional conditions. This indicates that the Building Memory Test involves several of the processes critical to the acquisition of spatial information; it also suggests a strong influence of visual memory in maze learning even under verbal instructions. Significant negative correlations were also found between scores on the Copying Test and both trials to criterion and errors to criterion measures under graphic instructions for the Maze Learning Task. This

finding indicates that flexibility of closure, defined as "the ability to hold a given percept or configuration in mind so as to disembed it from other well-defined perceptual material" [12] was involved to a much greater exten in maze learning under graphic instructions than under verbal instructions. It also provides some evidence that the same processes were not involved in knowledge acquisition under both instructional conditions.

The remaining two correlations were difficult to interpret. Scores on the Visual Digit Span Test correlated positively with number of errors in the Maze Learning Task under verbal instructions. It is not immediately clear why increased memory span for digits should be associated with poor performance of verbal instructions. Even less obvious is a rationale for the positive relationship between scores on the Object-Name Test and the trials to criterion measure of maze learning performance under verbal instructions. This result is uninterpretable in light of the fact that the test involved memory for word-digit pairs while the verbal instructions consisted of direction-distance pairs. These stimuli appear to be very similar.

V. RECOMMENDATIONS:

A. Implications. The results of the preceding studies have direct implications for the assessment of cognitive abilities and the consequences of such assessment for the acquisition of visuospatially-oriented procedural knowledge. After further research, these and similar findings could be incorporated into a modified scheme for the assessment of cognitive ability and the prediction of training success. With regard to

the initial study, it appears that macrospatial cognitive abilities may not be adequately assessed using available psychometric techniques. Thus it seems important to (a) replicate and extend this contention with additional studies, (b) identify and implement instruments that are useful for the assessment of macrospatial abilities, and (c) determine the extent to which such abilities contribute to the performance of Air Force tasks. It should be mentioned that the technology currently exists to present macrospatial cognitive tasks such as the Scrambled Route Task at computerized testing stations. Currently, the most effective means available for such presentation involves state-of-the-art videodisk technology, a method also recommended for the simulation of land navigation for map training exercise.[19] As such capabilities come to military experimental testing facilities, additional research focusing on the predictive and construct validity of macrospatial cognitive abilities will very likely ensue.

The findings of the second study suggest that the Maze Learning Task under graphic instructions may be an excellent test of visuospatial learning abilities. This task represents a short-term learning situation of high understandability and medium difficulty. With slight programming modifications, the task could be incorporated easily into ongoing experimental work such as the study of learning abilities at AFHRL Manpower and Personnel Division's Test and Training Research Branch. The results of the second study also suggest the importance of considering aptitude-treatment interactions in training situations. Procedural knowledge with important visuospatial components can be conveyed in either verbal and visuospatial format, and it is reasonable to assume that a

match between task demands and instructional format will yield the most rapid learning. However, it is also worth considering the proposition that the relative magnitude of verbal and visuospatial abilities at an individual's disposal affects that individual's rate of knowledge acquisition from various instructional formats. For example, an individual with low visuospatial ability but high verbal ability might benefit from verbal instruction even in the case of procedureal knowledge with considerable spatial content. This issue requires further investigation, preferably using experimental learning tasks.

B. Suggestions for Further Research. Data from both studies should be subjected to more sophisticated multivariate analytic techniques (e.g., multiple regression, factor analysis, clustering analysis, and multidimensionl scaling) as a prerequisite for experimental applications such as those listed in the previous section. In particular, data from the first study should be augmented with scores from tests of verbal and quantitative ability (e.g., ASVAB subtest scores) so that future analyses could reveal the "location" of the Scrambled Route Task in relation to the domain of cognitive abilities. Additional macrospatial tasks should be developed to pursue the three objectives mentioned previously in anticipation of technological advances that will permit their computerized administration.

The second study suggests an interesting line of research focusing on the role of verbal and visuospatial abilities in determining the rate at which procedural information with spatial content is acquired. Ideally, studies with this focus would include groups of individuals differentiated by their relative verbal and visuospatial abilities. These

groups would be tested on computerized experimental learning tasks (e.g., the Maze Learning Task) under different instructional conditions. In order to gain more insight into the dynamics of the learning situation, it would be useful to include some studies in which individuals would be allowed to select their own mode of instruction and control study time under various instructional conditions. Such studies would provide a better understanding of visuospatial learning abilities and their role in knowledge acquisition processes. This increased understanding might, in turn, eventually be incorporated into efforts to improve training strategies and procedures.

REFERENCES

1. Raymond E. Christal, "The Need for Laboratory Research to Improve the State-of-the-Art in Ability Testing," National Security Industrial Association-Department of Defense Conference on Personnel and Training Factors in Systems Effectiveness, San Diego, May 1981.
2. David L. Payne, "Establishment of an Experimental Testing and Learning Laboratory," Fourth International Learning Technology Congress and Exposition of the Society for Applied Learning Technology, Orlando, February 1982.
3. David F. Lohman, "Spatial Ability: A Review and Reanalysis of the Correlational Literature," Technical Report No. 8, Aptitude Research Project, School of Education, Stanford University, October 1979.
4. Mark G. McGee, Human Spatial Abilities (Praeger Publishers, New York, 1979).
5. E. E. Ghiselli, The Validity of Occupational Aptitude Tests (Wiley & Sons, New York, 1966).
6. Lauren J. Harris, "Sex-Related Variations in Spatial Skill," in L. S. Liben, A. H. Patterson, and N. Newcombe (Eds.), Spatial Representation and Behavior Across the Life Span (Academic Press, New York, 1981), pp. 83-125.
7. United States Employment Service, Estimates of Worker Trait Requirements for 4,000 Jobs (U.S. Government Printing Office, Washington, DC, 1957).
8. G. L. Allen, A. W. Siegel, and R. R. Rosinski, "The Role of Perceptual Context in Structuring Spatial Knowledge," J. Exp. Psych: Human Learning and Memory, Vol. 4, pp. 617-630, 1978.

9. Air Force Technical School Spatial Battery, Books I-V (Air Force Human Resources Laboratory, Lackland AFB, Texas, 1957).

10. R. B. Ekstrom, J. W. French, and H. H. Harman, Kit of Factor Referenced Cognitive Tests (Educational Testing Service, Princeton, 1976).

11. Nonverbal Aptitude Battery (Air Force Human Resources Laboratory, Brooks AFB, Texas, 1973).

12. R. B. Ekstrom, J. W. French, and H. H. Harman, Manual for Kit of Factor Referenced Cognitive Tests (Educational Testing Service, Princeton, 1976).

13. S. E. Goldin and P. W. Thorndyke, "Simulating Navigation for Spatial Knowledge Acquisition," Human Factors, Vol. 24, pp. 457-472, 1982.

1982 USAF-SCEEE SUMMER FACULTY RESEARCH PROGRAM

Sponsored by the

AIR FORCE OFFICE OF SCIENTIFIC RESEARCH

Conducted by the

SOUTHEASTERN CENTER FOR ELECTRICAL ENGINEERING EDUCATION

FINAL REPORT

THE EFFECT OF MODULATION TRANSFER FUNCTIONS ON FLASHBLINDNESS

Prepared by:	Dr. Silverio P. Almeida
Academic Rank:	Professor
Department and University:	Department of Physics Virginia Polytechnic Institute and State University Blacksburg, Virginia 24061
Research Location:	Air Force School of Aerospace Medicine Radiation Sciences Division/Laser Lab. RZL-803 Brooks AFB, San Antonio, Texas 78235
USAF Research Colleagues:	Lt Col Charles H. Bonney Dr. Ralph G. Allen
Date:	September 1, 1982
Contract No.:	F49620-82-C-0035

THE EFFECT OF MODULATION TRANSFER FUNCTIONS ON FLASHBLINDNESS

by

Silverio P. Almeida

ABSTRACT

The study of flashblindness is an important area of research since it can adversely effect normal vision. How an object is ultimately imaged through the visual cortex both under normal and flashblindness conditions is the subject of this study. It is believed by some researchers that image processing by humans and some primates is analogous to Fourier transform analysis. It is in this spirit that we investigated the possible effect of simulated flashblindness on various modulation transfer functions applied to an airplane instrument panel's Fourier transform. Preliminary results of this study are presented in this report. Also, further research is suggested for possible study.

I. INTRODUCTION:

A better understanding of flashblindness and its effects on vision is of prime importance to the Air Force. How would a given gauge on a fighter pilot's instrument panel be perceived if the pilot was suddenly exposed to a bright flash from a light source which, for example, came from a laser? This question involves many complicated aspects of the mechanism by which image processing is carried out by the brain. We shall assume in our discussion that the flash is from a uniform extended light source. In the first approximation the flash will be used as a linear superposition on the observed object. Also, assumed is the theory by Campbell[1], Ginsburg[2] and others that the image processing taking place in the visual path ways of the brain in humans is closely analogous to that used in Fourier analysis. That is, that the visual function in man processes incoming data from objects in terms of its spatial frequencies and varying levels of contrast. Sensitivity to the pattern of the object is based on its spatial frequency (cycles/degree) content. It is also known that the visual system is most sensitive to the vertical and horizontal spatial frequencies and to a lesser degree to those frequencies at oblique (45^{o}) angles.

By performing the Fourier transform of a given pattern, an instrument gauge of an airplane in our case allows us to separate out the various shapes, i.e., contours edges, letters, etc. of the pattern in terms of their spatial frequencies. Then by applying various frequency filters called Modulation Transfer Functions (MTF) to the Fourier transform plane and then taking the inverse Fourier transform we obtain a modified image of the original object. This, we assume is the type of vision processing which goes on in the brain. Given this system, how then would one perceive various images which have been modified by MTF after they have been exposed to varying degrees of flash? The next sections present some of the MTF applied to an instrument gauge and show which spatial frequencies tend to be seen the best. The results are preliminary but show a direction which one can pursue to gain further insights into image processing of flashed objects.

II. OBJECTIVES:

The main objectives of this project were:

A. Write software programs to display and analyze data on the Aydin monitor and PDP-11-34 computer.

B. Digitize pictures, in particular a gauge of an instrument panel in an airplane.

C. Perform the Fourier transform (F.T.) on the digitized data.

D. Apply various Modulation Transfer Functions (MTF) to the Fourier transform plane.

E. Perform an Inverse Fourier Transform (I.F.T.) to the modified F.T.

F. Apply a linear superposition of various flash intensities to the Inverse Fourier Transformed picture.

III. SOFTWARE PROGRAMS:

Several software programs were written in order to manipulate and analyze the data on the Aydin monitor. These were written in Fortran IV language and include the following:

A. RWSCN: One specifies a row (0-512) on the picture displayed on the monitor. This program then plots out on the monitor the intensity distribution of pixels along that row.

B. COLSCN: One specifies a column (0-512) on the picture displayed on the monitor. This program plots out on the monitor (along the right side, vertically) the pixel intensity distribution.

C. FLASH: This program superimposes on any specified monitor quadrant (1-4) an intensity specified by the operator. It was used to simulate flashblindness on a given picture. The pixel intensity range is from (0-255).

D. FLICK: This program allows operator to specify a given pixel (512X512) on the monitor screen and flicker it for identification purposes.

E. PWSPC: This program plots the power spectrum function along the X-axis in the spatial frequency domain.

IV. FOURIER TRANSFORM:

Given an input picture $g_1(x_1, y_1)$ located in the front focal plane of a lens. Its Fourier transform

$$G_1(u,v) = \mathcal{F}_1[g_1(x_1, y_1)] \tag{1}$$

will appear in the back focal plane of the given lens and is given by

$$G_1(u,v) = \iint_{-\infty}^{\infty} g_1(x_1, y_1)\, e^{-j2\pi(ux_1 + vy_1)}\, dx_1\, dy_1 \tag{2}$$

This representation is in the so-called spatial frequency domain when the spatial frequency values are

$$u = x_f / \lambda f_1 \quad ; \quad v = y_f / \lambda f_1 \tag{3}$$

and:

x_f = X- cooordinate in Fourier plane

y_f = y - coordinate in Fourier plane

λ = wavelength of light

f = focal length of lens used

The MTF of the Fourier Transform can be obtained by taking the product of eq (2) with the given transfer function say H(U, V) thus getting,

$$G_1'(u', v') = G_1(u, v) \cdot H(u, v) \tag{4}$$

Next, one would take the inverse Fourier Transform of eq (4) giving:

$$g_2(x_2, y_2) = \iint_{-\infty}^{\infty} G_1'(u', v')\, e^{-j2\pi(u'x_2 + v'y_2)}\, du'\, dv' \tag{5}$$

The steps discussed to get to equation 5 can be done either optically, via software or using a hard wired FFT board on line to an Aydin (1024X1024 pixel) monitor and a PDP-11-34 computer. For this project the latter method was used and the system is called the DIP (Digital Image Processor) located in the Laser Effects Branch of the Radiation Sciences Division.

The MTF curves were generated on the PDP-11 35 computer and form a part of the software package known as GIP (General Image Processing) also at this laboratory.

The MTF curves used are given in figures (1-2). They represent a 1^0

field of view (vision) and cut-off frequencies for LP = Low Pass Filters at HPS - High Pass Soft Filters and HP = High Pass Hand Clipped Filters.

V. RESULTS:

The results obtained are presented in figures (4-11) are preliminary. They represent the through-put of the instrument gauge pattern after a linear superposition of a given flash intensity on the gauge. Each set of the four picutres shown has had a given modulation transfer function applied to a particular element of the 2X2 picture matrix. Thus an LP=A+0 represents a low pass filtering (see Code A) + 0 (no addition of pixel intensity to the 2X2 matrix. An HPS+D+100 would represent a high pass (soft) filtering whose frequency cut-offs are given by Code D and a pixel flash intensity of 100 has been added to the 2X2 matrix. Using this scheme, one can then determine which modulated picture gauge can still be seen through a given flash superposition.

Some low pass MTF are seen to wash out quickly while the high pass filter MTF get through even at high intensity flash superportion.

VI. RECOMMENDATIONS:

The data and results obtained are only a first attempt at looking into the effects of flash on picture images. More study is needed on calibrations of the flash, total luminance of the picture, the flash distribution over the picture, the effect of the flashblindness on the aperture of the eye. These factors would then have to be related to how the model of the eye and its image processing actually does see the flashed image. Considerations to be taken into account would be the various contrast sensitivities of the eye as a function of the modulation transfer functions. Also, changes in pupil size due to various flash intensities and how the contrast sensitivity versus spatial frequency curves would be changed, if at all.

Then there is the whole question of color and its effect on the contrast sensitivity versus spatial frequency curves. Also, what happens if one has coherent (pure) colors versus a mixed spectrum as a flash on the gauge? The question of flashblindness and how it is perceived by the visual cortex is a complicated one to understand.

However, given the DIP (digital image processing) capability one hopefully should be able to obtain answers to some of these important questions.

REFERENCES

1. Campbell, F. W., and L. Maffei, "Evidence for the existence of orientation and size detectors in the human visual system," J. Physiol (London) 1970, 207 pp 635-652.

2. Ginsburg, A. P., "Visual information processing based on spatial filters constrained by biological data," 1978, AMRL-TR-78-129, Vol. I, II, Nat. Tech. Inf. Service, Springfield, Va 22161.

ACKNOWLEDGEMENT

The author would like to thank the Air Force Systems Command, the Air Force Office of Scientific Research and the Southeastern Center for Electrical Engineering Education for providing him with the opportunity to spend a very worthwhile and interesting summer at the Air Force School of Aerospace Medicine, Brooks Air Force Base, San Antonio, Texas. He would like to acknowledge the School of Aerospace Medicine Radiation Sciences Division, in particular the Laser Effects Branch for its hospitality and excellent working conditions.

Finally, he would like to thank Dr. Ralph G. Allen for suggesting this area of research and his collaboration and guidance, and he would like to acknowledge the interesting discussions with Lt Col Charles H. Bonney and Dr. Fred Previc. In particular he is very grateful to Mr. James Brakefield and Mr. Dave Schafer for their discussions and help in operating the Digital Image Processing (DIP) system.

FIGURE CAPTIONS

Fig. 1. Modulation-transfer functions for low pass filters. Amplitude versus spatial frequency (cycles/degree).

Fig. 2. Same as fig (1) but for rounded high pass filters.

Fig. 3. Shows the MTF used on each quadrant of figures 4-9.

Fig. 4. A. Low pass MTF-A flash = 0
B. " " MTF-B flash = 0
C. Flash Intensities added to MTF

Fig. 5. A. Low pass MTF-A + flash = 50
B. " " " " " = 100
C. " " " " " = 150
D. " " " " " = 200

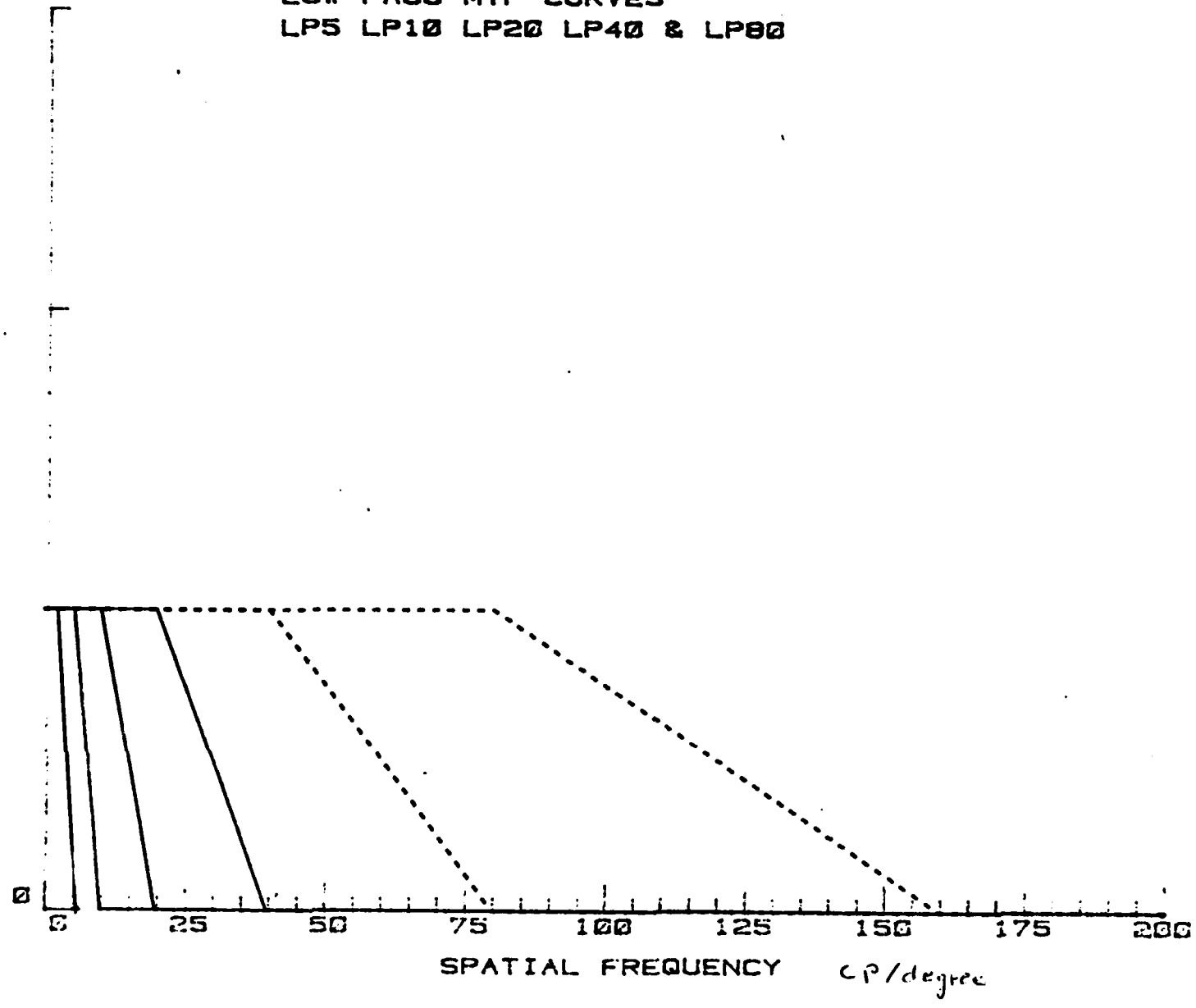
Fig. 6. A. Low pass MTF-B + flash = 50
B. " " " " " = 100
C. " " " " " = 150
D. " " " " " = 200

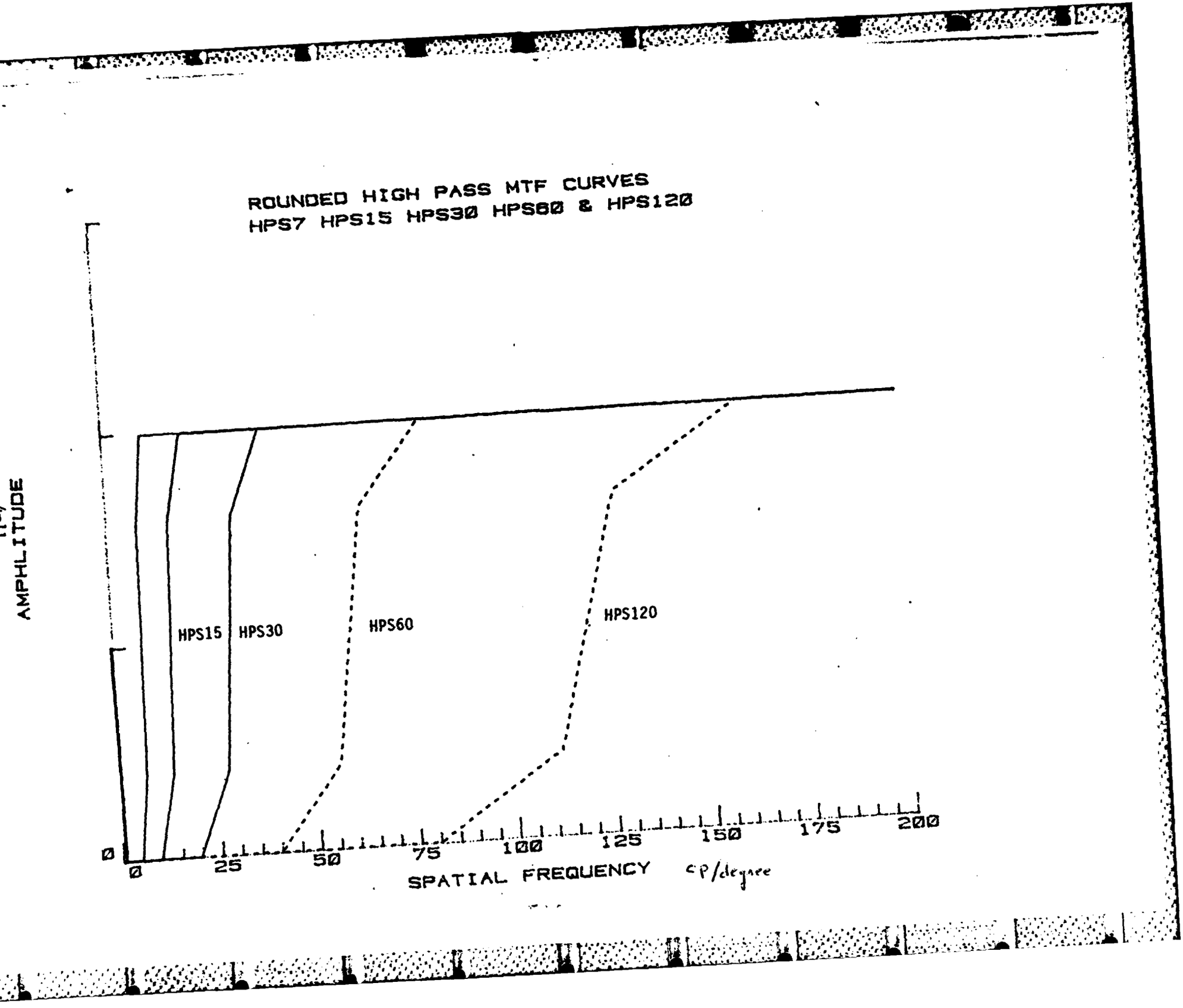
Fig. 7. A. High-pass rounded MTF-C flash = 0
B. " " " MTF-D flash = 0
C. Flash intensities added to MTF

Fig. 8. A. High pass rounded MTF-C + flash = 50
B. " " " " " " = 100
C. " " " " " " = 150
D. " " " " " " = 200

Fig. 9. A. High pass rounded MTF-D + flash = 50
B. " " " " " " = 100
C. " " " " " " = 150
D. " " " " " " = 200

LOW PASS MTF CURVES
LP5 LP10 LP20 LP40 & LP80

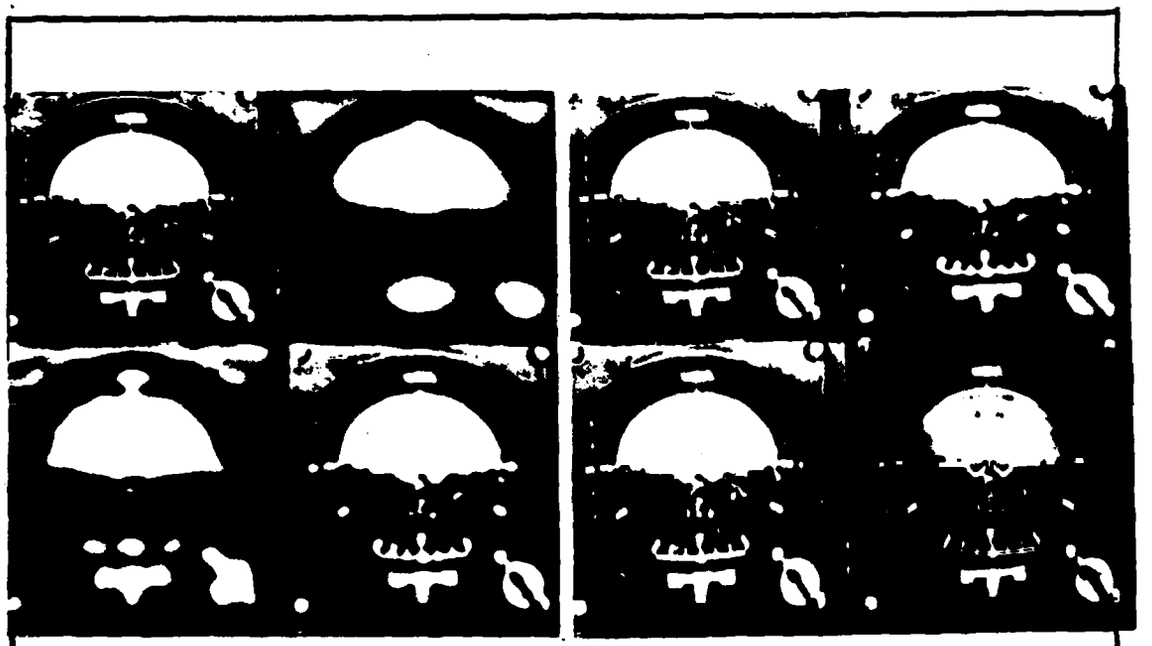



ROUNDED HIGH PASS MTF CURVES
HPS7 HPS15 HPS30 HPS60 & HPS120
AMPHLITUDE
1.1
HPS15
HPS30
HPS60
HPS120
0
0
25
50
75
100
125
150
175
200
SPATIAL FREQUENCY cp/degree

ORIGINAL GAUGE	5 CP/d	ORIGINAL GAUGE	20 CP/d	ORIGINAL GAUGE	7 CP/d	ORIGINAL GAUGE	30 CP/d
10 CP/d	20 CP/d	40 CP/d	80 CP/d	15 CP/d	30 CP/d	60 CP/d	120 CP/d
LOW PASS MTF-A		LOW PASS MTF-B		*HIGH PASS ROUNDED MTF-C		*HIGH PASS ROUNDED MTF-D	

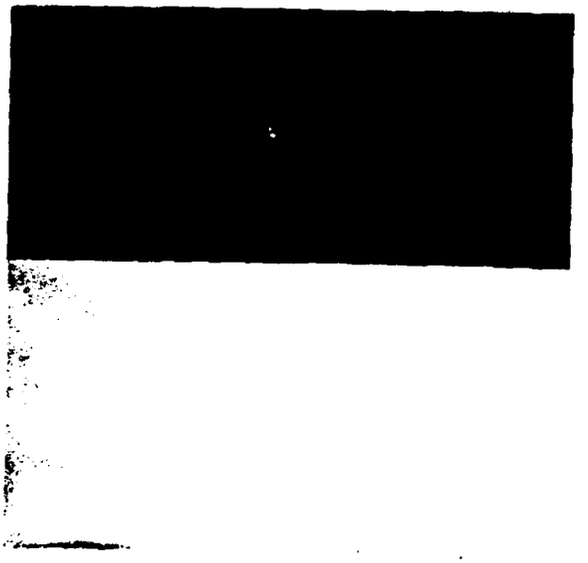
50	100	*Note: The HPS filter code refers to the midpoint spatial frequency on their respective curves in Fig. 2.
150	200	
FLASH INTENSITY		

Fig. 3.



A.

B.



C.

Fig. 4

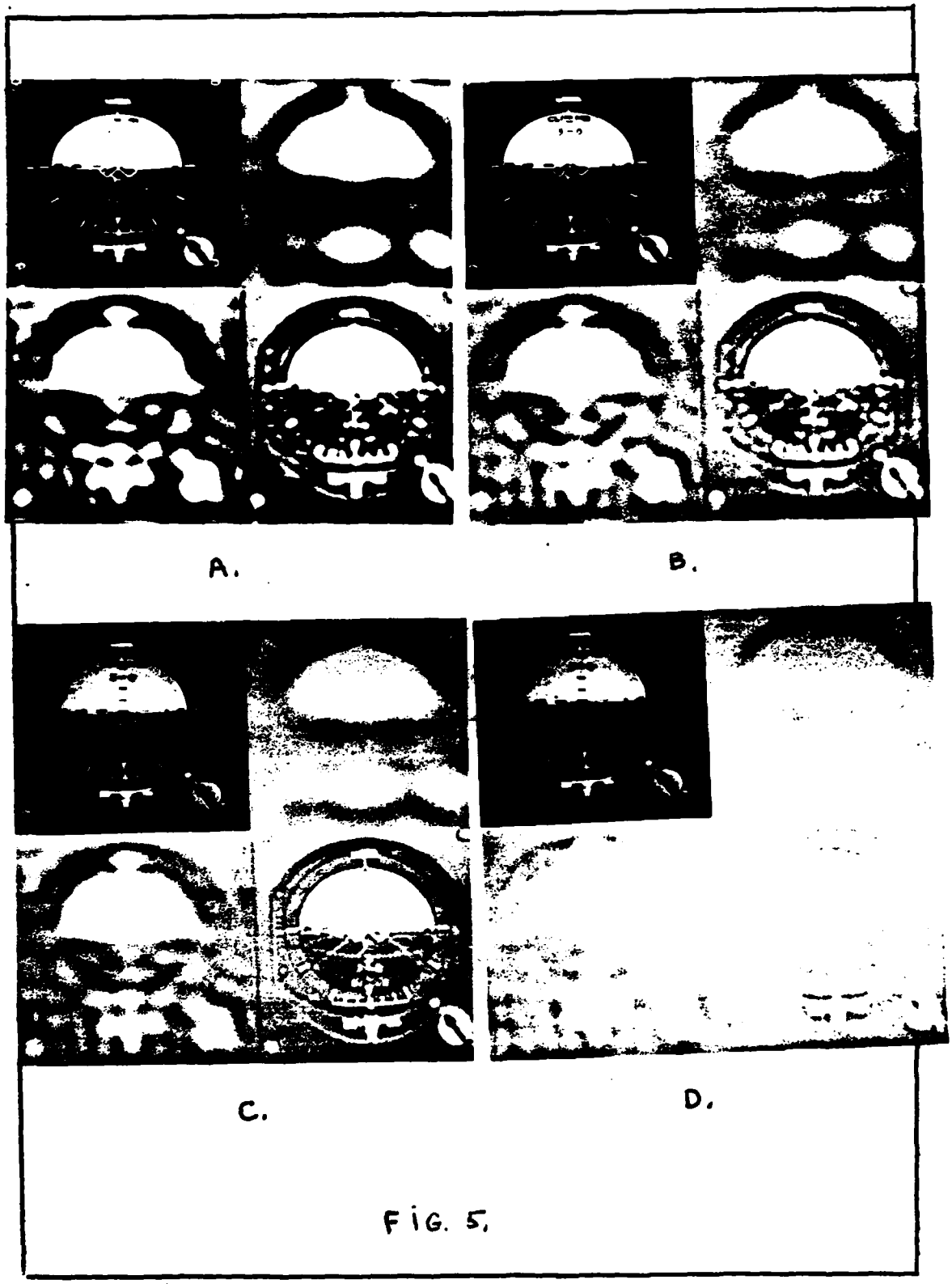


FIG. 5.

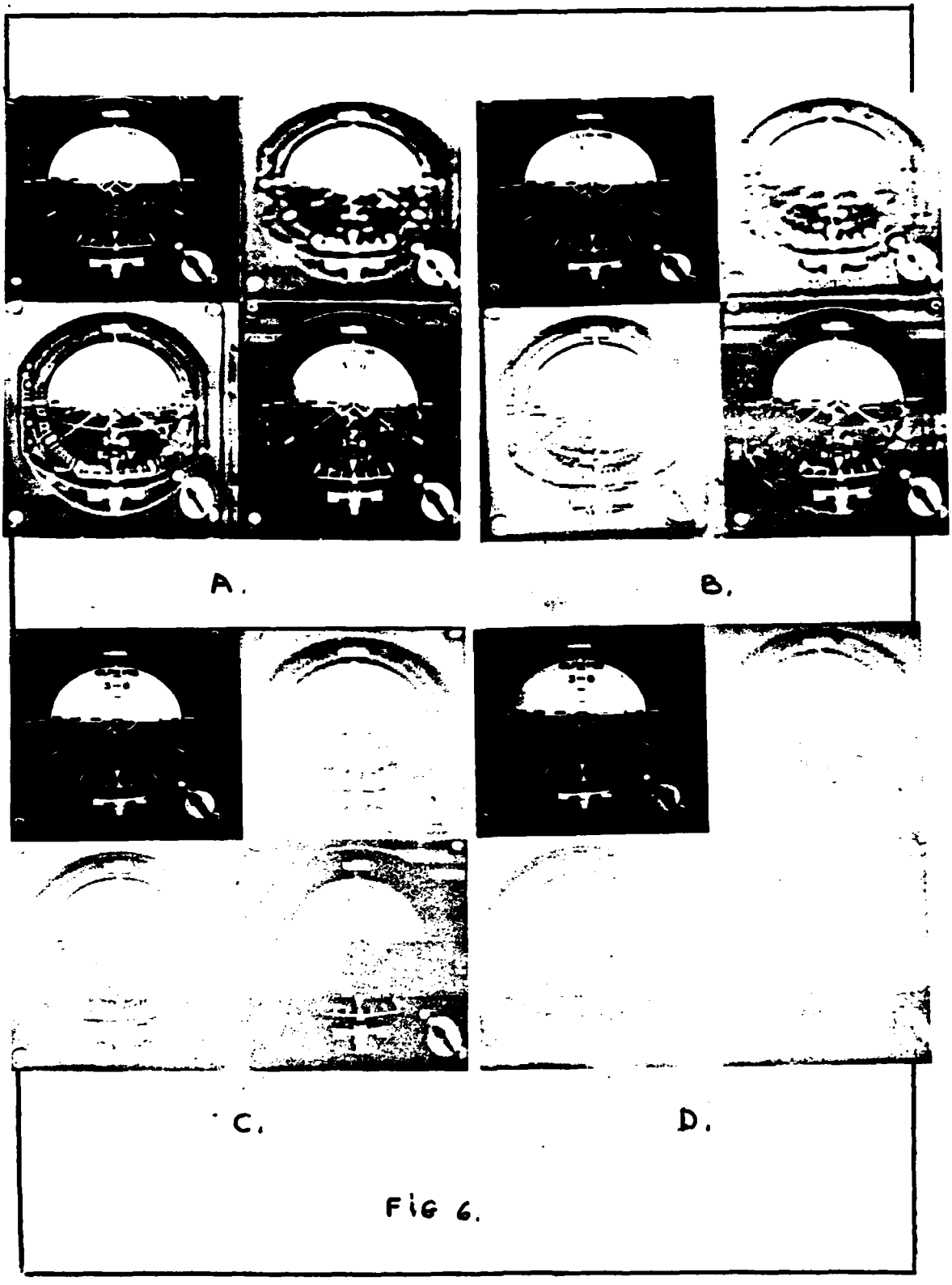
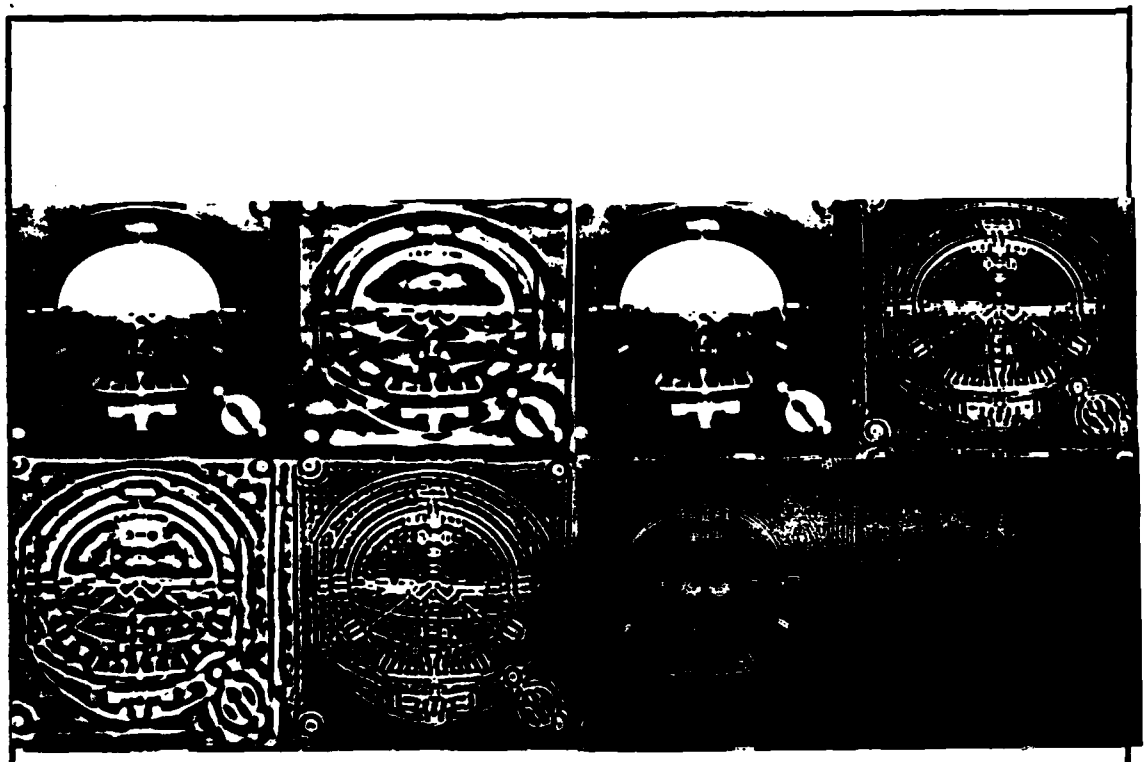


FIG 6.



A.

B.



C.

FIG. 7

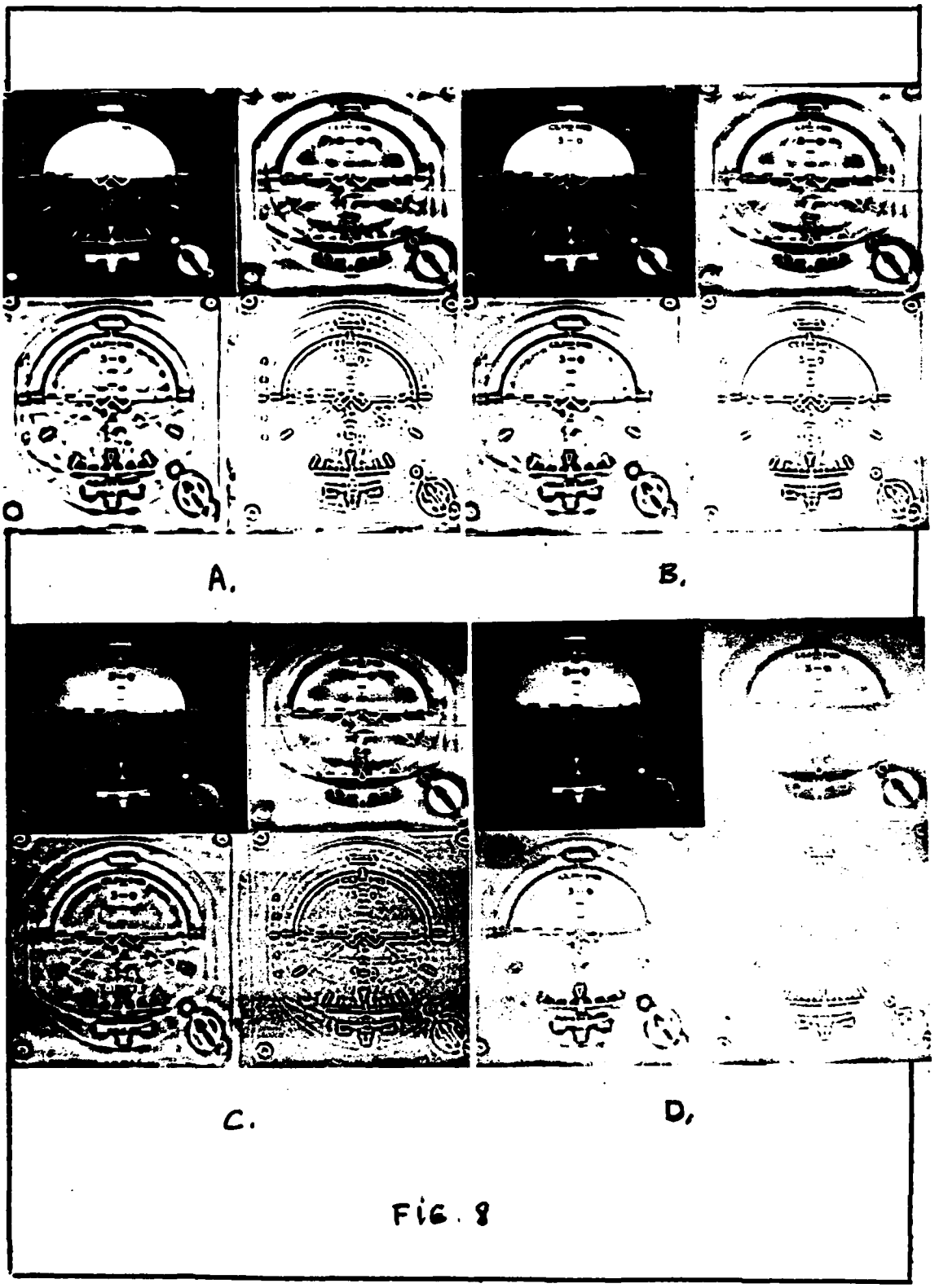


FIG. 8

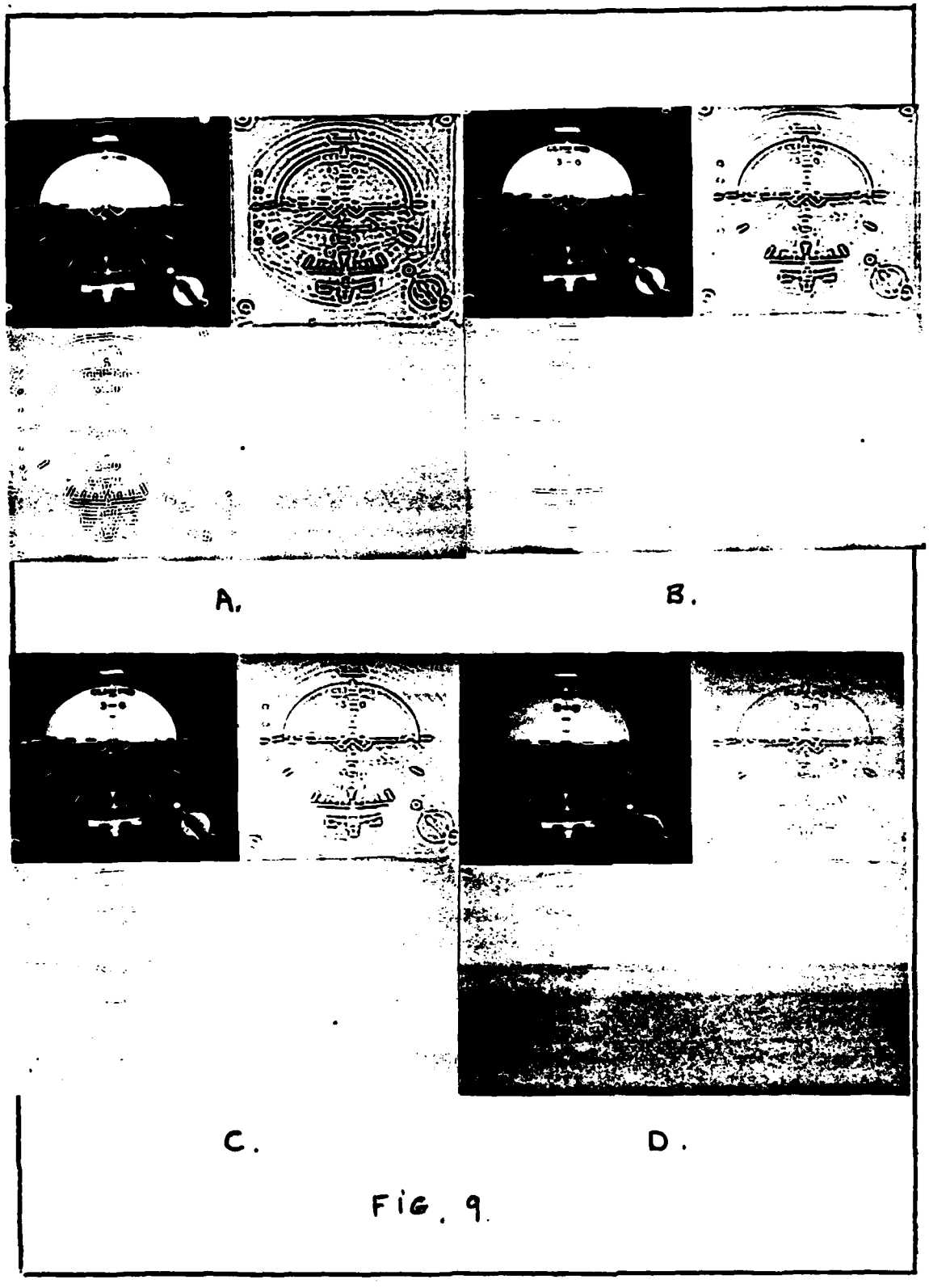


FIG. 9.

1982 USAF - SCEEE SUMMER FACULTY RESEARCH PROGRAM

Sponsored by the

AIR FORCE OFFICE OF SCIENTIFIC RESEARCH

Conducted by the

SOUTHEASTERN CENTER FOR ELECTRICAL ENGINEERING EDUCATION

FINAL REPORT

A THEORETICAL EVALUATION OF THE AIRFIELD PAVEMENT ANALYSIS (AFPAV) FINITE ELEMENT MODEL

Prepared by:	Dr. Muluneh Azene
Academic Rank:	Assistant Professor
Department and University:	Department of Civil Engineering Southern University
Research Location:	Engineering and Services Center Tyndall AFB, Florida
USAF Research Colleague:	Major T. Bretz
Date:	July 27, 1982
Contract No:	F49620-82-C-0035

A THEORETICAL EVALUATION OF THE AIRFIELD PAVEMENT ANALYSIS (AFPAV) FINITE ELEMENT MODEL

by

M. AZENE

ABSTRACT

The theoretical basis of the finite element model used in the airfield pavement analysis (AFPAV) code is studied. The scope of the study is limited to the mathematical model and does not attempt to investigate the programming aspect of the computer code.

On the basis of the study concluded, the semianalytical model used in AFPAV was found to be unsuitable for nonlinear analysis. For linear analysis the model provides a viable analysis technique. However, for improved accuracy some aspects of the idealization scheme utilized in the code need modification.

Alternate finite element idealization concepts are presented and guidance for implementing them are discussed.

Finally, material property characterization models are reviewed and suggestions and recommendation for continued effort outlined.

ACKNOWLEDGEMENTS

I would like to thank the Air Force Systems Command, the Air Force Office of Scientific Research, the Southeastern Center for Electrical Engineering Education and the Air Force Engineering and Services Center at Tyndall Air Force Base for the opportunity to work on this worthwhile project.

I am greatly indebted to Major T. Bretz for his valuable advice and oustanding hospitality and assistance in making this a very enjoyable and productive summer.

Finally, my thanks are also due to Captain J. D. Wilson and Captain H. Kelly for the discussions and useful information they have given me.

I. INTRODUCTION:

One of the primary objectives of the ALRS technical task group at the AFESC, Tyndall AFB, is the development of economical aircraft launch and recovery surfaces (ALRS) that are redundant to the primary airfield pavements and capable of supporting a limited number of aircraft passes. Towards that end, a research effort has been underway to develop reliable and cost effective experimental and numerical models for accurate prediction of pavement responses.

The numerical model provides capability for conducting parametric studies involving changes in the physical properties of pavement materials, pavement thicknesses and other pertinent variables affecting pavement behavior. It aids in understanding the relative influence of various parameters of the pavement components and helps supplement and validate experimental test results. An analysis technique capable of accurately predicting pavement response will also help reduce the need for expensive prototype experimental testing.

Currently a computer code designed for static analysis of flexible pavement structures is available. The airfield pavement analysis (AFPAV) code in its present form was written by J.E. Crawford (1) based on L. R. Herrmann's work (2) that was originally developed for the analysis of underground tunnel subjected to periodic loading. A modified version of the AFPAV Code, namely NMERI (BDR) is also used for investigating repairs on bomb damaged runways(3).

In order to ascertain the validity of the code several experimental tests have been conducted. For example, data from prototype pavement sections at the Waterways Experimental Station, Vicksburg, Mississippi were analyzed using the code (4). Similar other tests had also been performed elsewhere (5). Comparisons between calculated and observed values showed less than satisfactorry correlations. Errors as high as 50% or more were reported in some cases (5). The high discrepancy between observed and computed results have been attributed, by those who developed the code, to the difficulty associated with the characterization of the pavement material properties. However, no mention has been made on the nature of the mathematical formulation and the several simplifying asumptions that accompany it as possible contributing sources of error. This study attempts to examine the mathematical basis of the model and identify those simplifying assumptions that may be cause of error.

II. OBJECTIVE:

In the past, several full-scale experimental tests had been performed to validate the AFPAV Code. By contrast, very little effort had been directed towards examining the theoretical

background of the model. Effects of idealization such as: element size, displacement and load functions, number of Fourier terms, characteristic length, boundary condition specification, etc., on the accuracy of the solution have not been independently and sufficiently examined before. A study of some of the technical reports on the subject (1,3,4,5) and my discussions with Captain J. D. Wilson, who is presently using the code, indicated the need for an independent re-evaluation of the mathematical formulation so that a certain level of confidence can be established on the accuracy of the model. The objective of this study, therefore, is two fold:

a. To re-examine the theoretical background of the finite element model used in AFPAV and identify those simplifying assumptions that may be potential sources of error.

b. To recommend alternate approaches for improved analysis where feasible, and indicate the significance of these approaches relative to the accuracy of solutions.

III. BRIEF REVIEW OF THEORETICAL BACKGROUND:

The approach used in AFPAV code is a semianalytical finite element process using orthogonal functions. The basic element is a plane strain triangular element modified to account for variation in loading in the third direction by the introduction of Fourier series. A continuum is considered to be in a state of plane strain, say in the x, y plane, if the displacement component w in the z direction is negligible and the components u and v are functions of x and y only. An elongated body of uniform cross-section subjected to uniform strip loading in the longitudinal direction is an example of a plane strain problem. The plane strain method of analysis considers a simple slice normal to the longitudinal axis and solution is sought over the two dimensional space defined by the slice. If the continuum is of uniform cross-section but the loading is not, as in pavement structures, the plane strain model can still be used provided the field variables are adjusted such that functional dependence is established in the third direction. One of the common methods of accomplishing that is a semianalytical process of separation of variables, wherein the field functions and prescribed boundary conditions are expressed in terms of Fourier series of orthogonal circular harmonic functions in the longitudinal direction. For each harmonic of the series, the element stiffness matrices and the force vectors are assembled and the systems equations solved as many times as there are harmonics. Synthesis of the harmonic solutions leads to the final result. (A detailed treatment of the procedure for generating the finite element stiffness matrices, force vectors and systems equations is given in Reference (1)). Thus, the original three dimensional problem is substituted by a series of two dimensional problems. The semianalytical analysis scheme is considered economical for certain class of problems where

regular three dimensional idealization becomes expensive to set up and run. When the loading is complex and many harmonics need to be considered to achieve a specific degree of accuracy, then the advantages of the semianalytical approach vanish and the conventional three dimensional analysis becomes superior both in cost and accuracy.

IV. IMPORTANT FEATURES OF THE CODE:

The AFPAV code provides for linear and non-linear elastic material property characterization. It uses an efficient processing scheme for input and output data. A preprocessor program (AFPRE) generates finite element mesh, calculates the Fourier coefficients and computes various quantities needed by the main program. A postprocessor (AFPOST) determines displacements, strains and stresses and outputs numerical information according to specified formats and plots them on graphs. In general, the program contains a heavily automated data processing capability that very little effort is required for its application.

The finite element idealization used in AFPAV, while computationally efficient, uses simplifying assumptions that may adversely affect its ability to accurately predict pavement responses. The elimination or modification of some of these idealization schemes is important for improved degree of accuracy required for the design of economical pavement structures.

This report attempts to identify some of the idealization schemes considered to be potential sources of error. It also comments on the effects and significance of idelaization parameters such as element size, displacement function, loading function, number of Fourier terms, characteristic length, boundary conditions and material property characterization.

V. SIGNIFICANCE OF DESCRITIZATION AND FIELD FUNCTION:

The displacement finite element formulation in AFPAV employs a constant strain triangular element. Therefore, the accurracy of the model is greatly dependent on the fineness of the finite element grid.

In pavement structures where the wearing surface consists of very thin layer of asphalt concrete (of the order of 3 inches or less) a single row of finite element mesh would lead to constant strain value throughout the layer. Since the wearing surface is the most significant component of a layered pavement system receiving the load directly and distributing it to layers below it any stress aberration within the surface layer can easily result in very unrealistic and erroneous response predictions. An obvious way of improving this undesirable situation is the use of three or more rows of finite elements, as is done in AFPAV. The excessively

oblongated elements resulting from it, however, will have unacceptably large aspect ratio that impart directional bias. This undersirable effect associated with the linear displacement function, and therefore mesh sizes, can be minimized by using higher order elements. A highly refined stress element similar to the one described in Reference (6) and briefly outlined herein can be used to advantage.

Consider a self equilibrating stress function $\phi(x,y)$ defined over a triangular domain, and admitting the values of the function and its derivatives up to and including the second order as the nodal variables. The second order partial derivatives of the stress function (included in the nodal variables) are the nodal stress values. For the semianalytic finite element analysis, the function $\Psi(x, y, z)$ is interpolated from the nodal variables represented by a column vector $\{\phi_e\}$ such that

$$\Psi(x,y,z) = \sum_{n=0}^{N} \phi_n(x,y) G(z) \quad . \quad . \quad . \quad (1)$$

where $\phi_n = [N]\{\phi_e\}$ represents a set of quintic interpolation functions satisfying the usual requirements of interelement compatibility and G(z) are orthogonal circular harmonic functions.

The second order partial derivatives of equation (1) give the element stress vector such that

$$\{\sigma\} = \sum_{n=0}^{N} [B]\{\phi_e\}[g(z)] \quad . \quad . \quad . \quad (2)$$

The stress - strain relationships are

$$\{\epsilon\} = [C]\{\sigma\} \quad . \quad . \quad . \quad (3)$$

Where [C] is the compliance matrix.

Substituting equations (2) and (3) in the expression for the complementary strain energy function

$$U^* = \frac{1}{2}\int_V C_{ijkl}\sigma_{ij}\sigma_{kl}\,dV \quad . \quad . \quad . \quad (4a)$$

$$= \frac{1}{2}[\phi_e][f_e]\{\phi_e\} \quad . \quad . \quad . \quad (4b)$$

where $[f_e]$ is the element flexibility matrix.

The surface traction can likewise be expresses as

$$\{T\} = [S]\{\sigma\} \quad \cdot \cdot \cdot \quad (5)$$

in which [S] is a matrix of direction cosines of the outer normal to the surface. Minimization of the augmented total complementary energy functional will result in the desired element equations.

VI. SIGNIFICANCE OF BOUNDARY TRACTION AND FOURIER EXPANSION:

Another important factor that can seriously affect the accuracy of the solution is boundary traction and its representation. In AFPAV, the boundary traction, just as the displacement function, is expressed in terms of circular harmonic functions. The code expands the multiple wheel load assembly as a group in a single step. It generates the wheel load expansion for nineteen different type of aircrafts; with separate subroutines being provided for each aircraft gear assembly. This approach, however, may adversely influence the analysis scheme. The two most significant parameters influencing the solution are the characteristic length and the number of Fourier terms. The effect of these parameters can best be described using the results reported in Reference (4). For example, Figure 1 shows the effect of Fourier series expansion of four wheel loads of C-141A landing gear when the characteristic length is varied with the number of Fourier terms kept constant. Figure 2 shows expansion of four wheel loads of C-5A landing gear in which the characteristic length is kept constant and the number of terms varied. A close study of these figures and their comparison with the optimum representation indicates significant departure from the real situation. A small characteristic length causes negative traction, whereas a large characteristic length dampens the load amplitude by approximately 50 percent. Effects of a similar nature are observable for changes in the number of Fourier terms.

A numerical analysis technique can only be expected to be as accurate as the different assumptions and idealizations constituting it. Therefore, it becomes important to seek alternate means of idealizing the loading function described above so as to improve the input data. A single load expansion coupled with superpositioning scheme is helpful in that regard. The following advantages are expected to result.

a. The loading function can be more realistically represented with little or no negative stress or dampening effects on stress amplitude.

b. Interaction due to periodicity of loading function can be eliminated by taking sufficiently large characteristic length.

c. Separate load expansion for each type of aircraft will no longer be required. Consequently the several subroutines in AFPAV, designated for that purpose can be eliminated.

d. A single load expansion would make the program a multipurpose program capable of handling any loading. The present code is limited to nineteen different types of aircrafts.

e. It will permit the user more flexibility; such as the ability to lump together closely spaced loads, take advantage of symmetry in loading and disregard loads that have negligible influence on the solution.

f. For a given pavement no separate analysis will be needed for each aircraft type. One solution for a single wheel load is sufficient to predict responses for all types of loading conditions, i.e., the systems equations need not be solved more than once.

g. A single term Fourier series expansion is what will be needed for all types of loading, and the Fourier coefficients for the loads can be evaluated before hand and stored as permanent data without the need for re-evaluation.

h. Arbitrariness in the selection of characteristic length and number of terms can be eliminated.

A Fourier series representation for a single wheel load, hereafter referred to as basic load, is shown in Figure 3. The maximum ordinate is normalized but is not drawn to scale. These graphs depict the variation in the single load expansion when the number of cosine terms varies from 10 to 20 for L=120 inches. They give very close approximation to the actual load distribution which would be a single rectangular pulse with unit ordinate.

In order to illustrate some of the important aspects of what is described above, consider the simple example given in Figure 4a, in which a plan view of two isolated loads on a pavement surface is given. Suppose the combined response due to these two loads is to be evaluated at section A-A.

First, using one of the loads as the basic load, the usual computation for displacement harmonics is carried out. The origin of the global coordinate system is assumed to be positioned at the center of the basic load, as shown in Figure 4a . The influence due to another load at any point can be determined by translation of the coordinate system such that

$$\left.\begin{aligned} x &= x_i - x_p \\ y &= y \\ z &= z_i - z_p \end{aligned}\right\} \qquad . \quad . \quad . \qquad (6)$$

where x_i and z_i are the x and z coordinates of load i, whose influence is being computed and x_p and z_p are the coordinates of the nodal points where influence is being computed.

The response at section A-A due to load i is equivalent to the response of the basic load at section A'-A' or A"-A" with the x-coordinates of the points determined according to equations (6). In other words, the response at point P due to load i is equal to the response due to the basic load at any one of the points P_1', P_2', $P_1"$ or $P_2"$ as shown in Figure 4a. Because of double symmetry the solution space can be limited to the positive x, y, z quadrant and equation (6) can be modified as

$$\left.\begin{aligned} x &= |x_i - x_p| \\ y &= y \\ z &= |z_i - z_p| \end{aligned}\right\} \quad . \quad . \quad . \quad (7)$$

If the total depth of the pavement layers is less or equal to 1.75 times the distance from the section where stresses are computed to the edge of the distributed load, the effect of that load can be neglected as shown in Figure 4b.

The final solution is given by the cummulative solutions of the individual loads.

VII. NONLINEAR ANALYSIS AND MATERIAL CHARACTERIZATION:

The AFPAV code is unsuitable for nonlinear analysis, because of two main reasons. The first of which is the inevitable result of the semianalytical finite element formulation used in the code it has been alluded to in Reference (5) when the authors stated:

> "The prismatic formulation used in AFPAV imposes a significant limitation on the nonlinear analysis. The maximum shear strain, γ, is calculated as the absolute maximum of the shear strains which are computed at specified number of z stations (chosen by the user). γ, representing the largest strain, is derived only from the values of those strains at the selected z stations. Thus the selected Z sections must encompass the locations of the largest shear strains. Generally this is a conservative approach forcing the shear modulus of an element to be based on the greatest shear strain within that element. In the formulation of the element stiffness, the resulting shear modulus is applied as a constant over the entire element volume."

The simplification described above is generally acceptable provided fine mesh sizes are utilized in regions where the stress gradient is steep. In the semianalytical model, however, ones

ability to employ fine meshes is limited to the cross-sectional (x, y) plane. In the longitudinal direction, the characteristic length, which is also the element length, is fixed. The characteristic lengths used in the code are based on the type of aircraft analyzed and range between 100 to 300 inches; See Figure 5. Therefore, one connot justifiably consider the state of stress to be constant over the entire element volume of that size. That will be gross simplification and will inevitably lead to serious errors.

Figure 6 is reproduced from Reference (5). It shows a comparison of measured and computed vertical displacements for both linear and nonlinear elastic analysis. Since in most problems of this type, the effect of nonlinearity of the stress-strain relations appears in the horizontal stresses more strongly than it does in the vertical stresses a comparison of shear and horizontal stresses would have been more revealing. Nevertheless, the conclusions made in Reference (5) notwithstanding, the linear analysis shows a better correlation with observed values close to regions of high stress gradient. The large discrepancy between the linear solution and the observed values in the lower layers may be attributable to periodicity influence but needs further investigation. The implication is that the stresses and strains in the pavement except near the surface are so small that materials are stressed within or near their linear range, that linear analysis may not be the most critical factor in the disparity between the measured and predicted values.

Secondly, in nonlinear inelastic or elastoplastic analysis where the stresses are dependent on the loading path (i.e., the stresses and strains are related entirely by their differential behavior), the semianalytical model which inherently employs superpositioning of harmonic solutions to obtain the final solution, cannot be used. A much more realistic approach to nonlinear analysis is the regular three dimensional finite element model. The three dimensional model will in addition provide the capability to analyze effects of repeated loading, fatigue, permanent deformation, discontinuities, etc., in the pavement structure. However, any attempt to predict analytically the behavior of structures in the plastic range must begin with the choice, among the available theories, of one which successfully combines mathematical simplicity with a proper representation of experimentally observed material behavior. Some theories are best suited to certain type of problems than others; therefore, some research effort has to be directed to the study and development of the best theory applicable for pavement analysis.

Finally, another factor of significance needs to be mentioned. For nonlinear analysis where at every iteration step. stresses at every nodal point and the equivalent state of stress for each element have to be computed the complementary energy finite element formulation is superior to the displacement or potential energy approach. Therefore, the former approach merits serious consideration for future application.

VIII. RECOMMENDATIONS:

The two most important features of a good analytical model are: its ability to accurately simulate structural behavior and its computational efficiency. Both of these features depend, to a major extent, on the nature and type of simplifying assumptions made in the formulation. Oversimplification has an adverse effect on accuracy; but may or may not lead to computational efficiency. The guiding principle must always be to take simplifications consistent with the required degree of accuracy. For the type of analysis and application envisaged in the design of economical alternate launch and recovery surfaces, a high degree of accuracy is essential. The analysis tool must provide the capability to determine realistically the ultimate capacity of the pavement structure so that a viable and cost effective design criteria and procedure can be developed. Therefore, the need for improving the existing code or developing an improved model is evident. In connection with that the following recommendations will be pertinent:

a. Linear analysis: Conceptually the semianalytical finite element model is a viable tool for linear analysis, provided the loading function and other features of idealization mentioned earlier are realistically formulated. The accuracy of the AFPAV code, would greatly be enhanced if the single load expansion technique described in this report is implemented. The accuracy can further be improved if a higher order element is utlilized, instead of the linear displacement model presently employed. In this regard, employment of a highly refined stress model similar to the one in Reference (6) is advantageous. In particular, the combined application of the single load expansion scheme with the refined stress model is expected to give excellent results and is a subject deserving further investigation.

b. Nonlinear Analysis: As has been pointed out earlier the semianalytic model is unsuitable for both nonlinear elastic and inelastic analysis. It is unsuitable for nonlinear elastic analysis because it fails to realistically describe the state of stress within an element volume at every stage of incremental loading. It is also unadaptable to elastoplastic analysis because it is inherently a superpositioning scheme and therefore cannot be applied to path dependent nonconservative systems.

A reliable approach to nonlinear analysis of pavement structures is the more versatile regular three dimensional finite element model. The three dimensional model will provide the additional capabilities to analyze and study effects of repeated loading, fatigue, permanent deformation, discontinuities, etc., which the present code cannot perform.

Finally, on the basis of the study conducted, it is recommended that a three dimensional finite element model for nonlinear analysis be developed; until then application of the AFPAV Code for nonlinear analysis must be done with caution and if possible avoided.

REFERENCES

1. Crawford, J. E., An Analytical Model for Airfield Pavement Analysis, AFWL-TR-71-70, Kirtland Air Force Base, New Mexico, May 1972.

2. Herrman, L. R., Three-Dimensional Elasticity Analysis of Periodically Loaded Prismatic Solids, University of California, Davis, California, November 1968.

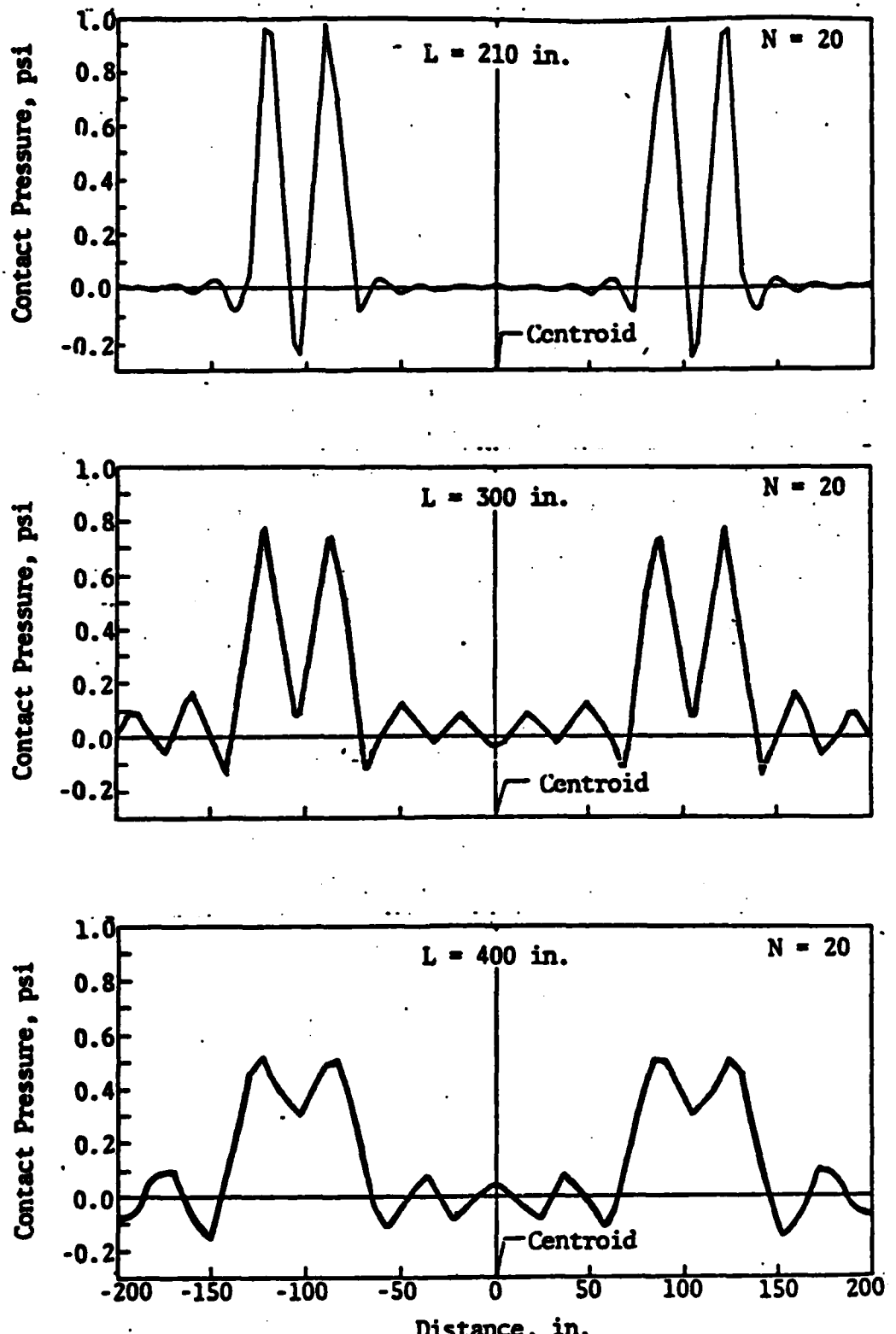
3. Baird, G. T., Bomb Damage Repair Code for Prediction of Repaired Crater Performance, ESL-TR-80-69, New Mexico Engineering Research Institute, University of New Mexico, Albuquerque, New Mexico, September 1980.

4. Pichumani, R., Finite Element Analysis of Pavement Structures Using AFPAV Code (Linear Elastic Analysis) AFWL-TR-72-186, Kirtland Air Force Base, New Mexico, May 1973.

5. Crawford, J. E., and Pichumani, R., Finite Element Analysis of Pavement Structures Using AFPAV (Nonlinear Elastic Analysis), AFWL-TR-74-71, Kirtland Air Force Base, New Mexico, May 1973.

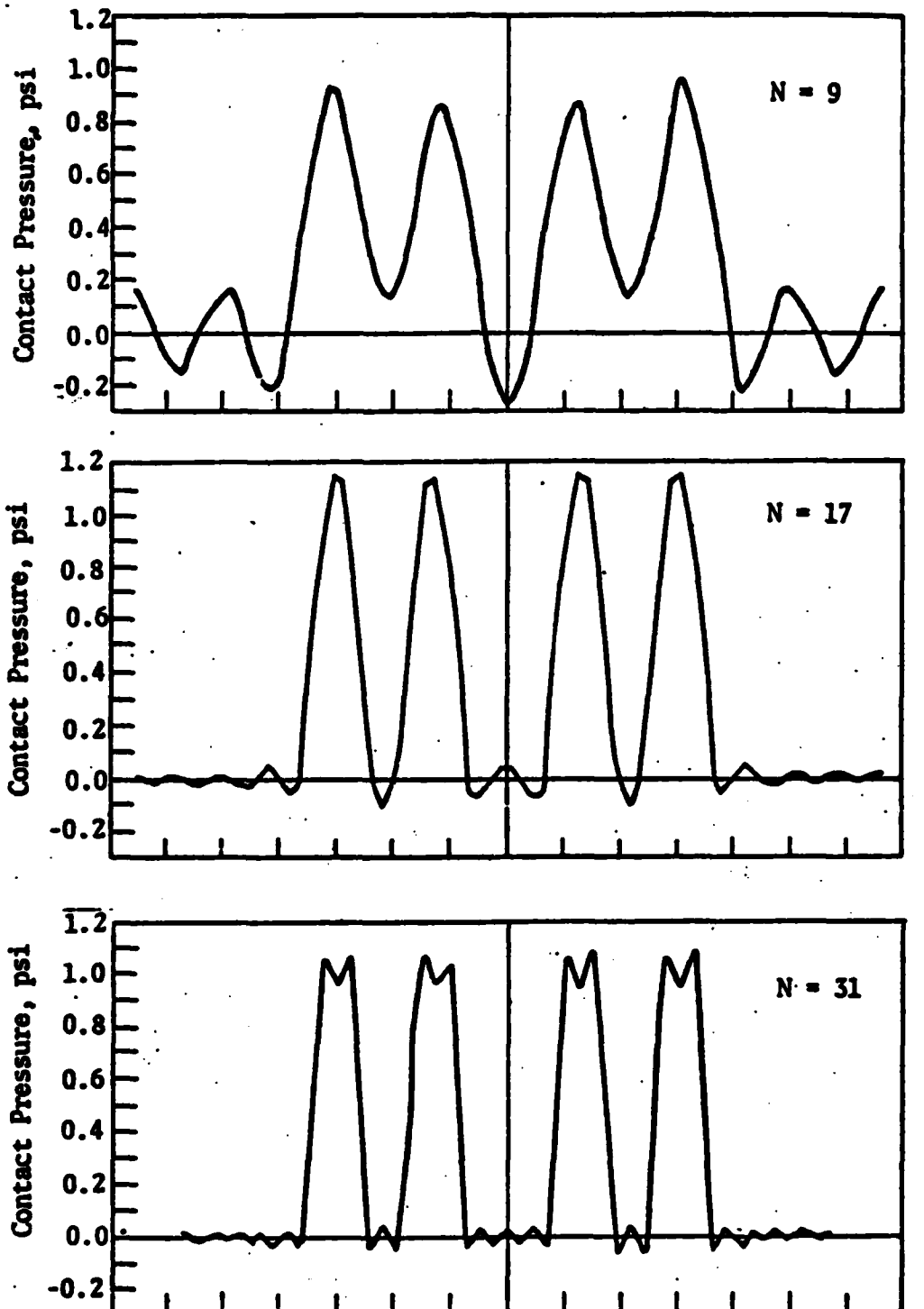
6. Vallabhan, C. V. G., and Azene, M., "A Finite Element Model for Plane Elasticity Problems Using the Complementary Energy Theorem", International Journal for Numerical Methods in Engineering, Vol. 81, 291-309, 1982.

7. Nielson, J. P. AFPAV Computer Code for Structural Analysis of Airfield Pavements, AFWL-TR-75-151, Kirtland Air Force Base, New Nexico, October 1975.



Note: N equals number of Fourier terms; L equals half-period.

Figure 1. Effect of Period on Fourier Series Representation of Four Wheel Loads of C-141A Landing Gear (Ref 4)



Note: N equals number of Fourier terms.

Figure 2. Fourier Series Representation of Four Wheel Loads of C-5A Landing Gear (Ref 4)

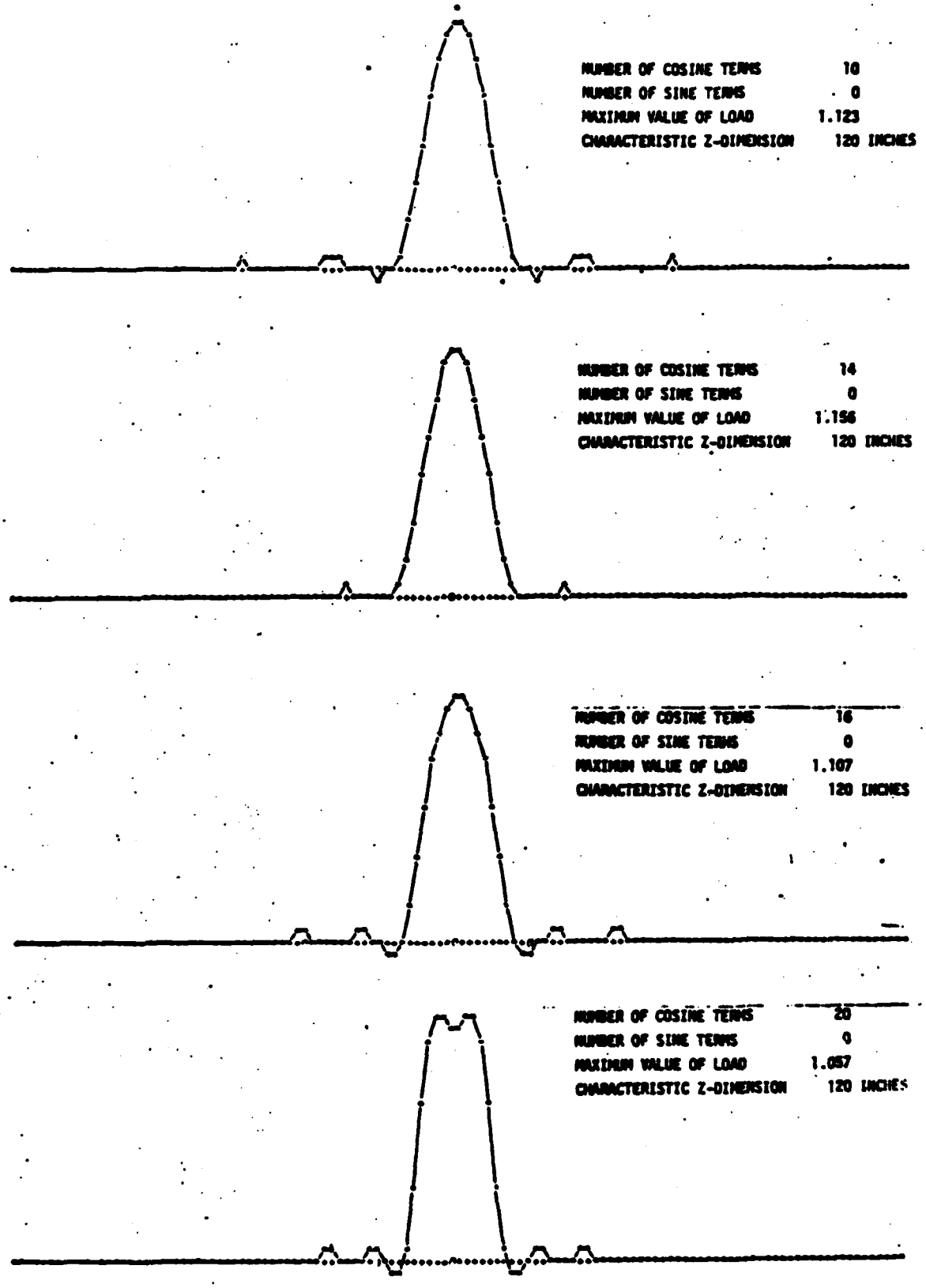


Figure 3. Fourier Load as a Function of Number of Cosine Terms (Ref 7).

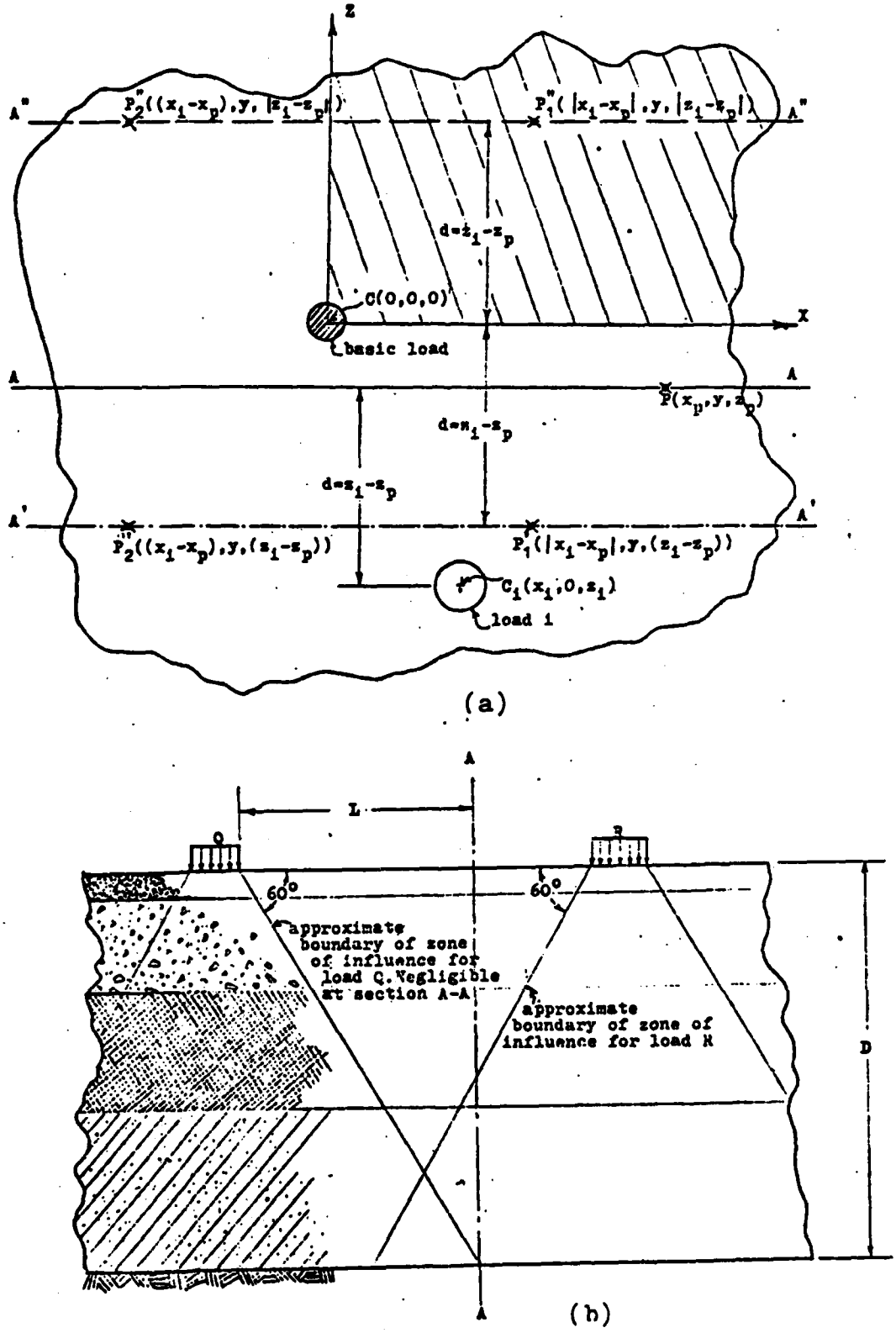


Figure 4. Single Load Superpositioning

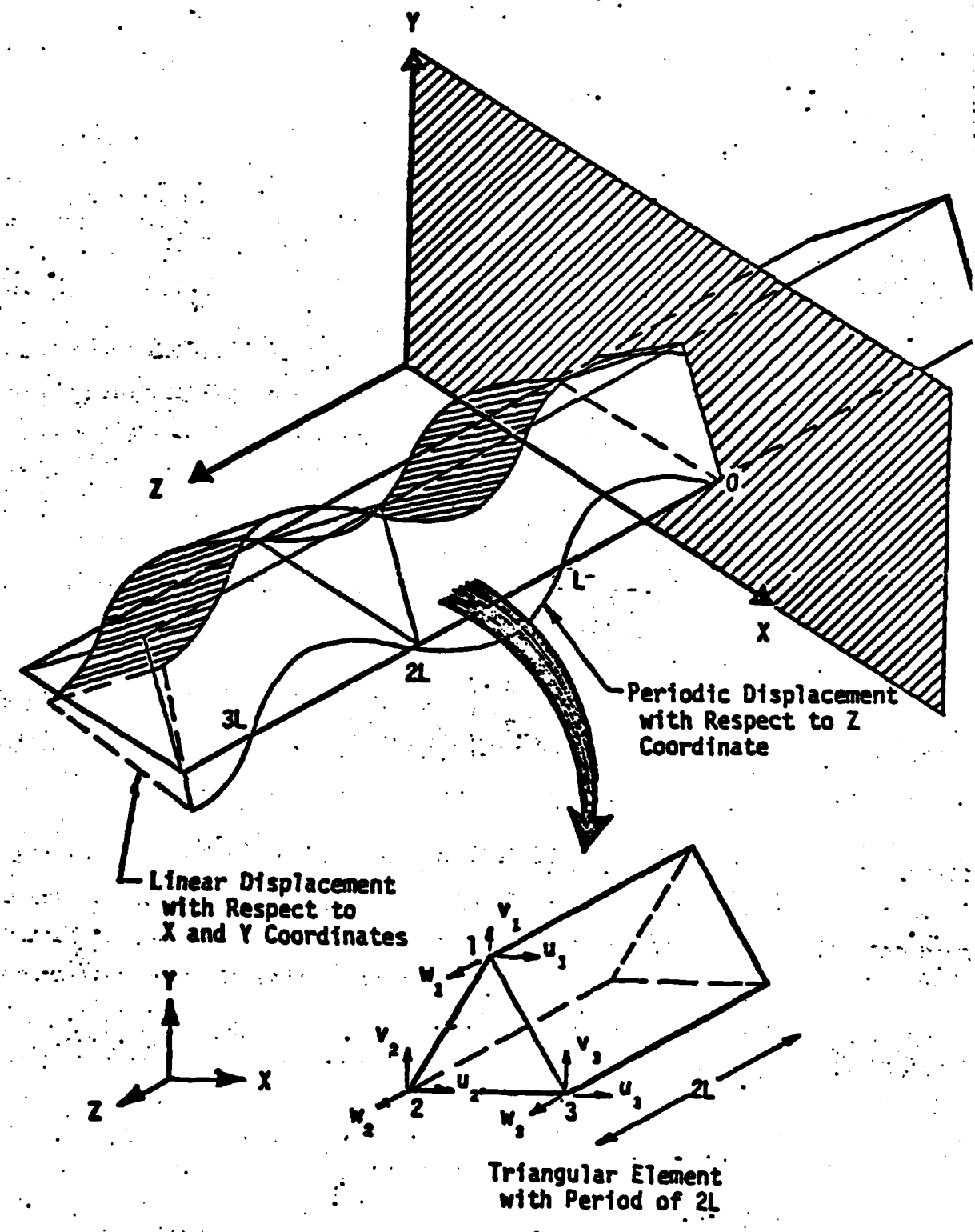


Figure 5. Periodic Deformation Pattern (Ref 5)

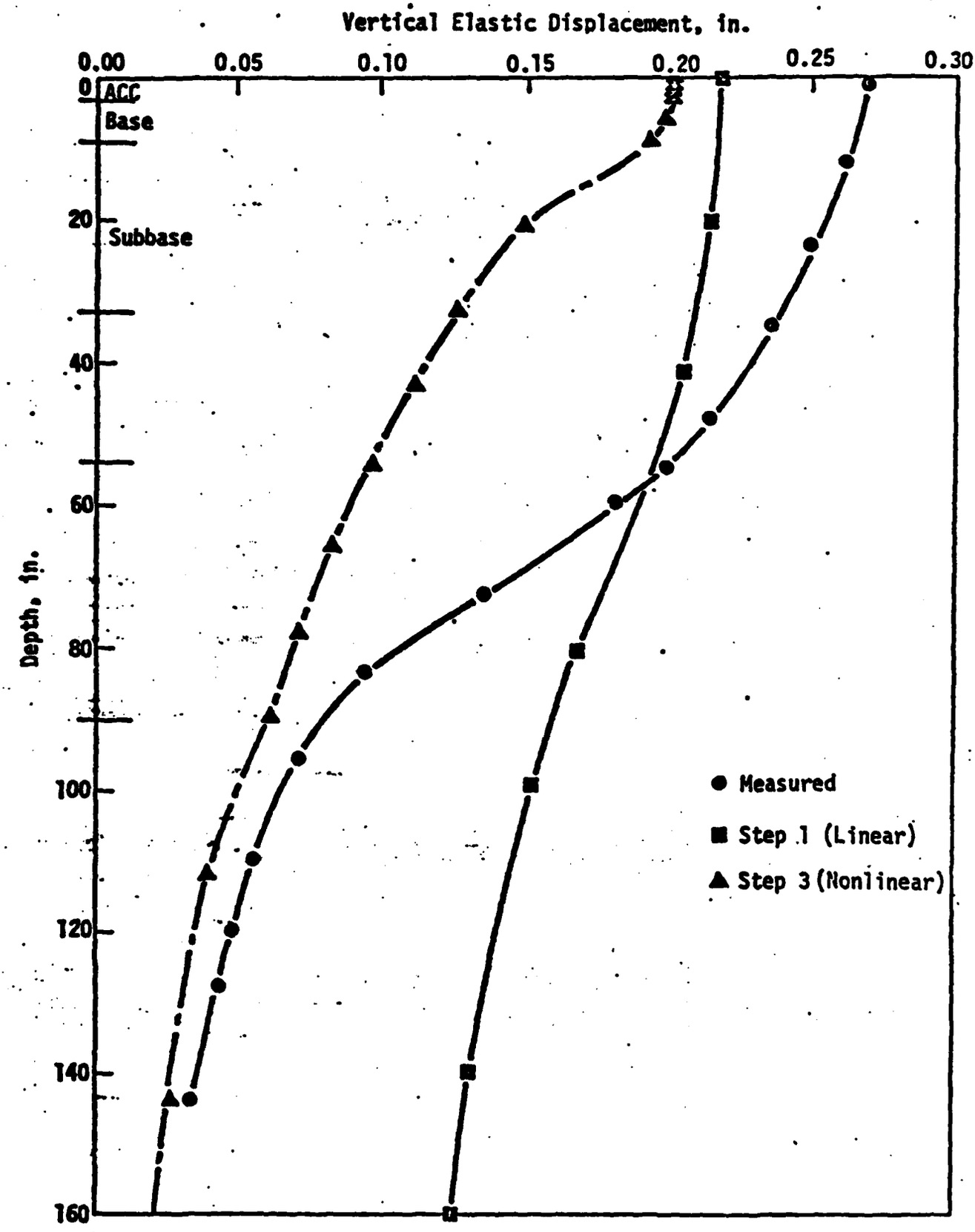


Figure 6. Comparison of Measured Data and Computed Response for WES Flexible Item 4 (Ref 5)

1982 USAF-SCEEE SUMMER FACULTY RESEARCH PROGRAM

Sponsored by the

AIR FORCE OFFICE OF SCIENTIFIC RESEARCH

Conducted by the

SOUTHEASTERN CENTER FOR ELECTRICAL ENGINEERING EDUCATION

FINAL REPORT

ORBITING GEOPHYSICS LABORATORY EXPERIMENT

Prepared by:	Dr. Francesco L. Bacchialoni
Academic Rank:	Associate Professor
Department and University:	Department of Electrical Engineering University of Lowell
Research Location:	Air Force Geophysics Laboratory, Aerospace Instrumentation Division, Sounding Rocket Branch
USAF Research Colleague:	Jack R. Griffin
Date:	September 9, 1982
Contract No:	F49620-82-C-0035

ORBITING GEOPHYSICS LABORATORY EXPERIMENT

by

Francesco L. Bacchialoni

ABSTRACT

This document reports the investigation on the potential utility and technical feasibility of a new self-contained support system to be utilized repeatedly for different AFGL experiments in space, using the Space Transportation System (Shuttle) for launch and retrieval. This support system is designed to operate independently of both the STS and ground stations, therefore, stores data rather than transmitting them by telemetry. Angular pointing is the only maneuver planned; no propulsion is designed into this system.

ACKNOWLEDGEMENT

The author would like to thank the Air Force Office of Scientific Research and the Southeastern Center for Electrical Engineering Education for providing him with the opportunity to spend a very worthwhile and interesting summer at the Air Force Geophysics Laboratory, Hanscom AFB, Massachusetts. He would like to acknowledge the laboratory, in particular the Sounding Rocket Branch for its hospitality and excellent working conditions. Finally, he would like to thank Mr. Edward F. McKenna for suggesting this area of investigation and for his guidance and collaboration. The author would also like to acknowledge many helpful discussions with Jack Griffin, Russell Steeves, Ray Wilton, William Miller, Roger Jacobs, Kenneth Walker, and several other members of the staff and the help of Dottie Boisvert in typing this report.

I. INTRODUCTION

With the Space Transportation System (Shuttle) beginning its operational activity, there is the practical opportunity of performing space experiments lasting up to a few days. A normal STS flight may last 7 days, which is a very long time compared with the typical 15 minutes flight time of a sounding rocket.

Several different techniques may be implemented to utilize the STS for scientific experiments. One technique aiming to avoid space contamination caused by the STS itself is to place the experiments in free space, outside of and away from the STS. A small package could be left detached from the STS for a long time, up to a few days, and retrieved by the STS for return to Earth. This study examines in some detail this particular technique.

II. OBJECTIVES

The main objective of this project was to investigate the technical and economic feasibility of building a space platform, to be utilized as a support system for AFGL space experiments.

Detailed objectives of this investigation were:

1. Flight Duration
2. Data Telemetry vs. Data Recording
3. Attitude Control System
4. Power Supply

In this investigation many decisions related to our objectives had to be taken by extrapolation from previous experience resulting from sounding rocket flights, applying engineering judgment.

III. GENERAL CHARACTERISTICS

This platform is to be designed as a free-flying support system for scientific experiments. The STS must supply mechanical support and transportation, deployment in orbit and retrieval by means of the Remote Manipulator System. The mission is envisioned in this way: when the STS is in orbit, the crew must activate an automatic test of the platform by radio link a switch and watching a Yes-No response before deployment; after this simple test, the STS crew may deploy the platform in orbit and then by radio link activate the experiment mode. The remaining action required of the STS crew is experiment turn-off by radio link, retrieval from orbit and stowage into the STS payload bay. This minimal dependence on the STS should allow for a wide range of experiments and offer a rapid response to opportunities for flight. Safety considerations should be present at every step of the design. This means that only manned flight-rated component units should be used, since testing a non-rated unit is a long, complicated, and expensive procedure.

The probable cost of a reusable support system seems to be lower than that of non-reusable packages even if it is difficult at this time to determine exact figures and the break-even point. Low cost of the platform is a very general design objective which has to be considered at each step, applying engineering judgment based on previous experience from sounding rockets.

IV. FLIGHT DURATION

In order to offer a substantial advantage with respect to a sounding rocket, it is clear that our space support system must be capable of operating for the major part of an STS flight, that is approximately 7 days. Experiment .ıpport and housekeeping must be available for this length of time, offering to the scientists the practical possibility of long experiments. Also, several different experiments can be supported in a single flight.

V. SCIENTIFIC DATA AND SUPPORT DATA REQUIREMENTS

It is considered essential to minimize the STS crew workload and also that of Earth-based telemetry sites. This last point means that all the data resulting from the experiments, plus some housekeeping information, must be recorded on-board. Magnetic tape recording is presently the best method to acomplish this objective. The obvious result of these considerations is that the tape recording system (one recorder or more) is one of the most important subsystems to be installed on the platform. Selection of a flight-approved tape recorder system is probably the first item to be considered when designing our space platform. Direct digital or analog recording choice remains undetermined at this time.

Major considerations are total recording capability and power absorption. It is extremely difficult to establish theoretically the data storage capacity needed for a typical platform mission, but it is possible to reach some reasonable numerical values by extrapolation from the Sounding Rocket Experiments. Engineering judgment based on previous experience should provide a reasonable starting point for the overall design.

A typical 16-minute rocket flight generates data which are recorded on one track of tape 9200 ft. long. These data include housekeeping data, and amount to approximately $2 \cdot 10^9$ bits of information. By engineering judgment it seems desirable to be able to store at least 10 times the above amount, that is a total of approximately $2 \cdot 10^{10}$ bits. This would allow the platform to support experiments with fairly fast data collection (2 Mbits/sec) for up to 160 minutes of active measurements. Different recording methods (direct, PCM, HDDR) may be used, but at this point only the total storage capacity is of interest. This value of $2 \cdot 10^{10}$ bits as an estimate for total storage capacity is compatible with existing data recorders; therefore, it can be accepted as a reasonable starting point.

VI. SUGGESTED DATA STORAGE SYSTEM

Several different methods could be applied in principle to provide our storage capacity of $2 \cdot 10^{10}$ bits. Conventional RAM chips or bubble memory chips could be used, but their capabilities are presently too limited. Bubble memory chips of 1 Mbit capacity exist, but it is clearly not practical to assemble a memory unit having 20,000 chips. Higher density chips may become available, but not in the near future. Optical recording has the potential for high capacity, but presently it is not available as a developed package. Some companies (e.g., Shugart Associates) are presently developing optical storage systems which will involve accurate positioning of laser beams on the recording medium. From a mechanical point of view, these systems seem similar to magnetic tape or disk recorders; therefore, it is reasonable to expect similar limitations, at least for the near future.

This leaves magnetic storage as the logical method to be considered. Disk storage can be quickly ruled out, again, for its too small capacity: typical 8" floppy-disk can store up to 12 Mbits, while 8" Winchester drives can store up to 160 Mbits, which is much too little.

This elimination process leaves the magnetic tape recorders as the only practical method for our purposes.

Several companies are presently offering space flight rated tape recorders, and some are also developing new models which are definitely of interest for our Space Platform application. Consideration has been given to the following manufacturers: Odetics, RCA, Lockheed, Honeywell, Ampex, EMI, and Bell and Howell. Information on their recorders is collected in an expanded version of this report, available from AFGL, Sounding Rocket Branch.

Again, engineering judgment must be exercised to formulate a reasonable suggestion of a tape recording system. The following characteristics are highly desirable:

a. Low power absorption
b. Variable speed
c. Two distinct recorders (to enhance reliability)
d. Reasonable price

It seems that the most balanced design at this time consists of a system made up by two Bell and Howell MARS 1428 recorders. Two recorders rather than one allow longer experiments and in the case of one recorder failing, the second one provides storage for part of the experiment. These recorders can be switched on and off so that only one at a time has to be active. One or two tracks on each recorder may be used for error correction, with a corresponding reduction of total storage.

This type of recorder requires power on (in STOP mode, power approx. 55W) for takeoff and landing of the STS, in order to avoid damage to the tape. While the energy consumption is negligible, there is the need of additional circuitry to turn on and off the recorders at the right times.

The required power is rather high but the recorder is proven and relatively inexpensive. The selection of the Bell and Howell MARS 1428 is valid only at this time, since several manufacturers are presently developing recorders worthy of consideration. Therefore, at design time, it will be necessary to reconsider the recorder selection, checking again the various units then available.

VII. ATTITUDE CONTROL SYSTEM (ACS)

This platform is designed to be a support system for a vast set of scientific experiments of different duration and pointing requirements. Typical desirable properties are:

pointing drift in 10 min. < 5 sec. of arc
outgassing as limited as possible
number of pointing maneuvers = 5 per orbit.
repositioning error < 20 min. of arc.

Specifications of this order, particularly low drift, require a rather elaborate active ACS. It is clear that in order to have low drift, a good quality inertial reference is required. The "tuned restraint" gyro systems typically can have drift less than 6 min. of arc/hr; therefore, this type of inertial reference seems adequate when used in connection with an acccurate star tracker. Laser gyros are presently becoming available and should be considered at final design time. Another typical mode of operation is target tracking with pointing error signals delivered by the scientific instruments. This tracking may be required by some experiments and should also be considered when designing the overall ACS. It has to be taken into account that any practical inertial reference required to operate through 7 days must be periodically realigned to an absolute reference. A star tracker can be designed to perform this job, and it appears from the technical literature (RCA Technical Communications, for example) that the design of this functional sequence has been successfully implemented. Therefore, no unusual technical difficulty is expected.

The repeated pointing maneuvers and the minimum outgassing requirements dictate the use of reaction wheels for most of the maneuvering. This technique also is well established and offers no technical surprise. Together with the reaction wheel subsystem there is need of a momentum desaturation subsystem, like gas jets or magnetic field torquers. Both momentum desaturation methods involve proven technologies. Gas-jets are quick acting and require reaction gas; magnetic field torquers develop small torques, therefore are slow in action and require electric energy, but no gas. This property is highly desirable, but their small torque may be a serious drawback. The residual tumbling of the platform when released in orbit by the Remote Manipulator System is probably very small (this estimate should be checked with NASA); however, the disturbance torques on the platform probably are rather high, particularly the aerodynamic torques, given the low altitude of the flight.

These considerations probably force selecting a gas-jet system rather than a magnetic field torque system. In order to be able to estimate the gas-jet system activity, a rather detailed analysis of the disturbance torques should be done. This in turn can only be done after the mechanical design is completed.

In conclusion, our ACS must include the following subsystems:

a. 3-axis stable platform
b. Star tracker
c. Gas jets
d. Reaction wheels

The entire set of these subsystems is necessary for high-accuracy pointing in a long flight. No additional maneuvering capability is planned at this time: the shuttle will take care of placement in orbit and recovery of the platform.

VIII. SYSTEM POWER REQUIREMENT

This standard platform is designed to support many different experiments, therefore, it is not possible to predict the exact energy requirements for any possible mission. However, it is possible to estimate the energy needed for housekeeping. Here it is in some detail.

ACS	28 W	Continuous
Star Tracker	14 W	Continuous
Reaction Wheels	25 W	Continuous
Tape Recorder	125 W	When Recording
Tape Recorder	0 W	On Standby
On-Board Electronics	25 W	Continuous
Contingency	20 W	Continuous

Total estimated energy for 24 hours, with only 2 hours of recorder operation:

$(28 + 14 + 25 + 25 + 20) \cdot 24 + 125 \cdot 2 = 2938$ Wh = Approx. 3 KWh

Every hour of additional recording requires 125 Wh more.

Notice that the above figures are rather rough estimates of the power requirement. At design time, a revision of these values is imperative. It is clear that it is desirable to reduce as much as possible the power consumption of the continuously running subsystems, even at the expense of some redesign. This point should be considered carefully at final design time.

The suggested type of tape recorder requires power (55W per recorder) applied during STS takeoff and landing. It appears possible to apply this power automatically, using accelerometers to close a time switch.

If these accelerometers are sensitive enough to operate during deployment in orbit and retrieval, no harm is done; only a small amount of electrical energy is lost. A small separate power supply (perhaps Ni-Cd batteries) is required to supply power to the Test Controller. The related energy requirement is very small (at most a few Wh) and poses no problem whatsoever. Another separate, very small power supply may be used to energize the system clock, in order to have a stand-alone time source. A small lithium battery probably will suffice for a very long time (thousands of hours).

IX. SUGGESTED POWER SYSTEM

Different types of energy souces have been considered. Here they are:

a. Lithium Cells - Non-rechargeable, high energy per unit mass (300 Wh/kg).

b. Lead-Acid - Rechargeable, medium energy per unit mass (40 Wh/kg).

c. Nickel-Cadmium - Rechargeable, medium energy per unit mass (40 Wh/kg).

d. Solar Cells - Virtually unlimited energy, low or moderate power levels. Rather complicated mechanical installation.

e. Fuel Cells - Possible weight advantage over rechargeable batteries. Expensive and critical in operation.

f. Silver-Cadmium and Silver-Zinc Cells - Rechargeable, high energy per unit mass (up to 160 Wh/Kg). Data from two manufacturers (Yardney and Eagle-Picher) indicate that they are available packaged as batteries, rated for space flight.

Since the total energy needed per each mission is relatively limited, solar cells and fuel cells may be ruled out, considering their mechanical complication and high cost. It is practical to expand the technique used in many sounding rockets, that is to use rechargeable batteries as power source.

Rechargeable batteries, compared with non-rechargeable ones, offer the advantage of allowing repeated tests of the entire system (platform plus experiment) before launch, without replacement of the batteries themselves. Their use is considered the best choice for our application.

It appears that the weight advantage of the Silver-Zinc cells dictates the use of this type of power source, when compared with the various different possible alternatives. Silver-Zinc cells develop a limited amount of gas (H_2 and O_2) during discharge; therefore, they are vented, but the battery container may be sealed. Venting space has to be provided inside the battery container, and a safety vent is installed on the container itself to protect it in case of abnormal development of gas. A manufacturer (Eagle-Picher) claims that it has succeeded in eliminating the hydrogen accumulation in a sealed battery container by having the hydrogen used up and converted into water by a nickel-hydrogen cell located inside the same sealed container. This technique or some equivalent one is highly desirable, in order to reduce the chance of hydrogen-oxygen explosions.

The energy density value of 160 Wh/Kg has been used in the following estimates. This value refers only to the cell mass (without container).

Applying the above indicated energy figures it results that 24 hours of operation, including 2 hours of recording, require a cell mass of approximately 19 Kg (41 lbs) plus an additional 0.8 Kg (1.75 lbs) for each hour of additional recording.

The estimated total mass for a 7-day mission, with a total of 14 hours of recording is approximately 129 Kg (285 lbs). The mass of the battery sealed container has to be added to this figure.

Notice again that this estimate does not include energy for the experiments.

X. SOME MECHANICAL DETAILS

The mechanical configuration of our platform is extremely important for many obvious reasons. Here are a few:

1. STS Compatibility - Our platform must be loaded into the STS payload bay, then deployed in orbit and later retrieved from orbit. After landing of the STS, our platform must be removed easily from the STS payload bay. Orbital deployment and retrieval require the existence of a mechanical grapple fixture to be utilized by the Remote Manipulator System of the STS. A support pallet attached to and remaining in the STS payload bay is very likely necessary.

2. Environmental Control - Pressurization must be supplied to the tape recorders and possibly to the electronic circuits. Temperature control is necessary for the tape recorders and the batteries and possibly also for the electronic circuits. A form of temperature control, active or passive, is needed. It seems at this point that passive temperature control may be realized by enclosing the whole platform into a thermally conducting shell, painted on the outside with an appropriate white/black pattern and properly insulated on the inside. The scientific instruments may be located in a compartment open to space and separate from the support equipment compartment.

3. Easy Accessibility - It is highly desirable to be able to replace defective units even a short time before take-off. This point does not lead to any preferred configuration, but must be kept in mind at every stage of the final design.

4. Testing - Attention should be given to laboratory testing of the entire unit. A specially designed mechanical support system should be available for extensive dynamic testing of the entire platform and particularly its ACS, offering three-axis freedom of motion without (or almost without) friction. A good dynamic test program for the platform should simulate all the events that it will see in a single flight; therefore, this test system should be capable of operating for up to 7 days without interruption. The platform test mode and its operational mode should be activated, the ACS should work, the recorders activated, etc.

XI. PROPOSED SEQUENCE OF EVENTS IN A FLIGHT

1. Platform is tested extensively on ground after installation into STS.

2. During STS takeoff recorders are automatically energized in STOP mode. Accelerometers determine the exact turn-on and turn-off instants. No crew action is required.

3. When STS is in orbit, its crew does the following:

a. By radio link closes switch 1 for system test. Platform responds YES or NO.

b. After YES response, crew releases mechanical latch, then by Remote Manipulator deploys platform in orbit.

c. When platform is released and off Remote Manipulator, crew by radio link closes switch 2, starting experiment.

4. The retrieval from orbit is done as follows:

a. By radio link, STS crew closes switch 3 turning off all systems and discharging residual ACS gas.

b. By Remote Manipulator, crew retrieves platform and secures it on pallet.

c. Pallet mechanical latch is automatically or manually latched.

5. Power is automatically supplied to recorders in STOP mode, for reentry and landing. No crew action required.

XII. TEST AND EXPERIMENT MODES

It is possible at this point to draw simple block diagrams of the automatic test and experiment modes of operation. Fig. 1, 2, and 3 show these block diagrams.

The Test Mode is activated by means of a remotely controlled switch which resets and starts the Test Controller. This mode is available for repeated tests. A diagnostic message for each tested unit will be issued, as a debugging help for ground tests. The same Test Mode will provide the STS operator with a YES or NO message. Eventually, after observing the YES message, the STS operator will deploy the platform in orbit and then initiate the Experiment Mode by remotely closing a separate switch. The Test Mode operation is planned as follows:

a. Software issues sequentially to port 0 different test codes, in order to activate test mode in each unit to be tested. Appropriate time delays are provided.

b. Hardware decoder activates test mode in unit corresponding to test code.

c. Each unit performs test, then issues response to corresponding port.

d. Test Controller reads all unit ports, stores their contents and then issues a diagnostic message for each unit.

e. After step d, Test Controller executes another check on stored inputs and issues a YES or NO message.

f. Test Controller halts, and it is ready to be reset and restarted. unless the Experiment Mode is activated.

The Experiment Mode is activated by a separate remotely controlled switch. A sequencer turns on the various units and the experiments at the appropriate times. A clock is designed into the system and its output is used to give a reference to the sequencer and to the recorders.

XIII. RECOMMENDATIONS

Increased effort in continuing the development of our Space Platform is in order, since the STS is now entering its routine operations. Economy of operation and possibility of long experiments in space will probably dictate the use of this platform or of a similar device.

The entire development effort should follow the outline here given:

Preliminary Study Concepts
Feasibility Study
Procurement
Preliminary Design
NASA Interface
Shuttle Integration
Design Review
Technical Design Review
Freeze
Fabricate
Integrate and Test
Readiness Review

This paper reports the Preliminary Study concepts and begins to develop the Feasibility Study. The remaining steps should be executed in order to arrive at a working model in a reasonable time, perhaps as soon as 1985.

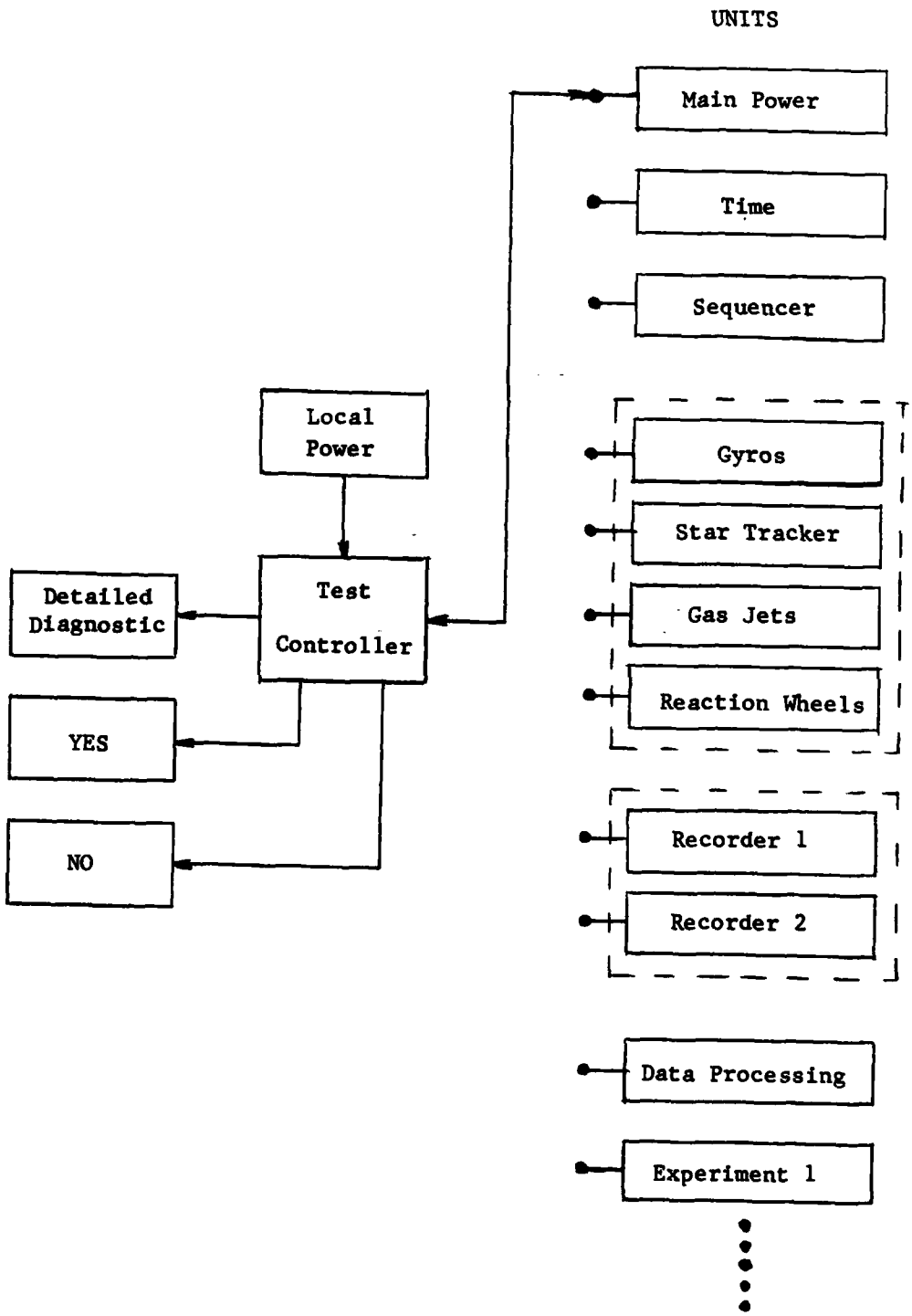


FIGURE 1. TEST MODE BLOCK DIAGRAM

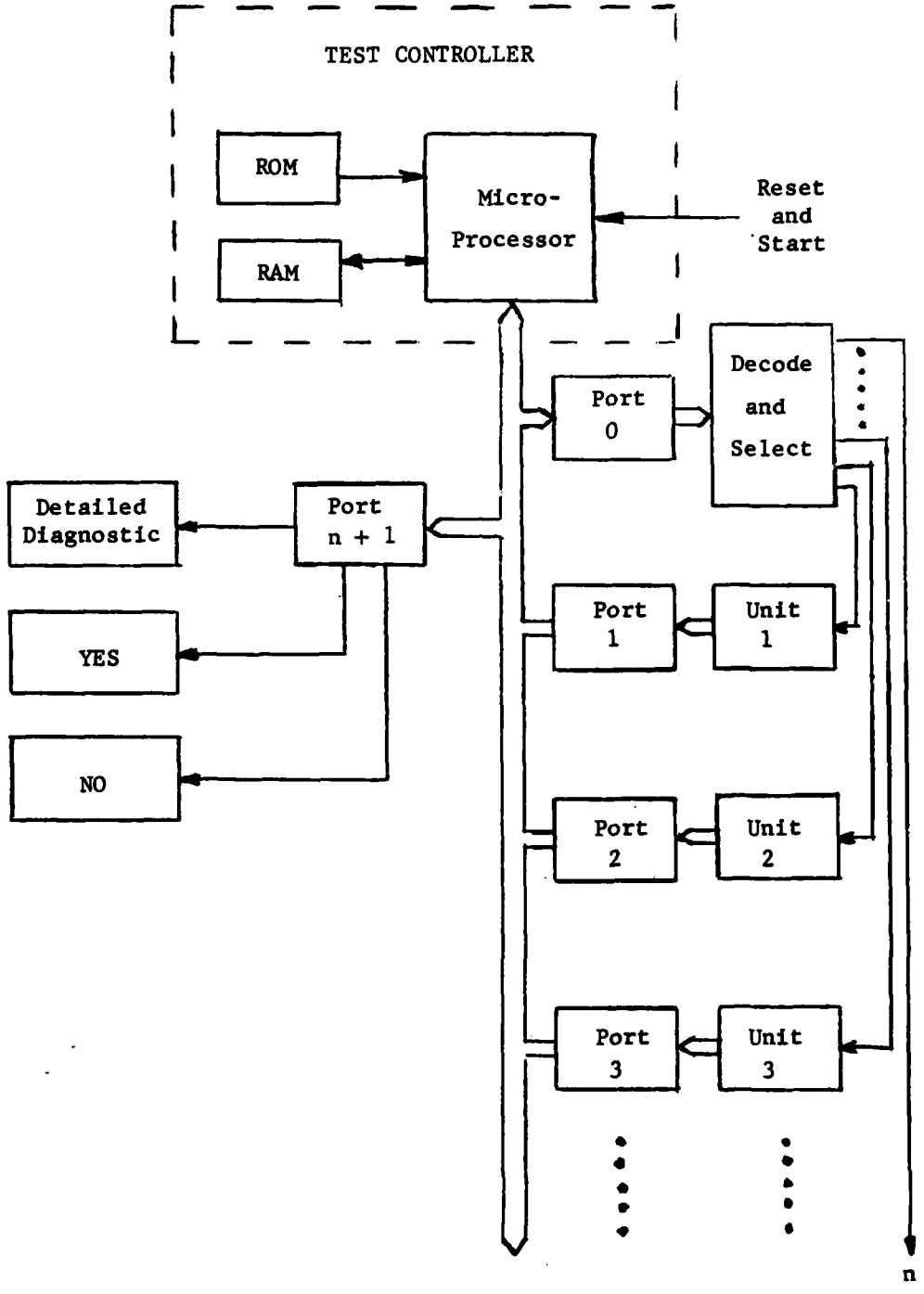


FIGURE 2. DETAILED HANDSHAKING TEST MODE

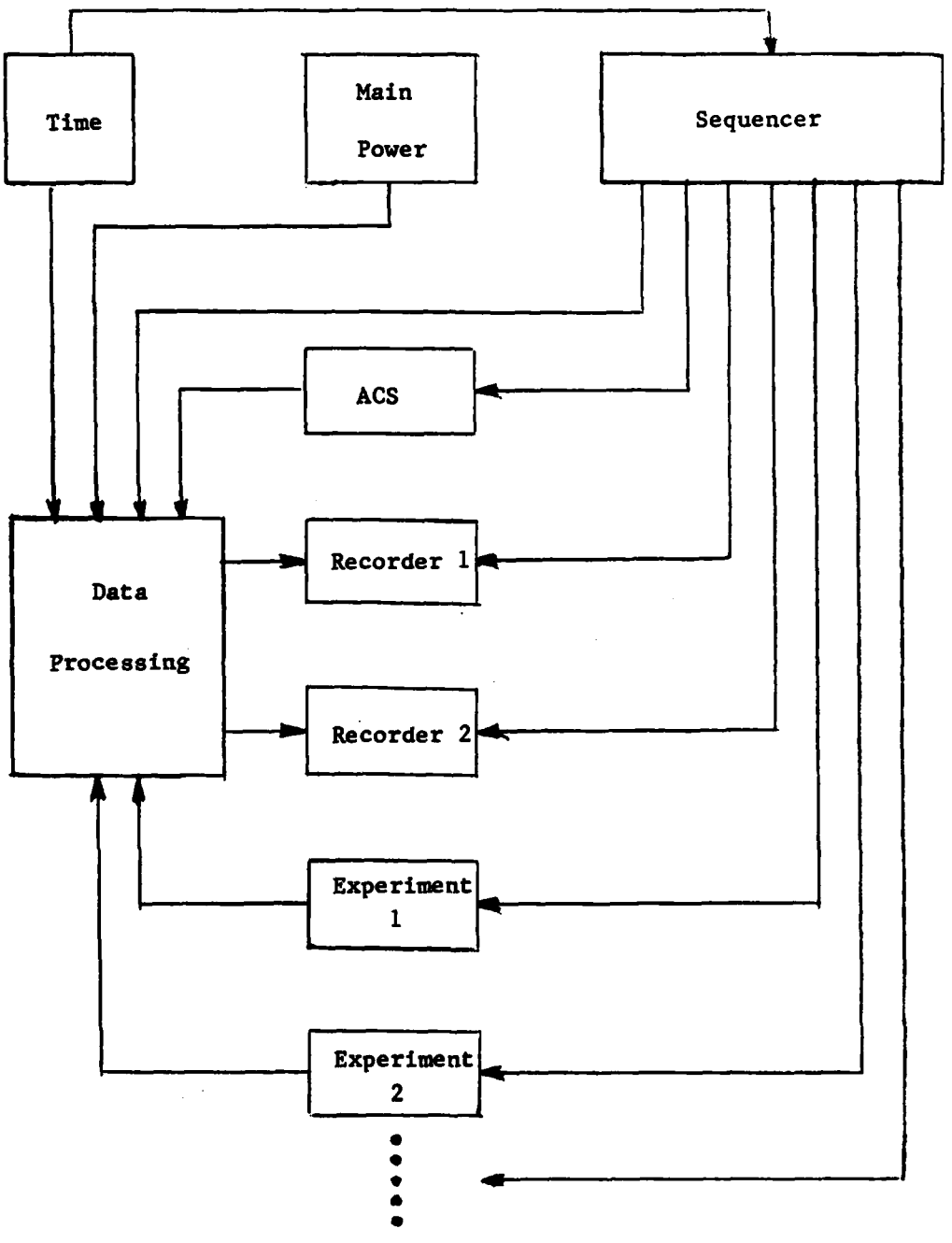


FIGURE 3. EXPERIMENT MODE BLOCK DIAGRAM

REFERENCES

1. Shrewsberry, D.J. and Olney, D.J., "Development of an Experiment of Opportunity Test Payload for the Space Transportation System," Seventeenth Space Congress, Cocoa Beach, Florida, May 1, 1980.

2. Muhlfelder, L., "Developments in Attitude Control Systems at Astro-Electronics," RCA Technical Communications, pp. 81-90, 1978.

3. Modern Instrumentation Tape Recording: An Engineering Handbook, EMI Technology, Inc., 1979.

4. Space Transportation System User Handbook, NASA, June 1977.
5. Ott, E.J., "The Get Away Special Program," AIAA 5th Sounding Rocket Technology Conference, March 7-9, 1979.

6. Hudgins, J.I., "An Autonomous Payload Controller for the Space Shuttle," AIAA 5th Sounding Rocket Technology Conference, March 7-9, 1979.

7. Ritz, W.F. and Whitsett, C.E., "A Detached Experiment Carrier Aids Adaptation of Experiments from Sounding Rockets to Space Shuttle," AIAA 5th Sounding Rocket Technology Conference, March 7-9, 1979.

8. Olney, D.J. and Cruddace, R.G., "Free-Flying Shuttle Payloads, an Extrapolation of Sounding Rocketry into the Shuttle Era," AIAA 5th Sounding Rocket Technology Conference, March 7-9, 1979.

9. Windsor, R.M., "Adaptation of Solar Sounding Rocket Payloads for Shuttle," AIAA 5th Sounding Rocket Technology Conference, March 7-9, 1979.

10. Roberson, R.E. and Farrior, J.S. (editors), Guidance and Control, Academic Press, New York, NY, 1962.

11. Cannon, R.H., Jr., "Gyroscopic Coupling in Space Vehicle Attitude Control Systems", Joint Automatic Control Conference, Boulder, CO, June 1961, and J. of Basic Engineering, pp. 41-53, March 1962.

1982 USAF-SCEEE SUMMER FACULTY RESEARCH PROGRAM

and

1982 USAF-SCEEE GRADUATE STUDENT SUMMER SUPPORT PROGRAM

Sponsored by the

AIR FORCE OFFICE OF SCIENTIFIC RESEARCH

Conducted by the

SOUTHEASTERN CENTER FOR ELECTRICAL ENGINEERING EDUCATION

FINAL REPORT

TRIALS AND TRIBULATIONS AT THE HELMET MOUNTED OCULOMOTOR FACILITY

Prepared by:	A. Terry Bahill & Jeffrey S. Kallman
Academic Rank:	Associate Professor & Graduate Student
Academic Department:	Electrical Engineering
University:	Carnegie-Mellon University Pittsburgh, PA 15213
Research Location:	Air Force Aerospace Medical Research Laboratory, Human Engineering Division Wright-Patterson AFB, Ohio
USAF Research Contact:	Dr. Ken Boff

Date:	August 27, 1982
Contract No:	F49620-82-C-0035

TRIALS AND TRIBULATIONS AT THE HELMET MOUNTED OCULOMOTOR FACILITY

by

A. Terry Bahill & Jeffrey S. Kallman

ABSTRACT

We spent most of the summer debugging the Helmet Mounted Oculometer Facility (HMOF) equipment. On our last day we were finally able to gather data on human head and eye coordination. We brought this data back to Carnegie-Mellon University; we were able to put it on our computer system and analyze it with our programs.

Acknowledgement

We thank the Air Force Office of Scientific Research and the Southeastern Center for Electrical Engineering for providing us with the opportunity to spend the summer at Wright-Patterson AFB and Yellow Springs, Ohio. We thank the many people from SRL who helped us and Dena Brooks for processing our letters and reports. Tom Furness's support and Ken Boff's enthusiam were appreciated. We are also grateful to Mike Haas for his efforts at making the oculometer work so that we could collect our data.

I. INTRODUCTION

At the beginning of the summer I stated that my objectives were

1 To present seminars to the Wright-Patterson AFB community. I presented the five seminars listed in Appendix A. The average attendance was 20.

2 To learn to use the Helmet Mounted Oculometer Facility (HMOF). The proceedures of operation that I wrote are included in Appendix B.

3 To record human head and eye movement data under a variety of target movement conditions. We have filled up a computer disk with data. It is presently in my Laboratory at Carnegie-Mellon University. I will analyze this data during the period of my minigrant.

The following narative written by Jeffrey S. Kallman summarizes our activity directly related to the Helment Mounted Oculometer Facility (HMOF).

The virtual cockpit is an idea that has existed for many years. In essence, the idea is to present a processed view of the world to a pilot. This view presents information to the pilot in the most usable form possible. Threats are emphasised, HUD information is available, displays can be task dependent, etc.. Unfortunatly, until recently, the technology and basic science needed to develop such a virtual cockpit was nonexistant. Not any longer. Currently, investigations are being made into artificial intelligence systems for threat evaluation, experiments are being performed in optimal display symbologys, and many other pieces of the virtual cockpit idea are being worked on.

One major piece of the virtual cockpit is the display system. Image

generation and display are among the most computer intensive tasks of the virtual cockpit. To use the virtual cockpit efficiently and, with present computer speeds, effectively, requires a minimization of image generation and display. The computers should only work on the virtual areas that the pilot is looking at.

Determining where a pilot is looking is an involved process. The direction of the eye in the head must be determined and the position and orientation of the head in space must also be determined. Given these, it is possible to determine where a person is looking, but in the case of a pilot, there are additional factors that must be taken into account. Neither the oculometer (device for determining eye direction in the head) or the sight (device for determining head position and orientation) can be either intrusive or obtrusive. This presents difficulties.

Occulometer and sight systems exist that are neither unacceptably intrusive or obtrusive. One such system is the Honeywell Helmet Mounted Occulometer and Sight (HMOS). The HMOS was delivered to the AFAMRL/HEA Helmet Mounted Occulometer Facility (HMOF) in November 1981. Unfortunatly, the HMOS was still not fully integrated into the HMOF in June 1982. In addition, the HMOS's performance characteristics were an unknown factor.

II. HMOF

This discussion of the Helmet Mounted Occulometer Facility comes in three parts: the hardware, the software, and the operation of the system.

Hardware

HMOF hardware can measure, record, and (if desired) can act upon the position and orientation of the human head and eyes. It has five main parts:

a helmet mounted oculometer (HMO), a helmet mounted sight (HMS), a Data General Eclipse minicomputer, a Network Systems HYPERchannel adapter, and a DEC PDP-11/34. This is a large, expensive and complex system.

The HMS provides a TV image of the subject's right eye illuminated by infrared light. The oculometer consists of an infrared light source, a CCD television camera, and associated optics. The light source is directed at the eye via beamsplitters and an infrared mirror. The TV camera sees the infrared light reflected from the eye. Ideally there are only two sources of infrared reflection from the eye: the corneal reflex and the bright pupil. The corneal reflex is the reflection of a bright light source off of the front surface of the cornea. The bright pupil is the effect caused by light entering the eye, bouncing off the retina and reemerging from the eye, lighting up the pupil. The corneal reflex and the bright pupil are picked up by the TV camera and then passed to the Eclipse computer.

The HMS provides head position and orientation data to the Eclipse. It works by using a transmitter to set up a magnetic field in the area the helmet will occupy. A receiver in the helmet senses the magnetic field and determines where the head is and how it is oriented.

The Eclipse computer collects the TV images from the HMO and the head position and orientation data from the HMS, computes direction of gaze, and sends it all to the HYPERchannel. The TV images are first processed to generate eye position (angular) in the helmet reference frame. Then eye position is 'added' to the head position and orientation to yield gaze angle (in universal coordinates). Finally, the Eclipse send all of the data and the results of its computations to the HYPERchannel.

The HYPERchannel allows the transfer of data from the Eclipse

minicomputer to the PDP-11/34 minicomputer. It is questionable whether this piece of equipment has helped or hindered the development of the HMOS facility.

The PDP-11/34 minicomputer is used for a variety of purposes in the HMOF. The PDP-11/34 generates targets, drives the target display system, takes data from the HYPERchannel adapter, and formats and stores the data on disk.

Software

This section of the report will cover the software that we either developed or helped to develop. All of our programs were written on the PDP-11/34. The Eclipse minicomputer was programmed by Honeywell and the HYPERchannel was programmed by its manufacturer. In the course of the work at the HMOF several programs were written for the 11/34. These programs were written for a variety of purposes: target generation, target presentation, data collection, error calculation, and demonstration. The programs were written in FORTRAN and assembly language. Some of the programs were designed to stand alone, while others were designed to fit into existing software. I'll discuss the programs that stand alone first.

DEMO

The demonstration program DEMO stands alone. It outputs a series of two dimensional target waveforms to a target generator (in our case, either an x-y scope or mirrors deflecting a laser beam). The targets presented are: a horizontal sinusoid, horizontal parabolic sections, horizontal cubic sections, circles, horizontal parabolic sections vs vertical sinusoids, and horizontal cubic sections vs vertical sinusoids. DEMO is a static program. Each time it is run, the same targets are presented at the same speed, and in the same order. The ordering, speed, and targets presented are the responsibility of

the FORTRAN part of the program. Acting on the ordering, speed, and target is the responsibility of the assembly language part of the program. The assembly langage subroutine accepts the number of ten thousands of a second between target updates as an argument. The subroutine takes the target from a buffer in a FORTRAN common block filled by the FORTRAN part of DEMO. As the FORTRAN program has no interaction with the outside world, the program is static.

TARGET

TARGET is a more dynamic stand alone program for horizontal target generation and display. It allows the user to pick up to thirty targets for display from a menu of five waveforms. In addition to waveform, the user also picks target frequency and duration. After the user's targets are displayed, the program allow the user to specify a new set of target waveforms.

The five waveforms are generated and stored in buffers when the FORTRAN part of TARGET is first started up. The program then asks the user to generate a target by picking waveforms, frequencies, and durations. After the target generation is finished, the target is displayed. The assembly language display subroutines are different from the single display routine in DEMO. Whereas in DEMO the display routine's buffers had to be refilled with each change in waveform, TARGET assigns one subroutine to each buffer, and has the buffers prefilled. Thus, while DEMO has delays between output of waveforms, TARGET displays waveforms continuously.

TARTTB

TARTTB is a flexible stand alone program for horizontal and vertical target generation and display. It is similar to TARGET in that it allows the user to specify the target, and it is similar to DEMO in that between displays of the target waveform it has to refill the display buffers. TARTTB is the

last of the stand alone programs.

SSCAN

SSCAN was designed to fit into the existing data collection program COLECT (sic). COLECT is the program that run on the PDP-11/34 which is responsible for collecting data from the HYPERchannel adapter, formatting it, and storing it on disk. SSCAN allows the user of COLECT to read the analog to digital (A/D) converters in the PDP-11/34. The user can select the number of A/D converter channels that are to be read.

MSE

MSE is a group of subroutines that fits into COLECT which computes and displays a short term mean square error of the form

$$mse = \frac{1}{T} \int_{t-T}^{t} (e_{EL}^2 + e_{AZ}^2)dt \qquad (1)$$

where t is time, T is a period of time, e_{EL} is elevation error, e_{AZ} is azimuth error, and mse is mean square error. There are three parts to MSE: MSESET which sets things up, MISER which computes mse, and MSEOUT which outputs the mse.

HMOF Operation

By far the most difficult part of using the HMOF is operating the HMOS. The HMOS operation proceedures are also the most difficult to describe. As a good description of the operating proceedures for the HMOS part of HMOF has been written by Dr. A. T. Bahill; they are included in Appendix B.

III. HMOS Evaluation

One of the most HMOS dependent developments in the virtual cockpit concept is the generic switch. Basically, the generic switch is a single switch on the stick that can represent any of a number of switches in the cockpit. In use, the generic switch represents which ever switch the pilot is currently looking at. The usefulness of the generic switch is dependent upon three HMOS parameters: resolution, drift, and noise. The resolution is the minimum angular separation that the HMOS can distinguish. In terms of the generic switch, this tells how far apart the switches the generic switch can represent must be. Drift is a measure of how incorrect HMOS determination of gaze can become over time. If the HMOS has a large drift, looking at a the same cockpit switch may not mean the same thing after an hour (i.e. the pilot looks at the radar switch, and the generic switch fires a rocket). Noise acts to degrade HMOS resolution. If the resolution of the HMOS allows switches to be separated by as little as three degrees of solid angle, but there is a jitter of five degrees, the generic switch will represent unexpected things at inconvenient times.

It turned out that we were unable to determine any of the aformentioned parameters. Because the HMOF was unable to collect and store data for ninty-nine percent of our time at WPAFB/AFAMRL-HEA, we collected approximately ten seconds of usable data. This allowed us to determine only one HMOS operating parameter; the noise in the HMOF system. This noise is large. Calculations based on the raw gaze angle data (see figure 1) yield mean square errors of 32.08 deg^2. When the data is filtered (as in figure 2) mean square error is 27.01 deg^2. Of our own experience in the Neurological Control Systems Laboratory (NCSL) at Carnegie-Mellon University in Pittsburgh, we know that people are capable of tracking with mean squared errors of less than 0.2 deg^2.

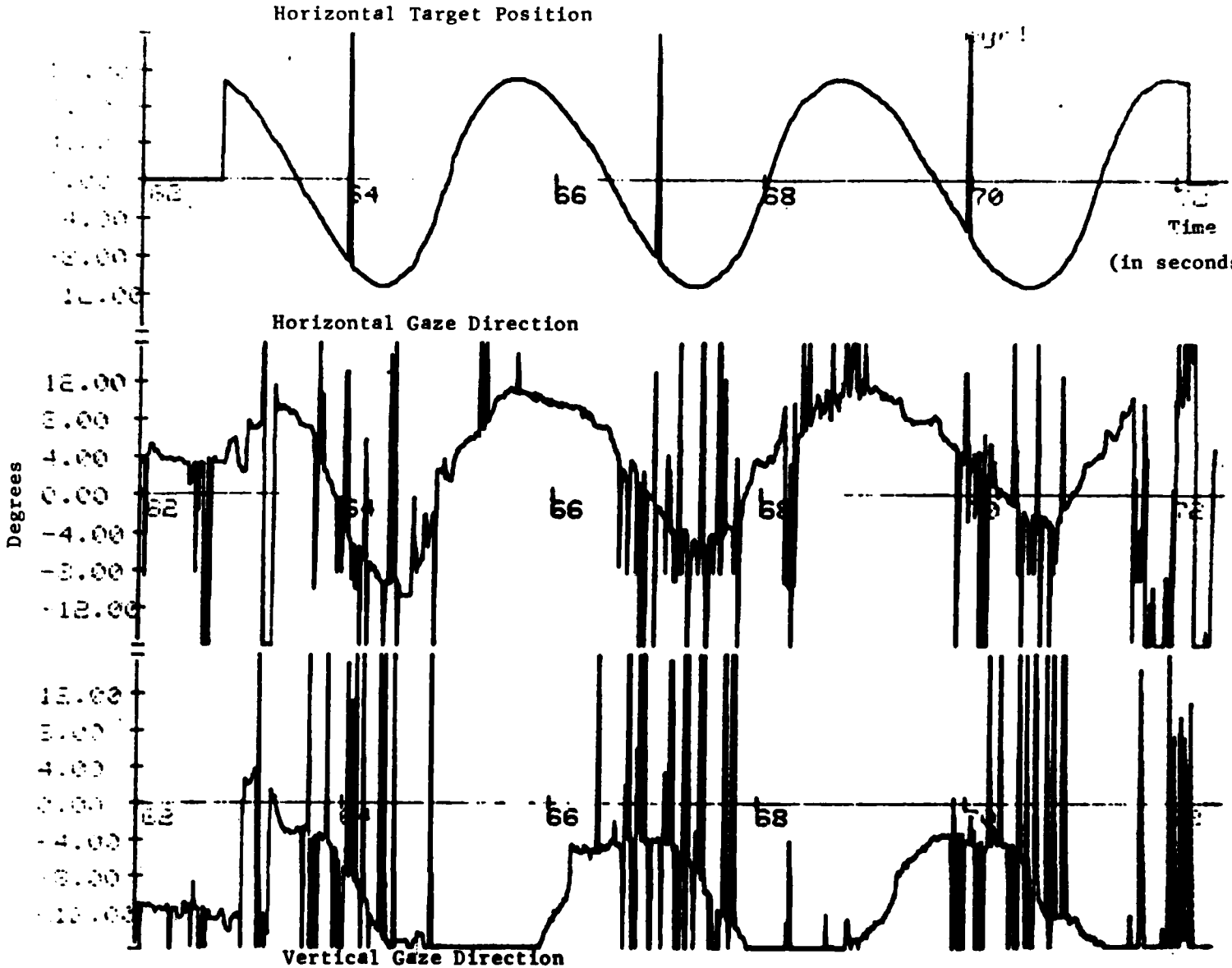
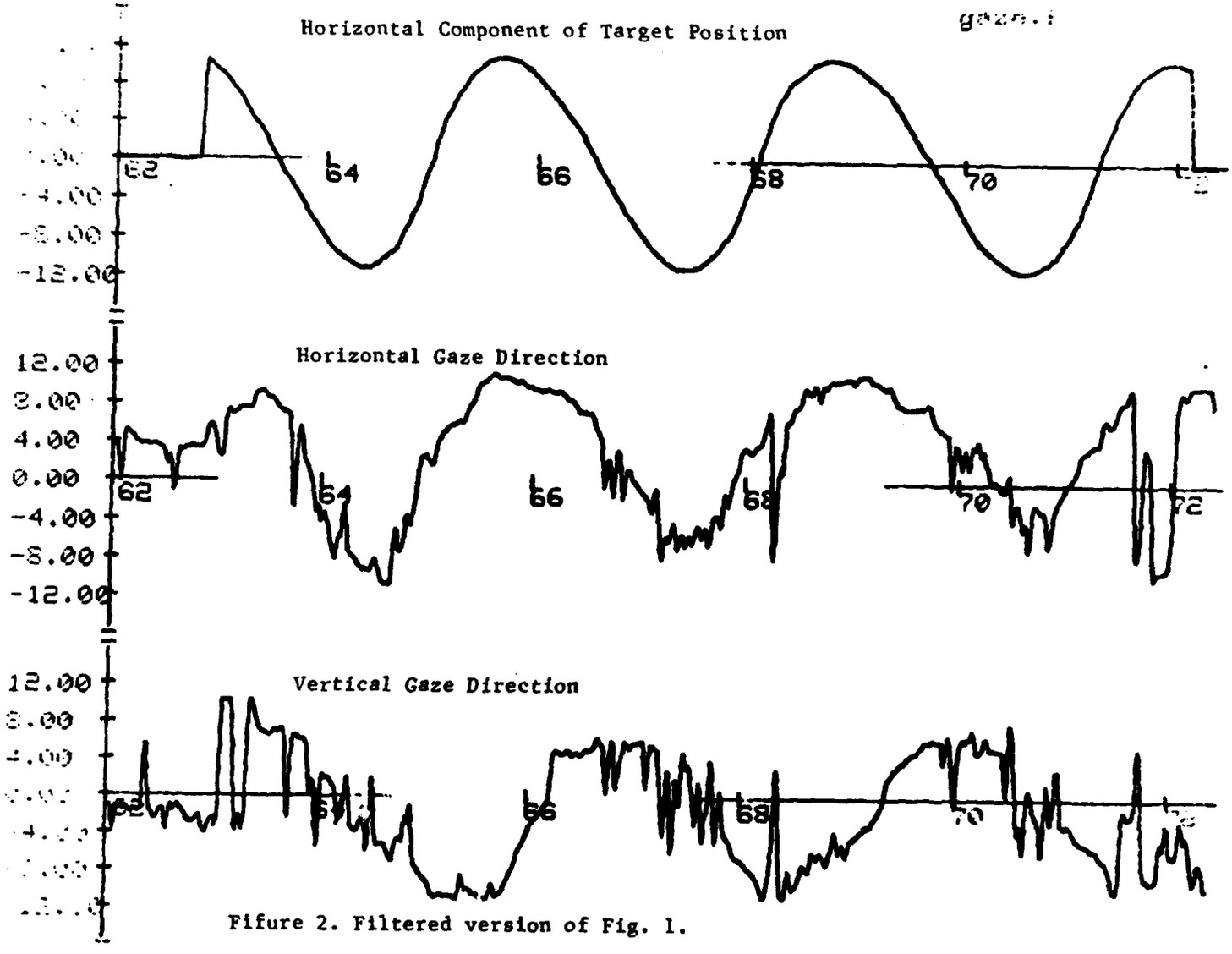


Figure 1. Target and Gaze directions as a subject tracked a target moving in a circle. Raw data.



Fifure 2. Filtered version of Fig. 1.

IV. Experiments Performed With HMOF.

As mentioned in the previous section, during 99% of the time we had at the HMOF we were unable to collect and store data. This severely cramped our style. We have ten seconds of usable data. This data needed to be processed a great deal to become usable (as figures 1 and 2, data before and after filtering, attest).

The filtering was done in two stages. The first stage of the filtering was performed when the data was transformed from the HMOF format to NCSL format. During the conversion, any data that passed a size threshold was dealt with by inserting in its place the value of the previous data point. The filtering was completed by running a simple digital lowpass filter over the NCSL format data.

Analysis of the data was performed using the Carnegie-Mellon University NCSL analysis programs ANA and SPA. ANA provided the graphic output of figures 1 and 2, and SPA provided the mean squared error numbers.

V. Summary and Conclusions

There is not a whole lot that we can say about the capabilities of the HMOF or the results of our head and eye coordination experiments. The HMOF's inoperability made it impossible to get data with which to work. In the the last four hours at HMOF we were able to get ten seconds of usable data. Even so, this snippet of data shows some of the possibilities inherent in a Helmet Mounted Occulometer Facility. As far as we know, there is no other facility where gaze can be monitored with as free a head with the types of targets we've used.

Appendix A

Seminars of Dr. A. Terry Bahill

ALL YOU EVER WANTED TO KNOW ABOUT EYE MOVEMENTS BUT WERE AFRAID TO ASK

by

A. Terry Bahill
Associate Professor of Electrical
and Biomedical Engineering
Carnegie-Mellon University

Building 33 Vault - 1330-1445

THURSDAY, JUNE 24, 1982

FOUR TYPES OF EYE MOVEMENTS

A general discussion of the saccadic, smooth pursuit, vergence and vestibulo-ocular eye movement control systems. We will discuss anatomical, dynamic and behavioral differences and the interactions between these systems.

****

TUESDAY, JULY 6, 1982

THE SACCADIC EYE MOVEMENT SYSTEM

A lecture based on the Scientific American paper by Bahill & Stark, January 1979.

Two tools, the main sequence diagrams and the reciprocal innervation model, will be used to explain the origin of dynamic overshoot, glissades, overlapping saccades and the curvature of oblique saccades.

****

THURSDAY, JULY 8, 1982

ZERO-LATENCY TRACKING OF PREDICTABLE TARGET WAVEFORMS BY THE HUMAN SMOOTH PURSUIT EYE MOVEMENT SYSTEM

This exciting lecture will show that the human can overcome an inherent time delay and track targets with no latency. An engineering model is developed that can do the same. Tracking of baseball players will also be shown.

****

THURSDAY, JULY 15, 1982

HEAD AND EYE MOVEMENTS WHILE WALKING

A human with a head rest and bite bar can track a target with a mean square error (mse) of 0.05 deg^2. As more freedom of movement is given to the subject the mse increases to 0.5 deg^2 for a subject standing with free head, and to 1.0 deg^2 for a subject who is walking.

****

THURSDAY, JULY 22, 1982

ADVANTAGES AND LIMITATIONS OF THE TWO-POINT CENTRAL DIFFERENCE DERIVATIVE ALGORITHM

This mathematical lecture will show the frequency limitations of this algorithm and it will show how noise and accuracy of the data influence the choice of the optimal sampling rate.

****

PLEASE RESERVE SPACE EARLY - CALL DR. KENNETH BOFF ON EXT. 54820/54693

****

Appendix B

The HMOS Aids of Dr. A. Terry Bahill

HMOS OPERATING PROCEDURES

by A. Terry Bahill

July 1982

Based on Sections 4.2 to 4.4, Volume III of Honeywell's HMOS system manual

4.2 Power-Up

1. Turn on circuit breakers #3 and #30 on Circuit Panel CPP-1.

2. Turn on power to instruments. There are 4 power switches: the CRT, the Eclipse, the Link tape, and the Electrohome panel (the Remote Electronics PWR switch and the Remote Electronics Breaker that turn the lamp on will be discussed later).

3. Mount the Linc Tape on the tape drive. Thread the tape through the tape head and put on adjacent spindle. Alternate between LOAD and REWIND positions on switch so that the tape load mark (the one-inch long silver strip) is to the right of the tape head. You may have to press the LOAD switch momentarily so that the tape is tensioned.

4. On the Eclipse front panel, depress the left most switch to the STOP position then raise to the RESET position. Set switches 10, 11, 12, and 13 to up position. Momentarily raise PR LOAD switch. After a short time delay, the computer will type -EXEC? on the CRT. If computer power has just been turned on, press Alpha lock key on CRT terminal. Now tell the computer which program you want to run, e.g. "HMOS", "TERRY", or "JEFF" as shown in the following line. Underlined items are things you type. Your response should be followed by a carriage return (CR).

EXEC? HMOS (CR)

When the tape stops spinning, you will be talking to the debugger. In many of the following examples you will be asked to press the ESC key on the CRT terminal. This key will be indicated as (ESC). Set the computer to decimal mode by typing:

(ESC)N 00000 1 (CR)
or, depending upon the computer's mode, perhaps
(ESC)N +1.1 (CR)

Set lamp brightness with

EGR4+22/-xxx.-yyy. (CR)

where -xxx. represents the old brightness level and -yyy. represents the new brightness level. The brightest possible value is -512. and the dimmest possible value is -0. A good range is -100. to -150.

Raise switches 0, 1, and 14 on the Eclipse front panel to their up positions, (lower switches 10, 11, 12, and 13 if they are still up). Start software with

RUN(ESC)R

(The first time you start the program HMOS you will have to type ZZZZ(ESC)R rather than RUN(ESC)R.)

You may verify that the software is working by observing that the ION light on the Eclipse is ON and that the tracking bars on the video screen are at the bottom and at the right side.

Turn on Remote Electronics breaker on video monitor panel. Push Remote Electronics PWR button to turn on lamp power. (If you did something wrong, the red overbrightness LED on the back of the HMOS control box may be on and it may be necessary to reset the adjacent circuit breaker.)

If at any time you wish to interrupt the program and get back to the debugger (BIDEB), raise, then lower switch 15 on the Eclipse. For example, to change bulb brightness, raise, then lower switch 15 and type

EGR4+22/-xxx.-yyy. (CR)

where -xxx. is the old brightness and -yyy. is the new brightness. Then type

RUN(ESC)R

4.4.1 Linearization

To determine the size and shape of each subject's eye, run the linearization program that collects data from 51 fixation points. Raise switch 12 on the Eclipse. The computer will tell you where the subject or artificial eye should be looking in terms of the coordinates described in the figure in Appendix D.

When the "eye" is at the correct location and the video monitor shows that it is locked on, raise switch 8. The machine will now take data. After 5 or 10 seconds check to see if it has taken enough data by lowering switch 8. If it is happy, it will now ask for the eye to be aimed at the next point, otherwise it will say nothing and you should return switch 8 to the raised position. If after 30 seconds of data taking, it still has not received a preset number of successive good fields of data it will give up, label the point BAD, and instruct you to proceed to the next point. If the computer will not give up, then you should move the eye slightly until tracking gate bars become stationary. At the end of the first pass, the computer will initiate a second pass where it tries to get data for all of the BAD points. The computer will ask you to aim the eye at the designated point; when this is completed, raise switch 8 as before. When it is through, it will rapidly list out a bunch of numbers.

To speed up the linearization data collection, you may want to force it to accept noisy data, by reducing the number of times the fixation data is averaged and by increasing the maximum acceptable variance. To accomplish this, enter the debugger, and type

FIXTST+441/+10. 3. (CR)

VARLMT+4/+1000. 32700. (CR)

VARLMT+5/+9000. 32700 (CR)

(Caution: Turning on the oscilloscope [or some other piece of equipment] may cause the program to quit.)

4.4.2 Calibration

Linearization is done only once for each subject. Calibration is done at the start of each run for each subject. To collect the calibration data, raise switch 13 and follow the computer's directions. Calibration only uses 7 fixation points and there is no second pass - if you blow a single point, do the entire calibration over again.

Creating a Version of HMOS Containing Linearization Data
by A. Terry Bahill
July 1982

1. To make room on the tape, you will probably have to delete some file using RUBOUT, SQUASH and TAPES.

2. Run HMOS and collect linearization data.

3. Enter debugger by momentarily raising switch 15 on Eclipse switch register.

4. On Eclipse front panel momentarily depress switch to STOP position, then momentarily raise it to RESET position. Set switches to 077377 and push "START" switch. LTOS should now be running, check to verify that LTOS prompt (EXEC?) is written on the TTY.

5. Put core image of HMOS into temporary file as follows:

```
EXEC-? SAVE
Filename TEMP, Ø
Addresses Ø, 74377, 44751
```

The above numbers represent the starting address and ending address of memory and the starting address of the program. This process takes approximately 3 minutes.

6. Run the program TAPES

7. Mak room on the tape by running RUBOUT, SQUASH and TAPES.

8. Run QSAVE as shown below.

```
EXEC-? QSAVE
Input file: TEMP
Output file: ARTEYE, Ø
```

This process takes approximately 10 minutes.

9. Run TAPES.

10. RUBOUT TEMP. Run the programs SQUASH and TAPES

11. The file ARTEYE can now be run just like HMOS. It contains linearization data.

12. If the file is valuable, you should make a backup copy using MOVER.

Collecting Data
by A. Terry Bahill
August 1982

1. Turn off room lights.

2. Turn on HMS power supplies (on the rear table).

3. Turn on PDP 11/34 computer and boot it.

4. Turn on Network Adapter (on the table) by pushing PWR switch on front panel.

5. Clear Network Adapter by pushing red M.C. button behind locked door on rear panel.

6. Have subject don helmet and sit in seat.

7. Turn on HMS (switch is on small 4x4x2 inch box).

8. Turn on circuit breaker #4 if laser is to be used. Do not let laser beam shine in your eyes.

9. Turn on HMOS equipment and run HMOS software as described on previous pages (keep switches 0, 1 and 14 up).

10. Run 7-point calibration routine.

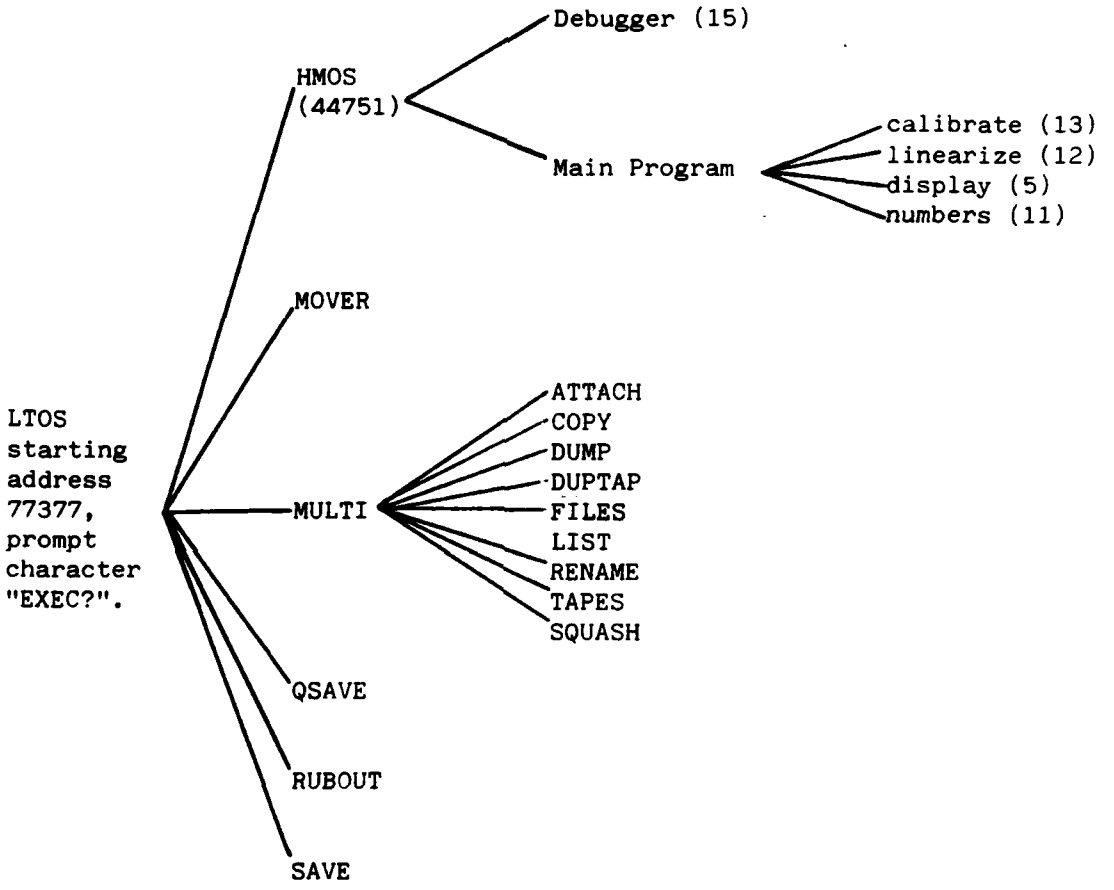
11. Run collect program on 11/34. (Type RUN COLECT.)

12. Lower switch 1 on Eclipse front panel.

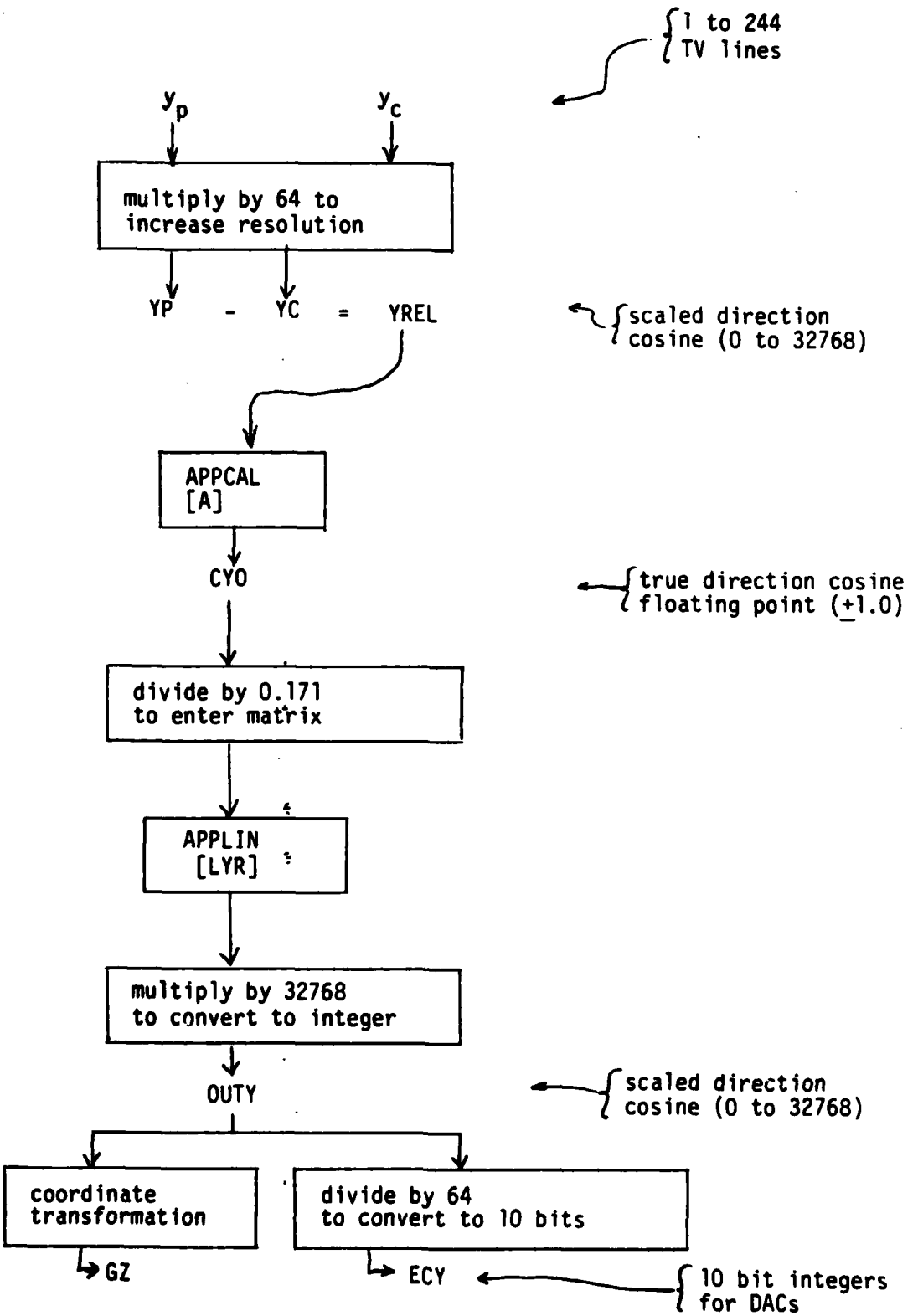
13. Lower switch 0 on Eclipse.

Bahill
6-30-82

HMOS PROGRAMS AND OPTIONS



Bahill
July 19



Appendix C

A History Of HMOF From June 1982 To September 1982

by J. S. Kallman

How do you solve a problem involving multiple computer interactions when you aren't familiar with two of the three computers comprising the system? With great difficulty. With ten weeks of great difficulty.

Step 1: Learn about the computers.
Step 2: Learn about the software running on the computers.
Step 3: Deduce the problem from data provided by altering software.

Debugging operations started with the Eclipse computer. The Eclipse refused to take a complete set of human linearization data. It was hoped that an artificial eye could be used to successfully model what the HMO wanted to see in a human eye (bright pupil and corneal reflex). This didn't work immediately. We though that perhaps the 'retina' of the artificial eye might be either reflecting too much light, or not enough light. We colored retinas, for a time, in search of a color that more closely approximated what the HMO was looking for. We never found such a color. Finally, knowing that the HMO wanted a bright pupil, we put a light bulb behind an artificial eye with a clear retina. By varying the voltage going to the eye, we could control the brightness of the pupil. We were able to make this work, and managed to get linearization tables. Soon thereafter we were able to obtain human linearization data. This was accomplished by turning down the room lights and moving the helmet to a new position on the human head. We then determined that human data yielded better HMOS responses with human linearization than with artificial eye linearization (no real surprize there). This shot down our hopes of being able to linearize an artificial eye and use that for everyone rather than putting all of our subjects through the linearization proceedure (a long, boring, and painful experience).

At this point we were ready to try sending data to the PDP-11/34 via the HYPERchannel. This yielded no results what so ever. The COLECT program would stop recording data for no apparent reason, the Eclipse computer would stop running the HMOS program for no apparent reason, and the whole system was fouled up. For no apparent reason. We got nowhere with resolving these problems until we made a small addition to the COLECT main program. This addition was a typical programmer's trick: add a print statement (in our case a bell ring). We set the program up to ring a bell each time it had received sixty pieces of data. This yielded some bizarre results. When the HMS data was 'added' to the HMO data, the system stopped dead after thirteen bells. When the HMS data wasn't 'added', the system stopped after thirteen bells, waited for a few seconds, and then restarted. Sometimes. Occasionally, the system died after only one or two bells. Every once in a while it wouldn't start at all.

After chasing bugs from the Eclipse to the 11/34 and back to the Eclipse, we determined that the Eclipse stack pointer had two words left behind on the stack after each data delivery. The stack was long enough to last for thirteen second. In addition we found that if HMS data is to be added to HMO data, the Eclipse cannot recover from a stack overflow, while if HMS data is not added, the Eclipse can recover. At this point we thought we had it licked. All we had to do was find a bad stack recovery. We found it and fixed it, but there was very little effect. The system still died after thirteen bells.

Two weeks were spent trying to get the system to work with little effect except a certainty that the problem was now resident in the 11/34. This was determined by inserting a HYPERchannel restart mechanism into the COLECT program. Once the system was started, the Eclipse put out data and didn't

stop. If the bells stopped, the HYPERchannel restart would get them going again. Unfortunately, the HYPERchannel was a sealed black box to us, so we couldn't attack it and see what gave.

In a fit of desperation, we decided to go over the software and manuals one last time. This is when we noticed that the COLECT program was instructing the HYPERchannel adapter to send data in burst mode. Burst mode allows the HYPERchannel adapter to grab hold of the PDP-11/34 UNIBUS and send a burst of data without being interrupted. Reading the HYPERchannel adapter manuals indicated that the burst length (the number of words sent per burst) was set by hardware switches. Looking at the HYPERchannel adapter card in the PDP-11/34 indicated that data was being sent and received in fourteen word bursts. Now, the Eclipse sends 32 words to the HYPERchannel adapter. If the HYPERchannel adapter wants to send them to the PDP-11/34 fourteen at a time, it's going to run into trouble on the third burst. We decided to pull out the HYPERchannel board in the 11/34 and switch select a burst length of eight words. The system worked. Or at least it seemed to work.

At this point we were forced to deal with a new and different type of problem. The bulb that supplied the infrared light used in the HMO blew out. Replacing this bulb turned out to be a difficult proposition because it was epoxyed into a special bulb holder, only one such bulb holder exists at the HMOF, and to replace the bulb you have to get a special solvent to eat the old epoxy so you can epoxy a new bulb into place. In addition we had to use a special epoxy. Getting the materials and replacing the bulb in the special fixture took two weeks. Fortunatly, the bulb had blown two weeks before we thought of the burst length fix.

At this point we tried to put it all together. We put a subject in the helmet, set the targets going were all set to take data, and didn't get any.

The system was completely intolerant of human data. We put the helmet on the artificial eye stand and tried to figure out what was wrong.

The next day the bulb blew. This was a particularly bad time for this to happen, as it takes a minimum of 48 hours to replace a bulb, and we were running out of time. In addition, the debugging was made more difficult because we didn't have real data to send over the HYPERchannel adapter.

On Wednesday of our last week at the HMOF we were once again prepared to try to take data. We started the system on the artificial eye, and within ten seconds, the bulb blew. We were in the ridiculous position of having ten weeks of work go down the tubes because some 50 cent light bulbs wouldn't last. It was too late to expoxy up a new bulb. We were at the end of our collective ropes. So what did we do? We performed several experiments in the following manner: The subject sat in the target presentation chair holding a bulb into the HMO with one hand and holding the HMS switch in the other hand. The 11/34 operator sat at the 11/34 console. The Eclipse operator sat at the Eclipse front panel. The Eclipse operator guided the subject in the placement of the HMO bulb. When the bulb was in an acceptable position, the Eclipse operator guided the subject through a calibration. Then the 11/34 operator started the target and data collection program. When the 11/34 was ready, the Eclipse operator opened the data passing gate and the data collection began. At several times during the data collection the HMOS would go into a "sight death" mode, at which time the Eclipse operator flipped two front panel switches and instructed the subject to hit the sight switch. The other major stoppage to data collection was the 11/34 death mode which was corrected by hitting a HYPERchannel init from the 11/34.

We filled up a computer disk with data. Upon analyzing the data at Carnegie-Mellon University we found that only ten seconds were valid and usable.

1982 USAF - SCEEE SUMMER FACULTY RESEARCH PROGRAM

Sponsored by the

AIR FORCE OFFICE OF SCIENTIFIC RESEARCH

Conducted by the

SOUTHEASTERN CENTER FOR ELECTRICAL ENGINEERING EDUCATION

FINAL REPORT

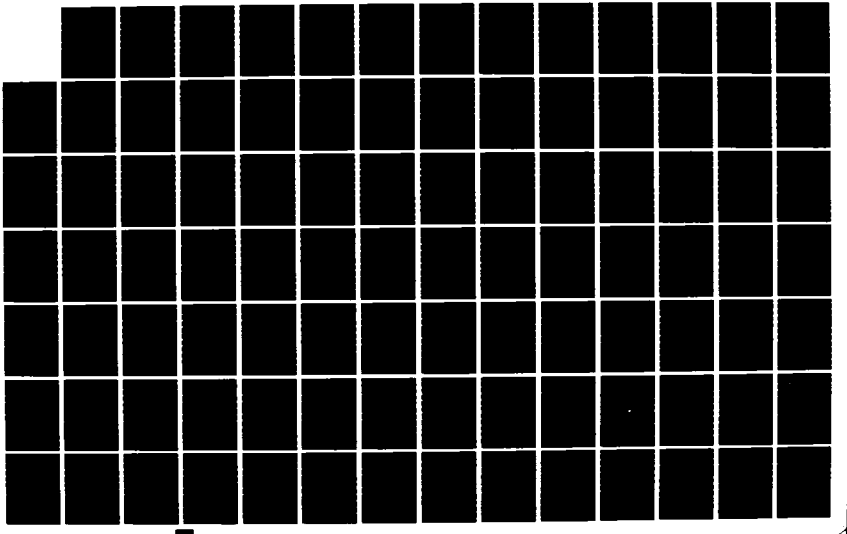
FEASIBILITY OF COMPUTER GRAPHICS AS AN AID TO AIRCRAFT BATTLE DAMAGE ASSESSMENT

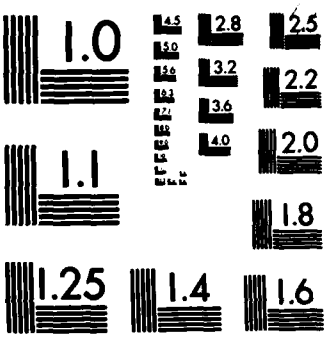
Prepared by:	Dr. M. Gene Bailey
Academic Rank:	Associate Professor
Department and University:	Computer Information Systems Department Western Carolina University
Research Location:	Air Force Human Resources Laboratory Logistics and Technical Training Division Logistics Research Branch Combat Maintenance Section
USAF Research Colleague:	Mr. Robert C. Johnson

Date:	August 13, 1982
Contract No:	F49620-82-C-0035

AD-A130 769 USAF/SCEEE SUMMER FACULTY RESEARCH PROGRAM RESEARCH REPORTS VOLUME 1 (U) SOUTHEASTERN CENTER FOR ELECTRICAL ENGINEERING EDUCATION INC S... 3/11

UNCLASSIFIED W D PEELE ET AL. OCT 82 AFOSR-TR-83-0613 F/G 5/1 NL





MICROCOPY RESOLUTION TEST CHART
NATIONAL BUREAU OF STANDARDS-1963-A

FEASIBILITY OF COMPUTER GRAPHICS AS AN AID TO AIRCRAFT BATTLE DAMAGE ASSESSMENT

by

M. Gene Bailey

ABSTRACT

The rapid and technically accurate assessment of the battle damage an aircraft has sustained is vital if our limited personnel and spare resources are to be used efficiently and effectively in a combat environment. Obviously, the capability to return damaged aircraft to a mission ready status has force multiplier implications. Rapid and accurate assessment is the first and perhaps the toughest aspect of the battle damage repair process.

The effort dissussed in this paper was designed to determine the feasibility of developing a computer-based, portable graphics device to aid in the assessment of aircraft battle damage. Suggestions for future research are offered.

1982 USAF - SCEEE SUMMER FACULTY RESEARCH PROGRAM

Sponsored by the

AIR FORCE OFFICE OF SCIENTIFIC RESEARCH

Conducted by the

SOUTHEASTERN CENTER FOR ELECTRICAL ENGINEERING EDUCATION

FINAL REPORT

FEASIBILITY OF COMPUTER GRAPHICS AS AN AID TO AIRCRAFT BATTLE DAMAGE ASSESSMENT

Prepared by:	Dr. M. Gene Bailey
Academic Rank:	Associate Professor
Department and University:	Computer Information Systems Department Western Carolina University
Research Location:	Air Force Human Resources Laboratory Logistics and Technical Training Division Logistics Research Branch Combat Maintenance Section
USAF Research Colleague:	Mr. Robert C. Johnson
Date:	August 13, 1982
Contract No:	F49620-82-C-0035

ACKNOWLEDGEMENT

The author would like to thank the Air Force Systems Command, the Air Force Office of Scientific Research and the Southeastern Center for Electrical Engineering Education for providing him with the opportunity to spend a most interesting and educational summer at the Human Resources Laboratory, Wright-Patterson AFB, Ohio. He would like to thank Mr. Robert Johnson for suggesting this area of research and for his expert guidance.

He would also like to acknowledge the kind cooperation of Dr. Don Thomas and Mr. Warren Payne for their willingness to share work they have initiated in ABDR and for their many excellent suggestions. He would like to express his appreciation to Susan Ewing for her diligent assistance in searching the literature and to all the HRL secretaries for not only their assistance but their patience as well.

Last, but certainly not least, he would like to thank the LRLC section (especially Lts. John Griffin and Nancy Fairchok) for their moral support and for creating a work environment that was most enjoyable.

I. INTRODUCTION

The rapid and technically accurate assessment of the battle damage an aircraft has sustained is vital if the limited personnel and spares resources available to repair the aircraft are to be used efficiently and effectively in a combat environment. Obviously, the capability to return damaged aircraft to a mission ready status has force multiplier implications. Rapid and accurate assessment is the first and perhaps toughest aspect of the battle damage repair process. Given the level of maintenance experience currently available in active duty maintenance units, it is extremely doubtful that sufficient personnel with adequate knowledge of all technical aspects of the assigned aircraft will be available. It is believed that a computer-based aid can be developed that will provide the technical information required to quickly and accurately assess battle damage. Such an aid would significantly increase the assessment capability of the maintenance personnel by providing them with rapid access to the information on the aircraft's systems and structures required to accurately and rapidly assess battle damage. The use of such an aid would reduce the need to rely on the technicians' knowledge and experience and would make it possible for less experienced personnel to accurately assess battle damage.

The Air Force Human Resources Laboratory (AFHRL), Logistics and Technical Training Division, has proposed development of a computer graphics based aircraft battle damage assessment system that would be ruggedized and would be portable to the extent that it could be used at the flightline. The system would have to be one that could be updated as aircraft undergo continual modification. Because of the increased pressure of the hostile environment induced by combat activities, the system would have to be very user-friendly, e.g., touch panels, voice recognition, simple commands, etc.

The primary objective of the system would be to rapidly provide the mechanic with the information required to allow him to determine quickly the nature of damage incurred, what repairs are required, and which damaged aircraft could be more expediently repaired and returned to full

or partial mission capability. In most cases, panels must be removed before an accurate assessment of damage can be made. By eliminating the need to remove most of the panels, computer graphics could reduce significantly the time required in making these assessments and thus enhance the capability to quickly assess damage. Ideally, the mechanic would be able to request a graphic display of a particular section. The computer would then "peel away" successive layers of the aircraft revealing the components behind the section. This would allow the technician to identify which systems may be affected so that operational checks of those systems may be conducted. Also, he would be able to determine if critical structural members are located in the damaged area and if closer examination (by removing the panel) is required. With additional information such as the type and angle of entry of the projectile, the computer could predict the possible path and tell the assessor which sections of the aircraft should be examined.

Such a system would allow the assessor to make decisions based upon more technical information. This would improve the probability of getting quick and accurate assessments. It would also allow the mechanic to rapidly locate required information and, in some cases, it would provide information not available from any other source. At present, the technician must search through a number of technical orders to find the required information. Also, some information is either not present in the technical data or is present in an inconvenient form. For example, there are diagrams showing where wiring is located, and diagrams showing where hydraulics are located, but there are no drawings showing them both together.

II. OBJECTIVE

The primary objective was to evaluate the state-of-the-art of computer graphics to see if current or near-term technology would support the development of a portable computer graphics battle damage assessment aid.

III. APPROACH

A three-step approach was taken to accomplish the above objective. The first step was to review the current literature to assess the research involving the use of computer graphics in aircraft design and battle damage. The second was to seek information relative to the feasibility of developing the system from the appropriate experts in both industry and academia. The last step was to attend the SIGGRAPH (Special Interest Group In Computer Graphics) conference, 26-30 July, in Boston. The purpose was to meet with vendors and to observe presentations of the most current research in computer graphics.

IV. FINDINGS

Industry has been using computer graphics to aid in the design of aircraft since the mid-1960's. Lockheed's CADAM and McDonnell-Douglas' CADD are among the best of the computer-aided design systems that have evolved from this early effort. Boeing, Hughes, and Rockwell International have also made extensive use of computer graphics in the design of aircraft. Engineering design areas have benefitted the most by a more accurate analysis through computerized structural definition and fewer design and manufacturing changes made possible by the use of CAD.

The graphics of the design systems consist principally of wire-frame drawings rather than 3-dimensional solids. The software and firmware which permit dynamic rotations of wire-frame figures in any plane are standard features on computer augmented design systems. Engineers have thus been able to design, using computer graphics, many of the complex systems (electrical, hydraulic, etc.) found in an aircraft. In most instances, these are designed as separate and distinct systems.

Some integration, however, of the different systems found in an aircraft have been made. John Zadarnowski demonstrates in his paper (1) an integration of the environmental control system, fuel-control system, electrical, fuel, flight-control, and hydraulic installations with the aircraft structure in predetermined system zones using 3-D CADD. In

particular, illustrations of the gun-bay door and an F-18 wing-leading edge both drawn with the 3-D CADD are given. The drawings have a "peel-away" effect similar to that desired by the Air Force for the proposed battle damage assessment aid.

In general, the use of computer graphics by industry has been for rather specialized purposes. Many different systems of the aircraft have been designed and analyzed using computer-aided design, but very little integration of systems has occurred. Very little research into battle damage assessment has been done using computer graphics, though some non-graphics use of computer aid has been done. In particular, the LOGMOD system being developed by the DETEX Corporation in California, will use a microcomputer to assist technicians in identifying systems which may have been affected by battle damage. Given that a bundle of wires is damaged, the system will be used to identify which of the aircraft systems may be affected.

Several of the leading software and hardware companies were contacted for their evaluation of the project and their products in relation to it. The following questions were asked of each:

(1) If the technology does exist, can the system be made portable and ruggedized or must it be relegated to shop maintenance efforts?

(2) Is color necessary?

(3) What kind of display resolution would be required?

(4) Is 3-D essential (i.e., is it essential to be able to rotate in all planes)?

(5) Can the displays be represented with wire-frame figures, or would solids be required?

(6) How flexible must the interface bewteen the system and the user be?

(7) How complicated would construction of the database be?

(8) Would a raster or stroke system be better?

(9) Would it be possible to integrate the Automated Tech Order System (ATOS) with a battle damage system?

(10) Should different levels of detail be available for the different levels of experience at the flightline?

(11) Is a "pure digital graphics" system necessary or would one with a video mix suffice?

The first question received a negative reply from all of the companies surveyed. All indicated that it would be possible to have the terminals operating from a van-like environment much like those used in the fields of health-care and in oil exploration. They indicated that though the development of a portable device is not possible in the current state-of-the-art, it should be possible in the near future. At the present, the main problem lies with the communications link between the terminal and the host computer.

The high data transmission speed required for computer graphics displays of any complexity is only possible with direct lines to the host. The highest of the current baud rates will not support this required speed. Industry is researching this problem and, as a result, has developed the technology for allowing "smart" terminals to do some of the processing locally. These are terminals that have either hardware or firmware ability to perform certain computations and data manipulations within the terminal and without the aid of the host computer. Technology is progressing rapidly in developing powerful microcomputer systems that could eventually eliminate the need for such a host system.

Ruggedization for the eventualities of a hostile environment would require a video display device more durable than the standard CRT. One suggestion made was to consider the use of flat panels, such as plasma panels, which have a better reputation for durability. Though the plasma panels have enjoyed popularity through application on the PLATO system at Illinois, they have not been part of the mainstream for the past few years. This is primarily an economic issue as the CRT has decreased greatly in cost. The use of plasma panels would mean that color would not be possible. However, the standard CRT is not a practical consideration for a combat environment. Other flat panel display technologies, such as electroluminescence displays, have promise but are not fully developed at this time.

Most of the companies indicated that the question of color was probably one that should be addressed by the Human Resources Laboratory

(HRL). All felt, though, that color would enhance comprehension. One comment made was that the use of color may not be realistic in that the actual parts of an aircraft (except for very specialized components such as emergency equipment) are usually drab.

The use of three-dimensional representations, at least in perspective, is a must (certainly at the database or modelling level, not the physical level, e.g., stereoscopic). Whether the technician would have the ability to view portions of the aircraft from any vantage point, i.e., rotating an image in all planes, is a human factors problem which will have to be resolved. It is important to note, however, that hidden line elimination (which allows an object to appear to be a 3-dimensional "solid") with dynamic viewing is extremely expensive in terms of memory and CPU time.

Much research is currently being performed in the area of surface modelling and 3-dimensional solid representations. The methods used involve a great deal of "number crunching" which requires a powerful CPU and a lot of CPU time. The time taken to complete a solid can be considerable, ranging from minutes to hours depending upon the complexity of the drawing. Ideally, solids would be best to use as the mechanic would actually "see" cross-sections as if he were looking at a photograph. However, the time presently required to generate solid representations would not be acceptable for operational use as a battle damage assessment aid. Thus, a tradeoff must be made between increased comprehension and expense and time. A possible solution would be to use a mixture of wire frame and solids.

The graphics system should be as user-friendly as possible, i.e., a minimal amount of training should be required to use it. The interface should be very flexible allowing for both voice recognition and touch panel. MIT has done a great deal of research using graphics and voice recognition and presented a video tape of this research at the 1982 SIGGRAPH conference in Boston. Keyboards have proven not to be user-friendly and their use in a hostile environment would increase even further the frustration of the operator (in this case, the battle damage assessor).

The construction of the database and its eventual management is probably singularly the most difficult task of the project. Without exception every organization expressed a great deal of concern about it. No aircraft has been completely "computerized", i.e., completely designed using computer graphics, though the aircraft industry indicated long-range goals to accomplish this. One representative commented that construction of the database for a battle damage assessment aid and its corresponding management system would essentially mean re-engineering the aircraft.

The type of system, raster or stroke or a mix, is an important issue because of physical as well as the human factors problems. For example, dynamic movements can be achieved much easier with stroke systems than with raster. Also, the use of solids is impractical on a stroke system. Depending on the complexity or detail required in the visual image, one system will be better than the other. The ultimate decision as to the type of display device to be used will, of course, be made by the supplier, but that decision will rest on a number of issues, such as those listed above, which still need to be resolved.

An integration of the Automated Tech Order System (ATOS) with the battle damage system would be feasible. Actually, once an aircraft has been "computerized", the system to do BOTH could be constructed and no integration would be necessary. ATOS is still in the development stage.

The companies were also asked to comment on the possibility of building an aircraft battle damage assessment system which integrates existing CAD graphics for systems such as hydraulic, electrical, structural, avionics, etc. One company, McDonnell-Douglas, indicated that they could integrate the systems that they had already computerized. However, the task of actually relating the drawings in the different systems would be a major one.

Although it adds to the complexity of the database management system, supplying different levels of information is a must. The responsibility for determining the actual necessity of providing this ability lies with the user. However, the manufacturers and software houses agreed that the concept is a necessary one.

Two of those interviewed indicated that a video disk might be a feasible alternative. An advantage to such a system would be that a mechanic would see an actual photograph of a cross-section of the aircraft rather than a computer drawing. A second advantage is found in the "minimal storage" concept of video disks, e.g., it is possible to store 55,000 full-screen images on a disk.

The principle disadvantage is in the inflexibility of the recording media. It is impossible (at this stage) to update the contents of a video disk. It is possible to do a form of updating by leaving blank spaces which could be written on at a latter time. However, this is not practical as updating would require the disks to be returned to a central location and saturation would eventually occur. The actual task of dissecting an aircraft to photograph the different components as they would appear installed is itself an expensive and difficult one. Modifications in the aircraft would necessitate future dissections in order to update the information. This problem could be solved by using drawings instead of actual photographs. Distributing current disks would be a major problem.

V. DISCUSSION

The state-of-the-art of computer graphics design indicates that it is feasible at this time to construct a version of an aircraft battle damage assessment system that would not be portable. It would be possible to develop a portable display device to present battle damage information. However, it would be dependepent upon and connected to a host computer (perhaps located in a van). The particular computer-aided system to be used needs further study. The video disk technology is advancing rapidly and will probably eventually allow updating the disks. Thus, it may be too early to completely disregard its possible use in ABDR. It would be advisable, too, to stay abreast of the use of video disks by the Navy. TERAK Corporation has just developed a package for Annapolis to be used in training cadets that uses video disk. The system is a high

resolution, touch panel, 64-color video graphics system that is totally interactive and user-friendly.

Although some information was gained in this study, there are several human factors issues which must be examined in more detail before a prototype can be developed.

(1) How important is color as an aid in comprehension? Could its use be actually more confusing?

(2) How important is hidden-line elimination? Are solids really necessary? Can approximate representations of components be used rather than exact drawings? How high should the resolution be?

(3) Is it essential that a technician be able to view sections of the aircraft from all possible vantage points?

(4) How much detail is required in each cross-section?

(5) What kind of user interface is best suited to a hostile environment? Is voice recognition required?

The answers to these questions bear greatly on the complexity of the database and its corresponding management system. They may also determine the physical representation of the system. For example, color would preclude the use of plasma panels. Voice recognition and computer graphics is just in its infancy stage and would require considerable more research in order to be used in ABDR. Once these questions have been satisfactorily answered, a proposal could be made to develop a prototype for a graphics system.

VI. RECOMMENDATIONS

The "state-of-the art" indicates that the technology exists to develop a computer graphics aid to battle damage assessment. The Air Force should develop a system with the available technology even though the system may not meet all of the software and hardware constraints. For example, the system may have to be located in a van or a shop and perhaps limit its scope to one section of one particular aircraft. As

more familiarity with the data and the database is obtained, the system could be expanded to include other sections. This prototype could be used to test the human factors constraints listed previously. As hardware and software technology progress, the physical components could be reduced and ruggedized to the portable requirements of the flightline. A second alternative would be to develop a video disk system. The state-of-the-art in video disk technology will more readily support the development of a small portable system.

REFERENCE

1. Zadarnowski, John H., "CADD on the F-18 Program," Astronautics and Aeronautics, March, 1980.

BIBLIOGRAPHY

1. Antl, V., W. Weingartner, "Computer Graphics and Related Design Process at MBB," AGARD Conference Proceedings, No. 280, Neubiberg, Germany, 3-6 September 1979.

2. Atherton, Peter R., "A Method of Interactive Visualization of CAD Surface Models on a Color Video Display," Computer Graphics, Vol 15, No 3, August 1981.

3. Beeby, William, "The Future of Integrated CAD/CAM Systems: the Boeing Perspective," IEEE CG & A , January 1982.

4. Burchi, R. S., "Interactive Graphics Today, "IBM System Journal, Vol 19, No 3, 1980.

5. Chasen, S. H., "Historical Highlights of Interactive Computer Graphics," Mechanical Engineering, November, 1981.

6. Drior, B., "Computer-Aided Design at Israel Aircraft Industries," Comput. & Graph, Vol 3, 1978.

7. Ebling, P., E. Pfisterer, "The Use of Computer Aided Design in Airborne Systems," AGARD Conference Proceedings No. 280.

8. Evans, D. C., "Computer Generated Images for Aircraft Use," Aeronautical Journal, August, 1978.

9. Foley, J. D., A. Van Dam, Fundamentals of Interactive Computer Graphics, 1982, Addison-Wesley Publishing Company.

10. Harris, David H. W., "Applying Computer Aided Design (CAD) to the 767," Astronautics & Aeronautics, September, 1980.

11. Krouse, John K., "Automated Factories; The Ultimate Union of CAD and CAM," Machine Design, November 26, 1981.

12. Newman, William A, Robert F. Sproull, Principles of Interactive Computer Graphics, 2nd Edition, 1979, McGraw-Hill Book Co.

13. Rawlings, J. S., "CAD/CAM' in British Aerospace - Aircraft Group," I MECH E (AIAA), 1980.

14. Raymer, Daniel, "Developing an Aircraft Configuration Using a Minicomputer," Astronautics and Aeronautics, November, 1979.

15. Smyth, S. J., "CADAM Data Handling from Conceptual Design through Product Support," J. Aircraft, Vol 17, No 10, October, 1980.

16. _____, "CAD - The Designer's New Tool," AIAA Annual Meeting and Technical Display, May 12-14, 1981, Long Beach, CA.

17. _____, A. N. Baker, "The CADAM System - The Designers' New Tool", Lockheed Horizons, Summer, 1980.

18. _____, and R. J. Ricci, "The CADAM System for Aircraft Structural Design", Society of Automotive Engineers, Meeting Oct 13-16, 1980.

19. Squier, Bailey,"Where Do We Stand On Programming Sculptured Surfaces?" CAM-I, Incorporated, Arlington, TX, 1981.

20. Wehrman, Marvin D., "CAD Produced Aircraft Drawings," J. Aircraft, Vol 18, No 7, July, 1981.

COMPANIES AND REPRESENTATIVES

CALMA, Bill Fernandez
CHROMATICS, John Pappas
COMPUTERVISION, Michael N. Schuh, Tom Sarvay
EVANS AND SUTHERLAND, Bob Stirland, Jim O'Malley
GENSICO, Jim Jones, Bob Diorio
GERBER SCIENTIFIC INSTRUMENT CO., R. W. Layton
GTE, Jim Vallenga
IBM, Michael W. Blasgen
IKONAS GRAPHICS SYSTEMS, J. N. England
INTERNATIONAL IMAGING SYSTEMS, Ted Dyer
LEXIDATA Corporation
LOCKHEED-CALIFORNIA/CADAM, Lee Whitney
LOCKHEED-GEORGIA, S.H. Chasen
MAGNAVOX, Donald Willis
MCAIR, Burt Birchfield
MCAUTO, David Shuey
MEGATEK, Maurice Katzman
PHOENIX COMPUTER GRAPHICS, INC., Lawrence D. Purcell
RAMTEK, Tom Peters, John Tothill
RASTER TECHNOLOGIES, Al Barr
SONY, D.C. Marro
SUMMAGRAPHICS, Dan Mullen
SYNERCOM TECHNOLOGY, INC, Ginger Juhl
TEKTRONIX, Harvey Betts
TERAK, Steve Rago
THREE RIVERS, Erin Coleman
VIRGINIA COMMUNICATIONS ASSOCIATES, Merv Norton

1982 USAF-SCEEE SUMMER FACULTY RESEARCH PROGRAM

Sponsored by the

AIR FORCE OFFICE OF SCIENTIFIC RESEARCH

Conducted by the

SOUTHEASTERN CENTER FOR ELECTRICAL ENGINEERING EDUCATION

FINAL REPORT

EFFECTS OF MAGNETIC SHEAR ON LOWER HYBRID WAVES IN THE SUPRAURORAL REGION

Prepared by:	Dr. Pradip M. Bakshi
Academic Rank:	Research Professor
Department and University:	Department of Physics Boston College
Research Location:	Air Force Geophysics Laboratory, Space Physics Division, Ionospheric Physics Branch
USAF Research Colleague:	Dr. John R. Jasperse
Date:	October 18, 1982
Contract No.:	F49620-82-C-0035

EFFECTS OF MAGNETIC SHEAR ON LOWER HYBRID WAVES IN THE SUPRAURORAL REGION

by

Pradip M. Bakshi

ABSTRACT

Effects of magnetic shear on lower hybrid modes are investigated. It is shown that due to non-local effects, even a small shear can lead to a significant reduction of their growth rate. These results are of importance in the context of the recently proposed mechanism of lower hybrid acceleration and ion evolution in the supraurora region. The non-local effects of magnetic shear are moderated if the width of the current sheet is not sufficiently large, and then the local growth rates are recovered.

I. INTRODUCTION

It has recently been shown[1] that ions can be accelerated perpendicularly to the magnetic field by resonant interactions with current-driven lower hybrid modes. This accelerated portion of the ions of ionospheric origin in the supraurоral region of the magnetosphere can evolve into conic distributions and propagate upwards along the magnetic field lines. These ions can reach the region where they can be strongly energized along the field lines by the electrostatic shocks, and it has been argued that the ion distribution resulting from the combination of these accelerated ions with the background ions can depart significantly from a thermal distribution, leading to the excitation of electrostatic ion cyclotron modes. This provides a plausible explanation of the simultaneous observation of the electrostatic ion cyclotron modes with the kev ion distributions in the supraurоral region.

Since the driving current also produces a magnetic shear, which generally exerts a stabilizing influence, it is quite important to investigate whether the lower hybrid mode remains unstable in spite of the influence of shear. The magnitude of shear is generally quite small, and it may seem reasonable to ignore it altogether. However, as we have shown earlier[2,3] in the context of the current-driven ion cyclotron instability, even a small shear due to non-local effects can sometimes produce a very significant reduction in the growth rate of an instability, and even stabilize it over a range of parameters.

The study of ionospheric instabilities has been an important area of research at the Air Force Geophysics Laboratory and the present author's background and recent contributions[2,3] in related areas as mentioned above led to the selection of objectives described in the next section.

II. OBJECTIVES

The main objective of this project is to investigate the effects of magnetic shear on the current-driven lower hybrid modes. The field aligned currents generate the shear and we would like to determine whether it can, through non-local effects of the type studied earlier in another context[2,3], lead to a reduction of growth rate and stabilization for some range of parameters. A complete treatment of the electrostatic modes dispersion relation would require an extended effort; due to the limited duration of this project only the classical lower hybrid mode dispersion relation will be analyzed here. Various extensions and generalizations are proposed in the last section of this report as future objectives.

Our specific objectives, then, were:

a. To formulate the non-local treatment of the lower hybrid mode, taking into consideration the magnetic shear.

b. To obtain the modified dispersion relation and to note its implications; in particular, to determine whether a significant reduction in growth rate takes place.

c. To examine the effects of the finite width of the current layer; this could moderate the non-local results due to shear.

d. Finally, to point out the limitations of the treatment adopted and to specify the approaches needed to go beyond the present level of description.

III. FORMULATION OF THE SHEAR PROBLEM

For electrostatic waves, the dispersion relation for the current-driven lower hybrid mode is given by[1,4]

$$\frac{f^2_{pi}}{f^2} + \frac{k^2_{\parallel}}{k^2}\ \frac{f^2_{pe}}{f^2} = 1 - \frac{n_b}{n_o}\ \frac{f^2_{pe}}{k^2 v^2_{tb}}\quad Z'\ \left(\frac{f - k_{\parallel} V_{eb}}{k_{\parallel} V_{tb}}\right) \qquad (1)$$

where the wave frequency f obeys the condition $f_{ci} \ll f \ll f_{ce}$, f_{ci} and f_{ce} being the cyclotron frequencies; $k_{\parallel} \ll k_{\perp}$; $k_{\perp} r_e \ll 1$, r_e being the electron Larmor radius; $f \gg k_{\parallel} V_{eo}$, $f \gg k\ V_{io}$, where V_{eo} and V_{io} are the thermal velocities of the ambient ions and electrons; f_{pi} and f_{pe} are the respective plasma frequencies, n_b the beam density, n_o the ambient density, V_{tb} indicates the thermal spread of the beam around the beam velocity V_{eb}, and we have assumed $f^2_{pe} \ll f^2_{ce}$. The real part of the plasma dispersion function Z is not significant in relation to the other terms when the beam density is small compared to the ambient density and the ambient thermal velocity is small compared to the beam thermal velocity.

The solution of the local dispersion relation (1) is given by

$$f_r^2 = f_{pi}^2 + (k_\parallel / k)^2 f_{pe}^2 , \tag{2}$$

and, assuming the growth rate $g \ll f_r$, we find

$$g = f_r \pi^{1/2} (n_b/n_o) (f_{pe}/kV_{tb})^2 \, ye^{-y^2} , \tag{3}$$

where

$$y = u - (f/k_\parallel V_{tb}) , \tag{4}$$

$$u = (V_{eb}/V_{tb}) . \tag{5}$$

The non-local formulation is achieved[2,3] by introducing (i) $k_\parallel = k_y(x/L_s)$, where x is the distance measured perpendicular to the current sheet and L_s is the shear length, and (ii) $k_x^2 = -\frac{d^2}{dx^2}$, which converts (1) into a differential equation. The magnetic field is along the z direction and $k_\perp^2 = k_y^2 + k_x^2 = k_y^2 - \frac{d^2}{dx^2}$. The resulting differential equation can be written in terms of the angle $a = x/L_s = Sx$ in the form

$$[(r_i S)^2 \frac{d^2}{da^2} + Q(f,a)]F = 0 , \tag{6}$$

$$Q = -(r_i k_y)^2 [1 + Aa^2 + ip(a)] ,$$

$$A = 1 + M (1 - f^2/f_{pi}^2)^{-1} ,$$

$$p = 2(g/f_r) (f_{pi}^2/f^2 - 1)^{-1} ,$$

where M is the ion to electron mass ratio, and g, f_r are as in (2) and (3) with $k^2 = k_y^2 + k_{||}^2 = k_y^2(1 + a^2)$. The local dispersion relation is recovered from (6) by setting S = o, i.e.,

$$Q(f, a) = o \ , \tag{7}$$

which is easily verified to lead to (2) and (3).

IV. SOLUTION OF THE SHEAR PROBLEM

The departure from the local dispersion relation Q = o can be investigated by solving the differential equation (6), subject to the boundary conditions that the electrostatic potential function remains bounded, or has outgoing energy boundary condition. In general the solution to the differential equation cannot be obtained in closed form, and numerical solution on a computer may be required. However, one can take advantage of the physical characteristics embodied in the Q function, and in particular, use the properties of the local solution to obtain an approximate form for Q which enables one to obtain an analytical solution. This is the approach adopted here.

The expression for the growth rate g indicates that the peak of the instability occurs near the angle a_o which corresponds to $y = y_o$ which maximizes the function $y \exp(-y^2)$. The normal modes of the local solution are in the vicinity of this angle a_o and if one waits long enough, the dominant mode at the angle a_o grows larger than all others. We take advantage of this property of the imaginary part of Q and expand it in the vicinity of this angle a_o to second order in the variable $(a-a_o)$.

After regrouping the terms and completing the square one obtains a Weber equation as shown in Reference 3, and the non-local dispersion relation is given by

$$Q(f,a_o) = \frac{Q_o'^2}{2Q_o''} + (2m+1)\,(r_i S)\,(-Q_o''/2)^{1/2}\,, \qquad (8)$$

where primes refer to differentiation with respect to the angle a and the subscripts indicate evaluation at $a = a_o$. Generally the m=o mode is the least damped by shear and we will set m=o in (8). The boundedness condition is satisfied if we take the branch for which

$$\text{Re}\,(-Q_o''/2)^{1/2} > o\,, \qquad (9)$$

with the solution of the form

$$F = \exp\,[-(\tfrac{1}{2})(a-a_1)^2(-Q_o''/2)^{1/2}]\,, \qquad (10)$$

with

$$a_1 = a_o - Q_o'/Q_o''\,. \qquad (11)$$

We omit the algebraic details and give here the main result:

(i) Even for small shear, the growth rate is reduced from its local value given in equation (3), evaluated at a_o, to

$$g_o \longrightarrow g_o\,[1 - 2(u-y_o)^2]\,. \qquad (12)$$

For typical parameters of this problem, u is in the range 1 to 3, and since $y_o = 2^{-(1/2)} \cong o{\cdot}7$, we have a significant reduction

of the growth rate, or even a sign reversal for higher currents indicating damping instead of growth. Thus, the shear produces a significant effect.

(ii) The real part of the frequency f_r moves closer to the ion plasma frequency f_{pi}.

(iii) The angle a_1 in (10) and (11) becomes complex, dominated by its imaginary part and with magnitude $|a_1| \ll a_o$.

According to this treatment the shear makes a significant difference. However, the large shift in the angle, away from a_o can render inadequate the second order expansion around a_o. As an improvement, one can determine a_1 as the solution of

$$Q'(f, a_1) = o \tag{13}$$

and expand Q to second order around a_1. Then the dispersion relation (8) simplifies to

$$Q(f, a_1) = (2m + 1)(r_i S)(-Q_1''/2)^{1/2} . \tag{14}$$

Now equations (13) and (14) simultaneously determine the complex frequency f and the complex angle a_1. While the full solution of (13) and (14) would require using a computer, an approximate analysis shows that the main results are essentially valid. We plan to solve equations (13) and (14) as an extension of the present work.

V. EFFECTS OF FINITE WIDTH CURRENTS

The treatment above assumes a uniform shear extending over all space. In reality, the current slabs in the ionosphere have a finite width of the order of a few kilometers for auroral arcs. The typical shear length is of the order of a few hundred kilometers. Thus the angular variation across the slab can be less than a degree. For some parameter ranges this will not be adequate to produce the non-local effect described in the previous section, and the local result will be recovered, as in the case of the current-driven ion cyclotron instability[5], when the slab width is much smaller than the shear length. We plan to investigate the demarcation boundaries in parameter space, separating the local and the non-local limits, as an extension of the present work.

VI. RECOMMENDATIONS

a. We have demonstrated, using an approximate analytical treatment for the non-local equation for the effects of shear, that the growth rate of the current-driven lower hybrid mode can be significantly reduced. An improved treatment, as indicated at the end of Section IV, requires a computer solution of two algebraic equations and can provide more accurate criteria for stabilization or significant reduction of the growth rate. We propose to carry out this extension in the context of the minigrant program.

b. The entire treatment in this report was based on the idealized lower hybrid dispersion relation, equation (1). The full electrostatic dispersion relation (e.g. equation (1) of Reference 3) should be employed to carry out a similar treatment. This will extend the results to a wider range of wavelengths, temperature ratios and other physical parameters. This is a major undertaking and we propose to carry out this generalization in the context of the minigrant program.

c. The interplay between the current width and the shear length determines whether the local theory prevails or whether the non-local shear effect comes into play. We propose a detailed investigation of this facet of the problem for realistic ionospheric parameters, varied as a function of height. This investigation can indicate whether or not the lower hybrid mode can be expected to occur at various heights. This also is a program contemplated in the context of the minigrant.

d. Finally, the methods described here are widely applicable to various other instabilities, and as a long range program, we would like to investigate the effects of shear and finite width currents on a variety of ionospheric instabilities.

ACKNOWLEDGEMENTS

The author would like to thank the Air Force Systems Command, the Air Force Office of Scientific Research and the Southeastern Center for Electrical Engineering Education for providing him the opportunity to participate in a very worthwhile summer program at the Air Force Geophysics Laboratory. He would like to thank Dr. John Howard and Dr. John Jasperse for their kind hospitality at the laboratory.

The author also wishes to thank Dr. J. Jasperse, Dr. B. Basu and Dr. T. Chang for suggestions in the selection of the area of research and for the many valuable discussions.

REFERENCES

1. T. Chang and B. Coppi, "Lower Hybrid Acceleration and Ion Evolution in the Suprauroral Region", Geophys. Res. Letters, Vol. 8, pp. 1253-1256, 1981.

2. P. Bakshi and G. Ganguli, "Non-local Aspects of Current-Driven Ion-Cyclotron Instability due to Magnetic Shear", Bull. Amer. Phys. Soc., Vol. 26, p. 913, 1981.

3. G. Ganguli and P. Bakshi, "Non-local Aspects of Electrostatic Current-Driven Ion-Cyclotron Instability due to Magnetic Shear", Phys. Fluids, Vol. 25, pp. 1830-1837, 1982.

4. K. Papadopoulos and P. Palmadesso, "Excitation of Lower Hybrid Waves in a Plasma by Electron Beams", Phys. Fuids, Vol. 19, pp. 605-606, 1976.

5. P. Bakshi, G. Ganguli and P. Palmadesso, "Interplay of Finite Width Current Channel and Magnetic Shear Effects on Current-Driven Ion-Cyclotron Instability", Bull. Amer. Phys. Soc., Vol. 27, p. 917, 1982.

1982 USAF-SCEEE SUMMER FACULTY RESEARCH PROGRAM

Sponsored by the

AIR FORCE OFFICE OF SCIENTIFIC RESEARCH

Conducted by the

SOUTHEASTERN CENTER FOR ELECTRICAL ENGINEERING EDUCATION

FINAL REPORT

A SIMPLE MODEL FOR IMPURITY PHOTO-ABSORPTION IN SILICON

Prepared by:	Gust Bambakidis
Academic Rank:	Assistant Professor
Department and University:	Department of Physics Wright State University
Research Location:	Air Force Wright Aeronautical Laboratories Electromagnetic Materials Divison Laser and Optical Materials Branch
USAF Research Colleague:	Gail Brown
Date:	Sept. 20, 1982
Contract No:	F49620-82-C-0035

A SIMPLE MODEL FOR IMPURITY PHOTO-ABSORPTION IN SILICON

by

Gust Bambakidis

ABSTRACT

A simple model for absorption of infrared radiation by impurity atoms in silicon crystals has been developed and applied to electronic excitations of the Group V donors Bi, Sb, As and P, and the Group III acceptors B, Al, Ga and In. The model is based on the quantum-defect method for approximating bound donor or acceptor wave functions outside the core region of the impurity. For each donor species, the relative oscillator strengths have been calculated for the transitions from the ground state to the first four excited levels. For each acceptor species, the relative oscillator strengths were calculated for transitions from the $P_{3/2}$ ground state to the first three $P_{1/2}$ excited levels. Comparison with high-resolution absorption spectra show qualitative agreement for the low-lying transitions.

I. INTRODUCTION

The identification of residual impurities as to type and concentration in silicon single crystals is an extremely important problem, since very small amounts of donors or acceptors can have a marked effect on the electrical properties of the crystal. For the Air Force in particular, the reliable characterization of silicon-based materials as to impurity type and content is necessary if these materials are to be used effectively in air-borne infrared radiation detectors.

The impurities most commonly found in silicon are carbon, oxygen, the Group III acceptors B, Al, Ga, In and the Group V donors Bi, Sb, As and P. The Group III and Group V impurities are infra-red active with respect to electronic excitation to discrete levels, and infrared absorption measurements have been used to identify the impurity types in the concentration range $10^{14}/cm^3$ to $10^{18}/cm^3$. The determination of impurity concentration using such measurements is more difficult but attempts have been made to use absorption peak areas of specific lines, since simple theory predicts that the absorption coefficient will be proportional to concentration. The proportionality constant is the absorption cross-section $\sigma(\nu)$. In practice, one proceeds by choosing one line for a specific type of impurity and calibrating it over the concentration range of interest by measuring the absorption in this line over a range of known impurity concentrations. In principle and accurate calculation of $\sigma(\nu)$, or more appropriately the integral of $\sigma(\nu)$ over the width of the line, would enable an absolute calibration of the line. However, $\sigma(\nu)$ depends on the effective electric field at the impurity relative to the macroscopic electric field in the crystal considered as a dielectric medium. This effective field is difficult to estimate. On the other hand, the ratios of the integrated cross-sections for two different lines belonging to the same impurity are independent of this quantity and therefore easier to calculate. Accurate values for these ratios would be useful in calibrating additional lines without the necessity of performing separate measurements for them.

II. OBJECTIVES

The objective of this work was to calculate the relative absorption strengths of certain lines associated with Group III and Group V dopants in silicon. In order to do this, one must evaluate the dipole matrix element for the transition between the initial and final electronic states of the impurity. The emphasis was on developing a simple model which would require only the use of a hand calculator. As described in the next section, the approach was to use the quantum-defect method (QDM) to obtain an analytic expression for the wave functions in the asymptotic region far from the impurity core.

III. FORMULATION OF THE MODEL

1. Assumptions

The basic assumptions made, in approximate order of decreasing validity are:

(a) the dipole approximation for the photon absorption process;

(b) the effective-mass approximation for the impurity wave function at large distances from the impurity (the asymptotic region);

(c) the silicon matrix can be regarded as a continuous medium characterized by its dielectric constant k and index of refraction n;

(d) any degeneracy in the Bloch functions and anisotropy in the effective-mass tensor at the band edge may be ignored.

(e) the major contribution to the absorption cross section comes from the asymptotic region.

The remainder of this section discusses these assumptions and their implications.

2. The Dipole Approximation

This approximation is a standard one when treating the interaction of radiation with matter. Classically it corresponds to treating the bound electron or hole as an oscillating dipole which absorbs energy in response to the electromagnetic field of the incident radiation. Quantum mechanically, absorption will occur only at discrete frequencies ν for which the photon energy $h\nu$ is equal to the energy difference $E_b - E_a$ between the final state $|b\rangle$ and initial state $|a\rangle$. Specifically, the power absorbed per unit frequency, $dP/d\nu$, in an atomic transition at the frequency ν, by a single impurity atom exposed to an incident

beam of intensity $I(\nu)$ per unit frequency, is[1,2]

$$\frac{dP}{d\nu} = I(\nu)\frac{n}{k}\left(\frac{\mathcal{E}_{eff}}{\mathcal{E}_o}\right)^2 \frac{\pi e^2 (E_b - E_a)}{3\epsilon_o \hbar c} g_b \delta(E_b - E_a - h\nu) \times \times \sum_{i=1}^{3} \left| \langle b | x_i | a \rangle \right|^2_{av} . \quad (1)$$

$\mathcal{E}_{eff}$ and $\mathcal{E}_o$ are the average electric fields at the impurity and in the medium, respectively. The initial state is assumed non-degenerate, while the degeneracy of the final state is g_b. The matrix element $\langle b|x_i|a\rangle$ is essentially that for the $i^{\underline{th}}$ Cartesian component of the dipole moment operator, and its magnitude squared is averaged over the g_b final states. Eq.(1) is a standard result but its derivation is rather involved and will not be reproduced here. The validity of the dipole approximation depends on the spatial extent of the orbitals being small compared to the wavelength. This condition is well satisfied here since the orbital size is at most a few hundred Å while the wavelength is in the range 10^4 to 10^5 Å.

3. Effective-Mass Theory

In effective-mass theory the electrons or holes move in the field of the impurity atom with an effective mass equal to that of the corresponding pure-crystal Bloch states at the top of the valence band (for holes) or bottom of the conduction band (for electrons). The attractive impurity potential is considerably weakened by the dielectric screening effect of the surrounding silicon atoms, resulting in bound donor or acceptor levels with binding energies, relative to the band edge, of order 10^{-2} to 10^{-1} eV (10 to 100 meV) and orbital extent of order 10 to 1000Å. The situation is complicated by the anisotrophy of the effective mass and, in the case of acceptor levels, by the degeneracy of the Bloch states at the symmetry point Γ at the top of the valence band. Specifically, the impurity states are expressed as

$$\psi(\vec{r}) = \sum_{j=1}^{q} F_j(\vec{r})\, \phi_j(\vec{k}, \vec{r}) , \quad (2)$$

where the $\phi_j(\vec{k},\vec{r})$ are the g_d - fold degenerate Bloch functions at the band edge and the coefficients $F_j(\vec{r})$ are the "envelope functions" which modulate the Bloch functions and which, for bound states, decrease rapidly with distance. The standard effective-mass result for determining the $F_j(\vec{r})$ is the set of g_d coupled equations,[3]

$$\sum_{j'=1}^{g_d} \left[D_{jj'}^{\alpha\beta} \left(\frac{1}{i}\frac{\partial}{\partial x_\alpha}\right)\left(\frac{1}{i}\frac{\partial}{\partial x_\beta}\right) + \left(u(\vec{r}) - E\right)\delta_{jj'} \right] F_{j'}(\vec{r}) = 0, \qquad (3)$$

where $u(\vec{r})$ is the impurity potential, E the energy of the state and the coefficients $D_{jj'}^{\alpha\beta}$ depend on the g_d different effective mass tensors at the band edge. These equations are valid at distances from the impurity large compared to the impurity-silicon nearest neighbor distance, in which case there are many Si atoms between the electron or hole and the impurity. The Si atoms then act simply to weaken by a factor 1/k the impurity potential, regarded as a singly charged coulombic center:

$$u(\vec{r}) = \frac{-e^2}{4\pi k \varepsilon_0 r} \quad . \qquad (4)$$

Effective-mass theory breaks down near the impurity core, but for electric dipole transitions from an s-like ground state, the final state must be p-like or f-like and therefore vanishes at the core. In this case one might expect the asymptotic region to give the major contribution to the transition matrix elements. A considerable simplification results when the effective-mass tensors are assumed identical and isotropic. Then

$$D_{jj'}^{\alpha\beta} = \frac{\hbar^2}{2m^*}\delta^{\alpha\beta}\delta_{jj'} \quad , \qquad (5)$$

and there is only one effective-mass parameter m* and one envelope function $F(\vec{r})$, determined from Schrödinger's equation with a hydrogenic potential:

$$\left[-\frac{\hbar^2}{2m^*}\nabla^2 - \frac{e^2}{4\pi k\varepsilon_0 r} - E\right] F(\vec{r}) = 0 \quad . \qquad (6)$$

4. The Oscillator Strength

The oscillator strength f_{ba} for the transition from state $|1a\rangle$ to state $|1b\rangle$, via photon absorption, is defined by,[1]

$$f_{ba} = \frac{1}{3}\left(\frac{2m^*}{\hbar^2}\right) g_b \left(E_b - E_a\right) \sum_{j=1}^{3} \left|\langle b|x_i|a\rangle\right|^2_{av} \tag{7}$$

In terms of f_{ba} the cross section $\sigma(\nu)$ for the transition, defined by

$$\frac{dP}{d\nu} = \sigma(\nu) I(\nu) \ , \tag{8}$$

is given by

$$\sigma(\nu) = \frac{n}{k}\left(\frac{\mathcal{E}_{eff}}{\mathcal{E}_o}\right)^2 \frac{\pi e^2 \hbar}{2\epsilon_o m^* c} f_{ba}\, \delta(E_b - E_a - h\nu) \ . \tag{9}$$

At impurity concentrations low enough for concentration broadening to be negligible, the cross section at frequency ν is related to the measured optical absorption coefficient $\alpha(\nu)$ by

$$\alpha(\nu) = N\sigma(\nu) \ , \tag{10}$$

where N is the impurity concentration, assuming only one impurity species to be active at that frequency. The area under an absorption peak is therefore proportional to the integrated cross section, which from Eq. (9) is in turn proportional to the oscillator strength:

$$\int_{\nu} \sigma(\nu)\, d\nu = \frac{n}{k}\left(\frac{\mathcal{E}_{eff}}{\mathcal{E}_o}\right)^2 \frac{\pi e^2 \hbar}{2\epsilon_o m^* c} f_{ba} \ . \tag{11}$$

For a given impurity, the ratio of the peak areas for transitions $|a\rangle \rightarrow |b\rangle$ and $|a\rangle \rightarrow |c\rangle$ is therefore equal to the ratio of the corresponding oscillator strengths. From Eq. (7),

$$\frac{f_{ca}}{f_{ba}} = \frac{g_c(E_c - E_a)}{g_b(E_b - E_a)} \frac{\sum_{i=1}^{3} \left|\langle c|x_i|a\rangle\right|^2_{av}}{\sum_{i=1}^{3} \left|\langle b|x_i|a\rangle\right|^2_{av}} \ . \tag{12}$$

It is this ratio which was calculated and compared to experiment.

5. Calculation of the Matrix Elements

For the asymptotic contribution to the matrix elements appearing in Eq. (12), only the envelope part $F(\vec{r})$ of the impurity state need be considered. The reason for this is that $F(\vec{r})$ changes very little over a unit cell volume of the Si lattice whereas the Bloch functions $\phi_j(\vec{k},\vec{r})$ are orthonormal within this volume.

Now if Eq. (6) were assumed valid over all distances $f(\vec{r})$ would be a pure hydrogenic orbital and the corresponding energy would be given by a simple Rydberg formula. This is the hydrogenic model of impurity states and is the simplest form of effective-mass theory. A more sophisticated form would incorporate mass anisotropy and band degeneracy via Eq. (3). In the present model one deals only with Eq. (6), but does not assume its validity at small distances; rather, an "effective" principal quantum number ν is determined from the Rydberg formula,

$$E = -\frac{1}{\nu^2} \quad , \tag{13}$$

using the experimental value for E expressed in units of the "effective" Rydberg R*,

$$R^* = \frac{e^2}{8\pi k \varepsilon_0 a^*} \quad , \tag{14}$$

where a* is the "effective" Bohr radius,

$$a^* = \frac{4\pi k \varepsilon_0 \hbar^2}{m^* e^2} \quad . \tag{15}$$

In terms of the quantum numbers ν, ℓ and m, the envelope function is

$$F_{\nu\ell m}(\vec{r}) = R_{\nu\ell}(r)\, Y_{\ell m}(\theta,\phi) \quad , \tag{16}$$

where

$$R_{\nu\ell}(r) = \left(\frac{2}{\nu a^*}\right)^{1/2} \frac{1}{r} P_{\nu\ell}\left(\frac{2r}{\nu a^*}\right) \quad . \tag{17}$$

The asymptotic form of $P_{\nu\ell}$ is given in the QDM[4] as

$$P_{\nu\ell}(\rho) \sim N_{\nu\ell}\, \rho^{\nu} e^{-\rho/2} \sum_{t=0}^{t_0} \beta_t \rho^{-t} \quad , \tag{18}$$

with $t_0 \leq \nu$. The QDM was first applied to this problem by Kohn and Luttinger[5] who used it to calculate corrections to the effective-mass value of the lowest excited donor levels. Bebb and Chapman[4] later adapted it to the calculation of photoioization cross sections of acceptors in Si and GaAs. Here the method is applied to photoexcitation, and it is necessary first to correct the expressions for $N_{\nu\ell}$ and β_t given in Ref. 4. The corrected expressions are

$$\beta_0 = \frac{\Gamma(\nu+\ell+1)}{\Gamma(\nu-\ell)} \quad ;$$

$$\beta_1 = \ell(\ell+1) - \nu(\nu-1) \quad ;$$

$$\beta_t = \beta_{t-1}\left[\ell(\ell+1) - (\nu-t+1)(\nu-t)\right]/t \quad , \qquad t \geq 2 \quad ;$$

$$N_{\nu\ell} = (-1)^{\nu-\ell-1}\left[\frac{\Gamma(\nu-\ell)}{2\nu\,\zeta(\nu)\,(\nu+\ell)\,\Gamma(\nu+\ell)\,\Gamma^2(\nu+\ell+1)}\right]^{1/2} .$$

$\Gamma(z)$ is the gamma function and the quantity $\zeta(\nu)$ is defined by

$$\zeta(\nu) = 1 + \frac{\partial\mu}{\partial\nu} \quad ,$$

where $\mu = n - \nu$ is the "quantum defect" parameter and n is the nominal principal quantum number of the state.

When ν is a positive integer, Eqs. (16) - (18) reduce to the hydrogenic case.

Evaluation of the QDM matrix element is lengthy but straightforward. The result for a transition between the ground state $|\nu s\rangle$ and excited state $|\nu' p\rangle$ is

$$\sum_{i=1}^{3}\left|\langle \nu' p|x_i|\nu s\rangle\right|^2_{av} = \frac{4\,a^{*\prime 2}}{3\nu\nu'}\left(\frac{a^{*\prime}}{a^*}\right)^{2\nu+1}\beta_0^2\left|N_{\nu' 1}\right|\left|N_{\nu 0}\right|^2\left(\frac{2}{\nu}\right)^{2\nu}\left(\frac{2}{\nu'}\right)^{2\nu'} \times$$

$$\times\left\{\sum_{t=0}^{t'_c}\beta'_t\left(\frac{\nu'}{2}\right)^t\frac{\Gamma(\nu+\nu'+2-t)}{\left[\left(\frac{a^{*\prime}}{a^*}\right)^{\frac{1}{\nu}}+\frac{1}{\nu'}\right]^{\nu+\nu'+2-t}}\right\}^2 , \qquad (19)$$

where primes refer to the excited state. For donors the ground and excited states have the same effective Bohr radius, but for acceptors the $P_{3/2}$ and $P_{1/2}$ states have different effective Bohr radii a* and a*' respectively. Fig. 1 shows schematically the transitions for the two cases.

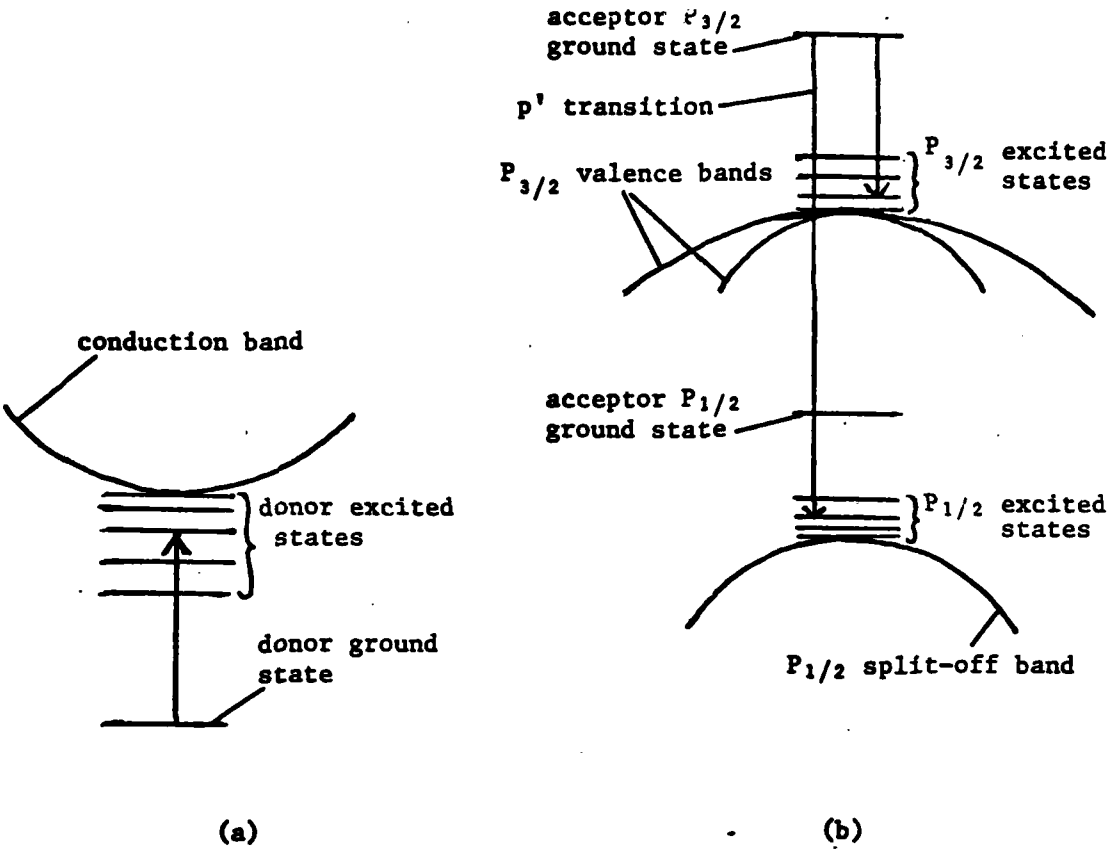


Fig.1 Schematic representation of (a) transitions between donor levels and (b) transitions between acceptor $P_{3/2}$ ground state and $P_{1/2}$ excited states, in silicon.

IV. NUMERICAL RESULTS

The model presented here requires a choice of the effective Rydberg R* or, equivalently, of the effective mass parameter m*. For donor electrons the value R* = 29.2 meV was used, based on the effective-mass calculation of Kohn and Luttinger.[5] This corresponds to $m^* = 0.294 m_o$, where m_o is the bare electron mass. For the $P_{1/2}$ states of acceptor holes we use R* = 26.15 meV, corresponding to $m^* = 0.250\ m_o$,[6] while for the $P_{3/2}$ states we use R* = 26 meV[3,4] ($m^* = 0.362\ m_o$). The positions of the Group V donor lines were taken from the tabulation by Kogan and Lifshits[7] and those for the Group III acceptor lines from Onton et al[8], Rome et al[9] and Rome.[10]

Table I shows the results for the donor line strengths relative to the $|1s\rangle \rightarrow |2p_{\pm}\rangle$ line. Also shown are the results of an effective-mass calculation by Kohn[11] for Si(P), which takes mass anisotropy into

account, and experimental values for Si(P) inferred from the linewidth measurements of Jagannath et al.[12] It is seen that the model overestimates by about a factor of two the $|1s> \rightarrow |3p_o>$ line strengh and underestimates by about 60% the $|1s> \rightarrow |3p\pm>$ strength.

Table II summarizes the results for the acceptors, normalized to the 2p′ line. The model underestimates the 3p′ line by about 50% and, except for In, the weak 4p′ line by a factor of ten. The experimental strengths have not been corrected for instrumental broadening, so are probably an overestimate.

Detailed calculations of line strengths for the transitions to $P_{3/2}$ excited states indicated in Fig. 1(b) have not been included because of the difficulty in describing these states as pure atomic-like orbitals.

Table I. Relative line strengths for Group V donors in Si, normalized to the $|1s> \rightarrow |2p\pm>$ line for each species. The "nominal" principal quantum numbers are used in labeling the states. The column labelled "expt." is inferred from Ref. 12.

Transition	Bi	Sb	As	P	P(Ref11)	P(expt)
$\|1s> \rightarrow \|2p_o>$	0.604	0.483	0.572	0.540	0.38	0.409
$\|1s> \rightarrow \|2p_\pm>$	1.000	1.000	1.000	1.000	1.00	1.000
$\|1s> \rightarrow \|3p_o>$	0.146	0.257	0.211	0.253	0.04	0.121*
$\|1s> \rightarrow \|3p_\pm>$	0.058	0.173	0.112	0.161	0.29	0.432

Table II. Relative line strengths for the p′ series of Group III acceptors in Si, normlalized to the 2p′ line for each species. The summetry of the final state was taken to be Γ_6 for all three lines[8].

	Calculated			Observed[10]		
	2p′	3p′	4p′	2p′	3p′	4p′
B	1.000	0.113	0.0037	1.000	0.174	0.044
Al	1.000	0.101	0.0018	1.000	0.231	0.040
Ga	1.000	0.107	0.0023	1.000	0.199	0.024
In	1.000	0.123	0.043	1.000	0.250	0.047

V. RECOMMENDATIONS

While it is possible that a more sophisticated model which incorporates band degeneracy and the anisotropy of the effective mass and which calculates accurately the ground-state wave function near the impurity would yield quantitatively correct results for the relative line strengths for photoabsorption, it is important to place this work in proper perspective. As an analytical tool, photoabsorption is of little value at concentrations below about $10^{14}/cm^3$ and also for optically thin films of thickness 1 micron or less. High-purity materials with impurity content as low as $10^{10}/cm^3$ are important for applications such as nuclear radiation detectors, while in the area of thin films, devices with film thicknesses of order 1000 Å are under development. A promising technique of high sensitivity for studying impurity excitation spectra in such cases is that of photothermal ionization. This is more complicated than photoexcitation, for it is a two-step process in which photoexcitation is followed by thermal excitation into the conduction band.

It is recommended that future work be directed toward developing a semi-empirical model for obtaining impurity concentrations in silicon from photothermal ionization spectroscopy. Recently Darken[13] has reported the successful use of this technique for acceptors in germanium of high purity. It may be possible to modify his method to make it suitable for analyzing high-purity silicon.

AKNOWLEDGEMENTS

The author would like to thank the Air Force Systems Command, the Air Force Office of Scientific Research and the Southeastern Center for Electrical Engineering Education for the opportunity of spending the summer at the AFWAL Materials Laboratory, Wright - Patterson AFB, where this research was performed.

He would like to express his gratitude to the staff of the Laser and Optical Materials Branch, in particular Drs. Melvin Ohmer, Patrick Hemenger, David Fischer and Gail Brown, for suggesting this area of research and for their very helpful guidance. Many thanks go also to John Rome for providing line strength data.

REFERENCES

1. Lax, M., "The Influence of Lattice Vibrations on Electronic Transitions in Solids," Proc. Photoconductivity Conf. Nov 4-6, 1954, Wiley, New York 1956, pp. 111 - 145.

2. Griem, H.R., Plasma Spectroscopy, McGraw - Hill, New York 1964.

3. Schecter, D., "Theory of Shallow Acceptor States in Si and Ge," J. Phys. Chem. Solids, Vol. 23, 1962, pp. 237 - 247.

4. Bebb, H.B. and Chapman, R.A., "Application of Quantum Defect Techniques to Photoionization of Impurities in Semiconductors," J. Phys. Chem. Solids, Vol. 28, 1967, pp. 2087 - 2097.

5. Kohn, W. and Luttinger, J.M., "Theory of Donor States in Silicon," Phys. Rev., Vol. 98, 1955, pp. 915 - 922.

6. Zwerdling, S., Button, K.J., Lax, B. and Roth, L.M., "Internal Impurity Levels in Semiconductors: Experiments in p-Type Silicon," Phys. Rev. Letts., Vol. 4, 1960, pp. 173 - 176.

7. Kogan, S.M. and Lifshits, T.M., "Photoelectric Spectroscopy - A New Method of Analysis of Impurities in Semiconductors," phys. stat. sol. (a), Vol. 39, 1977, pp. 11-39.

8. Onton, A., Fisher, P. and Ramdas, A.K., "Spectroscopic Investigation of Group-III Acceptor States in Silicon," Phys. Rev., Vol. 163, 1967, pp. 686-703.

9. Rome, J.J., Spry, R.J., Chandler, T.C. and Brown, G.J., "Additional $P_{3/2}$ and $P_{1/2}$ Infrared Excited State Lines of Gallium and Indium in Silicon," AFWAL-TR-81-4149.

10. Rome, J., (Unpublished).

11. Kohn, W., "Interpretation of Donor State Absorption Lines in Silicon," Phys. Rev, Vol. 98, 1955, pp. 1856 - 1857.

12. Jagannath, C., Grabowski, Z.W. and Ramdas, A.K., "Linewidths of the Electronic Excitation Spectra of Donors in Silicon," Phys. Rev. B, Vol. 23, 1981, pp. 2082 - 2098.

13. Darken, L.S., "Photothermal Ionization Spectroscopy of Acceptors in High Purity Germanium," J. App. Phys., Vol. 53 , 1982, pp. 3754 - 3764.

1982 USAF-SCEEE SUMMER FACULTY RESEARCH PROGRAM

Sponsored by the

AIR FORCE OFFICE OF SCIENTIFIC RESEARCH

Conducted by the

SOUTHEASTERN CENTER FOR ELECTRICAL ENGINEERING EDUCATION

FINAL REPORT

Prepared by:	Dr. Albert W. Biggs
Academic Rank:	Professor
Department and University:	Electrical Engineering Department University of Kansas
Research Location Branch:	Rome Air Development Center Electromagnetic Techniques Branch Hanscom AFB, MA 01731
USAF Research Colleague:	Dr. J. Leon Poirier
Date:	September 7, 1982
Contract No:	F49620-80-C-0035

Acknowledgement

The author would like to thank the Air Force Systems Command, the Air Force Office of Scientific Research and the Southeastern Center for Electrical Engineering Education for providing him with the opportunity to spend a very worthwhile and interesting summer at the Rome Air Development Center, Hanscom AFB, Massachusetts. He would like to acknowledge the Center, in particular the Electromagnetic Techniques Branch, for its hospitality and excellent working conditions.

Finally, he would like to thank Dr. J. Leon Poirier for suggesting this area of research and for his collaboration and guidance, and he would like to acknowledge helpful discussions with Mr. Otho E. Kerr, Jr.

FEASIBILITY AND IMPLEMENTATION OF A NEAR FIELD ANTENNA RANGE

by

Albert W. Biggs

ABSTRACT

Feasibility and implementation of a near field antenna range for large antenna arrays are investigated. The investigation also includes adaptive antenna arrays at near field ranges. Advantages and disadvantages of near field over direct far field antenna pattern measurements are compared. Descriptions of the basic theory of probe-compensated near field techniques and adaptive nulling are presented so that multiple usage of the near field range antenna arrays may be demonstrated.

I. INTRODUCTION

Most of the experimental measurements made on antennas relate to the fundamental characteristics of the antennas that determine their immediate application. Some of these characteristics are input impedances, far field antenna patterns, and gains or efficiencies. However there are occasions when it is necessary to have information about the current or charge distribution on the antenna, and the distribution of the near fields in the immediate vicinity of the antenna.

The near fields of the antenna can be divided into the "reactive near field" and the "radiating near field."[1] The reactive near field immediately surrounds the antenna with a usual outer limit approximately a wavelength. The radiating near field is beyond the reactive near field with electric and magnetic fields varying inversely with distance. It extends to a distance $2D^2/\lambda$ from a illuminated radiating aperture of diameter D, and much greater distances for noncophasal aperture distributions.

Far field antenna pattern measurements involve probing the field at a constant radius large enough to make the aperture resemble a point source. When the antenna is a large array, the required distance may be several thousands of feet and finding a suitable test site becomes a formidable problem. One solution to this problem is a physical modification of the antenna range or antenna under test. A second solution, which is discussed in this paper, is measurement of near field patterns or field distributions with computational techniques to predict approximate far field antenna patterns.

In addition to the far field range size limitation described above, several other advantages of near field measurements include the following.

(1) For large antenna systems, far field size limitations, transportation

and mounting problems, and the need for large positioners are eliminated.

(2) Near field measurements are time and cost effective. Accuracy of computed antenna patterns is equal to or better than that of the far field range.

(3) Near field ranges have controlled environments and all-weather capabilities.

The disadvantages of near field measurements are the following.

(1) More complex and expensive measurement systems are required.

(2) More extensive procedures are required to calibrate near field measurement probes than those for far field probes.

(3) The far field antenna patterns are not directly obtained in real time.

(4) Computer software is an essential factor in calculating patterns. As antenna arrays increase in size, similar increases occur in microprocessors and related computer software.

The theory, computer programs, and measurement capabilities for predicting far field antenna patterns by measuring near field coupling between test and probe antennas are adequate to develop a near field antenna range[2-10]. Near field measurements on planar surfaces[4-6] have attracted the most interest. Some of this interest is due to the degree of mathematical and computational simplicity. One major disadvantage is the limitation of calculating the antenna pattern only in a cone with an apex angle less than 180° without repeating measurements. This limitation is partially overcome with the cylindrical measurement surface[9]. The spherical surface is the most attractive because the complete 4π steradian pattern can be computed from one measurement[11]. However the computational limitations favor planar and cylindrical surfaces. In both

configurations all numerical integrations can be performed with the fast Fourier Transform (FFT) algorithm. This is not performable for spherical surfaces.

II. THEORY OF NEAR FIELD PROBE COMPENSATION

The theory of proble compensated measurements on planar surfaces is based on expansion of the antenna fields of test antenna and probe antenna into elementary plane waves or modes[7]. The modes are an angular spectrum of plane waves described by Booker and Clemmow[12]. According to the technique initially described by Brown and Jull[13], the Lorentz reciprocity theorem is then used to calculate the probe output as a function of an algebraic equation which relates the known field of the probe to the unknown fields radiated by the test antenna. The unknown mode amplitudes are then determined from this equation. The near field antenna pattern is finally calculated from the modal amplitudes.

Any arbitrary monochromatic wave may be seen as a superposition of plane waves. They have the same frequency, but travel in different directions with different amplitudes. The purpose of plane wave expansions is to find the unknown amplitudes and directions of the plane waves in the superposition. The resulting summation is a modal expansion of the original arbitrary wave.

In a linear, homogeneous, isotropic, and charge free region, and for harmonic time dependence $\exp(j\omega t)$, Maxwell's equations yield the vector Helmholtz equation

$$\nabla^2 \vec{E} + k^2 \vec{E} = 0, \qquad (1)$$

for the electric field $\vec{E}$, and the same equation for the magnetic field $\vec{H}$, where

$$k^2 = \omega^2 \mu \varepsilon - j\omega\mu\sigma, \qquad (2)$$

where ε, μ, σ are permittivity, permeability, and conductibity of the medium. In free space, $\sigma = 0$. The simplest solution of Eq. (1) in rectangular coordinates is

$$\vec{E} = \vec{A}(\vec{k})\, e^{-j\vec{k}\cdot\vec{r}}, \qquad (3)$$

where the exponent is

$$\vec{k}\cdot\vec{r} = (k_x\hat{x} + k_y\hat{y} + k_z\hat{z})\cdot(x\hat{x} + y\hat{y} + z\hat{z})$$
$$= k_x x + k_y y + k_z z. \qquad (4)$$

The propagation factor $\vec{k}$ is also called the vector wave number, while $\vec{A}(\vec{k})$ is the vector amplitude of the wave.

The dot product of the wave number $\vec{k}$ with itself yields

$$\vec{k}\cdot\vec{k} = k^2 = k_x^2 + k_y^2 + k_z^2 = \omega^2\mu\varepsilon, \qquad (5)$$

and only two of the components of $\vec{k}$ can be independently specified. If these are k_y and k_z, then the third component is

$$k_x = \sqrt{k^2 - k_y^2 - k_z^2}, \quad k^2 > k_y^2 + k_z^2,$$
$$= -j\sqrt{k_y^2 + k_z^2 - k^2}, \quad k^2 < k_y^2 + k_z^2, \qquad (6)$$

The relationship between $\vec{k}$ and $\vec{A}(\vec{k})$ is seen by

$$\begin{aligned}\nabla\cdot\vec{E} &= \nabla\cdot\vec{A}(\vec{k})e^{-j\vec{k}\cdot\vec{r}} \\ &= \vec{A}\cdot\nabla e^{-j\vec{k}\cdot\vec{r}} \\ &= -j\left[k_x A_x(\vec{k}) + k_y A_y(\vec{k}) + k_z A_z(\vec{k})\right] \\ &= 0, \end{aligned} \tag{7}$$

because the region is charge free, so that

$$\vec{k}\cdot\vec{A}(\vec{k}) = 0, \tag{8}$$

so that, like k_x,

$$A_x(\vec{k}) = -\frac{1}{k_x}\left[k_y A_y(\vec{k}) + k_z A_z(\vec{k})\right] \tag{9}$$

The magnetic field $\vec{H}$ is

$$\begin{aligned}\vec{H} &= -\frac{1}{j\omega\mu}\nabla\times\vec{E} = -\frac{1}{j\omega\mu}\nabla e^{-j\vec{k}\cdot\vec{r}}\times\vec{A}(\vec{k}) \\ &= \frac{-1}{j\omega\mu}\left[-j(k_x\hat{x} + k_y\hat{y} + k_z\hat{z})e^{-j\vec{k}\cdot\vec{r}}\right]\times\vec{A}(\vec{k}) \\ &= \frac{1}{\omega\mu}\vec{k}\times\vec{A}(\vec{k})e^{-j\vec{k}\cdot\vec{r}}. \end{aligned} \tag{10}$$

The general solutions for $\vec{E}(\vec{r})$ and $\vec{H}(\vec{r})$ are formed from summing over all values of k_y and k_z,

$$\vec{E}(\vec{r}) = \iint_{-\infty}^{\infty} \vec{A}(\vec{k}) e^{-j\vec{k}\cdot\vec{r}} \, dk_y dk_z,$$

$$\vec{H}(\vec{r}) = \frac{1}{\omega\mu} \iint_{-\infty}^{\infty} \vec{k} \times \vec{A}(\vec{k}) e^{-j\vec{k}\cdot\vec{r}} \, dk_y dk_z, \tag{11}$$

(12)

The function $\vec{A}(\vec{k})$ is the plane wave spectrum and is found analytically if the tangential fields are known at every point on the plane x = d. Thus,

$$E_y(d,y,z) = \iint_{-\infty}^{\infty} A_y(\vec{k}) e^{-jk_x d} \cdot$$

$$\cdot e^{-j(k_y y + k_z z)} \, dk_y dk_z, \tag{13}$$

with the same expression for E_z when A_y is replaced by A_z. Since Eq. (13) is a two dimensional inverse Fourier transform of A_y, then

$$A_y(\vec{k}) = \frac{e^{jk_x d}}{4\pi^2} \iint_{-\infty}^{\infty} E_y(d,y,z) e^{j(k_y y + k_z z)} \, dy dz, \tag{14}$$

with the same form for A_z when E_y is replaced by E_z.

The saddle point method[14], or method of steepest descent, is applied to Eq. (14) with the asymptotic solution,

$$\vec{E}(\vec{r}) = j \frac{2\pi}{r} k_{xo} \vec{A}(\vec{k}_o) e^{-jkr}, \tag{15}$$

where $\vec{k}_o$ and the unit vector $\hat{r}$ are

$$\vec{k}_o = k\hat{r},$$
$$\hat{r} = \sin\theta\cos\phi\,\hat{x} + \sin\theta\sin\phi\,\hat{y} + \cos\theta\,\hat{z}. \tag{16}$$

Knowledge of the tangential fields on a planar surface will provide the plane wave spectrum, and the plane wave spectrum will proide the field distribution in space. When a probe antenna is introduced to measure the tangential fields on the planar surface, the probe perturbs the fields on the surface so that the actual planar distribution is never seen. If negligible mutual coupling between probe and test antennas is assumed, probe perturbations can be compensated with the Lorentz reciprocity theorem.

Figure 1 is the coordinate systems for the test and probe antennas. The field radiated by test antenna A is measured on the plane $x = a + b = x_o$ by moving probe antenna over this plane. The source free volume V is bounded by a surface Σ, which is the infinite plane S_o at $x = a$, the surface S_1 at infinity, and the surface Σ_b around the probe antenna. The surface S_1 is an infinite hemisphere. The electric and magnetic fields are $\vec{E}_a$ and $\vec{H}_a$, primary fields from test antenna A, $\vec{E}_{as}$ and $\vec{H}_{as}$, secondary fields reflected or scattered by antenna A when radiated by transmitting probe antenna B, $\vec{E}_b$ and $\vec{H}_b$, primary fields from probe antenna B, $\vec{E}_{bs}$ and $\vec{H}_{bs}$, secondary fields reflected or scattered by antenna B when radiated by transmitting test antenna A, $\vec{J}_a$, $\vec{J}_{as}$, $\vec{J}_b$, $\vec{J}_{bs}$ are current densities associated with the above fields.

If we consider Green's theorem for the volume V covered by a surface Σ,

$$\int_{\Sigma} \vec{F}\cdot d\vec{S} = \int_{Vol\,V} \nabla\cdot\vec{F}\,dv\,, \tag{17}$$

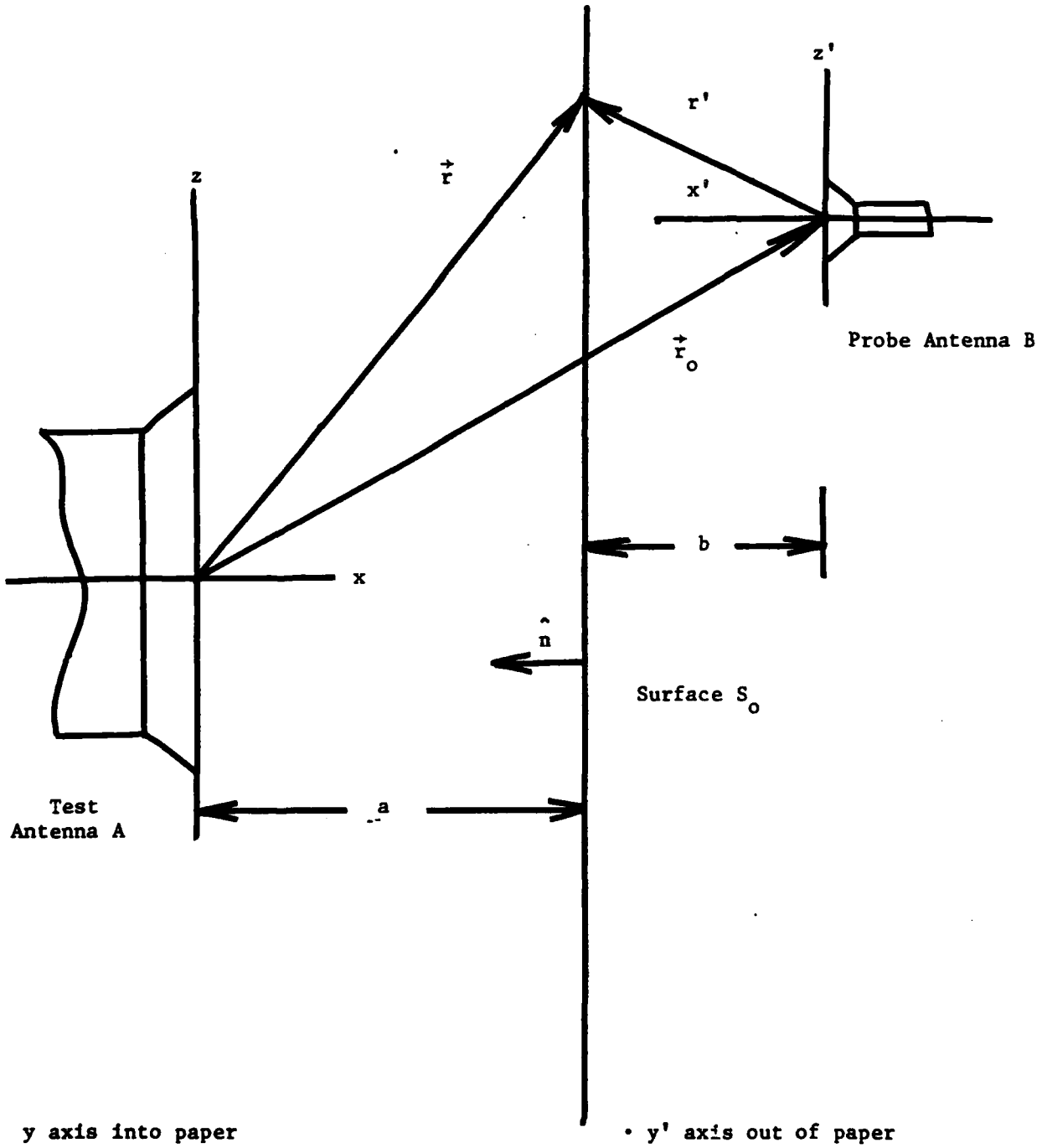


FIGURE 1: Test and Probe Antenna Coordinate System

where $\vec{F}$ is an arbitrary vector of surface and volume coordinates, and if

$$\vec{F} = \vec{E}_1 \times \vec{H}_2 - \vec{E}_2 \times \vec{H}_1, \tag{18}$$

then

$$\begin{aligned} &\int_\Sigma \{\vec{E}_1 \times \vec{H}_2 - \vec{E}_2 \times \vec{H}_1\} \cdot d\vec{S} \\ &= \int_V \nabla \cdot \{\vec{E}_1 \times \vec{H}_2 - \vec{E}_2 \times \vec{H}_1\} dv \\ &= \int_V \{\vec{J}_1 \cdot \vec{E}_2 - \vec{J}_2 \cdot \vec{E}_1\} dv, \end{aligned} \tag{19}$$

where Maxwell's equations were in the form

$$\nabla \times \vec{H}_1 = j\omega\epsilon\vec{E}_1 + \vec{J}_1, \quad \nabla \times \vec{E}_1 = -j\omega\mu\vec{H}_1, \tag{20}$$

with a second set formed by replacing subscript (1) by (2). Application of the Lorentz reciprocity theorem to the source free volume V enclosed by the surface Σ yields

$$\begin{aligned} \int_\Sigma \{&(\vec{E}_a + \vec{E}_{bs}) \times (\vec{H}_b + \vec{H}_{as}) - (\vec{E}_b + \vec{E}_{as}) \\ &\times (\vec{H}_a + \vec{H}_{bs})\} \cdot \hat{n}\, da = 0. \end{aligned} \tag{21}$$

The surface integral in Eq. (21) includes the infinite plane S_o, the infinite half sphere surface S_1, and the surface Σ_B. Thus the integral over S_o plus that over S_1 plus that over Σ_B equal zero.

The integral over the hemisphere S_1 vanishes because the fields are TEM waves as they approach the surface. With the relationships,

$$\vec{H} = \frac{1}{\omega\mu}\vec{k}\times\vec{E} = \frac{1}{\omega\mu}(k\hat{n})\times\vec{E}$$
$$= \frac{k}{\omega\mu}\hat{n}\times\vec{E} = \frac{1}{\eta}\hat{n}\times\vec{E}, \qquad (22)$$

where η is the characteristic impedance of free space, the integrand in Eq. (21) becomes

$$\left[(\vec{E}_a+\vec{E}_{bs})\times\left(\frac{1}{\eta}\hat{n}\times[\vec{E}_b+\vec{E}_{as}]\right)\right.$$
$$\left.-(\vec{E}_b+\vec{E}_{as})\times\left(\frac{1}{\eta}\hat{n}\times[\vec{E}_a+\vec{E}_{bs}]\right)\right]\cdot\hat{n}$$
$$=\frac{1}{\eta}\left[\left([\vec{E}_a+\vec{E}_{bs}]\times[\hat{n}\times(\vec{E}_b+\vec{E}_{as})]\right)\right.$$
$$\left.-([\vec{E}_b+\vec{E}_{as}]\times[\hat{n}\times(\vec{E}_a+\vec{E}_{bs})])\right]\cdot\hat{n}$$
$$=0, \qquad (23)$$

with use of the vector identity

$$\vec{X} \times (\vec{Y} \times \vec{Z}) = (\vec{X} \cdot \vec{Z})\vec{Y} - (\vec{X} \cdot \vec{Y})Z \,. \tag{24}$$

The surface integral over Σ_B surrounds the probe antenna, and the unit surface normal $\hat{n}$ points inward to the probe. If

$$-\hat{n}_B = \hat{n}, \tag{25}$$

is substituted into Eq. (21), the resulting surface integral over Σ_B becomes

$$\begin{aligned} &\int_{\Sigma_B} [(\vec{E}_a + \vec{E}_{bs}) \times (\vec{H}_b + \vec{H}_{as}) - (\vec{E}_b + \vec{E}_{as}) \\ &\qquad \times (\vec{H}_a + \vec{H}_{bs})] \cdot (-\hat{n}_B)\, dS \\ &= -\int_{V_B} [(\vec{E}_b + \vec{E}_{as}) \cdot (\vec{J}_a + \vec{J}_{bs}) \\ &\qquad - (\vec{E}_a + \vec{E}_{bs}) \cdot (\vec{J}_b + \vec{J}_{as})]\, dv, \end{aligned} \tag{26}$$

where the volume V_B covers the probe antenna. The scattered field $\vec{E}_{bs}$ is zero because it is not present in V_B, while $\vec{J}_a$ and $\vec{J}_{as}$ are zero because they exist on the test antenna. In addition to these terms, $\vec{E}_{as}$ can be neglected in comparison with the field $\vec{E}_a$, so that Eq. (26) becomes

$$-\int_{V_B} [\vec{E}_b \cdot \vec{J}_{bs} - \vec{E}_a \cdot \vec{J}_b]\, dv \simeq -P_B(x_o), \tag{27}$$

where $P_B(x_o)$ is proportional to open-circuit voltage. $P_B(x_o)$ is proportional to the measured signal. The surface integral over S_o is the only term remaining, so it is

$$\int_{S_o} [(\vec{E}_a + \vec{E}_{bs}) \times (\vec{H}_b + \vec{H}_{as}) - (\vec{E}_b + \vec{E}_{as}) \times (\vec{H}_a + \vec{H}_{bs})] \cdot \hat{n}\, da = P_B(x_o). \tag{28}$$

In Eq. (28), cross products and dot products of primary and scattered terms vanish, and products of only scattered terms may be neglected so that the result is

$$\int_{S_o} (\vec{E}_a \times \vec{H}_b - \vec{E}_b \times \vec{H}_a) \cdot \hat{n}\, da = P_B(x_o). \tag{29}$$

If the primary fields are expanded in their wave number spectra on the surface S_o, x = a, then

$$\vec{E}_a(a,y,z) = \int_{-\infty}^{\infty}\int \vec{F}(k_y,k_z) e^{-j\vec{k}\cdot\vec{r}}\, dk_y\, dk_z, \tag{30}$$

$$\vec{H}_a(a,y,z) = \frac{1}{\omega\mu}\int_{-\infty}^{\infty}\int \vec{k} \times \vec{F}(k_y,k_z) e^{-j\vec{k}\cdot\vec{r}} \cdot dk_y\, dk_z, \tag{31}$$

where $\vec{H}_a$ is expressed in terms of the spectrum of $\vec{E}_a$ with Eq. (10). From Eq. (8),

$$\vec{k} \cdot \vec{E}(k_y, k_z) = 0, \tag{32}$$

so that only two components of $\vec{F}$ are independent, similar to the situation with $\vec{A}$ in Eq. (9). Similar expansions for $\vec{E}_b$ and $\vec{H}_b$ in primed coordinates and wave number spectrum $\vec{G}$ are

$$\vec{E}_b(b, y', z') = \iint_{-\infty}^{\infty} \vec{G}(k_y', k_z') e^{-j\vec{k}' \cdot \vec{r}'} \, dk_y' \, dk_z', \tag{33}$$

$$\vec{H}_b(b, y', z') = \frac{1}{\omega\mu} \iint_{-\infty}^{\infty} \vec{k}' \times \vec{G}(k_y', k_z') \cdot e^{-j\vec{k}' \cdot \vec{r}'} \, dk_y' \, dk_z', \tag{34}$$

$$\vec{k}' \cdot \vec{G}(k_y', k_z') = 0. \tag{35}$$

If the wave number spectra are substituted into Eq. (29), the result is a series of six integrations,

$$\int_{S_0} (\vec{E}_a \times \vec{H}_b - \vec{E}_b \times \vec{H}_a) \cdot \hat{n} \, da = \int_{-\infty}^{\infty} \int (\vec{E}_a \times \vec{H}_b - \vec{E}_b \times \vec{H}_a) \cdot (-\hat{x}) \, dy \, dz$$

$$= \frac{1}{\omega\mu} \int\int\int_{-\infty}^{\infty} \int\int\int [\vec{F}(k_y, k_z) \times \{\vec{k}' \times \vec{G}(k_y', k_z')\} - \vec{G}(k_y', k_z') \times \{\vec{k} \times \vec{F}(k_y, k_z)\}] \cdot (-\hat{x}) e^{-j(\vec{k}\cdot\vec{r} + \vec{k}'\cdot\vec{r}')}$$

$$\cdot dk_y' dk_z' dk_y dk_z dy dz$$

$$= P_B(r_o). \tag{36}$$

Equation (36) is integrated with respect to y and z with the relationships

$$\vec{r}_o = \vec{r} - \vec{r}', \quad \vec{r}' = \vec{r} - \vec{r}_o,$$

$$\vec{r}\cdot(\vec{k} - \vec{k}') = a(k_x - k_x') + y(k_y - k_y') + z(k_z + k_z'), \tag{37}$$

so that

$$\int\int_{-\infty}^{\infty} e^{-j\vec{k}\cdot\vec{r} - j\vec{k}'\cdot\vec{r}'} dy dz = e^{j\vec{k}'\cdot\vec{r}_o - ja(k_x - k_x')} \cdot \int\int_{-\infty}^{\infty} e^{-j(k_y - k_y')y - j(k_z + k_z')z} dy dz. \tag{38}$$

In Eq. (38), the Dirac delta function,

$$\delta(x) = \lim_{L\to\infty} \frac{\sin Lx}{\pi x} = \frac{1}{2\pi}\int_{-\infty}^{\infty} e^{jxt}\,dt, \tag{39}$$

transforms the integral in Eq. (38) to

$$4\pi^2 e^{j\vec{k}\cdot\vec{r}_o - j\alpha(k_x - k_x')}\,\delta(k_y - k_y')\cdot \cdot\delta(k_z + k_z'). \tag{40}$$

The next integration is with respect to k_y' and k_z', at $k_y' = k_y$ and $k_z' = -k_z$, so that the resulting expression is

$$\frac{4\pi^2}{\omega\mu}\int_{-\infty}^{\infty}\int\{\vec{F}(k_y,k_z)\times[\vec{k}\times\vec{G}(k_y,-k_z)] + \vec{G}(k_y,-k_z)\times[\vec{k}\times\vec{F}(k_y,-k_z)]\}\cdot\hat{x} \cdot e^{-j\vec{k}\cdot\vec{r}_o}\,dk_y dk_z = P_B(r_o), \tag{41}$$

and with Eqs. (32) and (35), it simplifies to

$$\frac{8\pi^2}{\omega\mu}\int_{-\infty}^{\infty}\int\{\vec{F}(k_y,k_z)\cdot\vec{G}(k_y,-k_z)\}k_x \cdot e^{-j\vec{k}\cdot\vec{r}_o}\,dk_y dk_z = P_B(r_o). \tag{42}$$

Equation (42) is a two dimensional Fourier transform on the $x = x_o$ plane. The inverse Fourier transform is

$$k_x \vec{F}(k_y, k_z) \cdot \vec{G}(k_y, -k_z) = \frac{\omega\mu}{2\pi^4} \int_{-\infty}^{\infty}\int P_B(r_o) e^{-j\vec{k}\cdot\vec{r}_o} dy\, dz. \tag{43}$$

Equations (42) and (43) describe the result of probe compensation in rectangular coordinates. Similar expressions in spherical coordinates are more appropriate because antenna pattern measurements are made in these coordinates. Transformation to spherical coordinates is made by recalling Eqs. (11) and (15). Comparing Eqs. (30) and (33) for $\vec{E}_a$ and $\vec{E}_b$, respectively, with Eqs. (11) and (15) provide saddle point solutions,

$$\vec{E}_a(a, y, z) = j\frac{2\pi}{r} k_x \vec{F}(k_y, k_z) e^{-jkr}, \tag{44}$$

$$\vec{E}_b(b, y', z') = j\frac{2\pi}{r'} k_x' \vec{G}(k_y', k_z') e^{-jk'r'}, \tag{45}$$

where $\vec{F}$ and $\vec{G}$ become

$$\vec{F}(k_y, k_z) = \frac{re^{jkr}}{j2\pi k_x} \vec{E}(a, y, z), \tag{46}$$

$$\vec{G}(k_y,-k_z) = \frac{r' e^{-jkr'}}{j 2\pi k_x} \vec{E}'(b,y,z), \tag{47}$$

so that Eq. (43), in spherical coordinates, is

$$k_x \vec{F}(k_y,k_z)\cdot\vec{G}(k_y,-k_z) = -\frac{rr'}{4\pi^2 k_x} e^{jkr_o}\{\vec{E}(\theta,\phi)\cdot\vec{E}'(\theta',\phi')\}$$
$$= \frac{\omega\mu}{32\pi^4}\int_{-\infty}^{\infty}\iint P_B(r_o) e^{j\vec{k}\cdot\vec{r}_o} dy\,dz. \tag{48}$$

Since $\phi' = \theta$ and $\theta' = \pi - \theta$, and unit vectors are related by $\hat{\theta} = \hat{\theta}'$ and $\hat{\phi} = -\hat{\phi}'$,

$\vec{E}(\theta, \phi) = E_\theta(\theta, \phi)\hat{\theta} + E_\phi(\theta, \phi)\hat{\phi}$,

$\vec{E}'(\theta', \phi') = E_{\theta'}(\pi - \theta, \phi)\hat{\theta} - E_{\phi'}(\pi - \theta, \phi)\hat{\phi}$,

$\vec{k}\cdot\vec{r}_o = (k\sin\theta\cos\phi\,\hat{x} + k\sin\theta\sin\phi\,\hat{y} + k\cos\theta z)\cdot(x_o\hat{x} + y\hat{y} + z\hat{z})$

$= kx_o\sin\theta\cos\phi + ky\sin\theta\sin\phi + kz\cos\theta,$ (49)

Eq. (48) is written as

$$E_\theta(\theta,\phi)E_\theta'(\pi-\theta,\phi) - E_\phi(\theta,\phi)E_\phi'(\pi-\theta,\phi)$$
$$= C\sin\theta\cos\phi\, e^{jk_x x_o}\iint_{-\infty}^{\infty} P_B(x_o) \cdot e^{j(k_y y + k_z z)} dy\,dz, \tag{50}$$

where the constant C is

$$C = -\frac{15k^2}{\pi r r'} e^{-jkr_o}, \qquad (51)$$

and includes any instrument calibration.

III. THE PLANAR SURFACE

In a planar near field measurement, the probe antenna will respond predominantly to one of two preselected polarization components of the near field on the plane. These usually correspond to the horizontal and vertical components of the electric field. Determination of the test antenna far field requires that both polarization components of the near field be measured. This requires a rotational capability in the probe antenna.

The probe output is a sinusoidal signal whose amplitude and phase depend on location on the measurement plane. Amplitude and phase are detected with a coherent phase and amplitude receiver. This allows the detected signal to be described as a complex voltage which depends only on position. The probe output is indicated by $V_V(x_o, y, z)$ and $V_H(x_o, y, z)$, whre subscripts V and H indicate vertical and horizontal polarization, respectively.

Since $P_B(r_o)$ is proportional to the voltage induced in the probe antenna,

$$C P_B(r_o) = V(x_o, y, z), \qquad (52)$$

which represents the probe output. For the two polarizations, Eq. (50) becomes

$$E_\theta(\theta,\phi)E_\theta^V(\pi-\theta,\phi) - E_\phi(\theta,\phi)E_\phi^V(\pi-\theta,\phi)$$
$$= \sin\theta\cos\phi\, I_V(\theta,\phi), \tag{53}$$

$$E_\theta(\theta,\phi)E_\theta^H(\pi-\theta,\phi) - E_\phi(\theta,\phi)E_\phi^H(\pi-\theta,\phi)$$
$$= \sin\theta\cos\phi\, I_H(\theta,\phi), \tag{54}$$

where the far fields of the probe antenna are, with V and H for polarizations,

$$\vec{E}^V(\theta',\phi') = E_\theta^V(\pi-\theta,\phi)\hat{\theta} + E_\phi^V(\pi-\theta,\phi)\hat{\phi},$$
$$\vec{E}^H(\theta',\phi') = E_\theta^H(\pi-\theta,\phi)\hat{\theta} + E_\phi^H(\pi-\theta,\phi)\hat{\phi}, \tag{55}$$

and where the integals $I_H(\theta, \phi)$ and $I_V(\theta, \phi)$ are

$$I_V(\theta,\phi) = e^{jk_x x_o}\int_{-\infty}^{\infty}\int V_V(x_o,y,z) \cdot e^{j(k_y y + k_z z)}\,dy\,dz, \tag{56}$$

$$I_H(\theta,\phi) = e^{jk x_o}\int_{-\infty}^{\infty}\int V_H(x_o,y,z) \cdot e^{j(k_y y + k_z z)}\,dy\,dz. \tag{57}$$

$$E_\theta(\theta,\phi) = \sin\theta\cos\phi \cdot \frac{I_H(\theta,\phi)E_\phi^V(\pi-\theta,\phi) - I_V(\theta,\phi)E_\phi^H(\pi-\theta,\phi)}{E_\theta^H(\pi-\theta,\phi)E_\phi^V(\pi-\theta,\phi) - E_\theta^V(\pi-\theta,\phi)E_\phi^H(\pi-\theta,\phi)}, \tag{58}$$

$$E_\phi(\theta,\phi) = \sin\theta\cos\phi \cdot \frac{I_H(\theta,\phi)E^V_\theta(\pi-\theta,\phi) - I_V(\theta,\phi)E^H_\theta(\pi-\theta,\phi)}{E^H_\theta(\pi-\theta,\phi)E^V_\phi(\pi-\theta,\phi) - E^V_\theta(\pi-\theta,\phi)E^H_\phi(\pi-\theta,\phi)} \quad (59)$$

so that with E^V_θ, E^V_θ and E^V_θ, E^H_V for the probe antenna known, only the integrals I_V and I_H must be calculated in order to find the test antenna antenna pattern.

IV. SPATIAL SAMPLING IN NEAR FIELD RANGES

The space available for the near field antenna range is a rectangular room, 37 feet 6 inches long by 24 feet wide by 8 feet high. The exterior wall is 37 feet 6 inches long with a window 4 feet high by 6 feet 8 inches wide. The interior wall narrows to 32 feet 6 inches long with recesses for four doors, all 4 feet wide. These dimensions are described because they determine the configuration of the test antenna. An envelope specification of the test antenna is a planar array with maximum dimensions of 1 meter by 7 meters. The planar arrray will have its axis horizontal with the floor and perpendicular to the exterior wall.

The planar array will be located with its back side parallel to the rear wall (with two doors). The planar measurement surface is arbitrarily chosen to be 5 to 10 wavelengths from the array surface. With a frequency range 3-4 GHz, the wavelength is thus 7.5 - 10 cm, so the distance x_o becomes 0.75 - 1.00 meter.

The planar measurement surface, or sampling plane, has the coordinate system described in preceding sections. The vertical direction (up) is the

positive y-axis, the positive x-axis is normal from the planar surface, and the positive z-axis moves to the left across the face of the surface. The height and width of the sampling surface are Y and Z, respectively. The planar surface is also called the sampling surface because the probe antenna moves vertically and horizontally across the surface. As described in Section III, the detected probe output will be

$$V_V (x_o, y, z), V_H (x_o, y, z)$$

where subscripts V and H are vertical and horizontal polarizations of the probe, respectfully.

The two sets of measurements are made at a finite number of equally spaced intervals along the y and z axes so that Eqs. (56) and (57) may be numerically evaluated with the fast Fourier transform (FFT) technique. The sampling plane is divided into a grid of points defined by the coordinates $(x_o, m\Delta y, n \Delta z)$, where $0 \leq m \leq M-1$ and $0 \leq n \leq N-1$, and M and N are positive integers. These intergers are $m=Y/\Delta y + 1$ and $N = Z/\Delta z+1$. The probe responses at these grid points are $V_V(x_o, m \Delta y, n \Delta z)$ and $v_H (x_o, m \Delta y, n \Delta z)$. These responses are used with the FFT to compute Eqs. (56) and (57) at wave numbers defined by discrete Fourier transform theory and are

$$k_y = \frac{2m\pi}{M\Delta_y}, \quad -\frac{M}{2} \leq m \leq \frac{M}{2} - 1,$$

$$k_z = \frac{2n\pi}{N\Delta z}, \quad -\frac{N}{2} \leq n \leq \frac{N}{2} - 1. \qquad (60)$$

The spherical coordinates at these wave numbers are

$$\cos\theta = \frac{n\lambda}{N\Delta z},$$

$$\sin\phi = \frac{m\lambda/M\Delta y}{\sqrt{1-(n\lambda/N\Delta z)^2}}, \quad (61)$$

where spacings Δy and Δz must be less than $\lambda/2$, where λ is the signal wavelength. The spacings Δy and Δz are selected by the attenuation desired for evanescent waves[6],

$$\alpha = 54.6\,L\left[\left(\frac{\lambda}{2\Delta s}\right)^2 - 1\right]^{\frac{1}{2}}, \quad (62)$$

where $\Delta s = \Delta y = \Delta z$ and L is the number of wavelengths between the planar and the array surfaces, $x_o = L\lambda$.

V. NEAR ZONE MEASUREMENTS OF ADAPTIVE ANTENNA ARRAYS

The antenna array described here is an equispaced linear array with 2N + 1 isotropic elements spaced a distance d from each other. The space factor $S(\theta)$ is equivalent to the antenna pattern for isotropic sources, and in terms of θ and d,

$$S(\theta) = \sum_{m=-N}^{N} a_n e^{-jnkd\sin\theta}, \quad (63)$$

where a_n is the complex weight, phase and amplitude, of the nth array element. The pattern angle θ is measured from broadside. The array factor or power pattern is

$$|S(\theta)|^2 = \sum_{m=-N}^{N} \sum_{n=-N}^{N} a_m^* a_n e^{-j(n-m)kd\sin\theta} . \tag{64}$$

The maximum value of the mainlobe prior to adapting element weights to reduce power in a specific jamming region is in the broadside direction. This direction is chosen because a uniformly weighted array provides maximum signal to noise ratio (SNR) when noise interference levels are equal at each element and uncorrelated. With directional jamming, uniform weights do not optimize the SNR.

The space factor for a broadside array with uniform amplitude and zero phase element coefficients a_0 is

$$a_0 \sum_{n=-N}^{N} e^{-jkd\sin\theta} = a_0 \frac{\sin\left(\frac{2N+1}{2} kd\sin\theta\right)}{\sin\left(\frac{1}{2} kd\sin\theta\right)} . \tag{65}$$

The first nulls are at

$$\frac{2N+1}{2} kd\sin\theta = 0, \pi, \ldots, n\pi,$$

and if the mainlobe radiated field is replaced by a uniform field, the equivalent pattern lies in the interval between these nulls at $\pm \pi/2$. The mainlobe interval is then defined by

$$-\frac{\pi}{2N+1} \leq kd \sin\theta_M \leq \frac{\pi}{2N+1}, \tag{66}$$

where θ_M is

$$\sin\theta_M = \frac{\lambda/2d}{2N+1}. \tag{67}$$

Power P_M in the mainlobe is

$$P_M = \int_{-\theta_M}^{\theta_M} S(\theta) S^*(\theta) \cos\theta \, d\theta$$

$$= \frac{2\pi}{kd(2N+1)} \sum_{m=-N}^{N} \sum_{n=-N}^{N} a_m^* a_n \tag{68}$$

$$\cdot \frac{\sin\left[\frac{\pi(n-m)}{2N+1}\right]}{\left[\frac{\pi(n-m)}{2N+1}\right]}.$$

The jamming sector is

$$u_o - \Delta u \leq u \leq u_o + \Delta u, \tag{69}$$

where u_o is kd sin θ_o. The interference sector in Eq. (69) is symmetrical in "u space" but not in "θ space." If

$$\begin{aligned} \Delta u &= kd\left[\sin(\theta_o + \Delta\theta) - \sin\theta_o\right] \\ &= kd \sin(\theta_o + \Delta\theta) - u_o, \end{aligned} \tag{70}$$

where $\theta_o + \Delta\theta$ is the upper limit $\theta+$, then

$$kd \sin\theta^+ = u_o + \Delta u, \tag{71}$$

so that the lower limit $\theta-$ is

$$\begin{aligned} u_o - \Delta u &= 2u_o - kd \sin\theta^+ \\ &= kd \sin\theta^-. \end{aligned} \tag{72}$$

With these limits, the interference power P_N is

$$P_N = \int_{\theta^-}^{\theta^+} S(\theta)\, S^*(\theta) \cos\theta \, d\theta$$

$$= \frac{2\Delta u}{kd} \sum_{m=-N}^{N} \sum_{n=-N}^{N} a_m^* a_n e^{j(n-m)u_0} \cdot$$

$$\cdot \frac{\sin[(n-m)\Delta u]}{[n-m]\Delta u} \cdot \qquad (73)$$

The ratio of interference power P_N to the mainlobe power P_M is

$$p = \frac{P_N}{P_M} = \frac{(2N+1)}{\pi} \Delta u \cdot$$

$$\cdot \frac{\sum_{m=-N}^{N} \sum_{n=-N}^{N} a_m^* a_n N_{mn}}{\sum_{m=-N}^{N} \sum_{n=-N}^{N} a_m^* a_n M_{mn}}, \qquad (74)$$

where N_{mn} and M_{mn} are

$$N_{mn} = e^{-j(n-m)u_0} \frac{\sin[(n-m)\Delta u]}{[(n-m)\Delta u]}, \qquad (75)$$

$$M_{mn} = \frac{\sin\left[\frac{\pi(n-m)}{2N+1}\right]}{\left[\frac{\pi(n-m)}{2N+1}\right]} \quad . \qquad (76)$$

Equation (74) for p is wrtten as

$$p(A) = \frac{\Delta u}{u_M} \frac{A^+ N A}{A^+ M A} , \qquad (77)$$

where u_M is $\pi/(2N+1)$ and A is the column vector of complex weights a_n, and A+ is the Hermitian (complex conjugate) of A. It is a row vector.

A minimum value for p(A) is found when p(A) is stationary for small variations in A,

$$p(A) = p(A + \Delta A), \qquad (78)$$

so that Eq. (77) becomes

$$p(A + \Delta A) = \frac{(A + \Delta A)^+ N (A + \Delta A) \Delta u}{(A + \Delta A)^+ M (A + \Delta A) u_M} = p(A) = \frac{A^+ N A}{A^+ M A} \frac{\Delta u}{u_M} \quad . \qquad (79)$$

With cross-multiplying, cancelling terms, and dropping second order terms, the eigenvalue equation

$$p\frac{u_M}{\Delta u}MA = NA, \tag{80}$$

has 2N+1 independent eigenvectors satisfying

$$A_j^+ N A_i = 1, \quad i = j,$$
$$= 0, \quad i \neq j. \tag{81}$$

The smallest eigenvalue of Eq. (80) is the desired minimum interference power to mainlobe power (when multiplied by $\Delta u/u_B$).

This method is described for a three element array, N=1, with half wavelength spacing. The space factor is

$$S(\theta) = \frac{\sin\left(\frac{3\pi}{2}\sin\theta\right)}{\sin\left(\frac{\pi}{2}\sin\theta\right)}, \tag{82}$$

with maxima at $\theta = -90°$, $0°$, and $90°$, and minima at $\theta = -41.81°$ and $41.81°$. The mainlobe, at half intervals between the first nulls, has $u_M = \pi \sin\theta_M$ and θ_M selected to be 60° in the interference region and $\Delta\theta = 30°$,

$$u_0 = \pi \sin\theta_0 = 0.866\pi,$$
$$\Delta u = kd\sin(\theta_0+\Delta\theta) - u_0 = 0.134\pi,$$
$$\theta^+ = 90°, \quad \theta^- = 47.05°. \tag{83}$$

The ratio $\Delta u/u_B = 0.402$. The matrices N and M are

$$N = \begin{bmatrix} 1 & e^{-j u_0} \frac{\sin \Delta u}{\Delta u} & e^{-j 2u_0} \frac{\sin 2\Delta u}{2\Delta u} \\ e^{j u_0} \frac{\sin \Delta u}{\Delta u} & 1 & e^{-j u_0} \frac{\sin \Delta u}{\Delta u} \\ e^{j 2u_0} \frac{\sin 2\Delta u}{2\Delta u} & e^{j u_0} \frac{\sin \Delta u}{\Delta u} & 1 \end{bmatrix},$$

(84)

$$M = \begin{bmatrix} 1 & \frac{\sin \Delta u}{\Delta u} & \frac{\sin 2\Delta u}{2\Delta u} \\ \frac{\sin \Delta u}{\Delta u} & 1 & \frac{\sin \Delta u}{\Delta u} \\ \frac{\sin 2\Delta u}{2\Delta u} & \frac{\sin \Delta u}{\Delta u} & 1 \end{bmatrix},$$

(85)

The characteristic equations for these matrices are

$$[N-\lambda I]A=\left[\frac{\Delta u}{u_B}M-\lambda I\right]A=0, \tag{86}$$

and with the first form, the eigenvalues are $\lambda = 0$, 0.114, and 2,886. The eigenvectors for these eigenvalues are

$$X_1=\begin{bmatrix}-0.515e^{-j\mu_0}\\ 1\\ -0.515e^{j\mu_0}\end{bmatrix},\ \lambda=0,$$

$$X_2=\begin{bmatrix}e^{-j\mu_0}\\ 0\\ -e^{j\mu_0}\end{bmatrix},\ \lambda=0.114,$$

$$X_3=\begin{bmatrix}0.971e^{-j\mu_0}\\ 1\\ 0.971e^{j\mu_0}\end{bmatrix},\ \lambda=2.886, \tag{87}$$

and orthogonality is satisfied,

$$X_1 + X_2 = X_1 + X_3 = X_2 + X_3 = 0, \quad (88)$$

The smallest eigenvalue is zero, so

$$a_{-1} = -.515 e^{-j4\mu_0}, \; a_0 = 1, \; a_1 = -.515 e^{j4\mu_0}, \quad (89)$$

and the space factor is

$$S(\theta) = 1 - 1.03 \cos(\pi \sin\theta - .866\pi). \quad (90)$$

The antenna pattern before adaptive nulling is in Fig. 2. The scale is in dB. The region to be nulled lies between 47° and 133°, where the sidelobe maximum is 10 dB below the mainlobe maximum. After adaptive nulling the pattern degrades to Fig. 3, where the sidelobe maximum is 30 dB below the mainlobe. The beamwidth of the sidelobe decreased from 70° to 20°.

Degradation of the overall pattern after nulling is found in the shift of the mainlobe maxima to -10° and 190° from 0° and 180° before adaptively nulling. It is also present in the wider mainlobe beamwidth.

A simpler example is seen in Fig. 3, where a two element isotropic array has adaptive nulling in the shaded zones. The solid lines represent the pattern before nulling, and the degraded pattern after nulling is in dashed lines.

The preceding discussion of adaptive nulling was presented to show jamming or interference over an angular sector or solid angle. The jamming for a single angle, such as $\theta_0 = 0°$ and $\Delta\theta = 0°$, yields antenna weights

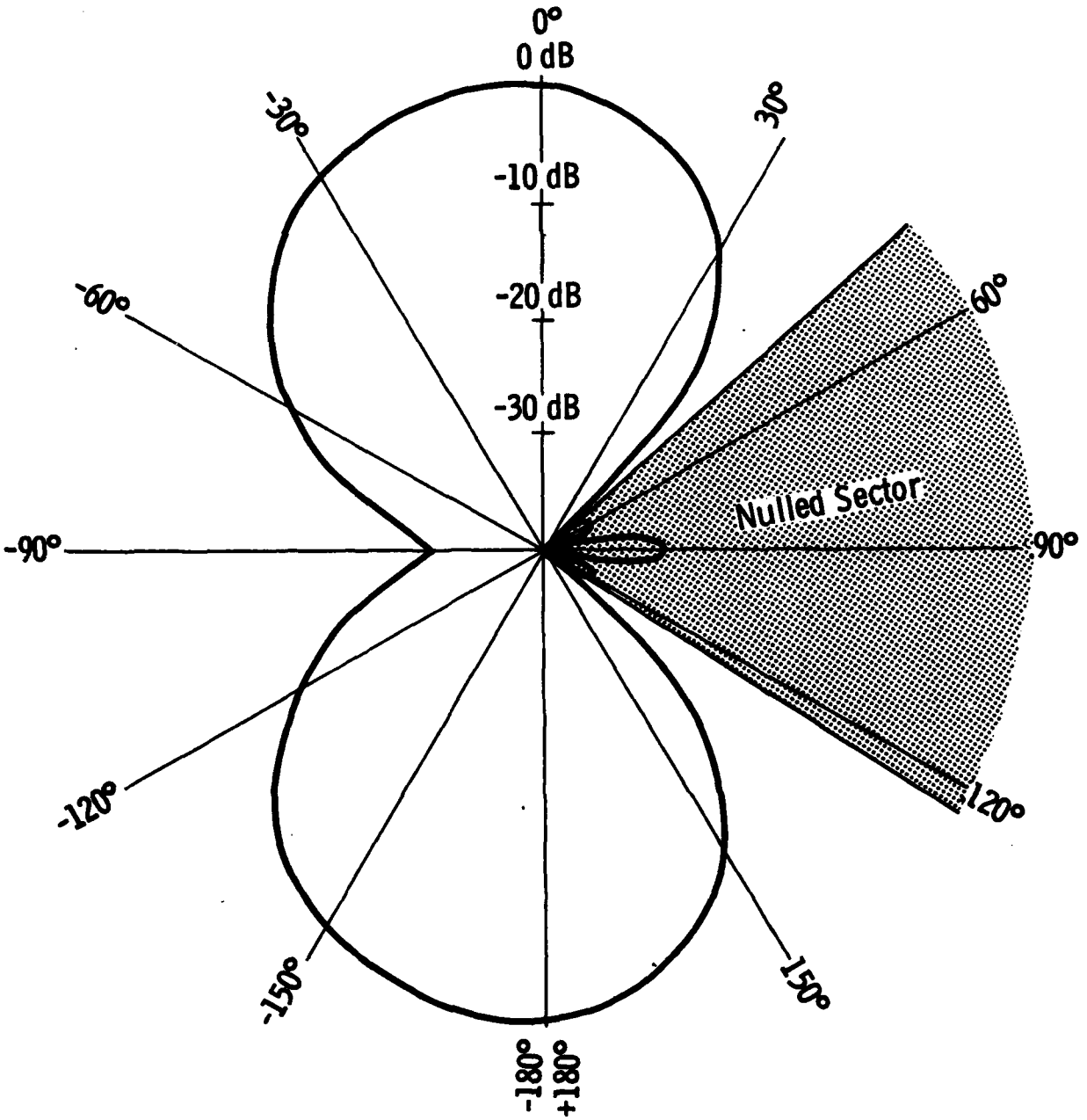


FIGURE 2: Adapted Pattern with Nulled Area

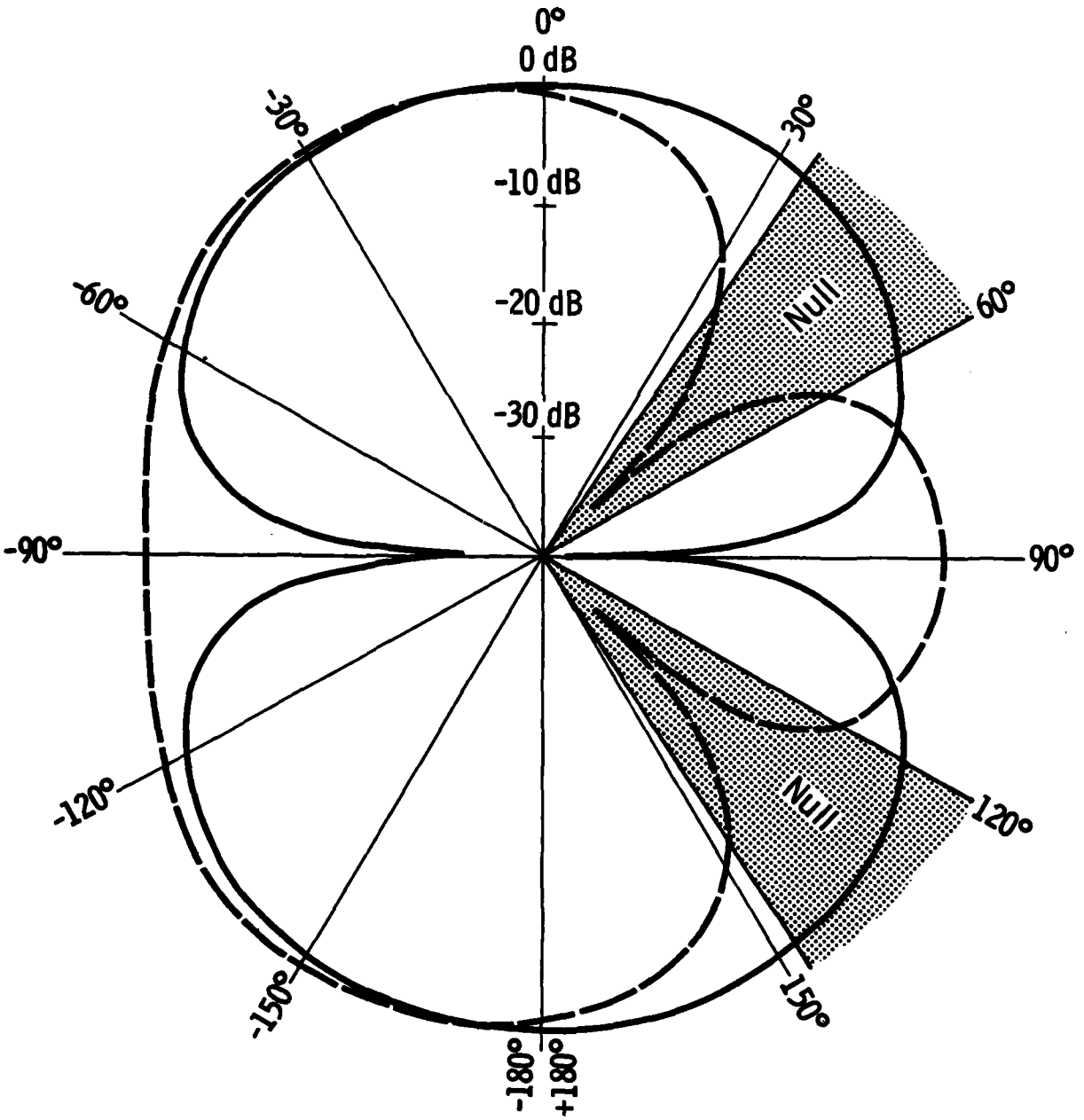


FIGURE 3: Broadside Pattern Before and After Adapting a Two-Element Array

$$a_{-1}=0.5,\ a_0=1,\ a_1=-0.5 \tag{91}$$

and the pattern is

$$S(\theta)=2\sin\left(\frac{\pi}{2}\sin\theta\right) \tag{92}$$

where the nulling weights cancel the desired signal at $\theta = 0°$. A jammer at $\theta = 90°$ yields weights

$$a_{-1}=1,\ a_0=2,\ a_1=1, \tag{93}$$

and the pattern is

$$S(\theta)=4\cos^2\left(\frac{\pi}{2}\sin\theta\right), \tag{94}$$

and if $\theta = 45°$,

$$a_{-1}=1,\ a_0=1.21,\ a_1=1, \tag{95}$$

with the pattern,

$$S(\theta)=2\cos(\pi\sin\theta)+1.21.$$

Adaptive nulling over an angular sector from $\theta+$ to $\theta-$ is more applicable to near field measurements of adaptive antennas than single angles with $\Delta\theta = 0$ because it simulates the pattern of a jamming antenna in the near field of the test antenna. Figure 4(a) shows rays from a jamming antenna, on the plane surface, to a test antenna. The rays are identified as 1, 2, ..., 6, where ray (1) represents $\theta+$, rays (3) and (4) to angle θ_0, and ray (6) to angle $\theta-$.

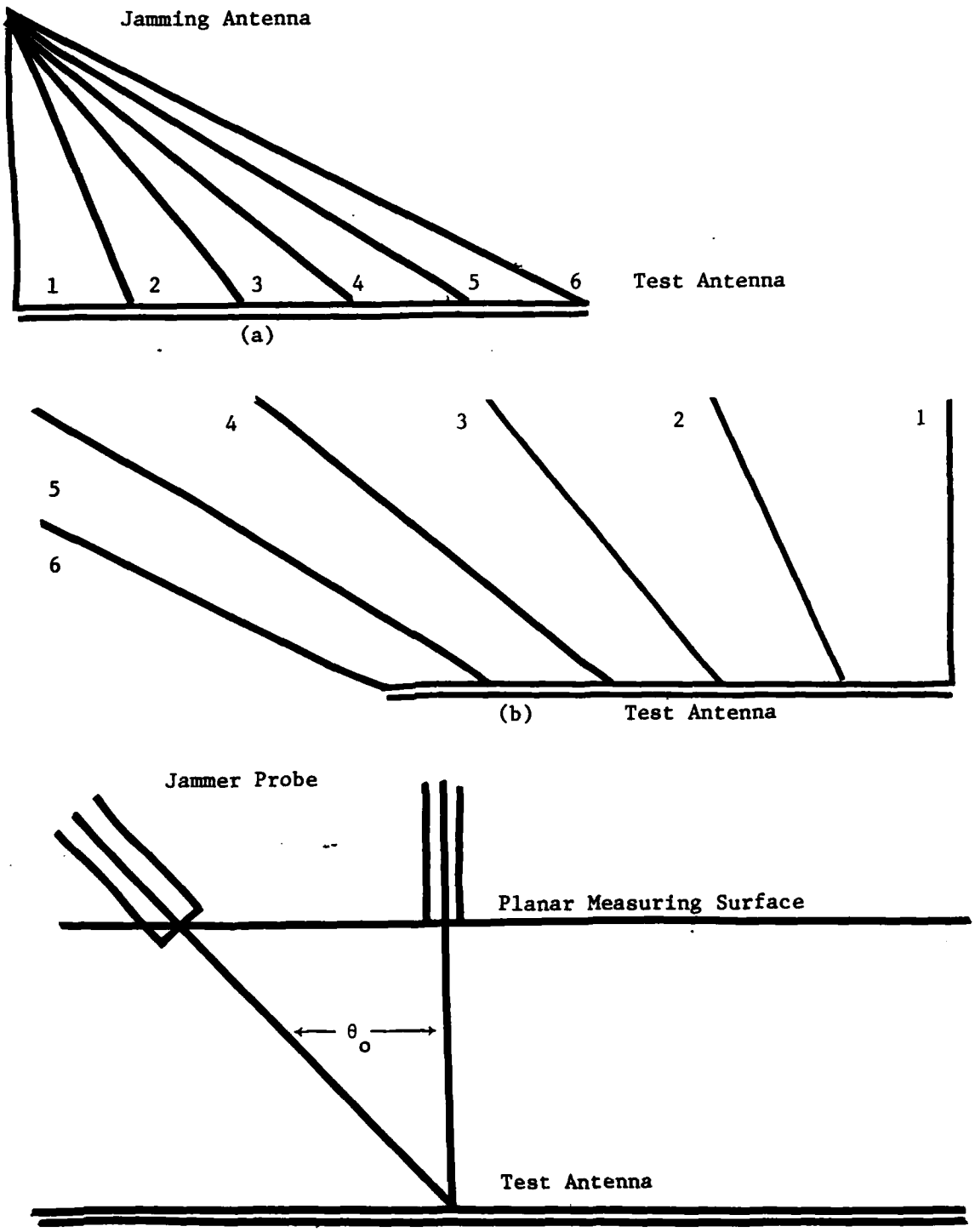


FIGURE 4: Adaptive Antennas in Near Fields

The direction of responsive nulls appear in Fig. 4(b), directed from the test antenna. The angular directions are numbered to correspond to the rays in Fig. 4(a).

When the jamming antenna, with its axis forming an angle θ_o with the axis of the probe antenna, transmits a coded signal to the test antenna, the test antenna pattern is adaptively weighted so that a null is created in the vicinity of angle θ_o. The jamming antenna transverses the planar surface, and the detected test antenna output is

$$V_{VN}(o,x,y),\ V_{HN}(o,x,y),$$

where the subscript N represents directional noise. Integrals similar to those in Eqs. (56) and (57), for

$$I_{VN}(\theta,\ \phi),\ I_{HN}(\theta,\ \phi),$$

are then calculated with the FFT method.

The probe antenna pattern is then obtained with the probe as a transmitter. The jamming antenna, located a fixed distance from the probe antenna, moves with the probe antenna but does not radiate. A third pattern is calculated with both jammer and probe antennas radiating. Orientation of probe and jammer antennas is in Fig. 4(c).

VI. RECOMMENDATIONS

Analytical studies of the jamming and probe antenna interactions with the test antenna should be conducted by Drs. Arthur Yaghjian, David Kerns, and Albert Biggs. Combined with these studies, coordination between Drs. Allen Newell, Charles Raquet and Albert Biggs on actual design and construction of a near zone antenna range should be initiated. Dr. Demetrius Paris should also be included in both efforts. Yaghzian, Kerns and Newell are with NBS-Boulder; Raquet is with NASA/Lewis, Biggs is with Kansas University, and Paris is with Georgia Tech University.

REFERENCES

1. "IEEE Test Procedure for Antennas, Number 149 (Revision of 48 IRE 282) January 1965," IEEE Trans., vol. AP-13, pp. 347-446, May 1965.

2. Arthur D. Yaghjian, "Efficient Computation of Antenna Coupling and Fields Within the Near Field Region," IEEE Trans., vol. AP-30, pp. 113-128, January 1982.

3. David M. Kerns, "Plane-Wave Scattering Matrix Theory of Antenna and Antenna-Antenna Interaction," National Bureau of Standards Monograph 162, June 1981.

4. David M. Kerns, "Correction of Near Field Antenna Measurements Made with an Arbitrary but Known Measuring Antenna," Electron. Lett., vol. 6, pp. 346-347, May 1970.

5. Ramon C. Biard, et al., "Recent Experimental Results in Near Field Antenna Measurements," Electron. Lett., vol. 6, pp. 349-351, May 1970.

6. Edward B. Joy and Demetrius T. Paris, "Spatial Sampling and Filtering in Near-Field Measurements," IEEE Trans., vol. AP-20, pp. 253-261, May 1972.

7. Demetrius T. Paris, W. Marshall Leach, Jr., and Edward B. Joy, "Basic Theory of Probe-Compensated Near-Field Measurements," IEEE Trans., vol. AP-26, pp. 373-379, May 1978.

8. Edward B. Joy, W. Marshall Leach, Jr., George P. Rodrigue, and Demetrius T. Paris, "Applications of Probe-Compensated Near-Field Measurements," IEEE Trans., vol. AP-26, pp. 379-389, May 1978.

9. W. Marshall Leach, Jr. and Demetrius T. Paris, "Probe Compensated Near-Field Measurements on a Cylinder," IEEE Trans., vol. AP-21, pp. 435-445, July 1973.

10. Allen C. Newell and Myron L. Crawford, "Planar Near Field Measurements on High Performance Array Antennas," National Bureau of Standards Report NBSIR 74-380, July 1974.

11. Paul F. Wacker, "Non-Planar Near Field Measurements: Spherical Scanning," National Bureau of Standards Report NB SIR 75-809, June 1975.

12. Henry G. Booker and Peter C. Clemmow, "The Concept of an Angular Spectrum of Plane Waves and Its Relation to that of Polar Diagram and Aperture Distribution," Journal IEE, vol. 97, part III, pp. 11-50, January 1950.

13. John Brown and E.V. Jull, "The Prediction of Aerial Radiation Patterns from Near Field Measurements," Journal IEE, vol. 108B, pp. 635-644, November 1961.

14. Albert W. Biggs, "Asymptotic Approximations for Surface Scattering Integrals," IEEE Trans., vol. AP-15, pp. 443-445, May 1977.

1982 USAF-SCEE SUMMER FACULTY RESEARCH PROGRAM

Sponsored by the

AIR FORCE OFFICE OF SCIENTIFIC RESEARCH

Conducted by the

SOUTHEASTERN CENTER FOR ELECTRICAL ENGINEERING EDUCATION

FINAL REPORT

COMPUTER SIMULATION OF CHANNELIZED RECEIVERS

Prepared By:	Dr Jack J. Bourquin
Academic Rank:	Associate Professor
Department & University:	Department of Electrical Engineering University of Missouri-Rolla
Research Location:	AFWAL Avionics Laboratory Electronic Warfare Division, Passive ECM Branch, ESM Technology Group Wright-Patterson Air Force Base OH
USAF Research Colleague:	Dr James B. Y. Tsui
Date:	16 August 1982
Contract No:	F49620-82-C-0035

COMPUTER SIMULATION OF CHANNELIZED RECEIVERS

by

Jack J. Bourquin

ABSTRACT

Development of computer subroutines applicable to the simulation of channelized receivers was continued. Some of the subroutines simulate the various blocks typical of a receiver, such as filters, detectors, and limiters. Others provide for diverse excitations, such as a pulse of CW carrier, or generate one of the types of displays available, such as the spectrogram of any signal in the system. The main (subroutine calling) program has a flow chart that closely resembles that of the system to be simulated.

Subroutines for several additional components were written and debugged. Progress was made toward converting the simulation package from FORTRAN IV to BASIC. Some of the subroutines were written in or converted to a modified simulation scheme whereby advantage is taken of the frequency characteristics of narrow band limited systems and of the cyclic properties of the discrete Fourier transform to greatly reduce computer memory requirements and running times. Thus, the simulation package was made more compatible to the desk top type of computer.

ACKNOWLEDGMENTS

The author would like to thank the Air Force Systems Command, the Air Force Office of Scientific Research, and the Southeastern Center for Electrical Engineering Education for providing him the opportunity of a very challenging yet educational and enjoyable summer at the AFWAL Avionics Laboratory, Wright-Patterson AFB OH. He is grateful to the Avionics Laboratory, especially the ESM Technology Group and the Passive ECM Branch, for its professional work environment yet very hospitable social atmosphere. He is particularly indebted to Dr. James B. Y. Tsui, who was the Effort Focal Point for the project, for his collaboration and guidance.

I. INTRODUCTION:

The primary thrust of this project was to continue the development of computer subroutines for the computer simulation of channelized receivers. Although the channelized receiver is presently the system of principal concern for this work, the same techniques could be applied to a large variety of systems and components. The ultimate goal is to be able to simulate the entire receiver from RF input to output displays under various excitations and operating conditions.

The motivation for such a simulation package is threefold: to provide a fast and inexpensive computer aid for

(1) the theoretical checkout of the basic receiver system concept and its block diagram,

(2) the checking of parameter specifications for the final design of the actual blocks chosen for the system, and

(3) the diagnosis and correction of whatever anomalies occur in the final constructed system.

By "fast and inexpensive" used above, we mean compared to the time and expense involved in a receiver design or redesign.

Toward this objective, a collection of 28 FORTRAN IV subroutines[1] for an IBM 370 (compatible) system had previously been prepared by the author and several M.S. students in Electrical Engineering at the University of Missouri-Rolla. Some of the subroutines simulate various blocks from the RF input to the output of the slot assembly of a channelized receiver, e.g., filters, limiters and detectors. Other subroutines provide various inputs, e.g., a rectangular pulse of a CW carrier. A final group of subroutines allows the output of any block to be displayed as (1) a time-domain transient response, (2) a frequency-domain spectrum, or (3) a time-frequency spectrogram surface[2,3,4].

This work has, for the most part, been supported under subcontract from the Engineering Experiment Station at the Georgia Institute of Technology under Air Force Contract No F33615-77-C-1253. Some of the basic concepts were an outgrowth of a project completed by the author in the 1977 USAF-ASEE Summer Faculty Research Program.

The original set of subroutines was developed on the University of

Missouri System - Wide Computer Network. The main computer is a virtual memory system and is relatively fast, except at predictable periods of peakload. Therefore, there was little effort to conserve memory requirements. However, since the termination of the above mentioned research contract, considerable effort[5] has been expended toward reducing the memory required for the subroutines, thus making them more compatible with smaller and slower computers. This reduction has been realized by taking advantage of the characteristics of band limited systems and the cyclic properties of the discrete Fourier transform. More on this will be discussed later.

Until recently the simulation package had been successfully run on only the Univer ty of Missouri computer system. Output display programs had been prepared for the Cal-Comp plotter and the Tektronix Series 4010 computer graphics terminal. When the ESM Group recently acquired a Hewlett-Packard Model 9826 computer system, there was considerable motivation for modifying at least some of the subroutines to make them compatible with that system. The computer graphics capability of the HP 9826 could greatly simplify and quicken the process of obtaining whatever graphical displays were desired. Therefore, a significant part of the author's work this summer has centered around making the simulation package operational on the HP 9826.

II. OBJECTIVES OF THE RESEARCH EFFORT

A. Conversion of the FORTRAN IV Subroutines to the HP 9826 BASIC Language

Dr James B.Y. Tsui, who is also the Effort Focal Point for this project, had already converted many of the original subroutines to the HP 9826 version of the BASIC programming language. What remained to be done was an extensive testing and debugging procedure to ascertain the validity of the subroutines. No attempt has been made to date to convert any of the subroutines associated with the spectrogram capability of the original simulation package. The reason is that these subroutines require larger arrays and take longer to run than the rest of the subroutines. And, although the HP 9826 is fast for a desk-top type computer, it is slow compared to the typical large computer system.

B. Subroutines Using Frequency Translation

The subroutines above were to be modified with an improved version of the frequency translation reported in reference 5 and extensively tested and debugged. The frequency translation allows smaller data arrays, thus reducing the memory requirements and the running time for each subroutine.

C. Computer Control of A Network Analyzer

A program was to be written that would allow the HP 9826 to control an HP 8505A Network Analyzer. The frequency response of a block could then be automatically and rapidly run and then stored on a mini-floppy disk. Those data could be used whenever that block was to be included in a simulation program.

D. Subroutines For Additional Components

Simulation subroutines for several additional components were to be written, tested and debugged.

E. Laboratory Check of Several Simulation Programs

The frequency response of several components would be run as in objective C. Then these data would be used in several simulation programs to predict the transient responses to various input signals. These simulated responses would be compared with actual responses to the same inputs observed and photographed in the laboratory.

III. THE GENERAL SIMULATION SCHEME

The general basis for setting up the simulation program for some system is that the block diagram of the program closely resembles that of the system. For example, suppose that the system to be simulated consists of component A in cascade with component B with some designated input signal, x(t), into A, as shown in Fig 1(a). A and B could be some combination of filters, limiters, diode detectors, etc. There must exist subroutines which adequately describe each device block (A and B) and each input signal (X), and the main-line program simply calls them in the right order, as shown in Fig 1(b). That is, if the output signal of A, y(t), is the input signal of B, the output array, Y(*), of SUB A(*) becomes the input array of SUB B(*). Of the CALL blocks shown, the least standard and well defined one is the CALL PLOT (*). This one

depends on the display medium and the application, and, in fact, may not be a subroutine at all but rather simply the last segment of the main-line program. It is shown here as a CALL block to demonstrate the idea of the procedure.

If a subroutine is to simulate a device, there are two possible domains. Some devices are better, if not only, described in the frequency-domain, such as a Butterworth filter. Others, like a limiter, are better described in the time-domain. Somewhat the same is true of the various input signals, X(*).

This means that the simulation block diagram in Fig 1(b) represents only a minimal diagram. Because if, for example, SUB A(*) implements a frequency-domain simulation and SUB B(*) implements a time-domain simulation, a call to a fast Fourier transform (FFT) subroutine operating in the inverse mode must be inserted between the CALL A(*) and CALL B(*) blocks to transform X(*) from the frequency-domain to the time-domain. Of course, the reverse could be true.

Furthermore, even if both subroutines are operating in the same domain but we wish to observe Y(*), for example, in the opposite domain, the FFT subroutine must be called after the CALL A(*) block, the data plotted in the desired form, and then the FFT subroutine called again to restore the data to the proper domain for the SUB B(*) implementation. An alternative to the second FFT subroutine call is to store the output of the CALL A(*) block in a second array and to use that for the input to the CALL B(*) block. The program runs faster but requires more memory. The typical FFT subroutine overwrites the input data with the output data in the same array.

A more subtle addition to the simulation block diagram is desirable for certain bandpass systems, such as the channelized receiver. Signals found in the RF and IF sections probably take the form of an amplitude modulated carrier. If one desires to observe or plot the computer simulation of such a (time-domain) signal, better results are probably obtained if the envelope of the carrier is detected (via an envelope detection subroutine) and displayed, rather than the complete carrier signal. Therefore, if the computer simulation of y(t), for example, is

to be displayed, the detection subroutine should be called af er Y(*) is in the time-domain and before SUB PLOT (*) is called.

IV. THE TWO PROGRAM STRUCTURES

Before describing the various simulation subroutines, the two fundamental program structures used in this simulation package are discussed and compared. But before that, several fundamental concepts are reviewed.

Since it is obviously necessary to be able to transform back and forth between the time and frequency domains, and since this is a computer simulation requiring discrete data, the properties of this simulation package are inexorably related to those of the discrete Fourier transform (DFT). The FFT is simply a fast algorithm for taking the DFT on a computer.

The various parameters associated with the DFT and the simulation package are defined here as follows:

N is the number of data in each domain, time and frequency (the same number for both),

DF is the frequency difference between adjacent data in the frequency-domain,

Dt is the time difference between adjacent data in the time-domain,

Fs is the sampling frequency or the length of the data record in the frequency-domain, and

Ts is the length of the data record in the time-domain.

In order to simplify the format of the numbers, we have found it convenient to use a time and frequency scale factor of 10^6. I.e., we measure frequency in MHz and time in μs.

The above parameters are related by the following:

$$Fs = N * Df \text{ and } Ts = N * Dt \quad (1)$$

and

$$Fs = 1/Dt \text{ and } Ts = 1/Df \quad (2)$$

Therefore,

$$N = Fs * Ts = 1/(Df * Dt) \quad (3)$$

Of these parameters, the user of the simulation package need specify only N and Df. However, it is important that he understand all

of the parameters when selecting values for N and Df.

One minor restriction on N is that the FFT subroutine we are using requires N to be an integer power of 2. There are subroutines available that do not require that restriction, but they require more memory and take longer to run.

A. The Original Structure

The spectra or Fourier transform of a real signal has a real part that is an even function of frequency, while its imaginary part is odd. The time-domain sampling involved in the DFT makes the DFT of a function of time periodic in frequency with a period of Fs. These two properties combine to require that the DFT of a real function of time has a real part that is even in frequency about the frequency

$$Fh = Fs/2 \qquad (4)$$

called the folding frequency, and that the imaginary part have odd symmetry about Fh[6].

This property requires that somewhere along the simulation procedure the frequency-domain data must receive a conjugate fold about Fh in order to obtain a real function of time when an inverse FFT (IFFT) is called. The user need not be concerned about this. One of the subroutines automatically includes this step.

However, the user must be sure that N and Df are large enough that no significant information in the spectrum input to any IFFT call be contained in any frequency greater (before the fold) than Fh; see equations (1) and (4). This eliminates irretrievable loss of information due to frequency-domain overlap of data called aliasing. Said another way, N and Df must be large enough for the desired resolution in the time-domain, i.e., Dt must be small enough; see equation (2). On the other hand, Df must be small enough for the desired frequency-domain resolution. Said another way, Df must be small enough to eliminate time-domain aliasing; see equation (2). These considerations determine an upper limit for Df and a lower limit for N.

Consider example 1:

Suppose that a band limited system has significant spectral components only in the band of from 330 MHz to 360 MHz, as shown in Fig 2.

These numbers are typical in a channelized receiver. The dotted portion of the spectrum is the complex conjugate of the solid portion. Suppose further that a visual inspection of the data indicates that the discrete data should be taken at frequency increments of no greater than 0.5 MHz, i.e., that

$$Df \leq 0.5 \text{ MHz} \tag{5}$$

Now in order to eliminate aliasing, it must be that

$Fh = Fs/2 = N * Df/2 \geq 360$ MHz i.e., that

$$N \geq 1440 \tag{6}$$

But since N must be an integer power of 2, we select

$$N = 2^{11} = 2048 \tag{7}$$

Checking back we find that

$$Fh = 2048 * 0.5/2 = 512 \text{ MHz} \tag{8}$$

The results of selecting Df = 0.5 MHz and N = 2048 are shown in Fig 2(b).

If we felt the 304-MHz "guard band" from 360 to 664 MHz to be excessive, we could reduce Df to possibly 0.4 MHz. This would reduce Fh to 409.6 MHz and the guard band to 99.2 MHz. The important thing here is that Fh must always be maintained to at least 360 MHz to eliminate aliasing.

Another effect of the above decrease in Df, of course, is that the frequency-domain resolution is better. However, one should remain mindful of the time-domain effects of changes in N and Df. From equation (3), we see that decreasing Df increases Dt and makes the time-domain resolution worse. This might be undesirable in some cases. On the other hand, from equation (2) we see that decreasing Df increases Ts, the time-domain record length, and this might be desirable in some cases. Any of the relationships in equations (1), (2), and (3) can be used in determining N and Df, and none of them should be completely ignored.

On examination of Fig 2(b), we observe that in this case, over 94% of the frequency record contains zeros. Furthermore, since the second half of the record is simply a conjugate fold of the first half, less than 3% of the entire record contributes uniquely to the output of the

IFFT call. This kind of inefficiency may be merely irksome (depending on who is paying the bill) on a large, fast computing system On a smaller, slower computer, it can be disastrous. This is one of the motivations for the modified program structure.

B. The Modified Structure

The concept of the modified structure will be illustrated first by example 2: Suppose that we start with the same system taken in example 1 whose spectrum is shown in Fig 2(a). This time in preparing the DFT for the IFFT call, suppose that we completely ignore the second half of the spectrum shown in Fig 2(b), since it contributes no new information anyway, and then translate the remainder down to near DC, as shown in Fig 3. To be sure, the output of the IFFT call is now a complex function of time since the real and imaginary parts of the DFT no longer have the proper symmetries for a real IDFT.

However, recall that the signal y(t) in the original system is probably of the form of a modulated carrier, such as

$$y(t) = m(t) \left[e^{j\omega_c t} + e^{-j\omega t_c} \right] \qquad (9)$$

since the system is band limited. Furthermore, we are probably mostly interested in m(t), the modulation signal. The typical diode envelope detector yields $|m(t)|$ as do our detection subroutines.

The frequency-shift theorem[6] for the Fourier transform states that if

$$F(t) :::: F(j\omega)$$

(":::" denotes a transform pair) then

$$e^{j\omega_o t} f(t) :::: F\left[j(\omega-\omega_o) \right] \qquad (10)$$

In other words, the two spectral bands in Fig 1(a) represent M(f), where m(t)::::M(f), translated to $\pm$ fc by the exponential terms in equation (9).

The DFT [y(t)] in Fig 3 represents the DFT of

$$e^{j(\omega_c-\omega_o)t} m(t) :::: M\left[j(\omega-\omega_c+\omega_o) \right] \qquad (11)$$

Note that the $e^{-j\omega_c t}$ term in equation (9) has been dropped; this is equivalent to dropping the second half of DFT [(y(t)] in Fig 2 for Fig 3. The ω_o term accounts for the downward frequency shift. For the

case shown in Fig 3

$$\omega_o = 2\pi \ 330 \text{ M R/s} \tag{12}$$

The detection subroutine written for the modified program structure takes the magnitude of the (complex) input function of time for the output. Therefore, if we take an IFFT of DFT $[y(t)]$ in Fig 3 and send that into our detection subroutine, we obtain a discrete but almost smooth version of

$$|e^{j(\omega_c-\omega_o)t}m(t)| = |m(t)| \tag{13}$$

the detected envelope, independent of ω_o. In order for the modified structure program for a simulation block diagram (Fig 1(b)) to be equivalent to the original system block diagram, we must be sure that the frequency shift, ω_o, is the same for all blocks.

Now to determine the values of Df and N for example 2. Whatever observations dictated inequality (5) would still be equally valid since the shape of the spectrum has not been distorted but simply translated in frequency. Since we no longer require the output of the IFFT of DFT $[y(t)]$ to be real, all we need for the prevention of a liasing is that Fs be at least the highest significant frequency in the record of DFT $[y(t)]$ in Fig 3, i.e., in this case, 30 MHz. Therefore,

$$Fs = N * Df \geq 30$$

gives

$$N \geq 60 \tag{14}$$

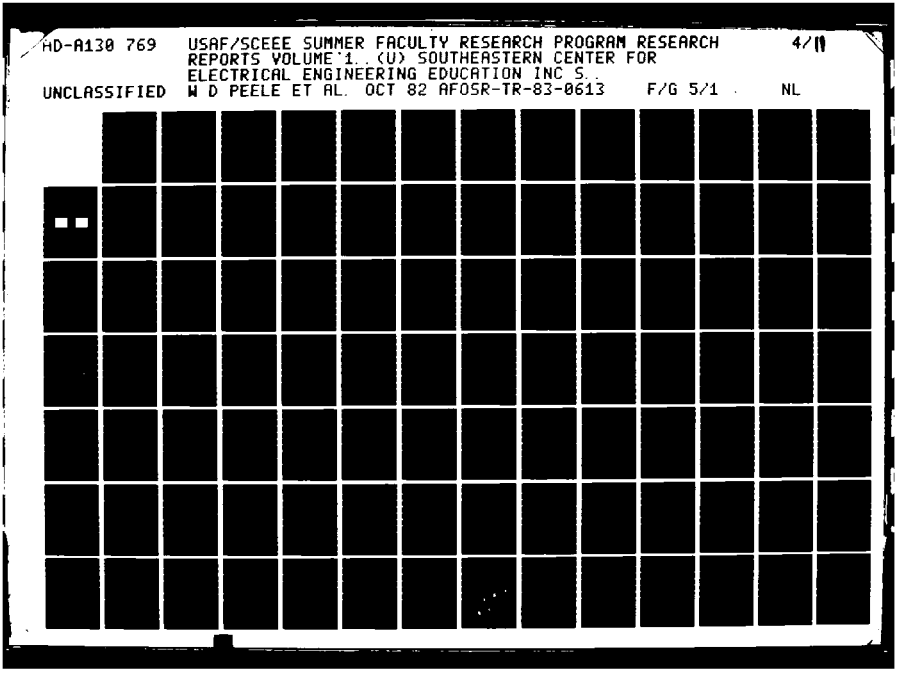
Again, since N must be an integer power of 2, we could select

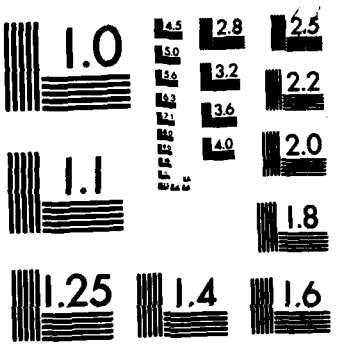
$$N = 2^6 = 64 \tag{15}$$

C. Comparison Between the Structures

In comparing examples 1 and 2 we will gain some insight into how the two structures compare. The most obvious advantage of the modified structure over the original is in the sizes of the required data arrays. Both real and imaginary components must be stored. Therefore, from equation (7) we see that we must reserve 4096 memory cells for the data arrays in the original structure while the modified structure requires only 128 memory cells (equation (15)).

A more subtle (until you run them once) difference is in the running times. Of course, for most subroutines in the simulation package the programs are relatively simple in loop structure, etc., and the


AD-A130 769 USAF/SCEEE SUMMER FACULTY RESEARCH PROGRAM RESEARCH 4/11
REPORTS VOLUME 1.. (U) SOUTHEASTERN CENTER FOR
ELECTRICAL ENGINEERING EDUCATION INC S..
UNCLASSIFIED W D PEELE ET AL. OCT 82 AFOSR-TR-83-0613 F/G 5/1 NL



MICROCOPY RESOLUTION TEST CHART
NATIONAL BUREAU OF STANDARDS-1963-A

running times are approximately proportional to N, another advantage for the modified program. The running time for the FFT, however, is not quite as simply related.

We have never timed a 2048-point FFT on the HP 9826 nor a 64-point FFT. But have timed a 256-point FFT to take 6.82 seconds.

The amount of time[6] it takes an FFT to run is approximately proportional to $N * \log_2 (N)$.

Therefore,

$$\frac{6.82}{256*8} = \frac{T(64)}{64*6} = \frac{T(2048)}{2048*11} \qquad (16)$$

gives the estimates of

T(64 pont) = 1.28 seconds

T(2048 point) = 75.02 seconds (17)

V. SUBROUTINES

This section briefly describes each subroutine and how to use it. Due to page limitations, the program listings are not included in this report. However, copies can be requested from the author. These subroutines have been extensively tested and debugged this summer and appear to be fully operational. Original structure and modified structure subroutines that simulate the same device or signal are paired together. A modified structure subroutine that simulates the same device or signal as an original structure subroutine takes the same call name with an "m" suffixed to it.

A. Rectangular Pulse of Carrier

1. Pam (Fc, Tau, Df, N, Resp 1, Resp 2 (*))

SUB Pam generates the frequency-domain spectrum of a time-domain rectangular pulse of carrier for the original structure.

Inputs:

Fc is the carrier frequency (in MHz)

Tau is the time width of the modulating pulse (in μs), and

Df and N have already been defined.

Outputs:

Resp 1(*) contains the real part of the spectrum, and

Resp 2(*) contains the imaginary part of the spectrum.

Arrays Resp 1(*) and Resp 2(*) should both be dimensioned to N in the main program. The subroutine analytically generates the sinc function displaced to $\pm$ Fc but fills only the lower half of the record in anticipation of the conjugate fold about Fh implemented in a subsequent subroutine.

2. Pamm (Fc, Fz, Fe, Tau, Df, Resp 1(*), Resp 2(*))

SUB Pamm is the counterpart of SUB Pam for the modified structure. All of the parameters and arrays are defined and dimensioned the same as before, except for the two new

Inputs:

Fz is the frequency by which the spectrum is translated downward.

Fe is the highest possible frequency of the spectrum generated.

This subroutine operates similarly to SUB Pam, except for the frequency translation by an amount of Fz. Furthermore, since there is no conjugate fold to follow, the entire frequency record is filled.

The lower end of the frequency record starts at Fz. As we proceed upward along the record, the frequency increases until Fe or the upper end of the record is reached, whichever occur first. If Fe is reached first, the rest of the record is filled with a cyclic rotation of the spectrum below Fz. See Fig 4.

B. Butterworth Band-Pass Filter

1. Btwth (Df, N, Fo, Nord, Bw, Resp 1(*), Resp 2(*))

SUB Btwth simulates a Butterworth band-pass filter for the original structure. The previously undefined parameters are:

Inputs:

Fo is the center frequency (MHz),

Nord is the order (number of poles) of the band-pass filter and

Bw is the bandwidth (MHz).

This subroutine operates entirely in the frequency-domain. The input data come stored in arrays Resp 1(*) and Resp 2(*) from the output of the previous block (Fig 1(b)). The output data of the subroutine overwrite the input data in Resp 1(*) and Resp 2(*). Both input and output arrays are in the frequency domain.

SUB Btwth first finds the poles of the (Nord/2) th-order normalized

low-pass prototype. Then the low-pass to band-pass frequency transformation is applied.

2. Btwthm (Df, N, Fo, Fz, Fe, Nord, Bw, Resp 1(*), Resp 2(*))

SUB Btwthm is the counterpart of SUB Btwth for the modified structure and operates in the same way, except for the frequency translation. All parameters and arrays are defined as before. See Fig 5.

C. Empirical Filter Data

Fildtm (N, Resp 1(*), Resp 2(*), Df, Fz, Fe, Freq(*), Mag(*), Phase(*))

This modified structure subroutine allows the simulation of a device for which the frequency response has been run in the laboratory. For each point of the response the frequency in Hz (Note: not MHz since the subroutine is presently compatible with the HP 8505A Network Analyzer), the gain (in dB), and the phase (in degrees) are stored in arrays Freq(*), Mag(*), and Phase(*), respectively, before the call to SUB Fildatm. All the rest of the parameters and arrays in the argument list have the same functions as in SUB Btwthm.

It is not necessary that the laboratory data be measured with any particular frequency spacing. The subroutine interpolates the data to a frequency spacing of Df. Nor is it necessary that the laboratory data span the entire frequency record. The subroutine pads the record with zeros below the lowest frequency of the measured frequency response and above the highest frequency in order to fill out the frequency record.

Subroutine knows that the measured frequency response data is over when it reads a zero from the Freq(*) array. Therefore, that array should be dimensioned to at least one more than the number of data points.

D. The FFT

Fouri (Resp 1(*), Resp 2(*), N, Isign)

SUB Fouri(*) is used in both program structures for taking FFT's and IFFT's. The only previously undefined term in the argument list is an

Input:

Isign = -1 to take an FFT (time to frequency transform)

= +1 to take an IFFT (frequency to time transform).

The output data overwrite the input data in the arrays Resp 1(*) and Resp 2(*). At the beginning of the subroutine, an internal work array is dimensioned. That array should be dimensioned to at least 2*N.

SUB Fouri(*) can be called directly in either program structure to find the frequency spectrum of a time signal without any additional data manipulation.

E. Frequency-To-Time Transform

1. Timrsp (N, Resp 1(*), Resp 2(*))

This subroutine takes the inverse transform of a frequency spectrum for the origjnal structure. This is where the conjugate fold discussed in section IV.A is implemented, after which SUB Fouri(*) is called to take an IFFT.

2. Since there is no conjugate fold required in the modified structure, this transform can be implemented directly by SUB Fouri(*).

F. Envelope Detection

In this case the subroutine naming policy stated at the beginning of Section V was not followed.

1. Detmm (N, Df, Resp 1(*), Detresp(*), Timer(*) Linsel, Rmax, Jcnt)

SUB Detmm(*) detects the envelope of an amplitude modulated carrier for the original structure. The yet undefined parameters and arrays in the argument list are

Inputs:

Limsel = 1 if SUB Detmm is to follow SUB Limtr, the limiter simulation,

= 0 if otherwise and

Rmax is limit level when Limsel = 1

Outputs:

Detresp(*) is the array containing the detected envelope,

Timer(*) is time array against which Detresp(*) can be plotted, and

Jcnt is the number of data in Detresp(*).

This subroutine determines the datum of maximum magnitude between adjacent zero crossings of the carrier. From this and the two adjacent data, the sinusoidal approximation of the peak value for that half cycle of the carrier is calculated and stored in Detresp(*). The calculated time at which that peak occurs is stored in Timer(*).

2. Dete (N, Resp 1(*), Resp 2(*), Detresp(*))

SUB Dete(*) detects the envelope of a carrier for the modified structure. The argument list has already been defined. This subroutine simply calculates

$$\text{Detresp}(I) = \text{SQR}(\text{Resp 1}(I)*\text{Resp 1}(I) + \text{Resp 2}(I)*\text{Resp 2}(I)) \quad (18)$$

as described in Section IV.B. Since these data occur every Dt seconds, a time array is not necessary. Another advantage of the modified structure is the simplicity of the detection scheme.

It should be noted here that both detection subroutines work strictly in the time-domain. However, the input data, Resp 1(*), for SUB Detmm is a real function of time, whereas the input data, Resp 1(*) and Resp 2(*), for SUB Dete(*) is a complex function of time.

G. RC-Diode Detector

Some diode detector circuits contain an RC holding circuit, as shown in Fig 6. The modified structure subroutine to simulate this circuit is

Rcdet (N, Df, Trc, Resp 1(*), Resp 2(*), Detresp(*))

Everything in the argument list has been defined except for the Input:

Trc is the RC time constant.

Depending on the value of Trc, the RC circuit can cause the leading edge of the detector response to be steeper than the trailing edge, as shown in Fig 7. Again, this is strictly a time-domain operation.

H. Single-Pole Low-Pass Filter

Low-pass (N, Df, Fb, Fr, Fz, Fe, Resp 1(*), Resp 2(*))

SUB low-pass(*) is a modified structure subroutine for simulating a single-pole low-pass filter for video signals. It is a frequency-domain operation. The yet undefined parameters in the argument list

are

Inputs:

Fb is the half-power frequency and

Fr is a reference frequency for centering the low-pass response. This is a filtering action on the detected envelope signal. But rather than transform the output of SUB Dete(*) into the frequency-domain for that filtering action, it is more effecient to implement the equivalent filtering action back in the frequency-domain preceding the detection step, i.e., preceding the IFFT just before the CALL Dete(*) line. For this, the low-pass response should be centered on the centroid of the original spectrum at that point by setting Fr equal to the mean frequency of the spectrum.

I. Centroid of A Spectrum

Meanfreq (N, Df, Fr, Resp 1(*), Resp 2(*))

This subroutine calculates the centroid, Fr, of the magnitude of a spectrum for use in the low-pass filter subroutines in the modified structure. The integration is performed by Simpson's rule.

J. Butterworth Low-Pass Filter

Lopasbut (Df, N, Fb, Fr, Fz, Fe, Nord, Resp 1(*), Resp 2(*))

This modified structure subroutine provides a low-pass Butterworth filter for video signals and is applied exactly the same as SUB Low-pass(*). The entire parameter list has been defined already.

K. Gaussian Low-Pass Filter

Gausslopas (Df, N, Fb, Fr, Fz, Fe, Resp 1(*), Resp 2(*))

This modified structure subroutine is applied exactly the same as the other two low-pass filter simulations. The actual filter simulated is an 8-th order 12-dB Gaussian transitional filter. This type of filter has superior pulse response characteristics. See Fig 8.

L. Limiter

Limitr (N, Rlimit, Resp 1(*), Kenabl, Mode, Rmax)

This original structure subroutine simulates an electronic limiter. The new parameters in the argument list are

Input:

Rlimit is either the value of the limit level or the percentage

the limit level is of the peak value of the input signal, depending on Mode,

Kenabl = 0 means there is no limiting

= 1 means there is limiting, and

Mode = 0 sets limit level as a percentage of the peak input value as specified by Rlimit

= 1 sets the limit level to the actual value of Rlimit.

Output:

Rmax is the actual value of the limit level

This is a time-domain clipping action.

M. Operational Amplifier

Opamp (N, Df, Tc, Kol, Kcl, Vbrk, Vlim, Detresp(*))

This time-domain simulation can work in either structure. It simulates the opamp inverter shown in Fig 9(a), except that the gain is taken as positive for convenience. The internal circuit is modeled as a first-order gain (real pole at -1/Tc) with saturation, as shown in Fig 9(b). The transition between linear gain and saturation is parabolic. The new parameters in the argument list are all Inputs:

Tc is the integrator constant,

Kol is the linear open-loop gain,

Kcl = R_2/R_1 is the closed-loop gain,

Vbrk is the output voltage at which saturation begins, and

Vlim is the final limit of the output voltage.

The integration is done by the traezoidal rule. Two responses are shown in Fig 10.

VI. TESTING

A. Subroutine Debugging

Each of the subroutines above underwent extensive debugging, either singly, in small meaningful groups, or even in parts. Many times a simple enough input signal or some other set of conditions could be devised that allowed the test results to be analytically checked or compared with other published results. Fortunately,

programming errors often manifest gross discrepancies in test results.

For example, in testing the opamp simulation in Fig 9. It was simple enough to test the integrator by integrating an easily analytically integrated function. The inner closed-loop around the integrator was easily tested with a rectangular pulse and then an exponential decay function. The same was true for the outer-loop in Fig 9(a) as long as the opamp remained linear. The nonlinearity by itself was tested by many plots of its transfer characteristics. Finally, when the entire circuit was forced into saturation (Fig 10), the response resembled that of a saturated opamp.

B. Experimental Verification

A program was written[9] that implements the computer control of the network analyzer. The frequency responses of several SAW filters were stored on a mini-floppy disk. Then by using SUB Fildatm and several other subroutines, the responses of the filters to various input signals were simulated and plotted. These plots were compared to photographs of actual responses taken in the laboratory. See Fig 11.

Then a detector and opamp were connected to the output of the SAW filter, and those responses were photographed. The opamp subroutine was added to the simulation program (the detector subroutine was already in place for the reasons given earlier), and the output of the opamp was simulated as shown in Fig 12. Both Fig 11 and 12 show good agreement between actual and simulated responses.

VII. RECOMMENDATIONS

The most immediate concern is that there are still several subroutines of the original structure that have been converted to BASIC but have not yet been thoroughly debugged. These programs include a Chebyshev bandpass filter, a comparator, a Gaussian transitional bandpass filter, and a subroutine that generates a trapezoidal or cosine-tapered envelope of a carrier. However, it should not take long to complete that part of the project. Furthermore, with what has been learned this summer, it should not be difficult to convert those to the modified structure. The limiter simulation may not be as easy.

It would probably be beneficial to have a subroutine by which one could specify a set of numbers for the shape of a filter, especially for a SAW-type response. SUB Fildatm could easily be converted to that use. Incidentally, if the phase function of a spectrum is a linear function with a slope of -m deg/MHz, the time delay for that filter is

$$Td = m/360 \ \mu s \qquad (19)$$

Other devices that should be investigated include the various logic gates fed by the comparator output of a slot assembly in a channelized receiver. The area of dispersive delay lines presents some interesting challenges.

Finally, these simulation subroutines should be assembled together to simulate larger parts of the channelized receiver, if not the entire system. The spectrogram may be helpful in answering some of the perplexing questions about receivers.

REFERENCES

1. Signorino, J. S., A FORTRAN Package for the Simulation and Spectr. l Analysis of a Channelized Receiver and Other Systems, Air Force Technical Report, AFWAL-TR-81-1278, June 1982.

2. Oppenheim, A. V., "Speech Spectrograms Using the Fast Fourier Transform", IEEE Spectrum, Vol 7, August 1970, pp 57-62.

3. Burbridge, T. E., The Effects of Window and Delay Selection on the Spectrogram of a Signal, Air Force Technical Report, AFWAL-TR-81-1279, June 1982.

4. Babiner, L. R. and Schafer, R. W., Digital Processing of Speech Signals, Prentice-Hall, Inc., 1978.

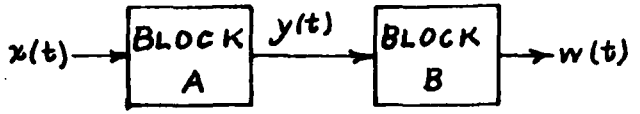
5. Cheng, Tsan-Huei, "Memory Reduction and Program Simplification in a Simulation Package for Band Limited System", M.S. Thesis, University of Missouri-Rolla, 1981.

6. Brigham, E. Oran, The Fast Fourier Transform, Prentice-Hall, Inc., 1974.

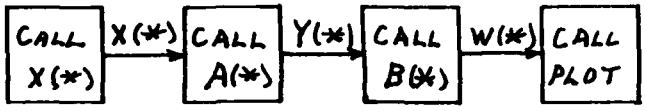
7. Budak, Aram, Passive and Active Network Analysis and Synthesis, Houghton Mifflin Company, 1974.

8. Zverev, Anatol I., Handbook of Filter Synthesis, John Wiley & Sons, 1967.

9. Programming Note: "Introductory Operating Guide for the HP 8505A RF Network Analyzer with the HP 9826A Desktop Computer (BASIC)", Hewlett-Packard Company, October 1981.

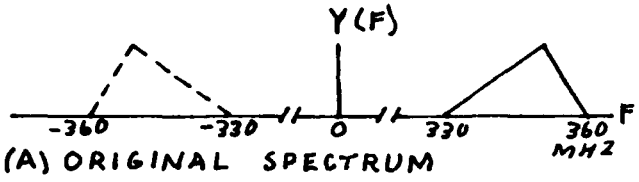


(A) SYSTEM BLOCK DIAGRAM

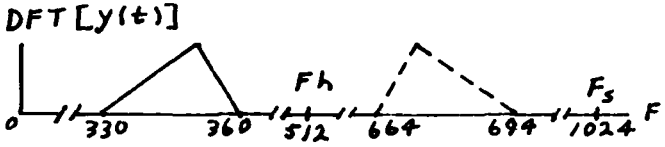


(B) SIMULATION BLOCK DIAGRAM

FIG 1. SIMULATION SCHEME.



(A) ORIGINAL SPECTRUM



(B) SPECTRUM: ORIGINAL STRUCTURE.

FIG 2. SPECTRA FOR EXAMPLE 1.

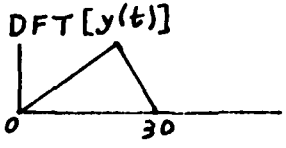
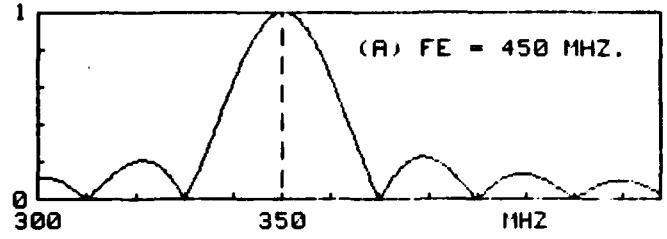


FIG 3. SPECTRUM: MODIFIED STRUCTURE.



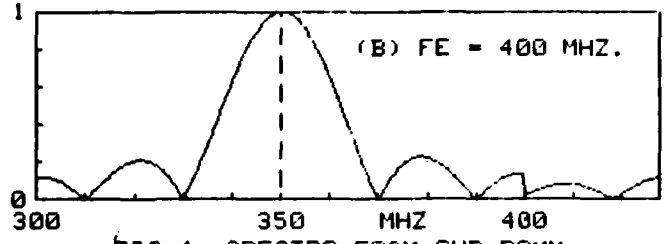
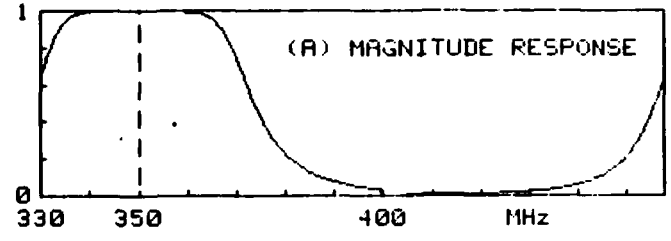


FIG 4. SPECTRA FROM SUB PAMM.



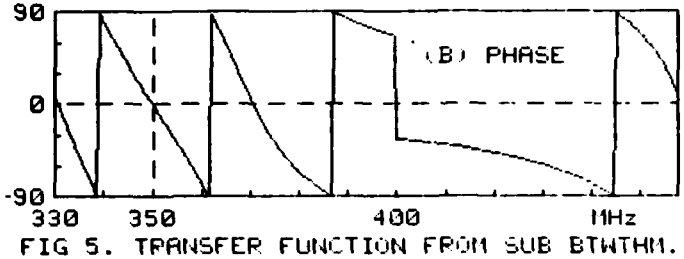
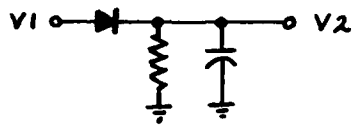
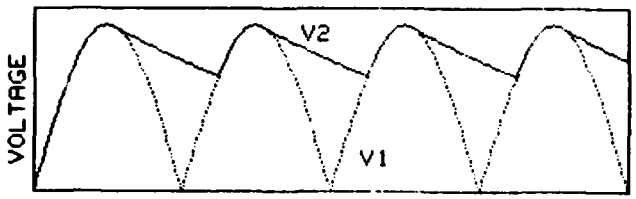


FIG 5. TRANSFER FUNCTION FROM SUB BTWTHM.



(A) CIRCUIT



(B) TYPICAL WAVEFORMS

FIG 6. RC-DIODE DETECTOR.

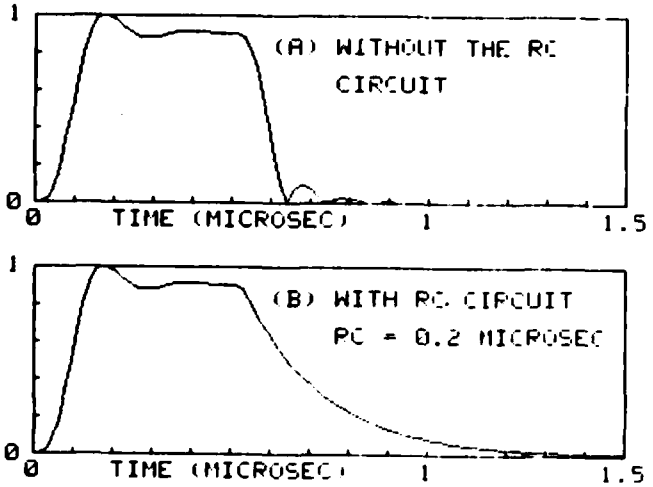


FIG 7. THE EFFECTS OF AN RC CIRCUIT.

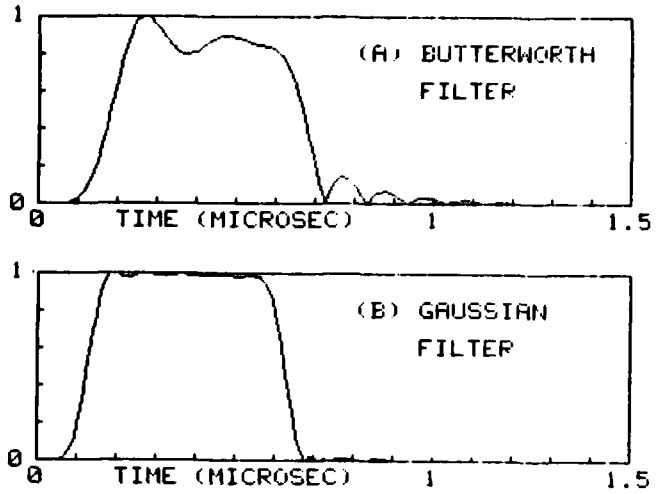
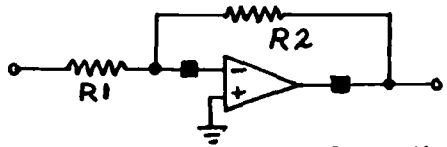
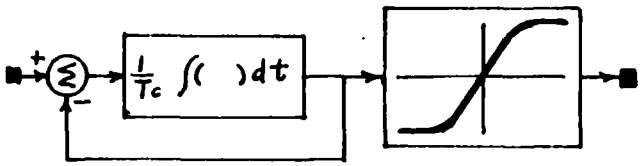


FIG 8. RESPONSE TO A 0.5-MICROSEC PULSE.



(A) EXTERNAL CIRCUIT



(B) INTERNAL CIRCUIT

FIG 9. OPAMP MODEL.

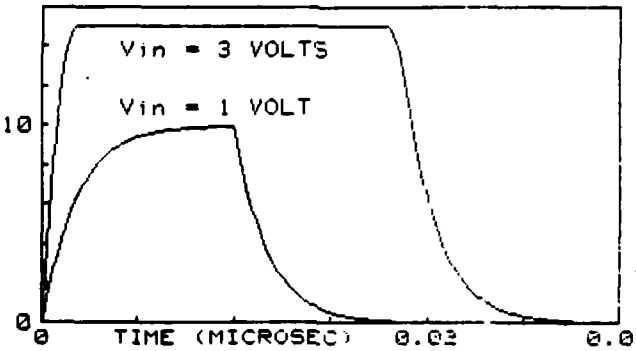
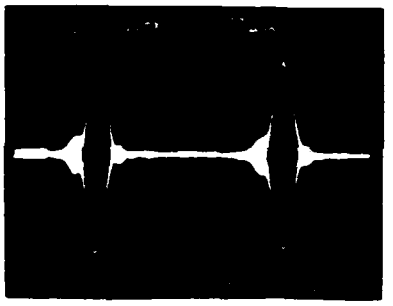
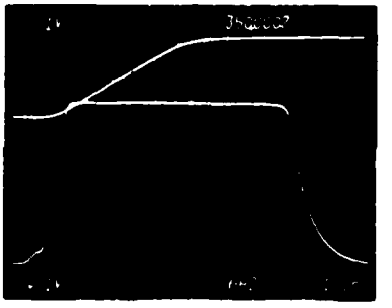


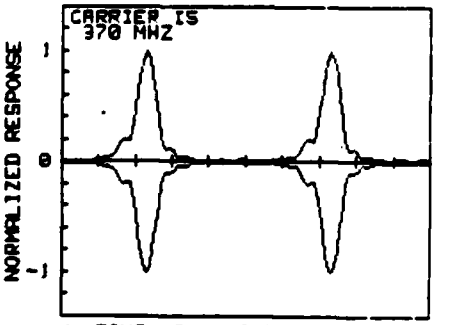
FIG 10. OPAMP RESPONSE TO A 10-NS PULSE.
Tc=500 NS Kol=3000 Kcl=10 Vlim=15



(A) ACTUAL

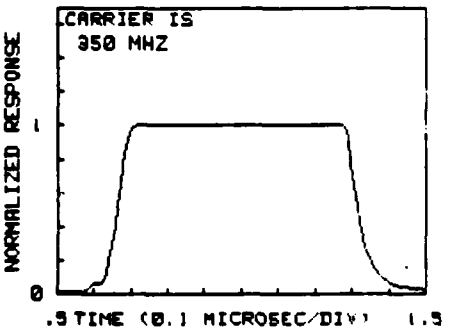


(A) ACTUAL (LOWER TRACE)



(B) SIMULATED

FIG 11. FILTER RESPONSE TO A 0.5-μSEC PULSE.



(B) SIMULATED

FIG 12. RESPONSE OF FILTER, DETECTOR, AND OPAMP TO A 0.5-μS PULSE.

1982 USAF-SCEEE SUMMER FACULTY RESEARCH PROGRAM

Sponsored by the

AIR FORCE OFFICE OF SCIENTIFIC RESEARCH

Conducted by the

SOUTHEASTERN CENTER FOR ELECTRICAL ENGINEERING EDUCATION

FINAL REPORT

FROM PETITE AVIATRIX TO USAF AIRCREW: HISTORICAL REVIEW AND CURRENT STATUS OF FEMALE FLIERS

Prepared by:	Dr. Willie A. Bragg
Academic Rank:	Assistant Professor
Department and University:	Department of Early Childhood and Special Education University of Cincinnati
Research Location: Beam	Neuropsychiatry Branch, Clinical Sciences Division, USAF School of Aerospace Medicine, Brooks Air Force Base, TX
USAF Research Colleague:	Drs. Bryce Hartman and David Jones
Date:	August 9, 1982
Contract No:	F49620-82-C-0035

FROM PETITE AVIATRIX TO USAF AIRCREW: HISTORICAL REVIEW AND CURRENT STATUS OF FEMALE FLIERS

by

Willie A. Bragg

ABSTRACT

A research project was conducted to investigate the integration of females into the United States Air Force. The focus of the investigation was to examine issues surrounding female entry into the undergraduate pilot training program. Historical data, attitudinal studies and policy guidelines are discussed as they relate to undergraduate pilot training. The results indicate that females have positively contributed to the field of aviation. In addition, female entries into undergraduate pilot training programs have increased. Recommendations for further research are outlined.

ACKNOWLEDGEMENT

This research project could not have been conducted without the sponsorship of the Air Force Systems Command, the Air Force Office of Scientific Research and the Southeastern Center for Electrical Engineering Education.

I would like to thank the Air Force personnel at the Clinical Sciences Division, especially the Neuropsychiatry Branch for their hospitality. I would also like to thank Dr. David Jones for his advice and support during this project.

Finally, my special thanks is extended to Dr. Bryce Hartman for his assistance and guidance throughout this endeavor.

I. INTRODUCTION

Historically, women have been received by society as a minority group. However, with the advent of the women's movement, women have become a more visible and vocal segment in the mainstream of society. Combined efforts of ERA posture and feminist litigation have positively affected the roles of men and women. Additionally, changes in lifestyles of women coupled with equal opportunity have resulted in the integration of women into traditionally male-dominated areas. Today, women have returned to institutions of higher education for advanced degrees, have entered highly specialized fields including science and engineering, have become business partners with men in corporate America and have shared political and judicial responsibilities with their male counterparts. Especially in the military, women's integration has not gone unnoticed. According to the Defense Advisory Committee on Women in the Services (DACOWITS), women account for 8.7% of the active force (1). However, since the signing of mandate P.L. 94-106 by former President Gerald Ford on October 7, 1975, modification of procedures and guidelines has been a primary concern of the military.

It is 1982 and crucial questions and issues continue to plague the implementation of P.L. 94-106 admitting women to the Department of Defense (DoD) service academies. For example, the Army is presently reassessing its military functions and the effect upon combat readiness with regard to women in combatant roles (2). Questions concerning draft status, interpretation of combat related assignments, physiological and psychological endurance standards have greatly influenced the extent of female participation and policy changes in all branches of the military.

Thus, the underlying concern seems to focus on what should remain military and what must be changed with the integration of women. More specifically, what posture has the United States Air Force taken to actually involve women in aviation training and what needs to be done in order to continue effective utilization of women in the United States Air Force.

II. OBJECTIVES

The primary purpose of the research project was to critically examine issues concerning female pilots from the inception of aviation to the present. However, the investigation was limited to American female pilots in the United States Air Force and did not include any material regarding upper body strength differences between males and females. The specific objectives were as follows:

1. present a historical perspective of women in aviation
2. critique studies related to women's entrance into undergraduate pilot training (UPT)
3. isolate problems concerning female participation in UPT programs
4. evaluate policy guidelines and procedures as they affect female pilots.

III. APPROACH

In order to accomplish these objectives, a comprehensive review of the literature was conducted, with the assistance of the Strughold Aeromedical, Human Resources Laboratory and Base libraries. Documents concerning the history of women pilots, studies involving women pilots

in training programs and policy statements of the United States Air Force were collected and reviewed.

In addition, structured interviews were conducted with personnel at Brooks AFB, Texas who were involved or who had previously participated in research concerning females in the undergraduate pilot training program. One interview was conducted with a female student pilot. This also aided in gathering valuable information about the current status of female student pilots.

A. History of Women Pilots

Although the literature is somewhat unclear as to whether Blanche Stuart Scott or Bessica Faith Raiche was America's first woman pilot, Blanche Scott was considered the woman to make the first international solo flight (3). Other American women who gained recognition and fame in the early years included Bessie Coleman, first black woman pilot, Harriet Quimby, Matilde Moisant, Katherine and Marjorie Stinson, Ruth Law, and Amelia Earhart (4, 5). Although a pilot's license was not a prerequisite for women pilots, some women took advantage of the opportunity to take the pilot test (6). Material published in the 1917 Aero Club of America Bulletin identifies the first ten women to receive pilot's licenses along with noteworthy accomplishments. These are shown in Table 1.

Perhaps one of the most well-known women pilots was Amelia Earhart. Although she received her license in 1923, she was considered the first woman to cross the Atlantic (7, 8).

During the early thirties, females were still viewed as record breakers. It was perhaps during the mid-thirties, that the focus

TABLE 1

WOMEN HOLDERS OF PILOT'S LICENSES

Certificate Number	Name	Accomplishment
37	Harriet Quimby	First to cross English Channel
44	Matilde E. Moisant	Piloted plane to 3,000 ft setting early world record
133	Julia Clark	First woman to be taught at Curtiss Flying School at North Island, San Diego, California
148	Katherine Stinson	Helped establish Stinson Aircraft Company in San Antonio, Texas. First woman authorized to carry air mail
173	Bernetta A. Miller	Qualified for license during night flight. Flew first monoplane demonstration flight for Gov't Officials
188	Ruth Bancroft Law	Set three new records: (1) Second best world nonstop cross country. (2) Women's world nonstop cross country. (3) American nonstop cross country
301	Richberg Hornsby	Graduated from Wright School in Dayton, Ohio
303	Marjorie Stinson	Trained cadets from Royal Canadian Flying Corps at San Antonio. Participated in exhibition flights
561	Dorthy Rice Peirce	Painter, Sculptor, Writer
633	Helen Hodge	First woman west of Chicago to receive license

changed for female pilots. During World War II under the supervision of Jacqueline Cochran, Woman's Air Force Service Pilots (WASP) was established to release male pilots from combat duty. The WASPs performed many tasks including ferrying, cargo carrying, and various other types of noncombat flying. The first step toward women's integration into the military came in 1948 with the passage of the Women's Armed Services Integration Act. Essentially, the act ensured women of both regular and reserve status in the Army, Navy, Marine Corps and Air Force. However, it must be pointed out that the act also imposed several limitations.

Gradual changes have come about with regard to women in the military. In 1977 Congress passed a bill militarizing women pilots who had participated during World War II, thus making them eligible for veterans' benefits and in 1976, the United States Air Force opened its academy to women and began its first undergraduate pilot training program for women pilots (9). A substantial portion of UPT students come from the Air Force Academy, following graduation. It is necessary, then, to examine the role of the Academy in providing students for UPT.

B. UPT Program

Presently, UPT programs are conducted at Williams Air Force Base, Mississippi, Vance Air Force Base, Oklahoma, Laughlin Air Force Base, Texas, and Reese Air Force Base, Texas. The academic and flying components of the UPT include approximately 750 hours of scheduled activities, 175 flying hours, 500 hours in ground training, and 72 hours in simulators and cockpit familiarization trainers. The initial flying phase is conducted using a T-37 subsonic jet and the second phase of training uses the supersonic T-38 Talon.

Academic training includes performance computation, flight planning, weather, aerospace physiology, aircraft systems operations, aircraft accident prevention, applied aerodynamics, flight instruments and instrument procedures. Students satisfactorily completing the one-year program receive silver pilot wings and begin their Air Force flying career. Additionally, navigator training on the undergraduate and graduate levels is also available to individuals interested in aircraft navigation (10).

Plans to admit women into the Air Force began as early as 1972. Academy officials initiated possible procedures for the admittance of women and appointed an ad hoc committee to focus on (1) utilization of women academy graduates in the Air Force, (2) appropriate selection criteria, (3) feasibility of a single-track program and (4) minimum number of women cadets (11).

C. Formal Studies

The first study was conducted outside of the Air Force. Its objective was to ascertain psychological data of potential female pilots. Novello and Youssef (12) administered the Edwards Personality Preference Scale (EPPS) and General Aviation Psycho-social Inventory (GAPSI) to 87 women general aviation pilots. The authors concluded that traits transcend sex differences in that female and male pilots showed more smiliarities ($p < .05$) than the general U.S. population of males and females.

Studies directly related to women's entry into UPT focused on attitudes and performance of women trainees. Kantor, Noble, Leisey and McFarlane (13) tested 30 women pilots who had entered UPT as of 1978. Data were also collected on 40 men, 16 of whom were co-students of women

trainees. The remaining 24 men were instructor pilots involved in the flight training program. Prior to training, all trainees were administered a battery of paper-and-pencil tests which included measures of verbal aptitude, non-verbal aptitude and psychomotor aptitude. Behavioral sample data were also collected from graduating women and men trainees and instructors. The findings indicated that men and women graduated from UPT at comparable rates, and more similarity rather than dissimilarity was evidenced. However, of particular interest is the instructor ratings. Although trainee attributes were seen similarly, instructors felt that men were more likely to become competent pilots.

In a follow-up study, Kantor and Ideen (14) surveyed the attitudes of 65 flight instructors who had participated in UPT, survival-resistance training, replacement training units and in-unit performance training. The performance of 22 female pilots who had completed UPT and were involved in advanced phases of flight related training was evaluated. Although the overall ratings showed a trend toward better male performance, instructors of first and second groups of females rated male co-students significantly better on their ability to manage stressful situations and overall performance.

These studies seemed to suggest that females were initially perceived as somewhat inferior during early phases of training, but these perceptions improved during the course of training. DeFleur, Gillman and Marshak (15) and Liang (16) found similar trends of changing attitudes toward females by male cadets at the Air Force Academy. DACOWITS (17) also reported problems during the test period of UPT (1976-79), but suggested a promising outlook toward normalization and

increase of female pilots.

D. Air Training Command Experience

According to the Air Force Training Command (ATC), Randolph Air Force Base, Texas, approximately 350 females have entered UPT. To date, 175 females have graduated and are pursuing flying careers. One has been medically disqualified. The overall attrition rate for women since the inception of UPT is 27.4% which compares favorably with the attrition rate for males. The number of females entering UPT is shown in Table 2. Inspection of the data shows that the number of female entries has increased. Additionally, the Air Force has substantially increased its total representation of women on active duty (11.2%) and leads all other services (18).

E. Policy Guidelines and Procedures

The underlying causes of increase, attrition and utilization of female pilots rest in major policy change and modification. During the experimental phase of UPT, the number of female entries were kept relatively low. The Air Force was also given latitude in constructing policies outlining the kinds of work available to females. Since the Air Force policy excludes females from duties involving such combat operations as actually engaging the enemy and/or delivering weapons upon the enemy, duties involving the operation of land-based missiles have also been limited to male pilots. In other words, females, continue to be excluded from flying combat coded aircraft.

In addition, the Air Force policy adheres to a fixed quota system. More specifically, the number of men trained as pilots and navigators must exceed the number of positions for these skills. This surplus

TABLE 2

FEMALES IN UNDERGRADUATE PILOT TRAINING

Fiscal Year	Number of Entries	Number of Graduates
1976	10	
1977		10
1978	10	6
1979	20	14
1980	24	20
1981	99	72
1982	110	53

ensures that pilots and navigators continually remain on flight duty and provides a mobilization base for wartime. Therefore, the imposed limitations require male entries to exceed female entries into pilot and navigator training. Although combat related duties have been limited to male fliers, gradual changes have been seen in the availability of other assignments for female fliers.

Another policy area involves modifications that have been made by the Air Force regarding join-spouse requests. Since females began to become pilot qualified, more requests to assign two people together have occurred. However, as married personnel progress and gain experience and rank, the question of optimum career progression for both members may complicate join-spouse requests. The mission and/or objective of the Air Force versus personal desire may also hamper join-spouse requests.

Finally, policy requiring automatic discharge of pregnant women has been reexamined. Pregnant women are immediately grounded and are assigned to other duties requiring flying personnel. This policy is based on medical considerations which place emphasis on the welfare of the mother and fetus, flying safety considerations and mission accomplishment. Increased fatigability, sudden and unpredictable onset of nausea and a variety of minor and inconsistent symptoms can interfere with flying duties and safe mission completion. Pregnant women pilots perform other flight related duties jointly determined by the attending physicians and supervisors or commanders, and continue to receive flight pay until the first day of the sixth month following medical disqualification. Based on the evaluation of the flight surgeon, women may

return to flying duties after pregnancy (19, 20).

IV. RESULTS

The results of this investigation showed that women have contributed to the field of aviation since its inception. Early pioneers such as Blanche Scott, Katherine Stinson, Jacqueline Cochran and Nancy Love paved the way for female participation in pilot and space training programs.

Studies related to UPT programs indicated that the gradual integration of females into the Air Force positively affected the attitudes of male students and staff personnel. It is unclear as to whether contact alone was sufficient to sustain attitude change within the Air Force population. Additionally, the number of females entering pilot training has increased.

Major policy changes have provided a wide array of opportunities for female pilots. In the Military Airlift Command, females have been assigned to cargo airlift, medical evacuation aircraft and aircraft used for weather reconnaissance. In the Strategic Air Command, females have gone to the air refueling tanker and the airborne command post aircraft. In the Air Training Command, females have been assigned to aircraft used to train student pilots and student navigators.

V. RECOMMENDATIONS

The material presented in this review clearly demonstrates that the Air Force has aggressively pursued the integration of women into its flying force. The recommendations which follow are in no way critical of the substantial progress the Air Force has achieved.

1. It is suggested that the Air Force reconsider its current policy restricting females from combat coded aircraft, particularly with regard to females at the Academy. Because the Air Force Academy has a mission of educating, training and preparing officers for various duties including combat, a diversion of females to a lesser mission is somewhat contrary to the philosophy. Additionally, some combat aircraft require pilot and co-pilot compatibility for mission completion.

2. It is suggested that the Air Force continue to conduct attidudinal studies of males and females during training. The material reviewed showed that early studies focused on female entries into UPT, with good results. In addition, the results of these studies should be disseminated to the Air Force staff so that they can continue to develop appropriate training, classes and personal development.

3. It is suggested that females receive systematic counseling concerning career options throughout UPT. Evidence from the present study showed that females entering traditionally male-dominated areas may encounter added emotional and psychological problems. Systematic counseling would aid in developing a strong self-concept which is vital to successful completion of training and continued pursuit of career goals.

4. It is suggested that tier relationships be developed. This can be done in several ways. Regular or weekly seminars can be conducted. During this time, females assigned to lower ranking females would serve as mentors. This procedure would also establish positive role models and provide emotional support. As an alternative, higher ranking males could also be assigned to females to develop protégé-

mentor relationships. The rationale underlying this suggestion is that physical proximity in addition to personal contact may positively sustain attitudes toward females in the Air Force.

5. A follow-on study to this review is strongly recommended. The current group of approximately 175 female graduates are a rich source of current information on job assignments, past and present experiences, problems encountered, and so on. This would enable the Air Force to evaluate the efficacy of pilot training programs and determine modifications needed in the total pilot program.

REFERENCES

1. Cutler, K., "All about Dacowits," Airman, April 1982, pp. 18-23.
2. Abrams, A., "Army examining readiness of women soldiers," San Antonio News, June, 1982, p. 6-B.
3. May, C., Women in Aeronautics, New York, Thomas Nelson and Sons, 1962.
4. Moolman, V., Women Aloft, Alexandria, Virginia, Time Life Books, 1981.
5. Boase, W., The Sky's the Limit: Women Pioneers in Aviation, New York, MacMillian Publishing Co., Inc., 1979.
6. Oakes, C. M., United States Women in Aviation Through World War I, Washington D.C., Smithsonian Studies in Air and Space, 1978.
7. Klaas, J., Amelia Earhart Lives, New York, McGraw-Hill Book Co., 1970.
8. St. Johns, A. R., Some Are Born Great, New York, Doubleday & Company, Inc., 1974.
9. Hodgman, A., and R. Dzabbaroff, Skystars: The History of Women in Aviation, Harrisonburg, Virginia, Canada-McClelland & Stewart Ltd., 1981.
10. Undergraduate Pilot Training, United States Air Force, Office of Public Affairs, Washington, D.C., October, 1981, pp. 1-2.
11. Wallisch, W. J., The Admission and Integration of Women into the United States Air Force Academy, (Doctoral dissertation, University of Southern California, 1977). Dissertation Abstracts, 1978, 38, 4619-A.

12. Novello, J. A., and Z. I. Youssef, "Psycho-Social Studies in General Aviation: Personality Profile of Female Pilots," Aerospace Medicine, June 1974, pp. 630-633.

13. Kantor, J. E., B. E. Noble, S. A. Leisey, and T. McFarlane, "Air Force Female Pilots Program: Initial Performance and Attitudes," AFHRL-TR-78-67, Brooks AFB, Texas, Personal Research Division, Air Force Human Resources Laboratory, February 1979.

14. Kantor, J. E., and D. R. Ideen, "Air Force Female Pilots Program: and Interim Report," Paper presented at 21st Annual Convention of the Military Testing Association," San Diego, California, 1979.

15. De Fleur, N. B., G. Gillman, and W. Marshak, "Sex Integration of the U.S. Air Force, Armed Forces and Society, August, 1978, pp. 607-621.

16. Liang, S., "Male-Female Differences in Variables Affecting Performance: Aeromedical Implication," Unpublished Paper, USAF School of Aerospace Medicine, Brooks AFB TX, June, 1982.

17. Hyatt, B., Performance of Women in Undergraduate Pilot Training and Follow-On Assignments," Proceedings from Defense Advisory Committee on Women in the Service Conference, Scottsdale, Arizona, November, 1980.

18. "Women on Increase in the Military," Medical Patriot, June, 1982, p. 25.

19. Binkin, M., and S. J. Bach, Women and the Military, Washington, D.C., The Brookings Institution, 1977.

20. Stiehm, J. H., Bring Me Men and Women: Mandated Change at the U.S. Air Force Academy, Berkeley, California, University of California Press, 1981.

APPROVAL SHEET

1982 USAF-SCEEE SUMMER FACULTY RESEARCH PROGRAM

Sponsored by the

AIR FORCE OFFICE OF SCIENTIFIC RESEARCH

Conducted by the

SOUTHEASTERN CENTER FOR ELECTRICAL ENGINEERING EDUCATION

FINAL REPORT

NAVIER-STOKES SOLVERS FOR RAMJET APPLICATIONS

Prepared by: Dr. E. F. Brown

Academic Rank: Associate Professor

Department and University: Mechanical Engineering Department
Virginia Polytechnic Institute and
State University

Research Location: Aero Propulsion Laboratory
Ramjet Engine Division
Ramjet Technology Branch

USAF Research Colleague: Dr. F. D. Stull

Date: September 14, 1982

Contract No.: F49620-82-C-0035

APPROVED: F D Stull (Signature)

NAME: F. D. Stull, Effort Focal Point

LOCATION: AFWAL/PORT

DATE: 16 Sep 82

1982 USAF-SCEEE SUMMER FACULTY RESEARCH PROGRAM

Sponsored by the

AIR FORCE OFFICE OF SCIENTIFIC RESEARCH

Conducted by the

SOUTHEASTERN CENTER FOR ELECTRICAL ENGINEERING EDUCATION

FINAL REPORT

NAVIER-STOKES SOLVERS FOR RAMJET APPLICATIONS

Prepared by: Dr. E. F. Brown

Academic Rank: Associate Professor

Department and University: Mechanical Engineering Department
Virginia Polytechnic Institute and
State University

Research Location: Aero Propulsion Laboratory
Ramjet Engine Division
Ramjet Technology Branch

USAF Research Colleague: Dr. F. D. Stull

Date: September 14, 1982

Contract No.: F49620-82-C-0035

NAVIER-STOKES SOLVERS FOR RAMJET APPLICATIONS

by

Eugene F. Brown

ABSTRACT

A typical Navier-Stokes solver (STARRC) was run in an attempt to simulate measured velocity and turbulence intensity measurements in a sudden expansion (dump) combustor. Failure to accurately predict the measured centerline velocity suggested that the turbulence model used in the calculation may be inadequate at low Reynolds numbers. Modifications to the program which allow the calculation of combustion efficiency and combustor pressure loss are described. Suggestions are made for improving the program and for implementing extensions to it. These include: an improved turbulence model, a more realistic combustion model, a hybrid algorithm, and a method of solution for high speed compressible flows.

I. INTRODUCTION:

Navier-Stokes codes offer a promising way to calculate the performance of ramjet combustors. AFWAL/PORT has acquired two state-of-the-art Navier-Stokes codes both of which are based on the TEACH/SIMPLE algorithm. One code is for two-dimensional flows (STARPIC) and the other is for three-dimensional flows (GARRETT). Both were originally developed for gas turbine calculations. The three-dimensional code is currently in the process of being modified for ramjet calculations. The two-dimensional program has already been modified and has been renamed STARRC. Although a number of runs have been made with this program, it has not been thoroughly validated, its limitations have not been fully examined, nor have extensions of its capabilities been explored. The purpose of the present project is to address these tasks. This is an important activity since without a thoroughly validated program, design decisions based on its predictions cannot be undertaken with confidence, and without a sufficiently complete model of the phenomena involved, predictions beyond the range of variables for which experimental data exists may be dangerously misleading.

II. OBJECTIVES:

The objectives of this project were to validate the operation of the STARRC program and to expand its capabilities. In order to accomplish this I undertook the following specific tasks:

- I familiarized myself with the ramjet literature in general and with the TEACH/SIMPLE algorithm in particular,
- I ran a number of test cases and compared the results with experimental data, and

- On the basis of these comparisons and my reading of the literature, I suggested ways of improving and expanding the capabilities of the program.

III. LITERATURE FAMILIARIZATION:

The bibliography which appears at the end of this report contains a list of references most of which I read during this portion of the project. I have placed in parentheses at various points throughout this section the identification numbers of those references which I found to be of greatest value.

The TEACH/SIMPLE algorithm is only one of a number of methods for solving the Navier-Stokes equations, and the Navier-Stokes equations are only one way of mathematically modelling ramjet combustors. Therefore, my initial objective was to obtain a general background in the subject of ramjet combustor modelling (3.1, 3.3, 7.1-7.4).

Proper characterization of the effects of turbulence is vital in obtaining good predictions of ramjet combustor performance since turbulent flows, in fact, turbulent-recirculating flows, dominate ramjet combustor flowfields. Since my background in this area was somewhat limited, I found the more basic references the most useful (4.3, 9.1, 9.6).

The TEACH/SIMPLE algorithm has been the subject of countless papers. All but the first papers assume a level of knowledge of the algorithm not necessarily possessed by the novice reader. I would, therefore, recommend one of the early papers (10.17) for a reasonably complete and straightforward explanation of the computational procedure. The recent book by Patankar (10.1) is also

excellent in this regard. On a more advanced level, the notes (10.9) and the description of STARPIC (10.15) are recommended reading.

A number of interesting applications of the TEACH/SIMPLE algorithm can be found in 10.11. This, as well as 6.1 and 6.6, provide a reference to or contain experimental data on ramjet combustors which may well prove of value in future validation studies.

The references listed in the bibliography were obtained from papers brought to my attention by my AFWAL/PORT colleagues, references cited in these papers, and books and papers which I had collected before coming here this summer. It can therefore not be considered an exhaustive list of references on the subject. Reference 11.1 is included for those who prefer a more systematic acquisition process. Several interesting references can be found there. See particularly those marked with a red dot.

IV. COMPUTER RUNS:

After becoming reasonably well informed about the theoretical background and operation of STARRC, I began to make some runs with the intent of simulating some sudden expansion (dump) combustor tests which had just been completed at AFWAL/PORT. In these tests, the expansion (area) ratio was 3.61 and air was the working fluid, being drawn through the test rig by a small fan. The inlet nozzle was 25.4 mm in radius. Mean axial velocity and turbulence intensity measurements were made with a single-component LDV system at 2, 2.5, 7, 12, and 17 nozzle radii downstream of the dump plane. A second nozzle was located several diameters

downstream of the last measuring station to control the mass flow rate. The inlet velocity (at the nozzle throat) was 25.2 m/s. In the calculations, the combustor was assumed to be 20 nozzle radii in length, the pressure at the inlet was assumed to be 100 kPa, and the inlet temperature was assumed to be 293 K. Only the upper half of the combustor geometry was used in the calculations and presence the second nozzle was ignored.

In the first calculations a 48 x 24 (axial x radial) point mesh was used and points were distributed in the radial direction with a packing factor of approximately 6 at the combustor wall and at radial locations surrounding an axial line corresponding to the inlet nozzle throat radius. The calculated velocity profiles are compared with the experimental data in Fig. 1. At the two measuring stations nearest the dump plane, the measured velocities are well predicted especially at the centerline. At the combustor wall, however, the measured profile is fuller than predicted and exhibits a reflex curvature not seen in the calculations. Away from the recirculation zone, the predictions of the velocities at the wall improve. This is shown by the results at the next two measuring stations; however, at the centerline, the measured velocities are considerably underpredicted by the calculations. At the farthest downstream station, the predicted velocities are in good agreement with the measurements both at the wall and the centerline. The disagreement at the centerline is particularly surprising since Harch* obtained much better

* "Computational Fluid Dynamics" at AFWAL/PORT/TMR Review, July 28, 1982.

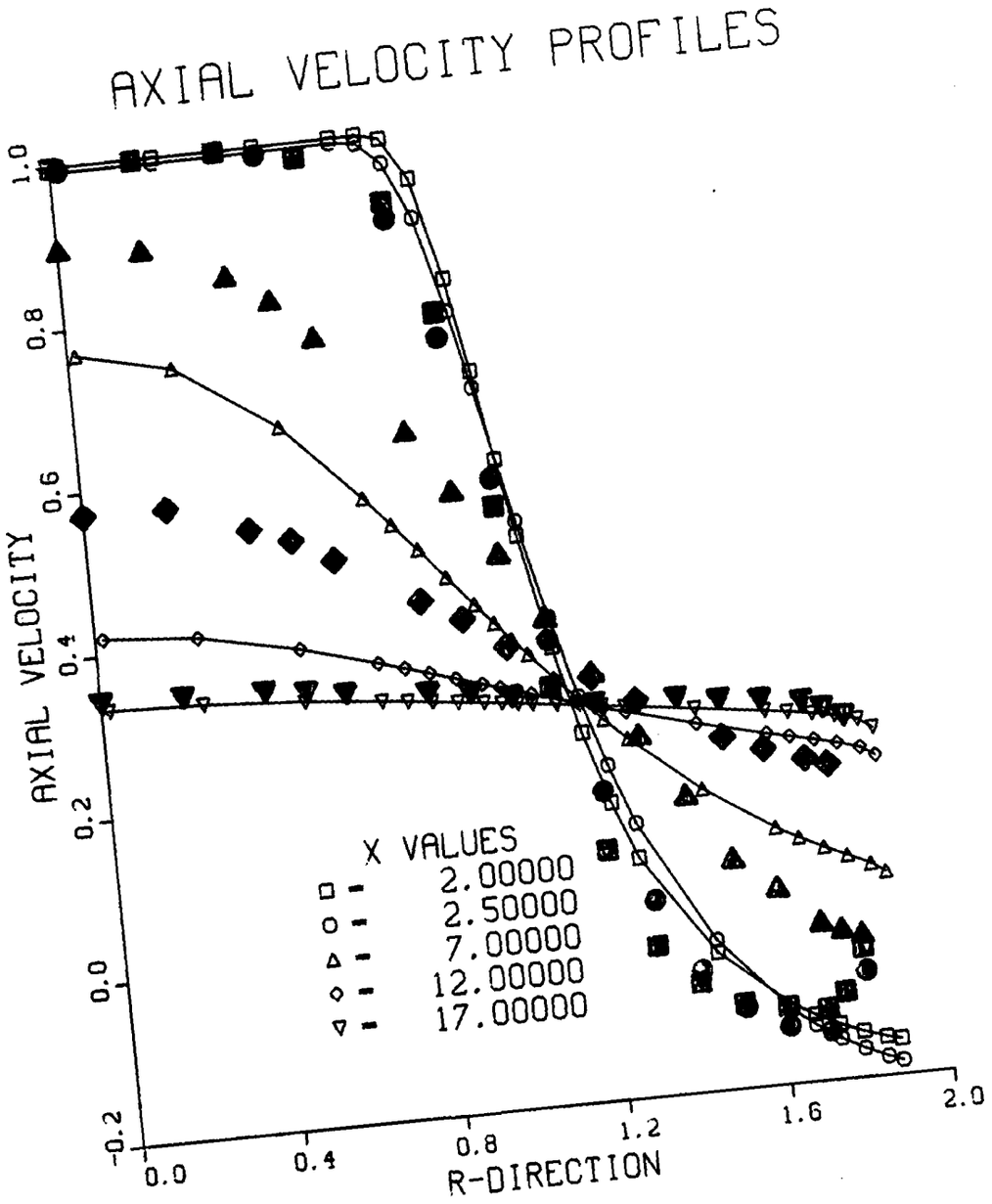


Fig. 1. Axial Velocity (Solid Symbols Are Experiments)

agreement in his simulation of Drewry's (6.1) data. A possible explanation for this situation lies in the fact that the inlet Reynolds number (based on nozzle radius) is more than 2.5×10^6 in Drewry's data and only 4.3×10^4 in the present case. Possibly the constants in the turbulence model are better suited for high Reynolds number calculations than they are for low Reynolds number calculations.

The measured and predicted value of turbulence intensity are compared in Fig. 2. The shape of the profiles are faithfully reproduced although the peak levels are consistently under-predicted. This discrepancy can be explained as follows. Experiments have shown that there is considerable non-isotropy exhibited by the turbulence in such flows (the axial turbulent velocity component being highly dominant). In computing the turbulence intensity from the predicted turbulence kinetic energy, this non-isotropy was ignored. If included, it would result in increasing the predicted turbulence intensity by as much as $\sqrt{3}$ and thus bring the predicted values into much more acceptable agreement with the measurements.

A second run was made in an attempt to improve the predicted velocity profiles in the recirculation zone. The difficulty was thought to be an insufficient number of mesh points in the near wall region. Accordingly, the packing factor was increased from 6 to 12. A 48 x 24 mesh was again used. Figure 3 shows the results. At the first two axial stations, a reflex curvature is clearly exhibited by the predicted velocity profiles in the recirculation region; however, its extent is considerably less than

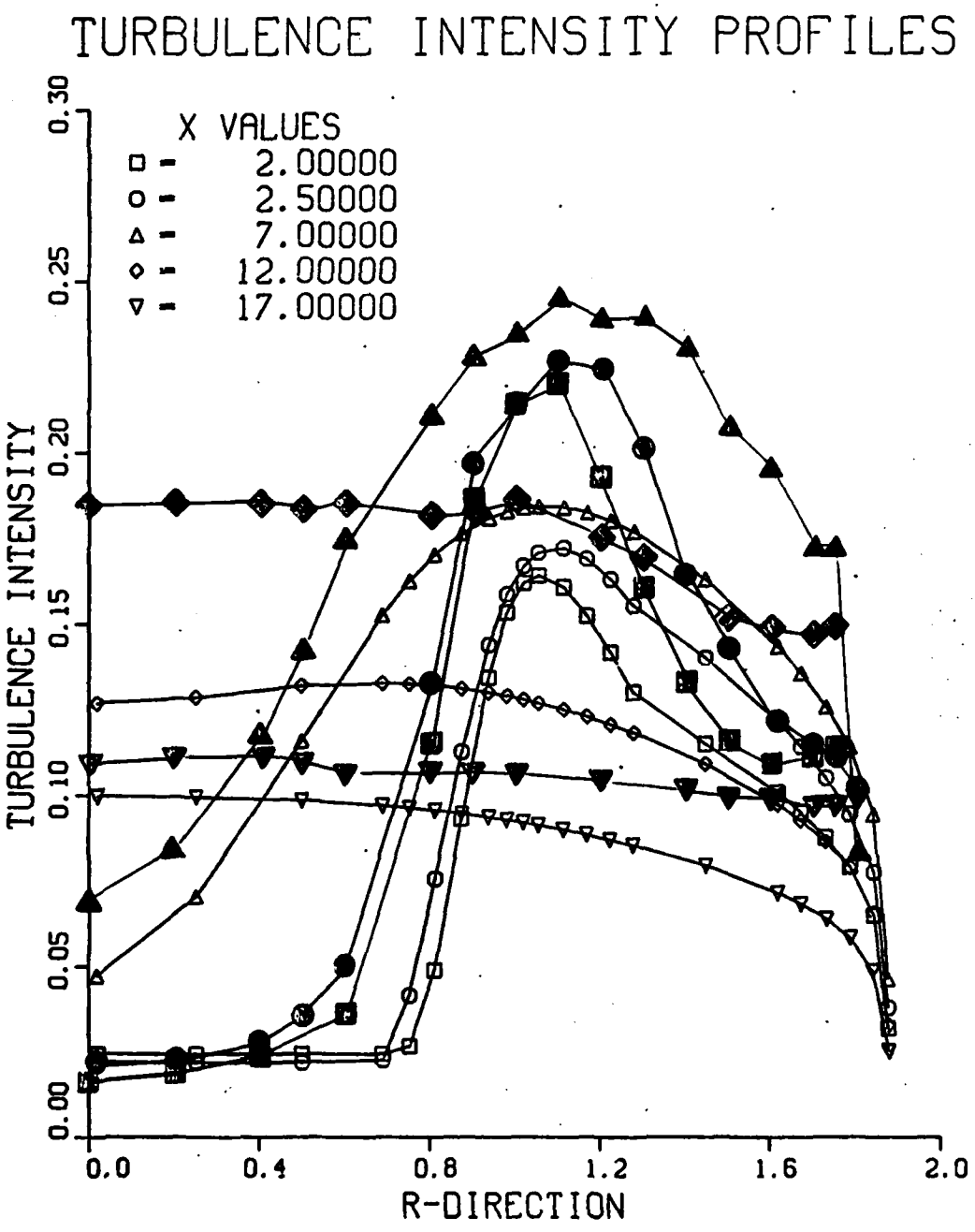


Fig. 2. Turbulence Intensity (Solid Symbols Are Experiments)

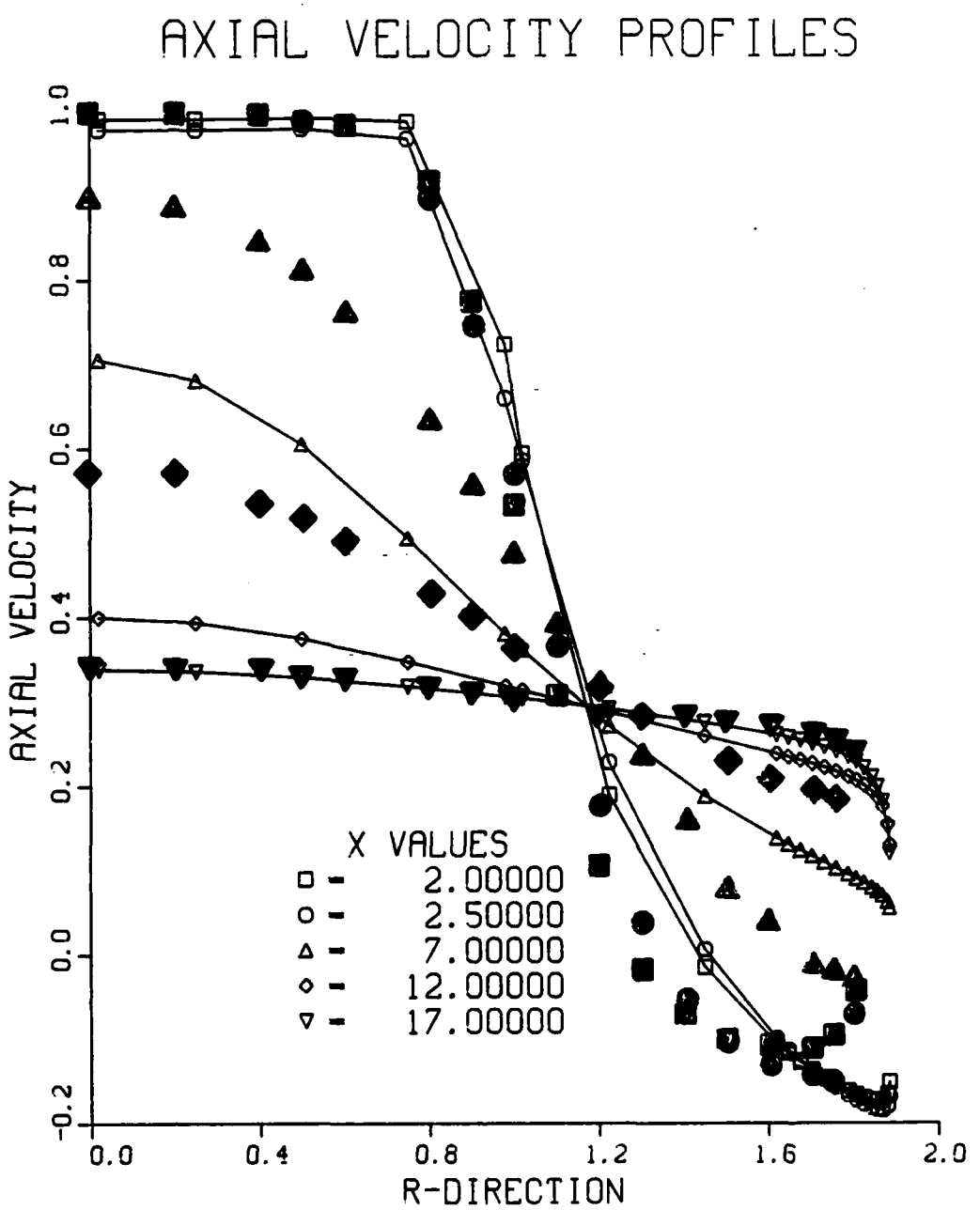


Fig. 3. Axial Velocity With Fine Mesh Spacing At Wall (Solid Symbols Are Experiments)

the experiments would suggest. In addition, the remaining velocity profiles show a boundary-layer-like character near the wall which is suggested by the measurements but not apparent in the previous calculations. Unfortunately, at the intermediate axial stations the centerline velocity is even more severely underpredicted than before. The turbulence intensity profiles were unchanged from the previous calculations.

A third run was made to examine the effect of compressibility on the calculations by invoking the compressibility option contained in STARRC. Since velocities of only a few meters per second are involved in these calculations (the inlet velocity is only 25.2 m/s), any significant change in the results from the previous calculations must be viewed with considerable suspicion. It is comforting to know that no differences whatsoever in either the velocity profiles or turbulence intensities were observed.

Finally a run was made with an inlet velocity of 252 m/s instead of 25.2 m/s in order to examine the Reynolds number sensitivity of the calculations. Surprisingly, this had no effect on the predicted velocity profiles and results identical to those obtained before were predicted. This is surprising since one would expect the reattachment point to move approximately 50 percent downstream due to such increases in inlet Reynolds number (10.12). This provides another indication that the failure of the calculations to properly predict the centerline velocities may be a Reynolds number related problem.

V. MODIFICATIONS TO STARRC:

As interesting and valuable as velocity profiles and turbulence intensities may be for validating the code and for providing detailed design information, of considerably greater interest in the applications area are such overall performance parameters as the combustion efficiency and the combustor (total) pressure loss. Accordingly, the calculation of these quantities was added to STARRC. The details of these calculations will now be described:

Combustion Efficiency: Combustion efficiency can be defined as the ratio of the actual to the ideal stagnation temperature rise of the working fluid as it flows through the combustor. Since in STARRC the flow is assumed to be adiabatic and constant specific heats are assumed, the combustion efficiency becomes the ratio of the actual mass of fuel burned to the total amount of fuel present. The combustion efficiency can, therefore, be expressed by the following equation:

$$\eta_C = \left. \frac{\Sigma\ (FR_j - FU_j)\ \delta m_j}{\Sigma\ FR_j\ \delta m_j} \right|_{i\ =\ NIM1}$$

Where the summations are taken across the combustor in the radial direction at the station adjacent to the exit (NIM1), FR_j and FU_j represent the local mixture fractions of total and unburned fuel, respectively, at radial location j, and δm_j is the mixture mass flow rate through the element. Station NIM1 was chosen for this calculation since the flow field there was expected to be more

accurately calculated than at the exit where extrapolation procedures were used.

Combustor Pressure Loss: Combustor pressure loss is defined as the ratio of the mass averaged total pressure at the exit to the mass averaged total pressure at the inlet. The combustor pressure loss can be expressed by the following equation:

$$\eta_P = \frac{\Sigma\ P_{oj}\ \delta m_j \Big|_{i = NIM1}}{\Sigma\ P_{oj}\ \delta m_j \Big|_{i = 1}}$$

where P_{oj} is the local total pressure, i = 1 represents the inlet station, and the remaining variables are as previously defined. For incompressible flow, P_{oj} is calculated from the local static pressure, P_j, and the local velocity by Bernoulli's equation. For compressible flow, the temperature ratio, T_j/T_{oj}, is first calculated from the energy equation, then the pressure ratio, P_j/P_{oj}, is calculated from the temperature ratio by the isentropic pressure temperature relationship for an ideal gas, and finally the total pressure is calculated from the pressure ratio and the local value of the static pressure. The equations used are the following:

$$T_j/T_{oj} = 1 - (u_j^2 + v_j^2 + w_j^2)/2H_{oj}$$

$$P_j/P_{oj} = (T_j/T_{oj})^{k/(k-1)}$$

$$P_{oj} = P_j/(P_j/P_{oj})$$

where k is the ratio of specific heats, H_{oj} is the local stagnation enthalpy, $(u, v, w)_j$ are the local velocity components, and

the remaining variables are as previously defined. (Note that since STARRC includes the enthalpy of reaction of the unburned fuel in the definition of stagnation enthalpy, this quantity must be subtracted from the computed quantity before the temperature ratio is calculated.)

Results: There are no results to present here for the combustion efficiency calculations since no successful combustion runs with STARRC have ever been made (see Recommendations section). Results from the pressure loss calculations, however, are available for both the 25.2 m/s cases and the 252 m/s case. For all 25.2 m/s cases the calculations predict a value of 0.9980. Although no experimental data is available for comparison, this result agrees well with a one-dimensional analysis of the problem (see 6.2) which gives 0.9979. This is not a very demanding test of the program, however, because the low velocities limit the pressure loss to a few tenths of a percent of the inlet total pressure. A better test of the capability of the program is the 252 m/s case. Here the program predicts a value of 0.8552; whereas, the one-dimensional analysis gives 0.7923. This may seem to be reasonably good agreement, but consider a more sensitive measure of the pressure loss, $(P_{01} - P_{02})/P_{01}$. In terms of this parameter, it appears that the pressure loss may be underpredicted by as much as 30 percent.

VI. RECOMMENDATIONS:

There is much which remains to be done before STARRC can be considered fully validated and fully capable of accurately simulating actual combustor performance. Both short and long range

tasks can be identified. It is my hope that I will be able to complete the short range tasks as a Senior Investigator under the terms of the Scholarly Research in Ramjet Technology Program. The long range tasks (involving basic research) I will include in a research proposal to the AFOSR Minigrant Program.

Short Range Tasks:

- From the runs made this summer, it seems that the low Reynolds number capability of STARRC may be in doubt. Accordingly, adjustments in the turbulence model will be sought to bring the predicted velocity profiles into better agreement with experiment.

- Runs at higher Reynolds numbers do not show the expected increase in reattachment length or the expected amount of pressure loss. The source of these difficulties will be investigated and may result in further modifications of the turbulence model.

- Another possibility is that the difficulty with the centerline velocity calculations may be due to an incorrect specification of the inlet conditions for the calculations. It is expected that such parameters as the inlet length scale will have a major effect on the results of the calculations (10.16). In light of the magnitude of the discrepancy and particularly since experimental measurements of the actual inlet conditions are unavailable, an investigation to determine the sensitivity of the calculations to the inlet conditions is called for.

- No successful runs of STARRC in the combustion mode have ever been run. This is because the instantaneous combustion model presently contained in STARRC produces such a rapid temperature increase that the calculations invariably diverge. An improved

combustion model with multi-stage reactions and rates controlled by the Arrhenius equation or eddy break-up model exists in the three-dimensional (Garrett) code. It is planned to transfer this model to STARRC.

- It is generally acknowledged that the k-ε turbulence model is inadequate in swirling flows because of the highly non-isotropic character of such flows. Algebraic turbulence models overcome this difficulty. Consequently, use of such methods in STARRC will be explored.

- A potentially promising way of reducing combustor pressure loss lies in the use of sloped-wall combustors equipped with swirlers; however, the effect of swirl on the fuel distribution in sloped-wall combustors is unknown. Such information is of great importance since it is essential that good combustion efficiency not be sacrificed in such designs. Runs are planned to provide this information. Comparisons with experimental data will be made.

Long Range Tasks:

- Current two-dimensional Navier-Stokes codes place severe demands on the capabilities of today's commonly available computing systems. For grids capable of even modest resolution of flow field details, computing times of several hours are not unknown and storage requirements close to total machine capacity are not unusual. In ramjet combustor applications, great computational time and storage requirement economies can be produced by using parabolic or partially parabolic methods instead of elliptic Navier-Stokes methods in those regions of the flow where no

recirculation takes place. Such "hybrid" solvers have the potential of halving the storage requirements for two-dimensional codes (reducing it by one-third for three-dimensional codes) and reducing computational time by an order of magnitude. Research is required to develop a means of judging in a dynamic fashion the local ellipticity of the flow and accordingly selecting the appropriate algorithm.

- Current Navier-Stokes methods used for ramjet calculations have evolved from algorithms originally designed to solve convection heat transfer problems. Although they are judged to be adequate for a wide variety of low speed applications, their performance is largely untried for high speed transonic applications. For short, high-technology combustors this is a severe shortcoming since accurate prediction of the performance of such combustors is certain to require the consideration of the transonic flow in the exhaust nozzle as a part of the calculations. This will at least require a modification of the TEACH/SIMPLE algorithm to include the effect of pressure corrections on the density calculations. It is even more likely that the TEACH/SIMPLE algorithm will be found fundamentally inadequate for such calculations. This is because use of this algorithm requires a prior specification of inlet mass flow rate; however, a well-known characteristic of transonic internal flows is that the mass flow rate cannot be prescribed in advance. The importance of high speed compressible flows in ramjet calculations combined with the suspected inadequacy of current calculation methods combine to make the discovery of a suitable algorithm a most challenging and valuable research activity.

ACKNOWLEDGEMENTS

I would like to express my gratitude to Dr. F. D. Stull, Branch Chief of AFWAL/PORT for inviting me here this summer and to AFSC, AFOSR, and SCEEE for providing me with the financial support which made my visit possible. I am particularly indebted to Dr. W. H. Harch, ARL, Melbourne, Australia and Dr. S. P. Vanka, ANL, Argonne, Illinois, who were at AFWAL/PORT on temporary assignment this summer, for many valuable technical discussions. Special thanks to Dr. Stull and Dr. R. R. Craig whose guidance and hospitality contributed greatly to making my visit a most enjoyable and rewarding experience.

BIBLIOGRAPHY

Categories:

1. Time-Dependent Navier-Stokes Calculations
2. One-Dimensional Ramjet Calculations
3. Modular Ramjet Calculations
4. Miscellaneous
5. Swirl
6. Ramjet Experiments
7. Surveys
8. Combustion
9. Turbulence
10. Steady Navier-Stokes Calculations
11. Computer Search

Location Key:

T - AFWAL Technical Library
B - Personal Library of E. F. Brown
W - Wright State University Library
P - AFWAL/PORT Ramjet Combustor Collection

1. Time-Dependent Navier-Stokes Calculations

Books

1.1 A Collection of Technical Papers, AIAA 3rd Computational Fluid Dynamics Conference, June 27-28, 1977, (532.05, AI11, 1977), T.

Papers and Reports

1.2 "A Navier-Stokes Solution for Cold Flow in an Axisymmetric Combustor," G. A. Hasen, AFWAL-TM-82-171-FIMM, March 1982, B.

1.3 "Navier-Stokes Solutions for an Axisymmetric Nozzle," G. A. Hasen, AIAA 81-1474, July 1981, B.

1.4 "Navier-Stokes Solutions for an Axisymmetric Nozzle in a Supersonic External Stream," G. A. Hasen, AFWAL-TR-81-3161, March 1982, B.

1.5 "A Numerical Method for Solving the Equations of Compressible Viscous Flow," R. W. MacCormack, AIAA 81-0110, January 1981, B.

2. One-Dimensional Ramjet Calculations

2.1 "Aerothermochemical Analysis to Predict Performance of Hypersonic Ramjet Combustion Systems," W. C. Colley, D. R. Ferguson, P. T. Harsha, M. J. Kenworthy, General Electric, R67FPD381, November 1967, P.

2.2 "Quantitative Predictions of Dump Combustor Flowfields," H. Viets and J. E. Drewry, AIAA J., Vol. 19, No. 4, April 1981, pp. 484-491, B.

2.3 "Analysis and Correlation of Sudden Expansion (Dump) Burner Data," R. B. Edelman and P. T. Harsha, SAI-77-002-WH, September 1977, P.

2.4 "A Generalized One-Dimensional Compressible Flow Analysis with Heat Addition and/or Friction in a Constant Area Duct," W. H. T. Loh, Int. J. Engng. Sci., Vol. 8, 1970, pp. 193-206, B.

2.5 "On the Addition of Heat to a Gas Flowing in a Pipe at Subsonic Speed," J. V. Foa and G. Rudinger, J. Aero. Sci., February 1949, pp. 84-94, P.

2.6 "Liquid Fueled Ramjet/Solid Fueled Ducted Rocket Analysis Methodology," Author Unknown, P.

2.7 "Analysis of Nonconstant Area Combustion and Mixing in Ramjet and Rocket Ramjet Hybrid Engines," A. Dobronolski, NASA TN D-3626, October 1966, B.

3. Modular Ramjet Calculations

3.1 "Application of Modular Modeling to Ramjet Performance Prediction," P. T. Harsha and R. B. Edelman, AIAA 78-944, July 1978, P.

3.2 "An Empirical/Analytical Design Methodology for Gas Turbine Combustors," H. G. Mongia and K. Smith, AIAA 78-998, July 1978, P.

3.3 "Modeling Techniques for the Analysis of Ramjet Combustion Processes," R. B. Edelman and P. T. Harsha, AIAA-80-1190, June 1980, P.

3.4 "Use of the Modular Model for Parametric Investigation of the Sudden Expansion (Dump) Combustor," Author Unknown, P.

4. Miscellaneous

4.1 Injection and Mixing in Turbulent Flow, J. A. Schetz, Vol. 68, Progress in Astronautics and Aeronautics, AIAA 1980, (TA 357, S3x, C.2), T.

4.2 Computational Fluid Dynamics, P. J. Roache, Hermosa Publishers, 1976, B.

4.3 Momentum Transfer in Boundary Layers, T. Cebeci and P. Bradshaw, Hemisphere Publishing Corp., 1977, P.

4.4 Engineering Calculation Methods for Turbulent Flow, P. Bradshaw, Imperial College of Science and Technology, I. C. Aero Tech. 77-102, September 1977, B.

5. Swirl

5.1 "The Structure of Vortex Breakdown," S. Leibovich, Annual Reviews of Fluid Mechanics, Vol. 10, 1978, pp. 221-246, P.

5.2 "Swirl Combustor Flow Visualization Studies in a Water Tunnel," J. A. Schetz, P. W. Hewitt, and R. Thomas, AIAA-82-1238, June 1982, P.

5.3 "Primitive Pressure-Velocity Code for the Computation of Strongly Swirling Flows," D. G. Lilley, AIAA J., Vol. 14, No. 6, June 1976, pp. 749-756, B.

5.4 "Swirling Jets With and Without Combustion," S. Fujii, K. Eguchi, and M. Gomi, AIAA J., Vol. 19, No. 11, pp. 1438-1442, B.

5.5 "On the Prediction of Swirling Flowfields Found in Axisymmetric Combustor Geometries," D. L. Rhode, D. G. Lilley, and D. K. McLaughlin, ASME Symposium on Fluid Mechanics of Combustion Systems, June 1981, P.

5.6 "Cyclone Design Fundamentals," F. Boysan, W. H. Ayers and J. Swithenbank, Source Unknown, P.

5.7 "Numerical Prediction of Confined Vortex Flows," F. Boysan and J. Swithenbank, Proceedings of the Conference on Numerical Methods in Laminar and Turbulent Flow, July 1981, P.

5.8 "Turbulent Swirling Flame Prediction," D. G. Lilley, AIAA J., Vol. 12, No. 2, February 1974, pp. 219-223, B.

5.9 "Swirl Flows in Combustion: A Review," D. G. Lilley, AIAA J., Vol. 15, No. 8, August 1977, pp. 1063-1078, B.

5.10 "Nonisotropic Turbulence in Swirling Flows," D. G. Lilley, Acta. Aero., 1976, pp. 919-933, B.

5.11 "Swirl Flow Modeling for Combustors," D. G. Lilley, AIAA 74-527, June 1974, B.

6. Ramjet Experiments

6.1 "Fluid Dynamic Characterization of Sudden-Expansion Ramjet Combustor Flow Fields," J. E. Drewry, AIAA J., Vol. 16, No. 4, April 1978, pp. 313-319, B.

6.2 "Pressure Losses in Dump Combustors," L. P. Barclay, AFAPL-TR-72-57, October 1972, B.

6.3 "In-Situ Measurements of Gas Species Concentrations (U)," C. Chang, G. D. Sides, and T. O. Tiernan, AFAPL-TR-78-64, August 1978, P.

6.4 "In-Situ Measurements of Gas Species Concentrations in Simulated Dump Combustor Flowfields," C. Chang, G. D. Sides, and T. O. Tiernan, AFAPL-TR-76-105, November 1976, P.

6.5 "Velocity Measurements in Confined Dual Coaxial Jets Behind an Axisymmetric Bluff Body: Isothermal and Combusting Flows," A. J. Lightman and P. D. Magill, AFWAL-TR-81-2018, April 1981, P.

6.6 "Laser Velocimeter Measurements in Turbulent and Mixing Flows - Part II," W. H. Stevenson, H. D. Thompson, R. Bremmer, and T. Roesler, AFAPL-TR-79-2009, Part II, March 1980, P.

6.7 "Laser Velocimeter Measurements and Analysis in Turbulent Flows with Combustion - Part I," W. H. Stevenson, H. D. Thompson, and T. S. Luchik, AFWAL-TR-82-2076, September 1982, B.

7. Surveys

7.1 "Numerical Solution of Compressible Viscous Flows," R. W. MacCormack and H. Lomax, Annual Reviews of Fluid Mechanics, Vol. 11, 1979, pp. 289-316, B.

7.2 "Computational Aerodynamics Development and Outlook," D. R. Chapman, AIAA 79-0129, January 1979, B.

7.3 "Prospects for Computer Modeling in Ramjet Combustors," D. G. Lilley, AIAA-80-1189, June 1980, B.

7.4 "Flowfield Modeling in Practical Combustors: A Review," D. G. Lilley, J. Energy, Vol. 3, No. 4, July - August 1979, pp. 193-210, B.

7.5 "Ramjets," G. L. Dugger, Ed., AIAA Selected Reprints, Vol. 6, June 1969, B.

8. Combustion

Books

8.1 Combustion, I., Glassman, Academic Press, 1977, T.

8.2 Turbulent Reacting Flows, P. A. Libby and F. A. Williams, Eds., Topics in Applied Physics, Vol. 44, Springer-Verlag, 1980, B.

8.3 Dynamics and Modelling of Reactive Systems, W. E. Stewart, W. H. Ray, and C. C. Conley, Academic Press, 1980, B.

8.4 Some Fundamentals of Combustion, D. B. Spalding, Butterworths Scientific Publications, 1955, B.

8.5 Introduction to Combustion Phenomena, A. M. Kanury, Gordon and Breach Science Publishers, 1975, (QD516, .K29), W.

8.6 Combustion and Mass Transfer, D. B. Spalding, Pergamon Press, 1979, (QD516, .S73, 1979), W.

8.7 Combustion Technology, H. B. Palmer and J. M. Beer, Eds., Academic Press, 1974.

8.8 Turbulent Combustion, L. A. Kennedy, Ed., Progress in Astronautics and Aeronautics, AIAA, Vol. 58, 1977, (TJ254.5, S95x, 1977, c.3), T.

8.9 Fundamentals of Combustion, R. A. Strehlow, International Textbook Co., 1968, (QD516, 589), W.

8.10 "Combustion Modelling in Two and Three Dimensions - Some Numerical Considerations," H. McDonald, Prog. Energy Combust. Sci., Vol. 5, 1979, pp. 97-122, P.

8.11 "The Theory of Turbulent Reacting Flows - A Review," D. B. Spalding, AIAA 79-0213, January 1979, P.

8.12 "Spray Combustion Models - A Review," G. M. Faeth, AIAA 79-0293, January 1979, P.

8.13 "Counter-Gradient Diffusion in Premixed Turbulent Flames," P. A. Libby and K. N. C. Bray, AIAA-80-0013, January 1980, P.

8.14 "Three-Dimensional Model of Spray Combustion in Gas Turbine Combustors," F. Boysan, W. H. Ayers, J. Swithenbank, and Z. Pan, Source Unknown, P.

8.15 "Fundamental Modelling of Three-Dimensional Two-Phase Reacting Flow Systems," J. C. Dutt, AFOSR-78-0072, January 1980, P.

8.16 "Fundamentals of Reactants Mixing in Reactor Systems," J. Swithenbank, F. Boysan, and W. H. Ayers, Source Unknown, P.

8.17 "Combustion in Swirling Flows: A Review," N. Syred and J. M. Beer, Combustion and Flame, Vol. 23, 1974, pp. 143-201, B.

8.18 "Some Implications of Recent Theoretical Studies in Turbulent Combustion," F. A. Williams and P. A. Libby, AIAA-80-0012, January 1980, P.

9. Turbulence

Books

9.1 Turbulence, P. Bradshaw, Ed., Topics in Applied Physics, Vol. 12, Springer-Verlag, 1978, (TA357, T87), T.

9.2 An Introduction to Turbulence and Its Measurement, P. Bradshaw, Pergamon Press, 1971, B.

9.3 Mathematical Models of Turbulence, B. E. Launder and B. Spalding, Academic Press, 1972, (532.0527, L371), T.

9.4 Turbulent Shear Flows, I, F. Durst, B. E. Launder, F. W. Schmidt, and J. H. Whitflaw, Eds., Springer-Verlag, 1979, (TA357, I59, 1977), T.

9.5 Turbulent Shear Flows, II, L. J. S. Bradbury, F. Durst, B. E. Launder, F. W. Schmidt, and J. H. Whitelaw, Eds., Springer-Verlag, 1980, (TA357, I59, 1979), T.

Papers and Reports

9.6 "Turbulence Modelling for Computational Aerodynamics," J. G. Marvin, AIAA-82-0164, January 1982, B.

9.7 "The Understanding and Prediction of Turbulent Flow," P. Bradshaw, Aero. J., July 1972, pp. 403-418, P.

9.8 "Use of Turbulent Kinetic Energy in Free Mixing Studies," S. C. Lee and P. T. Harsha, AIAA J., Vol. 8, No. 6, June 1970, pp. 1026-1032, P.

9.9 "Progress in the Modelling of Turbulent Transport," B. E. Launder, The Pennsylvania State University, College of Engineering, Supplementary Notes for Course: Turbulent Recirculating Flows - Prediction and Measurement, July 1975, P.

9.10 "The Numerical Calculation of Turbulent Flows," B. E. Launder and D. B. Spalding, Comp. Mthds. Appl. Mech. Eng., Vol. 3, 1974, pp. 269-289, B.

9.11 "Turbulence Transport Equations," F. H. Harlow and P. I. Nakayama, Physics of Fluids, Vol. 10, No. 11, November 1967, B.

9.12 "Turbulence Transport Modeling," F. H. Harlow, Ed., AIAA Selected Reprint Series, Vol. 14, February 1973, (620.1064, H227), T.

10. Steady Navier-Stokes Calculations

Books

10.1 Numerical Heat Transfer and Fluid Flow, S. V. Patankar, Hemisphere Publishing Corp., 1980, B.

10.2 Heat and Mass Transfer in Boundary Layers, S. V. Patankar and D. B. Spalding, Intertext Books, 1970, B.

10.3 Heat and Mass Transfer in Recirculating Flows, A. D. Gosman, W. M. Pun, A. K. Runchal, D. B. Spalding, and M. Wolfshtein, Academic Press, 1969, (QC151, H4), T.

10.4 Numerical Methods in Laminar and Turbulent Flow, C. Taylor, K. Morgan, C. A. Brebbia, Eds., John Wiley, 1978, (TA357, I566, 1978, C.2), T.

10.5 GENMIX - A General Computer Program for Two-Dimensional Parabolic Phenomena, D. B. Spalding, Pergamon Press, 1977, B.

Papers and Reports

10.6 "Prediction of Hydrodynamics and Chemistry of Confined Turbulent Methane-Air Flames with Attention to Formation of Oxides of Nitrogen," S. Elghobashi, D. B. Spalding, and S. K. Srivatsa, NASA CR-135179, June 1977, P.

10.7 "Prediction of Hydrodynamics and Chemistry of Confined Turbulent Methane-Air Flames in a Two Concentric Tube Combustor," N. C. Markatos, D. B. Spalding, S. K. Srivatsa, NASA CR-135412, June 1978, P.

10.8 "The Calculation of Turbulent Recirculating Flows in General Orthogonal Coordinates," S. B. Pope, J. Comp. Physics, Vol. 26, 1978, pp. 197-217, B.

10.9 "Bluff-Body Flameholder Wakes: A Simple Numerical Solution," G. H. Vatistas, S. Lin, C. K. Kwok, and D. G. Lilley, AIAA-82-1177, June 1982, P.

10.10 "Calculation of Annular and Twin Parallel Jets Using Various Discretization Schemes and Turbulence-Model Variations, M. A. Leschziner, W. Rodi, J. Fluids Eng., Vol. 10, June 1981, pp. 352-360, P.

10.11 "Validation Studies of Turbulence and Combustion Models for Aircraft and Gas Turbine Combustors," S. A. Syed and G. J. Sturgess, ASME Symposium on Momentum and Heat Transfer Processes in Recirculating Flows, HTD - Vol. 13, 1980, P.

10.12 "Computation of Flows in Ducts with Sudden Enlargements," A. D. Gosman, E. E. K. H. Khalil, and B. E. Launder, Pennsylvania State University, College of Engineering, Prepared for use in: Turbulent Recirculating Flows, June 1975, P.

10.13 "Three-Dimensional Flow and Thermal Development in Magnetohydrodynamic Channels," S. P. Vanka and R. K. Ahluwalia, J. Energy, Vol. 6, No. 3, May - June 1982, pp. 218-224, B.

10.14 "The Calculation of Local Flow Properties in Two-Dimensional Furnaces," E. E. Khalil, D. B. Spalding, and J. H. Whitelaw, Int. J. Heat Mass Transfer, Vol. 18, 1975, pp. 775-791, B.

10.15 "A Computer Code for Swirling Turbulent Axisymmetric Recirculating Flows in Practical Isothermal Combustor Geometries," D. G. Lilley and D. L. Rhode, NASA CR-3442, February 1982, P.

10.16 "The Calculation of Two-Dimensional Turbulent Recirculating Flows," A. D. Gosman, E. E. Khalil, and J. H. Whitelaw, Turbulent Shear Flows, I, Springer-Verlag, 1979, pp. 237-254, B.

10.17 "A Calculation Procedure for Heat, Mass and Momentum Transfer in Three-Dimensional Parabolic Flows," S. V. Patankar and D. B. Spalding, Int. J. Heat Mass Transfer, Vol. 15, 1972, pp. 1787-1806, B.

10.18 "Computations of Soot and NO_x Emissions from Gas Turbine Combustors," S. K. Srivatsa, NASA CR-167930, May 1982, P.

10.19 "TEACH-2E: A General Computer Program for Two-Dimensional, Turbulent, Recirculating Flows," A. D. Gosman and F. J. K. Ideriah, Dept. of Mech. Eng., Imperial College, June 1976, P.

10.20 "Turbulent Recirculating Flows - Prediction and Measurement," B. E. Launder, A. D. Gosman, and J. H. Whitelaw, July 1975, P.

10.21 "Combustion Diagnostics Application Analysis," L. Krishnamurthy, AFWAL Interim Technical Report, August 1982, B.

10.22 "Notes to Accompany TEACH - T (Combustion Version) Code Prepared for Dr. R. Craig," A. Salooja, December 1977, P.

10.23 "Three-Dimensional Analysis of MHD Generators and Diffusers," S. P. Vanka, R. K. Ahluwalia, and E. D. Doss, Argonne National Laboratory, ANL/MHD-82-4, March 1982, P.

10.24 "A Primitive Variable Computer Model for Combustion Within Solid Fuel Ramjets," C. A. Stevenson and D. W. Netzer, Naval Postgraduate School, NPS67-79-010, October 1979, B.

10.25 "An Adaption and Validation of a Primitive Variable Mathematical Model for Predicting the Flows in Turbo-jet Test Cells and Solid Fuel Ramjets," C. A. Stevenson, Naval Postgraduate School, Thesis, June 1979, B.

10.26 "Widely-Spaced Co-Axial Jet, Diffusion-Flame Combustor: Isothermal Flow Calculations Using the Two-Equation Turbulence Model," G. J. Sturgess and S. A. Syed, AIAA-82-0113, January 1982, B.

10.27 "Numerical Simulation of Combustor Flow Fields: A Primitive Variable Design Capability," A. S. Novick, G. A. Miles, and D. G. Lilley, J. Energy, Vol. 3, No. 2, March - April 1979, pp. 95-105, B.

10.28 "Isothermal Flowfield Predictions of Confined Coflowing Turbulent Jets in an Axisymmetric Bluff-Body Near Wake," L. Krishnamurthy, AFWAL-TR-2036, May 1981, P.

11. Computer Search

11.1 "Ramjet Combustion/Combustor," Dialog Data Base Search; NTIS, Compendex, DOE Files, August 1982, P.

1982 USAF-SCEEE SUMMER FACULTY RESEARCH PROGRAM

Sponsored by the

AIR FORCE OFFICE OF SCIENTIFIC RESEARCH

Conducted by the

SOUTHEASTERN CENTER FOR ELECTRICAL ENGINEERING EDUCATION

FINAL REPORT

DEVELOPMENT OF A MEASUREMENT TECHNIQUE FOR FIBER-MATRIX ADHERENCE IN BRITTLE-BRITTLE COMPOSITES

Prepared by:	Dr. S. D. Brown
Academic Rank:	Professor
Department and University:	Department of Ceramic Engineering University of Illinois at Urbana-Champaign
Research Location:	Air Force Wright Aeronautical Laboratory, Metals and Ceramics Division Processing & High Temperature Materials Branch
USAF Research Colleague:	Dr. Robert Ruh
Date:	September 9, 1982
Contract No:	F49620-82-C-0035

DEVELOPMENT OF A MEASUREMENT TECHNIQUE FOR FIBER-MATRIX ADHERENCE IN BRITTLE-BRITTLE COMPOSITES

by

Dr. S. D. Brown

ABSTRACT

Experimental measurement of fiber-matrix adherence was surveyed in the context of ceramic-ceramic and ceramic-glass composites. A literature search, and several letters and telephone calls yielded eight kinds of tests that held some promise of being adaptable to the specific case. These are listed and some are described. Of the eight, all but two were eliminated from consideration. The reasons for their being eliminated are given. Attempts to prepare test specimens and prove out selected tests proved futile. Said attempts are discussed. Finally, recommendations for further work are made.

ACKNOWLEDGEMENTS

The writer gratefully acknowledges the sponsorship of the Air Force Systems Command, Air Force Office of Scientific Research and the support and assistance of personnel of the Air Force Wright Aeronautical Laboratory/MLLM, Wright-Patterson Air Force Base, Ohio. Special thanks are due Robert Ruh and K. S. Mazdiyasni for stimulating technical discussions, and their help and encouragement throughout the period of the effort. Helpful technical discussions were had with Tai-Il Mah, Madan Mendiratta, Allan Katz, R. Kerans and Harold Gegel. Mr. Edward Hermes was helpful in the laboratory.

I. INTRODUCTION:

Fibrous composites offer a number of advantages in applications requiring light-weight materials that are stiff, tough, and/or strong. Fiber-reinforced polymers and metals have become important commercial materials. Now, ceramic-ceramic (i.e., brittle-brittle) composites --ceramic fiber-reinforced carbons, glasses and ceramics--are being developed that hold considerable promise for applications that require comparatively tough ceramic materials for service at elevated temperatures.

Reinforcement-matrix adherence is recognized as an important factor affecting the mechanical properties and performance of polymer-matrix and metal-matrix fibrous composite materials. This is expected to be so apropos of the brittle-brittle composites as well. Effective matrix-to-reinforcement load transfer must occur if the reinforcements are to function as the major load carriers. This, in turn, requires that an adequate bond exist between reinforcements and the matrix. Sometimes, composite toughness is enhanced owing to a frictional dissipation of strain energy at the reinforcement-matrix boundary during shear displacements of the reinforcements with respect to the matrix (e.g., during fiber pull-out). This mechanism requires that the reinforcement-matrix bond strength be such that the said frictional effect can occur; i.e., $\tau_{iu} < \sigma_{fu} D/2L$. Here, τ_{iu} represents the ultimate reinforcement-matrix shear bond strength; σ_{fu}, the ultimate tensile fracture strength of the reinforcement (fiber); D, the reinforcement diameter (ciruclar cross

section is assumed); and L, the reinforcement length. In any case, it is clear that a meaningful, quantitative, practical test that could be used to measure the reinforcement-matrix bond strength would do much to promote rational development, design, and application of brittle-brittle composites. Development of such a test is the general purpose of the present project.

Several kinds of adherence tests are reported in the literature. e.g., [1-16] However, only one or two of these are likely to be adaptable to cases involving brittle-brittle composites. Under scrutiny, most of them are seen to be inadequate. This matter will be discussed later in the report.

It needs to be pointed out that when reference is made in this report to the reinforcement-matrix boundary, what is envisioned is an interphase that lies interjacent to the reinforcement and the matrix. There is evidence that when adhesive failure occurs, the fracture surface passes through this interpahse.[17] Of course, composite failure is a comparatively complicated multibarrier rate process that involves competitive and/or sequential steps. Adhesive failure is but one of several reactions that may occur during failure of a composite material.[6,18]

II. OBJECTIVES OF THE RESEARCH EFFORT:

Originally, two objectives were selected for the research effort: The primary objective was to develop an experimental method by which a practical, quantitative measurement of matrix-reinforcement adherence can be made apropos of ceramic-ceramic composites. It was

recognized at the outset that achievement of this primary objective was not at all certain, that it was a most difficult research problem. Therefore, a secondary objective--development of a model based on multibarrier rate process theory for subcritical cracking and deformation of ceramic-ceramic composites under loads at elevated temperatures--was set forth as an alternate to the primary one in the event that reasonable efforts to develop a suitable adherence test proved fruitless. As things turned out, efforts to develop an adherence test were more successful than expected, and the entire focus was placed upon achievement of the primary objective.

Specific tasks were set up to accomplish the aforesaid objective. These were as follows:

Task One: Search the literature for adherence tests that might be adapted to the present case.

Task Two: Select a test: Scrutinize the tests reported in the literature to eliminate from further consideration all but the one or two that appear most promising.

Also, devise new tests, different from any reported in the literature, if none reported can be adapted to the present case.

Task Three: Prepare actual test specimens and prove out the test scheme.

What was achieved with respect to each of these tasks is described in the sections that follow.

III. TASK ONE--THE LITERATURE SEARCH:

In searching the literature for adherence tests that might be used and/or adapted for measuring the reinforcement-matrix bond strength in ceramic-ceramic composites, a wide range of methods was considered. Even techniques used to determine the adhesive strengths of coatings and films to their substrates were included in the hope that one of them might prove useful in the present case. The computerized search program available through the Wright-Patterson AFB library system was used extensively in connection with this task. Moreover, the library facilities at the University of Illinois were used and direct contacts were made with workers believed to be expert in areas pertinent to the study. The test methods finally considered are listed as follows:

1. Fiber pull-out[1,2]
2. Critical fiber length evaluation[2,3]
3. Coating pull-off/shear-off[4-6]
4. Fracture mechanics approaches to coating-substrate adherence[6-11]
5. Tests based on microhardness indentation[11,12]
6. Fiber punch-out[13]
7. Peel strength[14,15]
8. Dynamic Poisson's ratio[16]

IV. TASK TWO--TEST SELECTION:

All but two of the test methods in the foregoing list were eliminated from further consideration, at least during the term of

the summer fellowship program. The two selected were the fiber pull-out and the critical fiber length evaluation methods. In this section, the advantageous features of these two kinds of tests that led to their selection are discussed as well as their particular shortcomings. Moreover, reasons are given for the elimination of the other methods from present consideration.

The pull-out test is a particularly straightforward method. In principle, at least, test specimens should be comparatively simple to fabricate. A schema of a fiber pull-out test specimen is given in Figure 1. The experiment is performed by measuring the force necessary to pull fibers from the matrix, under carefully controlled conditions, as a function of the embedded fiber length. Assuming that the experiment proceeds according to design, a plot such as that

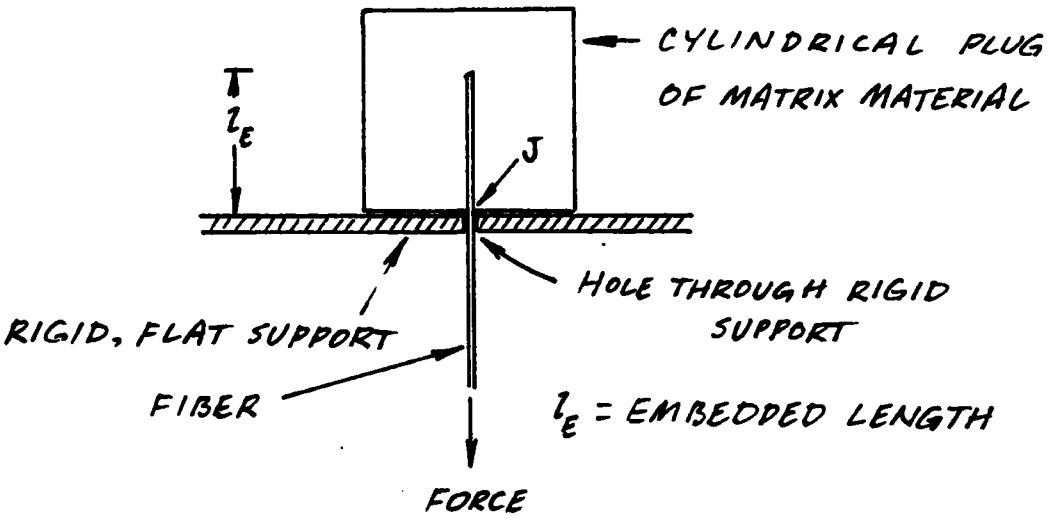


FIGURE 1 - SCHEMA OF FIBER PULL-OUT TEST SPECIMEN

shown schematically in Figure 2 will be obtained and the so-called critical length, l_c, thereby determined.[1,2] Then, the reinforcement-matrix shear bond strength is calculated from Eq. (1):

$$\bar{\tau} = \frac{\sigma_{fu}}{2} \frac{D}{l_c} \tag{1}$$

Here, $\bar{\tau}$ represents the <u>average</u> reinforcement-matrix shear bond strength.

This test is comparatively simple to do and should yield meaningful data provided it is performed correctly. Fiber alignment and straightness is crucial. Owing to the brittle nature of the fiber and the matrix, however, $\bar{\tau}$ can be expected to follow extreme value statistics; i.e., there will be a good deal of scatter in the data. Conditions at the fiber-matrix-environment junction (i.e., the region indicated by J in Figure 1) may dominate the results and must therefore be carefully considered and controlled.

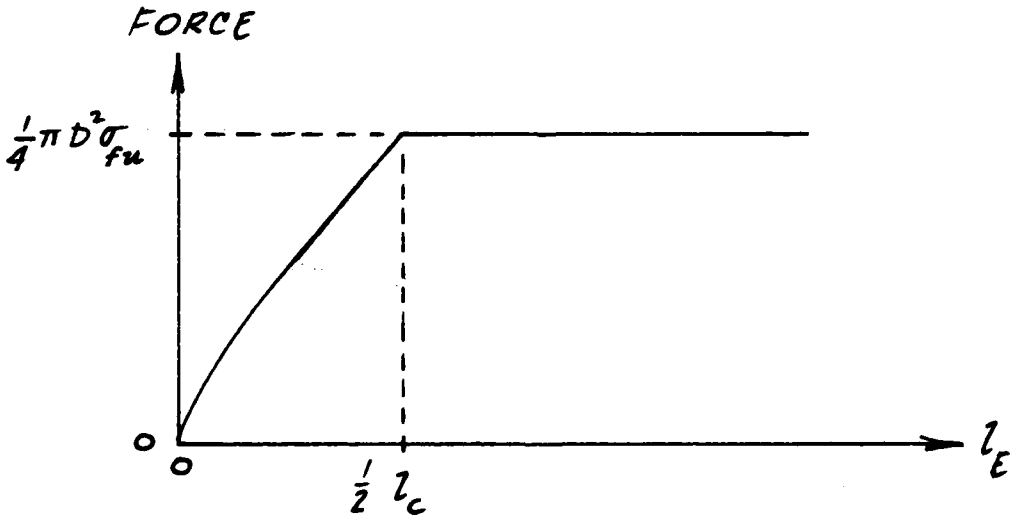


FIGURE 2 - PLOT OF THE FORCE REQUIRED TO PULL AN EMBEDDED FIBER FROM THE MATRIX VS. THE EMBEDDED LENGTH OF THE FIBER (ADAPTED FROM REFERENCE 1).

For instance, the initial stress concentration is located there and unless care is exercised to avoid spurious bending moments during testing, the fiber may break prematurely, resulting in an aborted test. Furthermore, environmental effects are expected to be an especially important factor in the pull-out test, requiring control of the test environment. Indeed, the pull-out test specimen may differ markedly from the actual composite material in regards to the access the environment has to the fiber-matrix interface. The value of $\bar{\tau}$ obtained from the test will depend upon the state of residual stress in the matrix. For example, if the stress state in the matrix is such that a radial compressive stress is imposed upon the fiber-matrix boundary, then frictional forces will result in a higher experimental value for $\bar{\tau}$ than would be the case were no such stress present. Finally, the loading mode in the fiber pull-out specimen is probably more simple than that encountered in the failure of an actual composite material. All of the aforementioned difficulties and drawbacks notwithstanding, the fiber pull-out adherence test is probably the best presently available for brittle-brittle composites.

The fiber pull-out test just described also can be classified a critical fiber length evaluation test. However, in this report this latter term is used more specifically to indicate the test reported by Drzal, Rich, Camping and Park.[3] In this procedure, which was devised to determine the strength of the bond between graphite fibers and resin matrices, a single, straight monofilament is embedded in the matrix which forms a standard dogbone specimen

(Figure 3). The monofilament lies coincident with the longitudinal axis of the specimen. This specimen is subjected to increasing uniaxial tensile stresses in the direction of the aforesaid axis until the monofilament has fractured into segments of critical length (Figure 4). The critical length is ascertained by means of an optical microscope while the specimen is still stressed, and the bond strength is calculated from Eq. (1).

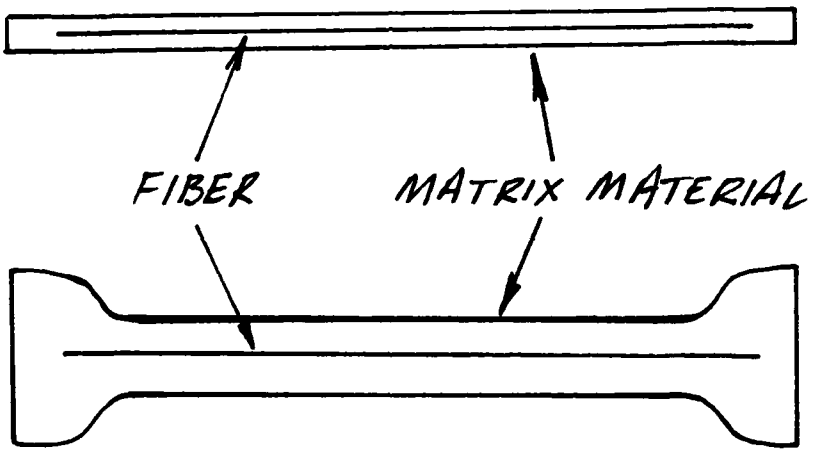


FIGURE 3 - DOGBONE SPECIMEN USED BY DRZAL, RICH, CAMPING AND PARK[3] TO DETERMINE THE CRITICAL FIBER LENGTH.

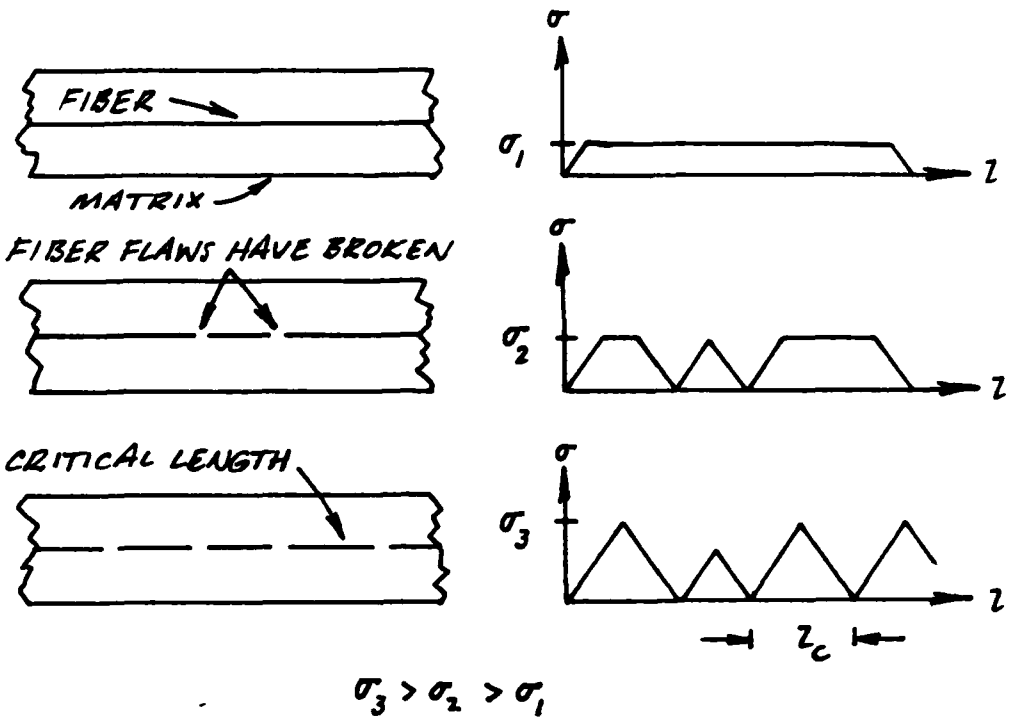


FIGURE 4 - FIBER FRACTURE AND STRESS DISTRIBUTIONS AT VARIOUS STAGES OF TESTING (ADAPTED FROM DRZAL, RICH, CAMPING AND PARK[3]).

The test just described has a number of important advantages. For instance, the environment vicinal the fiber-matrix interface is that which would be present in many (but not all) service failure situations apropos of the actual composite material. In contrast with the fiber pull-out test, there are no fiber-matrix-environment junction problems to contend with. The test is more efficient than the fiber pull-out method because it does not require the testing of several specimens with various embedded lengths of fiber to determine l_c. Depending upon the fabricability of the composite itself, test specimens should be comparatively simple to fabricate; surely no more difficult than those required for pull-out tests. In fact, achievement of the correct fiber alignment may be much easier for the specimens required in this test than for those needed in the pull-out method.

Two features of the critical fiber length evaluation test severely limit its usefulness in regards to ceramic-ceramic and ceramic-glass composites, its several advantages notwithstanding. The first of these is that the test requires that the strain to failure of the matrix material be greater than that of the fiber. That is, the fiber and matrix are strained equally in the test and the fiber must fracture into critical length segments before the matrix fails. This requirement will not often be met for ceramic or glass matrices. The second feature of the test that may present a problem with respect to its use with brittle-brittle composites is the fact that l_c must be measured *in situ*. If the matrix is sufficiently transparent, this can be done optically with a suitable cathetometer or traveling-tube microscope. While this may be possible with some glass matrices, ceramic matrices will almost always be optically opaque. An acoustic microscope might be considered for this purpose; however, commercial units currently available have lateral resolutions no better than 20 to 25 μm. The most advanced experimental units can do no better than 10 μm in this respect. Such resolutions will be inadequate in many cases. Nevertheless, some workers developing acoustic microscopes expect to achieve resolutions of less than 1 μm by using acoustic signals of extremely high frequency. If their efforts in this connection are successful, then the acoustic microscope may be useful for measuring l_c.

The coating pull-off/shear-off test[4-6] is a standard method that has been widely used and/or adapted for the measurement of

coating-substrate adherence in flame-sprayed ceramic-coated-metal systems. A schema of the test specimen is shown in Figure 5. Its use in the present context would require that the reinforcement material be obtained in the configuration of a film or tape. This may not always be practical. The results achieved would be strongly dependent upon the character of any flaws that may exist in the coating and/or at the coating-substrate-environment juncture (see J, Figure 5). This writer's experience with the method indicates that results may also be affected significantly by the rheological character of any adhesive used to attach the specimen to the load train. Spurious bending moments, which are difficult to eliminate in the uniaxial tensile pull-off version of the test, can affect the results.

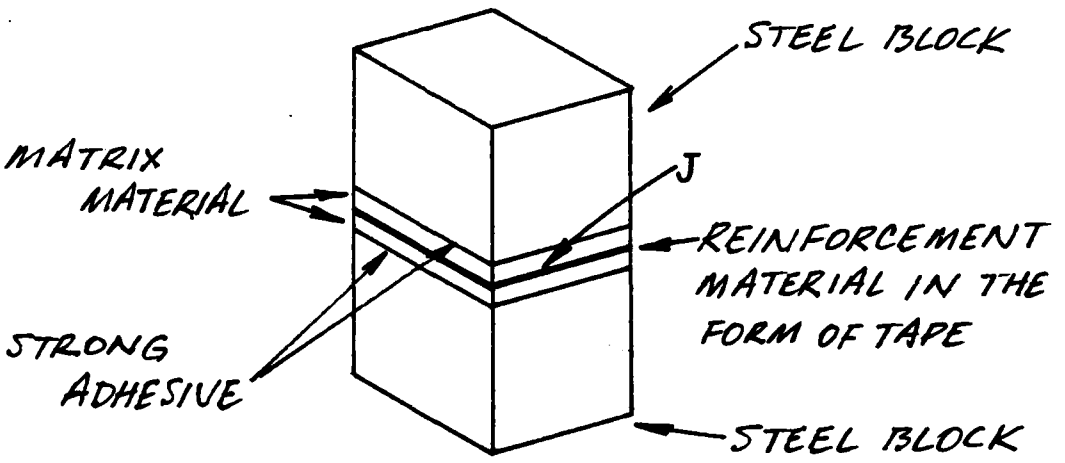


FIGURE 5 - SCHEMA OF THE SPECIMEN USED FOR THE COATING PULL-OFF/SHEAR-OFF TEST.

Finally, whether the failure obtained in the specimen during testing is adhesive in character, as is required for a valid measurement, or at least partially cohesive depends upon the loading rate and the relative humidity of the environment. Other factors not yet fully recognized seem to affect the extent to which the failure is adhesive or cohesive in nature. The problem is not simple or well understood. Owing to the foregoing difficulties which were expected with the pull-off shear-off test, no attempt was made to adapt it to the present case.

Fracture mechanics approaches to coating-substrate adherence measurement, with the exception of the microhardness indentation method of Chiang, Marshall and Evans,[11] are still somewhat controversial. Some workers have experienced difficulty in achieving valid results with certain fracture mechanics methods, others have not. In any case, the reinforcement material would have to be in the form of a film or tape just as in the coating pull-off/shear-off test. Therefore, these methods were eliminated from further consideration.

Tests based upon microhardness indentation[11,12] were not considered to be fully adaptable to the present case. The method devised by Chiang, Marshall and Evans[11] is an ingenious test for determining the adherence of thin films to hard substrates. However, after considerable study, the writer was constrained to conclude that it could not be made useful for fiber-matrix adherence measurement. The microdebonding test developed by Mandell, Chen and McGarry[12] likewise was a most interesting approach, especially for composites

having a resin matrix. However, stiffness and cracking problems expected apropos of brittle matrices and a potential lack of precision with regard to determination of the shear bond strength deterred further consideration of the method in the context of the short term of the summer program.

In the fiber punch-out test,[13] a thin section is made of the composite material such that the axes of the fibers are perpendicular to the plane of the section. Then a microhardness tester is used to measure $F_{min.}$, the force necessary to punch the fiber segments from the thin sections. The bond strength τ is then calculated from the formula

$$\tau = F_{min.}/\pi Dx \qquad (2)$$

where x represents the thickness of the thin section and D, the fiber diameter. This test is fraught with difficulties and to the writer's knowledge has never been used successfully. For one thing, fiber-matrix frictional forces are sure to confound the data. Moreover, providing the necessary support for the thin section during the punch out operation without blocking the exiting fiber segments poses a tricky problem. For these reasons, this particular method was not considered further.

Peel strength methods[14,15] have long been used to measure the bond strength between flexible polymer coatings and metallic or glassy substrata. In the adaptation of the peel strength approach to the measurement of fiber-matrix adherence, the fibers in question are bonded to the surface of a specimen of the matrix material, then the

force required to peel the fibers from the matrix material is measured by a standard technique. Optical microscopy is used to measure the fiber-matrix contact area once the fibers have been removed. A suitable dye is applied to the matrix surface prior to removal of the fibers to mark clearly the regions where no fiber-matrix had occurred. One of the serious problems with this scheme is that the kinds of fibers that need to be considered are too stiff and/or brittle to be peeled from the matrix surface in the fashion described. On this basis, consideration of this test was terminated.

Takemori's dynamic Poisson's ratio method[16] is a novel and promising approach. He measured the dynamic Poisson's ratio as a function of small static tensile strains, calculated the instantaneous macroscopic volume change in the composite, then related these results to microvoid formation. The microvoid formation occurred at the fiber-matrix boundary, allowing a relationship to interfacial adhesion to be inferred. While the writer maintains an interest in this test, the procedure was too involved to pursue further during the term of the summer fellowship program.

V. TASK THREE -- PREPARE TEST SPECIMENS & PROVE OUT SELECTED TEST SCHEMES:

Several attempts were made to prepare test specimens for the first, second and third kinds of tests described above. Said attempts either failed or were not completed by the end of the fellowship term. Fiber pull-out specimens consisting of SiC fibers in a silica glass matrix prepared by a sol-gel method were unsatisfactory owing to

shrinkage cracks. Specimens consisting of SiC monofilament and water glass ($Na_2O \cdot 3SiO_2$) did not cure properly and were loaded with bubbles. Moreover, the alignment of the monofilament was unsatisfactory and degradation of the filament at the filament-matrix-environment juncture was observed.

For the critical fiber length evaluation test, a SiC monofilament was cleaned and placed inside the bore of thin-walled, soft glass capillary tube, one end of which was subsequently sealed shut in a flame. A modest vacuum was then pulled with a small hand pump to evacuate the bore and a flame was moved along the tube beginning at the sealed end to collapse the glass upon the filament. Three problems developed: First, the glass collapsed in an uneven helical pattern upon the fiber. The wall of the capillary was too thin. Second, entrained bubbles of microscopic size were found scattered here and there along the embedded length of the filament. The vacuum was not sufficiently hard. Third, evidence of a chemical reaction between the glass and the filament was seen with a microscope. Some regions of the tube had been overheated. Limited time did not permit further pursuit of this effort.

Attempts to prepare specimens in the pull-off/shear-off test configuration were stymied from the outset by an inability to prepare or obtain the reinforcement material in the form of a film or tape.

VI. RECOMMENDATIONS:

It is recommended that the work started apropos of the fiber pull-out and critical fiber length evaluation be continued. Emphasis needs

to be placed upon the fabrication of suitable test specimens. The tests themselves require additional scrutiny. For instance, the fiber pull-out method should be subjected to a rigorous fracture mechanics analysis. That is, debonding is a type of fracture and it is expected that analysis in terms of fracture mechanics would prove useful.

Once the tests have been developed for the brittle-brittle case to the point that reliable, meaningful data can be obtained, experiments should be made to determine the effects of fiber surface treatments, pull-out rate, temperature and environments upon the bond strength. Moreover, experiments to ascertain the effects of the fiber-matrix bond strength upon the fracture characteristics of the composite should be made.

REFERENCES

1. P. Bartos, "Analysis of Pull-Out Tests on Fibres Embedded in Brittle Matrices," J. Mater. Sci., Vol. 15, pp. 3122-3128, 1980.

2. A. Kelly and W. R. Tyson, "Tensile Properties of Fibre-Reinforced Metals: Copper/Tungsten and Copper/Molybdenum," J. Mech. Phys. Solids, Vol. 13, pp. 329-350, 1965.

3. L. T. Drzal, M. J. Rich, J. D. Camping and W. J. Park, "Interfacial Shear Strength and Failure Mechanisms in Graphite Fiber Composites," 35th Reinforced Plastics/Composites Proceedings, The Society of the Plastics Industry, Inc., Section 20-C, pp. 1-7, 1980.

4. S. D. Brown, Room-Temperature Adhesive-Strength Tests of Various Flame-Sprayed and Flame-Plated Ceramic Coatings, Progress Rept. No. 20-374, Jet Propulsion Laboratory, California Institute of Technology, 1959, 16 pp.

5. ASTM Committee C-22, "Standard Method for Adhesion or Cohesive Strength of Flame-Sprayed Coatings, Designation C633-69," 1974 Annual Book of ASTM Standards, Part 17, pp. 630-633, 1974.

6. M. K. Ferber and S. D. Brown, "Delayed Failure of Plasma-Sprayed Alumina Applied to Metallic Substrates," J. Am. Ceram. Soc., Vol. 64, pp. 737-743, 1981.

7. P. F. Becher and W. L. Newell, "Adherence-Fracture Energy of a Glass-Bonded Thick-Film Conductor: Effect of Firing Conditions," J. Mater. Sci., Vol. 12, pp. 90-96, 1977.

8. P. F. Becher, W. L. Newell and S. A. Halen, "Application of Fracture Mechanics to the Adherence of Thick Films and Ceramic Braze Joints," Fracture Mechanics of Ceramics, Vol. 3, Edited by R. C. Bradt, D. P. H. Hasselman and F. F. Lange (Plenum Press, New York, 1978), pp. 463-471.

9. R. F. Lowell, Subcritical Crack Growth in Arc Plasma Sprayed Alumina on Titanium Alloy Substrates, M.S. Thesis, Department of Ceramic Engineering, University of Illinois, 1980, 78 pp.

10. J. H. Enloe, Slow Crack Growth Characteristics of Arc Plasma Sprayed Alumina on Stainless Steel Substrates, M.S. Thesis, Department of Ceramic Engineering, University of Illinois, 1981, 49 pp.

11. S. S. Chiang, D. B. Marshall and A. G. Evans, "A Simple Method for Adhesion Measurements," Surfaces and Interfaces in Ceramic and Ceramic-Metal Systems, Edited by J. A. Pask and A. G. Evans (Plenum Press, New York, 1981), pp. 603-617.

12. J. F. Mandell, J. H. Chen and F. J. McGarry, "A Microdebonding Test for in situ Assessment of Fibre/Matrix Bond Strength in Composite Materials," Int'l J. Adhesion and Adhesives, Vol. 1, pp. 40-44, 1980.

13. W. T. Petuskey, private communication to S. D. Brown, 16 June 1982.

14. D. H. Kaelble, "The Theory and Analysis of Peel Adhesion," Adhesion and Cohesion, Edited by P. Weiss (Elsevier Publishing Co., Amsterdam, 1962, pp. 74-88.

15. J. H. Engel, Jr. and R. N. Fitzwater, "Adhesion of Surface Coatings as Determined by the Peel Methods," ibid, pp. 89-100.

16. M. T. Takemori, "Dynamic Poisson's Ratio: A Novel Technique to Study Interfacial Adhesion," Polymer Eng. Sci., Vol. 18, pp. 1193-1199, 1978.

17. L. T. Drzal, private communication to S. D. Brown, 26 July 1982.

18. C. C. Berndt, N. R. Schankar and H. Herman, "Characterization of Mechanical Properties of Plasma Sprayed Coatings," presented at the conference Advances in Materials Characterization, Alfred University, Alfred, NY, 15-18 August 1982.

1982 USAF-SCEEE SUMMER FACULTY RESEARCH PROGRAM

Sponsored by the

AIR FORCE OFFICE OF SCIENTIFIC RESEARCH

Conducted by the

SOUTHEASTERN CENTER FOR ELECTRICAL ENGINEERING EDUCATION

FINAL REPORT

FORCE TRACKING PROFICIENCY IN OPERATING AIRCRAFT CONTROLS

Prepared by:	L. W. Buckalew
Academic Rank:	Assistant Professor
Department and University:	Department of Psychology Alabama A & M University
Research Location:	Air Force Aerospace Medical Research Laboratory, Human Engineering Division, Workload and Ergonomics Branch
USAF Research Colleague:	Dr. Joe McDaniel
Date:	August 4, 1982
Contract No:	F49620-82-C-0035

FORCE TRACKING PROFICIENCY IN OPERATING AIRCRAFT CONTROLS

by

L. W. Buckalew

ABSTRACT

This project is associated with the Air Force Aerospace Medical Research Laboratory's Pilot Strength Screening Program. An overview of static and dynamic strength is provided, with emphasis on relation to aircraft maneuvers. Research objectives were to determine the maximum strength applied to a wheel-type elevator and aileron control and to establish the relationship between tracking proficiency and control force resistance at variable submaximal strength levels. Corollary measures of heart rate and EMG frequency shift and amplitude were taken. Data collection is ongoing. Anticipated results should allow comparison of a wheel and stick-configured control system in terms of applicable strength. Based on tracking proficiency, results should provide insight into minimum and maximum control apparatus force resistances associated with adequate aircraft control, and will have relevance for design specifications. Several related research problems were developed.

I. INTRODUCTION:

All movement is behavior and is produced by muscle contractions. Detailed treatments of the operation of and influence on muscle behavior in a work situation have been provided.[1,2] The neuroanatomical level of this behavior ranges from the most basic system of spinal reflex pathways to complex cortical processes affecting pyramidal and extrapyramidal systems. The pyramidal system appears to mediate precise and skilled movements in man, while the extrapyramidal system is generally involved with the smoothness and continuity of limb movements, particularly arms and hands. Within these systems are three general types of muscle tissue: striated, smooth, and cardiac. Most movement directly involves striated muscles relaxing or contracting. Contractions are typically either isotonic (dynamic), wherein muscle tension is relatively constant and the limb moves, or isometric (static), wherein the muscle changes tension without the limb actually moving. The innervation, operation, and control of muscles and muscle systems is well established[3,4] and isometric exercise and the physiological responses during this form of exertion have been extensively treated.[2] Static or isometric strength has been defined as the single maximum force exerted by the subject in a fixed position.[5] Petrofsky[2] also noted that there exists a static component of most types of dynamic exercise, and the physiological responses to combined static and dynamic exercise are additive. The literature concerning the correlation of static and dynamic strength has been reviewed.[5]

There are several perspectives conventionally considered in investigations of isometric exercise: 1) strength usually expressed as maximum voluntary contraction or MVC, 2) endurance or fatigue, typically measured in terms of cardiorespiratory or electromyographic physiological substrates (heart rate, blood pressure, ventilation, EMG frequency shift, EMG amplitude), 3) recovery time from fatigue, and 4)

performance on some specified task.

Considering fatigue, the ultimately resulting physiological condition in endurance situations, the process and recovery from durations of submaximal sustained contractions have been investigated.[6] It was noted that recovery from fatigue was only about 75% complete after 40 minutes rest while recovery of ability to exert maximum tension was completed in 10 minutes. The assumption that, based on such findings, different muscles must be involved in a static strength vs endurance situation was confirmed,[2] and it was suggested that slow twitch muscles seem to be associated with low strength and high endurance while fast twitch muscles appear associated with low endurance and high strength. Petrofsky[2] summarized available evidence relative to endurance (sustained contractions) and provided time-based expectancies of endurance associated with proportions of MVC (maximum voluntary contraction) exerted. Evidence indicated a steep, negative, and generally linear relationship between muscle tension and endurance in situations involving greater than 15% MVC.[2,7] It was also noted that in an endurance to fatigue condition, approximately 80% recovery occured within a 20 minute period following fatigue, with complete recovery in 24 hours. Additional evidence reflecting on the development of and recovery from fatigue at different muscle tensions is available.[8] It is important to recognize that there is a clear relationship between maximum static strength (MVC) and endurance times at submaximal tensions, regardless of muscle group.[9]

The measurement of physiological responses and conditions in static strength or endurance situations typically is concerned with heart, neural, and muscle conditions. O'Donnell[10] contributed a thorough survey of psychophysiological techniques used in human engineering research, to include measures of cardiovascular function and electromyogram (EMG). Both heart rate and EMG were considered

viable measures of workload. Considering both static and dynamic exercise, a close relationship between varying muscle tensions and pulse rate has been noted, with the suggestion that fatigue caused from static effort could be reasonably well predicted from the rate of increase in heart rate.[9] This evidence does, however, suggest that heart rate may have a restricted sensitivity to muscle tension and fatigue. Another measure of the physiological conditions underlying endurance and fatigue situations is the electromyogram (EMG). The sensitivity of the EMG to small variations in stimulus conditions has been noted,[10] and EMGs taken from the forearm have been shown to correlate well with workload.[11,12]

Appreciable information exists relating static muscle exertion, fatigue, and recovery time and there are accepted techniques for measuring the physiological correlates of these behaviors and conditions. However, in assessing these conditions it is necessary to appreciate that exertion and fatigue are physiologic factors which set the relatively fixed and outmost limits of strength and endurance. Psychologic factors set the more proximate limits of strength and endurance; in this framework, capacity is the always undetermined measure of physiologic limits and performance is limited by psychologic factors.[13] Hence, the effect of motivation must be considered as a reservation in any conclusions of attempts to establish parameters of strength, endurance, fatigue, or recovery from fatigue.

Performance measures reflecting the effects of muscle exertion, strength, and fatigue are numerous. The task of present interest, tracking, has been extensively discussed, to include methodological considerations and theories of performance.[14] In the operation of an aircraft, the tracking task is both essential and critical, and any variables exerting influence on tracking proficiency are of appreciable importance. Aircraft controls which facilitate

tracking performance involve varying amounts of force resistance resulting in muscle tensions of different proportions of MVC. These strength and endurance demands logically influence tracking proficiency and should be reflected differentially in both heart rate and EMG measures.

II. OBJECTIVES:

Aircraft pilots must occasionally exert large forces on controls for brief periods of time and endure submaximal forces for lengthy periods.[15] Such strength and endurance requirements are necessitated by design standards for aircraft control resistance which are based on experience and performance of pilots in the mission environment. The controls requiring the exercise of strength and/or endurance include elevator and aileron manipulated by either a stick or wheel control, and rudder pedals. Pilots must often make precision adjustments with these controls, particularly in the pitch axis, during approach to landing and formation manuevers. Relevant precipitating conditions include out-of-trim, failed hydraulics, and engine out, and related maneuvers include cross-wind landing, extending flaps, dive recovery, and engine run-up.[15] These adjustments often require maintenance of a baseline force on the control apparatus. If the pilot were unable to track with the required precision (force and rate), the aircraft attitude may deteriorate to the point wherein the required corrective force would exceed pilot capability. Hence, it is important to have performance data on both the maximal static strength (MVC) that can be applied to aircraft controls and the relationship between tracking performance and predetermined increments of MVC.

The Aerospace Medical Research Laboratory's Pilot Strength Screening Program[15] was initiated in 1976, with the first phase devoted to accumulation of data on control accuation forces. The second phase of this program involves

developing, deploying, and validating a strength measuring technique for screening pilot candidates. Specific concerns of this phase include the measurement of relevant pilot strength characteristics. Previous efforts[16,17] have measured the strength characteristics of male and female subjects for operating a stick-type aileron and elevator control and rudder pedals. Muscle strength involving measures for which comparable data exist for men and women has been extensively reviewed.[18,19] Existing data are primarily concerned with measurement of maximal static strength (MVC) and static endurance of submaximal forces to fatigue. While essential, this information primarily reflects on strength or endurance limits, and is relevant to use of a stick-type control system. The next sequential step in developing a pilot strength screening program is to quantify control performance or the relationship between MVC and the ability to track with a variable submaximal force. Also, information on strength characteristics using a wheel-type aileron and elevator control are needed. Pointedly, what performance and physiological decrements are associated with specific aircraft control resistances? The objective of this study is to establish a quantitative relationship between variable submaximal force requirements and tracking proficiency, and to determine heart rate and EMG correlates to the variable force requirements.

III. METHODS AND MATERIALS:

a. Subjects

The subjects were 12 males who met the body size requirements for a Class 1 flying physical (Air Force Regulation 161-43), having heights in the range of 64-76 inches and within acceptable weight limits. Basic anthropometric characteristics of the sample are presented in Table 1. As the study required subjects to exert and maintain large proportions of their maximum arm strength, no one with a

TABLE 1

Characteristics of the Study Sample

Variable	Unit	Subject												Mean	SD
		1	2	3	4	5	6	7	8	9	10	11	12		
Age	yrs														
Weight	kg														
Stature	cm														
Sitting Height	cm														
Acromion-Radiale Length	cm														
Radiale-Stylion Length	cm														
Hand Length	cm														
Hand Breadth	cm														
Biceps, Flexed	cm														
Forearm, Flexed	cm														
Wrist	cm														
Triceps Skinfold	cm														
Thumb-Tip Reach	cm														
Arm/Forearm Angle	deg														
Handedness															

recent history of muscle or back injury was permitted to participate.

b. Apparatus

Strength testing and tracking were done using a Dynamic Strength Testing Cockpit consisting of a simulated aircraft cockpit, an adjustable C-130 aircraft seat, and wheel-configured elevator and aileron controls. The position of these manipulanda was controlled by a microprocessor data acquisition system. The force applied by subjects and the position of controls were monitored by the computer updated position signals sent to the hydraulic actuators as shown in Figure 1. An intercom permitted communication between the computer room and the simulator. During the maximum static strength tests, the wheel control was fixed and immovable in one of three distal locations medial to and forward of the subject. Position 1 (near subject) was used for the elevator pull test, Position 2 (center of range) was used for the aileron left and right tests, and Position 3 (most distant) was used for elevator push tests.

Data collection utilized an EMG Fourier Analyzer, Telectrode disposable electrodes (Johnson & Johnson), and amplifier (Grass Instruments Model PS 11 H) to obtain EMG center frequency and amplitude. A cardiotachometer with earlobe optic electrode was used to obtain heart rate data. Tracking proficiency was measured using the wheel-connected hydraulic actuators (Figure 1) and an oscilloscope to provide visual feedback of performance to subjects. All data were recorded on tape (Honeywell 5600B).

c. Procedure

Maximum Static Strength Tests. During testing, the subject sat in the simulator seat, restrained by a lap belt and shoulder harness, with feet placed on the rudder pedals. The subject was required to exert his maximum voluntary force for a period of 5 seconds, both push and pull, on the elevator control with right, left, and both hands. Subjects

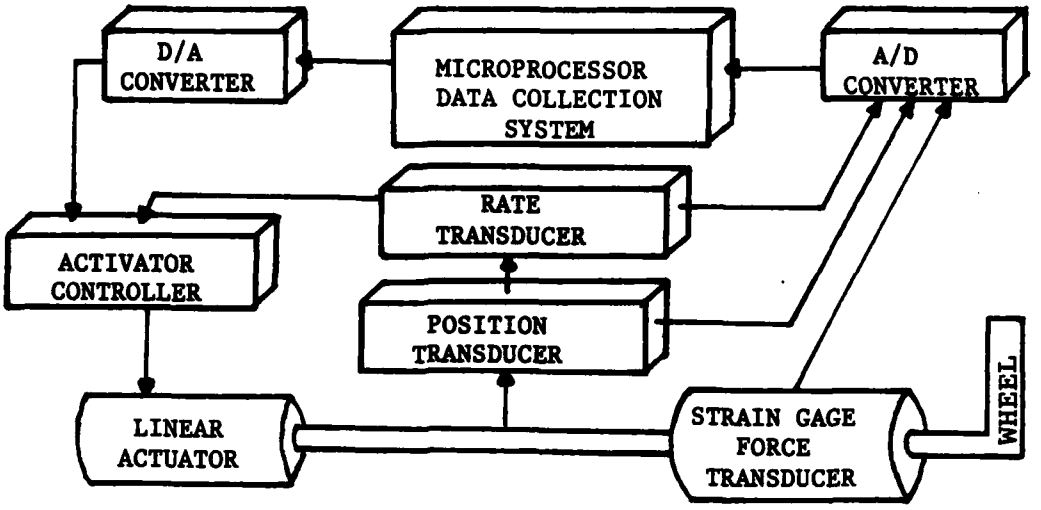


Figure 1 - Microprocessor data acquisition system.

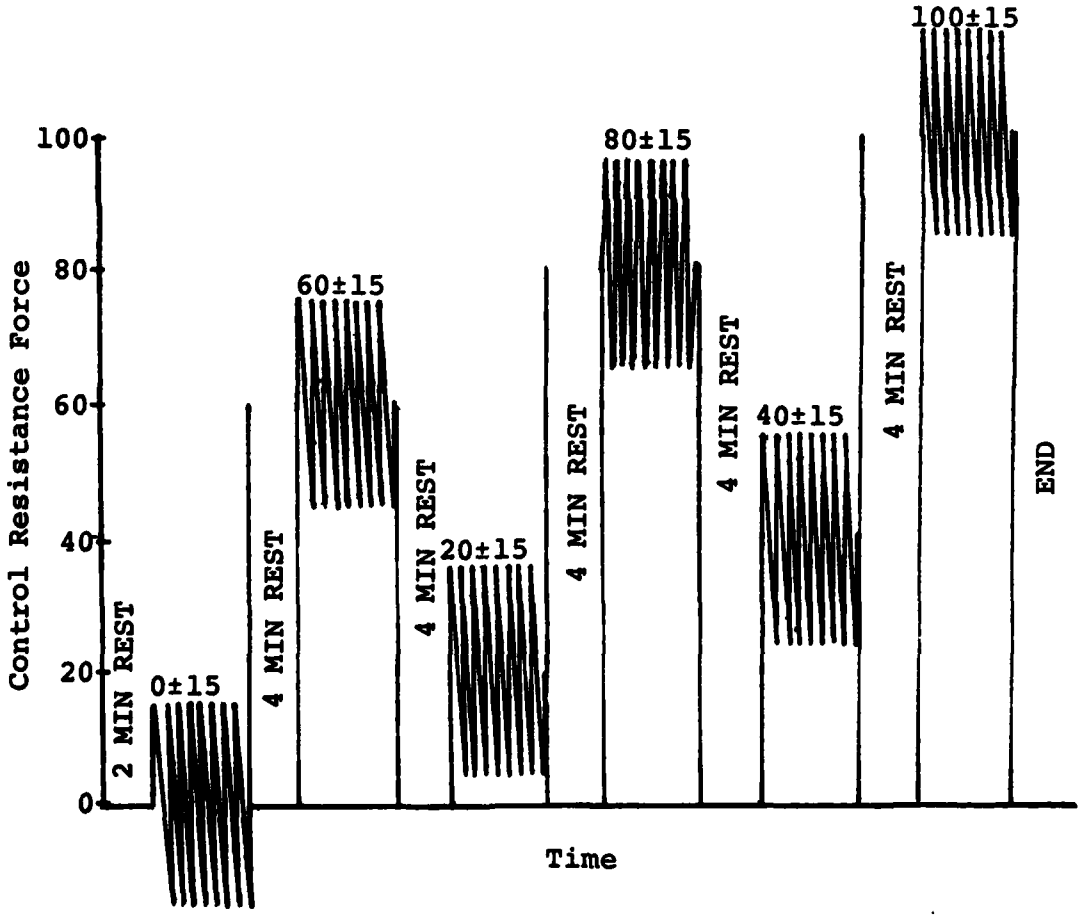


Figure 2 - Time profile of typical force tracking session.

also exerted maximum forces on the aileron to the left and right, using left, right, and both hands. Visual feedback of the amount of force exerted was displayed on an oscilloscope located above the cockpit wheel.

The orders of exertions were counterbalanced between and within subjects. The control (elevator or aileron) was counterbalanced between subjects (ABBA). For each control, the direction of force (push and pull for elevator, left and right for aileron) was counterbalanced (ABBA), and within each direction, the hand used (right, left, or both) was counterbalanced (ABCCBA). All static exertions lasted for a duration of 5 seconds, with a rest period of at least 2 minutes between exertions by the same hand.

Force Tracking Tests. The force tracking task required subjects to apply a variable force to null a sinusoidally moving target signal displayed on an oscilloscope. This task used only the elevator control, and forces were applied with both hands. A circle was displayed on the oscilloscope, offset vertically from the center of the display. Subjects were required to apply a force in the opposite direction until the circle was in the center of the display. Once centered, the amount of force needed to hold the circle on target oscillated ± 15 pounds at a rate of .25 hz. The force required to keep the target circle centered on the display oscillated sinusoidally according to the formula:

$$F = B + 15 \sin(R)$$

wherein F = force to be exerted by the subject, B = the baseline force, a multiple of 20 pounds, and R = angular velocity, 90^{o}/sec or $\pi/2$ radians/sec.

Subjects were allowed to practice the task with a baseline force of 0 ± 15 lbs. Baseline forces during formal testing increased in multiples of 20 lbs up to the largest multiple of 20 which was less than a subject's MVC or 100 lbs, whichever was the lesser. These baseline forces were presented to each subject in a different random order. Each

force tracking trial of a given multiple of 20 lbs was 32 seconds in length, and consisted of 8 oscillations. A rest period of 4 minutes was given between force tracking trials. Figure 2 illustrates a time profile of a typical force tracking trial block.

IV. RESULTS:

By design, data generated by this study are intended to be descriptive, hence no inferential tests are reported. Maximum Static Strength Tests produced 12 discrete MVC measurements for each subject. These data, in units of pounds force, are reflected in Table 2 which includes means and standard deviations for each measurement condition. The MVC measurements for each subject reflect individual means of 20 sampled values during the second through fourth seconds of each exertion. For many of the exertion conditions, these data are comparable to those previously reported.[16,17]

Force Tracking Tests, involving five different force resistance levels, were primarily concerned with tracking proficiency as a function of force resistance. For each subject under each resistance, an absolute error in pounds of force, offset by practice trial error, was computed and is presented in Table 3. Group mean absolute error for each force resistance condition is plotted in Figure 3 to show the relationship between tracking error and control apparatus force resistance. This data is amenable to the computation of a Pearson product-moment correlation coefficient to mathematically describe this association.

Heart rate and EMG measures were viewed as corollary measures relating to exertion and fatigue accompanying force tracking efforts. Heart rate presented in Table 4 are in terms of percent of change from immediate pre-tracking effort rate to immediate post-tracking effort rate. This transformation allows present data to be comparable to those previously reported.[9] For EMG measures, both amplitude and

TABLE 2

Static Strength Test Responses (MVC)

Subject	Elevator Control						Aileron Control					
	Right Hand		Left Hand		Both Hands		Right Hand		Left Hand		Both Hands	
	Push	Pull	Push	Pull	Push	Pull	Left	Right	Left	Right	Left	Right
1												
2												
3												
4												
5												
6												
7												
8												
9												
10												
11												
12												
Mean												
SD												

TABLE 3

Force Tracking Test Performance

Subject	Mean Absolute Error in Pounds Force				
	20 ± 15	40 ± 15	60 ± 15	80 ± 15	100 ± 15
1					
2					
3					
4					
5					
6					
7					
8					
9					
10					
11					
12					
Mean					
SD					

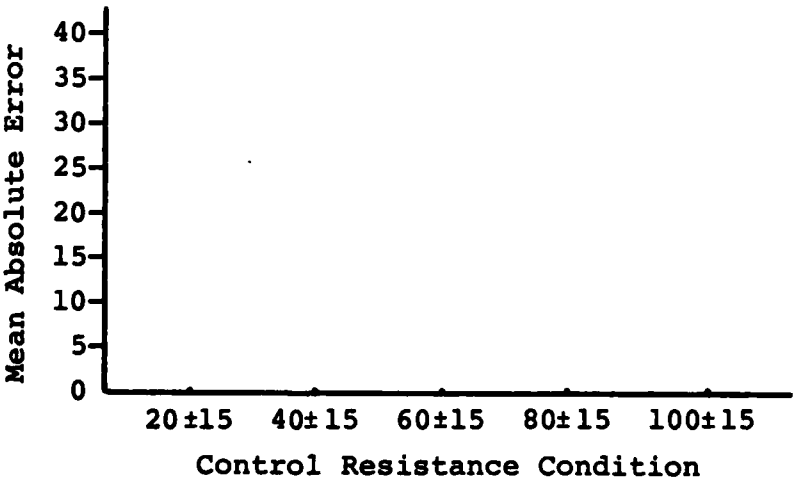


Figure 3 - The mean absolute tracking error in pounds force as a function of wheel control resistance in pounds.

TABLE 4

Heart Rate Response for Force Tracking Conditions

Subject	Heart Rate % Change				
	20 ± 15	40 ± 15	60 ± 15	80 ± 15	100 ± 15
1					
2					
3					
4					
5					
6					
7					
8					
9					
10					
11					
12					
Mean					
SD					

center frequency were recorded throughout tranking efforts. As measures were continuous, both frequency shift and amplitude could be directly correlated with absolute error in tracking over each force resistance condition.

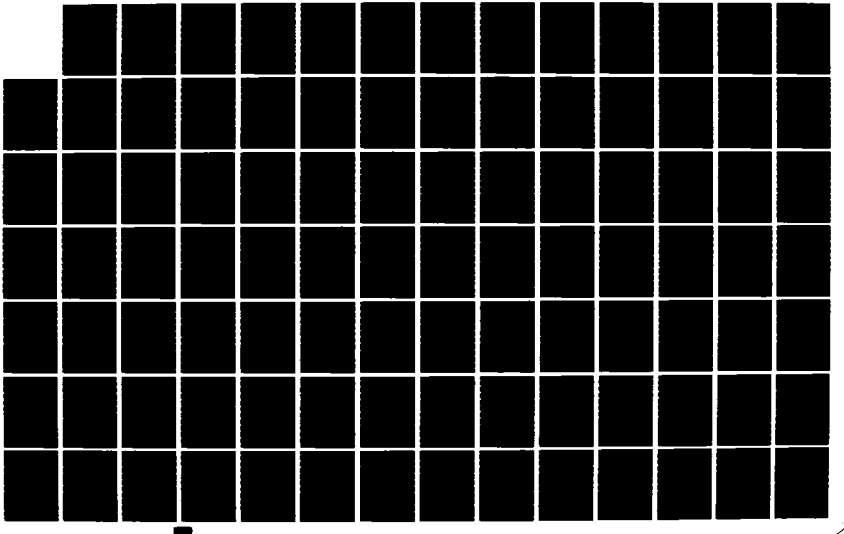
V. RECOMMENDATIONS:

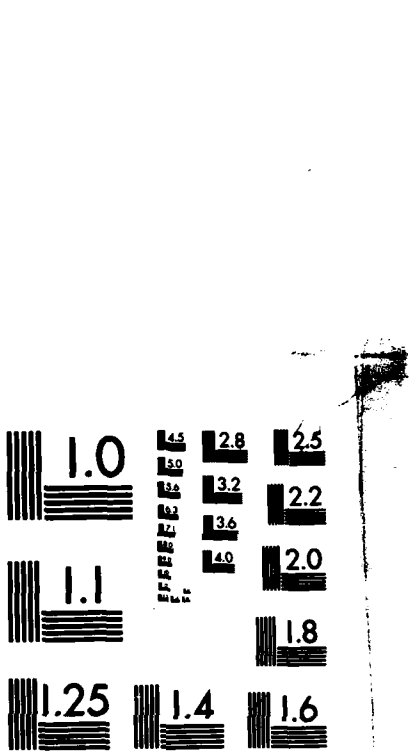
The planning, initiation, coordination, and conduct of this effort required appreciable time and effort of several individuals. Complex software had to be developed and refined, and several problems with hardware had to be resolved. Of particular note, software development took approximately thirty days longer than expected. At present, both hardware and software systems appear sound, and it is anticipated that data collection, likely to involve about three weeks, can begin. Due to the complexity of expected data, particularly for force tracking, it is projected that data analysis and synthesis will entail several weeks. The format, by design, of this Final Report should readily allow the integration of data and appropriate statistical and graphic description.

Anticipated data should be highly relevant to the Air Force Aerospace Medical Research Laboratory's Pilot Strength Screening Program. Not only will it provide pertinent information on strength characteristics associated with operation of a wheel-type air craft control, but should yield appreciable information of both a performance and physiological nature on the ability to maneuver an air craft under different force resistance conditions. It is strongly recommended that this research effort continue, with expansion to provide a data base for men and women relative to static strength and tracking proficiency using a wheel-type control apparatus. Given this base, comparisons of wheel and stick controls could be made to determine the most efficacious control system. Further, based on tracking proficiency data, minimum and maximum force resistances associated with

AD-A130 769 USAF/SCEEE SUMMER FACULTY RESEARCH PROGRAM RESEARCH REPORTS VOLUME 1. (U) SOUTHEASTERN CENTER FOR ELECTRICAL ENGINEERING EDUCATION INC S... 5/11

UNCLASSIFIED W D PEELE ET AL. OCT 82 AFOSR-TR-83-0613 F/G 5/1 NL





MICROCOPY RESOLUTION TEST CHART
NATIONAL BUREAU OF STANDARDS-1963-A

adequate air craft control could be determined and incorporated in design specifications.

The experience of this project has suggested several related research problems which appear to merit attention. Both static and dynamic strength characteristics are important considerations in air craft operation and man-machine interface. While dynamic strength exertions have static components,[2] no clear and predictive relationships between the two for specific exertions has been offered.[19] The literature reflects little data on even relationships between different static strength exertions. Determination of correlations between maximum voluntary contractions (MVC) of isometric efforts could provide utilitarian information of a predictive nature. Additionally, it has been noted that any static or dynamic performance is influenced by psychological conditions,[13] with the assumption that strength is amenable to psychologic manipulation. A study to determine the limits of psychological influence, such as through placebo treatment, on a range of static MVC exertions could prove valuable. Of particular concern would be efforts to maximize strength performance without the necessity of specific training programs.[16]

Acknowledgment

The author would like to thank the Air Force Systems Command, the Air Force Office of Scientific Research, and the Southeastern Center for Electrical Engineering Education for providing him with the opportunity to spend a very worthwhile, interesting, and productive summer at the Air Force Aerospace Medical Research Laboratory, Wright-Patterson AFB, Ohio. He would like to acknowledge the Human Engineering Division, and in particular the Workload and Ergonomics Branch, for its hospitality, support, and excellent working conditions.

A particular expression of appreciation and thanks is given Dr. Joe McDaniel for his collaboration and guidance in this research effort. Further acknowledged are the many helpful discussions with Mr. Charles Clauser whose personal and professional support contributed appreciably to the experience of this effort. Of particularly commendable nature is the cooperative and teamwork atmosphere which is so pervasive in this laboratory.

REFERENCES

1. Simonson, Ernst (Ed.), Physiology of Work Capacity and Fatigue, Springfield, Illinois, Charles C. Thomas, 1971.
2. Petrofsky, Jerrold, Isometric Exercise and Its Clinical Implications, Biomedical Engineering Laboratory, Departments of Engineering and Physiology, Wright State University, Dayton, Ohio, 1981.
3. Cotman, Carl, and McGaugh, Carl, Behavioral Neuroscience, New York, New York, Academic Press, 1980.
4. Thompson, Richard, Introduction to Physiological Psychology, New York, New York, Harper & Row, 1975.
5. Laubach, L., "Human Muscular Strength" in Churchill, Laubach, McConville, and Tebbetts (Eds.), Anthropometric Source Book, Volume I: Anthropometry for Designers, Webb Associates for National Aeronautics and Space Administration, 1978.
6. Lind, A. R., "Muscle Fatigue and Recovery from Fatigue Induced by Sustained Contractions," Journal of Physiology, Vol. 127, pp. 162-171, 1959.
7. Petrofsky, J. S., and Lind, A. R., "Aging, Isometric Strength and Endurance, and Cardiovascular Responses to Static Effort," Journal of Applied Physiology, Vol. 38, pp. 91-95, 1975.
8. Funderburk, C. F., Hipskind, S. G., Welton, R. C., and Lind, A. R., "Development of and Recovery from Fatigue Induced by Static Effort at Various Tensions," Journal of Applied Physiology, Vol. 37, pp. 392-396, 1974.
9. Simonson, E., and Lind, A. R., "Fatigue in Static Work," in E. Simonson (Ed.), Physiology of Work Capacity and Fatigue, Springfield, Illinois, Charles C. Thomas, 1971.
10. O'Donnell, R. R., "Contributions of Psychophysiological Techniques to Aircraft Design and Other Operational Problems," AGARDograph No. 244, Advisory Group for Aerospace Research and Development, Neuilly sur Seine, France, 1979.

11. Stackhouse, S. P., "The Measurement of Pilot Workload in Manual Control Systems," Minneapolis, Minnesota, Honeywell, Inc., F0398 FR1, 1976.
12. Cochran, D. J., Riley, M. W., and Scheller, W. L., "An Examination of Handle Size and Shape for Manual Material Handling Tasks," paper presented at the meeting of the American Industrial Hygiene Conference, Cincinnati, June 1982.
13. Ikai, M., and Steinhaus, A. H., "Some Factors Modifying the Expression of Human Strength," Journal of Applied Physiology, Vol. 16, pp. 157-163, 1961.
14. Poulton, E. C., Tracking Skill and Manual Control, New York, New York, Academic Press, 1974.
15. McDaniel, J. M., "Aerospace Medical Research Laboratory's Pilot Strength and Endurance Screening Program," AFAMRL-TR-78-112, Air Force Aerospace Medical Research Laboratory, Wright-Patterson AFB, Ohio, 1978.
16. McDaniel, J. W., "Male and Female Strength Capabilities for Operating Aircraft Controls," AMRL-TR-81-39, Air Force Aerospace Medical Research Laboratory, Wright-Patterson AFB, Ohio, 1981.
17. Laubach, L. L., Kroemer, K. H. E., and Thordsen, M. L., "Relationships Among Isometric Forces Measured in Aircraft Control Locations," Aerospace Medicine, Vol. 43, pp. 738-742, 1972.
18. Laubach, L. L., "Muscular Strength of Women and Men: A Comparative Study," AMRL-TR-75-32, Air Force Aerospace Medical Research Laboratory, Wright-Patterson AFB, Ohio, 1975.
19. Phillips, M. D., Bogardt, A., and Pepper, R. L., "Female and Male Size, Strength and Performance: A Review of Current Literature," Report No. 342-1, Naval Ocean Systems Center, Kailua, Hawaii, 1981.

1982 USAF-SCEEE SUMMER FACULTY RESEARCH PROGRAM

Sponsored by the

AIR FORCE OFFICE OF SCIENTIFIC RESEARCH

Conducted by the

SOUTHEASTERN CENTER FOR ELECTRICAL ENGINEERING EDUCATION

FINAL REPORT

SPARES SUPPORT USING CANNIBALIZATION

Prepared by:	Dr. Donald L. Byrkett
Academic Rank:	Associate Professor
Department and University:	Systems Analysis Department Miami University
Research Location:	Air Force Logistics Command Directorate of Management Sciences Management Sciences Division (XRSM)
USAF Research Colleage:	Dr. William E. Dickison

Date:	30 July 1982
Contract No:	F49620-82-C-0035

SPARES SUPPORT USING CANNIBALIZATION

by
Donald L. Byrkett

ABSTRACT

As an aircraft, weapon system, or other type of Air Force equipment reaches the latter phase of its life cycle there is a desire to spend less money in spares support due to the high risk of obsolescence. One approach to avoiding these expenditures is cannibalization, a process where several pieces of equipment are taken out of operation in order to provide spares support for the remaining pieces of equipment. This report describes the development of a mathematical model to predict the availability of equipment in the future where the sole means of support is cannibalization. This model is used to analyze data collected for the F-106 simulator. Suggestions for further extensions of the model are offered in the last section.

ACKNOWLEDGEMENTS

The author would like to thank the Air Force Logistics Command, the Air Force Office of Scientific Research, and the Southeastern Center for Electrical Engineering Education for providing him with the opportunity to spend a very worthwhile and interesting summer in the Directorate of Management Sciences (XRS) at Wright-Patterson Air Force Base. Special thanks are due to Dr. William E. Dickison for suggesting this area of research and for providing the author with a good introduction to the Air Force and logistics.

In addition, thanks are due to many other individuals in the Directorate of Management Sciences for their discussions concerning logistics modeling and to the individuals who helped me access data from the computer data bases. Thanks are also due to Dan Danishek, SCEEE coordinator at WPAFB, for providing opportunities to interact with other faculty researchers.

I. INTRODUCTION:

The Air Force Logistics Command is responsible for supporting Air Force equipment in such a way as to achieve certain levels of readiness or availability. One way in which this support is provided is by maintaining inventories of spares for components of the equipment that are subject to failure or condemnation. When a particular component fails, a spare is used to keep the equipment operational while the failed component is repaired. Numerous mathematical models [1], [2], [3], [4], [5] have been developed to compute spares requirements under varying sets of assumptions in order to achieve certain goals. Earlier models tended to focus on the goal of minimizing the number of occasions when equipment is idle due to the lack of an available spare and more recent models focus on the goal of maximizing equipment availability. (Though the availability of the equipment depends on many more factors than spares, generally this is the only factor considered. See Rich and Drezner[6] for a more integrated view of equipment availability.)

Fortuin[7] characterizes the life cycle of service parts (spares) into three phases; the initial phase, the normal phase, and the final phase. This life cycle description is particularly appropriate to Air Force spares. As a new aircraft model or equipment type enters the Air Force inventory, an initial buy of spares is made. This initial buy is made with little or no historic information available regarding component failure rates or repair times. As the equipment enters the normal phase, historic data becomes available and spares levels are adjusted to reflect this new information. One unique characteristic of Air Force spares requirements is that consideration must be given to both peacetime and wartime requirements. Thus, spares are purchased to support the equipment under normal peacetime conditions and additional

spares are purchased for wartime reserves. All of the mathematical models listed above are aimed at equipment primarily in the initial phase or normal phase of the life cycle. The research described in the report is primarily aimed at equipment in the final phase of the life cycle.

Spares of equipment in the final phase of the life cycle have several unique characteristics. Generally, the equipment is older, and thus, the components have higher failure rates. Spares are more difficult to obtain, since many of the components are no longer produced. The use of the equipment is generally declining. There is a tendency not to want to purchase too many spares, since in many cases they will soon become obsolete. One approach to dealing with the support of equipment in the final phase of the life cycle is to provide spares through the process of cannibalization. Under cannibalization, one or several pieces of equipment are taken out of operation in order to provide spares support for the remaining pieces of equipment. A particular goal of this research effort is to study the policy of using cannibalization to support equipment in the final phase of its life cycle.

A specific example of equipment in the final phase of its life cycle is the F-106 simulator. Originally, there were 14 simulators in active operation at various Air Force bases around the country (see Table 1 for current status). Three of these have been cannibalized (with the components stored at Hill Air Force Base in Ogden, Utah) to provide spares support to the remaining simulators and consideration is currently being given to cannibalizing another. The F-106 aircraft is an older model aircraft that is being gradually turned over to the Air National Guard. The aircraft's use and likewise the use of the simulators is expected to decline over a period of time.

TABLE 1

F106 SIMULATOR STATUS

Serial Number	Model	Location	Command	Power On Hours Per Month *
Active:				
62650001	MB42	Great Falls IAP, MT	ANG	175
62650002	MB42	Otis AFB, MA	ANG	100
61150002	MB42A	Atlantic City IAP, NJ	ANG	125
61150004	MB42A	McChord AFB, WA	TAC	150
61150005	MB42A	Griffiss AFB, NY	TAC	150
61150006	MB42A	KI Sawyer AFB, MI	TAC	125
61150007	MB42A	Jacksonville IAP, FL	ANG	100
61150008	MB42A	Minot AFB, ND	TAC	150
61150009	MB42A	Fresno IAP, CA	ANG	175
61150010	MB42A	Tyndall AFB, FL	TAC	350
61150011	MB42A	Tyndall AFB, FL	TAC	350
Inactive:				
62650003	MB42	Hill AFB, UT		
61150001	MB42A	Hill AFB, UT		
61150003	MB42A	Hill AFB, UT		

* Estmated from G033H, the equipment utilization data base.

II. OBJECTIVES OF THE RESEARCH EFFORT:

The major objective of this research effort is to determine at what point in the life cycle of an Air Force equipment type can the remaining spares needs of this equipment be supported by cannibalization. As a first step towards achieving this objective, the summer was spent developing a descriptive model to predict the future availability of a certain equipment type given a fixed initial level of spares and a support policy of "perfect cannibalization" (to be discussed later). The model assumes that repair time is

zero, and thus, in effect only predicts whether or not there are sufficient components (either serviceable or unserviceable) to support the equipment. This assumption represents a significant limitation of the model and as discussed in Section VI represents an important avenue of further research. The output of this model is a curve that for each point in the future gives the probability that N pieces of equipment are available, the expected number of pieces of equipment availble, and the standard deviation of the number of pieces of equipment available.

The steps followed in developing this model were:

(1) To review spares requirements computation models that are currently in use.

(2) To carefully review the computation and assumptions used in Dyna-METRIC[2] to compute availability (Secton III).

(3) To modify the Dyna-METRIC computations to encompass more general equipment and component configurations (Section IV).

(4) To apply the model to the F-106 simulator application (Section V).

III. DYNA-METRIC AND ITS ASSUMPTIONS:

After a careful review of existing spare requirement computation models, it was noted that Dyna-METRIC, under the assumption of instantaneous cannibalization, provided very nearly the computation of expected number of pieces of equipment available that is desired. Using a slight redefinition of symbols, the Dyna-METRIC computation proceeds as follows:

N = number of pieces of equipment available initially

C = number of mission essential components on each piece of equipment

S_i = initial number of spare components $i=1, \ldots, C$

q_i = number of units of component i on each piece of equipment i=1, ..., C

m_i = number of condemnations per 100 usage hours of each component i=1, ..., C

Normally, in Dyna-METRIC, m_i refers to a failure rate, but in this application, since repair time is being ignored and the goal is to predict the length of time sufficient components are available to support the equipment, a condemnation rate is used. If H(t) = planned hours of operation (in hundreds of hours) during quarter t for this equipment type, then the number of condemnations during quarter t of component i is calculated as follows:

$$d_i(t) = m_i * q_i * H(t) \quad (1)$$

These are then added up until time t to determine the total number of condemnations of components i through time t

$$L_i(t) = \sum_{p=1}^{t} d_i(p) \quad (2)$$

If it is assumed that condemnations occur in a random pattern, then the Poisson distributin is used to calculate the probability of K condemnations of component i at time t

$$P_i(K) = \frac{L_i(t)^K * \exp(-L_i(t))}{K!} \quad (3)$$

The cumulative distribution is:

$$CP_i(K) = \sum_{p=0}^{K} P_i(p) \quad (4)$$

These concepts are then combined to calculate the probability that the number of pieces of equipment available at time t (NA(t)) is greater than or equal to N-K:

$$P(NA(t)\ \ N\text{-}K) = \sum_{i=1}^{N} CP_i(S_i + q_i * K) \qquad (5)$$

Note that this is equivalent to calculating the probability that the number of pieces of equipment not available is less than or equal to K. From here it is a simple process to calculate the probability distribution, expected value, and standard deviation of NA(t).

$$P(NA(t)=N\text{-}K) = P(NA(t) \geq N\text{-}K) - P(NA(t) \geq N\text{-}K+1) \qquad (6)$$

$$E(NA(t)) = \sum_{k=0}^{N} (N\text{-}K)P(NA(t) = N\text{-}K) \qquad (7)$$

$$SD(NA(t)) = \sqrt{\sum_{K=0}^{N} (N\text{-}K)^2\ P(NA(t) = N\text{-}K) - E^2(NA(t))} \qquad (8)$$

Implicit in the calculations above are a numbr of assumptions which are discussed and evaluated with respect to the policy of supporting equipment for the remainder of its life through cannibalization.

Assumption 1: Condemnations are consolidated on as few pieces of equipment as possible. This is the assumption of perfect cannibalization. This assumption is probably more valid for equipment in the final phase of operation than equipment in other phases, since once the equipment is cannibalized it will not be brought back into operation.

Assumption 2: All components are equally mission essential. This depends on the application but is retained in the revised model.

Assumption 3: Component condemnations are independent. This also depends on the application but is retained in the revised model.

Assumption 4: The programmed hours of operation are fixed and will be carried out regardless of the number of pieces of equipment available. This is not a bad assumption as long as the expected number of pieces of equipment is not too small or if the programmed hours of operation are declining. For equipment in the final phase of operation, the number of pieces of equipment may be small but hopefully so are the planned hours of operation. This assumption is also retained in the revised model but represents a possible avenue of further research.

Assumption 5: Repair time is zero. This is not an assumption of Dyna-METRIC but is introduced in this study to focus on the problem of the sufficiency of cannibalization spares to support the equipment, rather than the availability of the spares. This likewise represents an important avenue of further research.

Assumption 6: The condemnation rate is constant over time. For equipment in the final phase of its life cycle, the condemnation rate is likely increasing. Allowing for a variable condemnation rate is a rather simple change which is implemented in the revised model.

Assumption 7: All pieces of equipment are identical with respect to components. This is not the case with the F-106 simulator appication described in section I. In this case, there are two models of equipment MB42 and MB42A. Some components are the same on both models, some are unique to MB42, and some are unique to MB42A. In addition, there is one component that is on both models but with a different quantity on each model. It is expected that other equipment types have this characteristic, so the revised model is designed to allow this generality.

IV. REVISED MODEL:

It is noted in the previous section that Dyna-METRIC did not allow for an increasing condemnation rate (Assumption 6) or for a variety of model types with different components (Assumption 7). This section describes how the Dyna-METRIC availability computation is revised to handle this greater degree of generality. For simplicity in explaining the revised model, it is assumed there are only two model types, though the extension to more than two types follows a similar line of reasoning.

The notation used in this section is the same as that used in Section III with the following additions and modifications:

N_j = number of pieces of equipment of model j available initially j=1,2. Assume $N_1 \quad N_2$. ($N = N_1 + N_2$)

C_o = number of components that are common to both equipment models

C_j = number of components that are unique to equipment model j j=1,2 ($C=C_o+C_1+C_2$)

q_{ij} = number of units of component i on equipment model j i=1, ..., C, j=1, 2. This will equal zero in some cases.

$m_i(t)$ = number of condemnations per 100 usage hours during quarter t for each component i=1,..., C. This takes care of Assumption 6.

To calculate $d_i(t)$, the planned hours of operation must be divided among the two equipment models as follows:

$$d_i(t) = \sum_{j=1}^{2} (N_j/N) * q_{ij} * m_i(t) * H(t) \qquad (9)$$

As in Section III, equations (2), (3), and (4) are used to calculate $L_i(t)$, $P_i(K)$, and $CP_i(K)$.

Unfortunately, the availability calculations are much more complicated, since one must consider specifically which equipment models are not available. If NMC_j = the number of pieces of equipment of model type j that are not mission capable at time t, then the probability that the number of pieces of equipment available at time t is greater than or equal to N-K is given below:

If $K \leq N_1$,

$$P(NA(t) \geq N-K) = P\left[(NMC_1 \leq K \cap NMC_2 \leq 0) \cup (NMC_1 \leq K-1 \cap NMC_2 \leq 1) \cup \ldots \cup (NMC_1 \leq 0 \cap NMC_2 \leq K)\right] \quad (10)$$

If $K > N_1$,

$$P(NA(t) \geq N-K) = P\left[(NMC_1 \leq N_1 \cap NMC_2 \leq K-N_1) \cup (NMC_1 \leq N_1-1 \cap NMC_2 \leq K-N_1+1) \cup \ldots \cup (NMC_1 \leq 0 \cap NMC_2 \leq K)\right] \quad (11)$$

In order to make this calculation, the random variable NMC_j must be translated into a random variable regarding the number of condemnations of individual components so that equation (4) may be used. If X_i = number of condemnations of component i at time t, than the following events are identical

$$(NMC_1 \leq Z \cap NMC_2 \leq K-Z) = ((X_1 \leq S_1 + Z*q_{11} + (K-Z)*q_{12}) \cap \quad (12)$$

$$(X_2 \leq S_2 + Z*q_{21} + (K-Z)*q_{22}) \cap \ldots \cap (X_c \leq S_c + Z*q_{c1} + (K-Z)*q_{c2}))$$

By substituting the relationship defined in equation (12) into equations (10) and (11) and by applying the probability laws involving the union of events [8], the desired probability is calculated. This result is substituted into equations (6), (7), and (8), as before, to obtain the final results.

The extension of this model to more than two equipment models is complicated but follows a similar line of reasoning. For example, if there are three equipment models equation (10) is as follows:

$$
\begin{aligned}
P(NA(t) \geq N-K) = P\,[&(NMC_1 \leq K \cap NMC_2 \leq 0 \cap NMC_3 \leq 0) \cup \\
&(NMC_1 \leq K-1 \cap NMC_2 \leq 1 \cap NMC_3 \leq 0) \cup \\
&(NMC_1 \leq K-1 \cap NMC_2 \leq 0 \cap NMC_3 \leq 1) \cup \\
&\quad \vdots \\
&(NMC_1 \leq 0 \cap NMC_2 \leq 0 \cap NMC_3 \leq K)]
\end{aligned}
\tag{13}
$$

V. APPLICATION TO F-106 SIMULATORS:

Though there are countless Air Force equipment types for which the models in this report apply, the primary motivation for the revised model of Section IV is the F-106 simulator. As was mentioned in Section I, spares for this group of simulators are being obtained by cannibalization. There are some individuals who feel that it is too soon to rely on cannibalization, since the F-106 aircraft, and hence simulators, may still serve a useful purpose for many years to come. Thus, it becomes important to predict the future availability of simulators using cannibalization support

The D041 data base which contains all the reparable stock numbers in use by the Air Force was searched to identify the components of the F-106 simulator. Seventy-nine stock numbers were obtained in this way. Of these, only 21 stock numbers (see Table 2) contained a non-zero failure rate, which indicates that the remaining 58 stock numbers did not experience any failures during the past two years. Of these 21 stock numbers, only 6 are unique to the F-106 simulator and only 7

contained a non-zero condemnation rate. For those stock numbers that are not unique to the F-106 simulator, the initial spares stock is pro-rated on the basis of programmed operating hours and for those stock numbers without condemnation during the past two years, the condemnation rate is arbitrarily set at 2% of the failure rate. Admittedly, this data is not as complete as desireable, but it is the best that could be obtained in such a brief period. Ideally, only components unique to the F-106 simulator should be used and more than two years of data are needed to accurately estimate condemnation rates. Additionally, it would be useful to be able to project condemnation rates into the future.

TABLE 2
COMPONENT DATA

	COMPONENT	UNIQUE TO F106	m_i	q_{i1} (MB42)	q_{i2} (MB42A)	S_i
1.	Indicator	Yes	.01183	2	2	28
2.	Generator	Yes	.00037*	6	0	5
3.	Converter	Yes	.00087*	1	1	4
4.	Amplifier	Yes	.00019*	2	0	4
5.	Indicator	Yes	.00048*	1	1	10
6.	Power Supply	Yes	.00032*	1	1	3
7.	Amplifier	No	.00015	38	8	11**
8.	Storage Me.	No	.00210	1	0	2**
9.	Indicator	No	.00029	2	2	3**
10.	Altimeter	No	.00199	1	0	1**
11.	Amplifier	No	.00006*	68	0	102**
12.	Climb Ind.	No	.00003*	2	0	35**
13.	Accelerometer	No	.00038*	2	2	12**
14.	Altimeter	No	.00005*	2	2	25**
15.	Tachometer	No	.00024	2	0	4**
16.	Amplifier Demod.	No	.00019*	4	0	4**
17.	ADI 2 Gumb	No	.00073	2	2	63**
18.	Gear Assy	No	.00001*	16	0	3**
19.	Motor Generator	No	.00016*	1	1	1**
20.	Indicator	No	.00016*	1	1	5**
21.	Indicator	No	.00004	1	0	14**

* Estimated as 2% of failure rate ** Spares allocated to simulator on basis of programmed operating hours

The projected training hour program for the F-106 simulator was also obtained from the D041 data base and is given below for the next 23 quarters starting with the first quarter of 1982.

TABLE 3
F-106 TRAINING HOURS (HUNDREDS)

QUARTER	1	2	3	4	5	6	7	8
HOURS	94	94	95	58	58	58	59	94
	9	10	11	12	13	14	15	16
	94	94	95	93	94	94	95	59
	17	18	19	20	21	22	23	
	59	59	59	94	95	95	95	

These figures conflict with the power on hours reported in Table 1. The power on hours indicate that the simulators operate an average of 40 hours per week or 57.2 (hundreds) hours per quarter.

To compute the expected number of simulators available at future points in time, the data provided in Tables 2 and 3 were plugged into the revised model of Section IV. Four cases were run using different combinations of components. In one case, all 21 components were used. In another, only components unique to the F-106 simulator (1-6) were used. In another, only components with actual condemnations rates (1,7,8,9,10,15,21) were used. And finally, a case was run with only component 1 which is both unique to the simulator and has an actual condemnation rate. The results in all four cases are almost identical and are indicated by curve A of Figure 1. The reason all four cases are nearly the same is that item 1 (which was included in all four cases) has

such a high condemnation rate that it is the dominating factor affecting the availability of the simulators.

Similarly, cases were run using a more realistic training hour program of 57.2 hundred hours per quarter. This result is indicated by curve B of Figure 1. Notice that using the more realistic training program, it appears that in spite of the high condemnation rate of component 1, there are sufficient simulators available for the next 23 quarters.

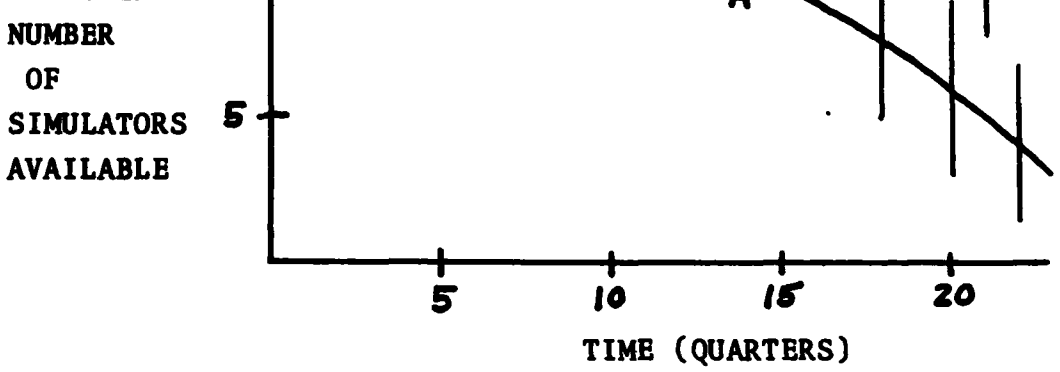


FIGURE 1 - EXPECTED NUMBER OF SIMULATORS AVAILABLE PLUS OR MINUS ONE STANDARD DEVIATION

Further investigation of component 1 indicated that it is an exhaust gas temperature indicator and, in fact, it does have a very high condemnation rate. So high that technicians have located a similar component on the F-102 simulator that may be substituted for this item.

Based on this brief analysis, it appears that cannibalization will produce sufficiient spares for the F-106 simulator. However, it must be remembered that as the number of spares

dwindles, repair time (which was ignored in the model) will become a much more significant factor affecting simulator availability.

VI. RECOMMENDATIONS:

It is clear from the attempt to apply the model to the F-106 simulator that it is an inadequate representation of equipment availability in the final phase. In fact, it is postulated that techicians will obtain replacement components for as long as the equipment is needed - even if it is necessary to make replacement components to specification on an as needed basis. This implies components can be made available indefinitely. However, as spares become fewer, the repair time is lengthened and equipment is unavailable while waiting for replacement components. To capture this reality, the model needs to be enhanced to include repair time, possibly allowing repair time to increase as the spares become less available.

A totally separate area of investigation involves the effect of the time sequence of component condemnations on equipment availability. At present, this effect is ignored but it can influence availability in a number of ways. For example, suppose there are two models of equipment. Model 1 contains 3 units of component A and Model 2 contains 5 units of component A. Under perfect cannibalization, if there are 4 condemnations of A, there would only be one piece of model 2 equipment down. However, suppose that the first condemnation occurred on a model 1 piece of equipment. It seems more likely that this piece of equipment would be the one cannibalized. Another example of where the time sequence of condemnations can be important is in the computation of the average condemnation rate, $d_i(t)$, specified by equation (9). This rate is computed using the original mix of equipment

assuming operating hours are the same on each piece of equipment. This is clearly not the case with the F-106 simulators (see Table 1). Actually, $d_i(t)$ depends on the exact sequence of equipment cannibalization and how the operating hours of cannibalized equipment are allocated to the remaining equipment. Furthermore, $d_i(t)$ depends upon whether the remaining equipment is capable of picking up the lost operating hours (see assumption 4, Section IV). This represents another interesting area of further research that could be investigated by comparing simulated and analytic results.

REFERENCES

1. T.R. Bridges and S. Schroeder, "Investigation of War Reserve Material Kit Objective Functions", Tech. Rep. XRS 79-243, September 1980.

2. R.J. Hillestad, "Dyna-METRIC: A Mathematical Model for Capability Assessment and Supply Requirements When Demand, Repair, and Resupply are Nonstationary", The Rand Corp., R-2785-AF (forthcoming)

3. R.J. Hillestad and M.J. Carrillo, "Models and Techniques for Recoverable Item Stockage When Demand and the Repair Process Are Nonstationary - Part I: Performance Measurement", The Rand Corp., N-1482-AF, May 1980.

4. J.A. Muckstadt, "A Model for a Multi-Item, Multi-Echelon, Multi-Indenture Inventory System", Mgmt. Sci., Vol 20, pp. 472-481, 1973.

5. C.C. Sherbrooke, "METRIC: A Multi-Echelon Technique For Recoverable Item Control", Mgmt. Sci., Vol 16, pp 122-141, 1968.

6. M.D. Rich and S.M. Drezner, "An Integrated View On Improving Combat Readiness", The Rand Corp., N-1797-AF, February 1982.

7. L. Fortuin, "The All-Time Requirement of Spare Parts for Service After Sales - Theoretical Analysis and Practical Results", Int. Jour. of Oper. and Prod. Mgmt., Vol 1, pp 59-70, 1980.

8. W. Feller, An Introduction to Probability Theory and its Appications, John Wiley and Sons Inc., New York, 1968.

1982 USAF-SCEEE SUMMER FACULTY RESEARCH PROGRAM

Sponsored by the

AIR FORCE OFFICE OF SCIENTIFIC RESEARCH

Conducted by the

SOUTHEASTERN CENTER FOR ELECTRICAL ENGINEERING EDUCATION

FINAL REPORT

ELECTRICALLY COMPENSATED CONSTANT SPEED DRIVE

Prepared by:	Dr. Jimmie J. Cathey
Academic Rank:	Associate Professor
Department and University:	Department of Electrical Engineering University of Kentucky
Research Location:	Air Force Wright Aeronautical Laboratories Aero Propulsion Laboratory
USAF Research Colleague:	Dr. William U. Borger
Date:	August 6, 1982
Contract No:	F49620-82-C-0035

ELECTRICALLY COMPENSATED CONSTANT SPEED DRIVE

by

Jimmie J. Cathey

and

Tim W. Krimm

ABSTRACT

The feasibility of designing a constant speed drive utilizing a mechanical differential in conjunction with a parallel electric drive speed compensation link is examined. Bidirectional power flow in the electric compensation link uses two high-speed, permanent-magnet, three-phase machines interconnected by a power conditioning network. One machine is operated as a brushless dc machine, while the other functions as a variable speed synchronous machine. Steady-state performance of two types of power conditioning are studied--a dc link inverter and a cyclo-converter link.

The dc link inverter with bidirectional power flow is found to require excessive values of current to allow full range reverse power flow. A mode switch to synchronous inversion is necessary to reduce current values, but it adds the penalty of increase in power electronic devices and control complexity. The cycloconverter link is found to offer the better full range bidirectional power flow. In addition, a dc link system is examined for a method of operation with unidirectional power flow through the compensation link at the expense of increased size of electrical machines, but offering simpler controls.

Suggestions are made for further research on this system concept.

ACKNOWLEDGMENTS

The authors extend thanks to the Air Force Systems Command, the Air Force Office of Scientific Research, and the Southeastern Center for Electrical Engineering Education for providing the opportunity to conduct research at the Air Force Wright Aeronautical Laboratories, Wright Patterson AFB, OH. A particular expression of gratitude is offered to the Power Systems Branch of the Aerospace Power Division of the Aero Propulsion Laboratory for provision of an excellent set of working conditions and facilities.

Further, the authors offer appreciative acknowledgment to Dr. William U. Borger for suggesting, encouraging, and guiding the work of this study.

I. INTRODUCTION

The need for a highly efficient link, capable of bilateral power flow, connecting a variable speed shaft to a constant speed shaft is manyfold. A particular Air Force need is to drive an onboard aircraft alternator at constant speed while the turbine engine speed varies. Presently, two methods are employed to provide a constant frequency on Air Force aircraft:

1. Constant Speed Drive (CSD)
2. Variable-Speed, Constant-Frequency (VSCF)

The VSCF system allows the alternator shaft speed to vary directly with turbine speed. The variable frequency alternator output is then conditioned by a cycloconverter to obtain a constant frequency. The VSCF system is not sensitive to attitude changes, and thus, functions well on highly maneuverable aircraft. However, total output power of the alternator must pass through the cycloconverter, leading to bulky and expensive power conditioning and filter circuitry.

The CSD scheme utilizes a mechanical differential to link the turbine engine and alternator. A constant alternator shaft speed is maintained by proper clockwise or counterclockwise rotation of the differential carrier housing through use of a reversible hydraulic pump-motor drive. For a 1.7:1 turbine speed range and a lossless system, a maximum of 21.5% of the alternator shaft power must pass through the compensating hydraulic drive, while 78.5% to 100% of the power is transmitted directly through the differential gearing. The CSD has been successful in flight operation except during maneuvers that produce negative gravity. In such cases, fluid level shifts can cause the hydraulic system to momentarily malfunction, creating an out of frequency range condition and leading to loss of electrical power.

Regardless of the above described potential failure mode, the concept of the CSD system has a quite desirable feature in that a large percentage of its output power is transmitted only through a low-order-mesh gear train which by nature is highly efficient. Replacement of the hydraulic compensation drive with an electric compensation drive can yield a CSD concept that is insensitive to aircraft attitude changes while preserving

the desirable feature. Further, a properly designed electric drive should offer an increase in overall efficiency, due to reduction in losses through the speed compensation path. Also, the potential exists for a greater interval between maintenance than for the compensating hydraulic drive system.

II. OBJECTIVES

The principal goal of this research was to study the feasibility of designing an electrically-compensated, constant-speed drive (ECCSD) that has potential for application as a drive link between a turbine engine and an aircraft alternator. Objectives were established to study the nature of ECCSD systems in the steady-state. Transient characteristics and parameter sensitivity evaluations were not possible within the research period time frame, and thus, were left for future investigation. The specific objectives that were pursued are enumerated below:

1. Define candidate electrical machinery and power conditioning circuitry arrangements suitable for use with an ECCSD system.
2. Determine nature of torques, currents, and voltages for each candidate system operating as an ECCSD.
3. Identify special requirements on machines, controls, and power electronic devices that result from the ECCSD application.

III. BASIC REQUIREMENTS AND CHARACTERISTICS OF ECCSD

An understanding of the power flow and torque requirements of the ECCSD concept underlies any study as these characteristics must serve as a basis for selection of candidate electric machine and power conditioning systems.

A. Nature of Power Flow. A physical arrangement of the ECCSD power level components is shown in Figure 1(a) where variable input speed n_1, constant output speed n_0, and differential carrier speed n_2 are related by:

$$n_2 = 1/2\ (n_1 - n_0) \tag{1}$$

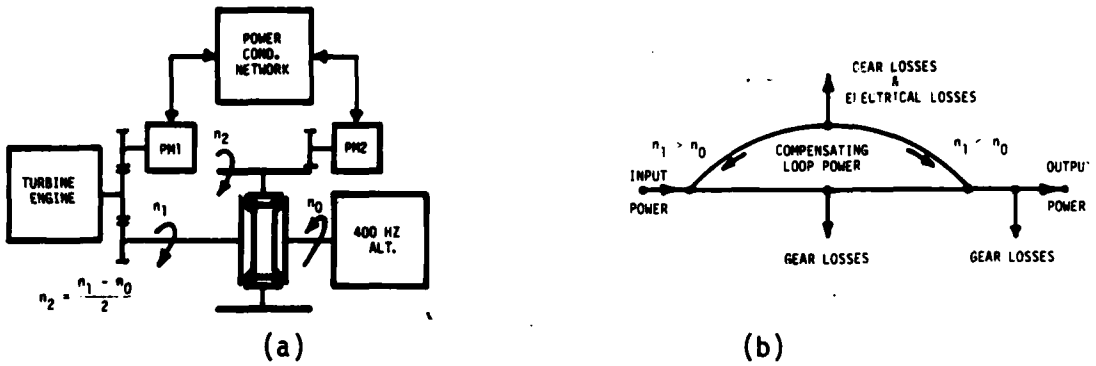


Figure 1 (a) Physical Arrangement of ECSD
(b) Power Flow Diagram of ECCSD

Speed compensation to maintain n_0 constant can be accomplished by two basically different control approaches:

1. Reversing differential operation. Ratios are selected so that n_0 lies between the extremes of n_1. Thus, from equation (1) it is apparent that n_2 can range from negative to positive values or that the differential carrier must be reversed to maintain a constant n_0 over the range of n_1 excursion.

2. Unidirectional differential operation. Ratios can be selected so that n_1 is always greater than (or always less than) n_0, leading to the conclusion from equation (1) that n_2 does not change sign as n_1 varies; or, the differential carrier is always rotated in the same direction for speed compensation.

For study of basic characteristics, a typical turbine speed range of 1.7:1 (10,588 to 18,000 rpm) was used. The 400 Hz alternator was modelled as a 44.444 KW load at a constant 12,000 rpm (40 kVA output at unity power factor operating at 90% efficiency). Constant efficiencies were assumed as follows:

1. Electric machines - 90%
2. Power conditioning units - 95%
3. Gear mesh - 99%

Energy balance equations were written for the arrangement of Figure 1(a) and turbine speed was incremented across its speed range to examine both the case of reversing differential carrier and the case of unidirectional differential carrier operations. A power flow diagram of the ECCSD system is shown by Figure 1(b) where the flow direction of compensating loop power (P_c) depends upon the polarity of ($n_1 - n_0$) as indicated on the diagram.

The reversing differential carrier results in minimum torque requirements for PM2 if the midrange speed of n_1 is set to equal n_0, which also gives a symmetric range on n_2 about the zero speed point. Figure 2 displays the performance results of this system. It is observed that the torque requirements of PM2 are nearly constant across the range of operation. However, the torque requirements of PM1 range from zero at the midrange speed point to a maximum value at the point of minimum turbine speed. It is further noted that the maximum torque requirement of PM1 is greater than that of PM2. The two maximum torque requirements could be made equal by an unsymmetric shift of the differential carrier zero speed point with a net result of increasing the torque requirement of PM2 while decreasing the requirement of PM1. The ratio of power flowing into the speed compensation loop to power delivered to the 400 Hz alternator (P_c/P_0) is plotted to use as an indication of power apportionment between that transmitted by the compensation loop and that transmitted in mechanical form through the ECCSD.

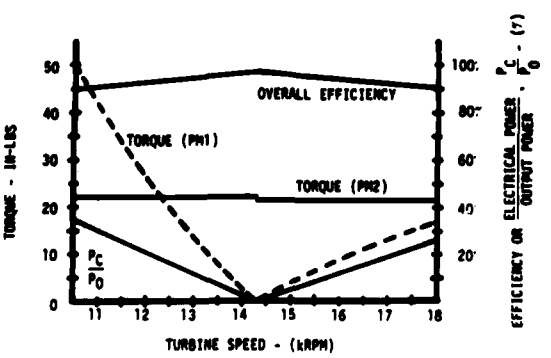


Figure 2 Calculated Performance Of Reversing Differential

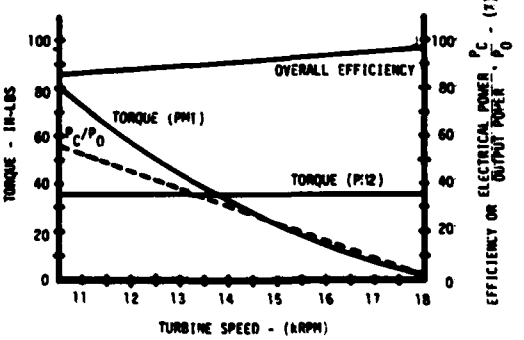


Figure 3 Calculated Performance Of Unidirectional Differential

Calculated torque requirements and performance results for unidirectional differential operation, if $n_1 < n_o$, are depicted by Figure 3. System gear ratios were selected so that n_2 ranges from 2% to 100% of PM2 base speed circumventing the necessity of dealing with low frequency torque pulsations at near zero speed.

B. Electric Machines. The wide speed range, constant torque requirements suggested for PM2 by the above work is the characteristic of a shunt dc machine; but, due to the brush-commutator maintenance requirement and poor adaptability to liquid cooling, the commutator dc machine is not suitable for aircraft application. However, the brushless dc motor offers the same desired speed-torque characteristics as the dc machine without the disadvantages of the commutator dc machine.[1-10] Further, use of a machine with a permanent magnet rotor offers two additional advantages:

1. Field excitation is eliminated which removes the complexity of supplying power to a rotating member. Also, machine efficiency is increased due to absence of field excitation losses.

2. Higher speed design is possible for permanent magnet rotors than is feasible with wound rotors permitting increased gear ratios and substantial reduction in electric machine size.

Some of the brushless dc motor performance reported in the literature is experimental data [1,3,5]. Others have presented calculations based on formulas derived using approximations of sinusoidal waveforms or neglecting commutation intervals giving results with some degree of correlation to test data but with appreciable error [2,8,9]. However, the nonlinearities introduced by the circuit switching leads to equations that are best solved by numerical techniques, and the reported performance data calculated by numerical solution of network differential equations show the least error between theoretical prediction and test results [4,10,11]. When analyzing PM machines with rare earth magnets and stainless steel retaining rings for rotor construction, Demerdash has reported [11] that rotor eddy current effects, armature reaction, and position dependence of inductances can be neglected leading to a simple third-order system of equations to describe a balanced, three-phase,

wye-connected PM machine:

$$\underline{v} = [R]\,\underline{i} + [L]\,p\underline{i} + \underline{e} \qquad (2)$$

where $\underline{v}$ is a vector of terminal phase voltages (v_1, v_2, v_3),
$\underline{i}$ is a vector of phase current (i_1, i_2, i_3),
$\underline{e}$ is a vector of phase generated voltages (e_1, e_2, e_3),
[R] is a diagonal matrix with each entry being phase resistance,
[L] is a diagonal matrix with each entry being half of line-to-line inductance, and
$p\,(\ )$ is understood to mean $\frac{d}{dt}(\ )$.

Since the equations given by (2) are decoupled, each can be used in networks formed by addition of the power conditioning circuitry with minimum difficulty.

C. Power Electronics. Obviously, the power conditioning circuitry of this application must be capable of bidirectional power flow when utilized in conjunction with the electric machinery. No reporting in the literature is available of an ac PM machine-to-brushless dc PM machine drive system. However, two basically different power conditioning links are candidates for use with this ECCSD under study:

1. A dc link inverter using a phase-controlled converter for rectification and synchronous inversion.
2. A cycloconverter link to perform ac-to-ac conversion.

Either of these power conditioning links can use thyristor or transistors as switching elements, but the practicality of transistors depends on values of voltage and current ratings dictated by the final system design. Much of the logic and signal manipulation of either power conditioning link will lend itself to digital processing and microprocessor control giving a finished product in which a large percentage of the signal level electronics is integrated circuits.

IV. DC LINK INVERTER WITH REVERSING DIFFERENTIAL

A. System Description. Power level components of a dc link drive system for use with the reversing differential are shown in Figure 4 where PM2 is operated as a brushless dc machine while PM1 functions as a variable speed synchronous machine.

In order to simplify the analysis, the phase-controlled converter and PM1 of Figure 4 are modelled as a dc source which, when coupled to the inverter and PM2, forms a nonplanar network. In this resulting network, the various SCRs (or transistors) and diodes are represented by nonlinear resistors the resistance of which are assigned small values

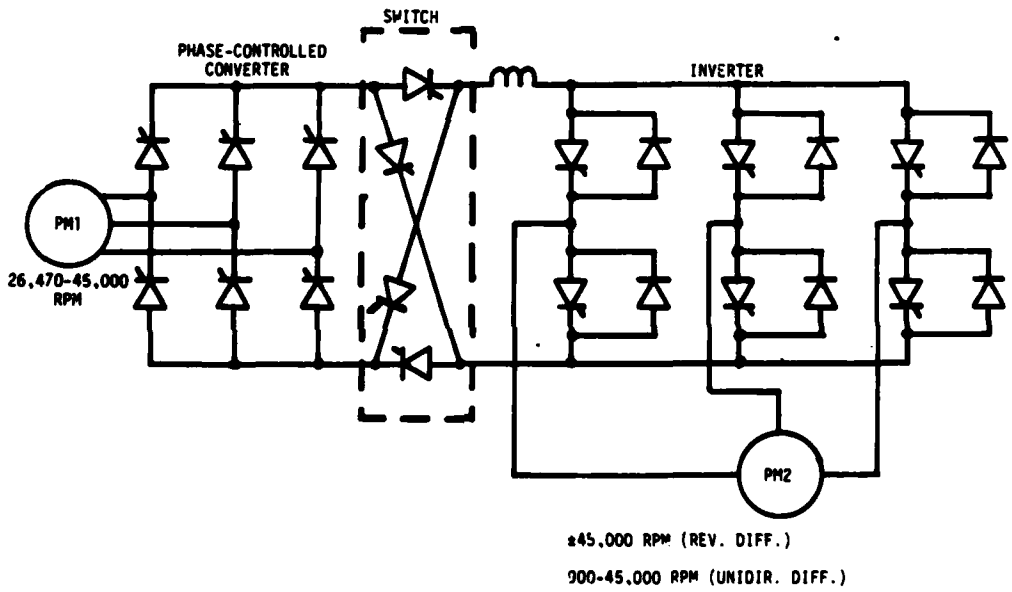


Figure 4 Power Components of DC Link Drive System

when forward conducting and large values when reverse biased. For a wye-connected PM2, the constraint that the phase currents must add to zero exists; thus, a system of two first-order differential equations is sufficient to describe the network. These equations have nonlinear coefficients due to the values of SCR (or transistor) and diode resistances being functions of the dependent variables (phase currents). Further, each 60° (electrical), a switching operation transpires in the inverter circuitry requiring a revised set of differential equations to describe the system; therefore, the differential equation coefficients

are also functions of the position (θ_2) and speed (ω_2) of PM2 rotor. In matrix notation, the network equations can be written as

$$p\underline{i} = [A(\underline{i},\theta_2)]\ \underline{i} + [B(\omega_2)]\ \underline{u} \qquad (3)$$

where $\underline{i}$ is a vector of two independent phase currents (i_1, i_2), and $\underline{u}$ is a vector the entries of which are phase generated voltages and the dc source which models the phase-controlled converter and PM1 combination.

B. Control Approach. A block diagram of a control approach that can be applied to this dc link drive system is displayed by Figure 5.

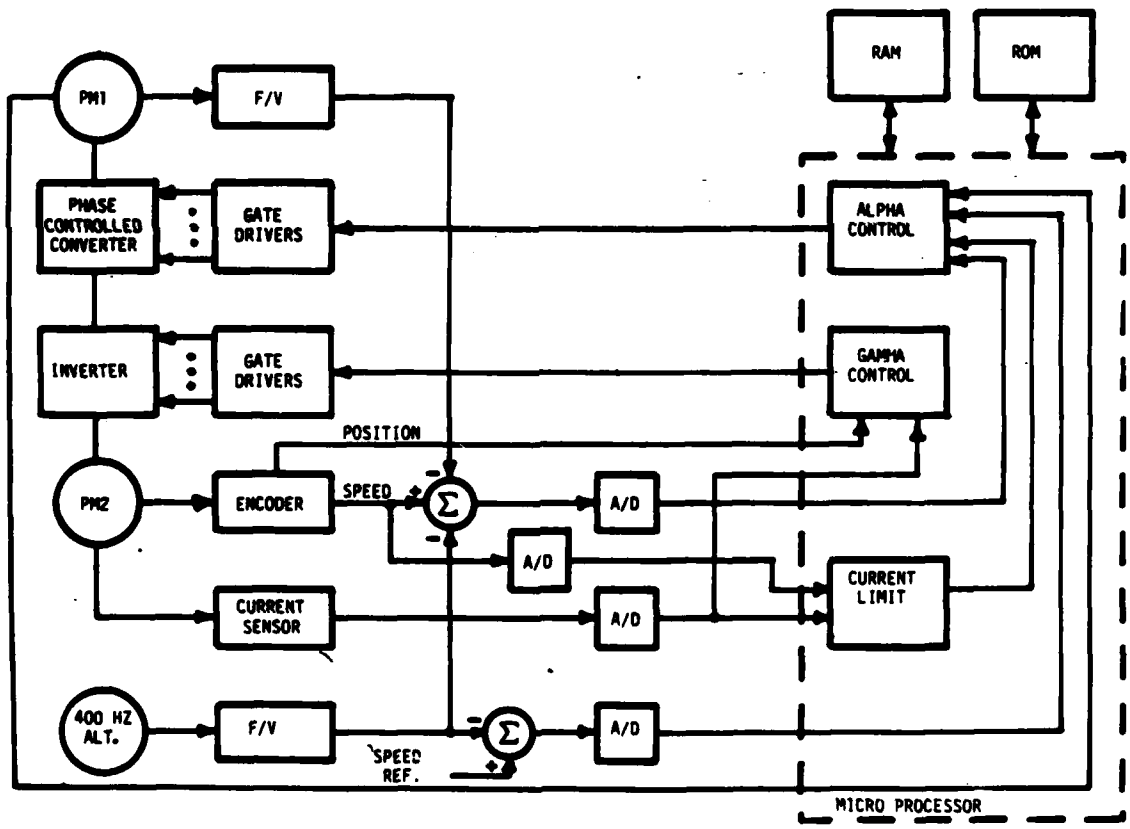


Figure 5 Block Diagram of DC Link Drive System

A primary control loop is established with a speed reference signal to assure that the 400 Hz alternator maintains rated speed. A secondary control loop is present to guarantee that equation (2) is satisfied. The SCRs (or transistors) of the inverter are fired in a manner to maintain a constant commutation angle γ, related to the angle between the mmf wave of the rotor and the no-load mmf wave of the stator. The delay angle of the phase-controlled converter is varied to regulate the value of dc link voltage applied to the inverter terminals. Steady-state characteristics of this drive are quite similar to those of a dc machine system [1-10] except for the extra degree of freedom that exists in selecting γ.

The block diagram of Figure 5 is shown with a microprocessor based control on current limit and SCR firing. It is likely that summing functions of the primary and secondary speed loops can also be handled as microprocessor operations if timing and sample rates do not become limiting factors.

C. Performance Results. Values were selected for motor and choke coil parameters as $R_a = 0.006\Omega$, $L_a = 25 \times 10^{-6}$H, $R_o = 0.003\Omega$, and $L_o = 43 \times 10^{-6}$H. A numerical solution of the equations represented by (3) was implemented using a fixed increment, fourth-order Runge-Kutta procedure to find performance of the dc link drive for various values of constant speed. A trial-and-error search was made for the average values of PM2 shaft torque (T_{sav}) to satisfy the requirements established by Figure 2. Results of points calculated across the speed range for forward flow of compensating loop power and partial range values for reverse flow of compensating loop power are shown in Table 1.

TABLE 1. PERFORMANCE OF DC LINK WITH REVERSING DIFFERENTIAL

Speed (rpm)	T_{sav} (N-m)	α (degrees)	γ (degrees)	I_{ave} (A)	I_{rms} (A)
45,000	2.46	18.2	45	56.4	69.5
22,000	2.48	61.6	45	56.2	69.2
5,000	2.51	82.8	45	56.4	69.8
500	2.24	88.2	45	55.2	66.3
50	2.53	88.5	45		
-500	-2.45	89.3	165	47.0	56.8
-5,000	-2.36	91.3	150	81.9	92.9
-10,000	-2.46	90.3	140	115.2	130.6

It can be observed that the values of average and RMS current required to produce the needed torque when PM2 is in the regeneration mode (reverse flow of compensating power) increase as speed becomes more negative. This increase in current values is attributable to a marked increase in the magnitude and time that current flows through the inverter shunting diodes. At some point for speed more negative than -22,000 rpm, the shunting diode current reaches a conduction angle equal to 60° at which point commutation failure occurs. A full range regenerative range operation with PM2 acting as a brushless dc machine is not possible. At some negative value of speed, it would be necessary to change modes of operation; PM2 would be allowed to operate as a variable frequency synchronous generator with the inverter shunting diodes acting as a three-phase, full-wave bridge rectifier and the phase-controlled converter could be controlled for synchronous inversion. However, use of a bridge switch as shown in Figure 4 would be necessary to establish proper polarity of dc voltage to the phase-controlled converter for synchronous inversion. Calculations show that the average values of current can be reduced to acceptable levels with the synchronous inversion operation; however, the mode change creates control complexities. Further, with addition of the bridge switch, the number (16) of power level switching devices has closely approached the quantity (18) necessary for the cycloconverter link which is capable of full speed range regenerative operation without a control mode change.

V. CYCLOCONVERTER LINK WITH REVERSING DIFFERENTIAL

A. System Description. Power level components of a cycloconverter drive system for use with the reversing differential are shown in Figure 6. As in the dc link case previously discussed, PM2 operates as a brushless dc machine while PM1 functions as a variable speed synchronous machine.

It is permissible to model PM1 as seen from the terminals of PM2 as a dc source that is magnitude dependent on both the speed of PM1 and an SCR firing delay angle α. However, since the response of PM2 due to the frequency of PM1 is desired it is necessary to describe V_d, the instantaneous waveform of PM1 generated voltage as seen from the terminals of PM2, in 60° increments of the PM1 voltage waveform giving the expression

$$V_d = V_m \sin(\omega_1 t - \phi + \frac{\pi}{3} + \alpha) \qquad (4)$$

where V_m depends on the speed of PM1, ω_1, is the electrical angular frequency of PM1 and ϕ is a phase shift angle that depends upon the

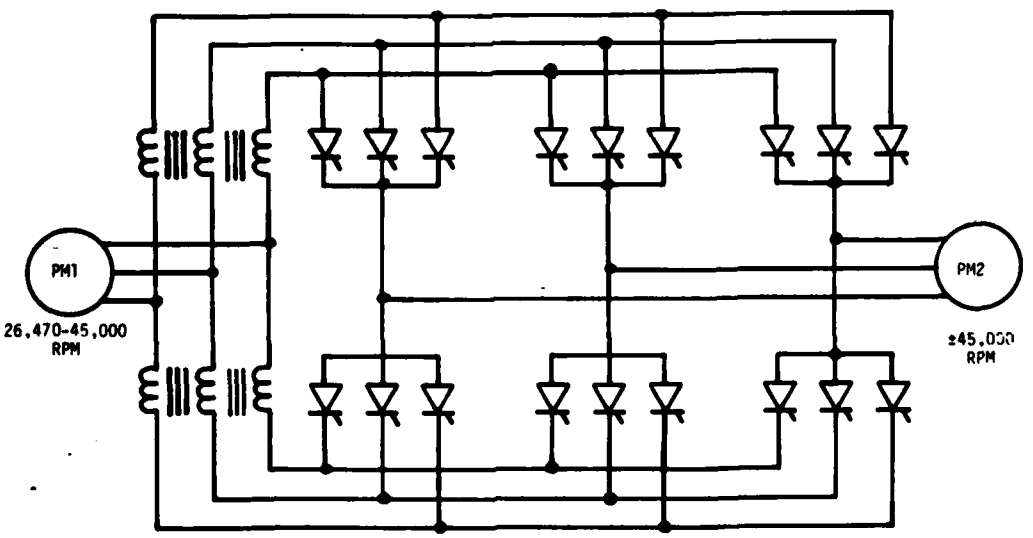


Figure 6 Power Components of Cycloconverter Link Drive

particular 60° increment of the PM1 waveform that is applicable at the instant of solution. The nonplanar network that results when V_d is coupled to PM2 through the cycloconverter is described by a set of two differential equations with nonlinear coefficients as discussed in section IV except that now the forcing function coefficient matrix has entries that depend on the electrical angular frequency of PM1:

$$p\underline{i} = [A(\underline{i},\theta_2)]\underline{i} + [B(\omega_1,\omega_2)]\underline{u} \qquad (5)$$

B. Control Approach. A control approach is suggested by the block diagram of Figure 7. The philosophy is basically that of the dc link system given by Figure 5 (discussed in Section IV) except that gating of the SCRs must be handled in such a manner to assure that both the commutation angle γ and delay angle α are both simultaneously satisfied.

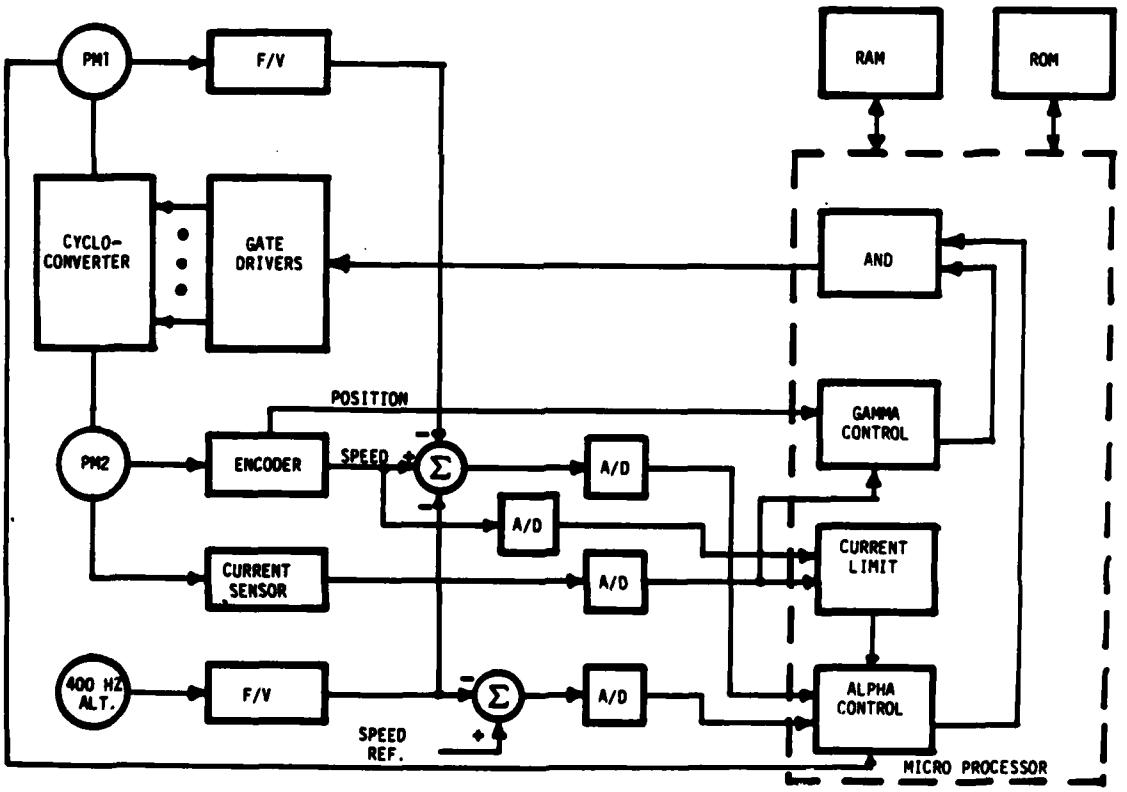


Figure 7 Block Diagram of Cycloconverter Drive System

C. Performance Results. The PM machine constants were unchanged from the dc link study. Values for the choke coil parameters were selected as $R_0 = 0.003\ \Omega$ and $L_0 = 150 \times 10^{-6}$ H. A numerical solution of the equations represented by (5) was implemented and a trial-and-error search made for average values of PM2 shaft torque (T_{sav}) to satisfy the requirements established in Figure 2.

Performance points across the speed range for forward and reverse flow of compensating power are tabulated in Table 2. It is observed that control across the region of reverse compensating power flow is nicely accomplished by shift of delay angle α greater than 90° and an additional forward shift of γ by 120°. No increase in PM2 phase current occurs as in the case of dc link when PM2 is regeneratively operated.

TABLE 2. PERFORMANCE OF CYCLOCONVERTER LINK WITH REVERSING DIFFERENTIAL

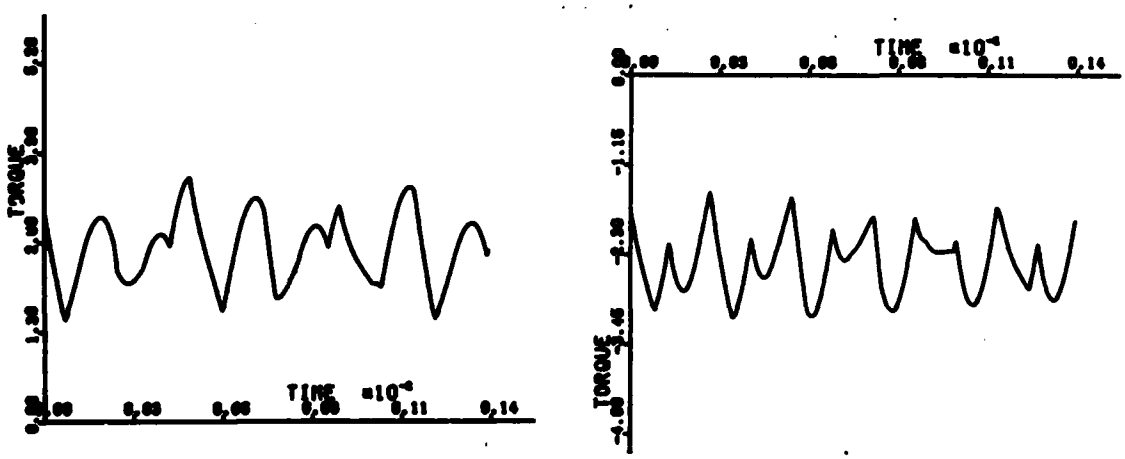
Speed (rpm)	T_{sav} (N-m)	α (degrees)	γ (degrees)	I_{ave} (A)	I_{rms} (A)
45,000	2.59	33.0	45	55.6	66.9
22,000	2.48	68.6	45	54.3	65.6
5,000	2.53	84.7	45	58.2	62.6
500	2.48	88.8	45	53.7	58.8
50	2.49	86.6	45		
0	2.49	89.1	45		
-5,000	-2.45	92.6	165	47.4	58.0
-22,000	-2.45	103.2	165	50.7	58.8
-45,000	-2.53	116.1	165	48.0	58.2
45,000	3.76	0	47	73.7	87.1

The last entry of Table 2 presents a set of control conditions and results for meeting a 150% load case (short time overload). Operation at such a point is automatically permitted by the control system unless prohibited by limits. Since current is monitored, the microprocessor can allow a timed interval of operation at any point above rated value before initiation of a limit action creating a quite flexible approach to overload management.

Figure 8 displays the steady-state instantaneous PM2 torque at a forward and a reverse compensating power flow point. There is inherently a pulsating torque component present in the brushless dc motor operation of a frequency that is six times the electrical angular frequency of PM2. At low speeds, this pulsation frequency can decrease to within a range at which the mechanical components respond. The control system will have a feature to assure that at low mechanical speeds, the gate drives are cyclically enabled and disabled at a frequency above that at which mechanical response is possible.

VI. DC LINK INVERTER WITH UNIDIRECTIONAL DIFFERENTIAL

A. System Description and Control. Power level component arrangement of a dc link drive system for use with a unidirectional differential is the same as shown in Figure 4 except that the bridge switch is not needed. The system equations are formulated as discussed in section IV and are given by (3). The block diagram of Figure 5 is applicable in describing a control system for this unidirectional differential drive.



(a) (b)

Figure 8 Calculated Torque For Cycloconverter Link with Reversing Differential
(a) Forward Compensating Power Flow (+22,000 RPM)
(b) Reverse Compensating Power Flow (-22,000 RPM)

B. Performance Result. The drive system must meet the performance criteria of Figure 3. Since the torques required are approximately 50% greater than for the reversing differential case, the PM machines will

necessarily be about 50% larger in size. The parameters for PM2 and the choke coil values are adjusted accordingly to give $R_a = 0.004\,\Omega$, $L_a = 15 \times 10^{-6}$ H, $R_0 = 0.003\Omega$, and $L_0 = 25 \times 10^{-6}$ H. A numerical solution for values of average torque to satisfy the requirements of Figure 3 and the results are presented in Table 3.

TABLE 3. PERFORMANCE OF DC LINK WITH UNIDIRECTIONAL DIFFERENTIAL

Speed (rpm)	T_{sav} (N-m)	α (degrees)	γ (degrees)	I_{ave} (A)	I_{rms} (A)
45,000	4.09	22.7	45	92.7	114.2
22,000	3.98	62.5	45	89.6	110.7
5,000	3.98	82.6	45	91.0	111.5
900	4.12	86.9	45	100.6	120.9

Inspection of Table 3 shows that average current values are approximately 60% greater than for the reversing differential case (See Table 1). Although this unidirectionally operated differential offers control simplification in that only one direction of compensating power flow is required and the necessity of dealing with torque pulsations at near zero speed is eliminated, the increased size requirements on the PM machines (to deliver approximately 50% more torque) and the increased current ratings on the SCRs or transistors (to conduct approximately 60% more current) are considered sufficient weight and cost penalties to abandon further study of this concept.

VII. RECOMMENDATIONS

Although this feasibility study uses specific examples, it is only possible to examine nonlinear systems of this complexity by numerical methods. The values of constants and parameters selected are believed to be sufficiently typical to identify problem areas and to allow formulation of general conclusions with reasonable confidence. The work leads to the conclusion that an ECCSD system is feasible and practical if PM machines are used in conjunction with a cycloconverter link and a reversing differential. Additional study is recommended in the areas enumerated below prior to and as an aid in forming specific guidelines for any prototype design.

A. Control system. Design and breadboard a microprocessor based control system to identify problems with timing and sampling rates.

B. PM Machines. Rough design PM machines of appropriate voltage rating and torque capability to verify that the needed parameters are practical and to establish approximate weights and sizes. Study the advantages and disadvantages of using identical machine sizes for both PM machines. Predict the approximate effects of magnetic saturation on performance.

C. Parameter Variation. Study the sensitivity of system performance to variation of design parameters.

D. Transient Performance. After a control system model has been formed and machine parameters and mechanical sizes determined, study the nature of response to step load changes and rapid turbine speed changes.

E. Operational Model. Fabricate a test bed model to further verify operational characteristics.

F. Transistor Switching Elements. Examine the increase in electrical machine utilization gained by transistor switching elements which allow operation at unity power factor without the danger of commutation failure that exists when SCRs are used.

G. Dual Function of PM1. Examine the feasibility of designing PM1 large enough to also serve as either a pilot exciter or primary exciter for the 400 Hz alternator.

REFERENCES

1. E. Ohno, T. Kishimoto, and M. Akamatsu, "The Thyristor Commutatorless Motor," IEEE Trans. Mag., vol. MAG-3, Sept. 1967, pp. 236 -240.

2. T. Tsachiya, "Basic Characteristics of Cycloconverter-Type Commutatorless Motors," IEEE Trans. IGA, Vol. IGA-7, No. 4, July-Aug. 1970, pp. 349 - 356.

3. N. Sato and V.V. Semenos, "Adjustable Speed Drive with a Brushless DC Motor," IEEE Trans IGA, Vol. IGA-7, No. 4, July - Aug. 1971, pp. 539 - 543.

4. E.P. Cornell and D.W. Novotny, "Commutation by Armature Induced Voltage in Self-Controlled Synchronous Machines," IEEE Trans. PAS, Vol. PAS-93, 1974, pp. 760 - 766.

5. N. Sato, "A Brushless DC Motor with Armature Induced Voltage Commutation," IEEE Trans. PAS, Vol. PAS-91, July - Aug. 1972, pp. 1485 - 1492.

6. J.M.D. Murphy, Thyristor Control of AC Motors, (Pergamon Press, Oxford, 1973), pp. 140 - 149.

7. F.J. Bourbeau, "Synchronous Motor Railcar Propulsion," IEEE Trans. IAS, Vol. IA-13 No. 1, Jan -Feb. 1977, pp. 8 - 17.

8. T. Maeno and M. Kobata, "AC Commutatorless and Brushless Motor," IEEE Trans. PAS, Vol. PAS-91, July - Aug. 1972, pp. 1476 - 1484.

9. Y. Shrinryo, I. Hosono, and K. Syoji, "Commutatorless DC Drive for Steel Rolling Mill", IEEE-IGA Conference Record, 1977 Annual Meeting, pp. 263 - 271.

10. A.C. Williamson, N.A.H. Issa, and A.R.A.M. Makky, "Variable-Speed Inverter-Fed Synchronous Motor Employing Natural Commutation," Proc. IEE, Vol. 125, No. 2, Feb. 1978, pp. 118 - 120.

11. N.A. Demerdash, T.W. Nehl, and E. Maslowski, "Dynamic Modeling of Brushless DC Motors in Electric Propulsion and Electromechanical Actuation by Digital Techniques," IEEE-IAS Conference Record, 1980 Annual Meeting, Sept. 28 - Oct. 3. 1980, pp. 570 - 579.

1982 USAF-SCEEE SUMMER FACULTY RESEARCH PROGRAM

Sponsored by the

AIR FORCE OFFICE OF SCIENTIFIC RESEARHC

Conducted by the

SOUTHEASTERN CENTER FOR ELECTRICAL ENGINEERING EDUCATION

FINAL REPORT

AN EXPERT SYSTEM FOR SYSTEMS RESEARCH IN COMMAND AND CONTROL

Prepared by:	Dr. Roger E. Cavallo
Academic Rank:	Associate Professor
Department and University:	Department of Computer and Information Sciences State University of New York College of Technology, Utica/Rome
Research Location:	Rome Air Development Center Command and Control Division
USAF Research:	David Craig
Date:	October 20, 1982
Contract No:	F49620-82-C-0035

by

Roger E. Cavallo

ABSTRACT

This report describes the basic issues related to complex systems associated with Command and Control. Rather than start with Command and Control as such, the underlying assumption is that problems associated with the area are prototypical of those which are being studied in a fundamental way in the field of systems theory.

The objective is to outline an operational framework which, when implemented on a computer, will serve as an expert system to aid users:

A. in characterizing and describing complex decision-making situations;

B. in the development, evaluation, and use of complex organizational and technical products associated with these situations.

The perspective taken in this report is that of systems modelling, defined in terms of an organized framework for recognizing and solving a comprehensive collection of interrelated systems problems which represent attempts to determine new knowledge about an object of interest. In this paper, "object" refers to the actual situation being investigated, on which systems (which carry most of the sense of the word "model" as it is often used) are defined.

Sections of the paper present the following: a general rationale for a comprehensive framework for systems investigation; the overall framework; the development of one component of the framework in some detail; a brief description of a number of possible studies using the framework.

ACKNOWLEDGEMENT

The author would like to thank the Air Force Systems Command, Air Force Office of Scientific Research, and the Southeastern Center for Electrical Engineering for creating and administering the program which made this summer research experience possible. He also thanks Al Barnum of the Command and Control Division of the Rome Air Development Center and a number of other very helpful people: John Huss, the Security Office, and the division secretaries.

Special thanks are also offered to Dave Craig and numerous others in the Command and Control Division for their openness in trying to develop approaches to some very complex problems.

I. INTRODUCTION

1. The Study of Wholes, of Method, and of Systems. Any attempt to function in interaction with complex, dynamic, not-well understood decision-making situations must be based on a solid understanding and well-founded capability for real-time modelling. With respect to Command and Control - the area of defense studies that is prototypical of such situations - there is a recognition that "building models for the immediate need at hand" and insisting upon "exclusively building system-unique models . . . will perpetuate our inability to develop a real understanding of command and control systems." (Van Trees, 1980). The current major need is for a "rich model environment" which utilizes generic models and which is based on a structure that relates these generic models and can evaluate their appropriateness for specific situations which arise.

Determination of whether or not a model is appropriate, however, depends on both the purposes of the investigation and the constraints (time, resources, quality of instruments, etc.) which are imposed on the investigator or modeller. Even with what seem to be simple objects which are relatively stable over the time frame of investigation (for example, the relation between the sun and the earth, studied to determine and predict relative positions) it may take years or centuries to settle on something which is widely accepted and useful. For situations which are more complex, which change and evolve during the time frame of study, and for which the time frame is highly constrained, classical methods of studying objects in isolation, are not adequate.

For many complex artificial objects (radios, weapons systems, communication networks, etc.) difficulties associated with the complexity can be skirted if enough essentially-the-same copies exist or can be made, to allow for adequate experimentation and development. However, there are many situations of interest which are not simple and are essentially one-shot in that experimentation with the overall situation is not possible. Such situations are often characterized by a complicated mixture of engineering and policy issues and issues associated with empirical investigation.

There are two distinguishing characteristics of modern science which have developed to deal with such objects and which have been made

operationally meaningful by technical advances in symbol-processing capability and in the ability to quickly access large quantities of information. These are:

(i) the "rediscovery of wholes" and the associated recognition of the need to augment the strong analytic and part-oriented capabilities that developed in the last two centuries;

(ii) a shift in emphasis toward a pragmatist philosophy, whereby the means and processes by which knowledge is obtained and used are considered to be as important to study and to understand as are any of the products which are produced by these means.

A result of the recognition of limits of the classical approach has been the development of areas of study such as systems theory, cybernetics, artificial intelligence, pattern recognition, and cognitive psychology which exhibit a well-established orientation "away from the traditional attempts . . . to represent knowledge as collections of separate, simple fragments" (Minsky, 1975) and which, in addition, assign a much more central role to procedural questions and to the importance of developing explicit representations of processes.

These developments are at the same time reflected in the philosophy of science, by the "rejection of the thesis of a scientific theory being a unit of methodological research" (Sadovsky, 1979) and by its gradual replacement in the past thirty years with the notion of system and of investigating the systems nature of objects of interest (see Cavallo, 1979a,b for a review of this development).

When dealing with complex one-of-a-kind objects under time constraint, the argument for emphasis on methodological issues is easy to make: it is necessary to be able to utilize insight, tools, and expertise that have developed in the study of other such objects. Because of this the notion of system has developed as a definable entity of study in its own right, essentially as a quasi-abstract construct which retains empirical significance but which at the same time provides a general representation of objects of investigation. This makes it possible to develop and study general concepts and principles - for example, memory, state, dynamics, organization, structure, complexity, performance, regulation and control - which are relevant to the systems nature of any object. This does not negate the need for disciplinary knowledge and real-world or object

expertise, but provides a mechanism for the synthesis of such knowledge and for the amplification of intuition which develops through contact with particular objects (see Cavallo and Pichler, 1979).

2. The Modelling Relation and the Integration of Methods. One aspect of the development and use of systems concepts as the basis for a comprehensive approach to modelling is the focus which it represents for integrating technical developments (e.g., in mathematics, computer science, and operations research). A common difficulty associated with specialization is that abstract areas such as mathematics generate many results whose utility for "real" problems is not always immediately apparent. A commonly recurring "discussion topic" for anything having to do with modelling (e.g., SIQAM, 1972) is the role that mathematics (formalisms and formal approaches, in general) has to play in building "real-world" (and hence, presumably, useful) models. Evidence of disillusionment with formal approaches is easy to find. There doesn't seem to be a strict logical necessity for the problem, but there also seems to be no way to avoid the empirical conclusion that such a problem exists; its essence was recognized at least in the last century by Goethe, commenting on the use of formalisms, that they themselves very often become the object of study and "an action which ought to be carried out for a certain aim becomes itself the aim, and no kind of purpose is fulfilled". On the other hand, almost everyone would accept the need to discover usable general principles and not to start from scratch on every new situation or class of situations.

The perspective which this evidence generates emphasizes the need to develop a coherent body of middle level concepts which can be used to investigate the logic of models as they are used and which will be useful for a wide range of practical research situations. The necessary link is provided by identifying general classes of system problems as requests for knowledge and by defining a problem-solving relation between these classes of problems and appropriately abstracted problem-solving tools which have been found useful in similar situations.

Systems Methodology as a level of abstraction that deals with problem characterization rather than specific content or purely formal results defines the use of abstract results and procedures for classes of problems that are meaningful over a spectrum of application areas. Conversely, it

also serves to motivate abstract results which have a high potential for widespread utility. This orientation can be depicted as in Figure 1, with the rectangle through the middle of the diagram representing the focus of systems research. A result of this emphasis is that modelling and design processes -- or the modelling relation -- are recognized as important areas that are worthy of study in their own right.

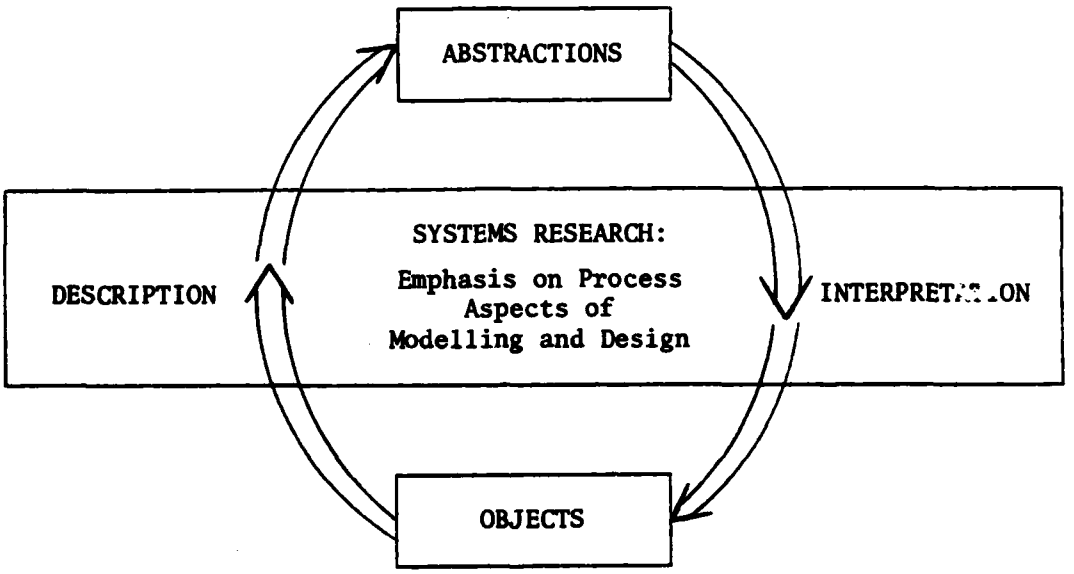


Figure 2. Systems Research / The Modelling Relation

For the study of the modelling relation as such to prove useful in associating abstract results with conctete objects of concern, the study of individual systems concepts and the development of isolated working methods cannot provide the only focus. The emphasis on modelling and design processes has to accept that "from the methodological point of view the essence of the problem is that every scientific concept exists in the language of science not in isolation, but only within a system of related concepts . . . and only within this system does it acquire its specific meaning and value" (Blauberg, Sadovsky, and Yudin, 1977). The need for methods has to be balanced by the need for their integration into a general and comprehensive characterization of the modelling process.

Command and Control and Command and Control Assessment have served as foci for many of the issues described here. Van Trees (1980), for example, directly states the need to develop a "framework to interrelate analytical findings, research results, empirical data, and judgement." His analysis highlights the need for the use of "generic models, in the plural" and numerous authors have concentrated on the need to develop assessment and analysis techniques for models based on function and utilization rather than on merely technical issues. Such needs, of course, require an understanding of the interplay of such system traits as structure, dynamics, and function, an understanding whose development requires investigation at a context-independent level.

Van Trees also emphasizes the need for a "thread of consistency" which can integrate various components of C^2 development and evaluation. Both he and others (e.g., Zraket, 1980) recognize the importance of system theoretic formulations but are unnecessarily restrictive by placing almost sole emphasis at the methodological level, on the concept of state and state-vector modelling. This is one of the oldest and most well-developed aspects of systems research, but a lot has been happening in the last decade or so. With respect to the larger notion of system investigation, state-vector modelling is only part of the picture, and it is reasonable to expect that a well-defined integrated framework which incorporates all systems concepts can itself more appropriately supply and serve as the "thread of consistency."

Systems Research, in the last ten years, has provided a tremendous increase in the understanding and development of systems concepts, and methodological issues associated with them. The level is such that a computer-implemented version of an integrated framework, which can serve as expert system giving users full access to latest advances in modelling and system evaluation techniques, is primarily a matter of implementation. Section III provides the outline for such a system.

II. OBJECTIVES

The central objective of this research project was to investigate broad areas of Command and Control from the perspective of modern systems research. Three lines of focus were identified:

1. Systems ideas are ubiquitous; it seems to be generally accepted that they are the proper source of a well-founded basis for the organized study of all Command and Control, yet their application to date has been spotty and ad hoc. One objective that we set was a presentation of systems ideas in a coherent manner and at high enough level to be suitable to serve as a basis for development of an expert system, which could be incrementally implemented, and which would operationally relate the full range of systems ideas to the full range of issues from Command and Control.

2. Systems research encompasses all aspects of interaction between investigators and objects, but probably the most characteristic is that which deals with representation of an overall situation of interest in terms of subsystems and relations among them. Because of its protypical and fundamental nature, it was decided to elaborate this aspect of the overall framework in greater detail. In doing so, a number of theoretical and computational questions associated with efficient implementation arose (see Section IV) and a number of these were investigated.

3. It is good to say, and make an abstract argument, that some general package will be useful for Command and Control; to illustrate this utility would be better. A third goal was to initiate preliminary development of a number of diverse application areas which would illustrate utilization of the expert system.

III. THE GENERAL SYSTEMS PROBLEM SOLVER (GSPS)

There are many recent developments which illustrate the benefits of the balance and methodological orientation described at the end of Section I; a number of these are presented in Cavallo (1982). They indicate that the integration of conceptual, mathematical, computational, and heuristic considerations can be accomplished to provide general system-modelling frameworks useful for a broad spectrum of applications. One such framework, which provides the background for the following sections, is the

General Systems Problem Solver (Cavallo and Klir, 1978; Cavallo, 1979). There are three major goals of GSPS:

(i) to provide a conceptual framework and investigative guide which incorporates as many as possible of the well-specifiable aspects of scientific investigation;

(ii) to provide an operationally-based language for the representation of systems knowledge;

(iii) to operate as an expert system which elicits from users appropriate descriptions of systems problems representing requests for information regarding an object of investigation; it then determines and utilizes appropriate system problem-solving tools (general tools, optimization algorithms, simulation packages, programming packages, decision-making aids, etc.) to provide this information.

At a general level of organization, GSPS depends on appropriate taxonomies -- of systems, objectives and constraints, system problems, and methodological tools -- and on relations among the various classes represented by these taxonomies.

The most fundamental classification used by GSPS is that of systems. The basis for the classification is a distillation and general integrated description of as many concepts as possible that have been found useful as elements of successful investigations in the past. There is a wide range of literature and work which supports this; that of Ross Ashby (e.g., Ashby, 1956, 1965, 1967) is especially noteworthy for its foundational approach to the methodological study of systems and cybernetic concepts. The work of Klir (e.g., Klir and Valach, 1965; Klir, 1969, 1970, 1976) provides the basis for the organization of these concepts into a well-defined hierarchy of levels of systems models suitable for symbolic description and manipulation by modern information processors. This has evolved to the emphasis placed here on characterizing the interrelatedness of different forms that are used to express knowledge about an object, and the interrelatedness of the processes which are used to determine or generate this knowledge.

The formal systems definitions used in GSPS thus serve as foci to which most investigative issues can be related and represent different levels at which one may "know" the objects of investigation. Conceptually, the basic systems levels are defined as follows:

A. Source Systems - primitive systems consisting only of attributes and their possible appearances (states).

B. Data Systems - source systems augmented by definition of a function from an appropriately defined parameter space to the set of possible overall observations.

C. Generative Systems - definitions at this level describe procedures which are parameter invariant, by which observed or desired data may be generated; such systems incorporate memory and dynamics by extending the definition of state.

D. Structure Systems - sets of subsystems together with some relation between them such that overall systems at level A, B, or C are described within acceptable tolerance determined by the demands of the situation.

E. Meta-Systems - descriptions of procedures which account for changes among systems at another level (for example, changes in structure).

As expert system, GSPS requires routines which interface with a user and effect the translation of knowledge regarding the object of investigation into an appropriate, formal system definition.

To provide further context, a description of the problem-solving orientation is given here. In order to encompass enough of the framework, the discussion is kept at an abstract level and implementation details are not described.

With respect to the utilization of various methodological tools, GSPS is organized around systems problems. These are defined as three-tuples which consist of the following basic entities: (i) initial system, (ii) terminal system or system type, (iii) objectives and constraints. These three entities formally and operationally represent the three elements which are generally agreed to be part of any problem situation:

(i) A state of knowledge which exists regarding the situation of concern. This state of knowledge is represented either (problem kind 1) solely in the definition of the initial system, or (problem kind 2) in both an initial system and a terminal system which are defined on the object of investigation.

(ii) A state of knowledge which is desired regarding the object

of investigation. For problems of the first kind, the request for this knowledge is represented by specifying the general type of the terminal system. The General System Problem Solver either: (a) provides a specific system definition of this type -- by determining and using appropriate problem solving tools on data derived from the object -- which represents the desired state of knowledge, or (b) responds with reasons that the problem cannot be solved. For problems of the second kind, specific definitions are provided of both an initial system and a terminal system. The desired state of knowledge is requested in an appropriate specification of objectives of the problem, which represent a request for determination of a relation between the initial and terminal systems -- see (iii) below and the following example.

(iii) Any objectives and/or constraints which are relevant to the information request. GSPS is intended to allow the full use of abstract tools while, at the same time, avoiding methodological faddism. System problem-solving in complex situations doesn't generally allow absolute solutions and does involve decisions and "extra-evidential" factors. By specifying objectives and constraints, the places where "assumptions . . . ambiguities and . . . arbitrariness" (Watanabe, 1969) may creep in are included as part of the problem. GSPS includes a catalogue of such objectives and constraints (referred to as requirements) as they motivate the use of particular tools.

For example, if a given object-problem translates to the system problem of design, a formal description of the overall desired behavior would be the initial system, structure system would be the type of terminal system, and requirements specification would elicit definition of available components, as well as design criteria such as whether to minimize cost or number of elements, etc. For problems of the second kind, where both initial and terminal system are given, the requirements specify a desired property to be determined of the relationship between the two systems. For example, determine the amount of information lost by using one (simpler) description of a system rather than another.

At its most ambitious level, GSPS is an attempt to construct an expert system which makes available to an investigator all of the problem-solving and methodological capability that has developed through various areas of investigation.

Example. The following is a simple illustration of a problem of the second kind; it also illustrates how contextually meaningful requests for information would be posed in terms of systems problems.

Imagine a decision-maker (DM) facing a situation with two binary input attributes, say v_1: flight pattern (0 = straight; 1 = zigzag) and v_2: terrain conditions (0 = smooth; 1 = rough). There are thus four input states — 00, 01, 10, 11 — and the decision-maker must continually decide from among four policies, each of which is most appropriate for a given situation. Using somewhat loose terminology, we can refer to the system defined by these attributes as S. Assume that the states of the input variables are recorded as they occur and that DM's decisions must be made without knowledge of the current values of v_1 and v_2 (assume also that previous decisions don't affect the current state). We can imagine the case that the time constraint is such that DM only has time to check the last record of one of the input attributes. The problem is to decide which one.

One solution to the problem is to answer the following question: based on the complete record of past patterns of occurrence of the two attributes, which of the two gives most information about what will happen next? Disregarding philosophical problems associated with inductive inference, the following approach using the standard entropy functional gives a reasonable solution.

Let $H(X) = -\Sigma\, p(x_i) \log_2 p(x_i)$ represent the amount of uncertainty regarding the value of a variable X. In our case assume that the data is stored sequentially and that the overall probability distribution is: $p(v_1v_2 = 00) = 1/8$; $p(v_1v_2 = 01) = 1/2$; $p(v_1v_2 = 10) = 1/8$; $p(v_1v_2 = 11) = 1/4$; then $H(v_1v_2) = 1.75$ bits.

Similarly, let $H(x/y) = -\sum_i \sum_j p(y_j)\, p(x_i/y_j) \log_2 p(x_i/y_j)$. One interpretation of H(x/y) is the amount of uncertainty about X, given knowledge of the value of y. If we let v_i represent, at any observation point, the value of v_i that occurred in the last record, then DM's problem can be interpreted as extending the system defined on the situation to include a new attribute and the problem boils down to whether to choose v_1' (system S_1) or v_2' (syatem S_2). Given easily implemented processing routines to sample the data, S_1 and S_2 can be defined in terms of probability distributions over the composite variables $v_1'v_1v_2$ for

S_1 and $v_1'v_1v_2$ for S_2. As a systems problem of the second kind, the requirements specification would ask for a comparison between $H(v_1v_2 \mid v_1')$ and $H(v_1v_2 \mid v_2')$. If we assume (to generate actual numbers) that the following portion of the record

t_0	t_1	t_2	t_3	t_4	t_5	t_6	t_7	t_8
0	0	0	1	1	0	1	0	0
1	1	1	0	1	0	1	1	1

represents the overall pattern, then $H(v_1v_2 \mid v_1') = 1.4512$ bits, and $H(v_1v_2 \mid v_2') = .9387$ bits.

The information measures can be normalized and presented in a suitable manner to indicate that the system utilizing past information regarding terrain removes almost three times as much uncertainty as that which keys on flight pattern.

Such simple examples are difficult because they seem not to warrant the complicated jargon and formalisms, but when the situation is extended to 5 or 6 attributes each taking 5 or 6 values, with options for including numerous past values, then some formal data compression and evaluation techniques must be used. Obviously, the principles in the more complicated case are identical to the simple one.

At its most ambitious level GSPS is an attempt to construct an expert system which makes available to an investigator all of the problem-solving and methodological capability that has developed through various areas of investigation. The programmatic aspects of GSPS imply that it can not be complete, but the top level design as described here allows modular and incremental implementation of all of its major components.

- Dialogue routines, which provide the interface with users. These are necessary primarily for elicitation of appropriate problem definitions including adequate explanations of different choices when they exist (e.g., descriptions of options in requirements specification which might represent various heuristics relevant to a given computationally complex problem). The structure of this component includes the ability to incorporate new independent developments (for example, Conversational Heuristics -- see Shaw, 1979), which facilitate man-machine interaction.

- Graphics routines, which can: aid in the elicitation of system and problem definitions; present the solutions to various problems in a manner

most suitable for interpretation; summarize, say, various simulation studies which explore the significance of different criteria under different conditions; and portray the effects of various decisions which the user may make.

· Library reference data base. Part of the solutions to many problems may involve reference to appropriate literature (some of which may be on line) which is relevant to those problems; this can include reference to similar examples either from the user's context domain or similar domains.

· Methodological Tools, to be used in the problem-solving process. While the other components are important for the overall package, the essence of the problem-solver is the ability to solve system problems. While many tools which can be incorporated already exist, many of the necessary tools are still in the process of development. This is the case because of the need for general problem solving tools and because the relatively short period of time that the study of systems as such has received major attention. A number of major issues such as complexity, fuzziness and imprecision, concurrency, the general theory of Petri-nets, the theory of loosely coupled systems, system evaluation, performance evaluation, autopoeisis, etc., all of which are associated with the study of systems, are new enough to regularly provide new and useful concepts and tools which should be incorporated.

With respect to the development of methodological tools, one of the major aspects of GSPS is that it provides a framework for this development as well as a means for comparison and evaluation of these tools. The conceptual and formal means for describing the systems nature of objects naturally identifies classes of problems and highlights existing deficiencies in concepts and tools to deal with them.

An important class of problems in GSPS is that associated with the relationship between parts and wholes, with the relationship between an overall (possibly dynamical) system and various conjunctions of parts (subsystems) which may be offered as models of such overall systems.

This class of problems is generic enough in nature and has such an extensive and diverse history of investigation to warrant consideration in its own right as a (the) fundamental system problem (Cavallo and Klir, 1981a). The next section describes some results in this area which form the basis for development of a package of tools for dealing with this problem.

IV. SYSTEMS, SUBSYSTEMS, AND STRUCTURE

1. General Structures. This section addresses the problem of determining and evaluating the adequacy of models of an overall situation in terms of a conjunction of partial models, each of which represents some portion of the overall situation. Over the past few years a general methodological area of investigation -- termed Reconstructability Analysis -- has developed to deal with this problem class (Cavallo and Klir, 1979, 1981a,b; Cavallo, 1980). Most generally it is defined as the process of investigating the possibilities of reconstructing or identifying desirable properties of overall systems from the knowledge of corresponding properties of their various subsystems. Collections of such subsystems have various interpretations such as structure systems, hypotheses, models, or designs.

Since the notion of system constitutes the basic methodological unit, it is necessary to have a definition which is general enough to serve to define both parts and wholes, emphasizing that from the methodological perspective overall-system/subsystem is a distinction which can be made only in terms of the relation between systems. In reference to the discussion of GSPS in the previous section, it is presumed for the considerations here that a number of other systems problems have already been solved which enrich the semantics of the primarily syntactical questions dealt with here. For example: choice of an appropriate set of attributes, decisions as to observation channels (well-defined, probabilistic, fuzzy) and resolution level, gathering of data (mapping from parameter space to state space), choice of state variables (time shifted values of attributes), etc. To allow concentration on the special issues associated with the system/subsystem relation, further reference to the more general context of GSPS will not be made.

Definition 1. A system is a six-tuple $(V, \mathcal{V}, s, A, Q, f)$, where

- $V = (v_1,\ldots,v_n)$ is an ordered finite set of variables representing attributes defined on the object of interest;
- $\mathcal{V} = \{V_1,V_2,\ldots,V_m\}$ is a set of finite sets, where each set represents a state set for one or more of the variables;
- $s: V \to \mathcal{V}$ is the mapping associating the appropriate state set with each variable;

- $A = s(v_1) \times s(v_2) \times \ldots \times s(v_n)$ is the set of all possible "overall states" of the system;
- Q is a set representing a measure; with the function f (below), Q determines whether the system is probabilistic, possibilistic (fuzzy), well-defined, etc.;
- f is a mapping from A to Q (which represents empirical observation and analytic determination of a parameter-invariant relation among the attributes).

Two points that are worth highlighting regarding this definition are:

(i) The set V may contain more than one variable representing the same attribute; that is, one variable may represent the same attribute as another at a different point in the parameter space (e.g., at a different time point). The structural considerations to follow may thus incorporate questions relating to dynamics.

(ii) The same general definitional form is used regardless of the type of systems, e.g., probabilistic or fuzzy, etc. This representational economy is important from both the implementation (data-base) point of view and from the methodological viewpoint, since it allows a clear focus on fundamental issues.

Definition 2. Given two systems, B and °B, then °B is considered to be a subsystem of B if the following conditions hold:

- Each variable in °V is also in V.
- Each state set in °V is also in V.
- °s is a restriction of s to °V.
- °f is the projection of f onto the variables in °V.

Definition 3. A structure system is a set of systems, say the set $k_B = \{(k_V, k_V, k_s, k_A, k_Q, k_f)\}$.

There are two fundamental investigative issues associated with an overall system/structure system relation. These are:

(i) Reconstructability Problem: given an overall system, determine which of the meaningful structure systems constitutes the "best" model of the overall system according to stated requirements.

(ii) Identification Problem: given a structure system, determine how much can be said regarding the overall system.

This section focusses on an issue associated only with the reconstructability problem, that of the generation of the meaningful structure systems or models which are to be evaluated. A structure system which is to serve as a meaningful hypothesis for an overall system must consist of subsystems of the overall system as given in Definition 2. If an overall system B is known, the only information relevant to characterizing a subsystem, °B, is the particular subset of V represented by °V. All other information of °B can be generated from this information. Thus, for most of what follows we represent structure systems merely by the family of subsets of V. The idea is to define the set of meaningful structure systems in a manner that makes it easy to generate (and search) this space of models and evaluate models when appropriate. The following considerations describe all classes of structure systems (or structures, since reference is only made to the pattern of interactions exhibited by the subsystems).

Definition 4. $S = \{S_i \mid S_i \subseteq P(V) - \emptyset\}$, where $P(V)$ represents the power set of V.

Models belonging to set S are very general and have mainly formal significance. The following restrictions can be placed on models to define meaningful subclasses of them. Some structures or models in S may not represent the original conception of the object of investigation in that not all variables in V are represented. Including this consideration gives the covering condition: that each variable in V appears in some subsystem. Also, in a model S_i containing two subsystems E_a and E_b such that $E_b \subset E_a$, all of the information contained in E_b can be obtained from the subsystem E_a. Thus, another meaningful restriction for models is that they satisfy the irredundancy condition: that no subsystem be properly contained in any other subsystem.

These restrictions lead to the definition of the following classes of structures:

Definition 5. $S_I = \{I_i \mid I_i \subset P(V) - \emptyset,\ E_a \not\subset E_b \text{ for each pair } E_a, E_b \in I_i\}$

Definition 6. $S_H = \{H_i \mid H_i \subset P(V) - \emptyset,\ \bigcup_{E_a \in H_i} E_a = V\}$

(Structures belonging to S_H are equivalent to mathematical objects studied as hypergraphs (Berge, 1973).)

There are situations for which it makes sense to consider models at the level of generality of S_I or S_H. This generality is not necessary, however, and structures at this level do not play a major role in the rest of this paper. Each structure which is considered here comes from a class of structures, referred to as general structures, whose elements satisfy both the covering and the irredundancy conditions.

Definition 7. $S_G = \{G_i \mid G_i \in S_I \text{ and } G_i \in S_H\}$

To describe a particular model, it is convenient to just list the variables in any subsystem, separating the subsystems by slashes, and also to have a visual representation of that structure. This is done by using boxes to represent the subsystems, with lines attached to them to represent variables. For example, the structure {{1,2},{2,3,4},{2,4,5}} can be written 12/234/245, and pictured as shown in Figure 2.

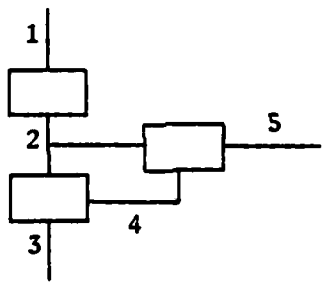


Figure 2. Representation of Structures

2. Structural and Contextual Complexity. Given an overall situation represented by a set of variables V, the set S constitutes the set of all models of that situation; as such, it is relevant to the situation from a number of perspectives. For example, some of the general questions which may motivate investigation of this set are:

- model the overall situation
- determine the (strength of) relationships which exist among variables of the overall system
- determine the subsystems, flow of control, communication patterns in the overall system
- determine the structural components of the overall system

- determine the simplest representation of the overall system which retains all the information, within a specified tolerance, that exists in the overall system
- determine which components of a complex system contribute most to the overall coordination which the system exhibits

When investigating the space of models, criteria must be chosen for evaluating the structure system associated with each structure. In general, more than one such criterion will be relevant to any given situation. These criteria will generally be of two types, those which relate to structure (the family of sets ^{k}V) and those which relate to context (the family of functions ^{k}f). There are obvious advantages to having as structurally simple a model to work with as possible -- for example, for policy- and decision-making purposes, system development and modification, information storage, retrieval and transmission, etc. Two difficulties associated with simple models, however, are: (i) conflict with contextual criteria -- simple models generally do not represent the overall situation as well as complicated ones do, (ii) adequate measures of structural complexity -- while it is clear that a model wherein every aspect of an overall system is considered to be independent of any other is simpler than the one which states that everything is interdependent with everything else, it is not obvious how to compare given models which lie between these two extremes.

In the framework of reconstructability analysis, the distinction between structural and contextual criteria is made in terms of the development of two sets of procedures, one for dealing with the generation of structures and one for the evaluation of a structure once determined. For this paper, issues associated with contextual criteria serve as background, and the focus is placed on structural issues. A general foundation for consideration of the issues associated with evaluation of models may be found in Cavallo and Klir (1981), and the problem is being dealt with in a number of projects.

Regardless of the motivating question, attempts to deal with general structures run into problems which stem from the inordinately large number of possible models or relationships which must be examined. Given the large size of this set of models, an exhaustive search is not computationally feasible. One solution to this problem has been to

impose some mathematical structure (usually through assumptions of linearity) on the form of the relationships among the variables. This makes a modelling exercise significantly easier, but in many situations the increased tractability does not justify the unrealistic nature of the assumptions.

Because of this, the development of systematic means or algorithms for generating and evaluating the set of models has been a long-standing problem, arrived at from a number of different lines of investigation. The noted statistician Kendall, for example, discusses the issue as one of the "Outstanding Problems of Multivariate Analysis." None of the approaches which have been proposed to deal with the complexity have been completely satisfactory; in general, past solutions are either limited with respect to the scope of the problem which they address or are unsatisfactory because of their ad hoc nature and lack of appropriate foundation.

In the first category we may consider a contribution of Ashby, who has provided many basic insights to the study of complex systems. Ashby (1965) elaborated the importance and main issues involved in answering the following question: Given an overall system, what is the most complex subsystem which must be involved in any description which allows reconstruction of all of the information present in the overall system. While this question is clearly important when interacting with a complex system, it also represents only a small portion of the structural information relevant to the system. In terms of the set S_G, this approach can be described as evaluating only those models which included all (and only) those subsystems with a given number of variables. Thus, for example, with five variables only five of the more than seven thousand G-structures would be considered.

Fienberg (1980) describes an extension of this approach, attributed to Goodman, which is also useful but which is also somewhat ad hoc and less than comprehensive. Let k be the number of variables (the dimension of) the subsystems of the acceptable model which has the lowest dimensional subsystems (for models of this type, models which involve k+1-dimensional subsystems will also be acceptable). This scheme is based either on adding k-dimensional subsystems to the structure which consists of all k-1 dimensional subsystems (eliminating these as necessary

to satisfy the irredundancy condition) or by eliminating them from the model with subsystems of dimension k. The fundamental nature of this aspect of modelling warrants a more thorough investigation of the set of models.

3. The Generation of G-Structures. The overall scheme described in Cavallo and Klir (1979) essentially provides a basis for the solution of this problem. Some of the theoretical components, as well as implementation questions and development and characterization of good heuristics, have not been developed as strongly as necessary and there are still a number of open questions. This section deals with these issues.

When dealing with structures, it is useful to consider that, given a set of variables V, each family of subsets of V representing a model defines a reflexive and symmetric binary relation on V. If R is the set of all reflexive and symmetric binary relations on V, there exists a mapping $r_G : S_G \rightarrow R$ where $r_G(G_i)$ is the binary relation in which variables v_j and v_k are related if and only if they each belong to at least one of the subsets of V through which G_i is defined. Also, to each element of R there corresponds a unique (undirected) graph drawn on the set of vertices V. The graph and the reflexive symmetric binary relation can be considered to be synonomous and in this paper the two will be used interchangeably (in depicting the graphs, the loops on each node, which are a consequence of reflexivity, will not be drawn).

Notice that the mapping r_G is not one-to-one; i.e., each graph corresponds to more than one structure or model, pointing out the by-now often recognized (but also still often not recognized) inadequacy of graphs (binary relations) as a basic modelling tool. Thus the mapping r_G imposes an equivalence relation on S_G where G_i is related to G_j iff $r_G(G_i) = r_G(G_j)$. Let the symbol S_G/r_G denote the set of equivalence classes imposed on S_G by r_G. The fact that r_G induces a partition on S_G can be exploited to introduce efficiencies in the model-generation process. It is first necessary to describe a natural structural property which relates the models in S_G.

Definition 8. For all pairs of structures G_i, G_j in S_G, G_i is said to be a refinement of G_j (denoted $G_i \leq_G G_j$) if and only if for each set $E_a \in G_i$ there exists a set $E_b \in G_j$ such that $E_a \subseteq E_b$.

The structure $(S_G, \leq_G)$ is a partial ordering and, in fact, is also a lattice with meet and join equal to GCR_G (greatest common refinement) and LCR_G (least common aggregate) defined as follows (Cavallo and Klir, 1979):

Given G_i and G_j, let $K_{ij} = \{E_p \cap E_q \mid E_p \in G_i, E_q \in G_i\}$ and let $L_{ij} = G_i \cup G_j$.

Then

$$GCR_G\ (G_i, G_j) = K_{ij} - \{E_a \mid E_a \in K_{ij}, \exists E_b \in K_{ij} \text{ such that } E_a \subset E_b\}$$
$$LCR_G\ (G_i, G_j) = L_{ij} - \{E_a \mid E_a \in L_{ij}, \exists E_b \in L_{ij} \text{ such that } E_a \subset E_b\}$$

The lattice structure which has just been defined represents an ordering which is natural from two points of view:

(i) It captures, in some sense, the notion of one model being simpler than another; i.e., it is simpler if all interconnections represented in it are also represented in the other.

(ii) It provides a natural scheme for generating the full set of models by "refining" each subsystem of a given model.

A significant reduction in generation complexity can be gained by taking advantage of the partition defined earlier.

For each equivalence class in the quotient set S_G/r_G there exists a simple graph and a unique representative of the class which consists of the set of all maximal cliques of the graph. This motivates the following definition of a subset of S_G.

INTERLUDE. Unfortunately, without writing a book (the reading of which would imply the ability to read the notation anyway), there seems to be no way to avoid a seeming barrage of symbolism. The formalisms clearly have a place, however, as it is unlikely that the results could possibly have arisen without them. It also serves to illustrate and strengthen the argument for the need of the middle-level concepts and GSPS as described in Section 4, whereby seemingly abstract results can be used, in terms of the systems concepts they represent, in any situation which is modelled through the concepts.

Definition 9. $S_c = \{C_i \mid C_i \in S_G$ and C_i consists of all and only the maximal cliques in some graph $R_i \in R\}$

Elements of S_c will be referred to as C-structures. There exists then a one-to-one onto mapping r_c: $S_c \rightarrow R$ from the set of all C-structures to the set R. Similarly as with S_G we can define the ordering $\leq_c$ on S_c and accept as meet (GCR_c) and join the operations of the subset lattice (and Boolean Algebra) of the set $\{\{v_i,v_j\} \mid v_i,v_j \in V, \ v_i \neq v_j\}$.

We now have a partition on the set S_G where each equivalence class has a canonical representative from the set S_c. We observe that S_c is not a sublattice of S_G (although $GCR_c(C_i,C_j) = GCR_G(C_i,C_j)$); however, we have the following:

Theorem 1. The mapping ϕ: $S_G \rightarrow S_c$, where $\phi(G_i) = (r_c^{-1} \circ r_g)(G_i)$ is a homomorphism (endomorphism) of the lattice of G-structures to the lattice of C-structures.

Theorem 2. The lattice (S_G, GCR_G, LCA_G) is modular.

This fact is useful since it bolsters the rationale for our approach to model generation and motivates a line of exploration regarding the evaluation of structures (utilizing some sort of "distance" from the least element in the lattice, $v_1/v_2/.../v_n$). It also makes it easy to show:

Theorem 3. The set of G-structures constituting any equivalence class in S_G/r_G is a sublattice of S_G (with greatest element the unique C-structure, say C_i, in the class, and least element the unique structure consisting of $\{\{v_i,v_j\} \mid (v_iv_j) \in r_c(C_i)\} \cup \{v_i \mid \nexists v_j (j \neq i)(v_iv_j) \in r_c(c_i)\})$.

Because of the isomorphism with the Boolean lattice of reflexive symmetric binary relations, the generation and examination of the lattice S_c is relatively straightforward and simple to implement. Theorems 1 and 3 allow consideration of the full lattice S_G in two stages:

1. Search the space S_c for the most suitable model.
2. Search the equivalence class (sublattice) of G-structures associated with the selected C-structure.

4. Some Questions Associated with Evaluation. This two-stage approach assumes that with respect to structural complexity, the goal is to get a model which is as "close" to the least element of S_G as possible. In such a case there is a straightforward relation with a number of suitable contextual measures (for example, amount of overall information lost by using the refinement representation) in that if $G_i \leq G_j$ then G_i cannot be a better model with respect to the contextual measure than G_j. This can be formulated as:

> Theorem 4. Let $m(G_k)$ be the amount of information regarding the overall system of interest that is contained in the structure system whose structure is represented by G_k (Kullback, 1959). If $G_i \leq G_k$, then $m(G_i) \leq m(G_k)$.

It should not be taken as automatically given, however, that the investigator will always choose, with respect to structural complexity, the most refined structure. For example, even with respect to structural complexity, the investigator may choose to reject a model which is a refinement of another if the refinement involves more interconnections among subsystems. This issue is a study in its own right and investigation has begun of a number of alternate measures of structural complexity. Under any conditions, even when all formal options are well understood, the meaning of the formalisms has to be developed by their proper integration into GSPS. It is safe to say that there will have to remain a number of questions which can only be resolved in context of characterization of specific investigations.

As a last word, we present the following common-sense observation and argument which supports the use of the lattice of G-structures and the associated lattice of C-structures (recall that a refinement of a C-structure involves removal of an edge of the graph).

> Observation: If a graph has enough lines, then every structure associated with it (i.e., all the G-structures) must be structurally-complex in one of the following ways: (a) it includes a high dimensional subsystem, (b) it involves a complex set of interconnections among the subsystems.

Argument: Consider the two canonical representatives of the G-structures in a given class, its associated C-structure and its associated most refined structure, call it L.

(a) When dealing with the C-structure, only maximal cliques (also known as maximal complete subgraphs) are allowed as subsystems. Let M(n,k) be the maximum number of edges that a graph with n vertices can have without containing a complete subgraph of order k. A basic result of Turan (1954) shows that M(n,k) is given by the following formula:

$$\frac{(k-2)(n^2-r^2)}{2(k-1)} + \binom{r}{2}$$

where r is equal to n mod (k-1). Since each maximal complete subgraph represents a subsystem of a C-structure, the result gives quantitative significance to the observation that at high levels of the lattice, associated C-structures must contain subsystems of "high" dimensions. His proof also shows how to construct D(n,k), a graph with n vertices, M(n,k) edges, and no complete subgraph of order k, and proves that, up to isomorphisms, it is the only such graph. Thus, all C-structures of systems with n variables whose associated graphs have M(n,k) edges (unless they are isomorphic to D(n,k)) contain a k-dimensional subsystem, as do all those with more than M(n,k) edges.

(b) When dealing with L, each edge of the graph represents a two-dimensional subsystem. Obviously, the more edges there are in the graph (the higher the level of the lattice), the more subsystems there are in L. But since the graph must contain a maximal complege subgraph of "high" order (k), then each low- (2-) dimensional subsystem must involve an intricate pattern of connection with at least the other $\frac{k(k-1)}{2} - 1$ subsystems represented in the clique.

V. INITIAL STUDIES

An important aspect of the framework described here is its intended usability in broad classes of actual situations. The time frame of the research period (as well as the length guidelines for this report) did not allow extensive development of any of these areas. However, the following four have been identified as promising to develop as test cases:

1. Determination for a Tactical Acquisition and Weapons Delivery Service (TAWDS) of the effects of different parameters on decision-making. The airborne unit of TAWDS, which is currently in flight test, will be simulated by the existing Dynamic Ground Target Simulator supplying movement scenarios and the existing Dynamic Data Generator (DDG) which can be used with different options for various parameters (e.g., beam width, flight path, error in ground truth). A number of interesting systems problems arise in this context. For example: determine a dynamical system definition which gives the least uncertainty in state-predictability, subject to the complexity-of-description tolerance of individual ground-station decisionmakers; with respect to some baseline initial system definition, calculate the distance from a terminal system which arises subject to constraints representing various combinations of the parameters; determine which decision-input form (e.g., well-defined, probabili tic, or linguistic variables), under which conditions allows the most regulation (or control) by the decisionmaker.

Given that the complexity of, say, "battle truth" is beyond that which can be completely dealt with by a decisionmaker, it is important to be able to determine, for given situations, a decisionmaker's model of the situation; that is, to determine what simplifications are being used (represented as a structure system). The argument is that decisions and actions are based on models and that these decisions, in turn, affect the "truth." The simulation set-up described here can provide an ideal setting to study this process.

2. Importance of strengths of various patterns in Indications and Warnings Scenarios. Define a primitive system on a given country's political situation in terms of attributes such as Inflation Rate, Legitimacy of Government (measured, say, by perception of corruption),

Rising Expectations Syndrome, Political Kidnappings, Changes in Size of Soviet and East European Embassies. Example system problems: determine quantization which gives least information loss; determine structure of the system as it relates to immediacy of a crisis as perceived by decisionmakers.

3. Determination of best parameter settings for algorithm-switching in an Automatic Tracking System; for given settings, determine which input attributes (flight: straight or zigzag; range; past error, etc.) are most related to current error (compare various structure systems).

4. One of the difficulties with product-oriented studies -- or, the system unique models of Van Trees, referred to in the introduction -- is that they do not lend themselves to increasing the conceptual base on which Command and Control is founded. The problem expresses itself in so-called "test-beds" which should serve a major function for experimentation but are in fact most often used for demonstration of products which already exist.

This last example is a proposal for an experiment motivated by a comment of Wohl regarding "how far we are from understanding the interaction between [v_1:] C^2 information characteristics, [v_2:] C^2 system design features, [v_3:] individual differences among decisionmakers (e.g., in experience, in cognitive or decision styles, etc.) and [v_8:] measures of military or mission effectiveness" (Wohl, 1981). The observation serves as an ideal focus for an experiment to develop the problem-solving framework and to make use of a number of products which already exist.

The main idea would be to consider each of the v_i as high-level concepts to be further elaborated and described as an overall system. Various concepts from literature and discussion with experts in given areas can be used to characterize and expand each of the four attributes. For example, the system design features attribute can be expanded by considering whether it is hierarchical or not, its level of redundancy, types of components, etc. -- each representing a variable with a number of possible appearances. Even for an

attribute such as measure of military effectiveness, which would be difficult to expand because of lack of knowledge or agreement, the attempt to characterize it for a particular experiment will help to focus theoretical issues and a number of alternatives can be used and their properties empirically investigated.

There are a number of ways that differences among decisionmakers can be characterized (e.g., using the concept of psychological types as developed by Jung). By preparing careful description, existing simulation products can be used to generate data and decisionmaking responses can be measured. The solution of systems problems, such as the determination of structure, will provide information regarding interaction among the characteristics, as well as motivate adapted descriptions and further understanding of each of the attributes and concepts involved.

It is also interesting to note that the theoretical focus of Wohl's paper -- utilizing uncertainty reduction (as the basis for mission-oriented measures of effectiveness) -- is one of the main analytical techniques involved in GSPS and has been implemented as an option for a number of the problem-solving tools. The direct interpretation of the tools and measures in terms of discussions such as Wohl's would be straightforward and interesting.

VI. RECOMMENDATIONS

A main reason for my accepting this research appointment was the perception that the field of Command and Control, coupled with official recognition that the field is so multi-faceted and that all of these facets are intimately related to each other, represents an ideal contextual area for implementation of the general program which has had more abstract development as systems methodology. The associated issues parallel those which face designers of large, complex software systems where there is clear recognition of the need for top-down design (or, better, recognition of the need to concurrently utilize both top-down and bottom-up techniques).

From the narrow point of view, in terms of classical areas of specialization and development, the ideas in this report may seem comprehensive to the point of precluding specific products and/or results. This is not the case, however. The modular aspects of the organization allow development of many pieces without sacrificing the overall integrability. A number of elements described in the report are either fully operable or in some stage of development and form a natural context from which to recommend further development.

For example, model generation algorithms based on the discussion of Section 4 (which in themselves represent the solution to a long-standing problem) have been implemented in Pascal, Fortran and C, and have run on the Apple microcomputer, PDP 11/45, VAX 11/780, as well as Honeywell, IBM, and Burroughs mainframes. In addition, the local design of these algorithms has stressed extensibility and they are constructed to allow the integration of appropriate heuristics as these are developed. In fact, one of my recommendations is that support be given to the development of such heuristics.

The algorithms have also been implemented to allow their utilization with any evaluation criteria and associated procedures which exist or are developed. A number of these are being used (for well-defined, probabilistic, and possibilistic systems), but there has, as yet, been no comprehensive and comparative study of various criteria. Such a study represents another recommendation of this report.

A third recommended area of development is for appropriate dialogue routines for elicitation of appropriate formal system problem descriptions to represent contextual situations. Preliminary versions of such routines exist, but a more intensive development effort is required.

Ultimately, the success of the overall program described here depends on the development of the semantics and pragmatics of the problem-solver by carrying through on a number of specific examples from the field of Command and Control. (It is also obvious that positive effects will indirectly accrue to further development of any of the component aspects. Each of the examples described in Section V represents a specific, easily developed area, with an almost guaranteed contribution. In addition, it would be fruitful to take a number of already existing studies (e.g., Wohl, et al., 1981; Callero et al., 1981) and translate them into the framework described here -- again with an almost guaranteed payoff in terms of additional contributions. The only problem might be institutional inertia which makes it difficult to generate cooperation at levels above the subsystem in which one is embedded. Stated more positively, in the short run if the goal is solely a better understanding of one component and there are limited units of resource available, it is likely that more benefits will accrue to devoting all the resources to direct "system-unique" study of that component. However, it is well known that most "greedy" algorithms which attempt to achieve local optima do not generate the global optimum. Fortunately, at RADC I developed contact with a number of groups who seemed enthusiastic about pursuing the line described here. This constitutes my last recommendation.

REFERENCES

Ashby, W. R., 1956, An Introduction to Cybernetics, London, Chapman and Hall Ltd.

Ashby, W. R., 1965, "Measuring the Internal Informational Exchange in a System," Cybernetica, Vol. VIII, No. 1.

Ashby, W. R., 1965, "Constraint Analysis of Many-Dimensional Relations," in N. Weiner and J. Schade (eds.), Progress in Biocybernetics, Vol. 2, Amsterdam, Elsevier.

Ashby, W. R., 1967, "The Set Theory of Mechanism and Homeostasis," in D. Stewart (ed.), Automaton Theory and Learning Systems, Washington, D.C., Thomson.

Berge, C., 1973, Graphs and Hypergraphs, Amsterdam and New York, North Holland/Americal Elsevier.

Blauberg, I. V., V. N. Sadovsky, and E. G. Yudin, 1977, Systems Theory: Philosophical and Methodological Problems, Moscow, Progress Publishers.

Callero, M., W. Naslund, C. T. Veit, 1981, Subjective Measurement of Tactical Air Command and Control, Vols. 1, 2, 3, Santa Monica, Rand.

Cavallo, R. E., 1979a, The Role of Systems Methodology in Social Science Research, Boston, Martinus Nijhoff.

Cavallo, R. E., 1979b, (ed.), Systems Research Movement: Characteristics, Accomplishments, and Current Developments, Special Issue of General Systems Bulletin, Vol. 9, No. 3.

Cavallo, R. E., 1980, "Reconstructability and Identifiability in the Evaluation of Structure Hypotheses: An Issue in the Logic of Modelling," in B. Banathy (ed.), Systems Science and Sciences, Society for General Systems Research, pp. 647-654.

Cavallo, R. E., 1982, (ed.), Systems Methodology in Social Science Research: Recent Developments, Boston and The Hague, Kluwer-Nijhoff.

Cavallo, R. E. and G. J. Klir, 1981a, "Reconstructability and Analysis: Evaluation of Reconstruction Hypotheses," International Journal of General Systems, Vol. 7, No. 1.

Cavallo, R. E. and G. J. Klir, 1981b, "Reconstructability Analysis: Overview and Bibliography," International Journal of General Systems, Vol. 7, pp. 1-6.

Cavallo, R. E. and G. J. Klir, 1978, "A Conceptual Foundation for Systems Problem Solving," International Journal of Systems Science, Vol. 9, No. 2.

Cavallo, R. E. and G. J. Klir, 1979, "Reconstructability Analysis of Multi-Dimensional Relations: A Theoretical Basis for Computer-Aided Determination of Acceptable Systems Models," International Journal of General Systems, Vol. 5, No. 2.

Cavallo, R. E. and F. Pichler, 1979, "General Systems Methodology: Designs for Intuition-Amplification," in Improving the Human Condition: Quality and Stability in Social Systems, Springer-Verlag, New York.

Fienberg, S. E., 1980, The Analysis of Cross-Classified Categorical Data, second edition, MIT Press, Cambridge, Mass.

Klir, G. J., 1969, An Approach to General Systems Theory, New York, Von Nostrand.

Klir, G. J., 1970, "On the Relation Between Cybernetics and General Systems Theory," in J. Rose (ed.), Progress in Cybernetics, New York, Gordon and Breach.

Klir, G. J., 1976, "Identification of Generative Structures in Empirical Data," International Journal of General Systems, Vol. 3, No. 2.

Klir, G. J. and M. Valach, 1965, Cybernetic Modelling, London, ILIFFE Books.

Minsky, M., 1975, "A Framework for Representing Knowledge," in The Psychology of Computer Vision, P. Winston (ed.), New York, McGraw-Hill.

Sadovsky, V. N., 1979, "Methodology of Science and Systems Approach," Social Sciences, 10, Moscow.

Shaw, M. L. G., 1979, On Becoming A Personal Scientist: Interactive Computer Elicitation of Personal Models of the World, London, Academic Press.

SIQAM, 1972, Special Issue of Quarterly of Applied Mathematics.

Turan, P., 1954, "On the Theory of Graphs," Colloq. Math., Vol. 3, 19-30.

Van Trees, H. L., 1980, "Keynote Address," Conference Workshop on Quantitative Assessment of the Utility of Command and Control Systems, Mitre Corp., McLean, VA, MTR-80W00025.

Watanabe, S., 1969, "Pattern Recognition as an Inductive Process," in Methodologies of Pattern Recognition, S. Watanabe (ed.), New York, Academic Press.

Wohl, J. G., 1981, "Rate of Change of Uncertainty as an Indicator of Command and Control Systems Effectiveness," in C^3 Theory, Vol. IV, M. Athans et al (eds.).

Wohl, J. G., D. Gootkind and H. D'Angelo, 1981, Measures of Merit for Command and Control, Mitre Corp., MTR-8217.

Zraket, C. A., 1980, "Issues in Command and Control R & D and Evaluation," in Quantitative Assessment of the Utility of Command and Control Systems, Mitre Corp., McLean, VA, MTR-80W00025.

1982 USAF - SCEEE SUMMER FACULTY RESEARCH PROGRAM

Sponsored by the

AIR FORCE OFFICE OF SCIENTIFIC RESEARCH

Conducted by the

SOUTHEASTERN CENTER FOR ELECTRICAL ENGINEERING EDUCATION

FINAL REPORT

ADAPTIVE KALMAN TRACKING FILTER FOR ARIS SYSTEMS

Prepared by:	Dr. Junho Choi
Academic Rank:	Assistant Professor
Department and University:	Department of Electrical and Computer Engineering, Florida Institute of Technology
Research Location:	Eastern Space and Missile Center Range Systems and Navigation
USAF Research Colleagues:	Mr. Charles D. Miller Mr. James E. Whiddon
Date:	August 27, 1982
Contract No:	F49620-82-C-0035

ACKNOWLEDGEMENTS

The author would like to thank the Air Force Systems Command, the Air Force Office of Scientific Research, and the Southeastern Center for Electrical Engineering Education for providing him with the opportunity to spend a worthwhile and interesting summer at the Division of Ships Engineering, Patrick Air Force Base, Florida.

He would like to thank the people at ESMC/RSN, Technical Lab Library, and RCA for their hospitality, in particular to Charles D. Miller and James E. Whiddon at RSN, Hank Henry and C. Welsh at RCA, and Kathleen Burgess at the Library for their help and collaboration.

He would like to acknowledge Chris Duhring at RCA for his help in programming the simulation study during the period of this research.

Finally, the author would like to thank Ms. Thelma Van Wagoner for typing this report.

Adaptive Kalman Tracking Filter for ARIS System

by

Junho Choi

ABSTRACT

As an extension of the Metric Accuracy Improvement Program (MAIP) at the Eastern Test Range (ETR), Patrick Air Force Base (PAFB) in Florida, the adaptive technique has been developed and simulated for the possible application to the existing ARIS systems.

Sklansky's model has been adopted for the Kalman filter simulation study, since this model has been widely used in this area and has also produced more errors when the straight Gaussian statistics are applied to the model. The feasibility of adaptive technique has been studied to update the measurement, driving, and state error covariance statistics. Results show that both measurement and driving (or process) noise covariances are very sensitive to the overall performance of the filter.

Several areas for the additional and continuing work are suggested and recommended to achieve the goals successfully.

I. Introduction.

On-axis tracking technique has been focused and applied to land, air, and shipboard radars for more than a decade and has shown more promising results and performances in real applications over the auto-tracking servo systems. As an example, the land-based on-axis tracking algorithm at Eastern Test Range is superior to the auto-tracking approach. The major problems of on-axis technique are the optimal real time adjustments of weighting factor (or gain matrix for Kalman filter) for the $\alpha-\beta$ tracker where the larger the weighting factor results in obtaining the better tracking capability and the smaller the weighting factor gives a better smoothing capability.

The development of optimum algorithm for both tracking and smoothing has been actively engaged in among the scientists and engineers in this area for the last several years. In general, the more heuristic approach has been adopted to achieve the better compromise for simultaneous tracking and smoothing.

As a part of the Metric Accuracy Improvement Program (MAIP) at Eastern Space and Missile Center (ESMC), Directorate of Range Systems, Ships Engineering Division (RSN), the recursive filtering (i.e., Kalman Filter) approach was proposed and the preliminary study was reported in[1] for the on-axis tracking of C-Band radar to improve the tracking performance.

As a continuing effort of MAIP program following[1], the adaptive Kalman tracking algorithm has been developed and tested through the simulation in this report to correct the divergence of error covariance, measurement noise covariance, and target dynamic covariance matrix for the real time application to both tracking and smoothing capability.

II. Objective

The main objective of this study is to correct and attack the problems found in the previous study for the on-axis application[1] to the USNS General H.S. Vandenberg and USNS Redstone, or possibly to the land-based radar system. The most common trackers, such as the Kalman filter, a simplified Kalman filter, an α-β filter, and a Wiener filter, can provide optimum estimates of the target's position and velocity if the dynamic model is a correct representation of the true state of the nature and a target moves a smooth trajectory with a constant velocity. However, when the target deviates from this type of flight path, all of the above trackers eventually lose the track and no longer perform their functions effectively.

In order to correct and improve those problems of maneuvering target, several approaches, such as linear and nonlinear acceleration model, or adaptive Sklansky model with measurement noise only, or state error covariance only, or target dynamic noise covariance only, have been proposed and showed a substantial improvement over the nonadaptive Kalman filters for the maneuvering target.

As pointed out in[2], all three covariances, state error, measurement noise error, and input noise error, are the main factors which contribute to the performance of Kalman tracking filter for the maneuvering target.

Our major objectives thus are:

1) to develop an adaptive algorithm which can monitor the update state error, measurement error, and input target dynamic noise covariance.

2) to determine and test the optimum approach for the required goals of MAIP program through the simulation or the real access to the existing systems.

An extended Kalman tracking filter with adaptive technique may be introduced in future and further investigation will be required for the possible application to the real system, if the time allows.

III. Mathematical Formulation.

The filtering theory developed to date assumes that system dynamics are completely known and are precisely modeled in the filter. Clearly, this is never true in practice and, furthermore, finite arithmetic precludes the exact computation of the filter state. The modeling and computational errors which are invariably present may not present particular difficulties when the noise inputs to the system are large. When these are small, however, when model errors such as dynamic biases exist, and when the filter operates over long time intervals, the operation is sometimes rendered totally unacceptable[3]. This is often the case in the determination of space vehicle trajectories via a modified Kalman filter[4]. The observed phenomenon is a divergence of the errors in the estimates to values totally inconsistent with the rms values predicted by theory[5]. If the covariance matrix becomes unrealistically small or optimistic, the filter gain thus becomes small and subsequent measurements are ignored. The state and its estimate then diverge due to model error in the filter.

To correct this phenomenon of Kalman filter which has been applied to the tracking of the airborne target, several approaches have been reported, such as Gholson and Moose[6], Thorp[7], Pearson and Stear[8], and many more.

As pointed out in[2], the complete information of state error covariance matrix, measurement error covariance matrix, and finally the maneuvering characteristics of the target (i.e., the acceleration input noise covariance) update should be available for tracking a maneuvering target if one wants an optimal tracking. However, most approaches cited above have assumed that at least one of the covariance matrices is constant or a known information.

Several schemes for dealing with the adaptive filtering to avoid the divergence problem involve increasing the size of the covariance matrix and the computational complexity with an additional computing time.

Some progress has been made in proposing filter designs by analyzing the properties of the actual error covariance matrix corresponding to estimates by a Kalman filter that is designed on the basis of an inaccurate system model[9],[10] or by modeling a maneuvering target using a semi-Markov process with the combination of Baysian estimation scheme[6], [7], [8], or by adopting the input estimation technique to correct the changing target characteristics[17].

III-1.Description of Target Model

As described above, several different models have been adopted and tested under certain circumstances in order to find the very close models to the actual maneuvering target. In this particular study, Sklansky[11] model has been adopted as in[1] to maintain the continuity and better performance comparison. For the review purpose, if we write the tracking equation[11] for the (range only) six-states model as follows:

$$\begin{bmatrix} X_1(n+1) \\ X_2(n+1) \\ X_3(n+1) \\ X_4(n+1) \\ X_5(n+1) \\ X_6(n+1) \end{bmatrix} = \begin{bmatrix} 1 & T & 0 & 0 & 0 & 0 \\ 0 & 1 & 0 & 0 & 0 & 0 \\ 0 & 0 & 1 & T & 0 & 0 \\ 0 & 0 & 0 & 1 & 0 & 0 \\ 0 & 0 & 0 & 0 & 1 & T \\ 0 & 0 & 0 & 0 & 0 & 1 \end{bmatrix} \begin{bmatrix} X_1(n) \\ X_2(n) \\ X_3(n) \\ X_4(n) \\ X_5(n) \\ X_6(n) \end{bmatrix} +$$

$$\begin{bmatrix} T^2/2 & 0 & 0 \\ T & 0 & 0 \\ 0 & T^2/2 & 0 \\ 0 & T & 0 \\ 0 & 0 & T^2/2 \\ 0 & 0 & T \end{bmatrix} \cdot \begin{bmatrix} U_x(n) \\ U_y(n) \\ U_z(n) \end{bmatrix} \quad --- \quad (1)$$

$$\begin{bmatrix} y_1(n) \\ y_2(n) \\ y_3(n) \end{bmatrix} = \begin{bmatrix} 1 & 0 & 0 & 0 & 0 & 0 \\ 0 & 0 & 1 & 0 & 0 & 0 \\ 0 & 0 & 0 & 0 & 1 & 0 \end{bmatrix} \begin{bmatrix} X_1(n) \\ X_2(n) \\ X_3(n) \\ X_4(n) \\ X_5(n) \\ X_6(n) \end{bmatrix} + \begin{bmatrix} 1 \\ 1 \\ 1 \end{bmatrix} v(n) \qquad \text{--- (2)}$$

where $X_1(n)$ = position of a target on x-axis

$X_2(n)$ = velocity of a target on x-axis

$X_3(n)$ = position of a target on y-axis

$X_4(n)$ = velocity of a target on y-axis

$X_5(n)$ = position of a target on z-axis

$X_6(n)$ = velocity of a target on z-axis

T = time interval between measurements (or a sampling time)

$U_x(n)$ = random acceleration of x-component

$U_y(n)$ = random acceleration of y-component

$U_z(n)$ = random acceleration of z-component

v(n) = random measurement error which is assumed to be the same in each coordinate.

This basic Sklansky model can be applied to several different applications, such as three dimensional case of the spherical coordinate system (r, θ, ∅), or only two dimensional case (r, θ) with the modified model of position, velocity, and acceleration in the spherical coordinate system. If we rewrite equations (1) and (2) in matrix form as

$$X(k+1) = \emptyset(T)X(k) + G(T)U(k) \qquad \text{--- (3)}$$

$$Y(k) = HX(k) + v(k) \qquad \text{--- (4)}$$

and $$\emptyset(T) = \begin{bmatrix} 1 & T & 0 & 0 & 0 & 0 \\ 0 & 1 & 0 & 0 & 0 & 0 \\ 0 & 0 & 1 & T & 0 & 0 \\ 0 & 0 & 0 & 1 & 0 & 0 \\ 0 & 0 & 0 & 0 & 1 & T \\ 0 & 0 & 0 & 0 & 0 & 1 \end{bmatrix}, G(T) = \begin{bmatrix} T^2/2 & 0 & 0 \\ T & 0 & 0 \\ 0 & T^2/2 & 0 \\ 0 & T & 0 \\ 0 & 0 & T^2/2 \\ 0 & 0 & T \end{bmatrix}$$

$$H = \begin{bmatrix} 1 & 0 & 0 & 0 & 0 & 0 \\ 0 & 0 & 1 & 0 & 0 & 0 \\ 0 & 0 & 0 & 0 & 1 & 0 \end{bmatrix} \qquad U(k) = \begin{bmatrix} U_x(k) \\ U_y(k) \\ U_z(k) \end{bmatrix}$$

where $\emptyset(T)$ is a state transition matrix obtained by a linear extrapolation, $U(k)$ and $v(k)$ are random variables which have to be specified and controlled by some priori or posteriori information of state variables.

The dependence of $U(k)$ and $v(k)$ has been studied exclusively by Choi[1] and later by Choi and Yildirim[12].

Most difficulties encountered in tracking a maneuvering target through ARIS system are uncertainties of $U(k)$ and $v(k)$ which are the focal points to be thoroughly investigated in this study.

III-2. Kalman Filter Equations.

K. F. Gauss introduced the theory of smoothing, prediction, and orbital determination in 1796 and dealt, at best, with the estimation of a set of random parameters (so called least square estimation). On the other hand, Wiener, Swerling, and Kalman have dealt with the estimation of the state of a ramdom process. It is the continuous introduction of new driving noise random variables into the process, in addition to the random observation noise, that distinguishes modern estimation theory from regression theory[13]. The addition of the driving noise has the desirable feature of compensating for inaccuracies in the model used. It permits handling a changing model, such as caused by a maneuver of the object being tracked and also ensures the stability of the filter.

The solution of equation (3) and (4) is given by [5].

Estimator: $$\hat{X}_{k+1} = \hat{X}^*_k + K_{k+1} (Y_{k+1} - H \hat{X}^*_k) \qquad --- (5)$$

Predictor: $$\hat{X}^*_{k+1} = \emptyset(T) \hat{X}_k \qquad --- (6)$$

Filter Gain: $$K_{k+1} = M_{k+1} H^T (H M_{k+1} H^T + R)^{-1} \qquad --- (7)$$

Predictor covariance: $M_{k+1} = \phi(T)P_k\phi(T)^T + G(T)QG(T)^T$ --- (8)

Error covariance: $P_{K+1} = (I-K_{k+1}H)M_{k+1}$ --- (9)

where $R = E(V_kV_k^T)$ is a measurement error covariance matrix

$Q = E(U_kU_k^T)$ is a driving noise error covariance matrix

$P_k = E((X_k-\hat{X}_k)(X_k-\hat{X}_k)^T)$: state error covariance matrix

As pointed out before, those three covariance matrices, R, Q, and P_k respectively, are required to correct their follow-up or divergence phenomena which is the main subject to be studied in this section.

III-3. Divergence of Kalman Filter Covariance Matrices.

Since the study of Schlee et al[14], several approaches have been developed and suggested to correct and bound the divergence of error covariance matrix K_{k+1} in equation (7) according to the abrupt variation of a target. However, no direct control technique and breakthrough have been proposed and applied to the actual problem except for a few suggestions like the semi-Markov approach[15] or the decision-directed[16] approach. As can be seen in the equations (5) - (9), covariance matrices and gain matrix can be computed without direct interference of the incoming data behavior except for the initial condition.

One of the major causes of divergence is inaccuracies in the modeling process used to determine the message or observation model, due to failure of linearization, lack of complete knowledge of the physical problem (in this case, the maneuvering target) or the simplifying assumptions necessary for mathematical tractability. Errors in the statistical modeling of noise variances and mean or unknown inputs may also lead to divergence. Another source of divergence is round-off errors, inherent in any digital implementation of the filter algorithm, which may cause the error-variance matrix to lose its positive definiteness or symmetry[5]. Based on the foregoing discussion of the cause of divergence, it is possible to postulate a number of modifications which may be made to the

Kalman filter to prevent divergence. Those can be placed into three broad classes:

1. Direct increase of the gain matrix[14].
2. Limiting of the error covariance[15], [16].
3. Artificial increase of the plant noise variance[17],[18].

Because of the inherent characteristic of the most recursive filter, the parameters involved in the Kalman filter equation are heavily interrelated, i.e., cause-effect. In other words, the effective control of gain matrix is required to satisfy those three classes described above by adapting error covariance of system model error or measurement errors.

1. Innovations Process:

One way to control the update covariances is to adapt the update information to the filtering process through the so-called innovation process.

Let us define $\hat{Y}_k = H\hat{X}_k$ --- (10)

and combine equations (4) and (10). Then we can introduce

$$\bar{Y}_k \triangleq Y_k - \hat{Y}_k = H(X_k - \hat{X}_k) + V_k \quad \text{--- (11)}$$

$$\bar{Y}_k = H\bar{X}_k + V_k$$

where $\bar{X}_k \triangleq X_k - \hat{X}_k$

and $V_k : N(0, R_k)$ = normal distribution with zero mean and variance R_k

$Y_k : N(H\bar{X}_k, HP_kH^T + R_k)$

$P_k = E(\bar{X}_k\bar{X}_k^T)$: error covariance of Kalman Filter

with a scalar observation, the maximum likelihood estimate of V_k in equation (11) becomes [18] [5].

$$\hat{R}_k = \frac{1}{N}\sum_{k=1}^{N}(\bar{Y}_k - H\bar{X}_k)^2 \quad \text{--- (12)}$$

After some manipulation, the sequential estimator is obtained as

$$\hat{R}_{k+1} = \frac{1}{N}((N-1)\hat{R}_k + (\bar{Y}_k - H\bar{X}_k)^2 (1 + HBH^T)^{-1})$$

where $$B = \frac{1}{N} \sum_{k=1}^{N} (H_k{}^T H_k)^2 \qquad \text{- - - (13)}$$

If we modify the equation (13) for our particular application, the empirical single stage sequential estimator of V_k is obtained as

$$\hat{R}_{k+1} = \hat{R}_k \pm \| Y_{k+1} - H\hat{X}_k \|^2 \, (\hat{R}_k + HP_kH^T)^{-1} \qquad \text{- - - (14)}$$

Equation (14) is very similar to equation (13) except for the weighting factor which is replaced by the variance of $\bar{Y}_k$ and $\bar{Y}_k$ and $\bar{X}_k$ into Y_k and $\hat{X}_k$ respectively in order to follow the update variation of the measurement and prediction difference. When the difference between the measurement and the radar prediction is getting larger, the variance of V_k increases by resulting in the reduction of the gain matrix. On the other hand, if the difference is getting smaller, the variance of V_k is unchanged which results in following the non-maneuvering target just like the smoothing Kalman filter, that is, the convergence of equation (14) is guaranteed for the large and steady state k.

2. Control of Driving Noise Variance

Singer model[19] will be applied to this particular study for the effective control of input noise variance since the straightforward Kalman filter application to the Sklansky model[11] performs very poorly, but performs very reasonably for the modified model and Singer's approach[2].

In order to utilize Singer's approach for the on-axis tracking, the technique should be modified in the sequential format which can recursively update and correct the divergence of the gain matrix. If we adopt the duality theorem proved by Kalman[20], then let us define

$$U_k \triangleq -K_k^T X_k + q_k \qquad \text{- - - (15)}$$

and

$\hat{U}_k \triangleq -K_k^T \hat{X}_k$ is deterministic, where q_k is a ramdom variable.

$$\bar{U}_k = U_k - \hat{U}_k$$

$$= -K_k^T (X_k - \hat{X}_k) + q_k \qquad \text{- - - (16)}$$

The covariance of $\bar{U}_k$ will be expressed as

$$E(\bar{U}_k \bar{U}_k^T) = Q_k = Q_{k-1} \pm K_k^T P_k K_k \quad \text{- - -} \quad (17)$$

The equation (17) is matching to the requirements of the increase of Q_k when the target starts maneuvering as shown by Choi[2]. In the beginning, Q_k starts increasing its quantity and when the value of k increases, the second term on the right hand side of equation (17) will be eventually diminishing for the steady state maneuvering (or the free-fall case), which implies the convergency of equation (17).

3. Update of Error Covariance Matrix.

Both dynamic error variance and measurement error variance update sequential estimates have been developed in the above. Those two parameters continuously influence the error covariance matrix equation(9).

The stabilized Kalman filter[5][21] will be applied to this update algorithm as

$$P_{n+1} = (I - K_{n+1}H)\, M_{n+1}\, (I - K_{n+1}H)^T + K_{n+1} R_{n+1} K^T_{n+1} \quad \text{- - -} \quad (18)$$

If we rewrite the Kalman filter equation with the proposed update algorithm as shown in the schematic flow diagram, Fig. 1,

$$\hat{X}_{n+1} = \hat{X}^*_n + K_{n+1}\,(Y_{n+1} - H\hat{X}^*_n) \quad \text{- - -} \quad (5)$$

$$\hat{X}^*_{n+1} = \phi(T)\hat{X}_n \quad \text{- - -} \quad (6)$$

$$K_{n+1} = M_{n+1}H^T\,(HM_{n+1}H^T + R_{n+1})^{-1} \quad \text{- - -} \quad (7)$$

$$M_{n+1} = \phi(T)P_n\phi(T)^T + G(T)Q_nG(T)^T \quad \text{- - -} \quad (8)$$

$$P_{n+1} = (I - K_{n+1}H)\, M_{n+1} \quad \text{- - -} \quad (9)$$

$$P_{n+1} = (I - K_{n+1}H)\, M_{n+1}\, (I - K_{n+1}H)^T + K_{n+1} R_{n+1} K_{n+1}^T \quad \text{- - -} \quad (18)$$

$$R_{n+1} = R_n \pm (Y_{n+1} - H\hat{X}^*_n)^2\,(HP_nH^T + R_n)^{-1} \quad \text{- - -} \quad (14)$$

$$Q_{n+1} = Q_n \pm K_n^T P_n K_n \quad \text{- - -} \quad (17)$$

IV. Simulation Results.

A step-by-step approach of a new adaptive scheme has been simulated in order to observe and compare the performance of the overall adaptive filter with either one or the combination of an adaptive measurement noise covariance, a stabilized state error covariance, and an adaptive driving noise covariance matrix approach.

Figure 2 shows the standard Kalman filtering process result without updating the initial conditions of P, Q, R matrices, while Figure 3 represents the standard Kalman filtering process result with updating the initial conditions of P, Q, R through the first 30- actual measurement data for X-coordinate only. Figure 4 shows the overall adaptive Kalman tracking filter process with the boundedness of Q and R as

$$0.0004 \leq R \leq 0.3 \qquad (K_m^2) \qquad \text{- - -} \quad (19)$$

$$0 \leq Q \leq 0.00083 \quad (\text{Km/sec}^2)^2 \qquad \text{- - -} \quad (20)$$

In the meantime, Figure 5 shows the results of the adaptive measurement error covariance matrix only, while Figures 6 and 7 represent the results of the adaptive driving noise covariance and stabilized covariance matrices only, respectively.

As pointed out in section 3, the adjustment of Q and R is required when the radar starts tracking a smooth trajectory from the recursive update relation as equations (14) and (17) into the constant value as

$$Q_{n+1} = Q_n = 0 \qquad \text{- - -} \quad (21)$$

$$R_{n+1} = R_n \qquad \text{- - -} \quad (22)$$

Finally, Figures 8 and 9 show the sum square residual of X-coordinate position and velocity between measurement (X_m) - predicted (X_p), measurement (X_m) - estimated (X_e), and estimated (X_e) - predicted (X_p) for all updated adaptive algorithms.

Several measures can be imposed to the algorithms developed to track the highly maneuverable target such as the equations (19) -

(22). In addition to those constraints, the predicted error, $\|Y_{n+1} - H\hat{X}_n^*\|^2$, can be a good candidate for monitoring the divergence or convergence of the filter. In such an event, the reinitialization or readjustment of the P, Q, R matrices are required to achieve both tracking and smoothing process.

As a conclusion of this study, two important factors should be pointed out: any one of the adaptive techniques can be applied for each different tracking situation, such as

1) Updating P, Q, and R covariances with some boundedness for some time-period according to each maneuvering case, i.e., whenever the target is lost.

2) Utilizing an adaptive Q-matrix when the target is highly maneuverable and an adaptive R-matrix when the target is not highly maneuverable.

3) Stabilizing the state error covariance through the stabilized Kalman filter in order to avoid the divergence of error covariance matrix and the computation time is increased remarkably when the adaptive technique is adopted. However, the on-axis applicability is high enough to meet the criterion because this filter does not require any storage and the mechanical timing is long enough to provide the update information to the servo-tracking system.

V. Recommendations.

The practical application and implementation will require the several intermediate technical developments and checkpoints.

Few of those requirements would be proposed to improve and guarantee the on-axis technique to be adopted.

1. The overall review of several tracking models is required, such as

a) Sklansky model (extrapolation method).

b) Singer model

which can be processed through the

a) α - β tracker

b) Standard Kalman filter

c) Extended Kalman filter

d) Adaptive Kalman filter

e) Combination of a) - d).

2. The reduced-order feasibility of the above mentioned tracking model should be tested for the simple and efficient algorithm to save processing computational time.

3. Decision theory adoption is required for the control of covariance matrix convergency and divergence such as equations (19) - (22). Those three areas of interest should be tested before the adoption of any on-axis tracking attempt and the author would like to recommend strongly the continuing research effort for the successful completion of MAIP program and the future application of any on-board aircraft and ship antenna tracking purpose.

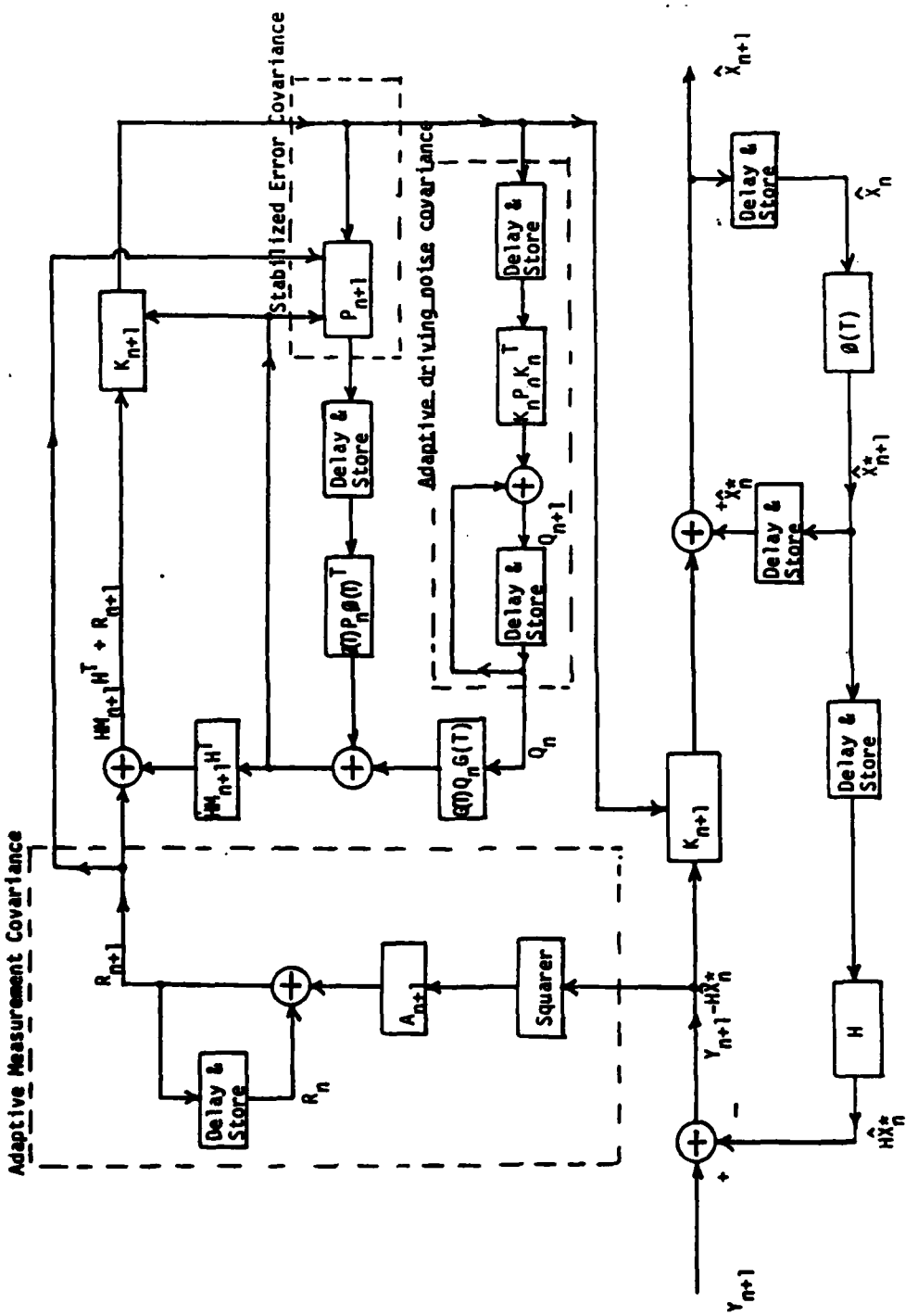


FIG. 1: Schematic Diagram for Adaptive Kalman Tracking Filter
$A_{n+1} = (Y_{n+1} - H\hat{X}_n^*)^2 - (HP_nH^T + R_n)^{-1}$

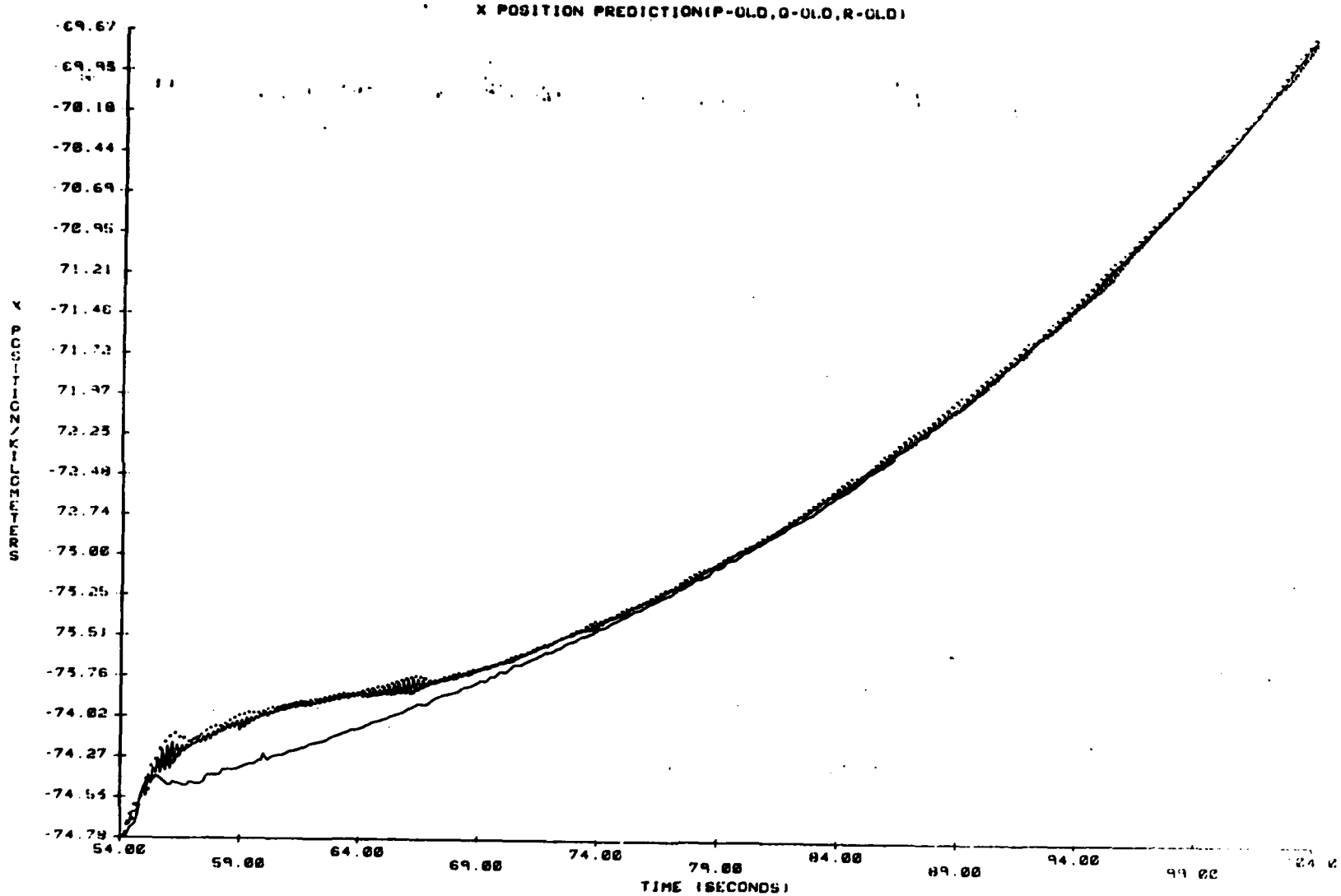


Figure 2. Standard Kalman Filter Without Update

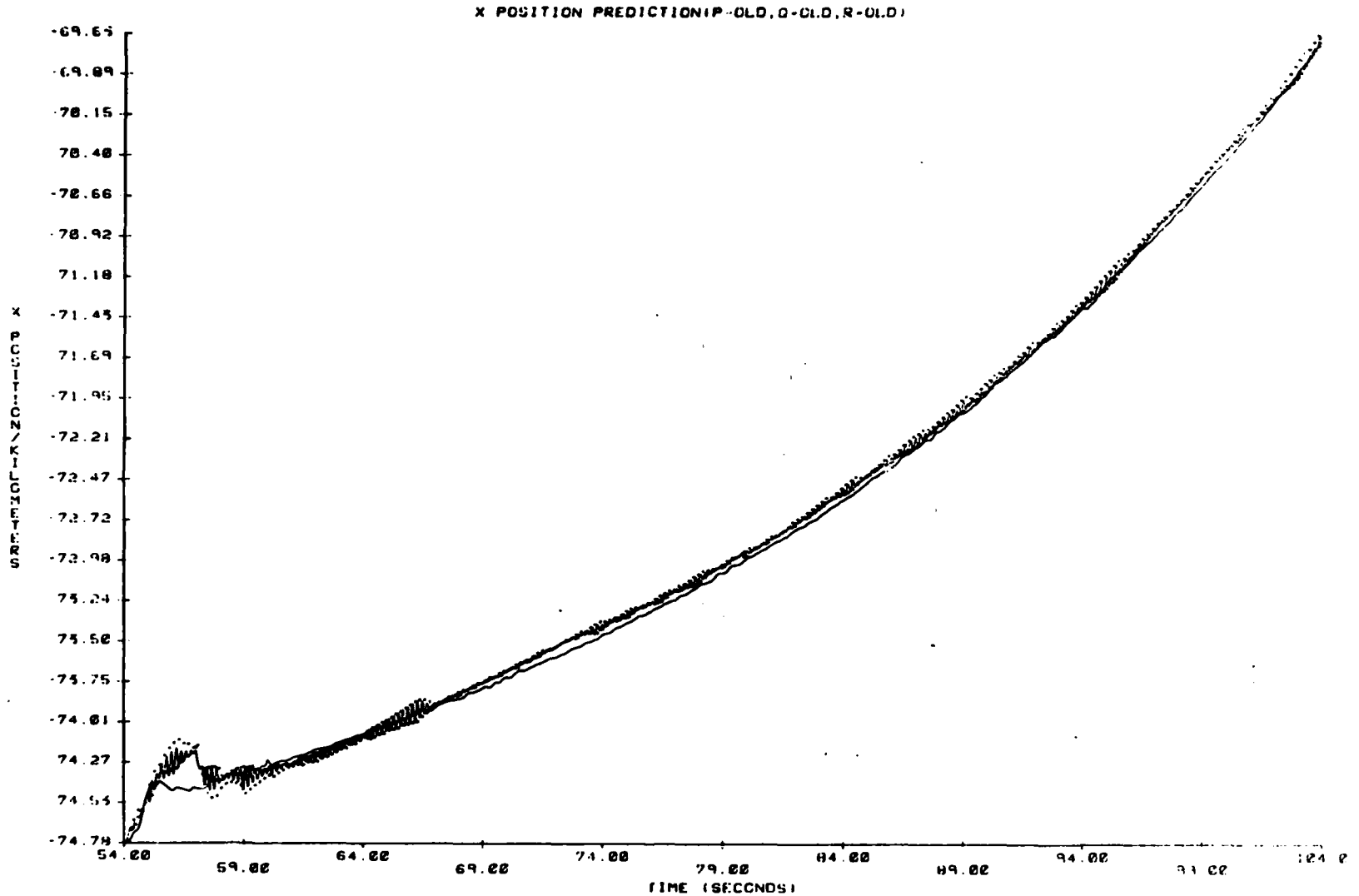
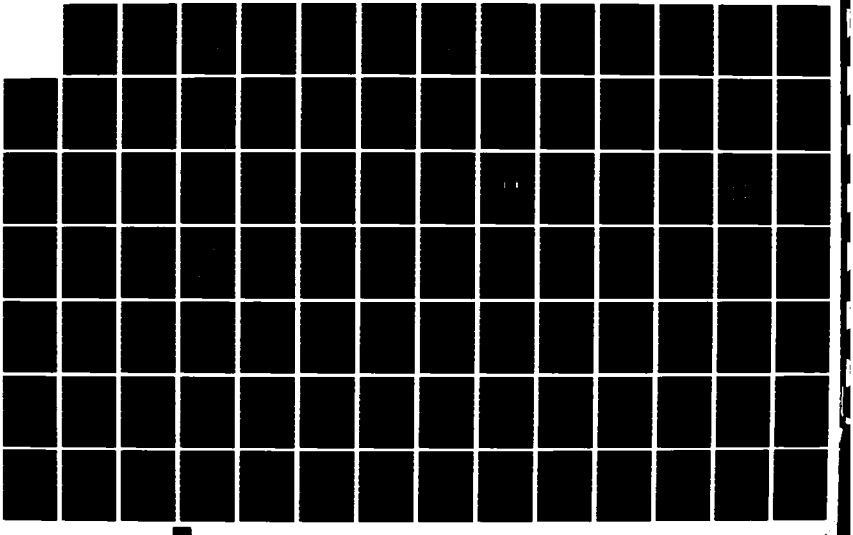
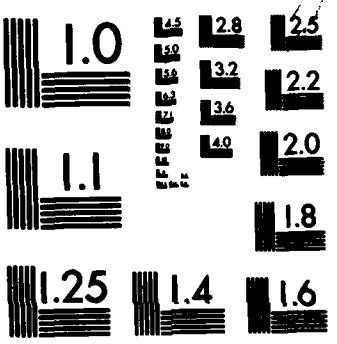


Figure 3. Standard Kalman Filter With Update

AD-A130 769 USAF/SCEEE SUMMER FACULTY RESEARCH PROGRAM RESEARCH REPORTS VOLUME 1. (U) SOUTHEASTERN CENTER FOR ELECTRICAL ENGINEERING EDUCATION INC S.. 6/11
UNCLASSIFIED W D PEELE ET AL. OCT 82 AFOSR-TR-83-0613 F/G 5/1 NL





MICROCOPY RESOLUTION TEST CHART
NATIONAL BUREAU OF STANDARDS-1963-A

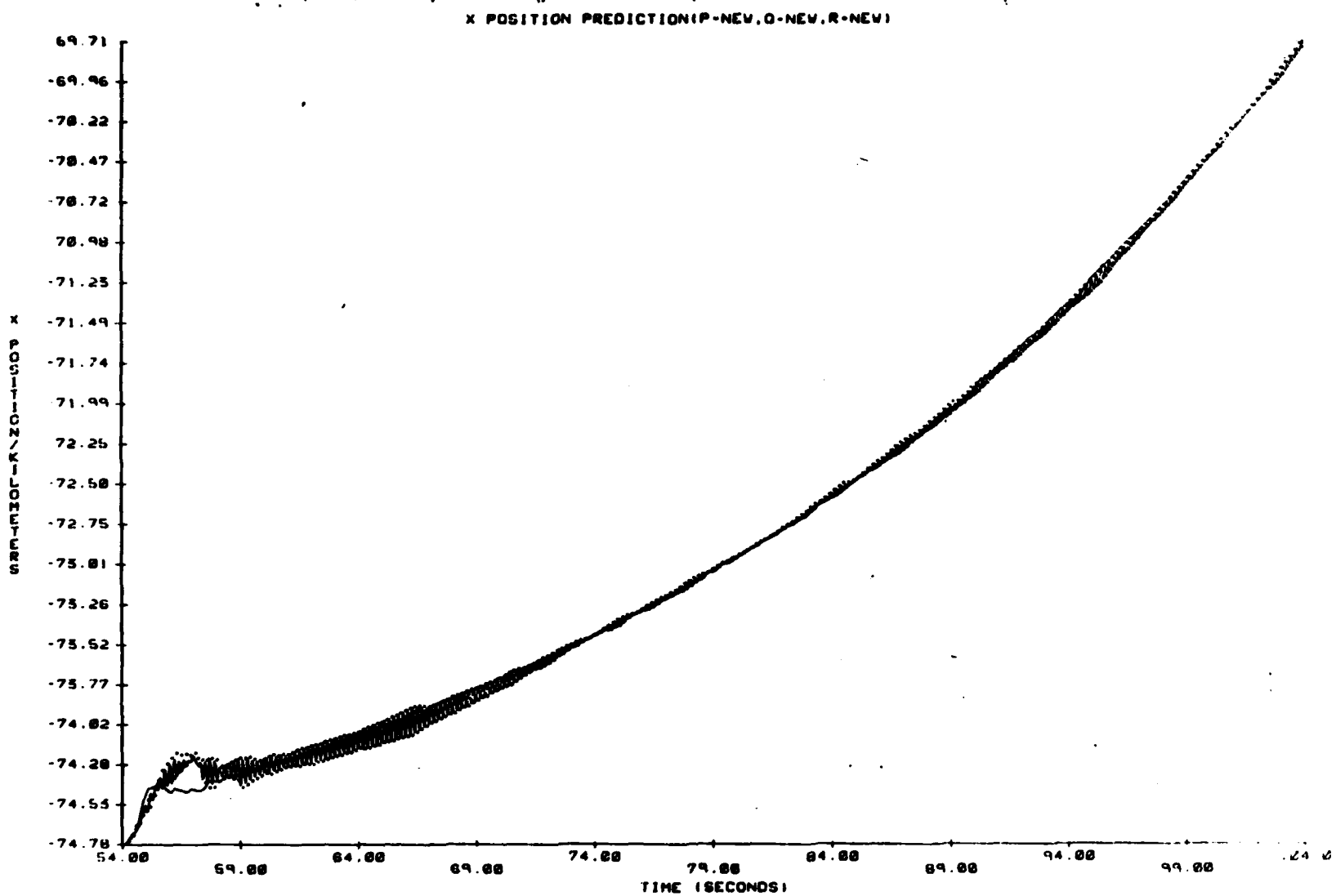


Figure 4. Whole Adaptive Kalman Filter

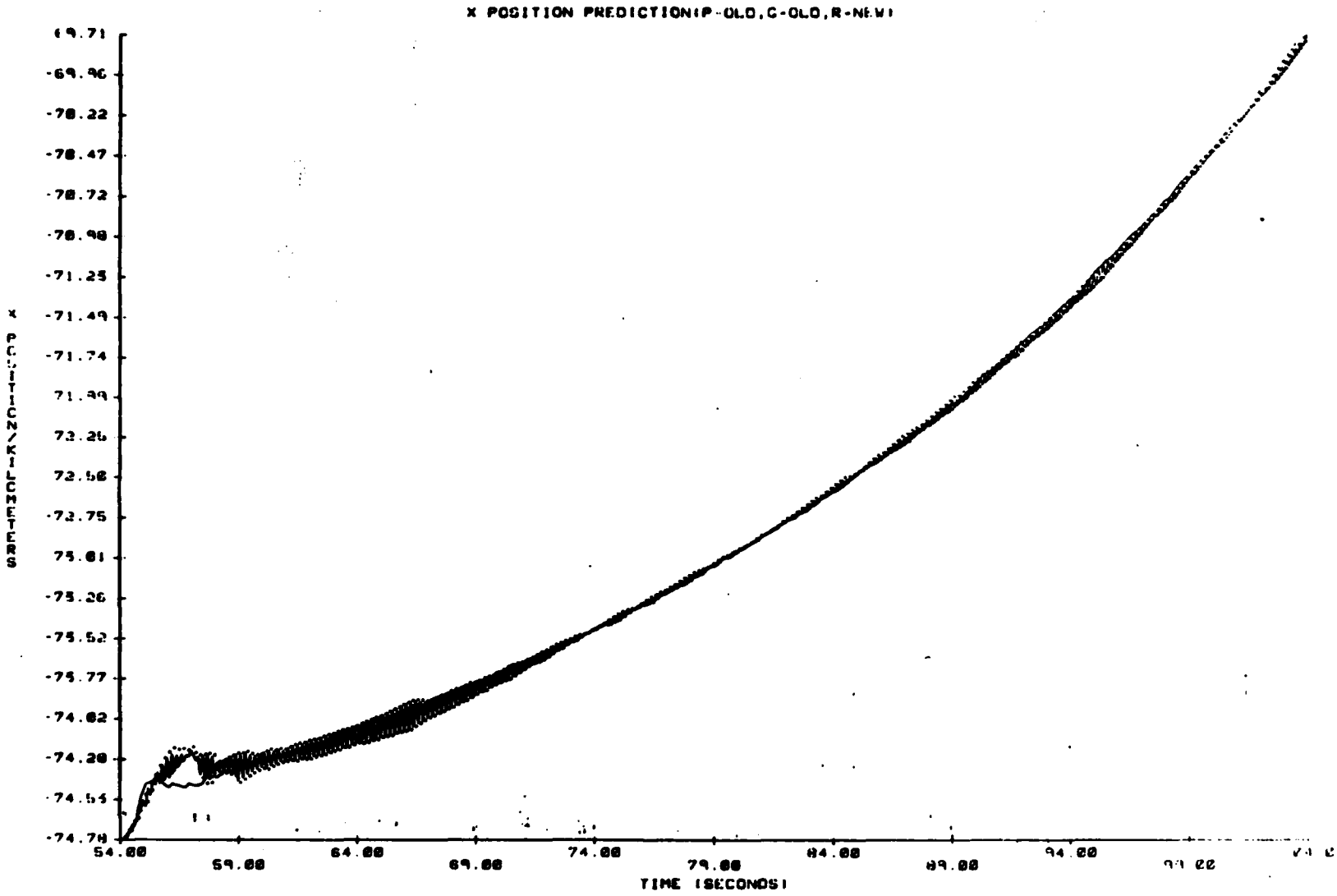


Figure 5. Adaptive Measurement Covariance Update Only

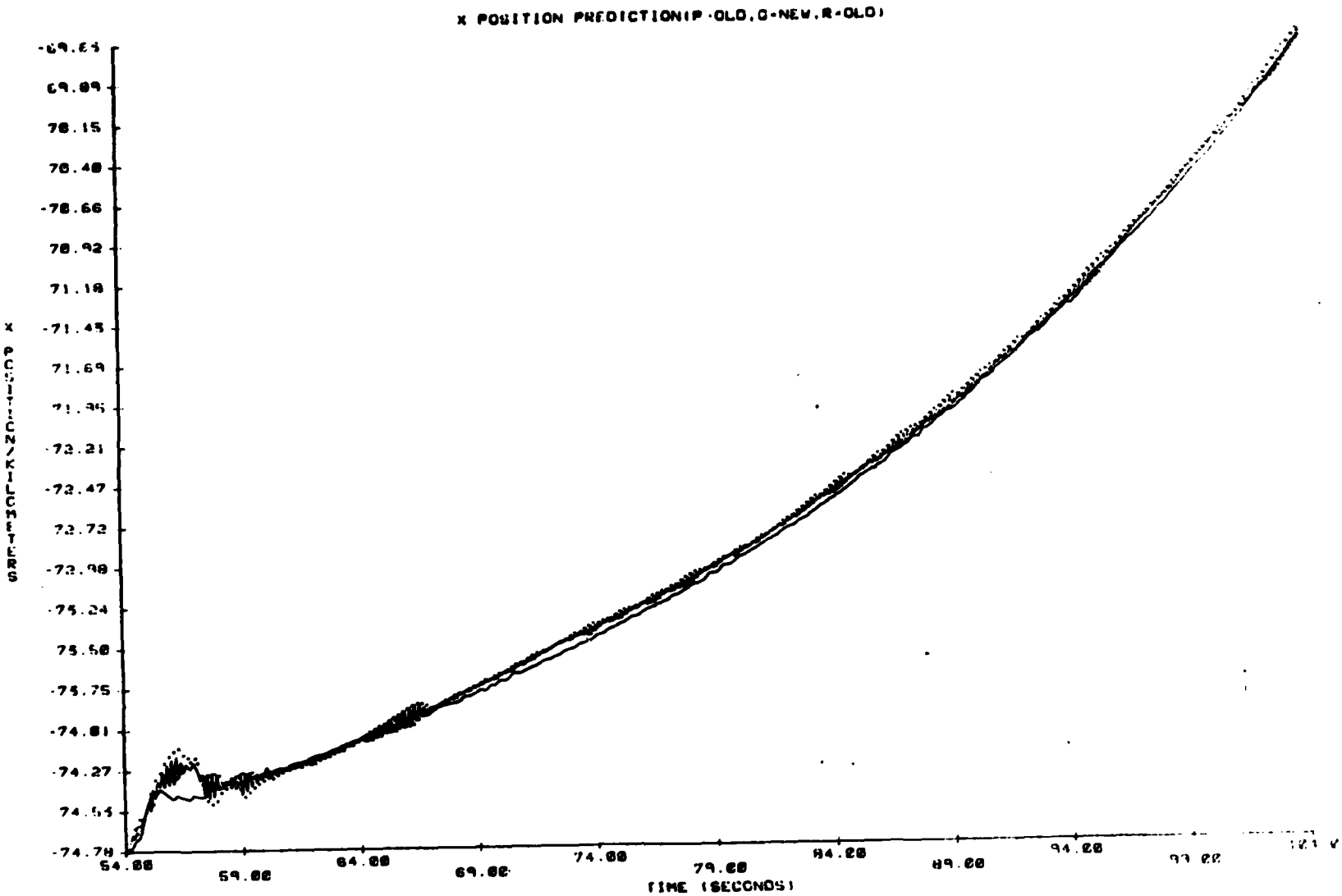


Figure 6. Adaptive Process Noise Covariance Update Only

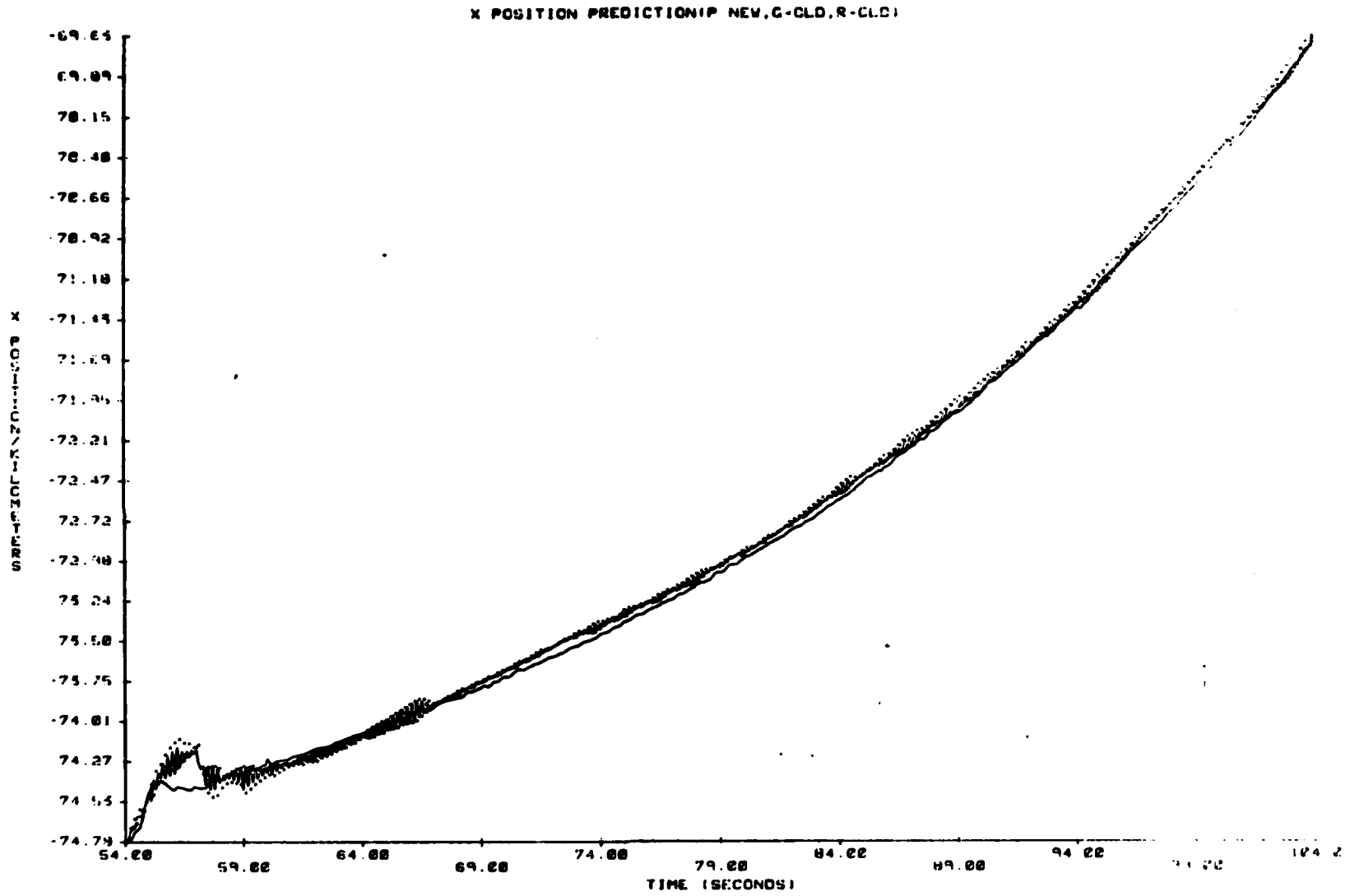


Figure 7. Stabilized Error Noise Covariance Update Only

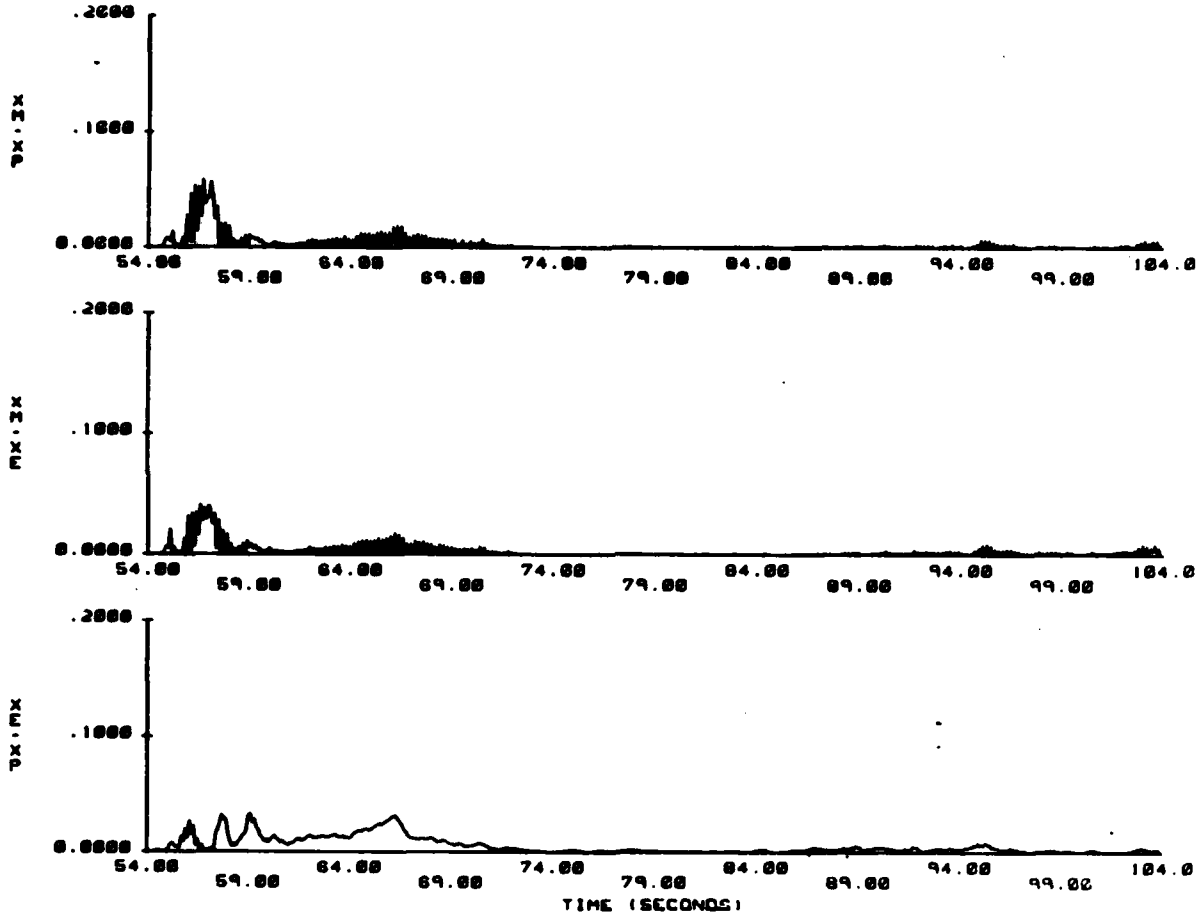


Figure 8. Sum Square Residual of X - Position Only

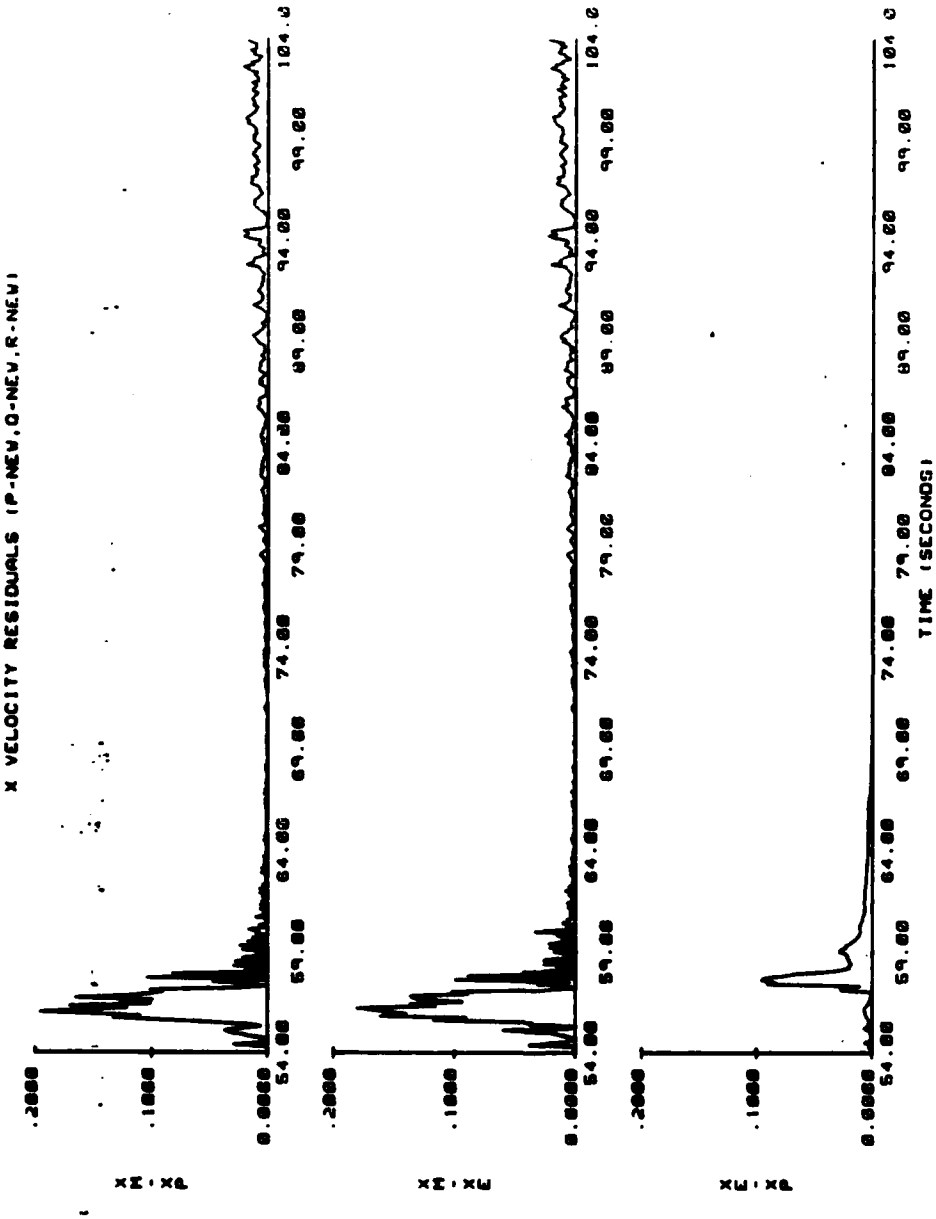


Figure 9. Sum Square Residual X - Velocity Only

REFERENCES

1. Choi, J., "On-axis Kalman Tracking Filter for H.S. Vandenberg ARIS System: A Final Report," AFOSR-SCEEE SFRP, Summer 1981.
2. Choi, J., "Performance Sensitivity of Kalman Tracking Filter for Maneuvering Target," Proceedings of IEEE Southeastcon, 1982. Sandestin, FL, pp. 441-444.
3. Jazwinski, A. H., "Limited Memory Optimal Filtering," IEEE Transactions on Automatic Control, Vol. AC-13, pp. 558-563, October 1968.
4. Jazwinski, A. H., "Adaptive Filtering," Automatica, Vol. 5, pp. 475-485, Pergamon Press, 1969.
5. Sage, A.P. and J.L. Melsa, "Estimation Theory with Applications to Communication and Control," McGraw-Hill Book Company, 1971.
6. Gholson, N.H. and R.L. Moose, "Maneuvering Target Tracking Using Adaptive State Estimation," IEEE Transactions on Aerospace and Electronic Systems, Vol. AES-13, No. 3, pp. 310-317, May 1977.
7. Thorp, J.S., "Optimal Tracking of Maneuvering Target," IEEE Transactions on Aerospace and Electronic Systems, Vol. AES-9, No. 4, pp. 512-519, July 1973.
8. Pearson, J. B. and E. B. Stear, "Kalman Filter Applications in Airborne Radar Tracking," IEEE Transactions on Aerospace and Electronics Systems, Vol. AES-10, No. 3, pp. 319-329, May 1974.
9. Price, C. F., "An Analysis of the Divergence Problem in the Kalman Filter," IEEE Transactions on Automatic Control, Vol. AC-13, No. 5, pp. 699-702, December 1968.
10. Heffes, H., "The Effect of Erroneous Models on the Kalman Filter Response," IEEE Transactions on Automatic Control, Vol. AC-11, No. 4, pp. 541-543, July 1966.

11. Sklansky, J., "Optimizing the Dynamic Parameters of a Track-While-Scan System," RCA Review, pp. 163-185, June 1957.
12. Choi, J., and E. Yildirim, "On the Relative Performance of Kalman Tracking Filter: Six-states and Four-states," to be published in IEEE Southeastcon 1983, Orlando, FL.
13. Schwartz, M., and L. Shaw, "Signal Processing: Discrete Spectral Analysis, Detection, and Estimation," McGraw-Hill, 1975.
14. Schlee, F. H., C. J. Standish, and N. F. Toda, "Divergence in the Kalman Filter," AIAA Journal, Vol. 5, No. 6, pp. 1114-1120, June 1967.
15. Moose, R. L., "An Adaptive State Estimation Solution to the Maneuvering Target Problem," IEEE Transactions on Automatic Control, Vol. AC-20, No. 3, pp. 359-362, June 1975.
16. Nahi, N.E. and B. M. Schaefer, "Decision-Directed Adaptive Recursive Estimators: Divergence Prevention," IEEE Transactions on Automatic Control, AC-17, No. 1, pp. 61-68, Feb. 1972.
17. Chan, Y. T., A. G. C. Hu, and J. B. Plant, "A Kalman Filter Based Tracking Scheme with Input Estimation," IEEE Transactions on Aerospace and Electronic Systems, Vol. AES-15, No. 2, pp. 237-244, March 1979.
18. Smith, G. L., "Sequential Estimation of Observation Error Variances in a Trajectory Estimation Problem," AIAA Journal, Vol. 5, No. 11, pp. 1964-1970, Nov. 1967.
19. Singer, R. A., "Estimating Optimal Tracking Filter Performance for Manned Maneuvering Targets," IEEE Transactions on Aerospace and Electronic Systems, Vol. AES-6, No. 4, pp. 473-483, July 1970.
20. Kalman, R. E., "A New Approach to Linear Filtering and Prediction Problems," Journal of Basic Engineering, Transactions of ASME, Vol. 82, pp. 35-45, March 1960.

21. Kortrum, W., Computational Techniques in Optimal State-Estimation - A Tutorial Review," Journal of Dynamic Systems, Measurement, and Control, Transactions of the ASME, Vol. 101, pp. 99-107, June 1979.

1982 USAF-SCEE SUMMER FACULTY RESEARCH PROGRAM

Sponsored by the

AIR FORCE OFFICE OF SCIENTIFIC RESEARCH

Conducted by the

SOUTHEASTERN CENTER FOR ELECTRICAL ENGINEERING EDUCATION

FINAL REPORT

INCENTIVE CONTRACTING IN MULTI-YEAR PROCUREMENT

Prepared by:	David L. Cleeton, Ph.D.
Academic Rank:	Assistant Professor
Department and University:	Economics Department Oberlin College
Research Location:	Air Force Business Research Management Center
USAF Research Colleague:	Captain Mike Tankersley
Date:	20 August 1982
Contract No.:	F49620-82-C-0035

INCENTIVE CONTRACTING IN MULTI-YEAR PROCUREMENT

by

David L. Cleeton

ABSTRACT

Using agency theory, insurance theory and results from economic incentive contracting models, this paper examines optimal risk sharing arrangements in multi-year contracting. While past models of incentive contracting have focused entirely on cost monitoring and performance evaluation, this research also looks at uncertainty due to demand fluctuations. Several alternatives are offered to supplement linear cost sharing devices in addresssing the risk sharing and moral hazard problem. The results suggest that a more flexible bargaining position may be achieved by the government through the use of multi-year procurement and that this advantage can be used to more closely evaluate contract performance. Lastly, suggestions for further research are outlined. An extended version of this report is given in (3).

Acknowledgement

The author wishes to express his thanks to the Air Force Office of Scientific Research, the Southeastern Center for Electrical Engineering Education and the Air Force Business Research Management Center for providing the opportunity and support for ths research effort. In addition, the kind co-operation of the University of Dayton and Wright State University in allowing the use of their library facilities was much appreciated.

Finally, an expression of gratitude is due to Capt Mike Tankersley for providing many helpful leads and contacts for ths research topic, and also Col Ronald Deep and Prof Hamed Eldin, Oklahoma State University, for their useful comments.

I. INTRODUCTION

Section 909 of the 1982 Department of Defense Authorization Act provides for the relaxing of several constraints which have limited the application of multi-year procurement (MYP). Currently the Department of Defense and the military services are developing and/or implementing policy guidelines for MYP. An examination of the policy environment today reveals that a conservative approach is being taken in the selection of possible programs for MYP and also toward the contractual features for these candidates.*

While the use of incentive contracting is not presently prominent in MYP policy, Deputy Secretary of Defense, Frank Carlucci, in his memorandum of 1 May 1981, encourages the study of innovative contractual terms which acknowledge contractor risk and the government's concerns over control. Given that incentive contracting is a much more flexible and adaptive contract form than other alternatives in handling risk sharing and cost monitoring, the role of incentive contracting in MYP is likely to increase steadily.

Recent modeling and empirical investigations of incentive contracting have focused on risk sharing, moral hazard issues, and cost control. This has been static analysis which looks only at the cost (supply) side for sources of uncertainty in programs. Demand uncertainty has been ignored. Yet demand uncertainty is very much a contractor concern and leads at least indirectly to increased costs via impacts on a firm's investment decision. MYP dirctly adddresses this source of risk and allows contract bargaining to be used more effectively to manage the cost sharing and cost monitoring functions.

Therefore, a need exists to investigate the role of incentive contracting in MYP. By doing so, we may be better able to understand how this form of contract can be used to improve contract performance and result in cost savings and improved budgetary planning.

---

*This area will be examined later, see (2), (8), and (9) for an historical guide to MYP, current policy developments, and heuristic arguments concerning the costs and benefits inherent in MYP.

II. OBJECTIVES OF RESEARCH EFFORT

This study has two main objectives. The first is to integrate current theoretical research in agency theory ((5), (6), (12), (14)), and insurance theory ((10), (13)), with the literature on economic incentive contracting ((1), (4), (11), (15)) and build a general model of optimal risk sharing and cost monitoring through linear cost sharing schedules. The analysis is simplified to two ways in order to accomplish this task. Only economic or profit incentives are modeled, i.e., performance and delivery incentives are not included in the analysis. Investment decisions by the firm are assumed to be exogenous.*

The second objective is to extend the analysis into a multi-period framework. Here the choice between using a series of single period contracts or a multi-period contract will be analyzed according to effects on risk sharing, expected cost, and contract monitoring.

Finally, a secondary objective is to outline areas of further research which are linked to the primary objectives. An example is the use of deductibles to make cost sharing schedules nonlinear and thereby alter the moral hazard penalty while preserving an adequate reduction in contractor risk.

III. RESULTS ON RISK SHARING AND MORAL HAZARD

The defense market is characterized by products requiring advanced technology which is highly uncertain, subject to rapid obsolescence, and demanding hugh capital investments. In addition, funding procedures lead to significant variations in product demand. Furthermore, the market is dominated by a single buyer, the federal government. All of these factors preclude the development of a competitive market process, and have led to the current reliance on a bilateral procurement contract. This contracting mechanism attempts to deal with two major problems which dominate in this environment. One is a concern over the cost risk sharing in programs. The second is the problem of monitoring cost growth, i.e., controlling those costs which are endogenously generated.

---

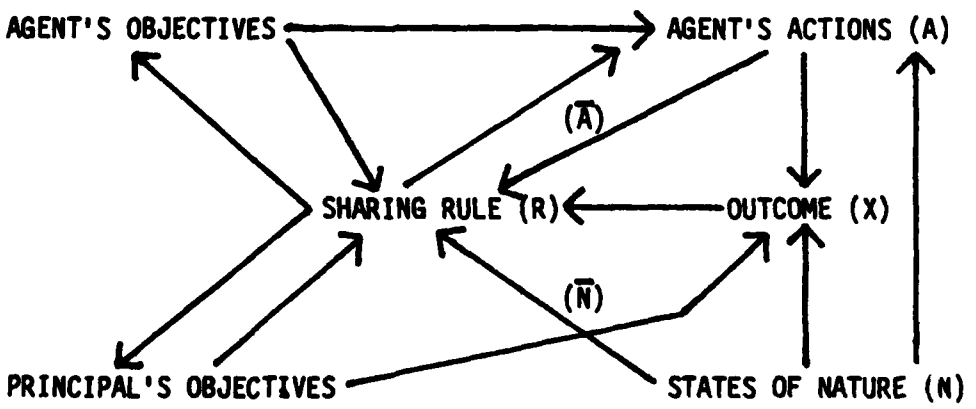
*This area will be mentioned later with respect to future research into MYP.

Private firms have a legitimate interest in reducing the cost risk associated with exogenous factors, e.g., changing input prices, technological uncertainty, etc. The government with its risk pooling abilities and wealth position is better able to take on these sources of financial risk. However, an incentive problem arises when the government shoulders the risk. Since it is difficult, costly, and perhaps informationally inefficient to completely sort exogenous and endogenous risk factors, firms are thereby relieved of incentives to control endogenous cost growth.

Agency Theory

Agency theory studies a broad class of problems which include the general framework of the defense contracting problem. (See Figure 1). A principal party engages an agent to perform duties on their behalf. The agent's actions (A) along with a random state of nature (N) jointly determine an outcome (X).* The outcome is divided between the principal and agent according to a given sharing rule (R). This sharing rule may have the outcome (X), an estimator of the agent's actions ($\bar{A}$), and an estimator of the state of nature ($\bar{N}$) as arguments. The estimators are called an information monitoring system.

FIGURE 1



*While the outcome is usually stated in terms of a monetary value, the defense problem involves the strategic bargaining over the value of the outcome.

Given the objective functions of the two parties which incorporate attitudes toward risk, the costs of various monitoring systems, subjective probability distributions of the states of nature, and any constraints which may be placed on the size or quality of the outcome, the solution to the agency problem involves identifying a Pareto Optimal contract, consisting of a sharing rule and an information monitoring system.* Thus, the problem is a game with a cooperative stage, choosing the sharing rule and monitoring system, and a non-cooperative stage, the strategic choice of actions by the agent.

Shavell (14) gives necessary and sufficient conditions for the optimality of a linear sharing rule. It is clear that these conditions are far too stringent to be satisfied in the defense contracting problem. We now turn to the defense contracting problem to formally set it up in the agency framework and show why the linear sharing arrangement can be dominated.

Incentive Contracting Theory

The literature on incentive contracting focuses on this gaming conflict through examining the objectives of the firm and government in light of the present set of contract forms which all can be represented as falling under a linear profit sharing rule. The firm's profit on a given project is given by:

$$P = aC_t + b(C_t - C)$$

where $0 \leq a \leq 1$, $0 \leq b \leq 1$

C_t = Target Cost

C = Actual Project Cost

a = Target Rate of Profit

b = Cost Sharing Rate

---

*See Gjesdal (5) for an elegant statement of the general problem and see Harris and Raviv (6) for some applications of results.

Contract types are determined by the specific values of the parameters a and b.* These are summarized in the table below:

TABLE 1

Contract Type	Parameter Values
FFP - Firm Fixed Price Contract	$0 < a < 1$ $b = 1$
FPI - Fixed Price Incentive Contract	$0 < a < 1$ $0 < b < 1$
CPFF - Cost Plus Fixed Fee Contract	$0 < a < 1$ $b = 0$
COST - Cost Type Contract	$a = 0$ $b = 0$

The government's cost in total is made up of the project cost plus any profit paid:

$$G = P + C$$
$$= (a + b)C_t + (1 - b)C \qquad \text{(II)}$$

Table II summarizes the variables which have been modeled by various authors into the two parties' objective functions. Most of these objectives are self explanatory, however, the terms capability and reputation effects should be expanded upon. Capability refers to expenditures taken on current projects which will improve the firm's ability to perform future contracts. Reputation effects are negative in that they refer to future consideration of cost overruns on current projects.

TABLE II

PRINCIPAL'S OBJECTIVES (Government)	AGENT'S OBJECTIVES (Contractor)
Minimizing Government Cost	Minimizing Profit
Meeting Program Performance Goals-Modeled as constraints on acceptable outcomes	Minimizing Financial Risk-Variance in profit
	Increasing Probability of Future Contract Awards-Capability effects and Reputation effects

*We will simplify and ignore any upper and/or lower bounds which may be placed on P or C. For details on models see (1), (3), (10), and (14).

Note that the government is assumed to exhibit risk neutral behavior and only considers capability and reputation effects as they might impact on expected government cost.

The major results of incentive contracting models can be summarized now. If the firm's choice of actions to be undertaken is independent of the sharing rule, although no necessarily independent of the distribution of the states of nature, then the optimal contract is of a COST or CPFF form wherein the government bears all of the project risk. This condition on the agent's strategy corresponds to an absence of moral hazard.

Moral hazard refers to the incentive problem which arises when program cost (C) is at least partially under the firm's control and the firm enjoys direct benefits from increasing cost. In particular, the alteration of acts by the agent in response to changed incentives after the purchase of insurance is referred to as the moral hazard problem. The purchase of insurance corresponds to any linear sharing rule where the agent does not bear the entire risk, i.e., any rule where $b \neq 1$.* Moral hazard can occur as long as monitoring the firm's future actions is costly, i.e., the government cannot freely observe the state of nature and the firm's actions independently.

A set of necessary conditions for moral hazard is that a firm derives some positive benefits from increasing costs, e.g., capability effects, and that it has at least limited ability to control costs. These are not sufficient conditions since the direct marginal benefits from increasing costs may not outweigh the indirect marginal loss which is manifested in terms of a reduction in the firm's profit or the awarding of future contracts. Readers are urged to refer to (1), (4), and (15) for details concerning these cost motivations for firms, e.g., private market spinoffs, managerial discretion, and capability effects.

---

*Another type of incentive conflict exists because there is a tendency for the worst risks to purchase insurance. This is termed the adverse selection problem. See McCall (11) for analysis of this problem and its effects on contract awards and cost overruns.

We can now see why the simple linear cost-or profit sharing rule is not optimal. The sharing rate (b) is the joint determinant of the degree of exogenous risk sharing (effects of the random state of nature) and at the same time the marginal cost in terms of profit from engaging in moral hazard behavior. One parameter cannot simultaneously perform these two conflicting roles. A high value for the sharing rate is desirable to combat against moral hazard behavior, when it is present, but results in the firm bearing a non-optimal amount of risk.

Solutions to the Risk Sharing and Moral Hazard Problem

Several directions can be offered toward the solution of this problem, some of which are drawn from insurance theory.* Basically there are two approaches that can be taken to preserve the simplicity of the linear cost sharing rule. The first involves preserving a high rate of risk reduction with a low value of the sharing rate, (b), while addressing the moral hazard problem with other mechanisms. Examples of other mechanisms would include increasing the reputation effects in contracting awards, decreasing the capability effect by providing separate funding for targeted capabilities, and providing tighter control over the ability of firms to profit from commercial applications. The second approach would provide a high penalty for practicing moral hazard by havnig a relatively high sharing rate, (b), while using other techniques to insure the firm against exogenous risk factors. Examples of these techniques include the use of escalation factors for input price increases, or the use of multiple contingent contracts which specify different target costs, ex ante, dependent upon the realization of various states of nature.** Both of these approaches depend upon the costs of identifying the sources of exogenous or endogenous risk and devising means to deal directly with those risk sources, thus allowing the usage of the sharing rate, (b), to be preserved for handling other sources of risk.

Insurance theory offers another solution which simply alters the linear sharing arrangements into a non-linear arrangement.

---

*See (10) and (13) for excellent surveys of the current status of insurance theory.

**See Cummins (4) for details on this contracting strategy.

This device is the use of minimums or deductibles in claims.* Firms with a low moral hazard potential would be expected to be more willing to accept a larger deductible in exchange for either an increase in (a) or a reduction in (b), the profit parameters, than would a firm with a high moral hazard potential. Experience ratings are also widely used in setting insurance premiums, and correspond to using an explicit reputation measure in awarding defense contracts. Experience ratings would involve increasing the value of (b), or decreasing (a), as a result of the contractor's past cost overrun record. It should be pointed out that in order to make all these effective, it is necessary that the negotiation of the target cost (C_t) be made independent of the contract type, i.e., independent of the values of (a) and (b). One method, which could be implemented to make this possible, is a two stage negotiation process in which the target cost is set in the first stage, leaving negotiations over the parameters (a) and (b), and the size of the deductible, until the second stage. This would involve a relaxing of the current reluctance on the part of DOD to allow a sizable variation in the target profit rate (a), but the potential savings in obtaining more reliable cost estimates for budgeting and meaningful cost overrun data, ex post, should far outweigh the misguided emphasis now placed on controlling the target rate of profit.

---

*See Mayers and Smith (10) for a discussion of the differential effects of deductibles versus minimums.

IV. MULTI-YEAR PROCUREMENT

Table III summarizes the major advantages and disadvantages which have been identified for MYP.*

TABLE III

ADVANTAGES	DISADVANTAGES
Reduction of repetitive contracting and administrative costs	Future competition impeded
Improvements in long range planning and forecasting	Increased leadtime for administration
Reduction in work force instability	Reduced discretion in decision making
Competition for initial award should increase	
Increased productivity due to capital investment	
Expansion and modernization of industrial base	
Increased quality and standardization	

There exists almost no documentation for any quantitative estimates of the size of any of the costs listed above. Modeling of MYP is at this point entirely informal and has lead to few if any empirically testable hypotheses. In addition, little data has been gathered to substantiate the claims of both opponents and proponents of MYP.

---

*Refer to (2), (8), and (9) for details.

When examining the advantages and disadvantages of the role of MYP, consideration of the critical importance of expectations is often lacking. In the absence of perfect certainty, economic agents form expectations about the future. Economists argue that these expectations must be rational. If expectations are biased over time, then parties with rational expectations will take full advantage and compete those with baised expectations out of the marketplace. Thus, the question becomes, how does the move toward MYP affect agents' expectations?

If for example, the government signs a multi-year contract, but can cancel at the end of any year, expectations may be unchanged and only minor administrative costs will be reduced. The debate over cancellation payment ceilings points out that the move to so called multi-year contracts may not be important enough in and of itself to alter rational expectations.

The answer concerning increased capital investment and resultant productivity gains is not optimistic. Since current DOD policy focuses on production contracts for MYP, the major inducement for investment lies in the possibility that current R&D work will in the future be extended to multi-year production contracts. It is doubtful that the marginal impact of this effect can change the overall investment strategy of the firm. If capital investment is of critical concern, it is easy to identify much more powerful policy tools, e.g., tax policy concerning depreciation and investment credits as well as funding subsidies via loan or borrowing privileges.*

---

*Regulated public utilities operate in a market which introduces similar biases in investment decisions. Since pricing is on a cost basis, many question the inducements for such firms to make productivity improving investments.

What then are the major impacts of MYP on the incentive contracting problem? All of the previously mentioned models focus on the motivations of contractors in the execution of a single project, with minor concerns, via capability and reputation effects, placed on future contract awards. Demand side risk is just as important to firms as is cost side risk. Both directly and substantially impact on profitability and its variance. MYP, to the extent that it actually smooths the expectation of demand variability, should lead to the acceptance by contractors of higher cost sharing rates and/or lower target rates of profit.

V. RECOMMENDATIONS

The use of simple linear cost sharing arrangements is not adequate to solve the optimal risk sharing problem when moral hazard is present. In those programs where it is relatively easy to identify exogenous sources of risk, e.g., the production of items classified as having stable configurations and requirements, these risk surces should be targeted and dealt with independently of the contract parameter negotiations, e.g., specifying escalator clauses for input price changes. This would allow the negotiation of a high sharing rate for costs. In addition, these programs are natural candidates for multi-year contracts. This situation would provide the largest inducement for productivity improving capital investments, since a firm could capture most of the returns on such investments over the entire contract period. Government cost savings should result due to its bearing the exogenous risks on both the demand and cost side and productivity savings could be captured in future contracts.

For programs where it is difficult to identify exogenous sources of risk, a low sharing rate would be negotiated, but independent devices to combat moral hazard should be implemented. These would include the specification of deductibles, the increased use of reputation effects in future contract awards, and perhaps a sharing in commercial applications of technology.

The deductible mechanism is very simple to implement and allows firms to signal jointly their attitudes toward risk and moral hazard. Research into the agency model incorporating deductibles should be carried out in order to recognize potential cost savings and improved budgetary planning resulting from the signaling process.

REFERENCES

(1) Blanning, R.W.; Kleindorfer, P.R., and C.S. Sankar, "A Theory of Multi-stage Contractual Incentives with Application to Design-to-Cost", Naval Research Logistics Quarterly, Vol. 29, No. 1, March 1982.

(2) Brearey, J.L., "An Analysis of the Impact of Multi-Year Procurment on Weapon System Acquisition", Master Thesis, AFIT School of Systems and Logistics, Sept. 1981.

(3) Cleeton, D.L., "Incentive Contracting: Moral Hazard and Risk Sharing Aspects", Working Paper, Oberlin College Department of Economics, 1982.

(4) Cummins, J.M., "Incentive Contracting for Natonal Defense: A Problem of Optimal Risk Sharing", Bell Journal of Economics, Vol. 8, No. 1, Spring 1977.

(5) Gjesdal, F., "Information and Incentives: The Agency Information Problem", Review of Economic Studies, Vol. 49 (3), No. 157, July 1982.

(6) Harris, M. and A. Raviv, "Some Results on Incentive Contracts with Applications to Education and Employment, Health Insurance, and Law Enforcement", American Economic Review, Vol. 68, No. 1, March 1978.

(7) Holmström, B., "Moral Hazard and Observability", Bell Journal of Economics, Vol. 10, No. 1, Spring 1979.

(8) Knittle, D.D., and A.J. Mandler, "Adapting to Multi-Year Procurement", Army Procurement Research Office, Sept. 1981.

(9) Lafors, K.P., "Selecting Programs for Multi-Year Procurement", Concepts, Vol. 5, No. 2, Spring 1982.

(10) Mayers, D., and C.W. Smith, Jr., "Contractual Provisions, Organizational Structure, and Conflict Control in Insurance Markets", Journal of Business, Vol. 54, No. 3, 1981.

(11) McCall, J.J., "The Simple Economics of Incentive Contracting", American Economic Review, Vol. 60, No. 5 , Dec. 1970.

(12) Ross, S.A., "On the Economic Theory of Agency and the Principle of Similarity", in Essays on Economic Behavior under Uncertainty, edited by M.S. Balch, D.L. McFadden, and S.Y. Wu, North-Holland, 1974.

(13) Rothschild, M., and J. Stiglitz, "Equilibrium in Competitive Insurance Markets", Quarterly Journal of Economics, Vol. 90, No. 4, Nov. 1976.

(14) Shavell, S., "Risk Sharing and Incentives in the Principal and Agent Relationship", Bell Journal of Economics, Vol. 10, No. 1, Spring 1979.

(15) Williamson, O.E., "The Economics of Defense Contracting: Incentives and Performance", in Issues in Defense Economics, edited by R.N. McKean, Columbian University Press, 1967.

1982 USAF-SCEEE SUMMER FACULTY RESEARCH PROGRAM

Sponsored by the

AIR FORCE OFFICE OF SCIENTIFIC RESEARCH

Conducted by the

SOUTHEASTERN CENTER FOR ELECTRICAL ENGINEERING EDUCATION

FINAL REPORT

BINARY CLASSIFICATION AND THE SUBTRACTIVE APPROACH

Prepared by:	Dr. Gregory M. Corso
Academic Rank:	Assistant Professor
Department and University:	School of Psychology Georgia Institute of Technology
Research Location:	Air Force Aerospace Medical Research Laboratory Human Engineering Division Technology Development Branch
USAF Research Colleagues:	Capt Richard J. Poturalski Sharon L. Ward
Date:	August 27, 1982
Contract No.:	F49620-82-C-0035

BINARY CLASSIFICATION AND THE SUBTRACTIVE APPROACH

by

Gregory M. Corso

ABSTRACT

Two experiments were performed using a modification of the subtractive approach to the partitioning of human reaction time. This investigation provided information concerning the effects of display load, classification rules, the proportion of target items, and interference stimuli on input and output latencies. The major findings from this investigation showed that input and output latencies were affected by different independent variables and provided information regarding the cognitive processes within a binary classification task not observed with previous methods. Suggestions for further research are presented.

ACKNOWLEDGEMENTS

I want to thank the Air Force Systems Command, the Air Force Office of Scientific Research, and the Southeastern Center for Electrical Engineering Education for providing me with a very worthwhile and unique summer experience at the Air Force Aerospace Medical Research Laboratory at Wright-Patterson Air Force Base. In particular, I want to express my appreciation to the Human Engineering Division and especially the Technology Development Branch.

I especially want to thank those individuals who assisted me in this research project, especially Capt Richard Poturalski, Sharon Ward, Dr. Erhard Eimer, and Walter Summers for their helpful suggestions and discussions; TSgt Danny Bridges for his tremendous assistance in generating the computer programs necessary to conduct this research; Suzanne Kelly for her assistance in subject running; and to Cheryl Dunaway for typing this report.

I. INTRODUCTION

Reaction time measures have commonly been used as estimates of the number (1), rate of processing (2) and duration (3,4) of cognitive processes. Reaction time, for the Air Force in particular, is one of the most important human performance measures, since the speed of human responding may either save or lose lives, and also contributes to system effectiveness.

The present project is concerned with the partitioning of reaction time into component processes within a binary classification task. Two different approaches have been identified in the literature (5).

The subtractive approach (3) suggests that the duration of a cognitive process can be estimated by subtracting the reaction times obtained from two different tasks, where one task involves an additional mental process that is lacking from the other task. The difference between the latencies resulting from each task can then be used as an estimate of the duration of the particular mental process under investigation. The major problem associated with this approach is determining whether one task in fact does not require the mental process under investigation.

A refinement of that approach, proposed by Teichner (4), appears to avoid that problem. The procedural modification involves the presentation of a matrix of stimuli, where each stimulus must be identified by separate and sequential responses. Using this procedure, the latency from the onset of the matrix to the performance of the first response is always longer than the latencies between any of the remaining sequential responses. Teichner (4) suggested that the longer first response latency was the result of additional processing times that are missing from the remaining response latencies. Specifically, because the matrix is not physically available for processing after the first response, all response latencies after the first response do not reflect processes required to encode and process the information into memory. That is, the latencies associated with these responses reflect only output processing. Following Donders' lead, separate times can then be derived for the encoding and processing functions and the output functions by subtracting the mean of the latencies associated with each sequential response

performed after the first response from the first response latency.

The additive factor approach (2;6) suggests that relative changes in the duration of mental processes can be estimated with a regression technique. Using a task specifically designed to test this proposal, subjects were required to remember a small number of items (the positive set). Then a series of items were presented to which the subjects were required to respond with either "yes", it was one of the items in the positive set, or "no", it was not one of the items in the positive set. Using the regression notion, the model proposed was:

$$RT = A + M(X) \qquad (1)$$

where A represents that portion of the latency associated with the processing involved in stimulus encoding, response selection and response execution; while M represents the processing time per element, or the central processing time per item (7;8;9); and X represents the number of items in the positive set. While several problems and criticisms of the additive factor method have been noted (5;10), its major deficiency for human performance rests with the fact that independent estimates of the stages cannot be determined. That is, with the additive factor approach the only latency measure available is the total latency associated with each response. Consequently, separate measures of each stage cannot be determined.

This shortcoming of the additive factor approach, does not appear to pose a problem for the subtractive approach (4). Furthermore, while the additive factor approach has been primarily applied to binary classification tasks, and while the modification of the subtractive approach proposed by Teichner (4) has been applied to identification tasks, Corso and Warren-Leubecker (11) have adapted the Teichner modification and applied it to binary classification tasks. Their procedure involves the use of a matrix of stimuli in which each stimulus is to be classified as either a positive set stimulus, or a negative set stimulus. If all the items in the matrix are from the positive set, the positive set key is depressed a number of times equal to the number of positive set stimuli. If the items in the matrix are all negative set items, then the negative set key is depressed a number of times equal to the number of negative set items in the matrix. Lastly, if some of the items are from the positive

set and some of the items are from the negative set, then each key is depressed successively for the number of times equal to the appearance of those items in the matrix. While the procedure has only been used with a matrix of two stimuli, there does not appear to be any reason why this procedure cannot be used for matrices larger than two items.

Corso and Warren-Leubecker (11) have demonstrated the validity of their approach against the classical Sternberg procedure. The results of their investigation have demonstrated the superiority of the Teichner modification over the Sternberg procedure. Specifically, the Teichner modification eliminates some masking effects that occur with the Sternberg procedure, and it allows for the independent assessment of the effects of the independent variables on input and output latencies.

II. OBJECTIVES

The present investigation was concerned with extending the modification of the subtractive approach in five different ways. Specifically, two experiments were designed to assess the effects of:

(1) display loads on input and output processing times,

(2) interference stimuli that occur between the onset and offset of the display;

(3) different decision rules for classification on those dependent variables;

(4) the proportion of targets on those dependent variables, and;

(5) different kinds of stimuli on input and output times.

III. EXPERIMENT 1

The purpose of this experiment was to assess the effect of two different types of stimuli on input and output latency. Sixteen right-handed volunteers from the Air Force military and DoD participated. Each subject viewed the word "initiate" or the letter "X" on a VT 11 CRT controlled by a PDP 11/34 mini-computer. The letter and word each appeared randomly five times. The participant was instructed to press one of two response keys, either the right or left key, once the stimulus occurred, and to continue depressing the key until the stimulus terminated. Unknown to the subject, the stimulus terminated when the subject performed ten key depressions. After the 10th key depression,

another stimulus occurred and another response sequence was executed in the same manner. After 10 stimulus trials, the sequence of events was repeated with the remaining key.

The right key was depressed with the index finger on the right hand, while the left key was depressed with the index finger of the left hand. The order of key use (right key then left key, or left key then right key) was counterbalanced between-subjects.

The first response latency and subsequent response latencies were subjected to separate two way ANOVAs (group to be placed in by hand by stimulus). The analysis of the latencies associated with the first response showed a significant interaction between the stimulus material and the hand used to perform the response, $F(1,14) = 5.10$, $p < .05$. This interaction showed no difference in latency between the right and left responses when the stimulus was the letter "X". However, when the stimulus was the word "initiate" the latency for the right response was shorter, by approximately 11 percent, than that for the left response (361 ms vs. 403 ms). The output latencies were influenced by the hand used $F(1,14) = 37.73$, $p < .01$. The right hand key was depressed faster than the left hand key (171 ms vs. 209 ms), an obvious finding since only right-handed subjects were used.

Following Teichner's approach, a subsequent analysis was performed on the input latencies, where the input latency is the first response latency minus the mean of the output latency for each trial. No significant main effects were observed. The previously observed significant interaction between stimulus material and the first response was not observed in this analysis.

IV. EXPERIMENT 2

The purpose of this experiment was to assess the effects of display load, classification decision rules, the proportion of targets, and interference stimuli on input and output latencies derived from the Teichner modification.

A. Method

The same sixteen volunteers used in the first experiment participated. The participants were randomly placed into two eight-member groups, with an equal number of males and females in each group.

One group of subjects viewed a four position columnar arrangement of Xs and Os. The remaining group of subjects viewed an eight position columnar arrangement of Xs and Os. The X was designated as the target letter and the participant's task was to identify the number of Xs contained in the column. For both groups, the proportion of Xs was .25, .50, and .75, and each occurred with a probability of 1/3.

The column of stimuli assumed two locations within a trial at different times. Position-1 was to the left of the center of the display. The duration of the column was 25 msec. Position-2 was to the right of the center of the display. Its onset occurred 3.525 sec after the onset of the first column and its duration was equal to the duration of the first column of stimuli.

Two different decision rule conditions were imposed. In condition-1, if the number of target items equalled or exceeded 50 percent of the total number of items displayed, then the target key was to be depressed a number of times equal to the number of target items that were presented.

In condition-2, if the number of target items equalled or exceeded 75 percent of the total number of items displayed, then the target key was to be depressed a number of times equal to the number of target items that were presented. These conditions were blocked within-subject factors and their order was counter-balanced between-subjects.

For condition-1 and condition-2 if the number of Xs was less than the designated proportion, the non-target key was to be depressed a number of times equal to the occurrence of the non-target letter.

The final independent variable was the occurrence of an interference stimulus. This stimulus was the sound generated by a VS11 terminal. It's probability of occurrence was .50 and if it occurred, it was initiated 250 msec after the onset of the left column and cycled on and off 12 times within a 1.54 sec interval. The interval between the onset of column 2 and column 1 was 7 sec.

Each participant received 144 trials for each decision rule condition for a total of 288 trials. Participants were run individually and were given a set of 18 practice trials of all combinations of the independent variables prior to the onset of the experimental conditions. The participant's station was situated in an acoustically treated room

and was monitored with a closed circuit TV. A mini-computer controlled the stimuli and recorded the sequence of responses and latencies associated with each response.

B. Results

The accuracy of the response and their associated latencies (first response latencies, output latencies and input latencies) were subjected to a 2 (display load) by 2 (decision rule) by 3 (proportion of targets) by 2 (side of display) by 2 (presence or absence of interference) split-plot analysis of variance. The raw data for the latency analyses were the mean of the latencies associated with each correct response over the 288 trials.

1. Percent correct. The percent correct was influenced by display load, $F(1,14) = 17.71$ $p < .01$, and the interference stimulus, $F(1,14) = 5.35$ $p < .04$. Both of these results were expected. Increases in display load resulted in decreases in accuracy, 92 percent for a display load of four items, and 57 percent for a display load of eight items. For those trials where the interference stimulus was absent, the percentage of correct responses was higher than those trials where the interferences stimulus was present, 77 percent versus 73 percent. Additionally, a significant interaction between the side of the display and the interference stimulus was observed, $F(1,14) = 9.05$, $p < .01$. This interaction, presented in figure 1, shows that on those trials where the interference stimulus occurred its effect was on the left display location. This effect was expected since the occurrence of the interference stimulus was during the presentation and response interval of the left display. No carry-over effect to the right display location was observed.

2. First response latency. The latency associated with a the first response when a correct series of responses occurred was influenced by display load, $F(1,14) = 20.07$, $p < .01$ and by the proportion of target items, $F(2,28) = 6.90$, $p < .01$. As expected, the first response latency was faster for a display load of four items than for a display load of eight items, 752 ms versus 942 ms. The function relating the proportion of target items to latency increased from 821 ms to 885 ms and then decreased to 835 ms for the .25, .50, and .75 values of the proportion of

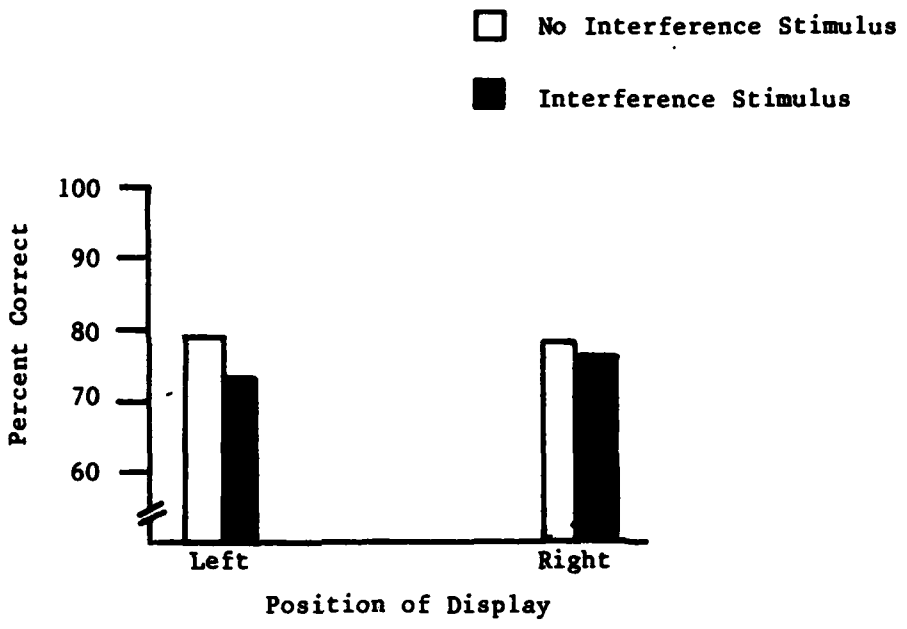


FIGURE 1. Percent correct as a function of the position of the display and the interference stimulus.

targets suggesting that the condition where the target and non-target items were evenly divided was a more difficult situation.

Significant two-way interactions occurred between the decision rule and the proportion of targets, $F(2,28) = 25.18$, $p < .01$ and between the location of the display and the interference stimulus, $F(1,14) = 6.97$, p .05. Significant three-way interactions occured a) between display load, the proportion of targets and the decision rule, $F(2,28) = 4.92$, $p < .02$, b) between display load, the proportion of targets and the interference stimulus, $F(2,28) = 6.61$, $p < .01$, and c) between the proportion of targets, the location of the display, and the interference stimulus, $F(2,28) = 8.56$, $p < .01$.

The display load by proportion of targets by decision rule interaction is presented in Figure 2. No interpretation of this interaction can be proposed at this time.

The proportion of targets by interference stimulus by display load interaction, presented in figure 3 suggests two points. First, when the proportion of targets is .50, the decision is the most difficult for both display conditions. Second, at that point the interference stimulus has both a facilitory effect for a display load of four items and an inhibitory effect for a display load of eight items. This interaction suggests that the time required to input the information and perform a classification is less for the smaller display size. Consequently, those processes are performed prior to the onset of the interference stimulus. For the larger display load, the amount of time to perform those processes increases, consequently the onset of the interference stimulus occurs with, and interfers with those input processes.

The proportion of targets by location of display by interference stimulus interaction, presented in figure 4, shows once again that the most difficult display condition is where the proportion of targets is .50. It is also at this value where the interference stimulus results in an effect. The onset of the interference stimulus occurs 250 ms after the onset of the left display location and is absent in all right display locations. The presentation of this stimulus facilitates the responses associated with the left display location but interferes with right display location responses. While it might be expected that the

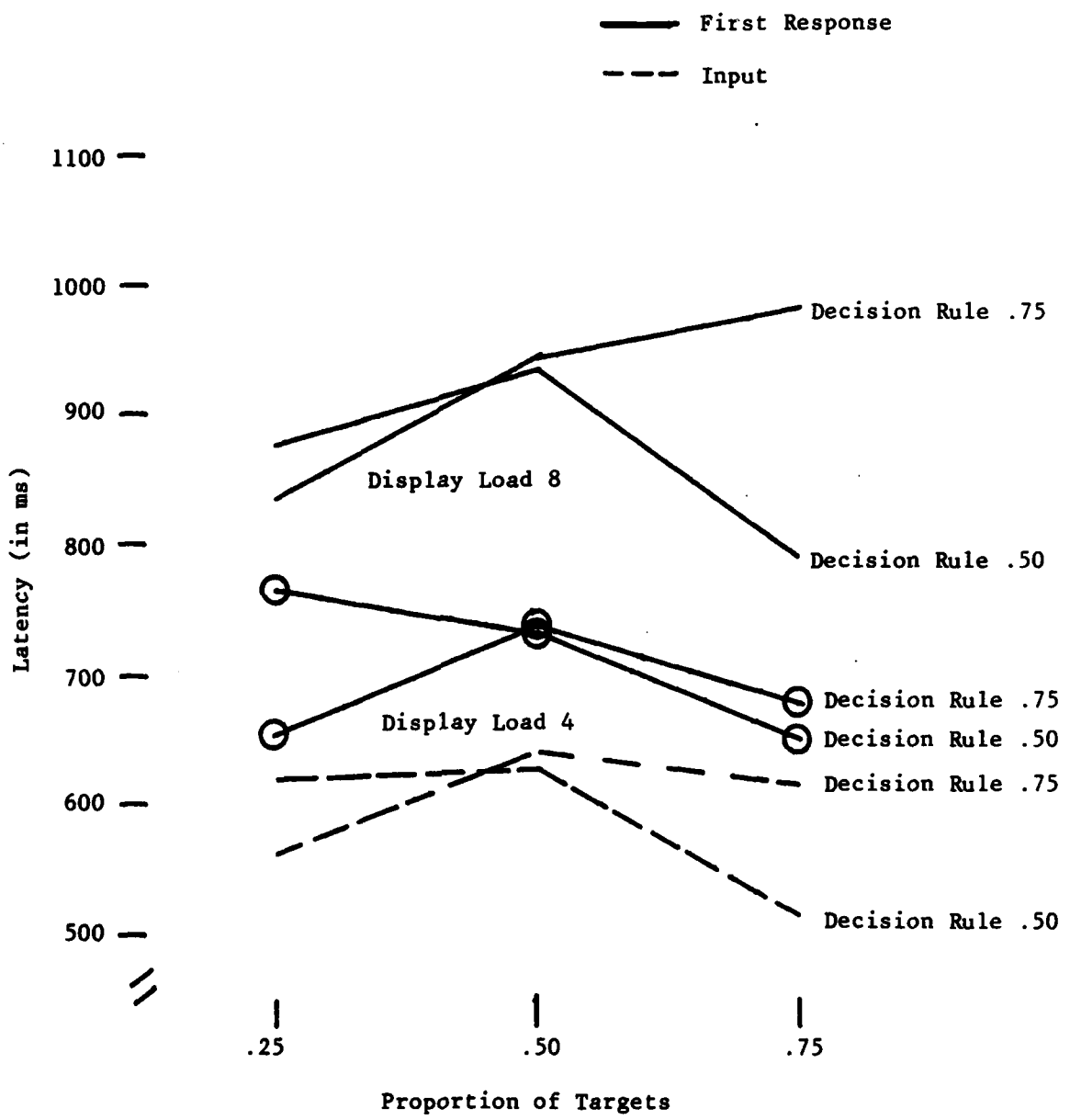


FIGURE 2. First response latency and input latency as a function of the proportion of targets with display load and decision rule as the parameters for the first response latency and with the decision rule as the parameter for the input latency.

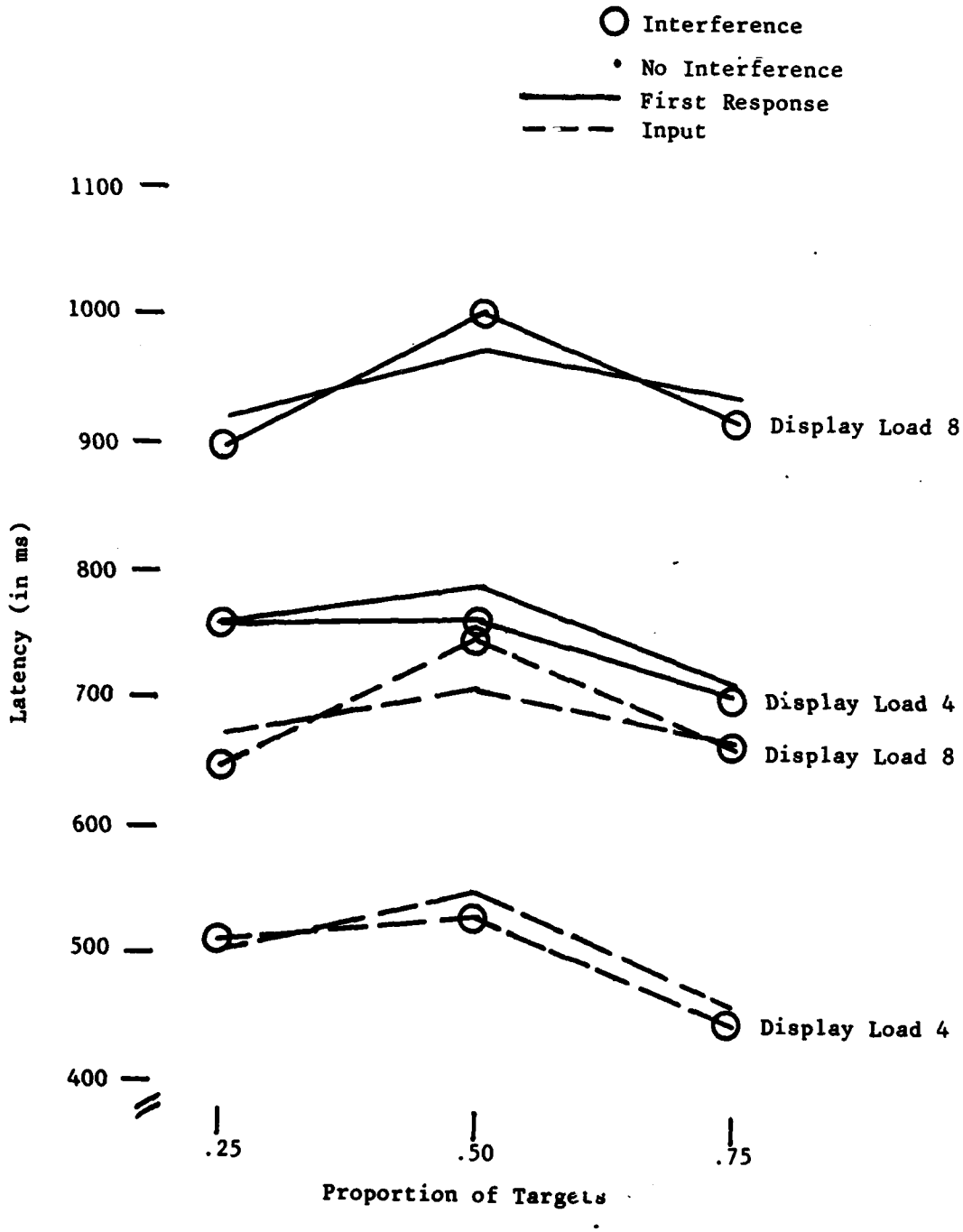


FIGURE 3. First response and input latencies as a function of the proportion of targets with display load and interference stimulus as parameters.

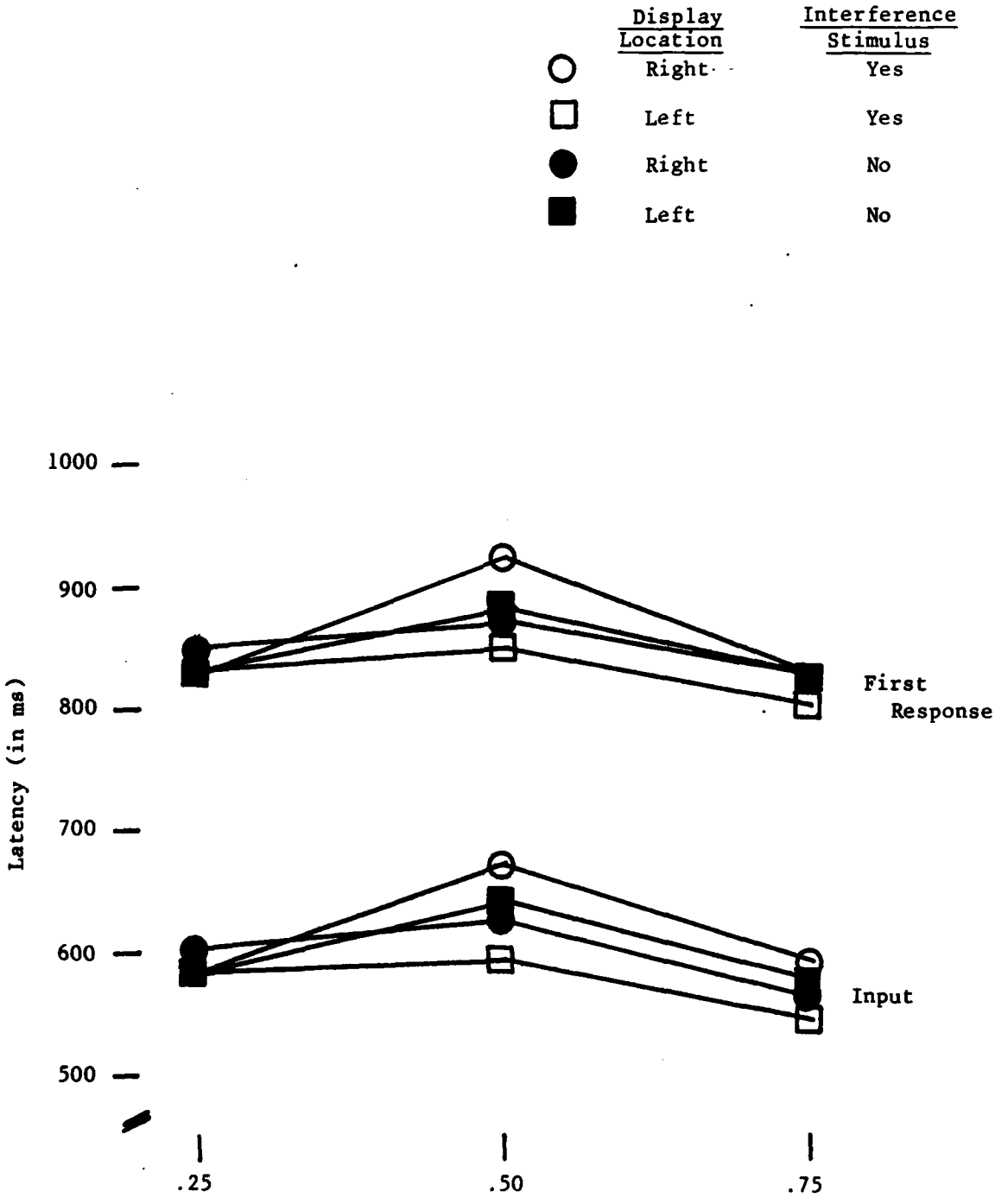


FIGURE 4. Latency as a function of the proportion of targets with display location and interference stimulus as the parameters.

12. G. R. Grice, "Stimulus Intensity and Response Evolution," Psychological Review, Vol 75, pp. 358-373, 1968.

13. W. H. Teichner, "Quantitative Models for Predicting Human Visual/Perceptual/Motor Performance," (NMSU-ONR-TR-74-3) New Mexico State University, Las Cruces, New Mexico, 1974.

REFERENCES

1. G. E. Briggs, "The Additivity Principle in Choice Reaction Time: A Functionalist Approach to Mental Processes," in R. F. Thompson & J. F. Voss (Eds.), Topics in Learning and Performance, (New York: Academic Press, 1972).

2. S. Sternberg, "The Discovery of Processing Stages: An Extension of Donders' Method," Acta Psychologica, Vol 30, pp. 276-315, 1969.

3. F. C. Donders, "Over de snekheid van psychische processen. Onderzoekinggen gecann in het Physiologisch Laboratorium der Utrechsche Hoogeschool," Tweede Reeks, Vol 2, pp. 92-120, 1868-1869, (Transl. by W. G. Koster, Acta Psychologica, Vol 30, pp. 412-431, 1969).

4. W. H. Teichner, "Temporal Measurements of Input and Output Processes in Short/Term Memory," The Journal of General Psychology, Vol 101, pp. 279-305, 1979.

5. R. G. Patchella, "The Interpretation of Reaction Time in Information-Processing Research," In B. Kantowitz (Ed.), Human Information Processing: Tutorials in Performance in Cognition, (Hillsdale, N.J.: Lawrence Erlbaum Associates, 1974).

6. S. Sternberg, "Memory Scanning: Mental Processes Revealed by Reaction Time Experiments," American Scientist, Vol 57, pp. 421-457, 1969b.

7. G. E. Briggs and A. M. Johnsen, "On the Nature of Central Processing in Choice Reactions," Memory and Cognition, Vol 1, pp. 91-100, 1972.

8. G. E. Briggs and J. M. Swanson, "Encoding, Decoding, and Central Functions in Choice Reactions," Journal of Experimental Psychology, Vol 86, pp. 296-308, 1970.

9. J. M. Swanson and G. E. Briggs, "Information Processing as a Function of Speed Versus Accuracy," Journal of Experimental Psychology, Vol 81, pp 223-229, 1976.

10. D. A. Taylor, "Stage Analysis of Reaction Time," Psychological Bulletin, Vol 83, pp. 161-191, 1976.

11. G. M. Corso and A. Warren-Leubecker, "Binary Classification: A Comparison of the Additive-Factor and Subtractive Method Approaches," submitted, 1982.

response demands. Nevertheless, this procedure may provide valuable information pertaining to cognitive processes that are either unobservable or masked using traditional partitioning methods.

This investigation has provided additional research questions such as the decrease in the latency to respond once the number of response items reached four. However, a much more interesting research idea stems from the finding that display load (when the proportion of targets is .50) and the presence of the interference stimulus interact on input latency. This finding suggests that variations in the onset of an interference stimulus may permit the identification of stages and the duration of those stages. If one assumes that the rate of accumulation of information about displayed items is constant, and that a certain amount of information must be accumulated prior to response initiation and that the criterion amount of accumulated information varies as a function of display load then the presence of an interference stimulus could have differential affects. For a display load of four items, the interference stimulus occurred after the information was accumulated thereby facilitating the response. However, for a display load of eight items, the stimulus occurred during information accumulation and, therefore, it inhibited accumulation. By keeping display size constant and varying the onset time of the interference stimulus, both inhibitory and facilitory effects should be found, and therefore, the time at which accumulation was complete could be identified. I propose to investigate this notion by varying the onset times of different types of interfering stimuli throughout the response latency interval. If variations in latencies as a function of the onset times occur throughout the response interval, then the total number and duration of stages of processing could be identified.

latencies for the response set of six items. One possible reason for this decrease in output latency may be due to the time available for responding. Since the inter-display interval was a constant the amount of time available for a response would decrease, and could, therefore, produce a decrease in the output latencies.

C. Discussion

The intent of this investigation was to apply a new method to the partitioning of binary classification latencies. The within-task subtractive method used in this study has provided information on output latencies and information on input latencies that was not obtained using a traditional reaction time method. In particular is the finding that the output latencies are sensitive to the number of response items, while input latencies are sensitive to the proportion of stimuli presented. While intuitively this finding would appear obvious, the within-task subtractive method supported that intuition. Other variables that would appear to influence input time but not output time, such as display load, on an intuitive level were experimentally supported.

On a theoretical level, the observed interaction between the interference stimulus, display load, and proportion of targets supports Grice's (12) notion of a variable criterion model, or Teichner's (13) A-component. Furthermore, the observed interaction between the proportion of targets, interference stimulus, and display location also supports the variable criterion model. The interference stimulus reduced the latencies when it occurred with the left display location. However, on those trials where the interference stimulus did occur, for the right display location, an inhibitory effect was observed. These findings would also support the variable criterion model in that the presence of the interference stimulus served to lower the response criterion and served to raise that criterion when the stimulus was absent.

V. RECOMMENDATIONS

The use of the within-task subtractive (WITS) method is recommended in all cases where reaction time measures might be collected. This procedure allows for the separation of input and output functions and permits investigations into these processes. However, it must be noted, that the use of multiple responses may change the task by increasing the

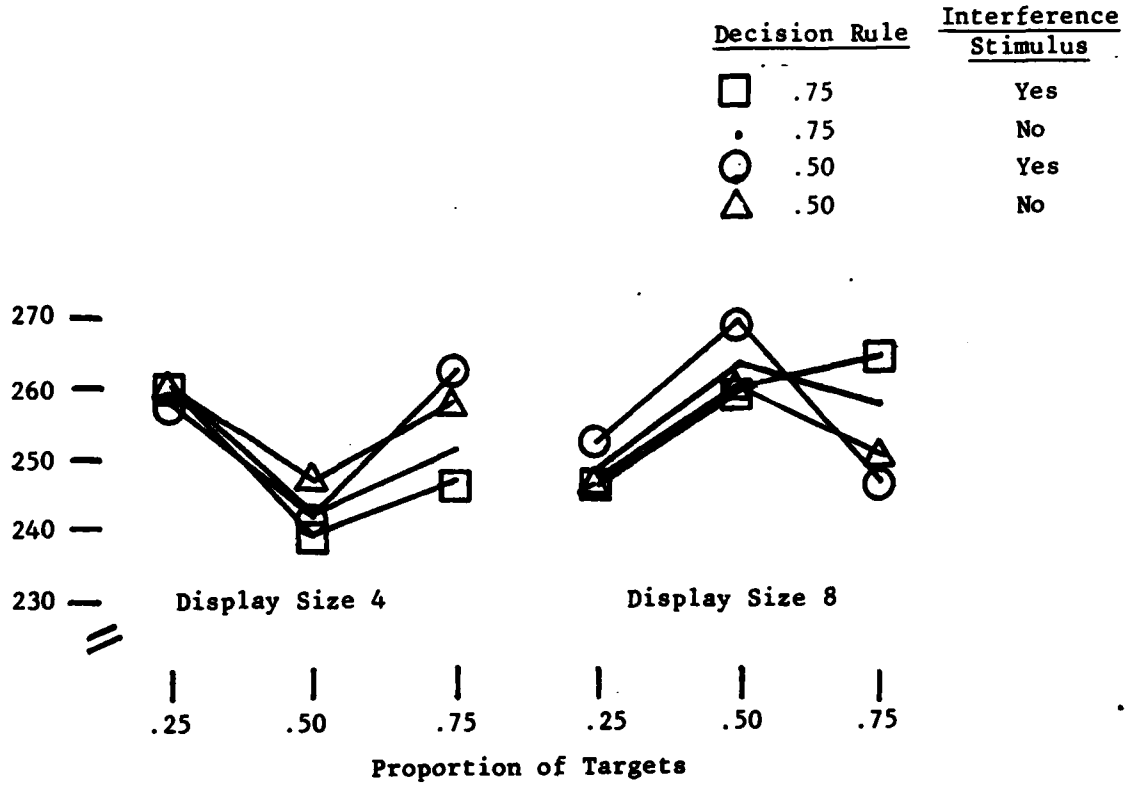


FIGURE 5a. Output latencies as a function of the proportion of targets with the decision rule and interference stimulus as parameters.

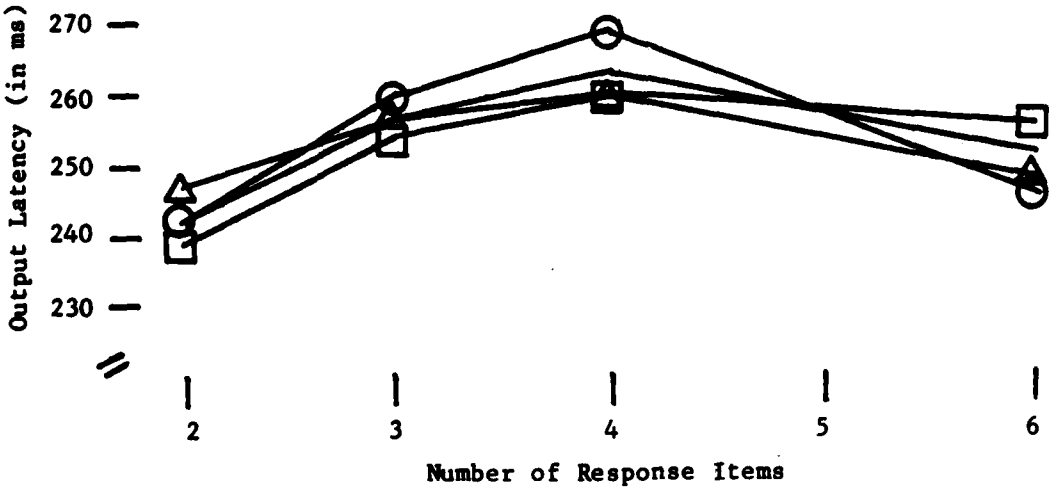


FIGURE 5b. Figure 5a recoded. See text for details.

by interference stimulus interaction, $F(1,14) = 8.08$, $p < .05$ was observed. A significant decision rule by proportion of targets interaction, $F(2,28) = 16.6$, $p < .01$ was also observed and is presented in figure 2.

The significant display load by proportion of targets by interference stimulus interaction, $F(2,28) = 6.18$, $p < .01$, and the significant proportion of targets by interference stimulus by display location interaction, $F(2,28) = 6.52$, $p < .01$ are presented in figures 3 and 4. The similarities between the first response and the input time latencies are obvious. The implications from the first response latency analysis appear to hold for the input latencies, suggesting that no information is lost using the Teichner procedure.

4. Output latencies. The analysis of the output latencies showed a significant main effect for the location of the display, $F(1,14) = 9.32$, $p < .01$. Output time was slower for the left display location than for the right display location (256 msec versus 251 msec).

The analysis also showed a significant display load by interference stimulus by proportion of targets by decision rule interaction, $F(2,28) = 3.82$, $p < .01$ and is presented in Figure 5a. The major portion of this interaction is, once again, where the proportion of targets is .5. There is an increase in output latency for a display load of eight items and a decrease in the output latency for a display load of four items. This interaction suggests that the proportion of target items is not the critical factor. In fact, by recoding the absissa to reflect the number of response items a better understanding of this function can be realized. Therefore, this interaction replotted as a function of the number of response items is presented in figure 5b.

Figure 5b suggests that the output latency is an increasing function of the number of items, up to and including four items. Newman-Keuls multiple-comparisons of the original interaction show that in general, ($p < .05$) the output latencies for the response set of two items for display load four are significantly different from the response set of four items for display load eight. However, the latencies associated with the three and six response items were not significantly different from any other conditions. This suggests a decrease in the output

latencies associated with the right display location on the interference stimulus trials should be equal to the latencies on those trials without the interference stimulus, this does not occur. This suggests that the interference stimulus when it is occurring reduces a criterion for responding but that the value assumed by the criterion changes when the stimulus changes. Furthermore, the sudden shift, from an interference stimulus to no interference stimulus within a trial results in a larger change, or a rebound effect in such a way as to overshoot the normal non-interference trial criterion position. However, an alternative explanation could also be that since the interference stimulus was also present during the response interval associated with the left display location, the interference stimulus was being processed and that it inhibited the encoding and processing of the visual stimuli in the right display location.

3. Input latency. The primary purpose of this investigation was to investigate a new method in the partitioning of latency, and to use the method to gather additional information that could not be gained by traditional approaches. A traditional approach was demonstrated with the analyses of the first response latency. It should be recalled that the first response latency contains both input processing time and output processing time. Therefore, the input latency was derived by subtracting the mean output latency for a trial from the corresponding first response latency. In relation to the first respone time analysis, all main effects and all interactions, with the exception of the display load by decision rule by proportion of target interaction which were found to be significant in the analysis of the first response latency, were also significant in the analysis of the input latencies.

The main effects of display load, $F(1,14) = 11.98$, $p < .01$ and the proportion of targets, $F(2,28) = 7.02$, $p < .01$ were significant. However, a third main effect, of the location of the display, was also significant, $F(1,14) = 5.49$, $p < .05$. The left display location was faster than the right display location, 587 msec to 603 msec. While this finding was not surprising, since the left display always occurred first, people read from left to right, etc., it is surprising that this effect was not observed in the prior analysis. A significant display location

1982 USAF-SCEEE SUMMER FACULTY RESEARCH PROGRAM

Sponsored by the

AIR FORCE OFFICE OF SCIENTIFIC RESEARCH

Conducted by the

SOUTHEASTERN CENTER FOR ELECTRICAL ENGINEERING EDUCATION

FINAL REPORT

EVALUATION OF THE NON-DESTRUCTIVE TESTING OF AIRFIELD PAVEMENTS: WAVE PROPAGATION ASPECTS

Prepared by:	Dr. Robert A. Douglas
Academic Rank:	Professor
Department and University:	Department of Civil Engineering North Carolina State University
Research Location:	Air Force Engineering and Services Center Engineering Research Division, Airbase Facilities Branch
USAF Research Colleague:	Major John Centrone
Date:	July 28, 1982
Contract No:	F49620-82-C-0035

EVALUATION OF THE NON-DESTRUCTIVE TESTING OF AIRFIELD PAVEMENTS: WAVE PROPAGATION ASPECTS

by

Robert A. Douglas

ABSTACT

Two different systems are currently being developed for the non-destructive testing (NDT) of airfield pavements. The two systems are evaluated here from the standpoint of their data collection schemes and the hypotheses on which the initial data processing is based. It is found that each system has critical points where understanding of the physical phenomena and of the fundamental nature of the mathematical processing of experimental data is yet to be fully established. Such points are identified and suggestions made for their resolution and for continued system development.

Next, it is suggested that it would be useful for the AF to possess an additional NDT system capable of being easily transported to airfields with which the AF has no experience, to be able to predict, in a matter of hours, runway carrying capacity for near term use. Requirements, functional hypotheses and system elements are described.

Finally, it is recommended that (1) research be initiated to establish a firm basis for the near-source use of Rayleigh waves to determine properties of the multi-layered and slabbed solids found in pavement systems, and (2) that exploratory efforts be undertaken to determine the feasibility of a light, rapid return NDY system. Of great importance,(3), an extension of time-signal analysis theory is needed to cover cases of separate signal entry times and multiple phasic discontinuities.

Acknowledgement

The author takes this opportunity to thank the Air Force Systems Command, the Air Force Office of Scientific Research, the Air Force Engineering and Services Center, and the Southeastern Center for Electrical Engineering Education for the opportunity to spend an interesting and enjoyable summer at Tyndall AFB FL. He wishes to make special mention of the hospitality and general helpfulness extended by all of his colleagues and associates at Tyndall.

In particular he wishes to thank Major John Centrone, his personal mentor, for the guidance, encouragement and unflagging help that was always available.

Finally, he must mention those very close associates whom he will miss as he returns to the cooler climates of North Carolina:

Lt Col J. E. Goin

Capt. J. D. Wilson

1 Lt R. A. McDonald

and two Good Samaritans:

Maj David Flaa

Mr. L. M. Womack

Mr. J. G. Murfee

Mr. H. R. Marien

I. INTRODUCTION:

Airfield pavements are the most important ground structures belonging to the Air Force. To the pilot they sometimes mean dangerous assaults on tires, on landing gear, and on the stability of his aircraft; yet in the larger sense, they are a magic skin laid over a generally hostile earth to provide smoothness and structural support found only occasionally in nature.

The airfield pavement is a multi-layered structure living in an environment of fluctuating temperatures and moisture, experiencing repeated dynamic loading of varying magnitudes. A permanent pavement is expected to last under continued service for many years; an alternate, emergency runway, may be designed to sustain only a few hundred loadings, perhaps only for a few days. Both systems experience a continuous chain of circumstances which tend to degrade them and therefore the engineer faces, about both, the same questions: What is its condition? Is it safe? How long will it last?

Those same questions are so continual and so widespread in the technological world that they have led past the dicipline and methods of initial quality control and on to the growth of an area of research, and to an industry and to widespread application of what is called nondestructive testing (NDT). The goals of the Air Force are precisely those of NDT; to find means to inspect the interior, the volume, of a part of structure and using the information obtained, determine its condition without altering the structure.

One of the principal tools of NDT is found in application of the theory and methods of the field of stress wave propagation in solids. Stress waves are used as part of an active diagnostic system, as invaders of the volume, so that by observing alterations of velocity and phase, or by reflection, refraction and diffraction effects, or by scattering theory, the condition of the interior may be determined.

The author's own qualifications are in the areas of impact and wave propagation, and as an experimentalist in those areas.

II. OBJECTIVES OF THE RESEARCH EFFORT

The objective of this effort were as follows:

1. Of the two NDT systems presently being developed for the Air Force, one of them employs wave propagation methods to generate data to be used subsequently in a finite element pavement model. The effort here was (a) to examine the hypothesis associated with wave propagation, (b) to examine the computational algorithms making use of the data gathered (c) to appraise the effectiveness of the signal generater and the overall experimental scheme, (d) make suggestions for continued development of the system.

2. The other NDT system is a "deflection basin" system, designed to move continuously along a runway, making semi-continuous measurements of the depth of its self-created deflection basin as it goes. The effort here again was directed to the data gathering portion of the system, but this time viewing it not with special experise but rather from the standpoint of an experimentalist familiar with hardware problems.

3. To suggest other application in which the theory and methods of stress wave propagation could be employed to the benefit of the Air Force and to outline the requirements and operating parameters for such systems.

4. To make recommendations for any research which is indicated as a result of the efforts above.

III. THE WAVE PROPAGATION SYSTEM OF NMERI-CERF

III.1. Introduction

The Civil Engineering Research Facility (CERF) of the New Mexico Engineering Research Institute at Albuquerque NM (NMERI) has been developing for the Air Force a self contained air-mobile pavement testing van which houses the data collection system and a computer for initial data analysis. This system employs a falling weight stress wave generator and functions by detecting the waves and analyzing them to determine elastic constants for the individual material layers that make up a particular runway. The elastic constants are employed later in a finite element program to produce the desired output. The system is described well by Wang (1981),(the author's predecessor, SCEEE Fellow 1981), by Marien and Baird (1981), by Baird (1981), and by Nielsen and Baird (1976).

Appraisal of the system followed study of the principal sources, (above), study of letter reports to AFESC Project Officers, discussions with AFESC personnel, and also involved a visit to UNMERI-CERF where the system was examined personally and was discussed with the principal investigator, Baird (1982).

III.2. Observations

The system is:
- (a) self contained
- (b) air mobile
- (c) capable of generating stress waves
- (d) equipped with hardware and softwave to
  - (i) detect stress waves
  - (ii) process the signals

III.3. Reservation, Questionable Points

The following points are to be resolved before the NMERI-CERF system becomes operational.

1. The only test results seen have been those obtained on one asphalt pavement. For several reasons such a pavement is more favorable to the system than is a rigid pavement, even though the system is directed specifically towards rigid pavements.

2. There is no evidence that tests are reproducible.

3. There is no evidence that tests give proper results.

4. It is not clear that the design of the signal generator and of the instrumentation system takes into account the nature of a rigid pavement, that its surface layer customarily is made up of imperfectly and variably joined slabs.

5. The signal generator does not seem to be designed to produce pulses with specific durations, with specific wavelength content.

6. It is not clear that the instrumentation array designed to maximize "clean time" and to define the character of joints.

7. It is not clear that individual frequencies of Rayleigh waves are all fully formed when picked up by the transducers. This is a fundamental point bearing on the permissible use of Rayleigh wave information.

8. Fourier tranform processing of received signals is being used as a step in determining a dispersion curve. It is pointed out here that the systems being studied are all layered systems and rigid pavements have slabbed top layers as well. The consequence is that every signal received by each transducer probably is a "dirty" signal, contains information from both direct waves and from reflected and/or

refracted waves; futhermore, that information comes in at different times within a given observational window. Use of the Fourier transform to analyse such a signal is improper.

9. It is not clear how the information is used to determine the condition of intermediate layers of a layered system. This too, is a critical point.

10. No evidence has been seen relating to resolution, sensitivity, and stability of the combined data collecting and processing system, or of its elements.

III.4. Plan for Continuing Development*

a. Initial tests.

i. Resolution

ii. Reproducibility

iii. Ability to determine layer parameters

iv. Comparison with known values

b. Engineering Development

i. Redesign and fabricate improved thumper

ii. Design and catalog accelerometer arrays and software routines tailored to pavement structures.

c. Project Related Research

i. Development of Rayleigh waves

ii. Relate despersion curve to intermediate layers

iii. Effects of slabbed surface layer

iv. Describe resolution, sensitivity, stability

* A separate, detailed version of this plan has been prepared for HQ AFESC/RDCF.

d. Project Related Research

i. Define geometry of pavement whose structure not well known.

ii. Determine the properties of multi-layered and buried pavement systems.

IV. THE HARR-PURDUE-W.E.S. DEFLECTION-BASIN SYSTEM

IV.1. Introduction

Professor M.E. Harr of Purdue Univerisity has been developing, over a period of a number of years, the background of research needed to permit the prediction of remaining life of flexible pavements, based on the measure of the total deflection that a pavement has undergone, determined by the current response of the pavement to a known load. This work over the years is documents (in part) by Harr and Elton (1981), Baladi and Harr (1978), Highter and Harr (1975), Boyer and Harr (1974).

Immediately pertinent here, Prof. Harr has proposed, and has done initial work at Purdue University on a system, also NDT, wherein a load vehicle is driven along a pavement to create a moving deflection basin. Central to this system is the use of laser deflectometers mounted on the load vehicle.

At present,four laser deflectometers are employed, mounted in a line in the direction of motion of the vehicle. Three of them, a foot apart, have the responsibility for establishing and maintaining a base line to which all subsequent measurements are referred, and of continually extending one "foot" out onto new territory and then moving that knowledge back to the next two.

The fourth laser deflectometer is at the location, fore and aft, of the deflection basin and makes a nearby measurement used to determine the maximum depth of the basin.

The laser deflectometer system is under development at the Waterways Experiment Station (W.E.S.) of the Corps of Engineers, Vicksburg, with Prof. Harr as consultant.

This limited appraisal of the system has followed study of the prinicipal documents, discussions with AFESC personnel, discussion with Prof. Harr, Harr (1982), and with Mr. Bush of Waterways Experiment Station, Bush (1982).

This author's experience only permits him to comment on a few aspects of the measuring system.

IV.2. The Measuring System.

This measuring system is a very clever and ambitious one. It proposes to make, on the fly, in real time, measurements of considerable accuracy. The measurement of the depth of the deflection basin should be sensitive to 0.001 inch and better. To establish a baseline that will hold up throughout a measurement distance of perhaps two miles along a runway, and for a time of perhaps 20 minutes or more, requires a high degree of accuracy.

The laser deflectometers are mounted one foot apart. If we, on this page, decide arbitrarily that the baseline may deviate from straightness by one foot over the 10,000 ft of a two mile runway, that corresponds, in the distance between two lasers (1 ft), to 0.001 ft or to 0.0012 inch.

The laser deflectometers are rated at 0.0005 inch/inch of standoff distance (laser to detector) and the 5 inch distance actually employed puts us at 0.0025 inch.

Here is the central hypothesis: By making repeated measurements and averaging them, it is possible to improve accuracy, to increase the number of significant figures.

This system employs that hypothesis by firing the lasers at a high repetitive rate and thus essentially making many measurements at the same spot.

IV.3. Reservations.

Repeated measurements are properly used to improve the accuracy of measurement. This author does not know the total number of laser firings at one point. His impression, Harr (1982), is a number in the thousands.

This author seems to remember a comment by one of his own professors when he was a student that as the number of repeated mearsurements becomes large, they no longer improve the accuracy; rather, the measurements begin to cluster about values corresponding to the consequences of individual sources of error.

A second factor that must be considered is that an on-board computer is continually reworking all the measurements and using them in simple computational algorithms. Of necessity, the algorithms are going to subtract one number from another, to subtract a measurement at one spot from a measurement at another spot, and since the numbers will be very close to the same value, many significant figures will be stripped away at each subtraction. This, done thousands of times, will do what?

The entire laser deflectometer system is mounted as a unit. It involves a "strong back", a truss stiff toward loading in one plane only. Transverse sway and torsion of the truss about its logitudinal axis may disturb the measurements.

It is not clear that the computational algorithm can successfully reject all frequencies of superimposed motion of the measurements sytem, caused by the motion of the vehicle, jar, shock, etc.

It is suspected that the measurement of laser spacing is a non-trivial matter, that both the actual physical location of a laser beam "center" and the pulse generated from a fifth wheel, used to define each new step forward, must be very percise.

IV.4. Recommendations.

This system is exceeding simple (brillant) in concept, sophisticated in operation, and hard to test. The accuracy with which it proposes to define a runway surface is beyond our ability to set up a suitable test track of a length to properly challenge the system. Accordingly it is suggested here that the following tests, rather simple, may help determine the response of the system.

1. Test the algorithm by a manufactured numerical input to the computer in which the (manufactured) input numbers (imaginary imput from the lasers,) oscillate back and forth by small amounts about a constant, E.A. 10.001, 10.002, 10.000, 9.998, etc. It will be known clearly what surface is being represented: flat, with irregularities of a chosen magnitude.

2. Test the overall system, data gathering and analysis, while not moving and aimed constantly at the same stretch of floor-preferably a plane target with the relative positions of the four spots to be queried by the lasers already established by careful measurement. Operate the system for a time period and in manner comparable to the act of traversing two miles of runway at (?) 5 mph.

   a. Repeat several times.

   b. Tilt the test bar very slightly, repeat several times.

3. Set up once more as 2. above, but with the laser deflectometer system suspended at its regular mounting points from springs, to be operated again for a time period and in a manner comparable to a runway test, this time to be jostled repeatedly, struck at the mounting points with a rubber mallet (automotive type), tugged, etc., to cause random motion with a variety of frequencies. This is not a destruct test. Abuse is to be directed at the algorithms, not at the structure.

IV.5. Some Expected Results.

1. The strong back will need to be made more torsionally stiff.

2. Spacings of the lasers along the strong back must be very carefully measured.

3. To accomplish 2. above, center of brilliance of laser must be determined very accurately.

4. The rotation of the fifth wheel be done very carefully.

V. AN NDT SYSTEM FOR RAPID RETURN PAVEMENT EVALUATION

V.1. Origin of Problem

Recent events (Falklands, Iran) make it seem inevitable that the Air Force will be asked to operate from airfields about which it has little information.

Add to that a reasonable possibility that the situation might call for a number of heavy aircraft (evacuation, catastrophe, reinforcement, etc.), that it might be desirable to start operations in 24-48 hours, and that the national or international pressure to do so might be very great.

Although the Air force has an extensive catalog of airfields world-wide, the catalog cannot be complete nor can the information be extensive enough to predict runway safety for repetitive use.

For one or two aircraft the Air Force might choose to go ahead and try. For ten aircraft the answer might have to be, with regrets, no.

The situation could be clarified to the better posture of the Air Force if quantitive information were available, describing subsurface conditions of the runways and in a matter of hours. But at this time the Air Force is limited to landing an experienced person to look at the field, drive over it, stomp on it, and make a pronouncement.

V.2. Action

It is suggested that the Air Force begin development of a non-destructive testing (NDT) system for rapid return pavement evaluation.

V.3. Requirements

1. Should be capable of providing evidence of subsurface conditions in a matter of several hours.

2. Should be very light-weight, a few hundred pounds, elements hand portable.

3. Jeep portable on site.

4. Two men maximum.

5. High degree of redundancy.

6. Data suitable for immediate evaluation and for later, more detailed analysis.

V.4. Solution

An NDT system to do such a job probably would be a wave propagation system drawing on NDT technology already in hand but far simpler than the NMERI-CERF system discussed earlier in this report. A possible configuration follows:

1. A man-portable falling weight stress wave generator would produce signals.

2. Signals would be detected by unbonded, grease coupled, dead weight loaded, piezoelectric transducers.

3. Signals would go directly to a portable storage oscilloscope with camera for trace recording.

4. Detected wave form signatures would be compared with "catalog" results to determine structure and condition.

V.5. Spinoff to Individual Airfields

The system described probably would cost less than $10,000 (without redundancy). Once a catalog of standard signatures has been prepared this single system could be a part of the equipment of individual Air force bases and civilian airfields for regular use between definitive inspections.

V.6. Acoustic Emission

Another wave propagation tool deserves to be looked at carefully as a possible candidate for airfield pavement evaluation. Acoustic emission (AE) is a relatively new experimental tool which is base on detecting self-generated internal noise produced by a structure or part as it is loaded. Such "noise" actually is the wave propagation from the growth of cracks, the tearing of inclusions, highly localized plastic deformation, etc. In the case of a rigid pavement system, it would be noise (probably high frequency) emanating from the concrete layer, noise (lower frequency) from the base course as gravel grates together.

AE holds the suggestion (not promise) that if it works at all, it could provide a means for continuous evaluation of rigid pavements akin to the Harr method for flexible pavements. In this on-the-fly application it would depend for success on an ability to detect waves coming to a pavement surface and coupling with the air, then detecting and analysing the air response.

VI. Recommendations

VI.1. Introduction

It is difficult for this author to conceive of the cost and value of the aifield pavements owned by the Air Force. He is convinced of their overall advanced age and that they are generally certain to be entering a stage of accelerated deterioration. He is convinced that NDT methods of pavement testing must be improved and their use extended so that deteriorations may be detected early and repairs effected in a planned and economical way rather than on an emergency (and costly) basis. The following recommendations are pertinent to the development of some, but not all, of the NDT methods involving wave propagation. Not mentioned, for instance, are the pulse transform methods and the potential for near surface reflection surveys.

VI.2. Research Associated with Rayleigh Wave Analysis

It has been recognized for sometime, Finn et al, Jones (1966) that the spectral study of Rayleigh waves, normally non-dispersive, dispersive in the presence of layered media, offers a way to determine the properties of individual buried layers of pavement systems otherwise inaccessible except by destructive tests. Baird (1981,1982) seeks to make use of Rayleigh wave dispersion. Heisey et al (1982) describe its potential use and describe the spectral analysis to determine constituent wave length velocity relationships. Just now, with recent developments in transducers and the astonishing computational ability of microcomputers, the use of Rayleigh wave dispersion analysis is

about to become a reality for the study of pavement systems.

There are several important questions to be answered by research before it will be possible to design instrumentation arrays properly for Rayleigh wave analysis. Until the questions are answered, some results will be valid, other results will be invalid and there will be no way of distinguishing between them.

These are the questions:

1. At what distance from the wave source have individual wavelengths become fully established?

2. What is the relationship between Rayleigh wave dispersion and the properties of intermediate layers?

3. When one layer of a layered system is made up of slabs, what happens to Rayleigh waves after reaching slab boundaries?

4. How do Rayleigh waves behave in the presence of buried surface layers?

VI.3. Research Associated with Suggested/Rapid Return NDT System

These are low intensity level efforts directed toward determining feasibility. Both should be done.

1. Wave propagation system:

a. Determine the level of visual discrimination that is possible, at the as-received waveform level between trial results for flexible and rigid pavement systems in various conditions.

b. Determine the extent to which results are reproducible.

2. Using a bread-boarded acoustic emission system:

a. Determine the level of response available and the possibility of attributing certain responses to certain layers.

b. Determine the possibility of detecting AE with a moving transducer.

c. Determine the possibility of associating levels of frequencies with certain layers and conditions.

d. Determine extent to which results are reproducible.

VI.4. Time Signal Analysis

A very fundamental problem relating to time signal analysis has surfaced in the method of analysis proposed by the contractor for the NMERI-CERF NDT pavement testing system. What they have done essentially, is to attempt to transfer from one successful experimental scheme and an appropriate method of analysis to a different experimental scheme together with what is intended to be an appropriately transformed (pun not intended) method of analysis. The entire effort is a desireable one and will be successful.

But the new method of analysis begins with Fourier transformation of a time signal in an interval during which different signals, each containing frequencies common to the others, enter at different times, and of course with different amplitudes and phases. Not only that, it is intended that the analysis produce and display discontinuities in phase of a well-ordered signal, in fact, as many as four discontinuities for significant frequencies.

This comes about basically as a result of signals of the same frequency but different wavelengths associated with the different layers of a layered half-space. The original system dealt with a single frequency at a time, physically, and systematically explored the number of wavelengths present.

What must be done is to examine the Fourier transform carefully to see if and how it may be possible to extract more information from the transform, for instance, to be able to identify and separate out multiple entries. And, with analysis and experimental scheme considered together, to learn how to modify the latter so that the information needed can become available.

REFERENCES

1. Baird, G.T. (1981), Letter Report to Capt J.D. Wilson, AFESC/RDCF Tyndall AFB FL, December.

2. Baird, G.T. (1982), Discussions held at the Civil Engineering Research Facility, U of New Mexico Research Institute, Albuquerque, June.

3. Baladi, G.Y., and Hann, M.E. (1978), "Nondestructive Pavement Evaluation: the Deflection Beam," Transportation Research Record 666, TRB-NAS.

4. Boyer, R.E. and Harr, M.E., (1974), "Predicting Pavement Performance," Trans, Engr. Jn., ASCE, May.

5. Bush, A.J. (1982), Discussions held at AFESC, Tyndall AFB FL in June. Represents Waterways Experiment Station, Corps of Engineers, Vicksburg MS. Directly concerned with development of Harr system.

6. Finn, F.N.; McCullough, B.F.; Nair, K.; Hicks, R.G.; (1966) "Plan for Development of a Nondestructive Method for Determination of Load-Carrying Capacity of Airfield Pavements," Final Report R.N. 1062-2(f), Materials Research and Development, Inc. to U.S. Nanal Civil Engineering laboratory, CR67.016, November.

7. Harr, M.E. (1982), Discussions at AFESC, Tyndall AFB FL, May.

8. Harr, M.E., and Elton, D.J., (1981), "Non-contact, Non-destructive Pavement Evaluation using Prototype Loads," TRB Task Force A2T56 Meeting, June.

9. Heisey, J.S.; Stroke, K.H., II: Meyer, A.H. (1982),"Moduli of Pavement Systems from Spectral Analysis of Surface Waves," Trans. Res.Bd, 61st Ann. Mtg, Jan.

10. Higher, W.H., and Harr, M.E., (1975), "Cumulative Deflection and Pavement Performance," Trans. Eng. Jn., ASCE, v.101, TE3, Aug.

11. Jones, R., (1966), "Measurement of Elastic and Strength Properties of Cemented Materials in Road Bases," Highway Research Record 128, HRB.

12. Marien, H.R., and Baird, G.T. (1981), "U.S. Air Force Nondestructive Airfield Pavement Evaluation Method," TRB Task Force A2T56 Meeting, June.

13. Nielsen, J.P., and Baird, G.T., (1976), "Pavement Evaluation System," Final Report 1 Dec 1975 - 30 Sep 1976, UNM-CERF to AFESC, Air Force Systems Command, Tyndall AFB FL, August.

14. Nielsen, J.P., and Baird, G.T., (1977), " Evaluation of an Impulse Testing Technique for Non-destructive Testing of Pavements and Recommended Follow-on Research," Report for period 18 Oct 1976 through 18 July 1977, by UNM-CERF for DET 1 (CEEDO) HQ ADTC, Air Force Systems Command, Tyndall AFB FL July.

15. Sun, G.T., (1970), "Surface Waves in Layered Media," Bull. of the Seismological Soc. of AM., 60,2,345, April.

16. Wang, M.C., (1981), "An Evaluation of the Air Force Pavement Non-destructive Testing Method," Final Report, 1981 USAF-SCEÉE Summer Faculty Research Program, Contract No. F49620-79-C-0032, Aug.

1982 USAF-SCEEE SUMMER FACULTY RESEARCH PROGRAM

Sponsored by the

AIR FORCE OFFICE OF SCIENTIFIC RESEARCH

Conducted by the

SOUTHEASTERN CENTER FOR ELECTRICAL ENGINEERING EDUCATION

FINAL REPORT

AMIS - ACQUISITION MANAGEMENT INFORMATION SYSTEM

PROBLEMS AND PROMISES

Prepared by:	Dr Hamed Kamal Eldin
Academic Rank:	Professor
Department and University:	Industrial Engineering and Management Oklahoma State University
Research Location:	Air Force Systems Command (AFSC/PMQ)
USAF Research Colleague:	Colonel John D. Voss
Date:	August 15, 1982
Contract No:	F49620-82-C-0035

AMIS - ACQUISITION MANAGEMENT INFORMATION SYSTEM

PROBLEMS AND PROMISES

by

Hamed Kamal Eldin

ABSTRACT

Due to the sophistication of modern military equipment, the Air Force acquisition cycle and the government contracts are complicated instruments involving large volumes of paperwork. In order to improve the contracting procedure, AFSC developed the Acquisition Management Information System (AMIS).

Like any relatively new system, AMIS has successes and failures.

The purpose of this report is to evaluate the positive and negative aspects of the system and to present recommendations for effective utilization of the system. The report also explores the future directions of AMIS and recommends short-term and long-range plans for its successful utilization.

ACKNOWLEDGEMENT

The author would like to thank the Air Force Business Research Management Center and the Southeastern Center for Electrical Engineering Education for providing him with the opportunity to spend an interesting and worthwhile ten weeks in Wright-Patterson Air Force Base, Ohio.

The author would like to thank Colonel R. Deep and his colleagues at AF/BRMC for their cooperation and providing excellent working conditions. He would also like to thank Colonel John D. Voss and his colleagues at AFSC/PMQ for their collaboration and assistance in conducting this study.

AMIS - ACQUISITION MANAGEMENT INFORMATION SYSTEM

PROBLEMS AND PROMISES

I. INTRODUCTION:

AMIS, like any relatively new system, has many successes and failures. AMIS management must spread the word about its achievements while trying to resolve the problem areas.

The purpose of this report is to discuss the present status of AMIS; the positive and negative aspects of the system, and to present recommendations for effective utilization of the system. The report also explores the future of AMIS and recommends short-term and long-range plans for its implementation.

II. PURPOSE OF AMIS:

AMIS has been developed by Air Force Systems Command (AFSC) to provide:

1. AFSC response to the Department of Defense Military Standard Contract Administration Procedures 4105.63M (DOD MILSCAP) effort.
2. Automated support for Air Force Contract Management Division (AFCMD) payment function.
3. On-line Management Information System (MIS) capability for AFSC users at all levels.

Did AMIS achieve its purpose?

Today, at its present status, AMIS is a straight retrieval system with capabilities to serve the first two objectives mentioned above. The main thrust of the system is to provide capabilities for exchanging existing contractual data in an automated standardized format with the other components of DOD.

AMIS is not a MIS; a more appropriate name for this system would be Contract Information Retrieval System. AMIS today does not effectively accommodate the third objective mentioned above. . .

III. PRESENT STATUS OF AMIS:

Prerequisites for a system's success

Most successful systems have the following prerequisites in common:

1. Top management support is essential.

2. A system succeeds when it satisfies users needs rather than a directive from above.

3. A good system documentation and training program.

These three yardsticks will be used in evaluating AMIS successes and failures.

A. AMIS ACHIEVEMENTS:

1. AMIS has been more effective in the divisions where management support has been observed. The Space Division, Los Angeles AFS, CA is an example where AMIS was accepted by top management. Consequently, frequent use and increased dependence on AMIS led to the success of its implementation.

2. To a great extent, AMIS successfully implements MILSCAP. If AMIS was not available, another automated system must be developed for this purpose.

3. AMIS has standardized the preparation of AFSC contracts in the Uniform Contract Format (UCF) as required by the Defense Acquisition Regulation (DAR). Source Data Automation (SDA) is the AMIS method of automatically capturing contractual data in UCF during the preparation of the forms.

4. AMIS provides support for AFCMD for the disbursement function. It provides complete funding data on the contract and serves as the check and balance on contract obligations and expenditures. A by-product of AMIS

compliance with DAR has made AMIS a useful tool in procurement training.

5. AMIS has provided valuable services for many users in the last few years. There is no doubt that it has been used more and more every year. Actually, in the last three years (May 79 to May 82) the number of queries received by AMIS increased from 5,000 to approximately 18,000 which is an indication of continued improvement of the system utilization.

B. PROBLEMS AND RECOMMENDATIONS:

Considering the above prerequisites for a system's success, AMIS needs improvements in top management support, users satisfaction and systems documentation and training. The following paragraphs will address these problem areas and present recommendations for system utilization/improvement.

1. Management Support

Top management support is the main prerequisite for a system's success. The Space Division is an example where top management support contributed to AMIS success.

Problems:

1. There appears to be a lack of HQ AFSC interest or emphasis on AMIS.
2. In the Comptroller's office top management expressed its support for AMIS. However, middle management seems less positive toward AMIS.

Recommendation: Start a vigorous campaign to publicize AMIS. Spend more time contacting and encouraging top and middle managers to use the system. Emphasize what is in it for them.

2. User Interaction

A successful management information system must be responsive to user needs. AMIS was designed to comply with the regulatory requirements of Uniform Contract Format and MILSCAP, not the information needs of its users. AMIS provides multi-users the ability to interact at near real

time through the common medium of automation. AMIS possesses the capability to provide accurate, complete contractual information to these users; however, its full potential has not been achieved.

Implementation of the accompanying recommendations in response to user needs will permit AMIS to achieve its MIS potential.

a. General Communications

Problem: The lack of interaction between AMIS users and the AMIS office contributes to the inability of the AMIS staff to appreciate user needs and thereby make clarifications and corrections to the system and its procedures.

Recommendations:

1. The AMIS office must seek dialogue with its users to ascertain their needs, problems, recommendations and experiences. The results of this communication should be used to design the required capabilities in AMIS.
2. Following the implementation of any changes, user feedback should be solicited to measure success or failure of the change.
3. Communications interaction between AMIS users should be encouraged to solicit and identify common problems, alleviate misconceptions or correct errors.
4. Identify new problem solutions, queries, capabilities and system status through a users' bulletin that can be accomplished by reinstating the now defunct NEWS data base.

b. Air Force

Problem: The Air Force is not totally in compliance with MILSCAP. AFLC and other AF Commands do not presently have a MILSCAP compatible system.

Recommendation: Perform analysis to determine if it is feasible to use AMIS as a MIS first at Air Force Logistics Command (AFLC) and, if successful, at all Air Force Commands.

c. AFSC HQ

Problem: AFSC's mission is to develop, acquire and deploy new weapon systems. However, AMIS does not provide AFSC management with accurate information concerning AFSC acquisitions. The data stored by AMIS does not accurately portray prior contract activity and current status at the time information is requested. The AFSC staff cannot rely on Command Management Information System-Contract (CMIS-K) products and therefore must use manual communications with each activity.

Recommendations:

1. Analysis be initiated to improve the quality of the AMIS data that underlies CMIS-K and Undefinitized Document Control (UDC) reports. Once the data provided by CMIS-K and UDC is reliable, AFSC can utilize AMIS as a true MIS without manual reports and telephone communication.
2. Implement a pre-award data base for each of the buying activites and AFPROs to give the AFSC staff a better view of the entire acquisition process from requirement initiation through contract award to contract closeout.
3. Analyze the needs of AFSC management and staff to perform its acquisition mission. Develop pre-award milestone tracking capability so that AFSC management can monitor contract placement, progress and thereby reduce the need to verbally contact each buying activity.

d. AFCMD

Problem: AFCMD has assumed a disproportionate role in the operation of AMIS. Its disbursement function has been the focus of AMIS programming and functional support and AMIS staff assistance visits. AFCMD has been permitted too much control over AMIS data. They have reassigned ACRNs, adjusted line item data, paid funds from wrong accounts and closed out contracts without the concurrence of the cognizant PCO or ACO. The emphasis on serving AFCMD has contributed to the buying activities resentment of AMIS.

Recommendation: Develop a more balanced support approach to all AMIS users. Require AFCMD to coordinate any proposed changes in AMIS data that is within ACO/PCO purview in accordance with AFSC Regulation 70-13. In those situations where obligations or fund citations in the data base are changed contrary to the written contractual document, PCO authorization must be required.

Problem: The number of documents requiring hand abstraction into AMIS exceeds the resources available.

Recommendation: Investigate why so many documents are not being entered through SDA procedures but are being mailed directly to AFCMD for input. Buying activities and AFPROs bypassing the SDA process need to be educated as to the system-wide advantages of SDA input.

Problem: AFLC Priced Spare Parts Lists (PSPLs) and Provisioned Item Orders (PIOs) are mailed to AFCMD for abstraction since AFLC

does not have SDA input capability. Due to the large number of line items associated with provisioning, the abstraction method of input is not efficient.

Recommendation: Develop direct input of PSPLs and PIOs to AMIS from the contractor's provisioning system.

e. AFPROs

Problem: The AMIS relationship with AFPROs is hindered by AFCMD's control of AFPROs. There is uncertainty as to who is responsible for AMIS training and staff support to AFPROs.

Recommendation: Authorize AMIS to deal directly with AFPROs in regard to AMIS matters.

Problem: AFPROs have complained that they do not have control of inputting some of their data into the data base as AFCMD has taken that responsibility away from them. This has caused errors in the input of data.

Recommendation: Determine what AMIS tasks of inputting data should be returned to the AFPROs from AFCMD.

f. AFSC Buying Activities

Problem: Large volume support equipment orders with hundreds of line items cannot be rapidly input into AMIS through use of Source Data Automation forms. The typing of hundreds of SDA forms and the resulting error messages can delay the order several weeks.

Recommendation: Develop a method to input Priced Support Equipment Lists (PSELs) and unpriced Provisioned Item Orders (PIOs) directly into AMIS via computer tape or from the contractor's computer system.

3. Systems Analysis

The problems related to the inputs, processing and outputs are:

a. Inputs

Problem: Users complain that the CMCT requires the user to align the forms in the typewriter perfectly.

Recommendation: IDI be implemented as quickly as possible, and word processors be made available to replace the CMCTs. In addition, provide like features/capabilities to all users.

b. Processing

Problem: The processing of batch jobs on the ITEL hardware (computer) requires the mounting of the correct tape or disc by a computer operator. When an incorrect tape or disc is mounted, the job will abort off the machine and this will require the job to be rerun.

Recommendation: Analysis of operator error be completed.

Problem: The End-of-Day (EOD) processing for AFCMD reports takes a tremendous amount of computer time. Improvement in EOD processing appears to take a long time, in some cases, over a year. The critical path has been reviewed several times and some changes have been made to improve the EOD processing.

Recommendation: Analysis be completed to see if a speedup in the throughput of data (I/O) can be improved. Dumping data into the data bases from EOD processing being done in parallel rather than serially would save some processing time.

Problem: The ASD/AD Computer Center ITEL system that processes the AMIS data has a limited number of channels for processing output data. This can be part of the reason the input/output (I/O) is bound up when there are heavy user requests.

Recommendation: Analysis be performed to see if more channels/discs could improve I/O functions.

c. Data Base

AMIS data base, or set of data bases, provides an outstanding source of information. However, there are problems that need immediate attention:

Problem: AMIS data bases are incomplete and to some extent incorrect. This leads to lack of credibility and confidence in the system.

Recommendation: Give top priority to resolving data base problems. To be more specific, the following problems with data bases are identified:

Problem: Are all the data bases really need to complete the AMIS mission? As new capability was needed, new data bases were added to AMIS. Many of these data bases did not have the necessary analysis performed to see how efficient they could be made, degree of access for I/O operation and query use.

Recommendation: Analysis of the data base be made to see if the critical path is as efficient as it could be and if the number of data bases could be reduced. In addition, the I/O should be addressed; possible more discs are needed to improve I/O capabilities.

Problem: Many abstractors at AFCMD insert data in the system that is incorrect or incomplete.

Recommendation: The AFSC Regulation 70-13 should contain specific instructions for when a contract could be abstracted into the data base. The above regulation should clearly state that any contract mailed around distribution should be returned to the Distribution Center for inserting the data into the AMIS. AFCMD should use AMIS to generate the error message thereby notifying the user of any errors or problems when abstracting data into the AMIS.

Problem: The data in the AMISDCAS data base is not complete and contains erroneous information. Many users have complained that administrative contract information from DCAS is not getting into the AMISDCAS data base.

d. Outputs

Problem: Queries are difficult to use, inflexible and work only in some of the data bases. Many users do not want to learn programming or make up natural language strings.

Recommendation: Analysis be performed to reduce the number but increase the flexibility of the queries. Users should be asked what types of queries are needed to do their job.

Problem: AMIS users complain that their request for strings/queries take too long to implement by the AMIS SPO. Some changes take up to a year to do. Coordination among the people in the AMIS office takes too long.

Recommendation: Workord data base is an automated version on how the AMIS office will complete a change or create a new string. In most cases, the coordination cycle takes far too long.

Getting things done by committee and requiring several coordinations is the wrong approach.

Problem: Many of the queries in the AMIS do not work. In an attempt to secure data the user will request the AMIS office to provide a natural language string to secure the contractual information from the data bases they need.

Recommendation: The queries should be reviewed and an analysis be performed on the buying activities to determine what strings they might need, then consolidate these findings to provide a flexible type string for the users. A COBOL program should be written so the strings/queries will work in the three data bases (CONTRACT, AMISDCAS and OTHRCONT).

4. Systems Support

a. Training and Orientation

A considerable effort has been expended in conducting training activities. However, these efforts are insufficient and lack the required follow-up.

Problem: Lack of formal structure of training programs with emphasis on user's benefits at different organizational levels.

Recommendations:

1. Develop a training package for top management, with emphasis on AMIS overview and management information needs for decision making.
2. Develop working level seminar/workshops; hands-on programs for:
   a. AFPROs
   b. BUYACs
   c. Monitors
   d. Program Control Personnel
   e. Budget Analysts (Comptroller)
   f. Production Specialists
   g. Contract Reviewers

Problem: Training programs lack a formal schedule for future user requirements.

Recommendation: Offer the above courses periodically with schedules and announcements at least a year in advance. This will allow managers and users to plan their training activities accordingly.

Problem: Training program contents.

Recommendation: Always emphasize user benefits. Toward this end get the users to determine their needs and then incorporate into the training course.

Problem: Use of outside resources for training.

Recommendations:

1. Augment AMIS training team with real front line experience systems contracting personnel to give credibility to the training program.
2. See to it that AFIT and Defense System Management College include discussions on AMIS in some of their courses.

b. AMIS Manuals

A successful system should be clearly documented. At least the following manuals are required:

(a) A Familiarization Manual
(b) A Training Manual for each level of user
(c) A User's Guide or set of guides

Problem: At present, AMIS manuals are too voluminous and its documentation is hard to understand. Potential new users have no manual for AMIS orientation; the available manuals dissuade rather than encourage use of the system.

Recommendation: Prepare a Familiarization Manual as soon as possible. Distribute the manual to candidates for future users.

Problem: Training manuals are not organized in accordance with the different levels of users.

Recommendation: Prepare different training manuals in accordance with the training needs at different levels of users. Include in the manuals step by step instructions related to the use of hardware equipment for input and output.

Problem: Have a professional agency rewrite the user manuals with the assistance of the previous authors.

c. AMIS Monitors

Problem: AMIS monitors lack the training, experience and professional status to be effective. They are AMIS' local representative yet they lack the necessary procurement and AMIS expertise to win their management's commitment to AMIS.

Recommendation: Upgrade the stature of the AMIS monitor by requiring a journeyman buyer or contract administrator to fill the position. The position should be defined as an ADP procurement analyst requiring full-time monitors at buying activities and large AFPROs and part-time monitors at smaller AFPROs. The grades of AMIS monitors must be comparable to the buyers or contract administrators they are dealing with. Require all monitors and their alternates to attend formal courses and workshops in AMIS and S2K. Each large SPO should have a full-time AMIS focal point to answer routine problems, obtain reports, and help with natural language queries.

d. System Awareness

Problem: There is a lack of awareness among top management and prospective

users with respect to the capabilities of AMIS and the benefits of its utilization.

Recommendations: Promote the utilization of AMIS among top management and prospective users.

1. Publish several articles, at different levels of sophistication, in appropriate journals to promote and encourage utilization of the system. For in-house publicity, short articles may be published in Air University Review and AFSC News Review. The National Contract Management Association would be appropriate for dissemination of information to a considerable number of contractors. In addition, technical articles emphasizing the computer capabilities of the system could be published in computer oriented journals such as Info Systems, MIS, Computer Design--etc. This will enhance the image of AMIS among the technical community.
2. Publicize new improvements in AMIS among top management and other users. A newsletter describing CMIS-K would be very informative and helpful in attracting more users for the system. Also, publicize the use of IDI in utilizing the CRT technology.

IV. FUTURE OF AMIS - RECOMMENDATIONS

A. IS AMIS AN ACQUISITION MANAGEMENT INFORMATION SYSTEM?

The acquisition cycle activities are:

Pre-Award

Approval of Requirement
Statement of Work Preparation
Purchase Request Preparation
Approval of Determinations and Findings
Issuance of Requests for Proposal/Solicitation
Commitment of Funds

Post-Award

Contract Award and Distribution
Obligation of Funds
Disbursement of Progress Payments
Delivery of Items/Services
Processing of DD250s (Material Inspection & Receiving Report)
Final Payment
Closeout of Contract

a. AMIS actually covers the activities related to the Post-Award portion of the acquisition cycle.

b. AMIS covers historical data and it gives information related to current transactions.

Conclusion:

AMIS, at the present is an Information Retrieval System for Post-Award Contract information.

B. AMIS - INFORMATION RETRIEVAL SYSTEM

AMIS should clearly define its system baseline. Determine the goal of AMIS.

Is AMIS a straight retrieval system or

Is it a management information system?

If AMIS decides to concentrate on pre-award information retrieval, it should concentrate on the following activities:

1 - Correcting and completing the data bases.
2 - Improving documentation.
3 - Improving training courses by tailoring the contents to audience comprehension.
4 - Identifying BUYAC products.
5 - Prioritizing IDI task to speed up incorporation of CRTs/word processors across the BUYACs.
6 - This will help in reducing dependence on the antiquated magnetic card typewriters.

7 - Improving the turnaround time on document validations by finding alternatives to the end-of-day processing, and finally,

8 - Advertise and encourage prospective users to utilize the system with a clear understanding of what the system can do for them; its capabilities and limitations.

C. AMIS MANAGEMENT INFORMATION SYSTEM

1 - Cons: AMIS drawbacks as a management information system:

a. AMIS data base was designed for information retrieval system, therefore it is inflexible for general use as a management information system.

b. From the BUYAC point of view, AMIS is not a viable MIS. It does not contain key pre-award milestones/data which the BUYACs require to manage on a daily basis. BUYACs rely on local MIS (LAMIS, Data Central, etc.) for pre-award information because they emphasize what BUYACs need to know to manage on a day-to-day basis.

c. AMIS could not serve as a MIS for the Comptroller because it does not contain the total financial program.

2 - Pros: The following are indicators which encourage the development of MIS:

a. AMIS data base, or set of data bases, provides an outstanding source of information. If properly designed, it can be used for a MIS.

b. AFSC achieved success in developing CMIS-K using some AMIS data bases.

c. AMIS is an expensive system; a lot of money has been invested to develop the system. ITEL AS-5 has been fully dedicated to the system. It makes sense to take advantage of these capabilities in expanding the present system into a viable management information system.

d. AMIS has potential as a MIS for AFCMD and eventually AFLC.

e. AMIS has the potential for providing a MIS for financial managers.

Conclusion:

If AMIS decides to be a viable management information system, it should concentrate on the following activities:

1 - Future plans should be focused on the pre-award activities and their integration with AMIS in order to develop a "total" system for contract acquisition. At the present time, there are several pre-award subsystems ranging from manual to fairly automated systems. An effort should be directed to standardizing this process towards an integrated system.

2 - AMIS/SPO should concentrate on being a central program management rather than central development. In this capacity it should coordinate the standardization of data definition to ensure data compatibility among the different systems.

3 - AMIS, at its present form, is a straight retrieval system. In order to upgrade it to a management information system, some decision support models should be developed and added to the system. The present AMIS data base is very rich with information that could be utilized for decision making by different management levels.

4 - Some divisions may prefer to develop their own decentralized management support systems. This trend is understandable due to the different styles of management and the continued reduction in hardware cost. This trend is also justifiable due to the fact that the acquisition process is not sufficiently standardized to satisfy all users. Again AMIS/SPO should coordinate efforts toward standardization and compatibility among systems. In other words, concentrate on the standards and policies required to assure smooth transfer of data between the different activities.

5 - Emphasize the role of AMIS as a service organization with a major function of coordinating inter and intra-AFSC acquisition information requirements.

REFERENCES

AMIS MANUAL, VOLUME I
INTRODUCTION 31 JUL 82

AMIS MANUAL, (DRAFT), VOLUME II
Source Data Automation 1 JUN 81

AMIS II MANUAL, (DRAFT), VOLUME III
Abstracting 1 MAR 82

AMIS II MANUAL, (DRAFT), VOLUME IV
Accounting and Finance 30 JUN 76

AMIS MANUAL, (DRAFT), VOLUME V
Precontract Management System (PMS)

AMIS II MANUAL, (DRAFT), VOLUME VI
Communications Instructions 31 JUL 82

AMIS II MANUAL, (DRAFT), VOLUME VII
Output Data Products 1 FEB 81

1982 USAF-SCEEE SUMMER FACULTY RESEARCH PROGRAM

Sponsored by the

AIR FORCE OFFICE OF SCIENTIFIC RESEARCH

Conducted by the

SOUTHEASTERN CENTER FOR ELECTRICAL ENGINEERING EDUCATION

FINAL REPORT

MODELING AND TRACKING SACCADIC EYE MOVEMENTS

Prepared by:	Dr. John D. Enderle
Academic Rank:	Assistant Professor
Department and University:	Department of Electrical Engineering North Dakota State University
Research Location:	Brooks AFB, Clinical Sciences Division, Neuroscience's Function
USAF Research Colleague:	Dr. James W. Wolfe

Date:	August 18, 1982
Contract No.:	F49620-82-C-0035

MODELING AND TRACKING SACCADIC EYE MOVEMENTS

by

John D. Enderle

ABSTRACT

Kalman filtering theory is applied to the tracking of horizontal eye movement during a saccade. Accurate estimates of position, velocity, and acceleration of the eye movement are calculated from infra-red reflection signals off the front surface of the cornea. The mechanical components and the control signal for the ocular motor system are developed and estimated using system identification techniques. The transfer function of the open-loop ocular motor system is calculated from the fast-eye response to step target displacements. The best fit as measured by the integral of the absolute value of the error squared between the model and data is with a second order linear model with real poles describing the mechanical components and a low pass filtered pulse-step descr.ing the control signal.

Acknowledgement

The author would like to thank the Air Force Systems Command, the Air Force Office of Scientific Research and the Southeastern Center for Electrical Engineering Education for providing him with the opportunity to spend a very worthwhile and interesting summer at the Clinical Sciences Laboratory, Brooks AFB, Texas. He would like to acknowledge the laboratory, in particular the Neurosciences Function branch, for its hospitality and excellent working conditions.

Finally, he would like to thank Drs. James W. Wolfe and J. Terry Yates for suggesting this area of research and for their collaboration and guidance, and he would like to acknowledge many helpful discussions with Mr. Edward Engelken and Mr. Kennith Stevens.

I. Introduction

Accurate estimates of position, velocity, and acceleration of eye movements are important in studies of vestibular and ocular motor system function and their neural organization. Specifically, a quantitative description of the input-output relationship between the stimulus and the eye movement response, serve clinical applications in assessing motoneuronal activity, and changes caused by fatigue, aging, alcohol, drugs, or pathology. For the Air Force in particular, quantitative measures of sensory function are important features for pilot evaluation, training, and treatment. Most of these applications involve an analysis of eye movements and their relationship to system performance. Typical sensory tests involve measurement and analysis of vestibular nystagmus (induced by either angular acceleration or bithermal caloric stimulation) and optokinetic nystagmus.[1,2] Eye movement analysis for these tests involve estimates of eye velocity and acceleration.

The present study is concerned with the application of Kalman filtering in the tracking of horizontal eye movements during a saccade. The basic task is to estimate, as accurately as possible, the position, velocity, and acceleration of the eye movement from infra-red reflection signals off the front surface of the cornea. These estimates, as mentioned, are the basis for most eye movement analysis systems. Applications involving Kalman filtering have appeared in satellite orbit determination, space flight and ballistic missile tracking. It seems appropriate to apply Kalman filtering theory to this problem. (Saccadic eye movements have even been described by many authors as ballistic.)[3]

One motivation for utilizing a Kalman filter in the study of eye movements is that it is a real-time system. Another is that the estimates for position, velocity, and acceleration are optimal estimates, given that the usual stipulations are true (these will be discussed in section).[4]

A first step in tackling the tracking problem is to derive a discrete-time model that describes horizontal eye movements during a saccade. A number of continuous-time models have been presented in

the literature, ranging in complexity and success from zeroth-order to sixth-order systems.[5,6,7,8] A model derived from the linear homeomorphic model by Bahill is incorporated in the recursive filter. System identification techniques were used to reduce the sixth-order linear homeomorphic model to a fourth-order model and to estimate the parameter values.

II. OBJECTIVES

The main objective of this project is to apply Kalman filtering theory to the tracking of horizontal eye movements during a saccade. The specific objectives were:

(1) Derive a discrete-time model that describes horizontal eye movements during a saccade.

(2) Estimate model parameter values using system identification techniques.

(3) Estimate position, velocity, and acceleration during a saccadic eye movement using a Kalman filter.

III. SYSTEM MODEL

The system model consists of defining a discrete-time state vector of position and velocity describing horizontal eye movement during a saccade. The mechanical components of the model are presented in Figure 1. The lateral rectus and inferior rectus muscles are modeled, (for the agonist muscle), with an ideal force generator F_{AG} in parallel with dashpot B_{AG} and an ideal spring K_{LT}, in series with another ideal spring K_{SE}. These components are then placed in parallel with another ideal spring K_{PE}. Equations describing the tension produced by the force generator on the eyeball for the agonist and antagonist muscle are

$$T_{AG} = \frac{K_{SE} F_{AG} - (K_{LT}(K_{PE} + K_{SE}) + K_{SE}K_{PE}) X_1 - B_{AG}K_{SE} \dot{X}_2}{K_{LT} + K_{SE}}$$

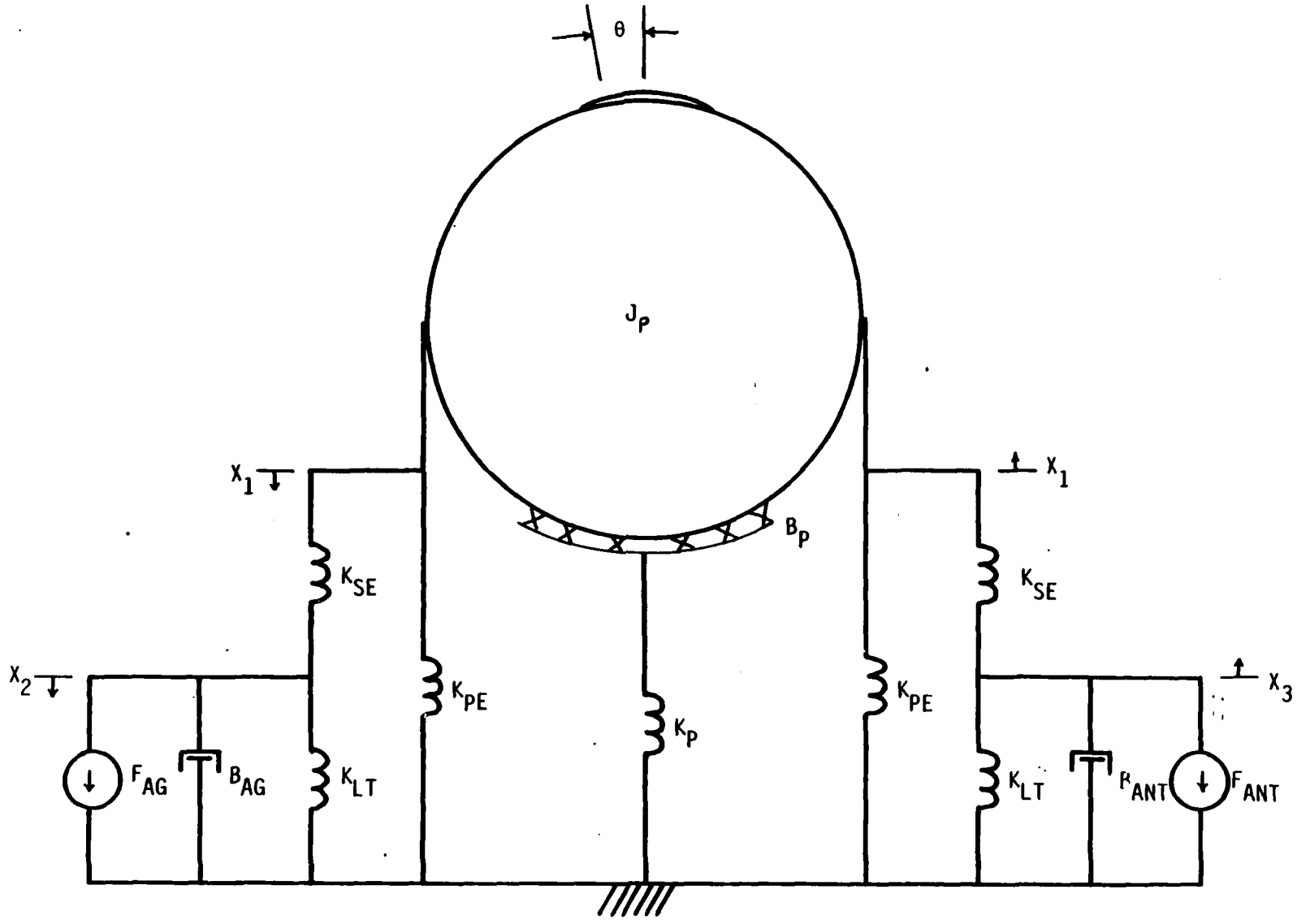
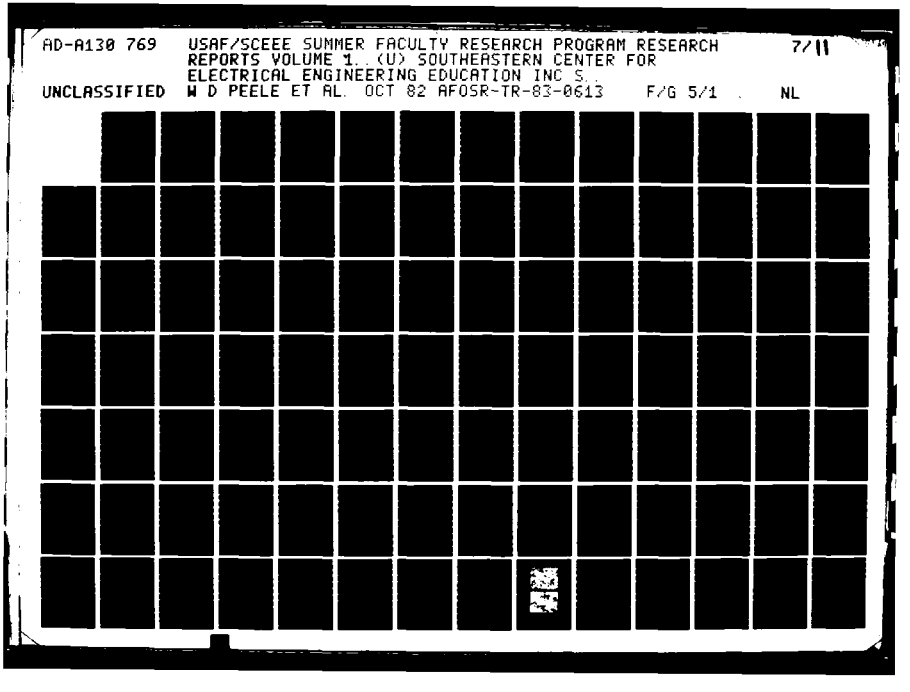
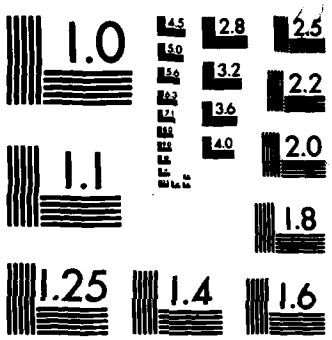


Figure 1. Mechanical components for eye model.


AD-A130 769 USAF/SCEEE SUMMER FACULTY RESEARCH PROGRAM RESEARCH REPORTS VOLUME 1.. (U) SOUTHEASTERN CENTER FOR ELECTRICAL ENGINEERING EDUCATION INC S..
7/11
UNCLASSIFIED W D PEELE ET AL. OCT 82 AFOSR-TR-83-0613 F/G 5/1 NL



MICROCOPY RESOLUTION TEST CHART
NATIONAL BUREAU OF STANDARDS-1963-A

$$T_{ANT} = \frac{K_{SE} F_{ANT} + (K_{LT}(K_{SE} + K_{PE}) + K_{SE}K_{PE}) X_1 + B_{ANT}K_{SE}\dot{X}_3}{K_{LT} + K_{SE}},$$

where X_1, X_2, and X_3 are displacements from equilibrium. The eyeball is modeled as a solid sphere with moment of inertia J_p, friction element B_p and elasticity element K_p. The equation for the model is

$$r(T_{AG} - T_{ANT}) = J_p\ddot{\theta} + B_p\dot{\theta} + K_p\theta, \qquad (1)$$

where r is the radius of the eyeball and θ is the angular deflection. It should be noted that at primary position, the ideal muscle springs are not at equilibrium, but are approximately 3mm longer.[9] Let X_p equal this displacement from equilibrium at primary position and

$$X = \frac{\pi}{180} r\theta,$$

the change of muscle length due to an angular deflection. The change in muscle length from equilibrium for an angular deflection for the agonist and antagonist are, respectively,

$$X_1 = X - X_p,$$

and

$$X_1 = X + X_p.$$

The velocity at nodes 2 and 3 for the agonist and antagonist are

$$\dot{X}_2 = \frac{\dot{T}_{AG} + (K_{SE} + K_{PE})\dot{X}_1}{K_{SE}},$$

and

$$\dot{X}_3 = \frac{(K_{SE} + K_{PE})\dot{X}_1 - \dot{T}_{ANT}}{K_{SE}}.$$

Substituting the previous equations into equation 1 yields

$$F_{AG} - F_{ANT} = P\dddot{\theta} + J\ddot{\theta} + B\dot{\theta} + K\theta, \qquad (2)$$

where

$$P = \frac{B_{AG} J_p}{r K_{SE}},$$

$$J = \frac{B_{AG} B_p}{r K_{SE}} + \frac{J_p (K_{SE} + K_{LT})}{r K_{SE}},$$

$$B = \frac{(B_{AB} + B_{ANT})(K_{PE} + K_{SE})\,\pi r}{180\,K_{SE}} + \frac{B_{AG}K_P}{r\,K_{SE}} + \frac{B_P(K_{SE} + K_{LT})}{r\,K_{SE}},$$

$$K = \frac{2(K_{LT}(K_{PE} + K_{SE}) + K_{SE}K_{PE})\pi r}{180\,K_{SE}} + \frac{K_P(K_{SE} + K_{LT})}{r\,K_{SE}}.$$

Equation 2 differs from equation 1 by the term

$$\frac{(B_{ANT} - B_{AG})}{K_{SE}}\,\dot{T}_{ANT}$$

which is assumed to be zero.

IV PARAMETER ESTIMATION

The ocular motor system undergoing saccadic eye movement operates in an open-loop mode as depicted in Figure 2.

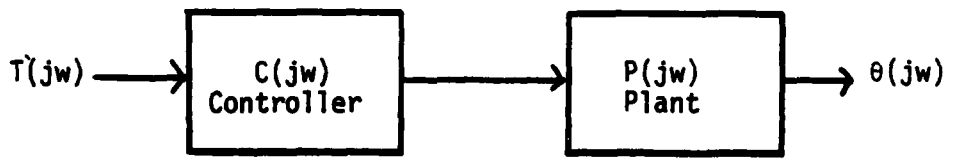


Figure 2. Block diagram of the ocular motor system for sacadic eye movements. The target displacement (T(s)) is the input to the system and the eye movement (θ(s)) is the output. H(s) is the transfer function of the mechanical components of the ocular motor system and C(s) is the neuronal control signal.

If a position error is observed between the fovea and the target, a control signal is sent that reduces the error to zero. The control signal is not a guided signal (there is no visual feedback), but a preprogrammed (ballistic) signal. Naturally when comparing the input with the output, this system acts like a feedback system, but this occurrs only at discrete-time intervals.[3] This type of behavior provides an excellent opportunity to study the ocular motor system using system identification techniques.

System identification techniques have been applied in a variety of disciplines, but not in the study of the ocular motor system.

Ideally, for a single input/single output system, the transfer function is equal to the ratio of the Fourier transform of the output to the system input

$$G(jw) = C(jw)\ H(jw) = \frac{\theta(jw)}{T(jw)}. \qquad (3)$$

Because of unequal time delays from saccade to saccade, it is not possible to use averaging techniques to reduce the effects of measurement noise.[10] Fortunately, the measurement noise is small relative to the input and output signals.

The transfer function of the open-loop ocular motor system is calculated from the fast eye response to a step target displacement. Measurements of position, as described by Young and Sheena, were obtained by sampling at a rate of 1,000 samples per second for one-half second from infra-red reflection signals off the front surface of the cornea.[11] The position measurements are first filtered using a Butterworth low-pass digital filter with a half-power point at 125 Hertz. Transforming the filtered measurements directly by the Fast fourier algorithm results in distortion due to truncation since the signal does not go to zero at steady state. This is circumvented by subtracting the steady state value from each sample and Fast Fourier transforming the modified signal. The Fourier transform of the fast eye response is equal to the Fast Fourier transform of the modified signal plus the Fourier transform of a unit step with amplitude equal to the steady state value. The input signal is a unit step function with amplitude equal to the steady state value. The transfer function is computed from equation 3.

Parameter estimates are calculated by fitting the transfer function computed from equations 3 to the transfer function for the model in equation 2. A conjugate gradient search Fortran program similar to Seidel's is used that minimizes the integral of the absolute value of the error squared between the model and the data.[12]

Results for a ten degree target displacement for the left eye are shown in Figure 3. Similar results were obtained for other target displacements of five, ten, fifteen, and twenty degrees for

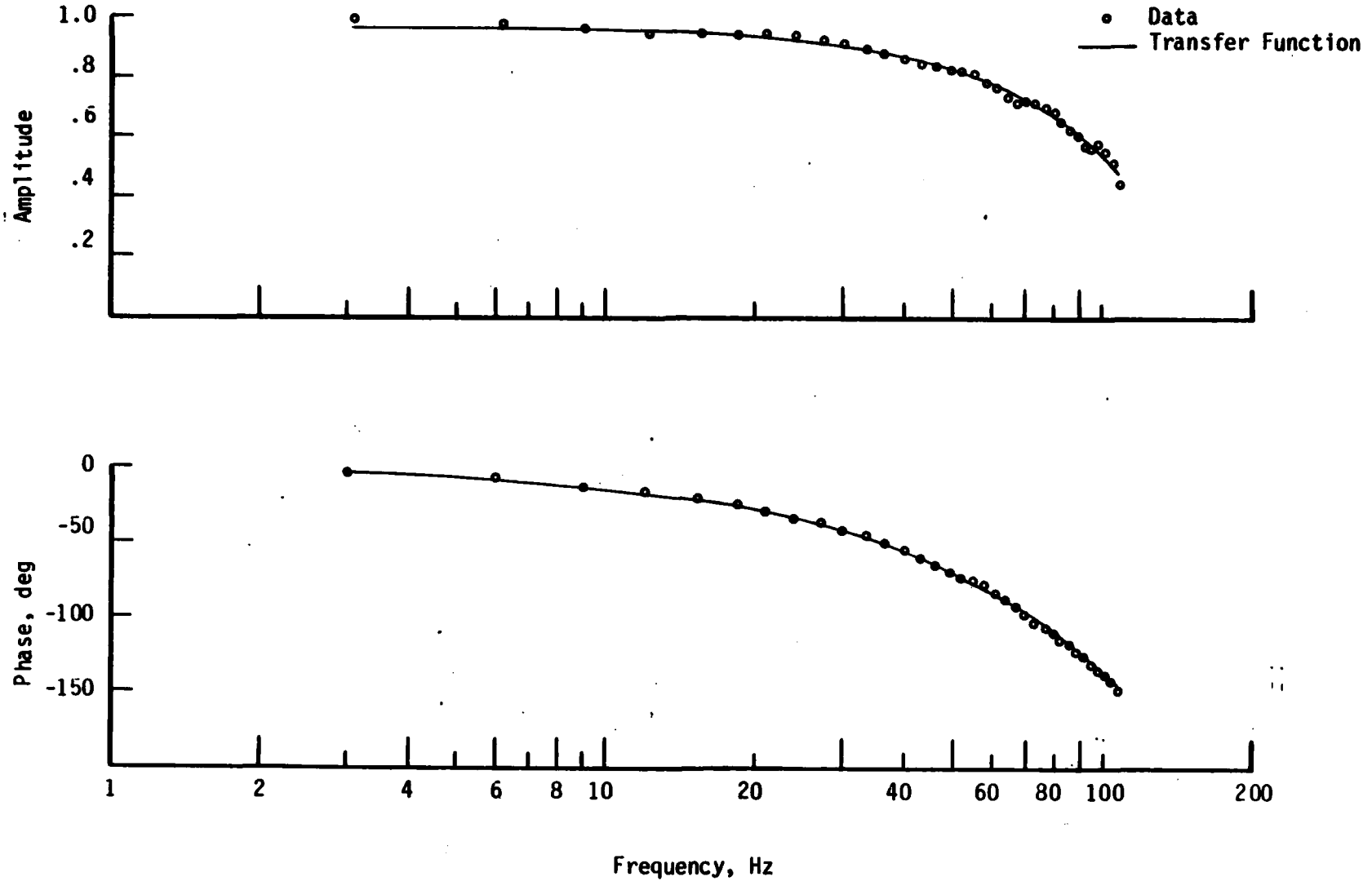


Figure 3. Left eye frequency response for a ten degree target displacement.

both eyes. The best fit to the transfer function data in Figure 3 is with a second order linear model with real poles describing the mechanical components and a low pass filtered pulse-step describing the control signal, $e^{-jt_0w}\left\{\frac{K_1}{(\frac{s}{P_3}+1)} - \frac{K_2e^{-jt_dw}}{(\frac{s}{P_4}+1)}\right\}$

$$G(jw) = \frac{}{(\frac{s}{P_1}+1)(\frac{s}{P_2}+1)}, \qquad (4)$$

where $P_1 = 68$, $P_2 = 152$, $P_3 = 90$, $P_4 = 500$, $t_o = .245$, $t_d = .037$, $K_1 = 1.2$, and $K_2 = .2$. The third pole in the model was made very large and was discarded. Returning to the time domain, the system model is now written

$$10\left\{K_1\,(1 - e^{-P_3(t - t_o)})\,U(t - t_o) - K_2(1 - e^{-P_4(t - t_o - t_d)})\,U(t - t_o - td)\right\} = \frac{(\ddot{\theta} + (P_1 + P_2)\dot{\theta} + P_1P_2\theta)}{P_1P_2}. \qquad (5)$$

The continuous-time state vector equation is

$$X(t) = AX(t) + B(t),$$

where

$$X(t) = \begin{bmatrix}\theta(t)\\ \dot{\theta}(t)\end{bmatrix}, \qquad A = \begin{bmatrix}0 & 1\\ -P_1P_2 & -(P_1 + P_2)\end{bmatrix}, \text{ and}$$

$$B(t) = \begin{bmatrix}0\\ 10P_1P_2\;\; K_1(1 - e^{-P_3(t-t_0)})\,(t-t_o) - K_2(1 - e^{-P_4(t-t_o-t_d)})\,(t-t_o-t_d)\end{bmatrix}$$

The discrete-time state vector of position and velocity written in terms of the state transtion matrix is for time zero starting at t_o

$$X(K + 1) = Q(K,K-1)X(K) + f(K+1),\ k = 0,1,\ldots \qquad (6)$$

where

$$X(K) = \begin{bmatrix} \theta(K) \\ \\ \dot{\theta}(K) \end{bmatrix}, \quad Q(K,K-1) = \begin{bmatrix} \dfrac{P_2 e^{-TP_1} - P_1 e^{-TP_2}}{P_2 - P_1} & \dfrac{e^{-TP_1} - e^{-TP_2}}{P_2 - P_1} \\ \dfrac{P_1 P_2 (e^{-TP_2} - e^{-TP_2})}{P_2 - P_1} & \dfrac{P_2 e^{-TP_2} - P_1 e^{-TP_1}}{P_2 - P_1} \end{bmatrix},$$

$$f(K+1) = 10\left\{ K_1 \begin{bmatrix} 1 + \dfrac{P_1 e^{-TP_2} - P_2 e^{-TP_1}}{(P_2 - P_1)} + P_1 P_2 e^{-KP_3} \left\{ \dfrac{(P_2 - P_3)e^{-TP_1} - (P_1 - P_3)e^{-TP_2}}{(P_2 - P_3)(P_1 - P_3)(P_2 - P_1)} \right\} - \dfrac{P_1 P_2 e^{-(K+1)P_3}}{(P_1 - P_3)(P_2 - P_3)} \\ P_1 P_2 \left\{ \dfrac{e^{-TP_1} - e^{-TP_2}}{(P_2 - P_1)} \right\} + P_1 P_2 e^{-KP_3} \left\{ \dfrac{P_2(P_1 - P_3)e^{-TP_2} - P_1(P_2 - P_3)e^{-TP_1}}{(P_2 - P_3)(P_1 - P_3)(P_2 - P_1)} \right\} + \dfrac{P_1 P_2 P_3 e^{-(K+1)P_3}}{(P_1 - P_3)(P_2 - P_3)} \end{bmatrix} U(K+1) \right.$$

$$\left. - K_2 \begin{bmatrix} 1 + \dfrac{P_1 e^{-TP_2} - P_2 e^{-TP_1}}{(P_2 - P_1)} + P_1 P_2 e^{-(K-K_d)P_4} \left\{ \dfrac{(P_2 - P_4)e^{-TP_1} - (P_1 - P_4)e^{-TP_2}}{(P_2 - P_4)(P_1 - P_4)(P_2 - P_1)} \right\} - \dfrac{P_1 P_2 e^{-(K+1-K_d)P_3}}{(P_1 - P_3)(P_2 - P_3)} \\ P_1 P_2 \left\{ \dfrac{e^{-TP_1} - e^{-TP_2}}{(P_2 - P_1)} \right\} + P_1 P_2 e^{-(K-K_d)P_4} \left\{ \dfrac{P_2(P_1 - P_4)e^{-TP_2} - P_1(P_2 - P_4)e^{-TP_1}}{(P_2 - P_4)(P_1 - P_4)(P_2 - P_1)} \right\} + \dfrac{P_1 P_2 P_4 e^{-(K+1-K_d)P_4}}{(P_1 - P_4)(P_2 - P_4)} \end{bmatrix} U(K-K_d) \right\},$$

and T is the sampling period of .001 seconds.

V. KALMAN FILTER

As mentioned previously, the main objective of this project is the application of Kalman filtering in the tracking of horizontal eye movement during a saccade. The discrete-time model developed in the previous section is not exact and small modeling errors result. Saccadic eye movement is more accurately modeled by the following stochastic vector difference equation

$$X_{K+1} = Q(K,K-1)\, X(K) + f(K+1) + \Gamma W(K+1),\ K = 0,1,\ldots, \quad (7)$$

where

$$\Gamma = \begin{bmatrix} T^2/2 \\ T \end{bmatrix},$$

and W_{K+1} is a modeling noise sequence. An equation describing the measurement model is

$$Z(K+1) = H\, X(K+1) + V(K+1),\ K = 0,1,\ldots, \quad (8)$$

where

$$H = \begin{bmatrix} 1 & 0 \end{bmatrix},$$

$Z(K+1)$ is the sequence of measurements and $V(K+1)$ is the measurement noise. Both the system noise sequence $W(k+1)$ and the measurement noise sequence $V(K+1)$ are assumed to be white Gaussian noise sequences, with zero mean and known uncorrelated statistics. If this is true, then the Kalman filter is optimum. Equations 7 and 8 were incorporated in a Kalman filter program written in FORTRAN.

The filtering results for the ten degree target displacement presented in Figure 3 are shown in Figure 4. Similar degrees of accuracy were obtained for other target displacements. The maximum modeling error was approximately one-half degree for any simulation. The maximum error usually occured at the start of the saccade and quickly went to zero during the course of the saccade. Improvements in modeling accuracy might be acheived by letting the antagonist force start 3 msec earlier as described by Bahill.[8]

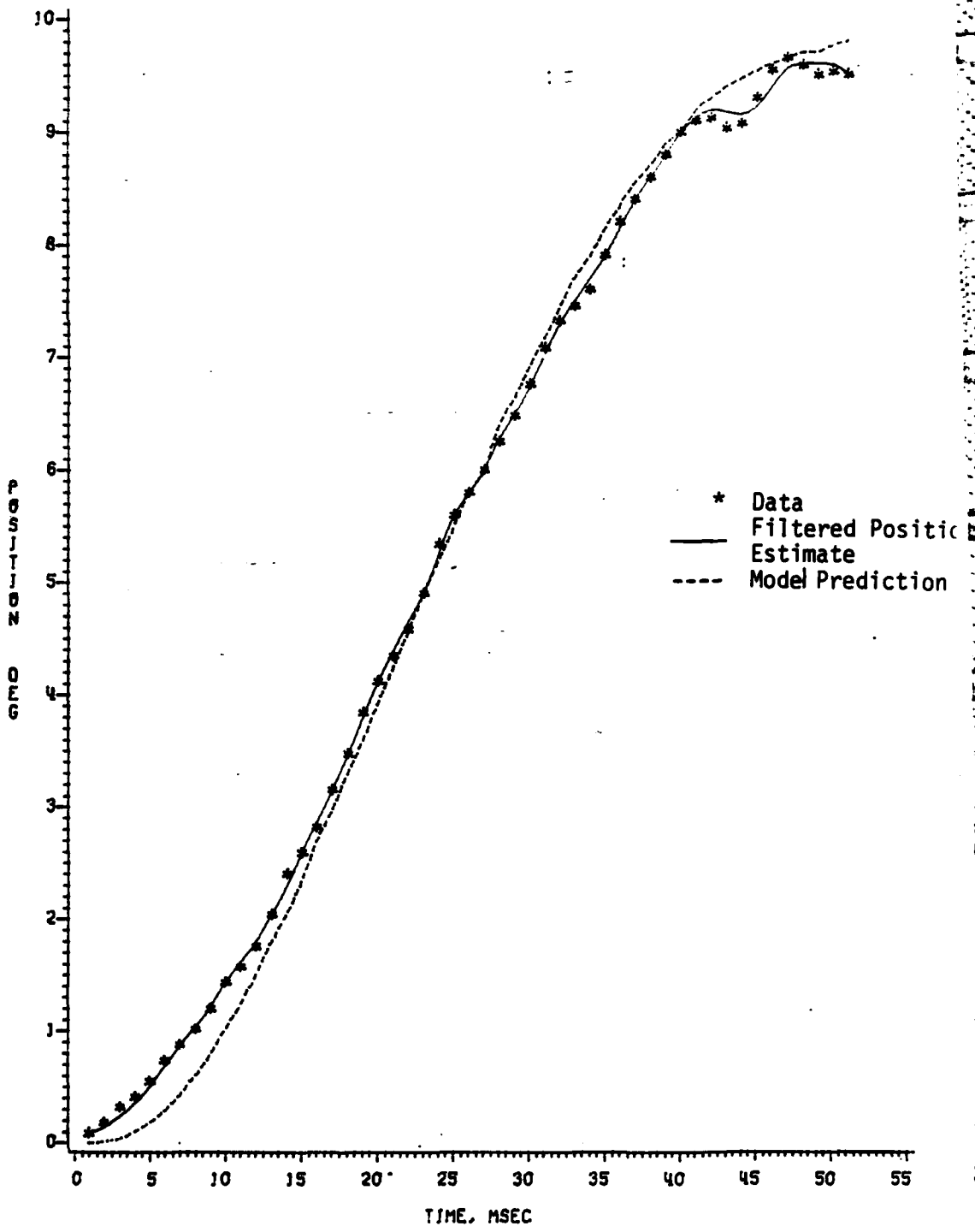


Figure 4a. Kalman filtering results for position tracking for a ten degree target displacement.

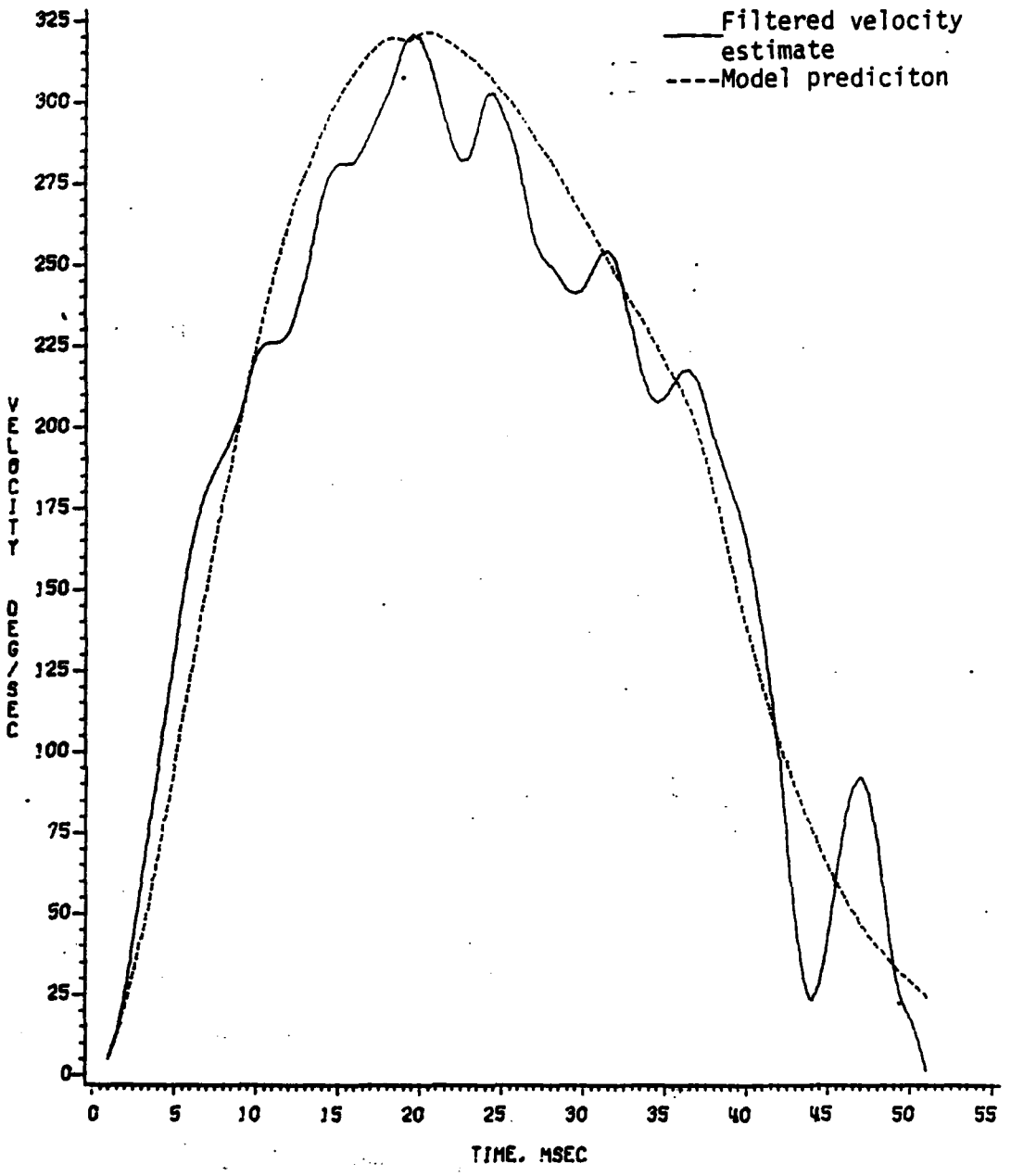


Figure 4b. Kalman filtering results for velocity tracking for a ten degree target displacement.

VI. RECOMMENDATIONS

All of the previously mentioned algorithms have been written in FORTRAN and implemented on a PDP 11/34 minicomputer as a cohesive unit. The program has been successfully run on a number of subjects in an off-line mode. Use of these analysis methods have resulted in optimal estimates for position, velocity, and acceleration. System identification techniques have been successfully employed to estimate parameters of the model. These estimates should provide additional insight into the study of ocular motor dysfunction.

Most sensory tests involve a combination of different eye movements (i.e., fast eye movements, slow eye movements, and vergence eye movements). In optokinetic nystagmus testing, both fast and slow eye movements are seen upon stimulation. A recommendation for follow-on research is to extend the present research and consider slow eye movements. This problem is much more difficult than the present one since we are dealing with a closed loop system. The end products of both of these projects can be combined and used in optokinetic and vestibular nystagmus testing.

REFERENCES

1. J.W. Wolfe, E.J. Engelkin, et. al., "Vestibular Responses to Bithermal Caloric and Harmonic Acceleration," Ann. Oto. Rhino. Laryng., Vol. 87(6), pp. 861-867, 1978.
2. J.W. Wolfe, E.J. Engelken, and J.E. Olson, "Low Frequency Harmonic Acceleration in the Evaluation of Surgical Treatment of Menieres' Disease," Adv. Oto. Rino. Laryng., Vol. 25, pp. 192-196, 1979.
3. Roger H.S. Carpenter, Movements of the Eyes, (Pion Ltd., London, 1977), p. 56.
4. Brian D.O. Anderson and John B. Moore, Optimal Filtering, (Prentice-Hall, Englewood Cliffs, N.J., 1979).
5. G. Westheimer, "Mechanism of Saccadic Eye Movements", Arch. Ophthalmol., Vol. 52, pp. 710-723, 1954.
6. D.A. Robinson, "The Mechanics of Human Saccadic Eye Movement," J. Physiol., Vol. 174, pp. 245-264, 1964.
7. G. Cook and L. Stark, "The Human Eye-Movement Mechanism: Experiments, Modeling and Model Testing, " Arch. Ophthalmol., Vol. 79, pp. 428-436, 1968.
8. A.T. Bahill, J.R. Latimer, and B.T. Troost, "Linear Homeomorphic Model for Human Movement," IEEE Trans. Biomed. Eng., Vol. BME-27, pp. 631-639, 1980.
9. D.A. Robinson, D.M. O'Meara, et al., "Mechanical Components of Human Eye Movements," J. Appl. Physiol., Vol. 26, pp. 548-553, 1969.
10. W.G. Halvorsen and D.L. Brown, "Impulse Technique for Structural Frequency Response Testing," Sound and Vibration, pp. 8-21, Nov. 1977.
11. L.R. Young and D. Sheena, "Survey of Eye Movement Recording Methods Behavior Research Methods and Instrumentation, Vol. 7, pp. 397-429, 1975.
12. R.C. Seidel, "Transfer-Function-Parameter Estimation from Frequency-Response Data - a FORTRAN Program," NASA TM X-3286, 1975.

1982 USAF-SCEEE SUMMER FACULTY RESEARCH PROGRAM

Sponsored by the

AIR FORCE OFFICE OF SCIENTIFIC RESEARCH

Conducted by the

SOUTHEASTERN CENTER FOR ELECTRICAL ENGINEERING EDUCATION

FINAL REPORT

DYNAMIC RESPONSE OF A DOUBLY CURVED CYLINDRICAL SHELTER

Prepared by:	Dr. Fernando E. Fagundo, Jr.
Academic Rank:	Assistant Professor
Department and University:	Department of Civil Engineering University of Florida
Research Location:	U.S. Air Force Engineering and Services Center, *Engineering and Services* Laboratory, Air Base Survivability Branch, Tyndall AFB, FL
USAF Research Colleague:	Lt. Cmdr. James W. Carl
Date:	July 23, 1982
Contract No.:	F49620-82-C-0035

DYNAMIC RESPONSE OF DOUBLY CURVED CYLINDRICAL SHELTER

by

Fernando E. Fagundo, Jr.

ABSTRACT

The United States Air Force is studying the feasibility of developing a protective structure for large aircraft such as the E-3A. The magnitude of the spans that must be considered in addition to the possible weapons effects makes an arch section the only feasible structural configuration.

The static and dynamic response of a double radius arch configuration is investigated. The applicability of current design provisions for the design of aircraft shelters subjected to conventional non-nuclear weapons is studied and recommendations are made for a more rational approach to describing load histories.

It is demonstrated that simplified mathematical models are not adequate for evaluating the response of the structure under consideration. Suggestions for further research in the area of conventional weapons effects are provided.

Based on the preliminary analysis performed in this project it appears that a double radius arch section could be successfully used for a Fourth Generation Aircraft Shelter. The feasibility of the shelter for large aircraft depends on the refinement of the analysis and design procedures.

ACKNOWLEDGEMENTS

The author is grateful to the Air Force Systems Command, the Air Force Office of Scientific Research, United States Air Force, and to the Southeastern Center for Electrical Engineering Education for providing this opportunity of professional growth during the 10-week Summer Faculty Research Program. He would like to acknowledge the hospitality of the members of the Air Force Engineering and Services Center, in particular those of the Air Base Survibability Branch for serving as hosts during his visit at Tyndall AFB, Florida.

The support and constructive comments of Lt. Cmdr. James W. Carl, Maj. Steve Hawn, and Cpt. Paul Rosengren are also acknowledged. Special thanks are extended to the personnel of the computer facilities for their cooperation during the many hours of computer usage.

Finally the author would like to thank Mr. David Israel for his cooperation and innumerable contributions throughout the course of this work.

1982 USAF-SCEEE SUMMER FACULTY RESEARCH PROGRAM

Sponsored by the

AIR FORCE OFFICE OF SCIENTIFIC RESEARCH

Conducted by the

SOUTHEASTERN CENTER FOR ELECTRICAL ENGINEERING EDUCATION

FINAL REPORT

USING HARD CRITERIA TO EVALUATE LEADERSHIP AND MANAGEMENT DEVELOPMENT CENTER CONSULTATIONS

Prepared by:	Dr. Hubert S. Feild
Academic Rank:	Professor
Department and University	Deparment of Management Auburn University
Research Location:	Leadership and Management Development Center, Directorate of Research and Analysis, Maxwell Air Force Base, Alabama
USAF Research:	Maj Lawrence O. Short, Ph.D., and Capt Janice M. Hightower, M.S.
Date:	August 20, 1982
Contract No:	F49620-82-0035

USING HARD CRITERIA TO EVALUATE LEADERSHIP AND MANAGEMENT DEVELOPMENT CENTER CONSULTATIONS

by

Dr. Hubert S. Feild

ABSTRACT

The purpose of the present research was to examine the applicability and analysis of hard or performance-based measures for evaluating consultation activities delivered by the Leadership and Management Development Center. Interviews with key personnel and analysis of available hard criterion measures for two selected Air Force groups suggested that certain measures might be useful for evaluation purposes. Interrupted time series analysis is offered as an appropriate analytical technique for determining any impacts of behavioral consultations on such data. Suggestions for selecting, applying, and analyzing hard criterion data from an evaluation perspective are made.

ACKNOWLEDGEMENTS

The conduct of any research project depends, in large measure, upon the cooperation and participation of numerous individuals. This project is no exception. Sincere appreciation is extended to Major Larry Short, Captain Janice Hightower, and Lieutenant Colonel David Wilkerson for providing the opportunity to work with an outstanding Air Force unit, the Directorate of Research and Analysis, and for their guidance during the course of the project. In addition, special thanks is also extended to Captain Bob Hodge, CMSgt Judy Vermilya, and Captain Mike Cox who greatly facilitated the retrieval of information used in the study. Appreciation is also given to Ms. Desjree Bradley who patiently and willingly typed and made numerous typed revisions in the report. Although the author is responsible for the research, certainly any successes enjoyed should be shared by the above named individuals. Without their help, such successes would not have been possible. Finally, appreciation is given to the Air Force Systems Command, Air Force Office of Scientific Research who made this summer research a rewarding experience.

I. INTRODUCTION

Role of the Leadership and Management Development Center (LMDC)

Establishment of the LMDC. As described by Mahr (1982, pp. 1-3), roots of the Leadership and Management Development Center (LMDC) can be traced to establishment of the all-volunteer force in 1973. Since the Air Force would need to compete for talented human resources, it was decided by Air Force leaders to study what makes the Air Force an attractive place to live and work. The Air Force Management Improvement Group (AFMIG) was established in 1975 to examine the non-technical aspects of Air Force life and to suggest how service life could be enhanced. Ideally, such a group would make the Air Force more competitive with the private and public sectors in attracting quality human resources.

Initially, AFMIG surveyed roughly 11% of the Air Force's world-wide active duty personnel in terms of their perceptions of the following areas: economic standards, economic security, free time, work, leadership/supervision, personal growth, personal standing, and health. An important finding of the survey was that although 81% of the respondents believed leadership and management were important, 71% indicated they felt the quality of Air Force leadership and management was poor to average (LMDC, 1981a, p. 1). In response to these findings the LMDC was created as part of the Air University at Maxwell Air Force Base, Alabama. Among others, two important purposes were to be served by the LMDC. These were:

1. to serve as the focal point for leadership and management education for the Air Force, and
2. to give leadership and management consultation to Air Force commanders upon request by providing these managers with systemic information on leadership and organizational trends (Mahr, 1982, p. 3).

For the objectives of this report, this latter purpose, that is, LMDC's consultation role in Air Force operations, is particularly significant. Due to its importance, it may be instructive to briefly review LMDC's consultation process.

LMDC's consultation process. The principal goal of LMDC is to ". . . help make the United States Air Force a more effective fighting force by focusing on the identification and solving of leadership and management problems, particularly, 'people problems'" (LMDC, 1981b, p. 3). LMDC addresses this goal by using organizational development (OD) consultants in collaboration with clients to identify and resolve leadership and management problems involving key organizational processes. The resolution of these problems is sought through six basic steps. (A more complete, thorough description of each of these six consultation phases may be found in Mahr, 1982 and Westover, 1979.) These steps are as follows:

1. Invitation--LMDC management consultation can only be offered following a written request for assistance from an Air Force commander or agency chief. Once contacted, an LMDC consultant reviews the services of the LMDC and explains the responsibilities of the client to the particular commander.

2. Initial Contact--The client group and the consultant continue to explore the suitability of an LMDC intervention. Once client responsibilities/expectations are clearly delineated, the client and LMDC negotiate a contract for consulting services. The contract represents the expectations, goals, roles, and methods to be used during the LMDC/client relationship.

3. Data Collection--The principal focus of this step is on the collection of information descriptive of a client group's work environment and leadership/management processes. Data are obtained from a variety of sources including formal organization charts, mission statements, interviews with key supervisors, an open-ended questionnaire assessing morale of the supervisor's work group, performance or attitude changes occurring in the last six months, the supervisor's leadership style, and objective or performance data, such as AWOL rates, drug and other arrest rates, and accident rates. In addition to these data, a key source of information is obtained from administration of the Organizational Assessment Package (OAP) to a sample of at least 60% of the people within each work group of a base or wing. The OAP is a 109-item, self-report questionnaire where respondents are asked to report on their

job/work environment in areas such as job satisfaction, organizational climate, supervisory leadership/management style, complexity of the respondent's job, and degree of job autonomy. Data obtained from the OAP serve as the principal basis for performing diagnostic/evaluation activities. (Additional information on the development, application, and scoring of the OAP may be found in Hendrix & Halverson, 1979; Short & Hamilton, 1981; Short & Wilkerson, 1981.)

4. Data Analysis--Upon collection of the data, the consultants prepare analyses to develop an initial assessment of the organization. The purpose of these analyses is to identify the strengths and weaknesses of the client organization as perceived by its incumbents. From these analyses, feedback materials or packages are created for all supervisors who had four or more subordinates complete the survey. These materials show how a supervisor's work group compared to other work groups in the organization as well as to similar groups in the Air Force on which data are available.

5. The Tailored Visit--At this point, a team of LMDC consultants is specially selected to return to the client organization to deliver particular consultation services. These services are tailored to address the specific problems identified in the preceeding phase, hence, the term "tailored visit." Once on location, the commander is briefed on the general condition of the organization. In turn, each supervisor is informed about his/her specific unit. Where major problems exist, consultants may work with an individual supervisor, using various OD intervention techniques such as team building, goal setting, job redesign and the like, to produce changes in the unit.

6. Follow-Up--After six weeks, the first step of the follow-up phase begins. LMDC mails survey questionnaires to the commander as well as all supervisors with whom the consultants worked. Generally speaking, these questionnaires solicit opinions concerning the performance of the LMDC consulting team. Approximately four to six months later, a second follow-up step is initiated. LMDC consultants return to the client organization to collect post-intervention OAP as well as objective data. This information when compared to that collected on the pre-intervention visit is used for determining the progress of the client

organization following an LMDC intervention. These comparisons are finally assembled into a report and submitted to the client organization commander. The submission of the report marks the end of the LMDC/ client group consultation.

Evaluation of LMDC's Consultation Process

One of the important mandates of the LMDC is to answer the question, "What effect(s), if any, did an LMDC consultation or tailored visit have on a client organization?" Obviously, such a question presumes that an integral component of the LMDC is to evaluate their behavioral consulting assistance offered to Air Force client groups. As suggested earlier, LMDC has incorporated the notion of evaluation into its consultation process. Since the principal emphasis of this report is on selected aspects of the LMDC evaluation effort, particularly as it applies to the use of performance data, the next section will focus on the types of data and nature of the research design employed.

Types of evaluation data. Three principal types of data are employed by LMDC: (a) anecdotal comments, (b) self-report data, and (c) performance data. Anecdotal comments have typically been collected by questionnaire from commanders following a tailored visit. Basically, these respondents are asked to report on the quality of consultation offered by the LMDC. Self-report data, a second type of evaluation information, have served as the principal data source for evaluation purposes. These data are collected primarily from the administration of the OAP. Since this type of information typically describes incumbents' perceptions of their organization (for example, organizational climate) and their reactions to it (for example, job satisfaction), these data could be labeled as being impressionistic or "soft" measures of individuals.

In the context of evaluation, the OAP has been administered on two occasions, once prior to an OD intervention and once after. Because these data are obtained from individual respondents, mean scores on OAP factors or dimensions are calculated for selected work groups. Significant differences in these paired mean OAP scores are treated as indices of organizational change.

The third form of data utilized by LMDC is performance data. To a lesser degree, performance data have also been incorporated as part of the evaluation effort. When employed, these data have focused principally on behavioral aspects of organizational performance. Due to their emphasis on work behavior, this type of information could be characterized as "hard" measures of organizational performance. Examples of such information would include the following variables: productivity, AWOLs, and retention rates. In contrast to the OAP measures that are available on individual respondents, performance data are generally available for an Air Force work group, unit, section, or branch. As such, these group data may require special forms of statistical treatment when used in evaluation research. (More will be said in a later section concerning the analysis of group data collected over time.)

Research design and statistical methods. In conducting an evaluation of OD projects, all empirical studies employ some form of research or experimental design. The design of a study represents the rationale for controlling a variety of variables while observing the effects of an independent variable(s) on a dependent variable(s). This rationale underpinning the design of a study determines the type of conclusions that may be drawn from the data collected.

The most prevalent research design used by LMDC to evaluate its OD efforts is the one-group pretest-posttest design (Campbell & Stanley, 1963). The nature of the design can be depicted as follows:

$$O_b - T_i - O_a$$

where: O_b is the pretreatment measure;
O_a is the posttreatment measure;
T_i is the treatment, that is, the OD intervention administered by LMDC.

Although the design is frequently used in OD evaluation studies, it has several limitations that hamper our ability to determine if the OD intervention produced any significant effects. From the perspective of evaluation research, these limitations are termed "rival hypotheses." These hypotheses simply represent alternative explanations for any noted organizational change other than the OD intervention. The one-group

pretest-posttest design is particularly susceptible to several rival hypotheses (Campbell & Stanley, 1963, pp. 7-12). The first of these is History. History represents any events occurring simultaneous to the introduction of the OD intervention. To the extent that the pretest-posttest design does not permit control of a history effect, then history becomes an alternative explanation for any noted organizational change.

A second limitation of this design is Maturation. The passage of time, independent of the intervention, may explain differences in pre- and post-intervention scores. Where respondents have changed over time due to biological and psychological processes which systematically vary with the passage of time, then maturation serves as another rival hypothesis.

Testing represents a third alternative explanation. This effect involves the reactions of respondents to simply being measured or tested. When respondents are aware of being tested, such as on a pretest, and this awareness influences respondents' scores over time, such as on a posttest, then testing serves as a confounding variable.

Instrumentation or changes in the measuring instrument that occur over time represents a fourth uncontrolled variable. When the measure shifts in the metric of measurement over time, then instrumentation has happened (Cook & Campbell, 1979, p. 52).

Finally, Regression poses a fifth problem uncontrolled for by the pretest-posttest design. Essentially, groups at the extremes on a pretest will demonstrate the most change on a subsequent posttest. When regression has occurred, these changes are due principally to statistical artifacts rather than to the OD intervention.

The important point to recognize from the above discussion is that the pretest-posttest design is not a particularly strong one. Since several rival hypotheses such as history, maturation, regression and the like, are not controlled for by the design, it is impossible to establish with any high degree of uncertainty that an OD intervention caused a particular organization change. LMDC has incorporated the pretest-posttest design using both self-report and performance data. When used with OAP or self-report data, independent *t*-tests have been calculated between two data points, that is, pretest and posttest means for specific OAP dimensions. Performance data have also been included in LMDC

evaluation activities, however, they have been used only to a limited degree. When employed, performance measures have generally been available over several points in time, prior to as well as after the OD intervention. In analyzing the pretest-posttest data where multiple measurements have been available, pretest and posttest measures have been averaged and the means compared in a descriptive manner. These procedures are not inherently "wrong," and they certainly provide some useful information. If, however, we are concerned with the certainty to which we can ascribe any recorded organizational change(s) to an LMDC intervention, then other alternative research designs and analyses should be considered. Attention will be given in this report to these alternatives. As will be seen, these alternative methods will not only help to control the rival hypotheses characteristic of the pretest-posttest design but will be particularly appropriate for analyzing hard criterion measures collected over time of work group performance. Such methods should be useful in evaluating the impact of an LMDC organizational development intervention using these hard criteria.

II. OBJECTIVES

As noted, the OAP dimensions or soft criteria have served as the principal basis for assessing the impacts of an LMDC organizational intervention(s). These perceptual measures are certainly important for characterizing changes in the quality of working life of Air Force incumbents. However, these soft measures alone do not give a complete account of the impacts of these interventions. Performance data are also needed for providing a clearer picture of organizational impacts and functioning. Such a need, of course, raises a number of important questions that will need to be addressed. These questions include but are certainly not restricted to the following: What performance measures should be used? Where can these data be obtained? What type of research design is most appropriate? How should such data be analyzed?

The principal concern of this report is to propose some alternative considerations for answering these questions. Although soft measures, such as OAP data, are recognized as being critical to OD evaluation efforts, performance data will be emphasized here. Thus, the focus will be on examining the feasibility of using existing performance-based measures for evaluating any impacts of LMDC organizational interventions

with selected Air Force client groups (Wilkerson, 1982). This emphasis will be given by the following research objectives:

1. to identify various variables or measures from existing sources of information that might be used as criteria for evaluating the impact of LMDC consulting activities on performance of selected Air Force units;
2. to propose methods for systematically collecting these criterion measures, the form of these data (that is, how measured), and the time interval covered by the data; and
3. to specify the research design and statistical analyses to be used in analyzing the data collected.

In addressing these objectives, several research steps will be taken. These steps include the following:

1. a review of selected, published literature concerning: (a) empirical evaluations of organizational development/consulting practices, (b) use of performance-based measures of organizational practices in evaluation research, (c) productivity measurement methods used in the Air Force, and (d) statistical treatment and research design of organizational development evaluation studies;
2. interviews/discussions with key personnel in selected Air Force organizational units chosen for study concerning the nature, availability, and quality of performance-based measures; and
3. interviews/discussions with selected LMDC personnel concerning the nature of the evaluation/consultation process.

Prior to discussing the major thrust of this report, it may be helpful to the reader to briefly review its five major sections. These sections are described below:

1. Hard Criterion Measures in Evaluating Organizational Development Programs. This section will briefly summarize the rationale as well as current practices/trends in using hard, performance-based measures for evaluating OD programs. These practices will be derived from published journal articles dealing with OD evaluation research.

2. Issues in Selecting Hard Criteria for LMDC Evaluations. One key ingredient of any OD evaluation system is the standard or criterion to be used for evaluating organizational change. This section will provide a broad overview of the relevant considerations to be taken in selecting or developing measures for use in evaluating an LMDC organizational intervention.
3. An Alternative Research Design and Analysis: Interrupted Time Series. Based upon the previous literature review and the nature of LMDC consultation, a suggestion will be made for using time series research designs to evaluate OD programs where hard, longitudinal measures are available. The nature and application of these designs will then be discussed in terms of their use with LMDC consultation activities.
4. Applications. If time series designs are to be used in OD evaluation, then longitudinal data must be available for use. By examining selected, specific work units of the Air Force, this section will describe what hard data are available, data requirements necessary for time series analysis, sources of data as well as other pertinent issues regarding the application of times series designs to these selected work units.
5. Recommendations. This final part of the report will present suggestions and recommendations for using hard criterion measures and implementing time series design and analysis for LMDC evaluation purposes.

III. HARD CRITERION MEASURES IN EVALUATING ORGANIZATIONAL DEVELOPMENT PROGRAMS

Need for Hard Criterion Measures

A common means used to evaluate OD programs is to collect information from program participants by using data sources such as questionnaires, interviews, or other self-report methods. These self-report methods are useful in that they provide data on such variables as incumbent attitudes and interpersonal behaviors. Few would argue that these soft or quality of work life measures (as some have termed them) are unimportant. However, these measures provide little information relative to other, important behavioral considerations such as productivity or organizational effectiveness and efficiency.

Of late, there appears to be an increasing reluctance on the part of OD practitioners and researchers to place sole reliance on soft measures to evaluate OD programs (Nicholas, 1978). Recent surveys indicate a developing interest in evaluating the role of OD in terms of hard measures of organizational performance (Jones, Spier, Goodstein, & Sashkin, 1980). Although interest in using hard measures for OD evaluation purposes is strong (particularly for longitudinal data), it is interesting to note that practice is rather rare (Nielsen, 1975, p. 194). While most administrators have good reason for interest in assessing the effects of OD on work group and/or organizational performance, most OD evaluation projects stop short of measuring these impacts. In general, there has been relatively little investigation of the impact of OD on system change using hard criteria. A recent review by Porras and Berg (1978) illustrates the paucity of OD evaluation research employing hard measures. Their study showed that only 20 of 160 evaluation research studies that assessed organization change employed hard criteria in their evaluations.

If hard criteria are so desirable, a question might be raised as to why they have not been more frequently used? As Nicholas (1982, p. 3) has noted, the almost exclusive emphasis on soft criteria for evaluating OD projects is not surprising since OD is aimed principally at individuals and work groups. Thus, changes in individuals' attitudes and behavior are primary targets. On the other hand, from an organizational or work group perspective, individual attitudes and perceptions are intervening variables, where changes do not necessarily translate into improvements in organization performance. Although many studies have assessed organization performance using soft criteria, perceived changes in performance do not necessarily lead to actual behavioral changes as assessed by hard criteria.

Another reason for using soft measures is that these measures are typically easier to collect. For example, most evaluation data are collected by questionnaire (Porras & Berg, 1978). Questionnaires are easy to administer, score, and are economical. The resulting data are easy to analyze, and a host of various questionnaires are available. Thus, from the perspective of ease of data collection, questionnaires are certainly desirable. Of course, these soft measures suffer from numerous limitations (see Webb, Campbell, Schwartz, & Sechrest, 1966, for a discussion of these problems).

In addition to providing behavioral data for evaluation purposes, hard criteria do not suffer from the same methodological problems as soft criteria in evaluating organizational change. For example, hard measures are not plagued with the difficulty of attempting to distinguish among alpha, beta, and gamma changes (Golembiewski, Billingsley & Yeager, 1976). Yet as Macy and Mirvis (1976) have noted, hard measures are subject to influence by variables both internal as well as external to the organization that affect their interpretability. Only by controlling these through statistical adjustments or through the research design can these effects be partialled out.

In sum, the issue that is being argued is that multiple measures of soft and hard criteria are needed to appropriately evaluate OD programs. As Campbell, Dunnette, Lawler & Weick (1970) suggest, program effectiveness cannot be measured by a single or global variable. Multiple measures are required. The criteria chosen for evaluation should be based on the problem setting, goals of the evaluation, hypotheses about the process (Nicholas, 1978, p. 32) as well as other critical factors. In light of the arguments presented here, Martin (1957) has similarly proposed that two kinds of criteria be used: (a) those linked to organizational processes involving people (for example, decision-making, motivation, leadership), and (b) those linked to actual behavior (for example, productivity). His arguments are consistent with those advanced here.

Regardless of their content, hard and soft measures have their unique assets and liabilities; both are needed to characterize organization/work group performance and quality of working life. As Webb (1970) has stated:

> Every data-gathering class--interviews, questionnaires, observation, performance records, physical evidence--is potentially biased and has specific to it certain validity threats. Ideally we should like to converge data from several data classes, as well as converge with multiple variants from within a single class (p. 450).

Use of Hard Criterion Measures

Although historical practices in the use of hard criteria for OD evaluation purposes are rather infrequent, recent trends indicate an increase in use of such criteria. In reviewing the OD evaluation

literature for the present research, it became apparent that studies utilizing hard criteria may not always be reported in professional journals. For instance, the literature review identified only three OD evaluation studies using hard criteria in a military setting (Adams, 1977; Lloyd, 1977; Rosenbach, 1977). However, these references were Ph.D. dissertation investigations that could not be retrieved in the time frame of the current project.

An important, unpublished paper by Nicholas (1982) was also identified in the review. This paper represents, perhaps, the best summary of some practices using hard criterion measures in OD evaluations.

Nicholas was principally interested in comparing the impact of three different classes of OD interventions on selected hard criteria. For the purposes of the current report, his few findings concerning the methodologies employed are of particular interest. Nicholas reviewed 65 studies that had used at least one of four types of hard criteria as a basis for evaluating an OD intervention: (a) work force behavior as measured by turnover, absenteeism, and grievances, (b) monetary performance as reflected in profits, operating costs, and dollar sales volume, (c) productivity including production quantity, efficiency, and effectiveness, and (d) output quality. Even though most of his research focused on the differential effects of various OD interventions, several methodological findings were of importance to this project. These included the following: (a) 80% of the studies employed quasi- or true experimental research designs, (b) 38% did not use comparison groups, (c) 93% used multiple hard criteria, (d) 22% did not use statistical tests, and (e) 12% relied upon single pretest-posttest measures for evaluating change.

In themselves, these results are certainly "sketchy" at best. However, they do, in part, suggest some considerations which should be taken as a methodology is proposed for LMDC to follow. This methodology for treating hard criteria in LMDC evaluations is proposed in the following sections.

IV. ISSUES IN SELECTING HARD CRITERIA FOR LMDC EVALUATIONS

A critical component for evaluating an LMDC consultation is the measure or criterion to be used for detecting organizational change. Theoretically speaking, some change(s), hopefully positive, should result from an LMDC intervention with an Air Force client group. The

criterion or criteria employed in an OD evaluation study represents the "yardstick" or measure to be used in identifying any possible changes. If these criteria are not thoughtfully chosen or developed, then any so called impacts of an intervention may go completely unnoticed. Thus, the choice of these measures is an important step in the evaluation plan.

The "criterion problem" has a long, tenuous history, particularly in the field of industrial/organizational psychology. Although significant inroads have been made at the conceptual, theoretical, and measurement levels, "the criterion" still presents formidible problems to personnel and organizational researchers. These problems are no less significant in the context of measuring organizational change(s) in the current setting.

Recently, through the research of Tuttle and his associates (Tuttle, 1981a; Tuttle, 1981b; Tuttle, Wilkinson, Gatewood & Luck, 1981), the Air Force has addressed the criterion problem. Even though a principal concern has been with the measurement of Air Force productivity, some of the work has important implications for the present research. By drawing upon the findings of Tuttle (1981a) as well as other investigators addressing the notion of criteria (A. T. Kearney, Inc., 1978; Hurst, 1980; Joint Financial Improvement Program, 1977), it is possible to identify a number of factors that should be considered in selecting or developing criteria for organizational change evaluations. It should be strongly emphasized that these criterion attributes are essential to effectively assess possible organizational changes. These factors or guides to developing and applying criteria for assessing LMDC consultations are as follows:

1. Reliability. The criterion should provide information that is dependable and accurate. Consistency of measurement that has a minimum of measurement error is a desired attribute. Thus, repeated application of a measure to the same level of organizational performance should yield the same scores.

2. Quantifiable. Quantitative criterion data are more desirable than are qualitative data. Criterion measures at an interval or ratio scale of measurement are preferred. These data will be appropriate for the types of statistical analyses to be performed on them.

3. Available on a frequent basis. Since an important interest is to evaluate organizational change over time, data should be available on at least a weekly or monthly basis.

4. Ease of retrieval. For criterion measures to be useful, they must be easily retrievable. As most hard criterion data will not be collected on-site by LMDC consultants, these measures must be retrievable via the mail. Most clients will willingly provide the necessary information assuming that the information is reasonably accessible. Furthermore, since information over time is going to be needed, archival data systematically reported to a centralized office is desirable.

5. Compatible with existing information sources. Criterion data developed from existing information sources rather than from new data sources are preferred. This policy will reduce the cost of measurement, increase the likelihood that data are available over time, and increase the probability that criterion measures based on these data will be accepted.

6. Sensitive to change. Variance in scores is an important measurement quality. That is, a criterion must be sensitive to detect and discriminate among differences in performance, yet not so sensitive as to be influenced by contaminating or external factors. If variance does not exist, then a measure would be useless for detecting organizational change.

7. Controllable by client group. Members of the group under study should be able to affect the outcome being measured. They should not be held accountable for results outside of their control.

8. Uniqueness. Multiple measures of organizational performance are needed to adequately capture an organization's effectiveness and efficiency. However, any measure employed should assess an important aspect of organization performance not measured by any other criterion indicator.

9. Comparable. Criteria should be comparable from one time period to another. If longitudinal analyses of organizational performance are to be made, then such measures should provide consistent methods of measurement over time.

10. Validity. Measures chosen should assess what they are supposed to measure. That is, they should reflect real changes in organization performance. They should be free from measurement biases such as omission of important aspects of performance or extraneous information unrelated to organization performance.

The above attributes taken in total represent the attributes of ideal criteria. In an operational context, some of the attributes may, at times, contradict others. On some occasions, it may be found that a criterion may possess some of the attributes but not others. Nevertheless, these characteristics serve as desired factors for choosing performance-based standard(s) for evaluating LMDC consultation activities.

V. AN ALTERNATIVE RESEARCH DESIGN AND ANALYSIS: INTERRUPTED TIME SERIES

In evaluating LMDC consultations using soft measures, it was noted earlier that a single group pretest-posttest design has been used. Subsequent statistical analyses have typically involved the calculation of t-tests between pre- and posttest means. Most often, these means have been derived from scores on the OAP administered to an Air Force client group. In contrast to treatment of soft measures, use of hard measures that are available in the Air Force poses some different problems and prospects. Some characteristics of such data are quite different from those found for soft measures. Thus, in the present context, a different form of research design and analysis will be required when performance-based data are employed. This section will provide an overview of an alternative design and analysis for treating hard measures in LMDC evaluation research. On the whole, the discussion will be presented at a conceptual level as it applies to LMDC. The statistical details are provided in a number of available sources (see, for example, Gottman, 1982; McClean & McCleary, 1979; McCain & Hay, 1980). The overview is organized in two sections: (a) nature of Air Force hard measures, and (b) interrupted time series design and analysis.

Nature of Air Force Hard Measures

A cursory review of selected Air Force documents and reports leaves any reader with the distinct impression that the Air Force routinely and

systematically collects a host of quantitative information. The quality of the data may vary from one measure or location to another; nevertheless, the quantity of data is impressive. Although much of the reported information has been used for monitoring purposes, some of the data have potential for evaluation applications as well.

Among others, there are two important traits of Air Force hard measures that have implications for evaluation research design and analysis. First, most data are collected and reported over time (such as, weekly or monthly intervals). Since time is a dimension of the data and many organizational changes may emerge only over time, then a suitable research design should incorporate time in it. Where time is included, a more sensitive test of organizational change can be made. Second, most hard measures are reported for a work unit. Whereas much of the soft criterion data collected by LMDC are available on individuals, most hard measures routinely collected by the Air Force are reported on work groups (such as, squadrons/wings, sections, or branches). When individual information is available, inferential statistics (such as t-tests) can be calculated. However, when group data are given, these procedures are not suitable. Therefore, any proposed analyses should facilitate the incorporation of group data. Finally, it should be added that any proposed design should compensate for inadequacies of the principal one in use, that is, the pretest-posttest design (Campbell & Stanley, 1963). Where research designs are subject to numerous rival hypotheses, the establishment of internal validity (that is, LMDC caused an organizational change) becomes questionable at best. If more robust designs can be employed that control for these rival hypotheses, then greater confidence in establishing cause and effect can be gained. One such robust design to be considered is the interrupted time series design.

Interrupted Time Series Design and Analysis

Given the weaknesses of the pretest-posttest design and the fact that multiple hard measures may be available on a client group, the interrupted time series design becomes a suitable option. A time series is involved when multiple measures collected over time are available for a group (Gottman, McFall & Barnett, 1969). The purpose of time series analysis is to determine whether a treatment or intervention (such as an

LMDC consultation) had any impact on the series. If measures in the series occurring prior to the intervention are different from those occurring after it, then it is assumed that the intervention (or interruption) had an impact. An example may help to clarify the application of a time series design to evaluation of an LMDC consultation.

Suppose LMDC had provided management consultation to an Avionics Management Squadron. Since it was hypothesized that the particular consultation should affect productivity of the branch, productivity measures were collected for 20 months prior to the consultation and 20 months after. The question to be answered is whether or not the consultation produced any significant organizational change. If it is inferred that change took place, then the series of observations should be different after the treatment (that is, consultation) than those before it. Interrupted time series or impact analysis (McCleary & Hay, 1980, pp. 141-201) permits the testing of the organizational change hypothesis.

Since the reader may not be familiar with the application of time series analysis, some details regarding the utility of the technique will be given. Again, the purpose is not to provide the statistical details of the method; only a general overview and some considerations are presented.

Cook and Campbell (1979, pp. 208-209) note that time series analysis permits a number of tests on a set of data. The following material borrows heavily from their ideas.

In evaluating a time series prior to and after an intervention, several types of effects in the series are tested. First, a change in the level or intercept of the series is made. For example, if preconsultation productivity data (monthly) in the example described above was 25, 26, 27, 28, 29, and 30 and the post-consultation series was 33, 34, 35, 36, 37, and 38, then it would be concluded that the consultation had an effect. Since the seventh observation was 33 and not the expected 31 and the pre- and posttreatment series have different intercepts, it may be concluded that the consultation enhanced productivity.

Additionally, changes in the slopes of a series may be tested. For instance, if the posttreatment series listed above was 33, 35, 37, 39, 41, and 43, it would be interpreted that the slope or trend in productivity measures had increased as well. Thus, productivity was increasing faster after the consultation than before it.

Effects can also be studied with respect to whether they are continuous or discontinuous. A continuous effect is a change that is produced over a long period of time. Conversely, a discontinuous effect is one lasting only a short period. Time series analysis may be used to isolate the duration of a particular effect.

Finally, time series effects can be tested in terms of whether they are instantaneous or delayed following an intervention. As a consequence of a consultation, change may occur immediately in group performance. On the other hand, the effects of the intervention may require some time to disseminate among group members. Therefore, the effects of a consultation may be delayed. Time series analysis could be used to identify such different impacts.

The principal threat to internal validity of the interrupted time series design is History (Campbell & Stanley, 1963, p. 39). History includes any factors occurring simultaneous to the treatment or consultation that may influence group performance. History can be controlled by adding a comparison group to the time series design; such a design is called the multiple time series design (Campbell & Stanley, 1963). In the earlier example, a comparison group could be added by selecting an Avionics Maintenance System squadron as similar as possible to the one receiving LMDC consultation. Performance data over identical time periods would then be collected. It would be expected that the client group (the one receiving the consulting service) would show improved productivity while the comparison group would not. Obviously, an important consideration in controlling history or any other factor is the comparability of the two groups. As group comparability decreases, control of the threat of history decreases. Where similar experimental and comparison groups can be used; however, the multiple time series design is a powerful alternative to the pretest-posttest design.

Some mention needs to be made concerning the requirements for conducting time series analysis in the context of LMDC evaluation. In addition to meeting the criteria for using hard measures listed earlier, a minimum number of observations are necessary. Although points of view differ, 40 to 50 observations seem to be the minimal requirement for estimating correlated time order of error and testing seasonality in the data (Cook & Campbell, 1976; McCain & McCleary, 1979; McCleary & Hay, 1980). Certainly, this number represents a considerable amount of data; yet, the utility of the procedure warrants careful consideration. Moreover, the nature of many available hard measures routinely reported by the Air Force suggests that the quantity (not necessarily the quality) of information needed may be available in current archival sources.

In some instances, it may not be possible to achieve the minimum number of data points even though a considerable number of pre- and posttest data are available. Cook and Campbell (1976) argue that a simple plotting of the data and observing the trends may be a reasonable option. More specifically, they state

> There are many situations in which it is not possible to collect data for so many time points. . . . We want to advocate the use of time-series designs even when no statistical test of the hypothesis can be carried out. In such a case, we consider it useful to plot the data and to 'eye-ball' whether there is a discontinuity in the time trend that cannot be readily explained in terms of the continuation of trends that are observable in the pretest time series, or in terms of statistical regression following from a deviantly low score just before the treatment is introduced. The most important feature of time-series designs is that there be a sufficient number of pretest data points covering a sufficiently extended time period so that all plausible patterns of variation can be ascertained. While it is undoubtedly advantageous also to be able to test whether an observed discontinuity at the time of the treatment can or cannot be plausibly attributed to chance, it should not be forgotten that chance is only one of many alternative interpretations that has to be ruled out. It would be a shame if time-series designs were not used because of 'too few observations for sensitive statistical analysis.' Even without tests of significance, they represent a powerful gain over designs with only one pretreatment observation (pp. 275-276).

Where other tests may not be appropriate, Cook and Campbell have proposed a possibility. Their proposal may not be an optimal one, but it may be a viable choice for some situations.

VI. APPLICATIONS

Time series or any other form of statistical analysis is no better than the data input to it. Clearly, if time series design and analysis are to be used, the hard measures employed should meet, at a minimum, the standards listed earlier for choosing hard criterion measures. As noted, one of the objectives of the present research was to examine the feasibility of using existing performance-based measures for evaluating LMDC organizational interventions with selected client groups. For the purposes of this study and given its associated time constraints, two client groups were chosen for investigation. This section of the report summarizes the hard criterion measures identified for these two groups. Selected hard measures are suggested as being appropriate for inclusion (along with soft measures) in a study to evaluate the effects of LMDC interventions with these client groups.

Consolidated Base Personnel Office (CBPO)

The initial client group chosen for review was the Consolidated Base Personnel Office or CBPO. This particular group was selected for two reasons: (a) the CBPO at Maxwell Air Force Base (where this research was conducted) was quite similar to CBPO operations at other bases and (b) LMDC staff members were available for consultation who had considerable experience with personnel and CBPO activities.

Collection of CBPO measures. Interviews/discussions were held with two LMDC staff members concerning CBPO operations. The objective of these discussions was to identify measures as well as data sources for evaluating a CBPO. The product of these discussions revealed that only one data source would possibly meet some of the 10 criterion characteristics described earlier. It is this source of data to which attention will now be given.

A review of the CBPO indicated that the Proficiency Status Reporting System (P-Status) might serve as a useful information source. The stated objective of the P-Status system is to ". . . improve the operating efficiency of base level military personnel operations through situation reporting by the CBPO chief" (AFM 30-130, 1981, p. 3-1). The system was introduced in 1972 in an attempt to provide some standardization across the Air Force in the evaluation of CBPO effectiveness. To

achieve this standardization, items called "trackers" were identified as symptomatic of performance problems of CBPOs. Examples of "trackers" are Late Airman Performance Reports, Late Officer Effectiveness Reports, Proportion of Personnel Files Containing Errors, etc. The P-Status system is applicable to all CBPOs regardless of their command affiliation. Furthermore, these data are reported monthly which facilitates the use of P-Status data for evaluation purposes.

Reviews of the P-Status reporting data suggested that four measures might be usable. (Other measures were available, however, these were eliminated. A cursory review of these variables indicated they would not meet most of the criteria established for a suitable evaluation standard.) These four measures and their associated CBPO branch responsible for these data are listed in Table 1. Several points should be made about the table and the measures. Looking at Table 1, it can be seen that certain branches of a CBPO are responsible for a specific measure. This responsibility may vary across CBPOs depending upon how they are organized, that is, whether they are a Class I or II CBPO (AFM 30-130, 1981, pp. 2-18-2-19). The use of these measures permits an evaluation to be carried to the branch level rather than limited to an overall section. Further, it should be pointed out that hard criterion data are not always currently available on all CBPO operations. Only four are noted here. Finally, the indices are constructed so as to range from 0 to 100. Presumably, the lower the score, the more efficient the CBPO branch. In general, these measures tend to place an emphasis on efficiency and less on effectiveness (Tuttle, 1981a).

Utility of CBPO measures. After identifying four possible measures for evaluating CBPO operations, it was necessary to investigate (a) the feasibility of obtaining these data, and (b) the quality of the reported measures. As a first step, a request was made to a CBPO at a large, midwestern Air Force base. Within one week, monthly P-Status reports were received, covering the period of 31 January 1981 to 31 May 1982. The response to the request suggested that it would be possible to obtain relevant hard measures through the mail.

An analysis of four potential measures (that is, Late Airman Performance Reports, Personal Reliability Program, Late Officer Effectiveness Reports, and Testing No-Shows) brought mixed results. No variance

Table 1

Selected Hard Criterion Measures for CBPO Operations

Evaluation Criterion	CBPO Branch		
	Quality Force	Personnel Utilization	Career Progression
1. Late Airman Performance Reports (APR) $\frac{\text{Number of APRs Received 30 days late}}{\text{Number of APRs Received/Accepted + Number of APRs Received 30 days late}} \times 100$	X		
2. Personal Reliability Program (PRP) $\frac{\text{Number of Errors Found}}{\text{Number of Errors Screened}} \times 100$		X	
3. Late Officer Effectiveness Reports (OER) $\frac{\text{Number of OERs Received 30 days late}}{\text{Number of OERs Received/Accepted + Number of OERs Received 30 days late}} \times 100$	X		
4. Testing No-Shows $\frac{\text{Number of 1st time no-shows}}{\text{Number of personnel tested}} \times 100$			X

(0 errors reported each month) was found with respect to the Personal Reliability Program (PRP) measure. Thus, if these data are typical for other time periods and/or other bases, then the PRP measure would not be a useful evaluation standard.

Although some variance was found for the measure Testing No-Shows, it tended to be rather limited or the number of no-shows was not reported. In fact, of the 17-month reporting period, it was noted that for 12 of the periods, the data were "not reportable this month." Therefore, Testing No-Shows was not considered to be a viable measure.

The final two measures hold promise for use as LMDC evaluation criteria. In addition to meeting most of the other evaluation factors, Late Airman Performance Reports (APR) and Late Officer Effectiveness Reports (OER) appeared to have meaningful variance and complete monthly data were reported. Split half reliability estimates (odd-even, Spearman-Brown corrected) for each of the measures were moderately high, .81 (APR) and .84 (OER) respectively. These estimates suggest reasonable consistency of measurement over time.

To examine the extent of dependence among these measures, a simple correlation was computed. This calculation produced a correlation of .38 (15), $p > .05$, indicating the criteria assessed different aspects of CBPO performance.

In sum, the P-Status report seems to be a useful vehicle for providing some hard criterion data on CBPO performance. Based upon data reported here, two measures seem to be particularly useful, that is, Airman Performance Reports and Officer Effectiveness Reports. The utility of the two other measures (Personal Reliability Program and Testing No-Shows) for LMDC evaluation purposes may vary across particular Air Force bases.

Aircraft Maintenance

The second unit chosen for investigation was Aircraft Maintenance. Essentially, this area was selected for two important reasons: (a) Aircraft Maintenance represents a major component of Air Force operations, and (b) resources were available locally (principally at Gunter Air Force Station) that could provide necessary information relative to this functional area. Since there are two major forms of maintenance organizations, the Standard Maintenance Organization (those

covered by AFR 66-1) was selected. Under this organization, the following squadrons are included: (a) Organizational Maintenance Squadron (OMS), (b) Field Maintenance Squadron (FMS), (c) Avionics Maintenance Squadron (AMS), and (d) Munitions Maintenance Squadron (MMS).

Collection of Aircraft Maintenance measures. Through the Maintenance Data Collection (MDC) and the Maintenance Management Information and Control System (MMICS), the Air Force collects a wealth of maintenance data. Since these data are routinely collected Air Force-wide, it was decided to attempt to utilize these existing measures in the present research. In that these information systems provide standardized data across a wide array of Air Force organizations and the information currently exists, there would be no need for a client to generate new information. Nevertheless, because existing data were going to be employed, the key problem was to identify those data that would be potentially most useful for the objectives sought.

As with the CBPO measures, tailored interviews/discussions were held with selected, key informants. These interviews were conducted with six interviewees: (a) a production maintenance analyst, (b) an aircraft maintenance superintendent, (c) a maintenance system director, (d) a civilian consultant working with Air Force maintenance information systems, (e) a maintenance management systems commander, and (f) a coordinator of DCM training. The informants were told about the purposes of the study and the criteria to be used in selecting an evaluation standard. Then, after reviewing the types of maintenance measures collected in the information systems, the respondents listed the measures they would recommend. Based upon their comments, the suggested measures of most of the respondents included the following:

1. Rate--Full Mission Capable
2. Rate--Partial Mission Capable-Maintenance
3. Rate--Partial Mission Capable-Supply
4. Rate--CMS Maintenance Cancellation
5. Rate--CMS Air Abort
6. Rate--Maintenance Late Takeoff
7. Rate--Scheduling Effectiveness
8. Rate--Sortie Cannibalization
9. Rate--Partial Mission Capable-Both

Initially, it was believed that it would be feasible to identify measures characteristic of maintenance squadron (OMS, AMS, FMS, MMS) performance. However, all informants reported that it would not be possible to use existing measures at the squadron level. It was noted that such measures would be influenced by numerous external factors. Based upon this point, it was concluded that any measure used would have to apply to an entire Aircraft Maintenance operation. The above measures were suggested as possible options.

Although there was not unanimous agreement on any one measure, a majority believed that each one offered some promise for the objectives of this study. Yet, it should be noted that several of the interviewees were uncertain as to whether the data would offer very much in the context of evaluation. In particular, one interviewee was very skeptical about the quality of the maintenance data entering the information systems. It was his belief that much of this information was so unreliable as to be of limited utility. Another reported that he did not believe that these measures would be sensitive enough to assess the impacts of an LMDC consultation. Alexander (1982) has also cautioned against the use of maintenance data. In a study of the accuracy of information entering the Maintenance Data Collection system, Alexander surveyed two large, TAC bases with two objectives: (a) to determine what percentage of actual maintenance data enter the information system, and (b) of the data that do enter, to determine their accuracy. His research yielded several important findings. First, only about 45% to 55% of available maintenance data were recorded and entered into the information system. Second, of these data, their accuracy ranged from 2% to 3%. If Alexander's results can be extrapolated to the present research, his findings would suggest that maintenance data would not offer a great deal of utility for evaluation purposes. Nevertheless, it was decided to investigate, in a limited way, the utility and feasibility of collecting information relative to these measures at an existing base.

Utility of Aircraft Maintenance measures. In order to investigate the dependability or reliability of actual measures of aircraft maintenance operations, contact was established with a large SAC base located in the northeast. A request was made for 20 months of maintenance data as reported in the Maintenance Monthly Summary (RCS: SAC-LGY

(M) 7902). Approximately one week later, the data, covering the period of 1 November 1980 to 30 June 1982, were received. From these reports, B-52 maintenance performance data were coded and submitted for analysis.

Preliminary review and analysis of the nine measures shows that four variables (Partial Mission Capable--Supply, Partial Mission Capable--Both, CMS Air Abort, and Sortie Cannibalization Rate) were not suitable for evaluation applications. Lack of variance in the scores as well as exceedingly small rates (in many cases, 0 rates) contributed to their lack of utility. On the other hand, the remaining five variables did not appear to suffer from these same problems. For these measures, subsequent analyses were designed and conducted to explore their uniqueness and reliability. The former analysis was performed to examine the extent to which the measures provided similar or unique maintenance information while the latter was used to test the dependability of the data.

As a first step, simple correlations were computed among the five variables. With the exception of a pair of variables, each of the maintenance measures was uncorrelated. Of the 10 intercorrelations computed, only one was significant. The lone exception was the relationship found between CMS Maintenance Cancellation Rate with Maintenance Late Takeoff Rate, $\underline{r}$ (18) = .63, $\underline{p} < .003$. These results suggest that, on the whole, different aspects of maintenance operations were measured by the five variables. Only a pair of variables appeared to share a common performance dimension in these operations.

Split half reliability estimates (odd-even, Spearman-Brown corrected) were also computed to determine the dependability of the variables. Three variables, Full Mission Capable (r_{tt} = .30), CMS Maintenance Cancellation Rate (r_{tt} = .16), and Maintenance Late Takeoff Rate (r_{tt} = .07), had very low reliability estimates. The low coefficients imply that these measures would be unacceptable for use as evaluation criteria. In contrast, two measures were found to be marginally acceptable, at least in terms of reliability estimation. Partial Mission Capable--Maintenance and Scheduling Effectiveness had reliability estimates of .74 and .63, respectively. Although these values are not as high as desired, they do suggest that these variables should receive strong consideration in evaluation criterion development/selection.

From an overall perspective, the quality of maintenance data studied in the present research was somewhat disappointing. Interview data, previous research, and the present data analyses have raised important questions about the applicability of maintenance data for LMDC evaluation purposes. Yet, one and possibly two measures (Partial Mission Capable--Maintenance and Scheduling Effectiveness) have some potential. Certainly, future evaluation research concerned with the use of hard criteria involving maintenance operations should at least consider these. As true of the CBPO data, the utility of any maintenance data may vary from one base to another.

VI. RECOMMENDATIONS

The preceeding analyses and results lead to several recommendations for LMDC to consider in implementing its evaluation strategies using hard criteria. Based upon the results of the present research, the following recommendations are offered:

1. Time series design and analysis should be employed as a method for analyzing hard criterion data collected for LMDC evaluation purposes. Time series designs can be used to control most of the rival hypotheses affecting the single group pretest-posttest design currently employed by LMDC. The rival hypothesis of History that characterizes the time series design can be controlled by one or a combination of the following: (a) keeping records of any possible events occurring during the LMDC intervention or over the study period that might produce changes other than the consultation effort, (b) using a monthly or, preferably, weekly time interval for collecting data on the evaluation standard (the shorter the time interval, the less possible the effect of History), and/or (c) incorporating a comparison group as similar as possible to the client group to which the consultation effort was given.

When time series designs are employed, no fewer than 40 observations or time periods should be used. For example, 20 time periods prior to an intervention and 20 after might be considered. Although this time interval represents a rather lengthy period, the present research suggests that the Air Force collects and retains the necessary information to meet this time requirement (at least on the criteria examined here). Thus, it should be possible for LMDC to obtain hard

criterion data on its previous consultations (say, those conducted prior to 1981) and examine efforts with respect to organizational change. When a statistical test is not desired or is not possible due to limited data, the criterion information should, at a minimum, be plotted with respect to time. Although inferences to similar situations about organizational change cannot be made, descriptions of change for the group under study can be given. In addition, the time series design will be useful when only group data (such as on an Air Force squadron or branch) rather than individual data are available. Current statistical tests employed by LMDC with OAP data are appropriate because they are collected on individual respondents. However, these tests are quite limited when used with data reported by group (which is characteristic of most Air Force hard measures). Time series analysis will help to resolve this limitation.

2. The evaluation standard or criterion is a critical ingredient to the success of time series analysis and evaluation of organizational impacts of LMDC consultations. In addition to data availability, it should be ascertained that evaluation criteria used have the following characteristics: (a) reliability, (b) validity, (c) ease of retrieval by a client group, (d) compatibility with existing management information sources, (e) sensitivity to organizational changes, (f) controllable by the client group, and (g) comparability across time periods. The LMDC evaluator should insure that the criteria chosen meet these standards. This assurance can be made through personal interviews with key informants of the client group (Tuttle, 1981a) and by empirical analyses (for example, reliability studies) of the data by the researcher.

3. Criterion information should not be collected and used simply because it is conveniently available. If there is not a sound rationale for choosing and linking a particular criterion with the specific consultation effort delivered by LMDC, then the detection of LMDC impacts on the client organization will be "guesswork" at best. Clearly, an evaluator should ask what effects should reasonably be produced by the intervention. Only those criteria representing those hypothesized effects should be considered.

4. The present research identified several, potentially-useful criteria for evaluation purposes. However, it may not be possible to consistently identify meaningful criteria from existing data sources. "Tailored" criteria may have to be developed to adequately assess organizational changes. Tailored criteria are those measures constructed specifically to assess organizational changes of a particular client group. Tuttle's (1981a) suggested procedure is one suitable option for developing these tailored measures. Although the tailored criterion development strategy may limit the external validity (generalizability of the findings from one group to another) of an evaluation study, the internal validity (establishment that an intervention caused or did not cause an outcome) of the research may be enhanced.

5. With respect to the present study, several criteria were identified as potentially useful for evaluating the efficiency of Consolidated Base Personnel Office (CBPO) operations. For the CBPO, Late Airman Performance Reports and Late Officer Effectiveness Reports were developed from monthly data systematically reported in the P-Status report system. (Analyses showed that CBPOs retain these data a minimum of 12 months.) Other P-Status report data were not found to be useful for evaluation purposes. When CBPO performance is to be evaluated, these two measures should be incorporated, at a minimum, in an evaluation plan (assuming of course that the type of consultation is logically related to the criteria).

6. Previous research (Alexander, 1982) as well as interview data collected from key informants in the present study have questioned the reliability of data reported in maintenance information systems. Based upon aircraft maintenance data reported in monthly maintenance summaries, the present research investigated the utility of nine measures for evaluating aircraft maintenance operations. On the whole, most of these measures were found to be unreliable and inappropriate for use as an LMDC evaluation criterion. However, two variables appeared to offer some utility. From the present analyses, when aircraft maintenance operations are to be evaluated, Partial Mission Capable Rate--Maintenance and Scheduling Effectiveness should be researched and considered for incorporation into an evaluation program. (As with the CBPO, these measures should only be used when it is reasonable to do so,

that is, measurements on the criteria are logically related to the type of intervention provided to the client group.)

7. Future research should investigate the applicability of time series analysis to previous LMDC consultations. The current findings suggest that relevant, historical hard data may be available for past LMDC clients. LMDC has historically conducted evaluations of their interventions with these clients using OAP or soft measures. Analyses using hard criteria for these same clients would help to answer the question of LMDC impacts on mission-oriented measures. Also, time series analyses would help to clarify the internal validity of LMDC evaluations that are somewhat limited due to the nature of the current research design. Prior to implementing such research, efforts should first be directed toward the selection/development of suitable evaluation criteria.

8. Current research is presently being conducted by the Air Force on productivity measurement. LMDC should carefully examine the utility of those measures developed by Air Force productivity researchers for possible inclusion in its evaluation program. These productivity measures are likely to have considerable face validity among Air Force managers and decision makers. Thus, if LMDC can incorporate such face-valid measures (where it makes sense to do so) in its evaluations, then the face validity and meaningfulness of LMDC and its evaluations will be enhanced. Although it will be some time before operational measures exist, LMDC should make plans to actively participate in Air Force productivity measurement programs.

9. Finally, future research should examine the relationships among various hard criteria and the dimensions of the OAP. Although cause and effect could not be established, any significant correlations would lend support to justify the importance of OAP dimensions used in evaluations. This evidence would be particularly important where hard measures are not available or are not used in an evaluation study but soft measures, i.e., OAP factors, are. In order to conduct such an investigation, a special study would likely have to be developed where individual OAP data and individual performance data could be collected. Alternatively, group OAP and group performance data could be employed; however, a large amount of data on numerous groups performing the same work functions

would be required. Whatever the option chosen, these data would seem to be invaluable to LMDC in discussing/presenting the importance of OAP information.

References

1. Adams, J. An evaluation of organization effectiveness: A longitudinal investigation of the effects of survey feedback as an action research intervention in unit efficiency, employee affective response, intergroup relations and supervisory consideration in the U. S. Army. Doctoral dissertation, Purdue University, 1977. Ann Arbor, MI: University Microfilms, No. 7813016.

2. Alexander, M. J. Personal Communication, August 2, 1982.

3. Campbell, D. T., & Stanley, J. C. Experimental and quasi-experimental designs for research. Chicago: Rand McNally, 1963.

4. Campbell, J. P., Dunnette, M. D., Lawler, E. E., & Weick, K. E. Managerial behavior, performance, and effectiveness. New York: McGraw-Hill, 1970.

5. Cook, T. D., & Campbell, D. T. The design and conduct of quasi-experiments and true experiments in field settings. In M. Dunnette (Ed.), Handbook of industrial and organizational psychology. Chicago: Rand McNally, 1976.

6. Cook, T. D., & Campbell, D. T. Quasi-experimentation: Design and analysis issues for field settings. Chicago: Rand McNally, 1979.

7. Golembiewski, R. T., Billingsley, K., & Yeager, S. Measuring change and persistence in human affairs: Types of change generated by OD designs. Journal of Applied Behavioral Science, 1979, 11, 331-347.

8. Gottman, J. M. Time series analysis. New York: Cambride University Press, 1982.

9. Gottman, J. M., McFall, R. M., & Barnett, J. T. Design and analysis of research using time series. Psychological Bulletin. 1969, 72, 299-306.

10. Hendrix, W. H., & Halverson, V. B. Organizational survey assessment package for Air Force organizations (AFHRL-TR-78-93). Brooks Air Force Base TX: Air Force Human Resources Laboratory, 1979.

11. Hurst, E. G. Attributes of performance measures. Public Productivity Review, 1980, 4, 43-50.

12. Joint Financial Management Improvement Program. Implementing a productivity program: Points to consider. Washington, D. C.: Author, 1977.

13. Jones, J. E., Spier, M. S., Goodstein, L. D., & Sashkin, M. OD in the eighties: Preliminary projections and comparisons. Group and Organization Studies, 1980, 5, 5-17.

14. Kearney, A. T. Measuring productivity in physical distribution. Chicago, IL: National Council of Physical Distribution Management, 1978.

15. Lloyd, R. F. Introducing model II survey feedback: A longitudinal investigation of the effects of traditional survey feedback and a proposed feedback style on job attitudes, employee affective reactions and organizational performance measures. Doctoral dissertation, Purdue University, 1977.

16. LMDC. History and structure of the Organizational Assessment Package survey. Maxwell Air Force Base, AL: Leadership and Management Development Center, 1981a.

17. LMDC. Consulting background and philosophy. Maxwell Air Force Base, AL: Directorate of Management Strategies and Education, Leadership and Management Development Center, 1981b.

18. Macy, B. A., & Mirvis, P. H. A methodology for assessment of quality of work life and organizational effectiveness in behavioral-economic terms. Administrative Science Quarterly, 1976, 21, 212-226.

19. Mahr, T. A. Manual for the Organizational Assessment Package survey. (Technical Report 82-1560). Maxwell Air Force Base AL: Leadership and Management Development Center, 1982.

20. Martin, H. O. The assessment of training. Personnel Management, 1957, 39, 88-93.

21. McCain, L. J., & McCleary, R. The statistical analysis of the simple interrupted time-series quasi-experiement. In D. Cook & D. Campbell (Eds.), Quasi-experimentation: Design and analysis issues in field settings. Chicago: Rand McNally, 1979.

22. McCleary, R., & Hay, R. A. Applied time series analysis. Beverly Hills, CA: Sage, 1980.

23. Nicholas, J. M. Evaluation research in organizational change interventions: Considerations and some suggestions. Journal of Applied Behavioral Science, 1978, 14, 23-40.

24. Nicholas, John M. The comparative impact of organization development interventions on hard criteria measures. Unpublished paper, Loyola University of Chicago, February, 1982.

25. Porras, J. I., & Berg, P. O. Evaluation methodology in organization development: An analysis and critique. Journal of Applied Behavioral Science, 1978, 14, 151-173.

26. Rosenbach, W. A. An evaluation of participative work redesign: A longitudinal field experiment. Doctoral dissertation, University of Colorado, Boulder, 1977. Ann Arbor, MI: University Microfilms, No. 77-24, 280.

27. Short, L. O., & Hamilton, K. L. An examination of the reliability of the Organizational Assessment Package (OAP). Maxwell Air Force Base, AL: Leadership and Management Development Center, 1981.

28. Short, L. O., & Wilkerson, D. A. An examination of the group differences aspect of construct validity of the Organizational Assessment Package. Maxwell Air Force Base, AL: Leadership and Management Development Center, 1981.

29. Tuttle, T. C. Productivity measurement methods: Classification, critique, and implications for the Air Force (AFHRL-TR-81-9). Brooks Air Force Base, TX: Manpower and Personnel Division, 1981a.

30. Tuttle, T. C. Manager's guide to productivity improvement resources and programs (AFHRL-TP-81-12). Brooks Air Force Base, TX: Manpower and Personnel Division, 1981b.

31. Tuttle, T. C., Wilkinson, R. E., & Gatewood, W. L. Measuring and enhancing organizational productivity: An annotated bibliography (AFHRL-TR-81-6). Brooks Air Force Base, TX: Manpower and Personnel Division, 1981b.

32. Webb, E. J. Unconventionality, triangulation, and inference. In N. K. Denzin (Ed.), Sociological methods: A source book. Chicago: Aldine, 1970.

33. Webb, E. J., Campbell, D. T., Schwartz, R. D., & Sechrest, L. Unobtrusive measures: Nonreactive research in the social sciences. Chicago: Rand McNally, 1966.

34. Westover, T. O. Consultant's guide to the management consultation process. Maxwell Air Force Base, AL: Air Command and Staff College, 1979.

35. Wilkerson, D. A. Personal communication, April 16; June 14, 1982.

1982 USAF-SEEE SUMMER FACULTY RESERACH PROGRAM

Sponsored by the

AIR FORCE OFFICE OF SCIENTIFIC RESEARCH

Conducted by the

SOUTHEASTERN CENTER FOR ELECTRICAL ENGINEERING EDUCATION

FINAL REPORT

AN EVALUATION OF INDICES OF CORONARY HEART DISEASE (CHD) IN A DISEASED FREE POPULATION

Prepared by:	Dr. Mack Felton, Jr.
Academic Rank:	Professor of Biology
Department and University:	Department of Biology Southern University - New Orleans
Research Location:	Brooks Air Force Base School of Aerospace Medicine Clinical Science Division Pathology Branch
USAF Research	Dr. R. G. Troxler/Mr. Lloyd L. Foster

Date:	August 16, 1982
Contract No:	F49620-82-C-0035

AN EVALUATION OF INDICES OF CORONARY HEART DISEASE (CHD) IN A DISEASED FREE POPULATION

by

Mack Felton, Jr.

ABSTRACT

Measurement of total serum cholesterol, high-density lipoprotein (HDL) and the ratio of total cholesterol to high-density lipoprotein (Total cholestrol/HDL) of 770 US Air Force aviators was determined seeking an improved index for predicting coronary heart disease. Measurement of all variables was expressed as percents. Each variable, total serum cholesterol, HDL, and the ratio, values were plotted in percent versus concentration (mg/dl). All the aviators used in the sample were free of any coronary heart disease. Plans were to obtain data from a diseased population, however, this informatin was incomplete.

An estimated cut point, determined graphically, for high-density lipoprotein (HDL) and the ratio total cholesterol/HDL was ninety percent (90%). There is an obvious question of confidence in the estimated cut point, however, data obtained from a diseased population will prove or dismiss the fit of the graphically determined cut points. The data obtained in this study support the use of the ratio, total cholesterol/HDL, as a clinical instrument for predicting coronary heart disease.

Age proved to be independent of the variables measured in this study. Use of the ratio as HDL/total cholesterol provided no measurable difference in the estimated cut point.

Acknowledgement

The author wishes to express his sincere thanks to the Air Force Systems Command, the Air Force Office of Scientific Research and the Southeastern Center for Electrical Engineering Education for providing an opportunity to spend a summer investigating a stimulating research problem at the Brooks Air Force Base School of Aerospace Medicine. He would like to extend his appreciation to the Clinical Sciences Division and particularly to the Pathology Branch, for its hospitality and excellent working conditions.

Finally, the author wishes to thank Dr. Raymond G. Troxler for his supervision of this project. Dr. Troxler shared his expertise generously. I would like to give credit to Mr. Lloyd L. Foster for his ceaseless efforts to make this summer's experience pleasant and profitable.

I. INTRODUCTION

A survey of the literature will indicate the long period of time in which total serum cholesterol was used as a strong indicator of coronary heart disease.[5,7,10] Several investigations revealed that the serum cholesterol could be divided into sub-fractions.[7] These sub-fractions are triglycerides, chylomicrons, very low-density lipoproteins (VLDL), low-density lipoproteins (LDL) and high-density liporoteins (HDL). Collectively, these sub-fractions comprise the plasma lipoproteins. The plasma lipoproteins do not circulate freely in solution in the blood. They exist in the form of complexes consisting of lipid and protein.

Plasma low-density lipoprotein (LDL) contains approximately 60 to 75% of the total plasma cholesterol. Therefore, LDL is considered a strong positive indicator of coronary heart disease.[7] Previously high-density lipoprotein (HDL) received much less attention than the heavy lipid containing low-density lipoprotein (LDL). HDL comprises approximately 20 to 25% of the total plasma cholesterol. High-density lipoproteins are the heaviest of the four lipoprotein classes. HDL has a density of 1.063 to 1.21 g/ml. This greater density reflects its greater protein and lower lipid content. Fifty percent (50%) of HDL is protein, thirty percent (30%) is phospholipid, twenty percent (20%) is cholesterol and five percent (5%) is triglyceride by weight. High-density lipoprotein is heterogenous, that is, in the ultracentrifuge it can be subdivided into two fractions. One fraction, HDL, has a density of 1.063 to 1.125, the other fraction, HDL_3 has a density of 1.125 to 1.21. HDL_3 contains the larger percentage of protein then HDL_2. HDL, is a fraction of HDL with a density of 1.063 to 1.125 and is precipitated by heparin and manganese.[7]

The exact nature of HDL metabolism is not known. It is known that both, the liver and the intestine, are involved in the production of HDL. Certain evidence indicates HDL is derived from a discoidal-shaped precursor form which is converted into a spherical particle by the action of an enzyme, lecithin-cholesterol acyl transferase (LCAT).[7]

It has been postulated that HDL plays a role in the efflux of cholesterol from tissues. Another hypothesis suggested that HDL may interfere with LDL cholesterol competitively for sites within tissues. Some investigators postulated a scavenger's role for HDL during VLDL lipolysis. Finally, another process ascribed to HDL function may be the reducing of arterial cellular uptake of cholesterol by interfering with LDL binding to the cell surface.[7] It is safe to state that HDL provides a protective effect in preventing coronary heart disease.

Uhl et.al.[9] in a cross sectional study of 572 asymptomatic airmen, who were screened for risk of coronary artery disease found the ratio of total cholesterol/HDL very useful in predicting disease regardless of age. Their findings indicated the ratio to be superior to total cholesterol or HDL cholesterol when either is used alone as a discriminator of coronary heart disease. The purpose of this study was to examine the total cholesterol/HDL ratios of 770 aircrew members who were free of coronary heart disease. Seeking to determine whether the ratio values, with concentrations expressed as mg/dl, if plotted against the values expressed as percents would reveal any enhancement of the ratio as a discriminator of coronary heart disease. Plans were made to contrast the same type of data obtained from coronary patients, however, the compilation of the data was incomplete. Along with the other variables evaluated in this study, the effect of age was considered.

II. OBJECTIVES

The techniques used to measure the serum cholesterol and lipoprotein of the 770 aircrew members are well documented at the research level.[3,5,7,9,10] Patient chemistry determinations were performed as described by Uhl et al.[9] These techniques are expensive and are not a part of the routine procedures available to clinical laboratorians. The application of ratio data routinely in the clinical laboratory would facilitate patient care and help prevent coronary artery disease.

The specific objective of this study was to determine if the percentage distribution of the total cholesterol/high-density ratio values, along with age, contrasted to the same ratio values measured in mg/dl, would yield any enhancement of the ratio as a strong index of coronary artery disease. To use data from a healthy population and coronary patient data to determine a cut point using the ratio values. To learn how well ratio values obtained by Uhl et al.[9] fit below the cut points obtained in this study.

Initially, the first task required examination of patient data so that healthy patients would form one population and coronary patients would comprise the second population. Ratio values were to be obtained for each population, so that cut points could be estimated.

III. STATEMENT ON THE NATURE OF THE PROBLEM

Classic risk factors used in determining coronary heart disease are total serum cholesterol, triglyceride, low-density lipoprotein, high-density lipoprotein and recently the ratio of total cholesterol/ high-density lipoprotein.[5,7,9,10] In addition to these classic risk factors, medical teams correlate factors such as age, sex, body mass, hormones, cigarette smoking, alcohol consumption, diet, physical activity,

socioeconomic status, race ethnicity, familial genetics, diseases such as diabetes, blood pressure and various medications when evaluating potential coronary risks.[5] Patients are counseled on managing the forementioned factors and how the factors relate in prevention of coronary heart disease. Patients identified as cardiovascular risks, upon entering the clinic, undergo cardiovascular screening. This requires physicians, specialist and a cadre of associated health professionals. The cardiovascular screening includes a chest roentgenogram, an electrocardiogram at rest, 16 hours of ambulatory electrocardiographic monitoring and a thorough history and physical examination. Patients who had abnormal tests underwent thallium perfusion scintigraphy and cardiac catheterization.[9]

Uhl et al.[9] cited the improved efficacy of the total cholesterol/high-density lipoprotein ratio over both, the total serum cholesterol and the high-density lipoprotein, when either was used alone. Their findings indicated persons with ratios above 6.0 had significant coronary artery disease. Their testing proved the ratio to be eighty seven percent (87%) effective. Had ratio data been employed initially, 508 treadmill test would have been eliminated. Ninety eight (98) men found free of coronary artery disease would not have been exposed to the risk of coronary angiography.[9]

The nature of the problem , then was to explore a means of improving the use of the total cholesterol/high density lipoprotein ratio in two select populations. If light can be shed on this problem the expense in the Uhl et al.[9] study could have been spared. Reliability in application of the totalcholestrol/HDL ratio moves closer to providing a simple routine test for predicting coronary heart disease.

IV. EXPERIMENTAL DESIGN

A decision was made to examine data from two populations of aircrew members. One population's medical histories indicated no measurable evidence of coronary heart disease. Required information was furnished by the Brooks Air Force Base School of Aerospace Medicine Division of Data Sciences which employs Statistical Analysis System of the SAS Institute Inc., Box 8000, Cary, NC, 27511.

Computer printouts, containing histories were examined, reviewing diagnosis to ascertain the population was free of any individuals that exhibited any significant symptoms of coronary heart disease. A computer compilation was made providing values for total serum cholesterol, triglycerides, high-density lipoprotein, the ratio of total cholesterol/high-density lipoprotein and the ratio of high-density/total cholesterol. The effect of the distribution of ratio values expressed in percent was plotted against ratio values expressed in mg/dl. Cut point was determined graphically, due to the incomplete data available on coronary patients. There is a method for estimating cut point when there is data from two groups as initially proposed. Computer data was obtained through use of a Univac 1100 Time Sharing Executive Multiple-Processor System.

There was an effort to determine if age correlated, according to Gaussian distribution, with the values of the variables, total cholesterol, triglycerides, high-density lipoprotein, the ratio of total cholesterol/high-density lipoprotein and the ratio of high-density lipoprotein/total cholesterol. (Table 1)

V. EXPERIMENTAL RESULTS

Upon reviewing the data which consisted of regression analysis plots of age versus values for concentrations of total serum cholesterol, triglycerides, high-density lipoprotein, the ratio of total cholesterol/high-density lipoprotein and the ratio of high-density lipoprotein/total cholesterol, age proved to be independent of the values of all the forementioned variables. Values for the slopes, R^2 (which indicates variance) and the correlation were very small. Slope values were too near zero to be of any significance. The value for the slope of high-density lipoprotein was a negative (-0.011767) (Table 1). Interpretation of the data means age was an independent variable. Further, this means the ratio, total cholesterol/high-density lipoprotein can be used as a coronary artery disease discriminator in populations of young people as well as in older groups.[3,6,9]

The total cholesterol/high-density lipoprotein values expressed as percent was plotted versus ratio values expressed as mg/dl. The graphically estimated cut point was ninety percent (90%). Ratio values up to the ninety percent level are within the range of ratio values reported by Uhl et.al.[9] (Table 2, Figure 3) as being safe from coronary artery disease. Williams et al.[10] studied normal populations, evaluating HDL concentrations and total cholesterol/HDL ratios as discriminators for coronary heart disease. In their study, mean high-density lipoprotein was measured as 59.2 mg/dl. The mean high-density lipoprotein in this study was 48.51 mg/dl. Williams et al.[10] reported a high-density lipoprotein ratio/total cholesterol expressed in percent as 27.9%. This value is much lower than the cut point in this study, but the value falls within the estimated range of ratio values considered safe from cardiac disease. In this study the 27.9% value would equal a ratio between 3.46 and

4.0 (Table 2, Figures 3 and 4). Most important is the approach measuring the ratio as a percent.

Lipinska and Gurewich[8] used electrophoresis and precipitation techniques to measure HDL. These investigators stated that expression of HDL-cholesterol expressed as a percent was a more critical measure than if expressed as mg/dl. Using a fully automated heparin-manganese precipitation technique they determined a mean HDL-cholesterol of 56.1 mg/dl. In healthy patients, using electrophoresis, HDL-cholesterol was measured at 32.6% with a cut point of 23.5% (by means of the polyacrylamide gel technique); HDL-cholesterol was measured at 27.9% with a cut point of 18.5% (by means of the cellulose acetate technique). Values for HDL-cholesterol and cut points were higher when measurements were expressed as mg/dl using the techniques forementioned. Their most significant finding was that when HDL-cholesterol was expressed as a percent, eighty two (82%) percent of their healthy sample were properly classified. Eighty three (83%) percent of their coronary patients were properly classified when HDL-cholesterol was expressed as a percent.[8] This data appears to be significant and supports the objectives of this study.

In this study, if the cut point of ninety percent proved to be real, the persons in the ninety to ninety-nine percentile would be critical. It could be hypothesized that these individuals will show disease later. Data from the coronary patient file will be used to clarify the question.

VI. RECOMMENDATIONS

The unique aspect of this study was seeking to establish two populations for study. The percent distribution of the values of total serum cholesterol, triglyceride, high-density lipoprotein, the ratios, total

cholesterol/high-density lipoprotein and high-density lipoprotein/total cholesterol were obtained. Analysis of the data revealed age as an independent variable from the variables cited above. Data showed that the correlation between age and the other variables did not reflect a Gaussian relation. Use of additional transformation techniques could possibly reveal the proper conditions when the parameters' relations might fit a Gaussian distribution (Table 1)

There is a need to continue this investigation so that data obtained from the coronary heart disease group can be correlated with the disease free group. There is a need to settle upon a means for measuring cut point for the two populations. The assumption, that if data from each group approaches Gaussian distribution there will exist an area of overlap consisting of individuals from each population. There is a need to provide aviators, as well as the public at large, with any risk of cardiac disease, a means of ascertaining their condition and initiating preventive measures.

On the other hand, persons free of disease need to be assured of their good health. More importantly, this experimental approach needs to be pursued if the graphically determined cut point of ninety percent (90%) is real. Predictability at the ninety percentile would make use of the ratio in the clinic a reality.

REFERENCES

1. Robert D. Abbot, Robert J. Carrison, Peter W. Wilson, and William P. Castelli "Coronary Heart Disease Risk: The Importance of Joint Relationships among Cholesterol Levels in Individual Lipoprotein Classes," Preventive Medicine Vol 11, pp. 131-141, 1982.

2. Tavia Gordon, William P. Castelli, Marthana C. Hjortland, William B. Kannel and Thomas R. Dawber "High Density Lipoprotein As a Protective Factor Against Coronary Heart Disease," The American Journal of Medicine Vol 62, pp. 707-714, 1977.

3. Tavia Gordon, William P. Castelli, Marthana C. Hjortland, William B. Kannel and Thomas R. Dawber "Predicting Coronary Heart Disease in Middle-Aged and Older Persons," The Journal of the American Medical Association Vol 238, pp. 497-499, 1977.

4. James Gutai, Ronald LaPorte, Lewis Kuller, Wanju Dai, Lorita Falvo-Gerard and Arlene Caggiula "Plasma Testosterone, High Density Lipoprotein Cholesterol and Other Lipoportein Fractions," Vol 48, pp. 897-902, 1981.

5. Gerardo Heiss, Norman J. Johnson, Susan Reiland, C.E. Davis and Herman A. Tyroler "The Epidemiology of Plasma High-density Lipoprotein Cholesterol Levels," Circulation Vol 62 (Supplement IV) pp. IV 116-136, 1980.

6. William B. Kannel, William P. Castelli and Tavia Gordon "Cholesterol in the Prediction of Atherosclerotic Disease," Annals of Internal Medicine Vol 90, pp. 85-91, 1979.

7. Robert I. Levy and Basil M. Riskind "The Structure, Function and Metabolism of High-density Lipoproteins: A Status Report," Circulation Vol 62 (Supplement IV) pp. IV 4-8, 1980.

8. Izabella Lipinska and Vistor Gurewich "The Value of Measuring Percent High-Density Lipoprotein in Assessing Risk of Cardiovascular Disease," Archives of Internal Medicine Vol 142, pp. 469-472, 1982.

9. Gregory S. Uhl, Raymond G. Troxler, James R. Hickman and Dale Clark "Relation Between High Density Lipoprotein Cholesterol and Coronary Artery Disease in Asymptomatic Men," The American Journal of Cardiology Vol 48, pp. 903-910, 1981.

10. Peter Williams, David Robinson and Alan Bailey "High Density Lipoprotein and Coronary Risk Factors In Normal Men," Lancet, Vol 8107, pp. 72-75, 1979.

Table 1. Relationship of Age to the Variables:
Total Cholesterol; Triglycerides; HDL; Total Cholestrol/HDL
HDL/Total Cholesterol

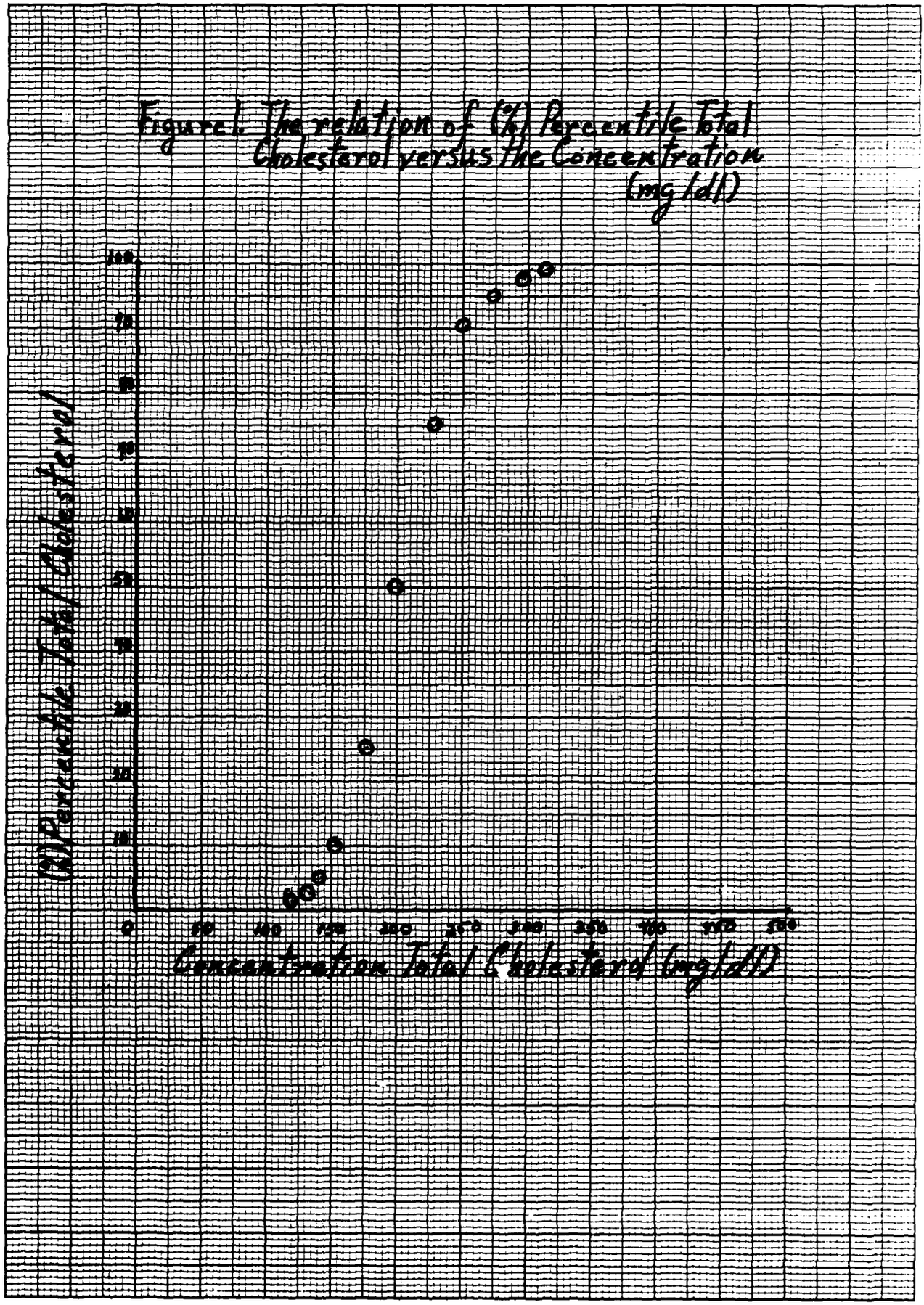
Variable	N	Mean	Slope	R^2	Correlation (Age)
Tot Chol	770	203.11	1.032	0.0453	0.2130
Tri Gly	770	103.73	1.384	0.0166	0.1288
HDL-Chol	767	48.51	-0.011	0.0001	-0.0100
TC/HDL	767	4.42	0.026	0.0187	0.1367
HDL/TC	767	0.24	-0.001	0.0244	-0.1562

Tot Chol = Total Cholestrol; Tri Gly = Triglycerides; HDL-Chol = Total Cholestrol/High-density lipoprotein ratio; HDL/TC = High-density lipoprotein/total cholestrol ratio.

Table 2. Relationship of The Percentiles of the Variables to their Concentrations

Variable	N	Percentiles of Variables											Mean
		0.010	0.025	0.050	0.100	0.250	0.500	0.750	0.900	0.950	0.975	0.990	
Tot Chol	770	122.00	132.00	143.00	154.00	176.00	200.00	229.00	253.00	275.00	296.00	314.00	203.11
Tri Gly	770	40.00	43.00	51.00	59.00	79.00	103.00	151.00	220.00	277.00	360.00	478.00	130.75
HDL-Chol	767	26.00	30.00	32.00	34.00	41.00	47.00	55.00	63.00	68.00	76.00	84.00	48.51
TC/HDL	767	2.17	2.40	2.64	2.94	3.46	4.13	5.11	6.18	6.84	7.44	8.80	4.42
HDL/TC	767	0.11	0.13	0.14	0.16	0.19	0.24	0.28	0.33	0.37	0.41	0.46	0.24

Tot Chol = Total Cholesterol; Tri Gly = Triglycerides; HDL -Chol = High-density lipoprotein cholesterol; TC/HDL = Total Cholesterol/High-denisty lipoprotein ratio; HDL/TC = High-density lipoprotein/Total Cholesterol ratio.



K&E 10 X 10 TO ½ INCH 7 X 10 INCHES KEUFFEL & ESSER CO. MADE IN U.S.A.
46 1320

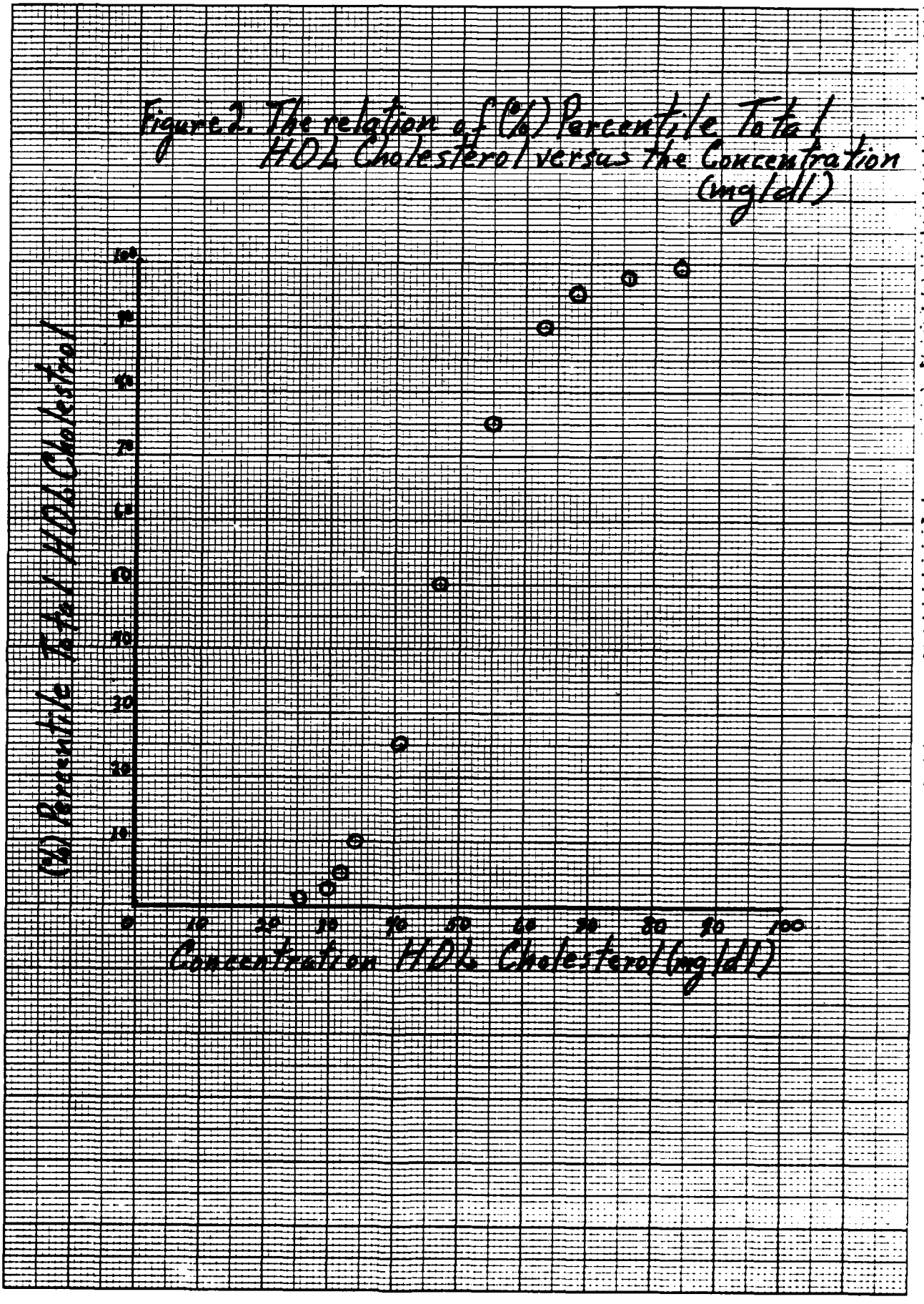


Figure 2. The relation of (%) Percentile Total / HDL Cholesterol versus the Concentration (mg/dl)

46 1320
K•E 10 X 10 TO ½ INCH 7 X 10 INCHES
KEUFFEL & ESSER CO. MADE IN U.S.A.

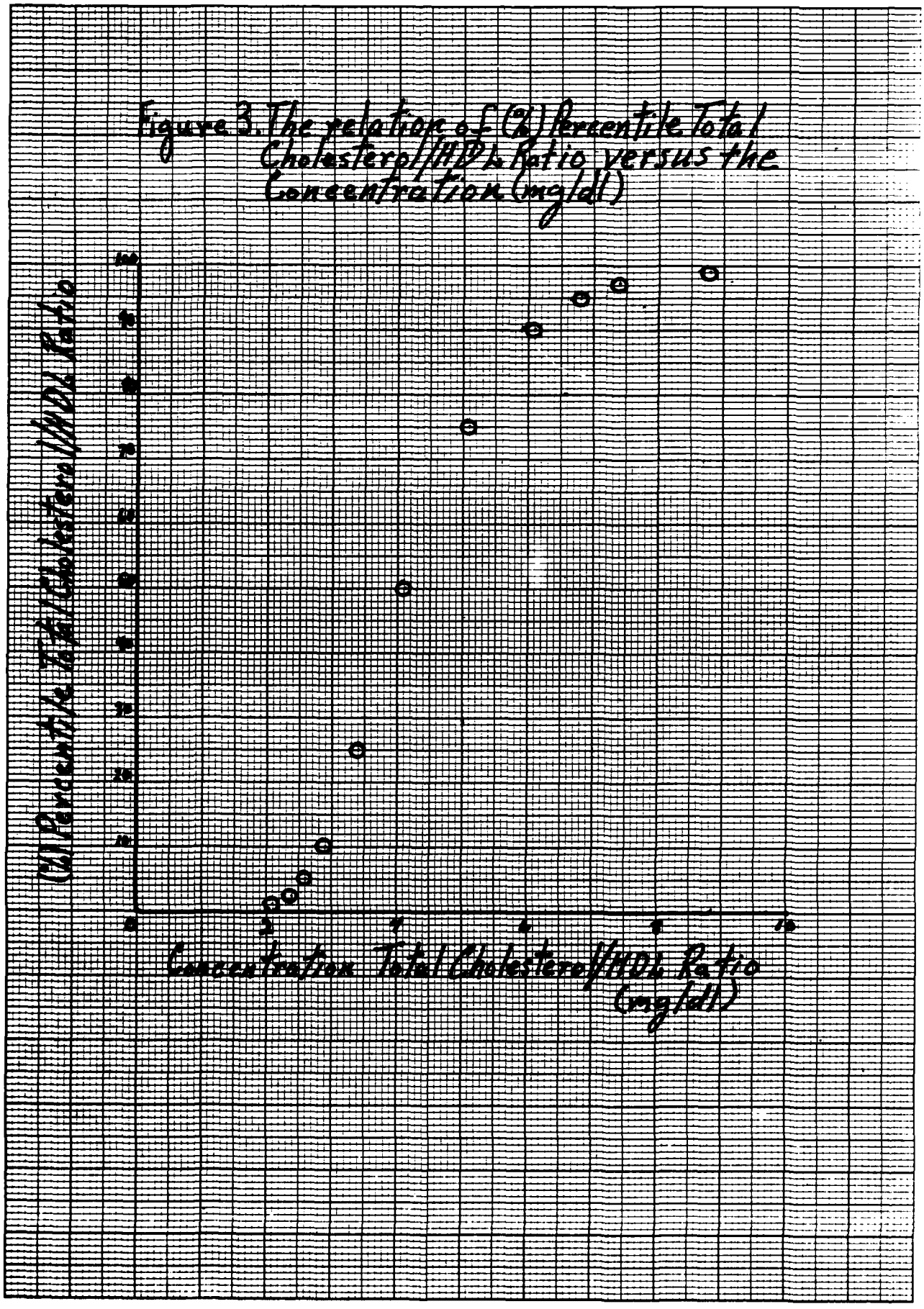


Figure 3. The relation of (%) Percentile Total Cholesterol/HDL Ratio versus the Concentration (mg/dl)

46 1320

K•E 10 X 10 TO ½ INCH 7 X 10 INCHES KEUFFEL & ESSER CO. MADE IN U.S.A.

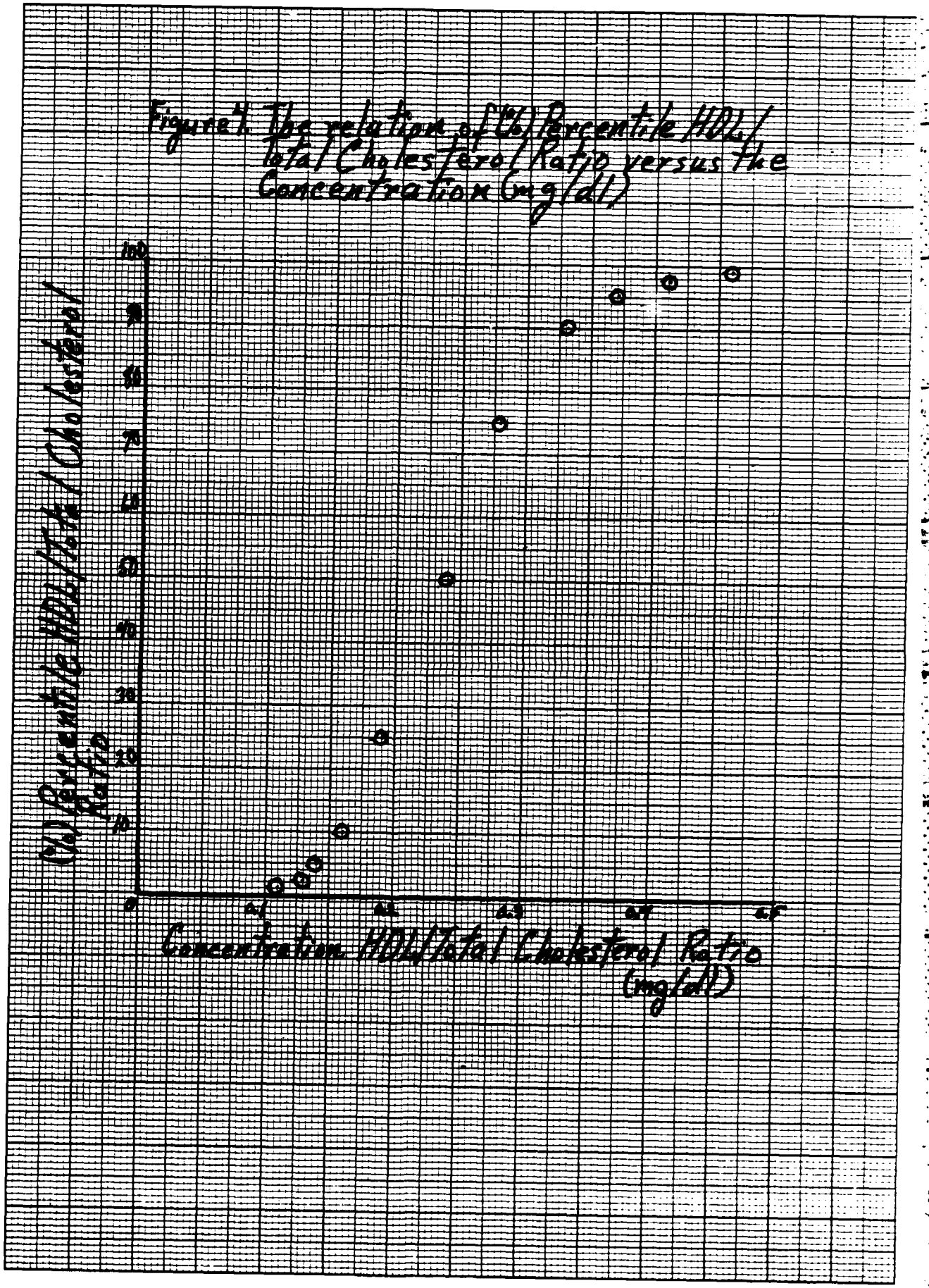


Figure 4. The relation of (%) Percentile HDL/Total Cholesterol Ratio versus the Concentration (mg/dl)

K+E 10 X 10 TO ½ INCH 7 X 10 INCHES KEUFFEL & ESSER CO. MADE IN U.S.A.
46 1320

1982 USAF-SCHEEE SUMMER FACULTY RESEARCH PROGRAM

Sponsored by the

AIR FORCE OFFICE OF SCIENTIFIC RESEARCH

Conducted by the

SOUTHEASTERN CENTER FOR ELECTRICAL ENGINEERING EDUCATION

FINAL REPORT

ELECTRON TRANSPORT CALCULATIONS USING THE METHOD OF STREAMING RAYS

Prepared by:	William L. Filippone
Academic Rank:	Associate Professor
Department and University:	Nuclear and Energy Engineering University of Arizona
Research Location:	Rome Air Development Center Solid State Sciences Division Radiation Hardened Electronic Technology Branch Radiation Effects Section
USAF Research Colleague:	Dr. John C. Garth
Date:	August 26, 1982
Contract No:	F49620-82-C-0035

ELECTRON TRANSPORT CALCULATIONS USING THE METHOD OF STREAMING RAYS

by

W. L. Filippone

ABSTRACT

The development of a new approach for solving problems of electron transport theory has been initiated. It involves using the streaming ray (SR) method to solve the Spencer-Lewis equation for the electron distribution in space, angle, and path length. The electron energy spectrum and energy deposition profile can then be determined using an appropriate stopping power formula.

Preliminary calculations have been carried out for idealized problems with energy independent cross sections and stopping powers. Several numerical methods for describing the anisotropy of the scattering process have been investigated. Those techniques that preserve the momentum transfer (rather than the total scattering cross section) appear to be most successful; however, more testing is needed.

ACKNOWLEDGEMENT

The author is grateful to the Air Force Systems Command, The Air Force Office of Scientific Research, the Southeastern Center for Electrical Engineering Education, and the Rome Air Development Center for making this research possible.

He would like to give a special thanks to Dr. John Garth for his suggestions and collaboration. Useful discussions with Drs. Edward A. Burke and Stanley Woolf, and the hospitality of Dr. Peter J. Drevinsky and the staff of the Radiation Hardened Electronics Technology branch are also appreciated.

I. INTRODUCTION

Electron transport theory plays an essential role in such diverse areas as plasma physics, lasers, and the study of radiation damage to electronic devices in space born vehicles. For many problems of practical interest existing electron transport calculational techniques are unacceptable. In theory, Monte Carlo computer codes could yield results to any desired accuracy; however, in many cases this would require a prohibitive amount of computer running time. Discrete ordinates (S_N) calculations are much more rapid, and there has been considerable progress in applying these techniques[1] to problems of electron transport. However, S_N calculations often produce unacceptable errors. Among the problems of S_N computations are energy straggling effects, dispersion of wave fronts (range straggling) and negative solutions along certain of the discrete ordinate directions. There is a definite need for computer codes that are accurate, reliable and relatively inexpensive to operate.

In recent years, several characteristic methods[2] have been developed for solving the transport equation. A major advantage of these methods is that they enable extremely good accuracy in numerically representing the streaming term of the transport equation. While some characteristic methods stress flexibility[3], the streaming ray (SR) method[4-8] stresses computational efficiency. It was developed as an alternative to the closely related S_N method, and has shown considerable advantage for problems involving the deep penetration of radiation, vacuum material interfaces, collimated beams, and wave fronts. Although the SR method was developed for two-dimensional problems of neutral particle transport, it appears that many of its advantages should carry over to the

charged particle case. In addition, SR computations can be performed at a fraction of the computer costs required by Monte Carlo calculations. An effective numerical electron transport method must be able to properly account for a huge number of very small deflections in both energy and angle.

Small Angular Deflections

In extreme cases, scattering can be so forwardly peaked that the probability of deflecting from one quadrature direction to another in a single collision is negligible. Straight forward application of a quadrature scheme for angular integrations would then lead to a diagonal scattering matrix. With such a matrix, scattering is modeled by straight ahead collisions alone, and there is no possibility for an electron to change directions. Another potential problem stems from the fact that the number terms required for an accurate Lagendre series representation of such a scattering kernel would be enormous.

The latter problem is eliminated by devices such as extended transport corrected cross sections[9,10], while the former problem can be eliminated by using mixed mesh[11], Fokker-Planck[1,12], or similar techniques. The Fokker-Planck and two new approaches described below, for defining the scattering kernel have been studied.

Small Deflections in Energy

When small deflections dominate the scattering process the relationship between an electron's energy and the distance it has traveled is well described by the continuous slowing down model. This stopping power information can be used in two different ways for determining the energy distribution of electrons. In the first approach the stopping power

formula would be used to generate multigroup cross sections. The multigroup transport equations would then be solved numerically. Alternatively one could first solve the Spencer-Lewis form of the transport equation for the electron distribution in space, angle and path length. The stopping power formula would then be used to relate the electron energy distribution to the path length distribution.

The former approach has the advantage that it is consistent with existing S_N codes and as the number of energy groups is increased the results converge to the solution of the Fokker-Planck equation[1]. However, due to the discrete energy groups, this approach is subject to energy straggling effects and a description of the energy spectra sometimes requires an inordinately large number of energy groups. For this reason the Spencer-Lewis approach has been adopted. Although a numerical solution of the Spencer-Lewis equation is subject to range (or path length) straggling effects we don't believe this would be a serious problem if the SR method of solution were used. Unlike other numerical techniques, time-dependent SR computations[8] have produced excellent results near wave fronts. In particular, SR calculations have been virtually free of straggling effects in the time variable.

II. OBJECTIVES

The principal objective of this research effort was to initiate the development of a method for solving electron transport problems based on the SR method, and to analyze its effectiveness with respect to accuracy and computational requirements.

The specific objectives were:

1. To develop a computer code for solving the one-dimensional Spencer-Lewis equation using the SR technique
2. To incorporate a subroutine for calculating electron energy deposition profiles
3. To find an effective method for describing anisotropic scattering
4. To compare the results with those obtained by other means.

III. THE SPENCER-LEWIS EQUATION AND ENERGY DEPOSITION

The electron distribution in space, angle and path length can be obtained by solving the Spencer-Lewis equation. In one dimension this equation is[13]

$$\left(\frac{\partial}{\partial s} + \mu \frac{\partial}{\partial x} + \sigma\right) \phi(x,s,\mu) = 2\pi \int_{-1}^{+1} \sigma(\mu' \to \mu)\, \phi(x,s,\mu')\, d\mu' + Q(x,s,\mu), \quad (1)$$

where

$\phi(x,s,\mu)$ = the density of electrons as a function of position, path length, and direction

σ = total interaction cross section

$\sigma(\mu' \to \mu)$ = differential scattering cross section

$Q(x,s,\mu)$ = the fixed source of electrons.

Equation (1) is similar to the two-dimension time-independent and the one-dimensional time-dependent Baltzman equations which have been accurately solved by the SR technique.

Existing SR computer codes have been modified to solve the Spencer-Lewis equation, and a subroutine has been added to calculate energy deposition profiles. The energy deposited, E(x) is given by

$$E(x) = \int_0^{s_{max}} \int_{-1}^{+1} \phi(x,s,\mu)\, d\mu \left|\frac{dE}{ds}\right| ds, \qquad (2)$$

where $\left|\frac{dE}{ds}\right|$ is the stopping power, and s_{max} is the electron range. To date, only calculations involving constant stopping powers have been carried out. The results are in good agreement with those obtained using the ONETRAN[14] S_N computer code (see Table I).

Tests have not yet been performed to see if the combined use of the Spencer-Lewis equation and a stopping power formula can ameliorate the energy straggling problem present in multigroup S_N computations.

IV. TREATING ANISOTROPIC SCATTERING

In both the S_N and SR methods, the integral term of Eq. (1) is approximated as

$$2\pi \int_{-1}^{1} \sigma(\mu' \to \mu_m)\, \phi(x,s,\mu')d\mu' \approx \sum_{m'=1}^{M} \sigma_{mm'}\, \phi(x,s,\mu_{m'})\, \omega_{m'}, \qquad (3)$$

where ω_m = the angular weight for direction μ_m

M = the total number of directions.

Several methods have been used to define the elements, $\sigma_{mm'}$, of the scattering matrix.

For many electron transport applications, scattering is extremely forward peaked, that is, $\sigma(\mu' \to \mu)$ is large only when $\mu' \approx \mu$. A straight forward quadrature scheme (putting $\sigma_{mm'} = \sigma(\mu_{m'} \to \mu_m)$) fails in this case since one obtains $\sigma_{mm'} \simeq 0$, $m \neq m'$ and there is no possibility of an electron changing its direction, as mentioned earlier.

To avoid this problem, the $\sigma_{mm'}$ were defined by assuming a representation of $\phi(x,s,\mu)$ of the form

$$\phi(x,s,\mu) = \sum_{m=1}^{M} \phi(x,s,\mu_m)\ g_m(\mu) \qquad (4)$$

where the g_m are a set of basic functions to be defined. From Eqs. (3) and (4) one obtains

$$\sigma_{mm'}\ \omega_{m'} = 2\pi \int_{-1}^{+1} \sigma(\mu \to \mu_m)\ g_{m'}(\mu)\, d\mu \qquad (5)$$

The g_m were chosen as follows

$$g_m(\mu) = \begin{cases} \dfrac{\mu-\mu_{m+1}}{\mu_m-\mu_{m+1}}, & \mu_{m+1} < \mu < \mu_m,\ m < M \\ \dfrac{\mu_{m-1}-\mu}{\mu_{m-1}-\mu_m} & \mu_m < \mu < \mu_{m-1}\quad m > 1 \\ 1 & \mu > \mu_m,\ m = 1 \\ 1 & \mu < \mu_m,\ m = M \\ 0 & \text{otherwise} \end{cases} \qquad (6)$$

Two problems containing screened-Rutherford scattering were used to test out the method. The first problem involved a slab thickness of two mean free paths, a screening factor of 10^{-4} and an isotropic electron source located at the center of the medium. For the second problem the slab thickness was 186 mean-free-paths, the screened factor was .000241, and an isotropic distribution of electrons was incident on one of the slab faces.

For the first problem an analytical solution is available and the numerical results were in excellent agreement with the exact solution. The second problem involved considerably more scattering due to its greater thickness. Here it appears (no exact solution available) that back

scattering is over estimated unless a very large number of quadrature directions is used (see Table I).

The SR calculations were repeated using the method of Morel[1] to define the scattering matrix. In this approach the scattering matrix is defined such that the Boltzman solution approaches the Fokker-Planck solution, which is known to be good for highly anisotropic scattering. The results for this case appeared significantly better and were much less sensitive to the number of quadrature directions. One drawback of Morel's method is that some of the elements of the scattering matrix turn out to be negative and this leads to negative solutions along certain discrete directions.

In was speculated that the success of Morel's scattering matrix was due to the fact that it preserves the momentum transfer[1],

$$\alpha = 2\pi \int_{-1}^{+1} \sigma(\mu_o)(1-\mu_o)d\mu_o \quad . \tag{7}$$

This leads to the following new definition of the scattering matrix

$$\omega_m,\sigma_{mm'}(\mu_{m'},-\mu_m) = \begin{cases} 0 \quad , \quad m = m' \\ 2\pi \int_{\mu_m}^{\mu_m+\frac{\omega_m}{2}} \sigma(\mu_{m'},\rightarrow\mu)\ (\mu_{m'},-\mu)d\mu \ , \ m = m' - 1 \end{cases} \tag{8a}$$

$$\omega_m, \sigma_{mm'}(\mu_m, -\mu_m) = \begin{cases} 2\pi \displaystyle\int_{\mu_m - \frac{\omega_m}{2}}^{\mu_m} \sigma(\mu_m, \to\mu)\ (\mu_m, -\mu)\, d\mu, & m = m' + 1 \\ 2\pi \displaystyle\int_{\mu_m - \frac{\omega_m}{2}}^{\mu_m + \frac{\omega_m}{2}} \sigma(\mu_m, \to\mu)\ (\mu_m, -\mu)\, d\mu, & \text{otherwise} \end{cases} \tag{8b}$$

One drawback of Eq. (8) is that an isotropic scattering cross section will not lead to an isotropic scattering source.

The back scatter fractions and energy deposition profiles are shown in Table I for the three different scattering matrices. An S_N calculation based on the ONETRAN code with Morel's scattering matrix is also included. The energy deposition profiles were determined using a constant stopping power value of 2.1882 Mev/(g/cm^2) and an incident energy of .2 Mev.

Equation (8) is seen to yield better agreement with Morel's method than does Eq. (6). However, a more conclusive evaluation of the various methods would require an accurate benchmark solution for the problem.

V. RECOMMENDATIONS

The method for solving the electron transport equation suggested in this report has been implemented in a computer code and some preliminary calculations have been carried out. The results are encouraging, however, considerably more testing and development are required before the suitability of the method can be determined. Some specific recommendations for follow-on research are outlined below.

A. Questions to be resolved:

1. Can a positive scattering matrix compete in accuracy and efficiency with the scattering matrix of Morel?
2. Are the energy straggling effects inherent in the multigroup approach eliminated by our procedure?

B. Code Modifications:

1. In the short run the capability to handle path length dependent cross sections and stopping powers should be incorporated.
2. Eventually, material interfaces, knock-on electrons and electron-photon interactions should be modeled.

C. Benchmark Solutions

There is an immediate need for accurate benchmark solutions to idealized problems so that the merits of alternative numerical techniques can be evaluated.

TABLE I

Energy Deposition Profiles and Backscatter Fractions Determined by the S_N Method and the SR Method with Three Different Scattering Matrices.

Method	SR			S_N	Distance from Source (g/cm^2)
Technique for Defining Scattering Matrix	Eq. (6)	Eq. (8)	Morel's	Morel's	
Energy Deposition Profile (Mev/g)	2.73	2.34	3.17	3.27	.0005
	3.28	2.55	3.51	3.68	.0015
	3.77	2.74	3.78	2.98	.0025
	4.23	2.92	4.03	4.24	.0035
	4.69	3.13	4.29	4.48	.0045
	5.15	3.40	4.58	4.72	.0055
	5.64	3.75	4.40	4.96	.0005
	6.17	4.22	5.26	5.20	.0075
	6.82	4.93	5.76	5.47	.0085
	7.07	5.45	5.88	5.83	.0095
Backscatter Fraction	.452	.289	.220	.257	

REFERENCES

1. J. E. Morel, "Fokker-Planck Calculations Using Standard Discrete Ordinates Transport Codes", Nucl. Sci. Eng. 79, 340 (1981).

2. R. E. Alcouffe and E. W. Larsen, "A Review of Characteristic Methods Used to Solve the Linear Transport Equation", Proc. International Topical Meeting on Advances in Mathematical Methods for the Solution of Nuclear Engineering Problems, Munich, 1, (3) 1981.

3. M. M. Halsull, "Cactus - A Characteristic Solution to the Neutron Transport Equation in Complicated Geometrics", AEEW-R 1291 (1981).

4. W. L. Filippone and S. Woolf, "A Streaming Ray Technique for Particle Transport Calculations", Trans. Am. Nucl. Soc., 33, 727 (1979).

5. W. L. Filippone and S. Woolf, and R. Lavigne, "Particle Transport Calculations with the Method of Streaming Rays", Nucl. Sci. Eng., 77, 119 (1981).

6. W. L. Filippone and S. Woolf, "Application of the Method of Streaming Rays to Particle Transport in Complex Geometries", Proc. International Topical Meeting on Advances in Mathematical Methods for the Solution of Nuclear Engineering Problems, Munich, 1, (69) 1981.

7. W. L. Filippone and S. Woolf, "The Linear Characteristic Scheme in the Two-Dimensional Streaming Ray Method, to appear in Trans. Am. Nuc. Soc., 41, 489 (1982).

8. W. L. Filippone and B. D. Ganapol, "Time-Dependence One-Dimensional Transport Calculations Using the Streaming Ray Method" to appear in Nucl. Sci. Eng.

9. G. I. Bell, G. E. Hansen and H. A. Sandmeier, Multitable Treatments of Anisotropic Scattering in S_N Multigroup Transport Calculations" Nucl. Sci. Eng. 28, 376 (1967).

10. J. E. Morel, "Validity of the Extended Trnasport Cross-Section Correction for Low-Energy Electron-Transport", Nucl. Sci. Eng. 71, 64 (1979).

11. W. L. Filippone and S. Woolf, "Description of Highly Anisotropic Scattering Using a Mixed Mesh Method", Trans. Am. Nucl. Soc., 27, 396 (1977).

12. J. Ligou, "Fusion Reactor Product Transport in Inertially Confined Plasmas", Proc. International Topical Meeting on Advances of in Mathematical Methods for the Solution of Nuclear Engineering Problems, Munich, 2, (385) 191.

13. H. W. Lewis, "Multiple Scattering in an Infinite Medium", Phys. Rev. 78, 526 (1950).

14. T. R. Hill, "ONETRAN: A Discrete Ordinates Finite Element Code for the Solution of the One-Dimensional Multigroup Transport Equation," LA-5990-MS, Los Alamos National Laboratory (1975).

1982 USAF-SCEEE SUMMER FACULTY RESEARCH PROGRAM

Sponsored by the

AIR FORCE OFFICE OF SCIENTIFIC RESEARCH

Conducted by the

SOUTHEASTERN CENTER FOR ELECTRICAL ENGINEERING EDUCATION

FINAL REPORT

VOLTAMMETRIC STUDIES OF THE LITHIUM/VANADIUM OXIDE ELECTROCHEMICAL CELL

Prepared by:	Dr. Dennis R. Flentge
Academic Rank:	Assistant Professor
Department and University:	Department of Mathematics and Science Cedarville College
Research Location:	Aero Propulsion Laboratory, Power Division, Battery Lab
USAF Research Colleague:	Dr. David Fritts
Date:	September 15, 1982
Contract No:	F49620-82-C-0035

VOLTAMMETRIC STUDIES OF THE LITHIUM/VANADIUM OXIDE ELECTROCHEMICAL CELL

by

Dennis R. Flentge

ABSTRACT

The electrochemical system composed of a lithium metal anode, a vanadium oxide (V_6O_{13}) cathode and a lithium hexafluoroarsenate/2-methyl-tetrahydrofuran electrolyte has been examined using cyclic voltammetry. Cells were found to discharge in distinct steps and to show fair rechargeability. Cell capacities were approximately 140 Ah/kg V_6O_{13}.

Acknowledgement

The author would like to thank the Air Force Systems Command, the Air Force Office of Scientific Research and the Southeastern Center for Electrical Engineering Education for providing him with an interesting and challenging summer in the Aero Propulsion Lab, Wright-Patterson AFB, OH. He would like to acknowledge the Battery Lab for its excellent facilities and for the hospitality shown by its workers.

He extends special thanks to John Leonard, Melvin French and David Stumpff for their excellent technical assistance.

Finally, he would like to thank David H. Fritts for his collaboration and guidance throughout this project.

I. INTRODUCTION

One of the goals in the development of a battery is to achieve the greatest energy output from the smallest weight and volume. Lithium metal is the lightest of all metals and has the largest electrode potential of all metals (E° = 3.045 volts). Primary lithium batteries have been developed which provide significantly longer useful life than the same size conventional dry cell batteries.

Development of ambient temperature secondary lithium batteries has been somewhat slower. In recent years, however, new solvents, electrolytes and electrode materials have been investigated and production of functional, safe secondary lithium batteries is an achievable goal. A solvent/electrolyte system whi :1 shows promise is 2-methyltetrahydrofuran/lithium hexafluoroarsenate (2-Me-THF/$LiAsF_6$).[1] Holleck, et al., have shown that 100-200 deep discharge cycles are possible in lithium/titanium disulfide cells using 2-Me-THF/$LiAsF_6$ as the electrolyte system.[2]

The lithium electrode has a tendency to interact with the solvent. This interaction is moderated by the formation of some type of passivating film on the lithium metal. Some attempts have been made to characterize the surface[3] but there has been no detailed work on an electrode which has been cycled extensively. While giving the system some kinetic stability, this film also acts to limit the cycling capabilities of a cell.

A useful cathode must be able to reversibly handle lithium. Solid state cathodes which undergo intercalation or topochemical reactions with lithium should adequately meet this need. Transition metal chalcogenides and oxides can be used to provide the cathodic reaction with lithium. One such material is vanadium oxide, V_6O_{13}.[4] It has a relatively open structure and this should allow movement of lithium cations throughout the material with a minor distortion of the crystal structure.

With these facts in view we felt that a study of the cell composed of a lithium anode, a vanadium oxide cathode and 2-Me-THF/$LiAsF_6$ electrolyte solution would be valuable.

II. OBJECTIVES

The overall objective of this work was to examine the quality of the Li/V_6O_{13} cell in 2-Me-THF. Specifically our objectives were:

(1) To determine the charge and discharge characteristics of the cell.

(2) To determine the ektent of rechargeability of the cell.

(3) To determine the overall capacity of the cell.

III. CELL PREPARATION AND CONSTRUCTION

Vanadium oxide, V_6O_{13}, was prepared by heating stoichiometric amounts of vanadium metal and vanadium pentaoxide at 650°C in a sealed, evacuated quartz tube for 24 hours. SEM photographs of the product material (Figure 1) show the material to have the same crystalline appearance as the material prepared by Abraham, et al.[5]

The cathode was prepared by mixing V_6O_{13} (70 weight percent) with Shawinigan black (20 weight percent) and Teflon-P powder (10 weight percent). This mixture was pressed onto an expanded nickel grid (Exmet Corp., 5Ni7-4/0) and was heated rapidly to 400°C under a low vacuum (P = 60 microns). Some samples were compressed using a hand press located within a Vacuum/Atmospheres dry box while others were prepared using a pressure of 1000 pounds per square inch generated by a hydralic press located outside the dry box. No difference in behavior was observed between the samples due to this variation in preparation technique.

The anode was prepared by pressing one square centimeter of lithium metal (15 mil thickness) into an expanded nickel grid. The total surface area of the anode was about two square centimeters. No separator was used.

The solvent, 2-methyltetrahydrofuran (2-Me-THF), was distilled under a dry helium atmosphere after standing for three days over calcium hydride. This distilled liquid was then cooled to slightly below 0°C and lithium hexafluoroarsenate ($LiAsF_6$) was dissolved in it. Vigorous stirring and a gradual warming of the solution was necessary to complete the dissolution of the electrolyte. The solution concentration was 1.5 molar.



(a)



(b)

Figure 1. SEM photographs of vanadium oxide. (a) Magnification = 1000x. (b) Magnification = 2000x.

The electrolytic cell, shown in Figure 2, was assembled in the dry box. It was made up of one electrode containing the vanadium oxide mixture pressed onto both sides of an expanded nickel grid, two lithium anodes and about 6 milliliters of the electrolyte solution. The total surface area of the cathode and the anode was approximately two square centimeters.

IV. DISCHARGE CHARACTERISTICS

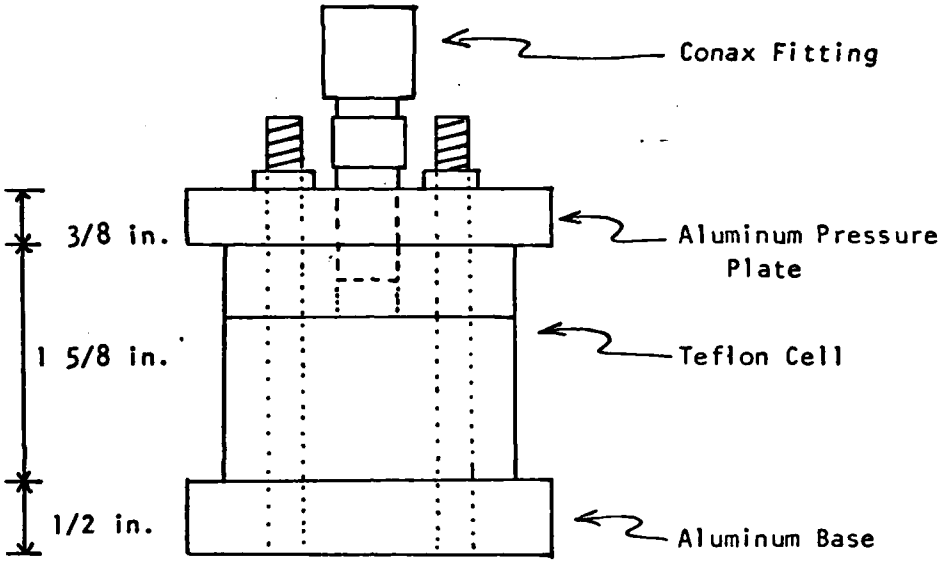
Figure 3 contains a series of discharge half-cycles for a typical cell. Each cell was discharged to 1.7 volts at a constant current of 1.0 milliamperes. The discharge current was generated by a Hewlett-Packard 6177C DC Current Source. The cell appeared to discharge in steps as shown by the plateaus at 2.65, 2.50, 2.25 and 2.00 volts.

There was a continuous decrease in the capacity of the cell as it was cycled. Figure 4 shows a plot of cell capacity vs. discharge number. This pattern was seen in all cells. The capacity of the cell during the initial discharge was typically 65-70% of the theoretical maximum capacity of the cell.

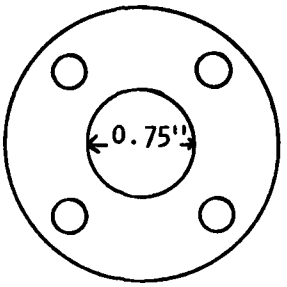
V. CHARGE CHARACTERISTICS

A series of charge half-cycles for a typical cell is shown in Figure 5. Currents of 1.0 and 0.5 milliamperes generated by a Hewlett-Packard 6177C DC Current Source were used to charge the cell. Cell performance did not seem to vary as the current was varied between these two values. A set of plateaus in the charge curves correlates well with the plateaus found in the discharge cycles. The upper limit for the cell potential during charge was 3.0 volts.

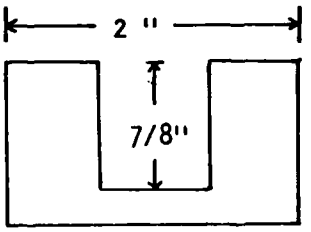
During the initial discharge/charge cycles the capacity of the cell during discharge exceeded the amount of energy supplied during the preceding charge. After 4-6 cycles the amount of energy removed during the discharge was approximately equal to the energy supplied during the preceding charge.



(A) Side view, Electrolytic cell



(B) Teflon cell, top view



(C) Teflon cell, side view, cut-away

Figure 2. Diagram of the electrolytic cell.

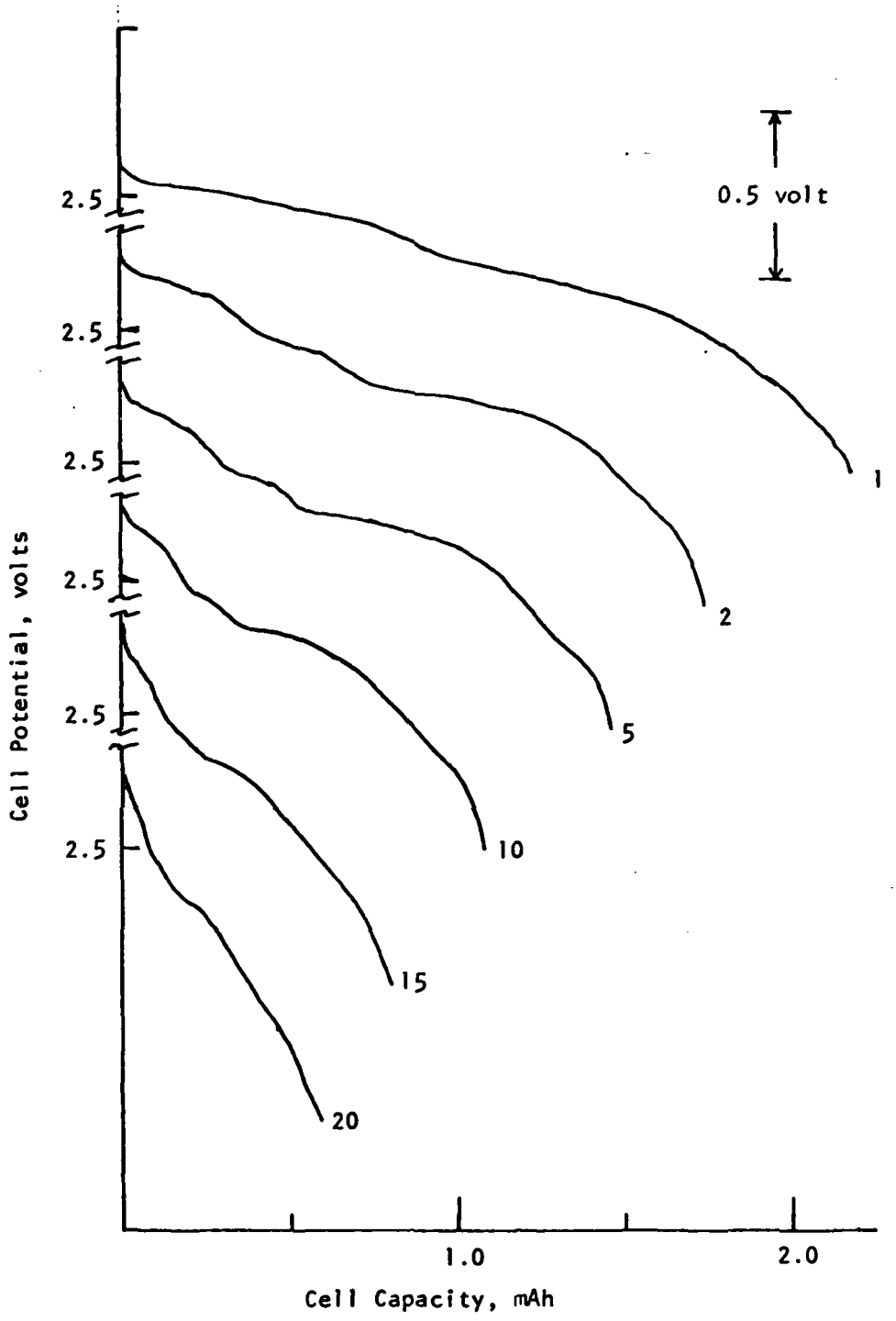


Figure 3. Discharge half-cycles for a cell. Lower potential limit = 1.7 volts. Numbers to the right of each spectrum represent the cycle number. Discharge current = 1.0 mA.

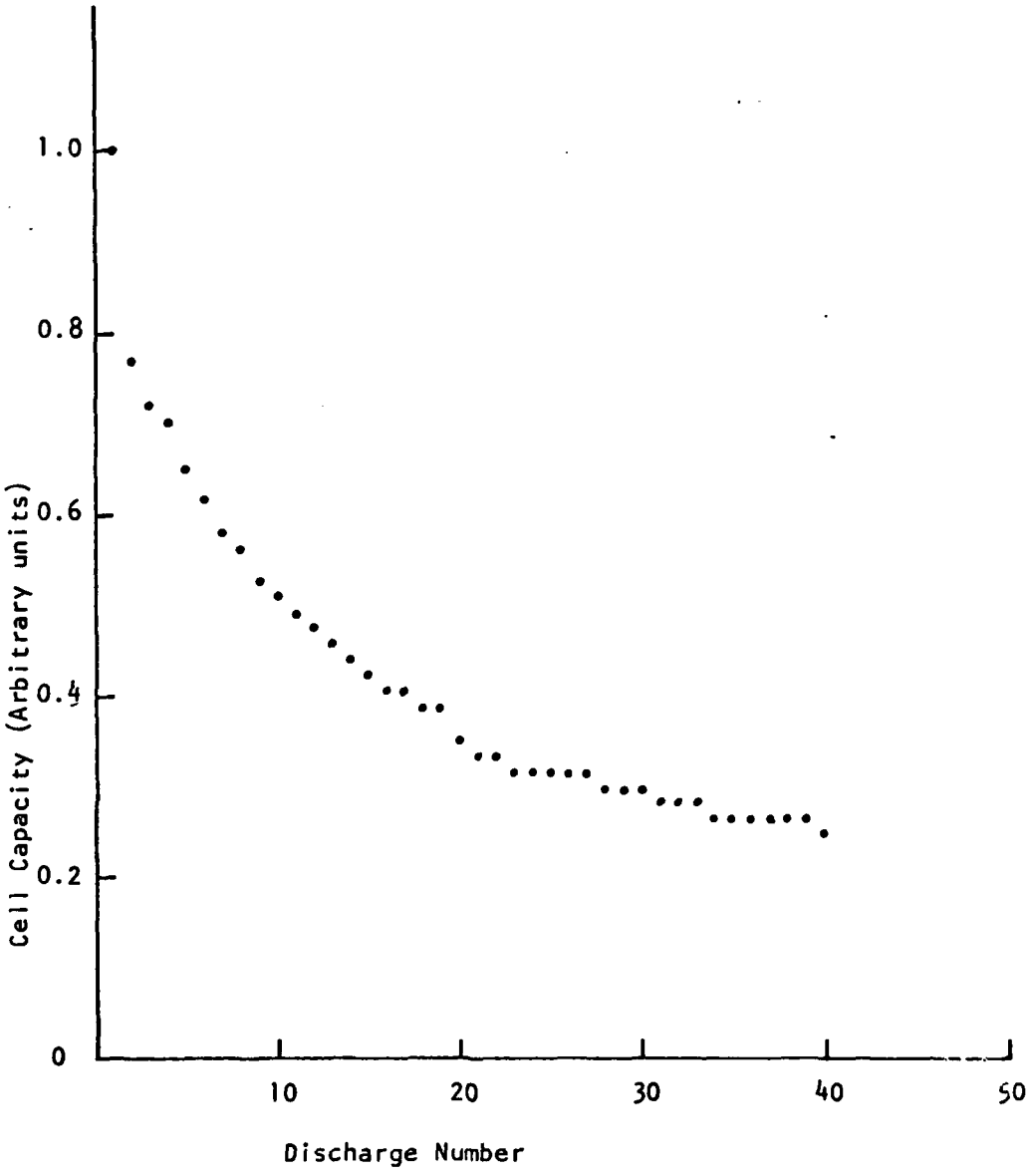


Figure 4. Cell capacity as a function of cycle number.

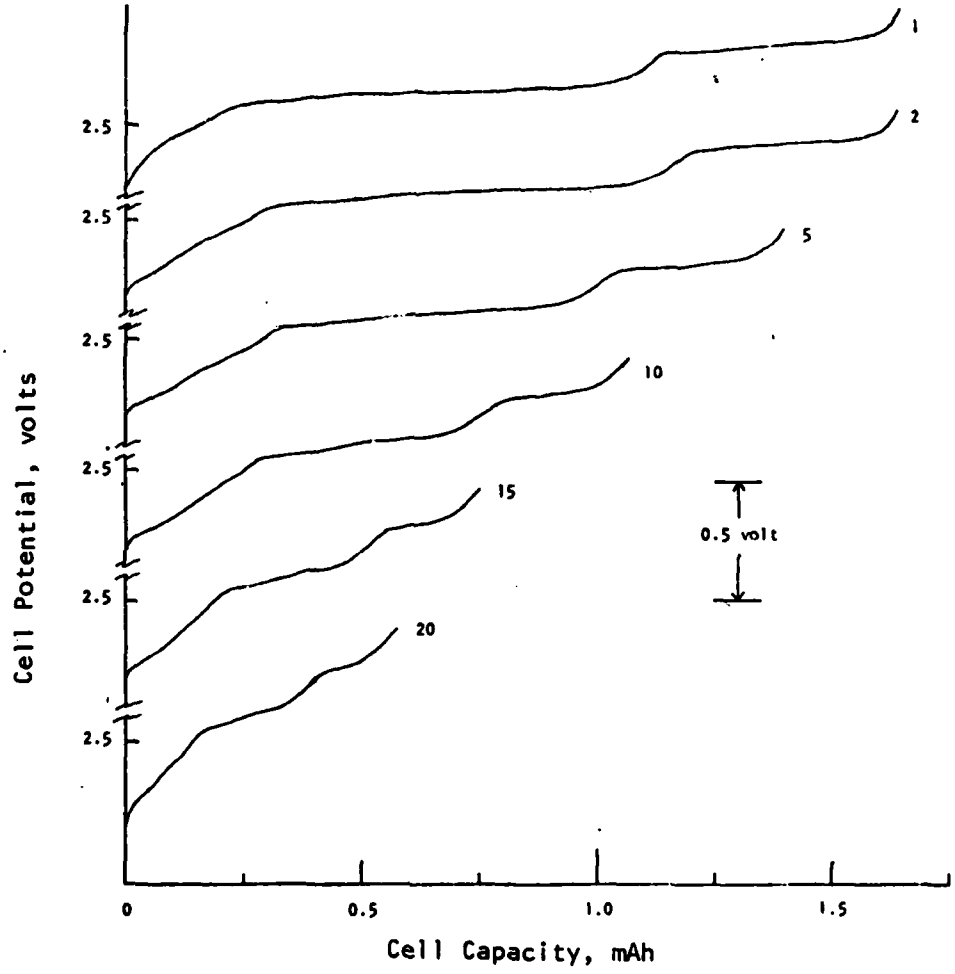
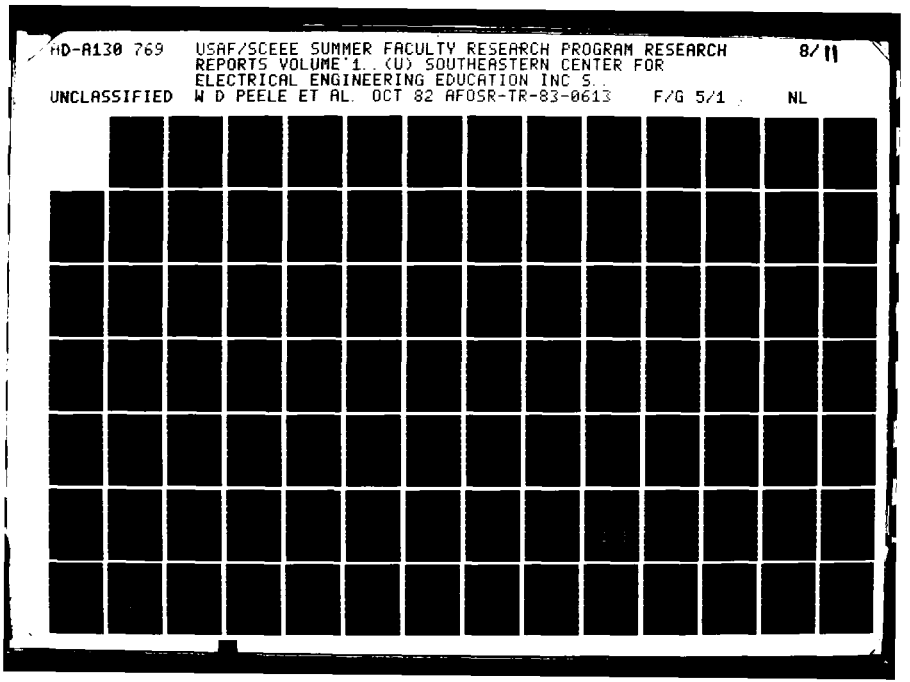
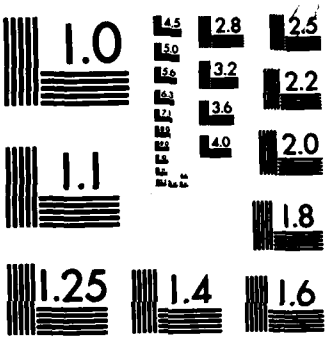


Figure 5. Charge half-cycles for a cell. Charge current = 0.5 mA. Potential limit was set at 3.0 volts. Numbers to the right of each spectrum indicate the cycle number.


AD-A130 769 USAF/SCEEE SUMMER FACULTY RESEARCH PROGRAM RESEARCH REPORTS VOLUME 1.. (U) SOUTHEASTERN CENTER FOR ELECTRICAL ENGINEERING EDUCATION INC S..
8/11
UNCLASSIFIED W D PEELE ET AL. OCT 82 AFOSR-TR-83-0613 F/G 5/1 NL



MICROCOPY RESOLUTION TEST CHART
NATIONAL BUREAU OF STANDARDS-1963-A

VI. CELL CAPACITY

The capacity of the cell whose discharge half-cycles are shown in Figure 3 was found to be 139 Ah/kg V_6O_{13}. This is representative of the capacities of the cells studied.

VII. CONCLUSIONS AND RECOMMENDATIONS

These studies show that the system Li/V_6O_{13}/1.5M $LiAsF_6$ in 2-Me-THF has good initial capacity and, in our system, showed limited rechargeability. Discharge and charge occur in distinct steps and the capacity of the cell shows a continuous decrease. Additional modification of the cell, better purification of the electrolyte system and perhaps more careful assembling of the cell could enhance the performance of the cell.

Future studies could include variation of the cathode composition by incorporation of other metals into the vanadium oxide structure or by introduction of these metals directly into the cathode mixture.

REFERENCES

1. (a) J. L. Goldman, R. M. Mank, J. H. Young and V. R. Koch, "Structure and Reactivity Relationships of Methylated Tetrahydrofurans with Lithium," J. Electrochem. Soc., 127, 1461 (1980). (b) V. R. Koch and Y. H. Young, "2-methyltetrahydrofuran/lithium hexafluoroarsenate: A Superior Electrolyte for the Secondary Lithium Electrode," Science, 204, 499 (1979).

2. G. L. Holleck, K. M. Abraham and S. B. Brummer in Proceedings of the symposium on "Power Sources for Biomedical Implantable Applications; Ambient Temperature Lithium Batteries," B. B. Owens and N. Margalit, eds., The Electrochemical Society, PV80-4, 1980.

3. S. P. S. Yen, D. Shen, R. P. Vasquez, F. J. Grunthaner and R. B. Somoano, "Chemical and Morphological Characteristics of Lithium Electrode Surfaces," J. Electrochem. Soc., 128, 1434 (1981).

4. D. W. Murphy, P. A. Christian, F. J. DiSalvo and J. N. Carides, "Vanadium Oxide Cathode Materials for Secondary Lithium Cells," J. Electrochem. Soc., 126, 497 (1979).

5. K. M. Abraham, J. L. Goldman and M. D. Dempsey, "Rechargeable Lithium/Vanadium Oxide Cells Utilizing 2-Me-THF/$LiAsF_6$, J. Electrochem. Soc., 128, 2493 (1981).

1982 USAF - SCEEE Summer Faculty Research Program

Sponsored by the

AIR FORCE OFFICE OF SCIENTIFIC RESEARCH

Conducted by the

SOUTHEASTERN CENTER FOR ELECTRICAL ENGINEERING EDUCATION

FINAL REPORT

INTEGRAL PRINCIPLES AS APPLIED TO ELECTROMAGNETIC ENERGY PROPAGATION

Prepared by:	W. A. FORDON
Academic Rank:	Associate Professor
Department and University:	Electrical Engineering Michigan Technological University
Research Location:	ESD/XR
USAF Research Colleague:	Dr. D. B. BRICK
Date:	13 August 1982
Contract No:	F49620-82-C-0035

INTEGRAL PRINCIPLES AS APPLIED TO ELECTROMAGNETIC PROPAGATION

by

Wilfred A. Fordon

ABSTRACT

The application of the theory of the propagation of electromagnetic energy to communication systems has been hampered when an inhomogeneous, anisotropic medium is involved. The prediction of the performance of such systems has relied traditionally on well-developed techniques such as ray-tracing and, if necessary, full-wave solutions. The resulting computational difficulties often become intractable when serious discontinuities in the medium are encountered - such as the case where communication over moderate-to-long distances at HF, (3 MHz - 30 MHz), is required.

In addition to these computational difficulties, the previously-mentioned techniques are extremely sensitive to the choice of a system of coordinates.

By reverting to fundamental energy considerations and applying variational techniques, (integral principles), an alternative approach can be developed which obviates the theoretical difficulties and may alleviate the computational problems. This approach, though well-known, has not been heavily exploited. The simple and elegant formulations that ensue should enhance the capability to interpret more precisely the physical phenomena involved, and enable more sophisticated use of the propagation medium.

Acknowledgment

The author would like to thank the Air Force Systems Command, the Air Force Office of Scientific Research, and the Southeastern Center for Electrical Engineering Education for providing an extremely worthwhile opportunity this summer to crystallize a number of diverse concepts. He would like to thank the Electronic Systems Division, Hanscom Air Force Base, Massachusetts, for the opportunity to interchange ideas, and particularly for the warm hospitality afforded.

The helpful discussions with Mr John Rasmussen, Dr Gary Sales, and Dr Paul Kossey at RADC are gratefully acknowledged. In addition, the assistance afforded by many of the ESD personnel - a list too large to individually mention - is much appreciated.

Finally, this summer's work would have been impossible without the advice and support of Dr Donald B. Brick.

1.0 Introduction

A large class of problems in communications deals with the prediction of the performance of a communications system as it traverses an inhomogeneous, anisotropic medium - such as the ionosphere. Since the time of Maxwell and Hertz, electrical engineers and physicists have attempted to solve these problems by applying Maxwell's equations in time-differential form.

If the characteristics of the medium through which the electromagnetic energy passes are sufficiently "well-behaved," the application of the techniques developed in geometric-optics, such as ray-tracing, has proven to be of great practical use - especially since the development of modern computers has made rapid computation feasible.

In the event that the medium must be considered "disturbed," conventional techniques become more difficult to apply - even with increased capability of computation.

There is a technique available for electromagnetic problems which has not received as much attention as the previously-discussed approaches. This technique is based upon the application of an "integral principle" - also referred to as a "variational principle."[14]

It is the objective of this report to lay the groundwork

in defining the various approaches mentioned, leading to a careful study and comparison of the advantages and disadvantages of each.

Having laid the groundwork in this report, a plan of future work is proposed to uncover the complementary advantages that may be afforded by the variational approach.

Future work is divided into three phases. In the first phase, a digital computer program will be developed to illustrate the variational principle. Using a modern ionospheric model, this program will be used to compare the computational efficacy and accuracy of the variational principle with full-wave and ray-tracing techniques.

The frequency range at which the performance will be initially calculated is the HF, (3-30 MHz), portion of the RF spectrum. Included in the ionospheric model will be anisotropies and inhomogeneities which lead to caustics and other computational difficulties.

The second phase of the study will attempt to focus on the problems related to diffraction and scattering - such as those which arise in the VHF/UHF spectrum in the ionosphere and troposphere.

Since the variational technique should be applicable to radiation problems, the third phase of the study will be devoted to these.

2.0 Ray-Tracing Procedures

The "granularity" of the medium through which electromagnetic energy is passing and the information required determine the math-

ematical technique to be employed in a given situation. For example, at HF the ionosphere presents a medium, (most of the time), whose electron-density variations in time and space are relatively small.

Generally speaking, spatial electron density variations in the ionosphere are used as the criterion for determining the analytical technique. If the relative change in refractive index along the energy path is a small number of vacuum wavelengths of the transmitted energy, the technique usually employed is called "ray-tracing." That is to say, geometric-optical principles can be employed.[4]

Oblique ray-tracing at radio frequencies by means of large-scale general-purpose digital computer programs is becoming a well-developed technique -- useful to a large number of propagation problems once the characteristics of the ionosphere are known. Commonly used parameters include ground range traversed, the group time delay along the ray path, the number of wavelengths along the ray (phase path), Faraday rotation and absorption.[11]

3.0 Full-Wave Solutions

When geometrical-optical conditions do not exist, ray-tracing cannot be used to obtain quantitative results. A so-called "full wave" technique is then necessary. This name is usually applied to solutions of Maxwell's equations in differential equation form, supplemented by appropriate constitutive relations and boundary conditions.[17]

By applying numerical techniques, the full-wave solution can be programmed for a large-scale general-purpose digital computer -- as with the ray-tracing technique. The amount of computation involved, as compared with ray-tracing, is large.[25,26]

Full-wave solutions, in principle, are exact. As with ray-tracing, they are limited by the accuracy with which the medium is specified. Both ray-tracing and full-wave solutions do not readily lend themselves to deducing the physical characteristics of the transmission medium when the input and output conditions are known. They are better in deducing the output, when the input and transmission medium is specified. Since the former is the general problem for radio communications, the field is wide open for new analytical techniques which contribute to the solution.

4.0 The Variational Approach

4.1 Introduction

Physicists and engineers are well acquainted with Newton's equation of motion in differential form. The statement $\bar{F} = \frac{d}{dt}(m\bar{v})$ needs no introduction. The solution of Newton's equations, supplemented by equations describing the constraints in the system, can satisfactorily predict the performance parameters of a mechanical system at an arbitrary time when the parameters are known at a specified time.

It is desirable to generalize the equations of state to consider arbitrary coordinate systems, instead of the usual Cartesian rectangular coordinates. It is also desirable to incorporate the equations of constraint. In addition, equations

directly applicable to a system containing a large number of particles are more useful. By applying "D'Alembert's principle,"[19] mechanics can be formulated so that the forces of constraint disappear, since they are generally unknown 'a priori.' Defining a Lagrangian (L),

$$L = T - V$$

where

$T \equiv$ Kinetic energy,

and $V \equiv$ Potential energy

Lagrange's equations:

$$\frac{d}{dt}\left(\frac{\partial L}{\partial \dot{q}_j}\right) - \left(\frac{\partial L}{\partial q_j}\right) = 0 \qquad (4.1)$$

are the result of transforming Newton's equations to a generalized system of coordinates, (q_j), and their velocities, $(\dot{q}_j)$. These mechanical equations are most useful when system forces are conservative. They can also be applied to non-mechanical systems, where electromagnetic energy systems are prime examples, since they are usually conservative and can be expressed in terms of potentials.[19]

Lagrange's equations were derived from a consideration of the instantaneous state of the system and small virtual displacements about the instantaneous state - a "differential principle" such as D'Alembert's principle. It is also possible to obtain Lagrange's

equations from a principle which considers the entire motion of the system between times t_1 and t_2, and small virtual variations of this motion from the action motion. Such a principle is called an "integral principle." An example is "Hamilton's principle" which states that "the motion of the system from time t_1 to time t_2 is such that the line integral, (Action Integral),

$$A = \int_{t_1}^{t_2} L dt \tag{4.2}$$

is an extremum for the path of motion, ($\delta A=0$).* Thus, out of all possible paths by which the system point in configuration space, (the space described by the q_j's), could travel from its position at t_1 to its position at t_2, it will actually travel along that path for which Equation (4.2) is either a maximum, minimum, or stationary point. This principle is both a necessary and sufficient condition for Lagrange's equations. Thus, Lagrange's equations can be used to derive Hamilton's principle, and conversely, Hamilton's principle can be used to derive Lagrange's equations.

The importance of the latter is that Hamilton's principle can be used as a basic postulate to Newton's equations of motion in mechanics. One advantage is that it is invariant to coordinate transformation. Even more important, it can be formulated in a relativistically invariant manner quite readily for systems not

*Fermat's principle, used in geometrical optics and in radio ray-tracing is a specific example of an integral principle.

strictly classified as "Newtonian mechanical." For example, an electromagnetic system whose potentials ϕ and $\bar{A}$ describe the electromagnetic energy, and which interact with particles in the system, result in a Lagrangian (L)

$$L = \iiint \frac{\varepsilon_0}{2} (\bar{E}^2 - c^2 \bar{B}^2) - \rho\phi + \bar{J}\cdot\bar{A} \; dV + \Psi_0 + \Psi_1 + Q, \qquad (4.3)\ *$$

where

$\varepsilon_0 \equiv$ Electric permittivity of free space,

$\bar{E} \equiv -\nabla\phi - \frac{\partial \bar{A}}{\partial t}$ = Electric Field Intensity

$\bar{B} \equiv \nabla \times \bar{A}$ = Magnetic Field Intensity,

$\rho \equiv$ Net volumetric charge density,

$\bar{J} \equiv$ Surface current density,

$dV \equiv$ Infinitesimal volume element

$\left.\begin{matrix}\Psi_0 \\ \Psi_1 \\ Q\end{matrix}\right\} \equiv$ Terms describing the kinetic energy of the particles[17]

Deriving Lagrange's equations from L; as an example (for ϕ and $\bar{A}$), and substituting in Equation (4.3)

$$\frac{\partial L}{\partial \phi} = -\rho \qquad (4.4)$$

$$\frac{\partial L}{\partial \left(\frac{\partial \phi}{\partial X_j}\right)} = \varepsilon_0 E_j \quad \frac{\partial E_j}{\partial \left(\frac{\partial \phi}{\partial X_j}\right)} = \varepsilon_0 E_j. \qquad (4.5)$$

Since $\frac{\partial L}{\partial \dot{\phi}} = 0$, the equation is

$$-\rho + \sum_j \varepsilon_0 E_j = 0, \qquad (4.6)$$

* ϕ and $\bar{A}$ refer to the conventional scalar electric and vector magnetic potentials, respectively.

which leads to

$$\nabla \cdot \bar{D} = \rho \tag{4.7}$$

Considering derivatives of A_1, (one component of $\bar{A}$):

$$\frac{\partial L}{\partial A_1} = J_1, \tag{4.8}$$

$$\frac{\partial L}{\partial \dot{A}_1} = - \varepsilon_0 E_1 \tag{4.9}$$

$$\frac{\partial L}{\partial \left(\frac{\partial A_1}{\partial x_2}\right)} = - \varepsilon_0 c^2 B_3 \frac{\partial B_3}{\left(\frac{\partial A_1}{\partial x_2}\right)} = - \frac{1}{\mu_0} B_3 \frac{\partial B_3}{\left(\frac{\partial A_1}{\partial x_2}\right)} = \frac{-1}{\mu_0} \frac{\partial B_3}{\partial x_2} \tag{4.10}$$

$$\frac{\partial L}{\partial \left(\frac{\partial A_1}{\partial x_3}\right)} = \varepsilon_0^2 B_2 \frac{\partial B_2}{\left(\frac{\partial A_1}{\partial x_3}\right)} = \frac{1}{\mu_0} B_2 \frac{\partial B_2}{\left(\frac{\partial A_1}{\partial x_3}\right)} = \frac{1}{\mu_0} \frac{\partial B_2}{\partial x_3} \tag{4.11}$$

This leads to:

$$\frac{1}{\mu_0}\left(\frac{\partial B_3}{\partial x_2}\right) - \left(\frac{\partial B_2}{\partial x_3}\right) - \varepsilon_0 \left(\frac{\partial E_1}{\partial t}\right) - J_1 = 0, \text{ which} \tag{4.12}$$

a component of

$$\nabla \times \bar{H} - \frac{\partial \bar{D}}{\partial t} - \bar{J} = 0. \tag{4.13}$$

Equations (4.7) and (4.13) describe the generation of fields by external charges and currents and are seen to be identical with Maxwell's differential formulation.

4.2 Application of the Integral Principle

Conventionally, the solution of practical problems, whether formulated initially from an integral principle or formulated directly via a differential principle, has ultimately led to the integration of Maxwell's differential equations with suitable boundary conditions. As seen in section 4.1, this is not necesarily the case. Since the integral principle results in Maxwell's equations, it appears possible to integrate δA directly without differentiating first to derive Maxwell's equations. The formulations being mathematically equivalent, the results should be identical.

It will be assumed initially that the second and third virial coefficients (Ψ, and Q) are negligible in order to simplify further calculations. This assumption is not essential to the development of the integral technique, since the coefficients can be considered later and the results recalculated with little or no change in form. Because first considerations are to be given to the ionospheric medium, (which is the most general case of interest), the electrostatic problem for an ionized medium will be first investigated. Later work will consider, in turn; magnetostatics, stationary fields, quasi-stationary fields, and finally -- rapidly time-varying fields.[36]

The concept of action at a distance has failed to account for the mechanism of radiation. In order to include this mechanism, both advanced and retarded potentials will be introduced into the integral formulation, following a suggestion made by R. P. Feynman.[41] Due to the symmetry introduced, an added ad-

vantage could be the easing of the practical problem of directly integrating the variation of the action integral.

A retarded potential is more familiar than an advanced to those working in electromagnetic theory. In brief, if the electromagnetic effect of a particle is desired at some point A, from a particle at B, the potential function must consider the separation between A and B and the finite propagation time, (usually the speed of light), for a cause at B to be an effect at A. The result has been potential functions of the form:

$$\phi(q_i^{(A)},t) = \iiint \frac{\rho(q_i^{(B)},\ t = \gamma_{AB}/c)}{4\pi\ \varepsilon_0\ \gamma_{AB}}\ dV \qquad (4.14)$$

where γ_{AB} = Distance between A and B,

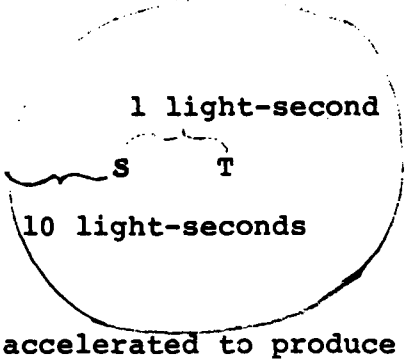
c = Speed of light, and

dV = Volume differential, and ϕ is the scalar potential.

A similar expression exists for $\bar{A}$, the vector potential.[37]

The formulation of the potential function in terms of retarded potentials alone is in accord with convention and is usually satisfactory for problems not related to radiation. Advanced potentials, although mathematically satisfactory for the solution of Maxwell's equations, have generally been rejected on the ground of physical intuition. This is mainly due to the usual way of relating earlier times to causes and later times to effects. This is the non-relativistic, (or non-covariant) way of describing events. When relativistic, (covariant), formulations are required, as in radiation problems, time and space are intertwined and the postulation

of advanced potential becomes a necessity for a principle of stationary action, (integral principle).[42] To illustrate this, consider two charged particles S and T in otherwise charge-free space separated by one light-second and surrounded by atmosphere consisting of perfectly absorbing walls at radius 10 light-seconds from one of the particles (see below).



At t=o, let S be accelerated to produce electromagnetic radiation. It will be shown below that the effect produced by S within the sphere can be described by a field equal in magnitude to one-half the difference between a retarded and an advanced field, where the retarded field is the conventional outgoing field, and the advanced field is an incoming field, (i.e., toward S), equal in magnitude to the retarded field but of opposite sign.

$$F_T = 1/2\ (F_R - F_A), \text{ where} \qquad (4.15)$$

F_T = Total field,

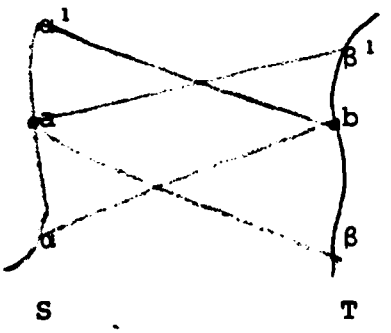
F_R = Retarded field, and

F_A = Advanced field.

At t=o, at S, there is a field of F_T due to S. S also induces motions at the wall at t = +10 seconds. At T, these motions can be seen by advanced effects as early as 11 seconds earlier, or

t = -1 seconds. This is the time at which the direct advanced effects from S can first be seen at T. Since the effects are equal and opposite at T, they cancel out, and there is no field. At t= +1 seconds, the direct retarded effect first arrives at T from S. The direct advanced effect has also arrived at T, but is of opposite sign. Thus, the total field at t= +1 seconds is seen at T to be a full retarded field, $F_T = 1/2\ [(F_R) - (-F_R)] = F_R$. At later times this remains the case, and the model gives a true picture at all times, where the field appears to be travelling outward from S.

It therefore becomes necessary for an integral principle in considering the influence of matter at a given point in phase space from another point to know at least a segment of the world lines for both points contained between light cones connecting the two world lines, S & T (see below):



In the figure, a and b represent events at the same proper times on their respective world lines. The light cones from a and b, intersecting the world lines at retarded proper times β and α, and advanced proper times β^1 and α^1 represent all the possible

time-like events in space-time. Thus, knowledge of both of the intervals $\alpha - \alpha^1$ and $\beta - \beta^1$ is necessary to characterize the entire continuum.

4.3 Integration of the Variation of the Action Integral

Several practical questions arise in the integral formulation. One question might be, "Can the integration be carried out?"

That is is possible to integrate the action, integral is readily verified by the literature.[27]

Another question might be, "How is this method superior to the time-differential approach?" Several reasons appear to make a strong case. For one thing, if the integral formulation is carried out, the boundary conditions will be automatically included in the limits of the integral; whereas the time-differential approach requires supplementary equations which must be incorporated, sometimes with difficulty, into the differential equations. Another argument is that the numerical solutions of a system of differential equations describing (for example) ionospheric propagation inherently require dividing the ionosphere into path segments small enough to make the path appear to be linear. At 2 MHz, as many as 100,000 steps are needed to traverse the ionosphere on a one-hop path.[25,26] The number of steps required increases as the frequency, making the amount of computer calculation impractical for a significant number of runs and higher frequencies.

On the other hand, it appears intuitively that the integral would only be limited insofar as the medium itself is discontinuous. Thus, even where an ionosphere consisting primarily of relatively

small moving irregularities of scale size on the order of 5 km along the magnetic field and 1 km across is considered it appears possible to reduce the step-size (hence the processing time), by at least an order of magnitude. Since full-wave solutions are relatively practical up to frequencies of 1 MHz or so, this advantage could make feasible the analysis of electromagnetic frequencies well into the HF region -- higher than present applications have reached. This is especially important, since modern communication requirements are placing greater emphasis on finer detail and precision.[17]

4.3.1 The Rayleigh-Ritz Method[10]

The Rayleigh-Ritz method provides a direct solution to the variational problem. It is based on the consideration of the variation problem in the form $D[\phi]$ = minimum, where the functional $D[\phi]$ is an integral of a given expression containing the function ϕ and its derivatives up to the k-th order, and where the region of integration and the domain of admissible functions, ϕ, are given. It does not matter whether $D[\phi]$ is a simple or a multiple integral. It is assumed that the set of values of $D[\phi]$ for the admissible argument functions ϕ possess a greatest lower bound, (GLB), d. Then, there exist sequences $\phi_1, \phi_2, \ldots$ of admissible functions such that $\lim_{n\to\infty} D[\phi_n] = d$, while the relation $D[\phi] \geq d$ holds for every admissible function ϕ. Such sequences of functions are called minimizing sequences of the variational problem. A direct solution of the variational problem always consists in the construction of minimizing sequences and the attempt to secure the solution based upon this sequence.

The method consists of the following steps:

(1) Start with a fixed complete system of coordinate functions $W_1, W_2, \ldots$, defined in the region of integration, which has the property that all linear combinations $\phi_n = C_1 W_1 + C_2 W_2 + \ldots + C_n W_n$ of a finite number of the functions are admissible comparison functions for the problem, and such that for every admissible function ϕ there is a suitable combination ϕ_n of this kind for which $D[\phi]$ differs arbitrarily little from $D[\phi_n]$. Then, there exist minimizing sequences $\phi_1, \phi_2, \ldots$ in which ϕ_n is a linear combination

$C_1W_1+C_2W_2+\ldots+C_nW_n$ of the functions $W_1, W_2, \ldots, W_n$.

(2) We obtain an even better minimizing sequence if for every n we determine the function ϕ_n, i.e. the parameters $C_1, C_2, \ldots, C_n$, by the requirement that $D[\phi_n] = d_n$ be a minimum. This requirement represents an ordinary minimum problem for $D[\phi_n]$ as a function of the n parameters $C_1, C_2, \ldots, C_n$ and can always be fulfilled. The values C_i are determined by the n simultaneous equations $\frac{\partial D[\phi_n]}{\partial C_i} = 0$ $(i = 1, 2, \ldots, n)$. We may now expect the resulting minimizing sequence to converge to the desired solution. There are, however, difficulties with this expectation, as discussed in reference 10. We can only state that the values $D[\phi_n] = d_n$ obtained in this way converge to the desired GLB, or minimum.

In some cases the method may prove useful for numerical calculations, even though its convergence is improved. Its success in any particular case will depend on the proper choice of coordinate functions W_i. Reference 10 gives some examples.

4.3.2 Dynamic Programming[14]

The calculus of variations is a mathematical discipline that treats certain problems in the area of optimization theory. A more recent mathematical formalism, dynamic programming, is also applicable to optimization problems. There is a strong relationship between the two techniques.

A rule to associate a numerical value with each function in a given set of functions is called a functional. The calculus of variations considers problems in which the functional is expressed as a definite integral. Then, that function is sought which has

associated with it, by the given rule, a numerical value less than that associated with any other function in the specified set of functions.

Thus, the calculus of variations follows from the principle that a minimizing function must yield, at the least, a smaller value of the criterion functional than that associated with any neighboring function. Neighboring functions are constructed by varying the candidate function; hence, the name calculus of variations. Attention is focused upon the function yielding the minimum value of the functional, rather than the actual numerical value of the minimized functional. This is a reasonable approach, since the value of the functional can be easily found, in theory, once an argument-function is specified. On the other hand, the shape of the minimizing function cannot be deduced from the minimum value of the functional.

Recently, a new approach to a wide variety of optimization problems, including as a special case those usually associated with the calculus of variations, has been developed. In this approach, a particular optimization problem is solved by studying a collection, or family, of problems which contains the particular problem as a member. (As an example, consider the problem of finding the curve of shortest length connecting two specified points, A and B. The family of problems for this example might be the problems of finding the minimum-length curves connecting any given initial point and B.) Each member of the family of problems has its own solution curve, and that curve has a value. (In the example, for any given initial

point C, the solution curve is the straight line connecting C with B and the value of the curve is given by the distance from C to B.) In this manner, an optimal value can be associated with each member of the family of problems and each member can be identified by its initial point. The rule associating an optimal value with each initial point is called the optimal value function. Dynamic programming studies the optimal value function, rather than the solution curve yielding the value.

The dynamic programming approach is appealing because the optimal value function has certain intuitive local properties in the space of points on which it is defined that allow it to be mathematically characterized, usually as the solution of a partial differential equation. Knowledge of the optimal value associated with a particular problem that has particular initial and terminal points provides no clue for determining the minimizing curve itself. However, knowledge of the more optimal value function associated with a family of problems having a variety of initial points does allow one to determine the minimizing curve for any particular member of the family or problems.

Thus, the dynamic programming viewpoint centers its attention upon a function - the optimal value function - and upon its attributes. The classic variational theory, on the other hand, studies minimizing curves and their properties.

The classical theory eliminates all explicit appearances of the neighboring comparison functions from its results and transforms statements about definite integrals into conclusions concerning properties that hold at each point of the minimizing function. However, in doing so, it gives up much of its intuitive content. The existence of an intuitive geometric appreciation of almost every

derivational step and conclusion constitutes a strong justification for the dynamic programming approach.

5.0 Summary, Conclusions, and Recommendations

As stated in the introduction, this report has attempted to formulate the basis for the application of integral principles to electromagnetic propagation problems. In order to accomplish this, a brief review of the principles underlying the more well-known techniques was considered necessary. Thus, discussions about ray tracing and full-wave solutions of Maxwell's equations were included.

Having established the theoretical and practical limitations of ray tracing and full-wave approaches, a discussion about integral techniques has been composed, and some justifications for the consideration of this approach have been developed.

In order to justify the practicality of the integral principle approach, a few of the techniques which could be used to perform computations have been included - the Rayleigh-Ritz method, and dynamic programming.

It is the conclusion of this summer's study that further development of the integral principle approach can lead to significant insight into the solution of many difficult problems encountered when an inhomogeneous, anisotropic medium must support electromagnetic energy.

The writer recommends a three phase study as a follow-on to this report.

The first phase involves the development of algorithms illustrating the integral principle and comparing the output of the algorithm with other established techniques, such as ray

tracing and full-wave solutions, to provide a reference point for further study. The model employed in this phase could be a fairly simple model of the medium in order to lend confidence to the integral principle algorithm.

Having developed the algorithm and compared it to other techniques using a relatively simple model of the medium, the algorithm can then be applied to a more complex model of the medium, one which has anisotropies and inhomogeneities.

The second phase of the study can then be concentrated on problems arising when diffraction and scattering are encountered.

In the third phase, a study of radiation problems as analyzed by the integral principle algorithm would be included.

It is the conviction of the writer that this three-pronged approach should allow more definitive conclusions about the integral principle - and hopefully result in a practical complementary approach to communication problems.

References

1. Bahar, E., (1976), "Electromagnetic Waves in Irregular Multi-layered Spherical Structures of Finite Conductivity - Full wave solutions," Radio Science, 11, (2), pp. 137-148, Feb 1976.

2. Bennett, J. A., (1969), "On the Application of Variation Techniques to the Ray Theory of Radio Propagation," Radio Science, 4, (8), pp. 667-678, Aug 1969.

3. Bennett, J. A., (1973), "Variations of the Ray Path and Phase Path: A Hamiltonian Formulation," Radio Science, 8, (8,9), pp. 737-744, Aug-Sep 1973.

4. Born, M. & E. Wolf, (1965), "Principles of Optics - 3d rev. Ed." Pergamon Press, London and New York.

5. Brandstatter, J. J., (1963), "An Introduction to Waves, Rays, and Radiation in Plasma Media," McGraw-Hill, New York.

6. Brekhovskikh, L. M., (1960), "Waves in Layered Media," Academic Press, New York.

7. Bremmer, H., (1949), "Terrestrial Radio Waves," Elsevier Publishing Co., Amsterdam.

8. Bremmer, H., (1958), "Propagation of Electromagnetic Waves," Handbuch der Physik, 16, Springer - Verlag, Berlin.

9. Budden, K. G., (1961), "Radio Waves in the Ionosphere," Cambridge Univ. Press, London.

10. Courant, R. & D. Hilbert, (1953), "Methods of Mathematical Physics - Vol I," Interscience Pub., Inc.

11. Croft, T. A., (1966), "A Review of Oblique Ray-tracing and its Application to the Calculation of Signal Strength," Stanford Electronics Lab., Presented at 11th EPC AGARD Symposium, Leicester, England, 26 Jul 1966.

12. Croft, T. A. & H. Hoogasian, (1968), "Exact Ray Calculations in a Quasi-Parabolic Ionosphere with no Magnetic Field," Radio Science, 3, (1), pp. 69-74, Jan 1968.

13. Dandekar, B. S. (1982), "Ionospheric Modeling," AFGL-TR-82-0024, Environmental Research Papers, No. 768, 27 Jan 1982, Space Physics Divison, Project 4643, Air Force Geophysics Laboratory.

14. Dreyfus, S. E., (1965), "Dynamic Programming and the Calculus of Variations," Academic Press, New York and London.

15. Fante, R. L., (1972), "Propagation of Electromagnetic Waves in Media Which Vary Slowly With Position and Time," Radio Science, 7, (12), pp. 1153 - 1162, Dec. 1972.

16. Feynman, R. P., Leighton, Sands, (1964), "The Feynman Lectures on Physics - Vol. II," Addison-Wesley.

17. Fordon, W. A., (1966), "The Theoretical Basis of HF Propagation Experimentation," MITRE WP-845, 15 October 1966.

18. Geisler, J. E. & S. A. Bowhill, (1965), "Ionospheric Temperatures at Sunspot Minimum," JATP, 27, pp. 457-474.

19. Goldstein H., (1959), "Classical Mechanics," Addison-Wesley.

20. Hammond, P., (1981), "Energy Methods in Electromagnetism," Clarendon Press, Oxford.

21. Haselgrove, J., (1957), "Oblique Ray Paths in the Ionosphere," Proc. Phys, Soc. London, Ser B, 70, (7), pp. 653-662.

22. Haselgrove, J. & C. B. Haselgrove, (1960), "Twisted Ray Paths in the Ionosphere," Proc Phys, Soc London, 75, (3), pp. 357-363.

23. Hildebrand, F. B., (1958), "Methods of Applied Mathematics," Prentice-Hall.

24. Hill, J. R., (1979), "Exact Ray Paths in a Multisegment Quasi-parabolic Ionosphere," Radio Science, 14, (5), pp. 855-861, Sep. - Oct. 1979.

25. Inoue, Y., & S. Horowitz, (1966), "Magneto-Ionic Coupling in an Inhomogeneous Anisotropic Medium," Radio Science, 1 (4), pp. 427-440, Apr 1966.

26. Inoue, Y., & S. Horowitz, (1966), "Numerical Solution of Full-Wave Equations with Mode Coupling," Radio Science, 1, (8), pp. 957-970, Aug 1966.

27. Jeffreys, H. & B. S. Feffreys, (1956), "Mathematical Physics - Third Edition," Cambridge University Press.

28. Jones, R. M., (1968), "A Three-Dimensional Ray-tracing Computer Program, (digest of ESSA Technical Report, ITSA, No. 17)," Radio Science, 3, (1), pp. 93-94, Jan 1968.

29. Kelso, J. M., (1964), "Radio Ray Propagation in the Ionosphere," McGraw-Hill, New York.

30. Kline, M. & I. W. Kay, (1965), "Electromagnetic Theory and Geometrical Optics," Interscience Publishers.

31. Lemanski, T. J., (1968), "An Evaluation of the ITSA 3-D Ray-Trace Program," Radio Science 3, (1), pp. 95-100, Jan 1968.

32. Morse, P. M. & H. Feshbach, (1953), "Methods of Theoretical Physics," McGraw-Hill, New York.

33. Nagano, I., M. Mambo, & G. Hatatsuishi, (1975), "Numerical Calculations of Electromagentic Waves in an Isotropic Multi-layered Medium," Radio Science, 10, (6), pp. 611-617, June 1975.

34. Philips, M., (1962), "Handbuch der Physik, 4," Springer-Verlag, Berlin.

35. Rektorys, K., (1977), "Variational Methods in Mathematics, Science, and Engineering," D. Reidel Pub. Co.

36. Sommerfeld, A., (1964), "Lectures on Theoretical Physics - Electrodynamics - Vol III," Academic Press.

37. Stratton, J. A., (1941), "Electromagnetic Theory," McGraw-Hill New York.

38. Weber, E., (1965), "Electromagnetic Theory - Static Fields and Their Mapping," Dover Publications.

39. Wentzel, G., (1949), "Introduction to the Quantum Theory of Fields," Interscience Pub. Co., Inc.

40. Westover, D. E., (1968), "Exact Ray-path solutions in a Quasi-linear Ionosphere," Radio Science, 3, (1), pp. 75-79, Jan. 1968.

41. Wheeler, J. A. & R. P. Feynman, (1945), "Interaction with the absorber as a Mechanism of Radiation," Rev. of Modern Physics, 17, (2, 3), pp. 157-181, April, July 1945.

42. Wheeler, J. A. & R. P. Feynman, (1949), "Classical Electrodynamics in Terms of Direct Interparticle Action," Rev. of Modern Physics, 21, (3), pp. 425 - 433, Jul 1949.

43. Yourgrau, W. & S. Mandelstam, (1968), "Variational Principles in Dynamics and Quantum Theory," W. B. Saunders Co, Phila.

APPENDIX 1.0 - Electromagnetic Theory[36]

In order to present an orderly plan for developing the variational technique, consider the usual progression in studying electrical problems of varying degrees of complexity. The following basic parameters are used in studying an electromagnetic problem -- $\bar{E}$, $\bar{B}$, $\bar{D}$, $\bar{H}$, $\bar{J}$, and ρ. For convenience, let us also define an auxiliary vector:

$$\bar{S} \equiv \bar{E} \times \bar{H}. \tag{1.1}$$

Maxwell's equations, in differential form are:

$$\nabla \times \bar{E} = -\frac{\partial \bar{B}}{\partial t} \tag{1.2}$$

and

$$\nabla \times \bar{H} = \frac{\partial \bar{D}}{\partial t} + \bar{J} \tag{1.3};$$

with supplementary equations

$$\nabla \cdot \bar{B} = 0 \tag{1.4},$$

by taking the divergence of equation (1.2). By applying the principle of charge conservation

$$\nabla \cdot \bar{D} = \rho \tag{1.5}, \text{ and}$$

$$\frac{\partial \rho}{\partial t} + \nabla \cdot \bar{J} = 0 \tag{1.6} \text{ result.}$$

Also, taking the scalar product of $\bar{H}$ in (1.2), $\bar{E}$ in (1.3) and adding gives

$$\bar{H} \cdot \dot{\bar{B}} + E \cdot \dot{\bar{D}} + \bar{E} \cdot \bar{J} + \nabla \times \bar{S} = 0. \tag{1.7}, \text{ which}$$

is Poynting's theorem, expressing energy flow.

Appendix 1.0 (Cont.)

As discussed in reference 2, $\bar{E}$ and $\bar{B}$, which express the basic characteristics of the electromagnetic energy, can be expressed in terms of potentials ϕ and $\bar{A}$:

$$\nabla \times \bar{A} + \bar{B} \qquad (1.8), \text{ and}$$

$$-\nabla \phi - \frac{\partial \bar{A}}{\partial t} = \bar{E} \qquad (1.9).$$

Thus, if ϕ and $\bar{A}$ can be found, the electromagnetic energy is also determinate.[19,34]

Static fields will first be considered, then stationary, quasi-stationary, and rapidly varying fields in turn. The following conditions apply:

.1 Static Fields:

$$\dot{\bar{B}} = \dot{\bar{D}} = \dot{\rho} = \dot{\bar{J}} = \dot{\bar{S}} = 0.$$

In addition for

.1.1 Electrostatic Fields

$\nabla \times \bar{E} = 0$, $\nabla \cdot \bar{D} = \rho$ in non-conductors

$\bar{D} = \bar{E} = 0$ in conductors

$\bar{H} = 0$ in all cases, and

.1.2 Magnetostatic Fields

$\nabla \times \bar{H} = 0$, $\nabla \cdot \bar{B} = 0$, $\bar{E} = 0$.

.2 Stationary Fields

$\dot{\bar{B}} = \dot{\bar{D}} = \rho = 0$. Current fields $\bar{J}$ are prescribed in conductors. $\nabla \times \bar{E} = 0$ always, and $\nabla \times \bar{H} = 0$ only outside the currents.

.3 Quasi-Stationary Fields

Appendix 1.0 (Cont.)

These are determined as in .2 but time-dependence is accounted for in first approximation.

.4 Rapidly-Varying Fields

These are determined with the full system of equations (1.2) through (1.6).

The expressions for the potentials at a point P are given as:

$$\phi(P) = \frac{1}{4\pi\epsilon} \iiint \frac{\rho}{r}\, d\tau + \frac{1}{4\pi\epsilon} \iint \frac{\sigma}{r}\, da \qquad (1.10),$$

$$\text{and } \bar{A}(P) = \frac{\mu}{4\pi} \iiint_{\tau} \frac{\bar{J}}{r}\, d\tau + \frac{\mu}{4\pi} \iint \frac{\bar{K}}{r}\, da \qquad (1.11),$$

where static fields are considered, and

$d\tau$ ≡ Element of volume,

da ≡ Element of surface,

$\bar{K}$ ≡ Sheet current density,

σ ≡ Surface charge density,

r ≡ Distance to P.

APPENDIX 2.0 - Ionospheric Models

2.1 Electron Density Versus Height

The key to describing the ionsphere is the electron density (n) versus height (H) profile. Many analytical expressions which approximate the actual profile are available in the literature. The ultimate limitation to the precision of the calculation of EM propagation problems remains in the accuracy of actual measurements of this profile, or parameters describing it.

This being so, if a relatively simple analytical expression for n versus H is used, it should be sufficient to assist in the development of the variational technique.

The ionosphere for analytical purposes will be arbitrarily divided into two height regions: 60-160 km - covering the so-called D, E, and F, layers, and 160-660 km covering the F_2 layer. This loose subdivision has been made because the 60-160 km region can generally be classified as "weakly ionized," (<1% ionization) as opposed to the 160-660 km region, which is "highly ionized," (>1% ionization). Thus, on a microscopic basis, the lower region behaves roughly in accordance with the Boltzmann equation; and the upper region behaves in accordance with the Fokker-Planck equation. The major constituents are also quite different in the two regions. In the lower, the main components are N_2, O_2 and A. In the upper region, they are O, N_2, O_2 and electrons.

From the foregoing, an analytic expression describing a "parabolic" layer will be employed initially. This model approximates the physical conditions. An example would be:

$$n/_{n_m} = 1 - \left(\frac{H}{T}\right)^2 \quad \text{, where}$$

n_m = Maximum electron density, and

T = Parabola half-thickness = 1.848 H units.[29]

2.2 Temperature Versus Height

Since, initially Ψ, and Q are to be assumed = 0, the full expression for the Lagrangian (Equation 4.3), requires a measure of Ψ_0. This expression is given by:

$$\Psi_0 = \frac{3}{2} N k T_M \text{ . where}$$

N = Particle number density,

k = Boltzmann's Constant, and

T_M = Particle ambient temperature.[17]

There are, in general, three types of particles to consider: electrons, ions, and neutrals. The technical literature contains many analytical and experimental determinations of the behavior of ambient temperature versus height in the ionosphere.[18] A temperature versus height model will be extracted from such literature.

GLOSSARY

Parameter	Definition	Units
A	Action Integral	(J.s)
$\bar{A}$	Vector Magnetic Potential	(Wb/m)
$\bar{B}$	Magnetic Flux Density	(Wb/m^2,T)
c	Speed of light in free space = 2.99729×10^8	(m/s)
$\bar{D}$	Electric Flux Density	(C/m^2)
$\bar{E}$	Electric Field Intensity	(V/m)
F_A	Advanced Field	(-)*
F_R	Retarded Field	(-)*
F_T	Total Field	(-)*
$\bar{F}$	Force	(N)
$\bar{H}$	Magnetic Field Intensity	(A/m)
$\bar{J}$	Current Density	(A/m^2)
k	Boltzmann's Constant = 1.3803×10^{-23}	($J/^oK$-Hz)
$\bar{K}$	Surface Current density	(A/m)
L	Lagrangian	(J)
m	Mass	(K_g)
n	Electron density	(e/m^3)
N	Particle density	(Particles/m^3)
Q	Virial Coefficient	(J)
$\bar{S}$	Poynting Vector	(W/m^2)
T	Kinetic Energy	(J)
T_M	Particle Ambient Temperature	(^oK)
$\bar{v}$	Velocity	(m/s)

GLOSSARY (Cont.)

V	Potential Energy	(J)
ε	Permittivity	(F/m)
μ	Permeability	(H/m)
ϕ	Potential Function	(v)
Ψ_0, Ψ_1	Virial Coefficients	(j)
ρ	Volume Charge Density	(C/m^3)
σ	Surface Charge Density	(C/m^2)

*Depends upon the field quantity described.

1982 USAF-SCEEE SUMMER FACULTY RESEARCH PROGRAM

Sponsored by the

AIR FORCE OFFICE OF SCIENTIFIC RESEARCH

Conducted by the

SOUTHEASTERN CENTER FOR ELECTRICAL ENGINEERING EDUCATION

FINAL REPORT

SCALING LAWS FOR PARTICLE BREAKUP IN NOZZLE GENERATED SHOCKS

Prepared by:	Dr. L. J. Forney
Academic Rank:	Associate Professor
Department and University:	School of Chemical Engineering Georgia Institute of Technology
Research Location:	Arnold Engineering Development Center Technology Division Advanced Propulsion Diagnostics Group
USAF Research Colleague:	W. K. McGregor
Date:	August 26, 1982
Contract No:	F49620-82-C-0035

SCALING LAWS FOR PARTICLE BREAKUP IN NOZZLE GENERATED SHOCKS

by

L. J. Forney

ABSTRACT

Conditions for the onset of particle breakup in normal shock waves have been investigated. Including appropriately defined particle Knudsen and Reynolds numbers into analytical expressions for the drag coefficient, a normalized particle drag behind the shock has been determined in terms of gas stagnation conditions and particle diameter for a range of gas Mach numbers $1 \leq M_1 \leq 5$. Numerical computations of the particle drag, normalized with gas stagnation pressure and particle area, indicate a peak at a gas Mach number $M_1 \sim 2.2$. The magnitude of the peak was found to decrease with increasing particle diameter and reservoir gas density.

Criteria for the onset of agglomerate breakup were defined in terms of a modified Weber number for the adhesion mechanisms due to Van der Waals forces, electrostatic attraction and adsorbed surface films. These results indicate that larger more closely packed agglomerates made up of smaller constituent particles have a greater tendency to resist breakup for a given set of gas stagnation conditions and shock Mach number.

Acknowledgment

The author would like to thank the Air Force Systems Command, the Air Force Office of Scientific Research and the Southeastern Center for Electrical Engineering Education for providing him with this excellent opportunity to address a current research topic. He would also like to thank W. K. McGregor and P. T. Girata, Jr. of the Propulsion Diagnostics Group for many helpful discussions and to Marshall K. Kingery for his assistance in the coordination of the summer appointment.

I. INTRODUCTION

Particle agglomerates and small liquid droplets are prevalent in the atmosphere and in the by-product gases from combustion processes. These micron and submicron size particles are formed by condensation of supersaturated vapor and coagulation of existing aerosol. Common combustion devices responsible for the formation of large numbers of particle agglomerates are the internal combustion engine, power plants, jet engines and solid fueled rocket motors.

In many types of supersonic flows such as wind tunnel testing, jet and rocket engine plumes and high speed flight, the small agglomerates and droplets encounter both normal and oblique shocks. These resulting particle-shock interactions subject the particles to sudden large stresses which may result in particle breakup. Specific problems of interest to the Air Force in this case are the impingement of water droplets on supersonic airfoils (1) and particle sampling with supersonic probes in jet and rocket motor plumes (2).

In the present report, the analysis of particle breakup is restricted to the interaction of particles with normal shocks, specifically, normal shocks in isentropic supersonic flows generated by a converging - diverging nozzle. The nozzle configuration was chosen since it is the basic aerodynamic element used to obtain prescribed flows in wind tunnels (3) and is similar to the design of rocket motor nozzles.

II. OBJECTIVES

The objective of this project was to determine the appropriate scaling laws for the onset of particle breakup at a normal shock. The specific objectives were:

(1) Define particle parameters behind a normal shock.

(2) Relate particle parameters and maximum drag to nozzle stagnation conditions and gas Mach number.

(3) Outline the strength of agglomerates for various adhesion mechanisms.

(4) Establish criteria for particle breakup.

III. NOZZLE GENERATED SHOCKS

The basic aerodynamic element used to obtain prescribed supersonic flows is the converging - diverging channel of the type shown in Figure 1. The nozzle is supplied with gas at high pressures and temperatures or stagnation

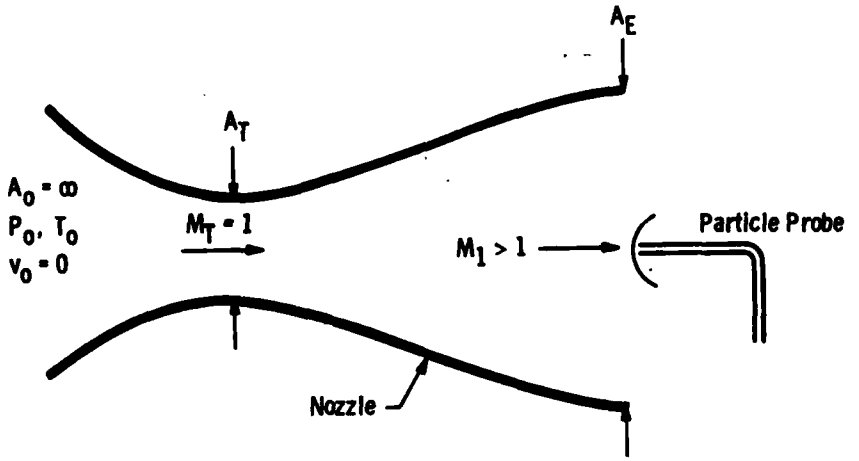


Figure 1. Schematic of Laval Nozzle.

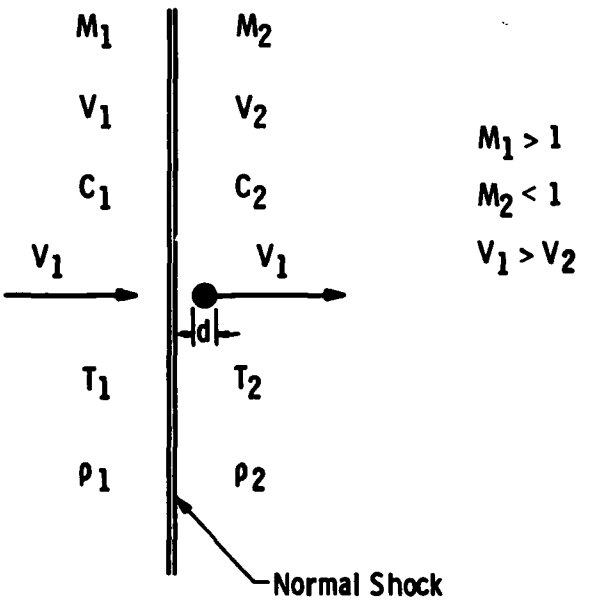


Figure 2. Particle Moving Behind Normal Shock Wave.

conditions at the inlet. Provided the exhaust pressure is sufficiently low, sonic conditions exist in the throat and the gas Mach number at any position along the axis of the nozzle is determined by the ratio of the local cross sectional area to that of the throat. The same basic configuration also exists in the nozzle of a solid fuel rocket motor.

If the nozzle of Figure 1 is designed to function without significant separation along the inside walls and we assume a perfect gas with constant specific heats, the flow is assumed to be isentropic and the gas properties are related to stagnation conditions by the following expressions (3),

$$\frac{T_o}{T_1} = 1 + \left(\frac{\gamma-1}{2}\right) M_1^2 \tag{1}$$

and

$$\frac{\rho_o}{\rho_1} = \left[1 + \left(\frac{\gamma-1}{2}\right)M_1^2\right]^{\frac{1}{\gamma-1}} \tag{2}$$

Stationary test objects such as airfoils or probes placed in the supersonic region of the nozzle flow as shown in fig. 1 will create discontinuities in the flow field. These shock waves may be normal or oblique to the direction of flow. Assuming a thermally and calorically perfect gas and restricting the discussion to normal shocks, the ratio of gas properties across the shock wave in terms of the gas Mach number ahead of the shock are

$$\frac{\rho_1}{\rho_2} = \frac{v_2}{v_1} = \frac{(\gamma-1)\ M_1^2 + 2}{(\gamma+1)\ M_1^2} \tag{3}$$

and

$$\frac{T_2}{T_1} = \frac{\left[1 + \left(\frac{\gamma-1}{2}\right) M_1^2\right]\left[\left(\frac{2\gamma}{\gamma-1}\right) M_1^2 - 1\right]}{\frac{(\gamma+1)^2}{2(\gamma-1)} M_1^2} . \tag{4}$$

Equations (1)-(4) will be used in the discussion that follows and refer to those properties shown in fig. 2.

IV. PARTICLE PARAMETERS AND STAGNATION CONDITIONS

When a particle encounters a shock front as indicated in fig. 2, it projects ahead of the carrier gas moving behind the discontinuity because of its inertia and the sharp decrease in gas velocity. This phenomenon subjects the particle to a large drag force behind the shock wave and the particle motion relaxes to that of the carrier gas.

To predict the drag on the particle behind the shock it is necessary to define at least two dimensionless groups of the three discussed below. These particle parameters are expressed in terms of the gas stagnation conditions of the nozzle and the gas Mach number M_1 upstream of the normal shock.

a. Reynolds Number

The particle Reynolds number which represents the ratio of inertial to viscous forces acting on the particle is defined in terms of the particle diameter and its local velocity relative to the ambient gas. The Reynolds number is a maximum behind the shock front and subsequently approaches zero as the particle equilibrates to the gas velocity. Thus behind the shock wave, one obtains

$$Re = \frac{\rho_2 (v_1 - v_2) d}{\mu_2} . \tag{5}$$

Introducing the gas stagnation conditions into Eq. (5) by writing all gas properties in the form

$$\rho_2 = \left(\frac{\rho_2}{\rho_1}\right)\left(\frac{\rho_1}{\rho_o}\right)\rho_o$$

where the ratios of gas properties are given by Eqs. (1)-(4), one obtains

$$Re = \gamma^{1/2} \left(\frac{d\rho_o}{k}\right) f_4 \ (M_1) \tag{6}$$

where

$$f_4 \ (M_1) = \frac{M_1 \ (M_1^2-1)}{\left[1 + \frac{\gamma-1}{2} \ M_1^2\right]^{\frac{\gamma}{\gamma-1}}} \left(T_{1/T_2}\right)^{3/2} \left[\left(\frac{T_2}{T_1}\right) + \left(\frac{T_o}{T_1}\right)\left(\frac{T_\theta}{T_o}\right)\right] \ , \tag{7}$$

$k = b/R^{1/2}$, R is the specific gas constant, and $b = \mu_r \ (1/T_r)^{1/2}\left(1 + \frac{T_\theta}{T_r}\right)$.

Here the quantity b appears in Sutherland's formula for viscosity where

$$\mu = \frac{b \ T^{3/2}}{T + T_\theta} \ , \tag{8}$$

$\mu_r = \mu \ (T_r)$ is a reference viscosity and T_θ is Sutherland's constant (4).

Numerical solutions to Eq. (7) are plotted in fig. 3 for constant gas stagnation conditions and particle size. Figure 3 demonstrates that Re increases to a maximum at $M_1 \sim 2$ and decreases for larger gas Mach numbers as the gas becomes less dense. It is also noted that the parameter $d\rho_o/k$ appearing in Eq. (6) is proportional to the ratio of particle diameter to the gas mean free path in the stagnation reservoir.

b. Knudsen Number

The particle Knudsen number is defined as the ratio of the mean free path of the gas to the particle diameter. From kinetic theory (5) one obtains

$$Kn = \left(\frac{\pi}{2}\right)^{1/2} \gamma^{1/2} \frac{\mu_2}{C_2 \ \rho_2 d} \tag{9}$$

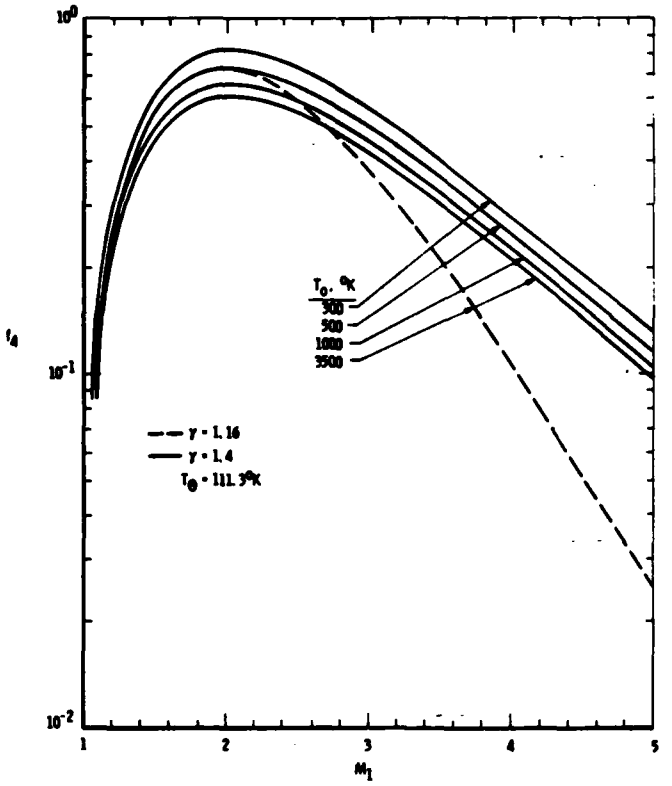


Figure 3. Dimensionless Function Proportional to Particle Reynolds Number.

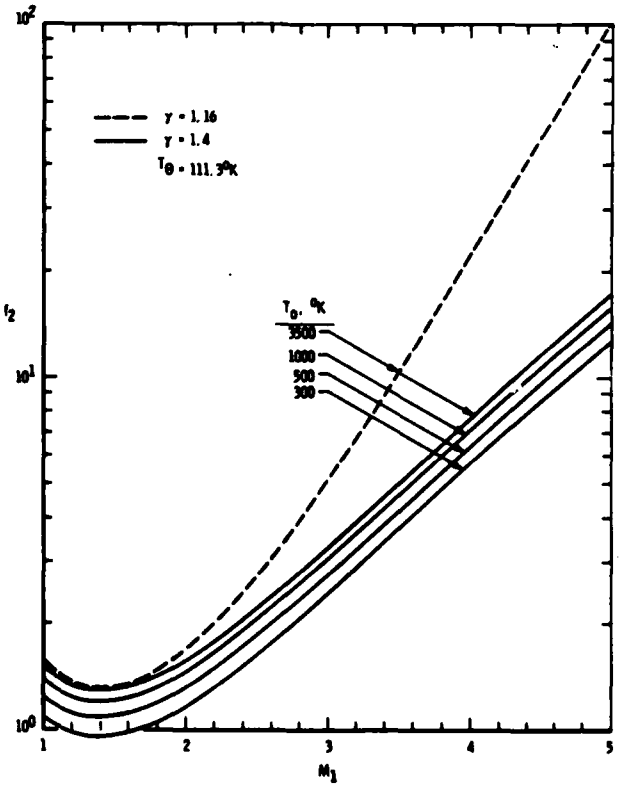


Figure 4. Dimensionless Function Proportional to Particle Knudsen Number.

where $C_2 = (\gamma R T_2)^{1/2}$ is the speed of sound back of the shock. After some rearrangement using the procedure of the previous section, one obtains

$$Kn = \left(\frac{\pi}{2}\right)^{1/2} \left(\frac{k}{d\rho_o}\right) f_2\ (M_1) \tag{10}$$

where

$$f_2\ (M_1) = \frac{(T_2/T_1)}{\left[\left(\frac{T_2}{T_1}\right) + \left(\frac{T_o}{T_1}\right)\left(\frac{T_\theta}{T_o}\right)\right]} \quad \frac{\left[1 + \left(\frac{\gamma-1}{2}\right) M_1^2\right]^{\frac{\gamma}{\gamma-1}}}{\left(\frac{\gamma+1}{2}\right) M_1^2} . \tag{11}$$

Numerical solutions to Eq. (11) are plotted in fig. 4 where the effect of decreasing gas density with larger gas Mach numbers is again demonstrated.

c. Particle Mach number

The particle Mach number is defined as the ratio of the relative velocity of the particle with respect to the ambient gas to the local speed of sound. Thus one obtains

$$M_p = \frac{v_1 - v_2}{c_2} = \left(1 - \frac{v_2}{v_1}\right)\left(\frac{T_1}{T_2}\right)^{1/2} M_1 . \tag{12}$$

where M_p increases over the limits $0 \leq M_p \leq \left(\frac{2}{(\gamma-1)\gamma}\right)^{1/2}$

for $1 \leq M_1 \leq \infty$. From kinetic theory M_p is not independent of Re and Kn as discussed above since $M_p = Kn\ Re \left(\frac{2}{\pi\gamma}\right)^{1/2}$.

V. MAXIMUM DRAG

The maximum drag on a particle immediately behind the shock wave is defined as

$$D = \frac{\rho_2}{2} A_p C_D (v_1 - v_2)^2 \tag{13}$$

where C_D is the drag coefficient and A_p $(=\pi d^2/4)$ is the cross sectional area of the particle. Defining local gas properties in terms of the stagnation conditions and the gas Mach number M_1 upstream from the shock as done in Sec. IV, one obtains

$$\frac{D}{A_p P_o} = C_D \left[\left(\frac{\gamma}{\gamma+1}\right) \frac{(M_1^2 - 1)^2}{\left(1 + \left(\frac{\gamma-1}{2}\right) M_1^2\right)^{\frac{2\gamma-1}{\gamma-1}}}\right] \tag{14}$$

or

$$\frac{D}{A_p P_o} = C_D \, g\,(M_1) \tag{15}$$

where P_o is the gas stagnation pressure. Since $g \to o$ for $M_1 \to o$ or ∞, $g\,(M_1)$ has a maximum at $M_1 = (3+2\gamma)^{1/2}$ (i.e. if $\gamma = 1.4$ for air, one can show that $g_{max} = 0.42$ at $M_1 = 2.4$).

Numerical solutions are now sought for the normalized drag of Eq. (15). In this report we use the functional form of the drag coefficient proposed by Crow (6). Contours of C_D for constant Knudsen number are plotted in fig. 5. Also shown in fig. 5 is the inequality $Kn\ Re \leq [\frac{\pi}{\gamma - 1}]^{1/2}$ determined from the maximum particle Mach number M_p discussed in the previous section. Since the drag coefficient $C_D = C_D(Kn,Re)$, expressions for Kn and Re were introduced as defined by Eqs. (6) and (10).

Numerical results for the normalized particle drag are presented in fig. 6 for contours of constant $\frac{d\rho_o}{k}$ defined by a fixed set of nozzle stagnation conditions and particle size. These results demonstrate that particles experience the largest stresses at a gas Mach number in the range $2 < M_1 < 2.5$ with the maximum value decreasing with increasing particle diameter. These results proved to be insensitive to the stagnation temperature over the range $500^oK < T_o < 3500^oK$ and to changes in Sutherland's constant, T_θ.

VI. STRENGTH OF AGGLOMERATES

We assume that large agglomerates consist of small constituent particles which are uniform spheres of size d_D in the following treatment. An example of an aggomerate is shown in fig. 7. Following the treatment of

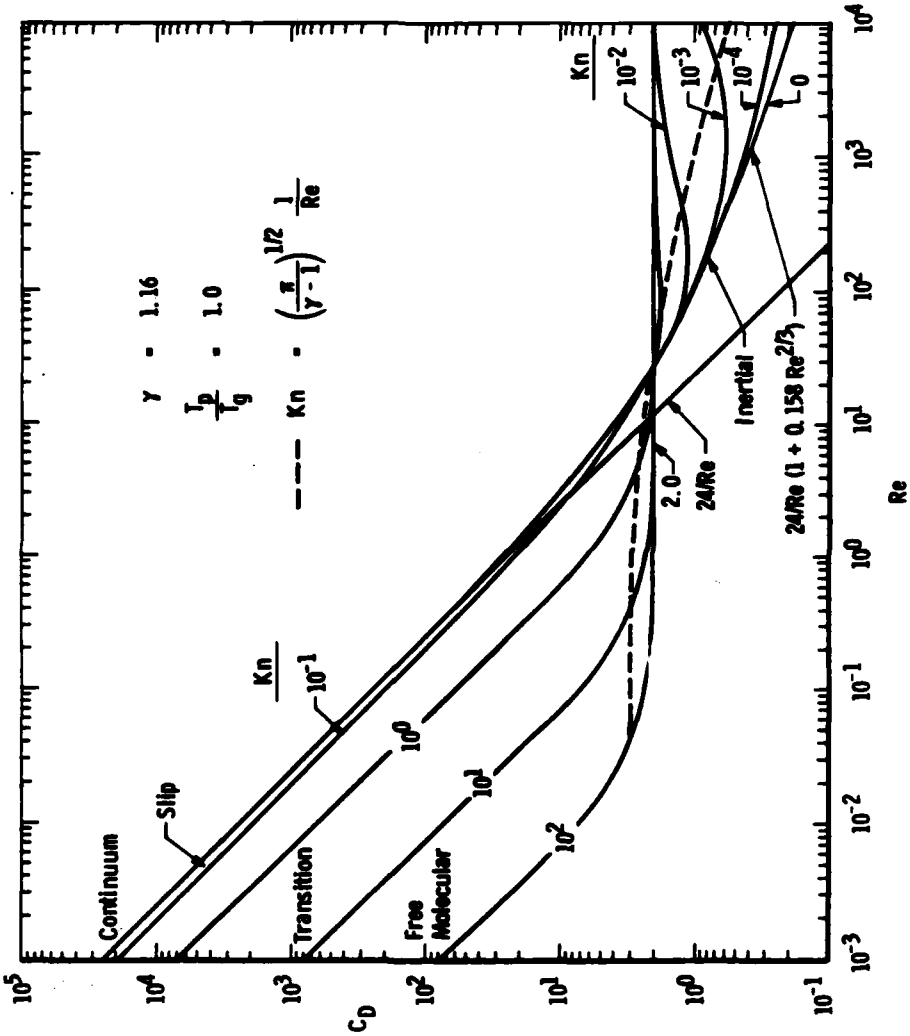


Figure 5. Particle Drag Coefficient After Crowe (1967).

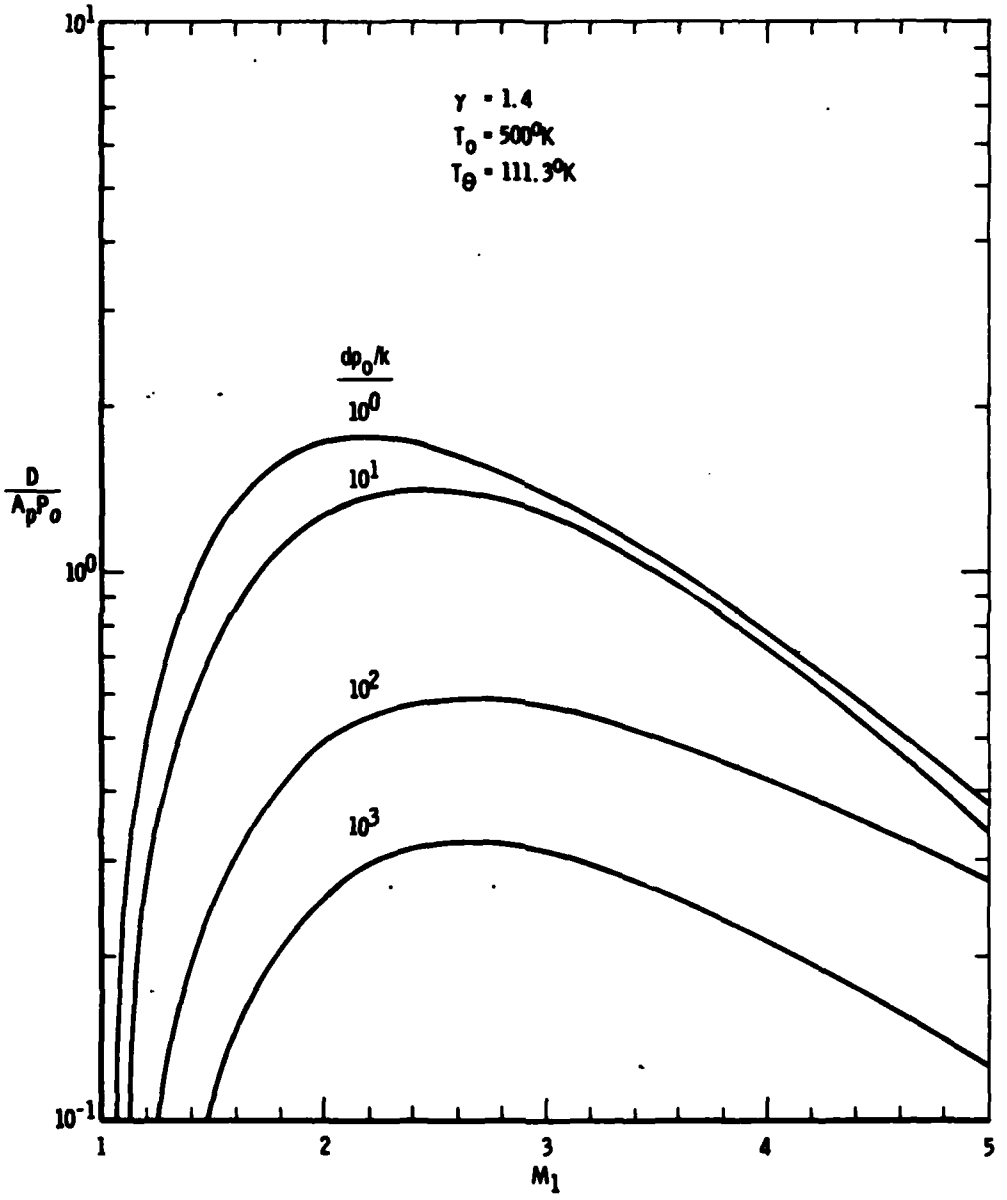


Figure 6. Normalized Particle Drag.

Rumpf (7), we assume that the force of adhesion between two constituent particles is F and that each small sphere of size d_D has z contacts (coordination number). If the voidage is $1-\phi$, the number of spheres per unit

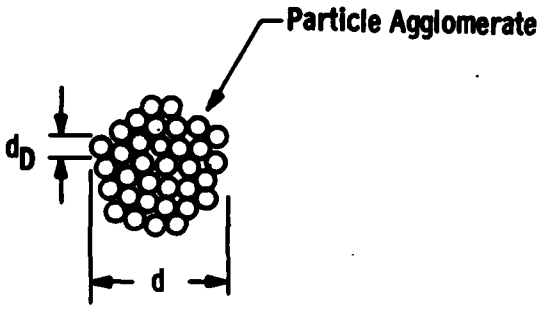


Figure 7. Schematic of Particle Agglomerate.

cross sectional area of the large agglomerate is

$$n = \frac{\phi}{\pi d_D^2/4} \quad . \tag{16}$$

Thus, the number of contacts per unit cross sectional area becomes

$$\frac{nz}{2} = \frac{2\phi z}{d_D^2} \tag{17}$$

The factor of 1/2 is introduced above in Eq. (17) since each contact is shared by two spheres.

One can now write the total force of adhesion per unit cross sectional area of the agglomerate as

$$\frac{P}{A_p} = \frac{2\phi z\ F}{d_D^2} \tag{18}$$

where P is the total force of adhesion. Rumpf (7) demonstrates that $z(1-\phi) \simeq 3.1$ for common coordination numbers so that Eq. (18) simplifies to

$$\frac{P}{A_p} = 6.2 \frac{\phi}{1-\phi} \frac{F}{d_D^2} \tag{19}$$

a. London-Van der Waals Forces

The force of adhesion between clean, dry, uncharged particles and surfaces are due to London-Van der Waals attractive forces. Nonpolar, electrically neutral atoms and molecules have momentary dipoles over short periods of time due to the movement of their electrons. Integrating the attractive forces between all of the molecules in two small spheres separated by a distance "a" gives an attractive force of the form

$$F_{v1} = \frac{B_1 d_D}{a^2} \quad . \tag{20}$$

The distance in the denominator of Eq. (20) is restricted to a <2000 A^o and B_1 is typically in the range $10^{-13} < B < 10^{-11}$ ergs (8) depending on the nature of the material and the media separating the spheres.

For larger separations a >2000 A^o, Lifshitz equation (8) between two spherical particles of equal diameter is

$$F_{v2} = \frac{B_2 d_D}{a^3} \tag{21}$$

where $B_2 \sim 10^{-20}$ erg-cm and depends on particle composition and the media separating the spheres.

It should be noted that the extensive literature available on the subject of Van der Waals forces demonstrate that the calculations suggested above are only approximate, at best, as reviewed by Davies (8). Electrostatic charge and adsorbed liquid on particle surfaces can make the simple calculations above greatly in error. A more complete discussion of experimental results for the crushing strength of metal oxide agglomerates is given in Forney et. al. (10).

b. Electrostatic Forces

Suspended particles carry electrostatic charge. There are many mechanisms of charging and these are reviewed by Davies (8). The important mechanisms fall into one of two categories. The particles are either charged during their formation or are exposed to electrons or ions carried by the ambient gas. Assuming two spheres with a surface charge density q, separated by a distance much smaller than the diameter of the spheres d_D, the force of attraction is

$$F_e = \frac{\varepsilon \pi^2 d_D^2 q^2}{a^2} \tag{22}$$

where $\varepsilon = 9 \times 10^{18}$ dynes-cm^2/couls is Coulomb's constant.

Electrostatic mechanisms have been shown to have a large effect experimentally on the magnitude of the force of adhesion between particles. This effect is much larger than expected assuming normal charge distributions. This suggests that the details of surface irregularities and nonuniform charge distributions at the contacting surface are not properly accounted for in existing theories.

c. Surface Films

When particles are suspended in a condensible vapor, a film of liquid develops on the surface. If the vapor pressure is near its saturated value, the force of adhesion between two spheres of equal diameter with smooth clean surfaces is estimated to be (7)

$$F_s = 2.2 \sigma d_D \tag{23}$$

where σ is the surface tension of the liquid film. In practice, the force of adhesion decreases sharply below the value given by Eq. (23) if the vapor pressure is below 90% of its saturated value. Surface contaminants and the non-submergence of surface irregularities will also reduce the expected force of adhesion (8).

d. Strength of Liquid Droplets

Uniform liquid spherical droplets are held together by surface tension forces. Surface tension σ has units of force per unit length. The strength of the droplet is thus the product of σ and the circumference or

$$P = \sigma \pi d \quad . \tag{24}$$

Writing Eq. (24) in the form of Eq. (9), one obtains a strength per unit cross sectional area of the droplet or

$$\frac{P}{A_p} = \frac{4\sigma}{d} \quad . \tag{25}$$

Caveny and Gany (9) have studied the breakup of molten AL/AL_2O_3 droplets in accelerating flow fields.

VII. CRITERIA FOR PARTICLE BREAKUP

From the foregoing, we are now in a position to establish criteria for particle breakup. The discussion is restricted to the possibility of breakup behind nozzle generated, normal shocks. We hypothesize that the onset of particle breakup occurs when the drag force exceeds either the agglomerate or droplet strength. Thus one obtains the inequality

$$D > P \tag{26}$$

where D is given by Eq. (15) and the particle strength P by Eqs. (19) or (25). In Eq. (19) the constituant particle adhesive force F which appears in P is given by either Eqs. (20), (21), (22), or (23). Equation (26) is the same argument used to predict breakup in the definition of a droplet Weber number (9).

Substituting for particle drag and strength in eq. (26), the following criteria are established for each of the adhesive mechanisms discussed in Sec. VI. Thus, particle breakup is expected to occur for the conditions listed below.

Van der Waals:

$$\frac{d_D P_o C_D g (M_1)}{B h_1 (\phi)} > 1 \qquad (27)$$

where $B = B_1/a^2$, $a < 2000\ A^o$

$B = B_2/a^3$, $a > 2000\ A^o$

and $h_1 (\phi) = 6.2 \left(\frac{\phi}{1-\phi}\right)$,

electrostatic:

$$\frac{d_D P_o C_D g (M_1)}{\varepsilon q^2 h_2 (\phi)} > 1, \qquad (28)$$

where $h_2 (\phi) = 6.2 \pi^2 \left(\frac{\phi}{1-\phi}\right)$,

surface films:

$$\frac{d_D P_o C_D g (M_1)}{\sigma h_3 (\phi)} > 1, \qquad (29)$$

where $h_3 (\phi) = 13.64 \left(\frac{\phi}{1-\phi}\right)$,

and liquid droplets:

$$\frac{d P_o C_D g (M_1)}{4 \sigma} > 1. \qquad (30)$$

It should be noted that Eq. (30), above, represents the Weber number for a liquid droplet.

Equations (27), (28), and (29) indicate that the likelihood of particle breakup increases significantly as the volume fraction of solids ϕ decreases. Larger gas stagnation pressures P_o or constituent particle sizes d_D also contribute to agglomerate breakup. Moreover, the product C_D g (M_1) in fig. 6 increases with smaller agglomerate sizes d. Thus, we can conclude that larger more closely packed agglomerates made up of smaller constituent particles will have a tendency to resist breakup for a given set of gas stagnation conditions and shock Mach number.

VIII. RECOMMENDATIONS

The following recommendations are made for future work from the foregoing discussion:

1. Conduct controlled experiments with nozzle generated shocks to determine if the onset of particle breakup occurs as predicted by Eqs. (27) - (30).
2. Determine in what manner the experimental methods and results may be used to improve the current understanding of the forces of adhesion between constituent particles of an agglomerate.
3. Determine the effect of the unsteady Basset term on particle relaxation behind normal shock waves. The Basset term has been neglected in this report as is customary but it may be of importance in large particle acceleration behind normal and oblique shocks.

REFERENCES

1. Serafini, J. S., "Impingment of Water Droplets on Wedges and Double-Wedge Airfoils at Supersonic Speeds," NACA Report 1159 (1954).

2. Smith, P. W., Stety, G. A. and Delaney, L. J., "Impulse Scaling Predictions," AFRPL-TR-66-297, Air Force Rocket Propulsion Laboratory, Edwards AFB, Edwards, CA (1966).

3. Leipmann, H. W. and Roshko, A., Elements of Gasdynamics, John Wiley, N.Y. (1957).

4. Jeans, J., An Introduction to the Kinetic Theory of Gases, Cambridge University Press (1940).

5. Vincenti, W. G. and Kruger, C. H. Jr., Introduction to Physical Gas Dynamics, John Wiley, N.Y. (1965).

6. Crowe, C. T., "Drag Coefficient of Particles in a Rocket Nozzle," AIAA J. 5, 1021 (1967).

7. Rumpf, H., "Mechanics of Granules", Chem.-Ingn.-Tech. 30, 144 (1958).

8. Davies, C. N., Aerosol Science, Academic Press, N.Y. (1966).

9. Caveny, L. H. and Gany A., "Breakup of AL/AL_2O_3 Agglomerates in Accelerating Flow-Fields, AIAA J. 17, 1368 (1979).

10. Forney, L. J., McGregor, W. K. and Girata, P. T., "Particle Sampling with Supersonic Probes: Similitude and Particle Breakup," AEDC report (to be published).

1982 USAF-SCEEE SUMMER FACULTY RESEARCH PROGRAM

Sponsored by the

AIR FORCE OFFICE OF SCIENTIFIC RESEARCH

Conducted by the

SOUTHEASTERN CENTER FOR ELECTRICAL ENGINEERING EDUCATION

FINAL REPORT

OXYGEN-18 IMPLANTATION IN GaAs

Prepared by:	Dr. Albert Frasca
Academic Rank:	Associate Professor
Department and University:	Department of Physics Wittenberg University
Research Location:	Avionics Laboratory Wright-Patterson AFB
USAF Research Colleague:	Dr. Y. S. Park
Date:	August 25, 1982
Contract No:	F49620-82-C0035

OXYGEN-18 IMPLANTATION IN GaAs

by

Albert J. Frasca

ABSTRACT

The role of oxygen in the GaAs lattice has been studied for over a decade. The experimental results are very dependent on the anneal temperature, dose, dopant, and implant energy. This paper is concerned with the further investigation of oxygen in GaAs. Both electrical and lattice damage measurements were made. The electrical study was done using C-V techniques and the lattice damage study was done using proton backscatter techniques. Results are given for annealed and as implanted samples.

ACKNOWLEDGEMENT

The author would like to thank the Southeastern Center of Electrical Engineering Education for providing the opportunity to work in the Avionics Laboratory at W-P AFB. The ten week period was most beneficial in terms of research as well as permitting the opportunity to work in an area which is at the forefront of surface physics research.

In particular I would like to thank the following people for their excellent cooperation and interest.

Y. S. Park

P. Pronko

P. Stover

R. Bhattacharya

J. Ehret

D. Hurley

Y. K. Yeo

C. Geesner

A. Ezis

I. INTRODUCTION:

During the early 1970's oxygen was one of many elements implanted in n-type GaAs in order to evaluate its ability to resistively compensate the material. Implant energies ranged from 50 to 1000 keV with implant doses ranging from $1x10^9$ O^+/cm^2 to $1x10^{15}$ O^+/cm^2. C-V, C-f, and Hall probes techniques were used for electrical measurements and photoluminescence for optical spectra analysis. In the mid-1970's, the use of SIMS became popular as an oxygen profiling tool.

The fact that oxygen could compensate n-type GaAs and could produce highly resistive layers made it a prime candidate for device isolation. It was found that compensation occurred because of lattice damage and by oxygen acting as a "dopant" (double electron trap).[1] Also, it was found that implant damage compensation could be annealed away as it is with hydrogen implantation. However, the compensation due to the "dopant" contribution was thermally stable to at least 800°C if the implant exceeded a threshold dose of $1x10^{13}$ O^+/cm^2. Further research with oxygen implants revealed another interesting characteristic of considerable importance for device production. It was found that before annealing, the oxygen formed highly resistive layers centered at the mean range for defects and at the mean range for ions.[2] The fact

that two regions exist explains the earlier results of having two separate resistance regions.

In the most recent articles, it has been reported that implanted oxygen redistributes (after anneal) and seems to be drawn together (cluster) at R_p thus reducing the width of the implant and increasing the oxygen concentration of the highly resistive layer.[3,4] This characteristic is highly desirable for production of very thin devices.

II. OBJECTIVES

Many techniques for developing GaAs devices are presently being studied and developed by research organizations and electronic companies. One aspect of this broad research area centers on the role of implanted oxygen in the GaAs lattice. A desire to more fully understand how the implanted oxygen is able to develop highly resistive material is of primary importance. Obviously the answer lies in knowing its lattice location and atomic interactions. The objective of this project was the further investigation of implanted oxygen in GaAs using the following techniques:

a) C-V measurements for electrical compensation

b) Rutherford backscatter measurements for lattice damage analysis.

It is further planned to continue this study by extending the research to nuclear reaction profiling of the same oxygen-18 samples.

III. C-V MEASUREMENTS

Capacitance-Voltage measurement is a method for determining carrier concentrations of doped and implanted samples without using layer removal techniques. Since oxygen can compensate n-type GaAs at the mean range for ions, a rapid change in carrier concentration is expected as the R_p is exceeded. Since high dopant level n-type material ($3.12 \times 10^{17}/cm^3$ Si) is being used, the implant range must be shallow in order to avoid avalanche breakdown as the reverse bias is increased. The depletion layer width should be about 0.15 μm for 3.12×10^{17} Si/cm^3 material, thus, implant energies of 120 keV were used.

The backside of the samples were coated with Au-Ge ohmic contacts and the implanted side used aluminum Schottky contacts. The presence of Schottky contacts generates a depletion layer which is controlled with the reverse bias. Thus the space between the contact and the n-type material acts as a dielectric sheet between plates of a capacitor. The capacitance of such a device is given below:

$$C = \frac{\varepsilon A}{x} \qquad (1)$$

A=area of Schottky contact
ε=dielectric constant of GaAs
x=depth of depletion zone.

As the reverse bias is increased, the value of x can be determined by measuring C. Thus a profile can be obtained as a function of reverse bias. The net carrier concentration is obtained using the capacitance measured above.[5]

$$N(x) = \frac{2}{\varepsilon q A^2}\left(\frac{d}{dV}\left(\frac{1}{C^2}\right)\right)^{-1} \quad \text{or} \quad N(x) = \frac{C^3}{\varepsilon q A^2}\left(\frac{dC}{dV}\right)^{-1} \qquad (2)$$

where N(x) = carrier concentration

ε = dielectric constant

A = area of Schottky contact

C = capacitance

V = applied reverse voltage.

The C-V results are given below:

TABLE I

OXYGEN COMPENSATION DEPTH

Sample	10^{14} O^+/cm^2	10^{15} O^+/cm^2
as implanted	.30μm	.30μm
400°C anneal (20 min.)	.34μm	.32μm
800°C anneal (20 min.)	.45μm	.75μm

As can be seen, the compensation resulting from the high dose implants has produced compensation far beyond the implant range (120keV≈.15μm). The very high anneal temperatures caused additional diffusion and compensation well beyond that for the as implanted and 400°C annealed samples.

IV. RUTHERFORD BACKSCATTER

Rutherford backscatter is a common means for analyzing damage in crystalline materials. The technique utilized for this study was bombardment of 340keV protons to observe the channeled and random backscatter spectra. The channeled vs. random spectra were used to evaluate damage. Both the <110> and <100> spectra were recorded for the as implanted, 400°C and 800°C annealed samples. Since oxygen is a very light nucleus compared to gallium or arsenic, very little information can be obtained concerning its presence, only the damage can be evaluated. Calibration testing using argon implants in carbon illustrated the difficulty of separating the argon backscatter peak from the carbon spectrum. The energy of the backscattered proton from carbon and argon differ by less than 20% for a detector angle of 170° with 340keV protons. Thus, all the recoil protons from oxygen backscatter should be in the low energy end of the GaAs distribution. Likewise, since the percent abundance of oxygen is small, the oxygen profile is not observed.

The actual procedure for analyzing damage utilizing this technique requires locating the 100 axis and then recording the backscatter high energy yield and comparing it to the high energy yield for a random angle. The ratio of channeling yield to unchanneled yield is referred to as χ_{min}.

$$\chi_{min} = \frac{\text{channeled yield}}{\text{unchanneled yield}} \times 100\%$$

If the channels are clear of displaced atoms then χ_{min} will be small which implies low damage. However if the crystal has a large number of interstitial atoms then χ_{min} will be large. Typical values for χ_{min} made on unimplanted GaAs range from 3 to 5 percent. The results obtained from our measurements are given below.

TABLE II

χ_{min} FOR OXYGEN-18 SAMPLES

Sample	10^{14} O^+/cm^2	10^{15} O^+/cm^2
as implanted	8.1%	11.3%
400°C (20 min.)	5.9%	6.7%
800°C (20 min.)	4.9%	5.0%

The small amount of damage is typical of light ion implants. As can be seen, the 800°C anneal is capable of removing most of the damage caused by the implantation. However, this technique does not give any information on the lattice location of the oxygen.

V. RECOMMENDATIONS

The C-V measurements confirmed the ability of oxygen to compensate n-type GaAs and to retain the ability after high temperature annealing. The Rutherford backscatter study confirmed that low damage profiles result in GaAs

after oxygen implantation and that annealing removes most of the damage caused by the implant.

It is now a question of locating the oxygen both in depth and in proximity to its lattice neighbors. This last study can be done using nuclear reaction techniques.

An extensive literature search resulted in finding several nuclear reactions which could be utilized for oxygen-18 detection.[6]

TABLE III

Reaction	$O^{18}(p,\alpha)N^{15}$	$O^{18}(d,\alpha)N^{16}$	$O^{18}(d,p)O^{19}$
Cross-section (mb)	75	5	10
Incident energy (MeV)	.6	.6	.9
Particle	α	α	p
Estimated sensitivity (gm)	2×10^{-12}	3×10^{-10}	2×10^{-11}
Q(MeV)	3.97	4.24	1.7

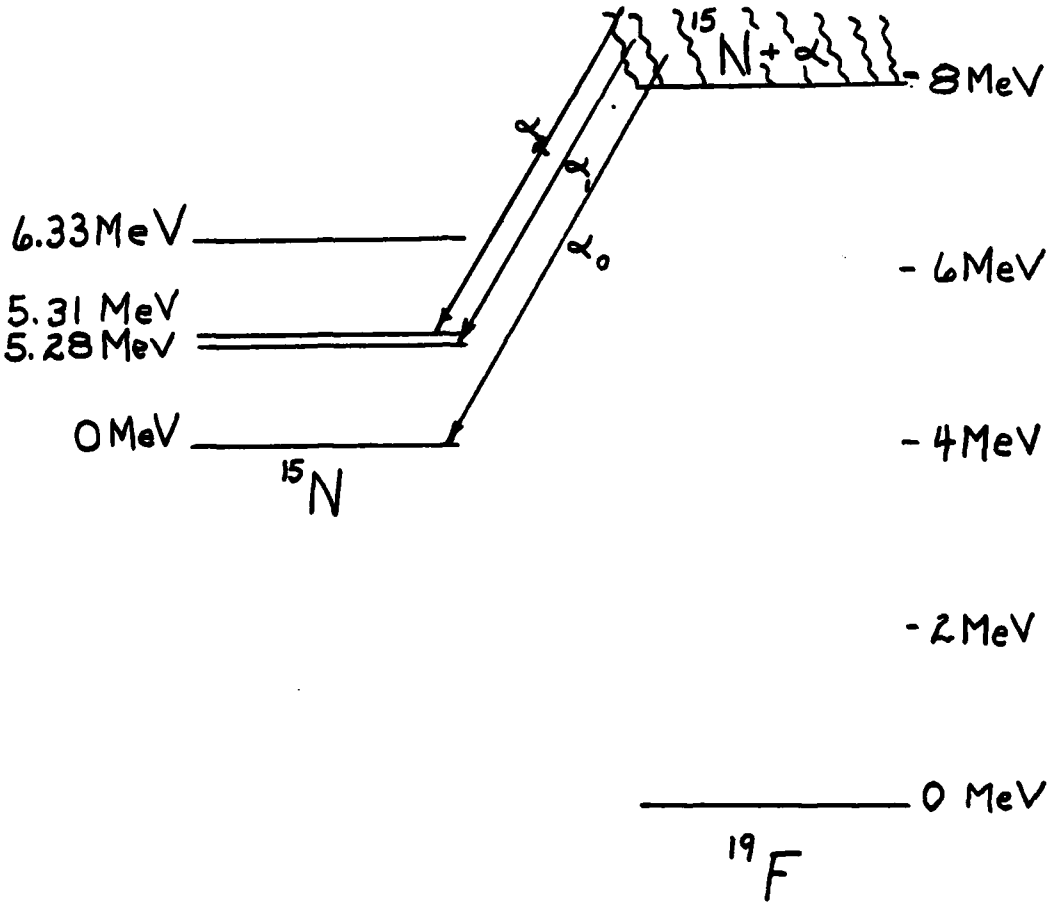
The oxygen-18 reaction proposed is the first one listed with a resonance energy of 630keV. The resonance is very narrow (2.6keV) which allows for a depth resolution of <500Å for shallow implants of oxygen-18. Since the isotope (oxygen-18) is not abundant in nature, the background from abundant oxygen-16 is not a problem. Also, protons and not deuterons are used which reduces the

probability of neutron generation in the accelerator due to deuteron-deuteron collisions around the collimating slits.

The reaction has a high cross-section and results from proton absorption and the formation of fluorine-19. The fluorine is unstable and decays forming nitrogen-15 and an α particle.

$$^{18}_{8}O + ^{1}_{1}H \rightarrow {}^{19}_{9}F^{*} \rightarrow {}^{15}_{7}N + {}^{4}_{2}He \qquad Q=3.98MeV \qquad (3)$$

The nuclear level decay scheme is shown below.[7]



Since the energy release is large (3.98MeV) and the recoil nucleus ($^{15}_{7}N$) is large, the alpha particle immerges with most of the kinetic energy (~3.3MeV). Another beneficial relationship about the reaction is the number of sharp resonances (35) at low proton energies up to 3.5MeV. The lowest ones are listed for reference.[8]

TABLE IV

Proton energy for resonance (keV)	Resonance width (keV)
630±2	2.6±1.0
844±6	40±5
1165±1	±.5
1399±5	±15
1685±5	±15
1769±2	4.0±1.0
1931±2	1.5±1.0

It should be noted that all the resonances listed have narrow widths which makes them ideal for profiling oxygen. The first resonance at 630±2KeV is of primary concern because of its sharpness and being the lowest allowed resonance. The yield jumps from about 7mb/ste to almost 60mb/ste at 630keV. At resonance an increase in count rate of approximately nine should be experienced. The emerging α particle will have an energy of about 3.3MeV and will be able to travel through several microns

of GaAs. The maximum range is about 10μm and the differential range is $dE/dx \approx .5MeV/\mu m$. The loss of energy with depth is a problem in selecting a mylar foil that passes α's and stops backscattered protons. The 630keV resonance is sufficently narrow (2.6keV) that good depth resolution can be obtained. The differential energy loss for protons in GaAs is about 68keV/μm. Thus, the resonance will only occur in a thin section of the sample.

$$\frac{2.6keV}{68keV/\mu m} = .038\mu m = 380\mathring{A} \qquad (4)$$

Calculations performed by Ansel and Samuel[6] (1967) imply a sensitivity of $1x10^{-12}$ grams/cm^2 to oxygen-18 for shallow implants. Work performed by Gass and Müller[7,8,9] (1973) show depth profiles of oxygen-18 in silicon for thick (5000Å) and thin (70Å) specimens.

Thus it is recommended that the study be continued using the same specimens and their oxygen-18 depth profile be obtained by using channeling techniques and nuclear reactions, the oxygen atom locations can be confirmed as interstitial or substitutional.

REFERENCES

1. Favennec, P. N. and E. V. K. Rao, "Compensating Layers in GaAs by Ion Implantation: Application to Integrated Optics," Proceedings from the Fourth International Conference on Ion Implantation in Semiconductors and Other Materials, Osada, 1974, pp. 65-71.

2. Favennec, P. N., "Semi-Insulating Layers of GaAs by Oxygen Implantation," Journal of Applied Physics, Vol. 47, 1976, pp. 2532-2536.

3. Favennec, P. N., M. Gauneau, H. L'Haridon, B. Deveaud, C. A. Evans, Jr., and R. J. Blattner, "Chromium Gettering in GaAs by Oxygen Implantation," Applied Physics Letters, Vol. 38, 1981, pp. 271-273.

4. Favennec, P. N., B. Deveaud, M. Salvi, A. Martinez, and C. Armand, "Redistribution of Implanted Oxygen in GaAs," Electronics Letters, Vol. 18, 1982, pp. 202-203.

5. Blood, P. and J. W. Orton, "The Electrical Characteristics of Semiconductors," Reports on Progress in Physics, Vol. 41, 1978, pp. 158-257.

6. Amsel, G., D. Samuel, "Microanalysis of the Stable Isotopes of Oxygen by Means of Nuclear Reactions," Analytical Chemistry, Vol. 39, Dec. 1967, pp. 1689-1698.

7. Carlson, R. R., C. C. Kim, J. A. Jacobs, and A. C. L. Barnard, "Elastic Scattering and Reactions of Protons on ^{16}O," Physical Review, Vol. 122, Number 2, April 15, 1961, pp. 607-616.

8. Butler, J. W., H. D. Holmgren, "Radiative Proton Capture by ^{16}O," Physical Review, Vol. 116, Number 6, Dec. 15, 1959, pp. 1485-1489.

9. Gass, J. E., H. H. Müller, "Measurement of Oxygen-Diffusion-Profiles in Silicon-Single-Crystals by Means of the Nuclear Reaction $^{16}O(p,\alpha)^{15}N$," Nuclear Instruments and Methods, Vol. 106 (1973), pp. 109-113.

1982 USAF-SCEEE SUMMER FACULTY RESEARCH PROGRAM

Sponsored by the

AIR FORCE OFFICE OF SCIENTIFIC RESEARCH

Conducted by the

SOUTHEASTERN CENTER FOR ELECTRICAL ENGINEERING EDUCATION

FINAL REPORT

MODELING OF ACTIVE NEUROMUSCULATURE RESPONSE TO MECHANICAL STRESS

Prepared by:	Dr. Andris Freivalds and Mr. Jeffrey L. Harpster
Academic Rank:	Asst. Professor, Industrial Engineering Graduate Student
Department and University:	Dept. of Industrial & Management Systems Engineering The Pennsylvania State University
Research Location:	Air Force Aerospace Medical Research Laboratory, Biodynamics & Bioengineering Division, Modeling & Analysis Branch (AFAMRL/BBM)
USAF Research Colleague:	Dr. Ints Kaleps
Date:	August 13, 1982
Contract No:	F49620-82-C-0035

MODELING OF ACTIVE NEUROMUSCULATURE RESPONSE TO MECHANICAL STRESS

by

Dr. Andris Freivalds

and

Mr. Jeffrey L. Harpster

ABSTRACT

The Articulated Total Body (ATB) Model, based on rigid-body dynamics with Euler equations of motion and Lagrange type constraints, was used to predict the forces and motions experienced by air crew personnel in typical flight operations. To provide a more realistic representation of human dynamics, an active neuromusculature was added to the ATB Model via the newly developed advanced harness system. The lumped three parameter muscle model included a contractile element, a damping element and a parallel elastic element.

Two validation studies were performed. The first simulated elbow flexion with one muscle/harness system representing the biceps brachii and the brachialis. The results indicated that the force velocity effects produced the greatest changes in force, with significant force changes due to the damping element and length tension relationship and no force changes due to the parallel-elastic element. The second study simulated the whole body response to a 2-G_y lateral force utilizing trunk musculature. Although the musculature did not completely prevent the lateral deflection of the body, the response is significantly delayed compared to a control response, with the head and neck maintaining the upright posture for a longer period of time.

ACKNOWLEDGMENTS

The work described in this report was performed under the Air Force Office of Scientific Research and the Southeastern Center for Electrical Engineering Education Summer Faculty Research Program at the Air Force Aerospace Medical Research Laboratory, Wright-Patterson Air Force Base, Ohio. The authors express their sincere thanks to these organizations for a very productive and enjoyable summer research program and to the Modeling and Analysis Branch of the Biodynamics and Bioengineering Division for supporting this project.

The authors would also like to thank Dr. Ints Kaleps, Chief, Modeling and Analysis Branch, for suggesting this interesting topic and encouraging further challenging pursuits, Dr. Eberhardt Privitzer, Mr. Ric Rasmussen and Mr. Mark Hoffman for their assistance, Mrs. Elizabeth Alder and Ms. Brenda Martin for their typing and Lt. Thomas Gardner for his patient assistance and the many miles run together.

This research was sponsored by the Air Force Office of Scientific Research under Contract F49620-82-C-0035.

I. INTRODUCTION:

The use of biodynamic computer-based models for the prediction of human body response to mechanical stress has become an extremely useful and cost-effective research and developmental tool, especially as an alternative to direct experimentation with humans and animals. These models attempt to simulate or predict the forces and motions experienced by a body in high-acceleration events such as impacts or from sudden forces such as wind shear. In particular, the Air Force is interested in the reactions of aircrew personnel to such forces typically encountered in various phases of flight operations, including emergency ejections from high-speed aircraft. Such a hazardous environment is well suited to computer modeling, and with proper execution considerable insight of body motion and stresses developed in the body can be gained.

The Modeling and Analysis Branch of the Air Force Aerospace Medical Research Laboratory (AFAMRL) has been using a human body modeling program known as the Articulated Total Body (ATB) Model for several years. The model is based on rigid-body dynamics using Euler equations of motion with Lagrange-type constraints. The specific configuration uses 15 body segments (head, neck, upper torso, center torso, upper arms, lower arms, upper legs, lower legs, and feet) and 14 joints between the segments. Although it was originally developed by the Calspan Corporation for the study of human-body and anthropometric-dummy dynamics during automobile crashes for the United States Department of Transportation (Fleck et. al., 1974; Fleck, 1975), the ATB Model was sufficiently general to allow simulation of whole-body articulated motion resulting from various impacts or abrupt accelerations applied to the body. Furthermore, modifications involving special joint forces, aerodynamic forces and a complex harness system were added to accommodate specific Air Force applications (Fleck and Butler, 1975).

The ATB Model, although realistically reflecting human body structure, mass distribution and tissue material properties, presently has the serious limitation of only simulating events with passive internal responses. The gross, whole-body motion is no different for human aircrew personnel data than for anthropometric dummy or cadaver data. What is needed is the implementation of an active neuromusculature to simulate both voluntary and

reflex responses of the human subject to externally imposed forces.

II. OBJECTIVES:

The objective of this Summer Faculty Research Project has been to define and formulate methodologies for implementing active muscle effects such as body pretensing and time varying forces into the present ATB Model. Several considerations were involved: (1) the present model was not to be altered, (2) basic muscle phenomena such as the length-tension and force-velocity relationships and passive viscoelastic properties were to be included, and (3) particular emphasis was to be placed on muscles acting in the torso and neck region which affect flexion, extension and lateral motion of the trunk.

The objective was approached as follows: (1) A detailed literature search on muscle functions and current techniques used was performed. (2) Based on the results from the literature and theoretical principles, muscle models were formulated. (3) The new muscle models were implemented into the existing ATB model structure. (4) Simulation of available experimental results were performed.

This final report follows the approach used in fulfilling the objectives and therefore will be organized in a similar fashion.

III. BACKGROUND:

Skeletal Muscle - Skeletal muscles usually originate on the skeleton, span one or more joints and insert into a part of the skeleton again. Each muscle is enclosed in a connective tissue sheath called the epimysium and is held in its correct position in the body by layers of fascia. The muscle is attached to the bones via tendons, while the interior is compartmentalized into longitudinal sections called the fasciculi, each containing many individual muscle fibers. The fibers are enveloped by a connective tissue called the endomysium, which transmits the force of the muscle contraction from individual fibers to the tendons (Fung, 1981).

The muscle fibers do not always run parallel to the force transmitting tendons, as they do in fusiform muscles. They can be arranged in unipennate, bipennate or multipennate form, thus altering the force transmitting charac-

teristics (Fig. 1).

The muscle fiber, although the basic structural unit, with a diameter of 10-60 μ and length from several millimeters to several centimeters, can be subdivided further into myofibrils of 1μ diameter. These myofibrils comprise the hexagonal array of protein filaments that are directly responsible for the contractile process and give rise, with appropriate stains to the peculiar striations that are characteristic of skeletal muscle (Fig. 2). A repeating unit known as the sarcomere is defined by the vertical z-disk. Two types of protein filaments are distinguishable in each sarcomere, thin ones about 5μ in diameter and thicker ones about 12μ across. The thin filaments contain actin, globular molecules in a triple helix, while the thick filaments contain myosin, long molecules with globular heads. The thin filaments are each attached at one end to a z-disk and are free at the other to interlace with the thick filaments. The A-band is the region of overlap between thick and thin filaments, the I-band contains solely the thin filaments, while the H-band is the middle region of the A-band into which the actin filaments have not penetrated (Fung, 1981).

The actual contractile process takes place at the junctions between the myosin and actin in a process known as the sliding filament theory first presented by H.E. Huxley (1953). The myosin molecules consist of a long tail piece and a "head". The tails lie parallel in a bundle to form the core of the thick filament while the heads project laterally from the filament in pairs, rotated with respect to its neighbors to form a spiral pattern along the filament. These heads seem to be able to nod; they lie close to their parent filament in relaxation, but stick out to actin filaments when excited. Thus, during muscle contraction the muscle fiber shortens as the filaments slide over each other, forming, breaking and reforming chemical bonds between the myosin heads and the globular actin molecules.

IV. STRUCTURAL MODEL OF SKELETAL MUSCLE

If a muscle is not stimulated neurally, its tension, due to the contractile process, is extremely small. Practically all the tension observed when stretching the resting muscle will be due to elastic

structures which lie in parallel to the force-producing sarcomeres: the sarcolemna (sheath) of the individual fiber and all outer connective tissue sheaths (fascia, endomysia, perimysia). Thus, a set of parallel elastic elements (PEs) some of which are to be considered in parallel with each sarcomere of each fiber and others only in parallel with the whole muscle. Because these tissues move in fluid, appropriate damping elements (DE) also need to be included when stimulation takes place. The contractile proteins produce tension which, via elastic components such as tendons, is transferred to the end points of the muscle. These components are termed series elastic elements (SEs) Hatze, 1981).

Thus the following model based on Hatze (1981) can be constructed (Fig. 3). At both ends of each fiber are lightly damped SEs representing the tendinous parts of the fiber, and for each sarcomere two lightly damped SEs representing the elastic structures within the cross bridges (BE_i) and the z-disk (SE_i). The parallel elastic elements for each sarcomere (PS_i) do not individually contain the damping components, since the sarcolemna attached to the z-discs does not allow appreciable movement. The damping element is contained in the fiber external structure and is thus placed parallel to the entire fiber. The DE_i represent the purely contractile elements of the protein. Any mass of the sarcomeres is disregarded, especially when compared to the much larger external mass that the muscle contraction must move (Hatze, 1981).

Obviously such a distributed model for a complete muscle would be much too complicated to use in a multilink system of the human body such as the ATB model. Thus, a transition from the distributed system to a simpler lumped system must be made. One justifiable assumption is that all the sarcomeres in a fiber are more or less identical and activated at approximately the same time. It follows then that all the SE_is for one fiber can be replaced by an equivalent single element SE of length λs_i, the same procedure can be applied to the elements CE_i, BE_i and PS_i, resulting in equivalent lumped elements.

A similar process is applied in lumping fibers into motor units. The nervous system does not control single muscle fibers, but sets of fibers in the form of a functional unit, the motor unit. Each motor unit consists of the motor neuron producing the neural input signal to the unit, and all

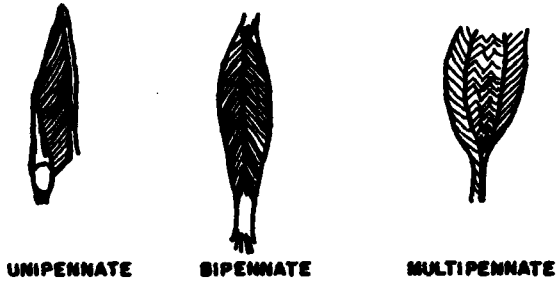


Fig. 1 Schematic representation of skeletal muscle fibre arrangement.

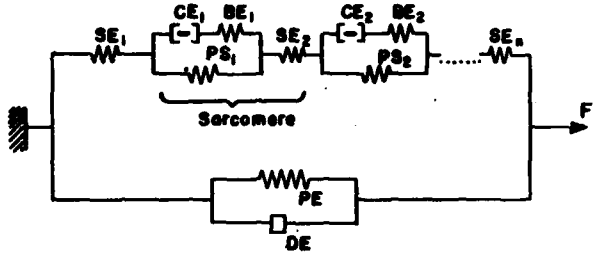


Fig. 3 Distributed model of skeletal muscle.

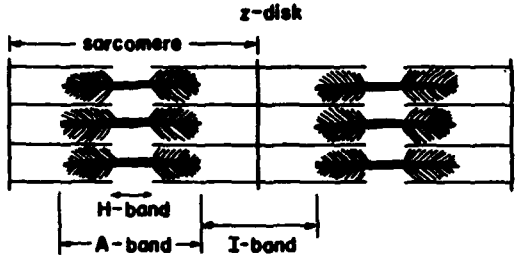


Fig. 2 Molecular substructure of mammalian skeletal muscle.

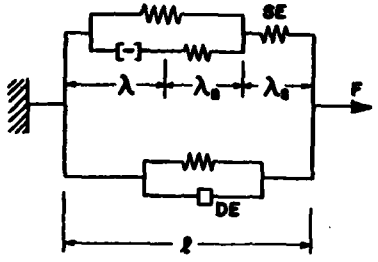


Fig. 4 Lumped model of skeletal muscle.

of the fibers that are innervated by branches of the motor neuron. In general, the motor unit fibers are distributed randomly over a certain volume of the muscle and all have similar morphological contractile and histochemical profiles (Close, 1972). Also, assuming BE to be very stiff, as suggested by Hatze (1981, p. 66), results in the final lumped model (Fig. 4).

For the parallel elastic element, extensive tests on the tensile properties of resting skeletal muscle carried out by Yamada (1970) indicate an exponential force-straint function:

$$f_{PE} = \alpha e^{\beta(\varepsilon-1)} - 1 \tag{1}$$

where f_{PE} is the force developed by the PE normalized with respect to maximum isometric tension in the muscle, α and β are constants and is the strain:

$$E = \frac{l - l_o}{l_o} \tag{2}$$

where l is the instananeous muscle length and l_o is the resting length. Fitting Eq. 1 to the data of human sartorius muscle from Yamada (1970, p. 95) yields values of $\alpha = .0016296$ and $\beta = 7.6616$. This typical force-strain curve is shown in Fig. 5. The SE and PS elements exhibit force-strain functions similar to the PE (Hatze, 1981) and will be discussed in more detail later.

The velocity dependence of the damping element (DE) can be expressed as for a simple mechanical dashpot:

$$f_{DE} = B\dot{\varepsilon} \tag{3}$$

where f_{DE} is the normalized force and B is the viscous damping coefficient. For the plantaris muscle of the cat, Bawa et.al. (1976) have determined B = 6.4 g sec/mm which if normalized to the plantaris resting length (l_o = 50 mm) and maximum isometric tension (F_{MAX} = 1000 gr) yields B = .32 sec. (Fig. 6).

The contractile element is the only active component in the model. Its behavior is extremely complex and depends nonlinearly on its length, contractive history, velocity of movement, the degree of stimulation and its temperature. However, for practical purposes and as discussed later, only the basic functions will be considered: the length-tension relationship and the force-velocity relationship.

The length-tension relationship is determined by the number of active cross links or filamentary overlap and can be adequately expressed from the data of Gordon et.al. (1966) by the function suggested by Hatze (1981, p. 42):

$$f_L(\xi) = .32 + .71e^{-1.112\ (\xi-1)} \sin\ (3.722\ (\xi-.656)) \qquad (4)$$

here $f_L(\xi)$ is the normalized force due to length-tension relationships and $\xi = \lambda/\bar{\lambda}$ with $.58 \leq \xi \leq 1.8$, where λ is the instantaneous length of CE and $\bar{\lambda}$ is the resting length of CE. This function is shown in Fig. 7.

The force-velocity relationship is determined by the rate of breaking and reforming the cross bridges with higher rates producing less effective bonds. To account for the whole range of negative velocities (shortening or concentric contractions) as well as positive velocities (lengthening or eccentric contractions) Hatze (1981, p. 44) has defined the following expression:

$$f_v(\dot{\eta}) = .1433\ \{.1074 + e^{-1.409 \sinh\ (3.2\dot{\eta} + 1.6)}\}^{-1} \qquad (5)$$

where $f_v(\dot{\eta})$ is the normalized force due to the force-velocity relationship and

$$\dot{\eta} = \dot{\varepsilon}/V_{MAX} \qquad (6)$$

where V_{MAX} is the maximum concentric velocity in muscle lengths/sec. and $\dot{\varepsilon}$ is the velocity again in muscle lengths/sec. This relationship is shown in Fig. 8.

Scrutinizing Figs. 5-8, several important conclusions can be drawn. The passive force-strain property (Fig. 5) shows an exponential increase with very small values (compared to the maximum isometric tension or maximum voluntary contraction (MVC)) for strains less than 50% and very large values for strains greater than 50%. However, strain values of 50% would not be reached during normal movements and thus the passive force-strain effect should be negligible in the normal neuromuscular response.

The passive viscous damping forces (Fig. 6) show a linear increase with strain rate ($\dot{\varepsilon}$). Force values equal to MVC are obtained for $\dot{\varepsilon}$ = 3.125/sec. Since the maximum velocity for slow fibers is 2.9 muscle lengths/sec (Hatze, 1981) fairly substantial viscous damaging forces can be obtained.

The active length tension relationship (Fig. 7) shows a fairly peaked

Fig. 5 PASSIVE MUSCLE FORCE - STRAIN FUNCTION

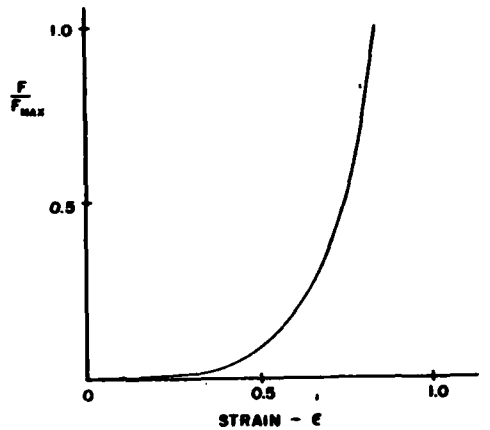


Fig. 6 PASSIVE MUSCLE VISCOUS DAMPING FORCES

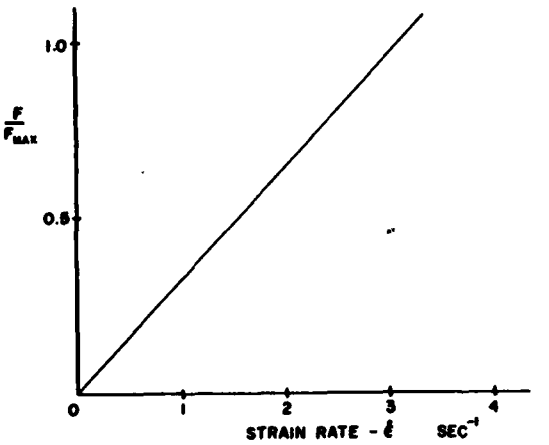


Fig. 7 MUSCLE LENGTH TENSION RELATIONSHIP

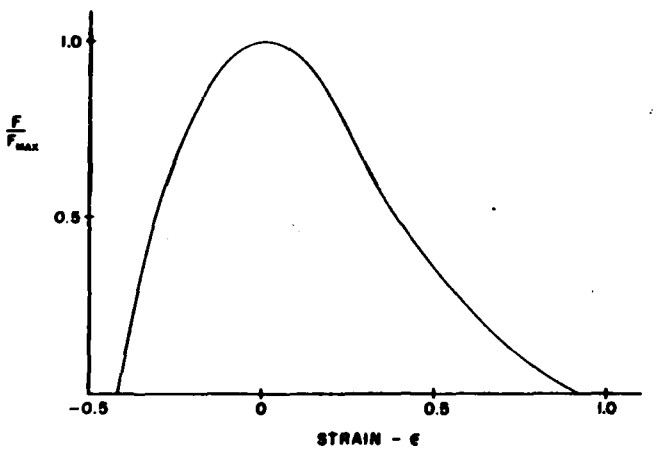
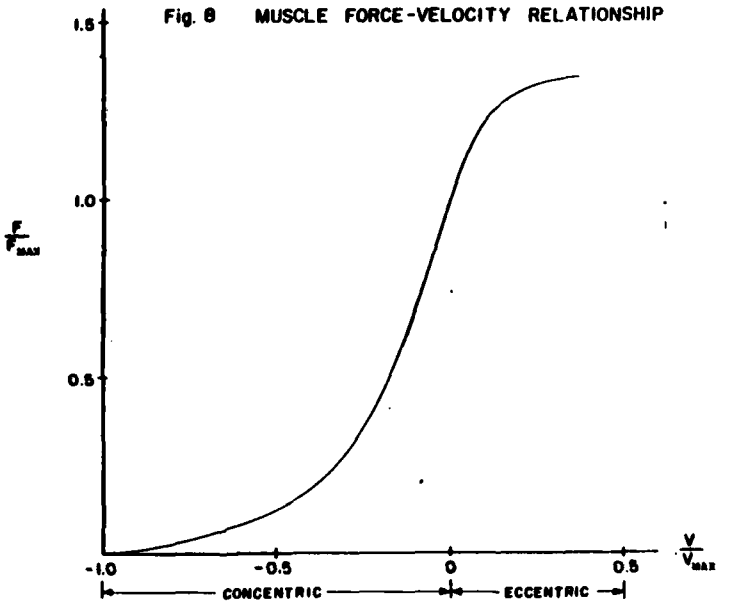


Fig. 8 MUSCLE FORCE-VELOCITY RELATIONSHIP



response with a 20% reduction in force for $\varepsilon = \pm$ 20%. Therefore, the length tension relationship shows a significant effect that should be accounted for.

The active force-velocity relationship (Fig. 8) shows a rapid increase up to an asymptotic value 34% greater than the MVC for eccentric contractions and a very rapid decrease in force (down to zero) for concentric contractions. Therefore, the force-velocity relationship should have a very significant effect in normal human movements.

Now, combining the model in Fig. 4 with the above-derived Equations 1-6 yield the following overall force equations

$$f_{SE} = f_{CE} + f_{PS} \tag{7}$$

$$f = f_{SE} + f_{PE} + f_{DE} \tag{8}$$

V. INCORPORATION OF THE MUSCLE MODEL INTO THE ATB MODEL:

With the consideration that existing features of the ATB model were to be used for the incorporation of muscle elements, two possibilities arose: (1) to use the spring-damper routine or (2) to use the advanced restraint system of harness and belts. The spring damper routine was quickly discounted because, as the name implies, only a direct spring force proportional to displacement were available. Other functions such as the length-tension or force-velocity relationships could not be accounted for. Furthermore, the spring-damper functions were limited to second power polynomials, which would be insufficient to fit the required forms of the muscle properties.

The harness routines provided a much better alternative. First of all, the functional form of the harness forces allowed the use of four terms:

$$NF(\varepsilon,\dot{\varepsilon}) = NF_1(\varepsilon) + NF_2(\varepsilon)NF_3(\dot{\varepsilon}) + NF_4(\dot{\varepsilon}) \tag{9}$$

where ε = strain, $\dot{\varepsilon}$ = strain rate and NF = functional form of force. Secondly, each of the terms could be expressed either as a fifth order polynomial or as a tabular function for more complex simulations.

On the other hand, there are still limitations within the harness routine that restrict the effectiveness of the muscle model. Obviously, from the functional form of Eq. 9 only three elements can be modeled

adequately. Furthermore, all three of these have to be in parallel, since forces add directly only in parallel. Series elements would require complex integro-differential equations in NF which can not be replicated with Eq. 9. Thus, the series elastic element (SE) needed to be eliminated.

The elimination of SE can be rationalized by considering SE to be a very stiff spring which is supported by Bawa et.al. (1976) who found K_{SE} = 380 g/mm as opposed to K_{PE} = 103 g/mm. Eliminating SE yields four elements in parallel, two of which are parallel elastic elements. This can be combined into one parallel elastic element, yielding the final simplified model in Fig. 9. The functional forms for each of these elements have been given previously in Eq. 1,3,4, and 5.

Simulation of Elbow Flexion - The simulation of elbow flexion (Fig. 10) consisted of three segments: the upper arm, the lower arm including the hand and a mass held at the center of gravity of the hand; and three joints: the shoulder which is fixed to an inertial reference frame, the elbow modeled as a hinge joint and an unconstrained joint acting as the attachment between the hand and the mass. One muscle was attached to act as the combination of elbow flexors, the biceps brachii and the brachialis. Anthropometric values for the segments and centers of gravity were taken from the data of Dempster (1955). The origin of the elbow flexor was put at the shoulder joint since the long head of the biceps even crosses the shoulder joint (McMinn and Hutchings, 1977). The insertion was set at 1.8 inches from the elbow corresponding to the biceps data of Wilkie (1950).

The maximum isometric tension of the elbow flexor was calculated from the data of Wilkie (1950). His subjects maintained a 20kg weight at the wrist with a lever ratio between muscle insertion distance and the moment arm of the weight of .15, yielding a maximum isometric tension of 133.3kg or 293 lbs. This result is confirmed using cross-sectional areas of 4.6 cm^2 and 7.0 cm^2, respectively, for the biceps and brachialis (An et.al., 1981) multiplied by the maximum muscle force of 10 kg/cm^2 (Hatze, 1981) to yield 255 lbs. This value is remarkably close to the more direct value, considering that other minor flexors which produce additional torque are not accounted for. As a result, a value of 300 lbs. was selected as the maximum isometric tension for the elbow flexors.

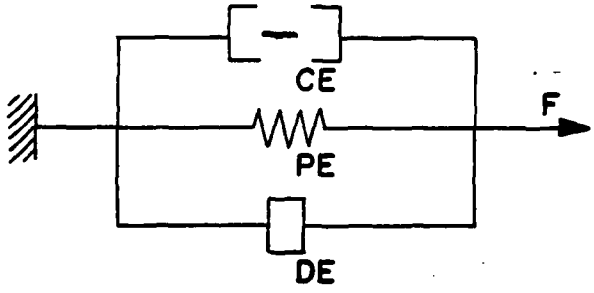
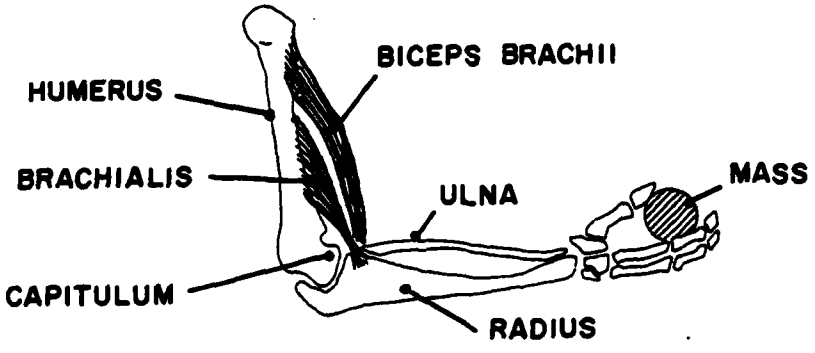


Fig. 9 Simplified muscle model.

Fig. 10 ANATOMY OF THE ELBOW FLEXORS



Special modifications needed to fit the four muscle functions to the ATB model included the following. At present, the ATB model doesn't allow negative strain which does occur during a concentric contraction, it was necessary to pretighten both the length-tension function and the muscle-spring function so that under extreme concentric contractions, the calculated strain would still be positive. Strain under pretensioning is calculated as follows:

$$\varepsilon' = \frac{1}{l_o + s} - 1 \tag{10}$$

where s = slack (negative if pretensioned). During a resting state when normal strain $\varepsilon = 0$ a pretensioning of $s = l_o/2$ yields $\varepsilon' = 1$. Then ε and ε' are related by:

$$\varepsilon' = 2\varepsilon + 1 \tag{11}$$

Thus for normal strain (ε) ranging from -.4 to .8, pretensioned strain (ε') would range from .2 to 2.6.

The velocity dependent functions are calculated based on strain rates. Thus a strain rate of 1/sec. would be equivalent to a muscle velocity of one muscle lenth per second. For slow twitch fibers, as typically found in the trunk musculature, the maximum velocity is approximately 2.9 muscle lengths/sec (Hatze, 1981). Thus Eq. 6 can be used to define $\dot{\eta}$ needed for the force-velocity function in Eq. 5.

The elbow flexor simulations utilized a fixed upper arm, a freely pivoting elbow joint (i.e. pin joint) a fixed wrist joint and a mass held in the hand. The upper arm is fixed vertically while the lower arm starts out horizontally (i.e. elbow angle = 90%). The mass in the hand is varied and the lower arm is allowed to move under the combined effects of gravity and the elbow flexor forces. For a large mass, the torque around the elbow created by the mass exceeds the maximum voluntary torque produced by the elbow flexors and the lower arm pivots down, lowering the mass. For a small mass, the maximum voluntary muscle torque exceeds the externally produced torque and the arm pivots up lifting the mass.

Muscle forces as a function of time for various masses and conditions are shown in Figs. 11-15. Figs. 11-14 show the effects of isolated muscle

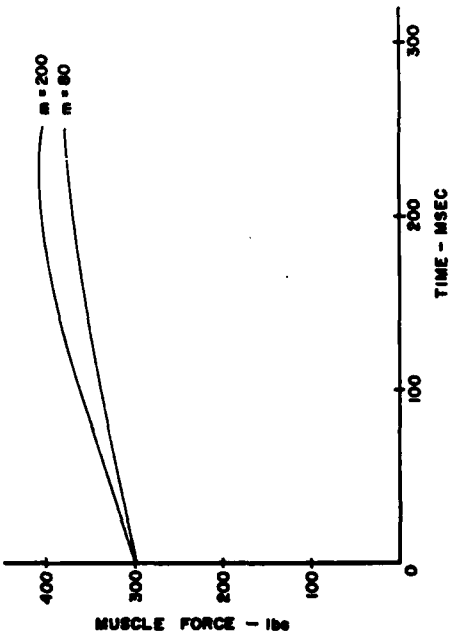


Fig. 12 FORCE vs. TIME FOR ISOLATED MUSCLE DAMPER

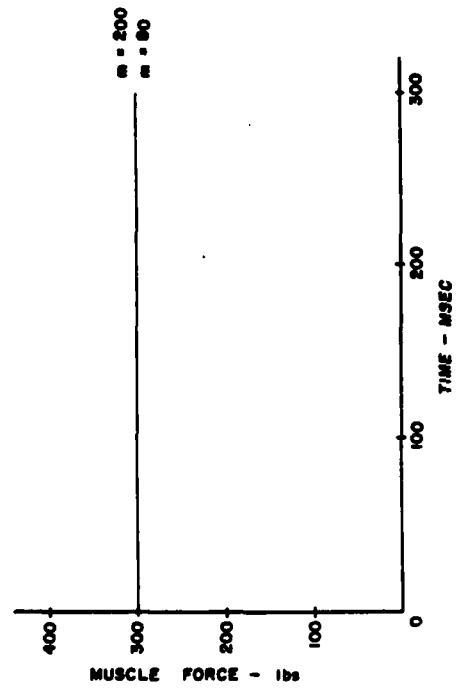


Fig. 11 FORCE vs. TIME FOR ISOLATED MUSCLE SPRING FUNCTION

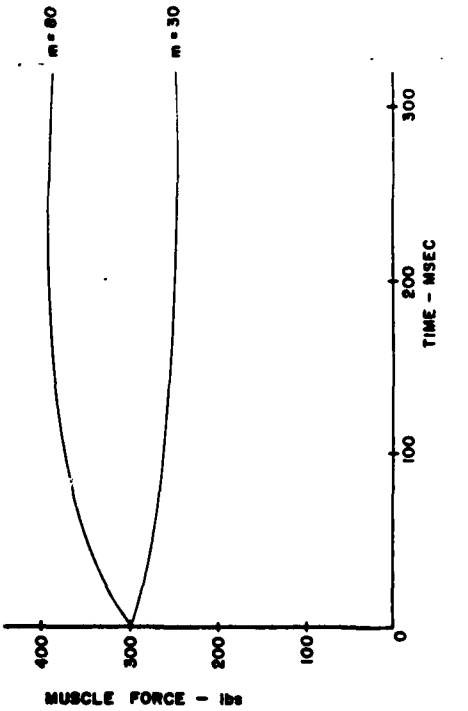


Fig. 14 FORCE vs. TIME FOR ISOLATED MUSCLE VELOCITY FUNCTION

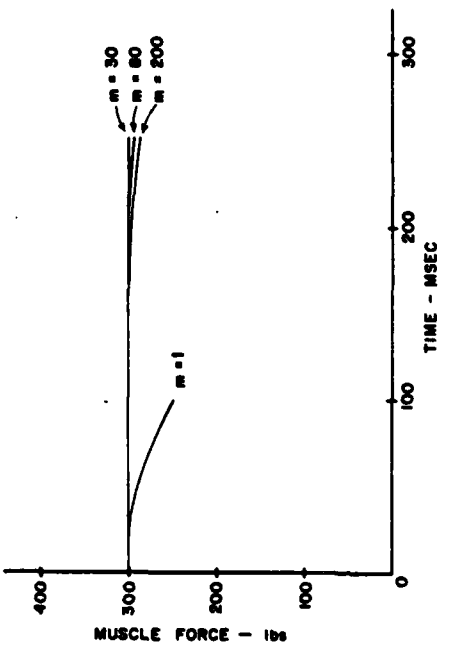


Fig. 13 FORCE vs. TIME FOR ISOLATED MUSCLE LENGTH FUNCTION

functions (the other functions are replaced by dummy variables) while Fig. 15 shows the effects rising the complete elbow flexor. More complete results including the angular displacement and strain at 256 msec, and the maximum linear muscle velocity and resulting $\dot{\eta}$ for the various conditions are summarized in Table 1.

The conclusions drawn in Section IV from theoretical muscle function relationships are definitely supported by these simulations. For example, Fig. 11 shows a constant muscle force over time for the isolated muscle-spring function for two different masses (m = 80 and m = 200). In both cases the lower arm pivots down (39° and 43° respectively) but the resulting muscle strain is too small to produce any significant increase in muscle force. In fact for a completely extended forearm, the resulting strain of 13.9% is insufficient to produce a significant muscle-spring force. On the other hand, the forces produced by the passive damper amount to a significant 30% increase above the maximum isometric tension (Fig. 12), which results in a substantial slowed descent and reduced angular displacement (Table 1).

The reduction in muscle force due to the length tension relationship amounts to approximately 16% of the maximum isometric tension at full flexion as shown for condition m=1 at time = 100 msec in Fig. 13. Full extension would result in a 10% decrease in force. Since these are the maximum decrements possible, the length-tension relationship seems less important than the passive damper effect. This, however, is slightly misleading in that the present case is not a completely realistic simulation of elbow flexion. Nearing full extension of the elbow, the biceps tendon tends to be distended by the capitulum of the humerus (Fig. 10) accentuating the length-tension relationship.

The active force-velocity relationship produces a 30% increase in force for a eccentric contraction (m=80) and a 16% reduction for a concentric contraction with mass = 30 lbs. However, a smaller mass would have resulted in a much faster contraction and consequently greater force reduction as shown more clearly in Fig. 15 for the force histories for the complete elbow flexor. A concentric contraction with mass = 1 lb. at maximum velocity results in an 84% reduction in muscle force. This predominant dependence of the muscle force on the velocity of contraction is shown even more distinctly in Fig. 16 in which the time plots of force strain and strain rate are

TABLE 1 - SUMMARY OF ELBOW FLEXION SIMULATIONS

	Mass (lbs)	Parameter	Spring	Damper	Length	Velocity	Complete Muscle
CONCENTRIC	1	Angular Disp. (°)			-90.0		-79.0
		Strain			-.162		-.159
		Muscle Velocity $\frac{in}{sec}$			-27.8		-8.65
		Strain Rate			-.805		-.250
	30	Angular Disp. (°)			-12.0	-6.0	-5.9
		Strain			-.031	-.016	-.015
		Muscle Velocity $\frac{in}{sec}$			-3.04	-1.05	-1.04
		Strain Rate			-.088	-.03	-.03
ECCENTRIC	40	Angular Disp. (°)					1.8
		Strain					.005
		Muscle Velocity $\frac{in}{sec}$					.330
		Strain Rate					.010
	80	Angular Disp. (°)	39.0	26.0	28.4	24.0	20.9
		Strain	.090	.063	.069	.059	.052
		Muscle Velocity $\frac{in}{sec}$	6.08	5.39	6.08	4.99	4.36
		Strain Rate	.176	.156	.176	.144	.126
	200	Angular Disp. (°)	43.0	41.0	43.0		39.0
		Strain	.097	.0935	.097		.090
		Muscle Velocity $\frac{in}{sec}$	7.65	7.39	7.65		7.12
		Strain Rate	.221	.213	.221		.206

Fig. 15 FORCE vs. TIME FOR COMPLETE ELBOW FLEXOR

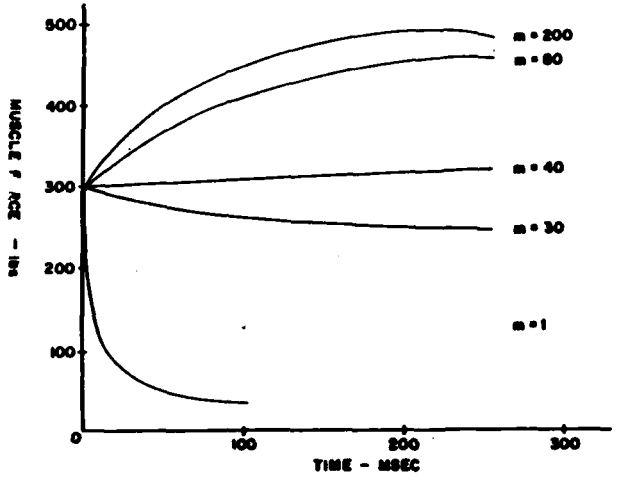


Fig. 16 FORCE, STRAIN AND STRAIN RATE vs. TIME FOR COMPLETE ELBOW FLEXOR

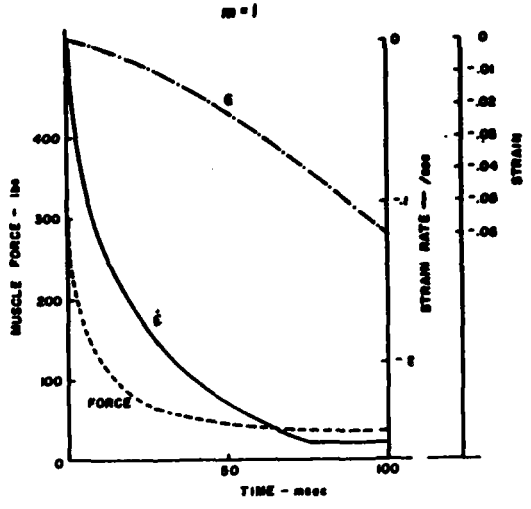


Fig. 17 ANATOMY OF THE TRUNK AND NECK MUSCULATURE (POSTERIOR VIEW)

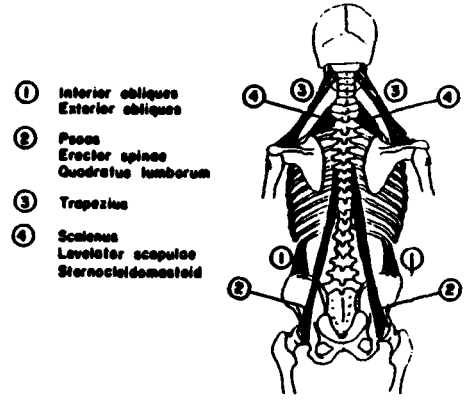
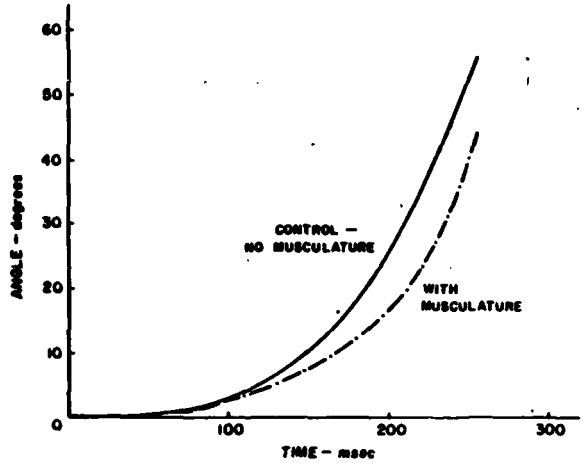


Fig. 19 ANGULAR DISPLACEMENT (ROLL) OF UPPER TRUNK DUE TO LATERAL G-FORCES



superimposed. Force and strain rate follow almost identical curves as compared to the strain function. Thus, for the present simulations, muscle force is determined primarily by the strain rate functions.

Simulation of Trunk Musculature - Simulation of the trunk musculature is a much more difficult undertaking than simulation of the elbow flexors. First of all, there are many more muscles involved, close to 20 for the lower back and trunk and equally many for the neck region. Secondly, some of the muscles, such as the erector spinae, have many attachment sites betwen the different vertebrae. Thirdly, the lines of action of the muscle forces are not always in straight line, e.g., the interior and exterior obliques. Fourthly, the vertebral joints are complicated by the ligaments and their additional force-bearing capabilities. Another restricting factor was the limit of five muscle harness systems for the recently added feature on the ATB model (Butler and Fleck, 1980). Therefore, for the present effort most of the above complications were avoided and a very simple model of the trunk musculature was constructed.

The model as shown in Fig. 17 consisted of four muscle-harness systems representing the major lateral bending muscles. One harness system was used to restrain the seated operator and since only lateral forces were of concern, all four muscle-harness systems were placed on the same side as the force being applied. The four major muscle groups used - two for the trunk, two for the neck - were as follows:

1) Interior and exterior obliques - which tend to curve around the trunk at the abdomen but act over a fairly short distance vertically.
2) Psoas, erector spinae, quadratus lumborum - which tend to be longer, originating in the pelvic area and inserting in the thoracic area.
3) Trapezius - originating laterally on the shoulders and inserting on the skull.
4) Scalenus, levator scapulae, sternocleidomastoid - which originate closer to the midline than trapezius and insert at various levels of the cervical spine.

A procedure similar to the elbow flexor simulation was followed using cross-sectional areas from Takashima et.al. (1979) to determine maximum isometric tension for the neck muscle groups, maximum lateral bending forces

(225 lbs) from McNeil et.al. (1980) proportioned between the two trunk muscle groups according to Rab (1979) (which is more accurate than using the first technique) and finding insertions and origins in Takashima et.al. (1979), Williams and Belytschko (1981) and Rab et.al. (1977). This information is summarized in Table 2.

The study of trunk musculature simulated the conditions experience by a 95% male air crew personnel in a series of tests run in the Dynamic Environment Simulator at Wright-Patterson AFB, OH. The full ATB Model with 15 body segments and 14 joints was used along with the addition of the four muscle groups described previously. The body segments were arranged in the semi-reclining posture maintained by air crew personnel in the cockpit (Fig. 18). The lower trunk was restrained by a lap belt; any other restraints, such as shoulder pads or hands placed on controls, were eliminated. A 2 Gy lateral force was applied to the body and the acceleration; velocity and displacement of various body segments was recorded.

A graphical display of the whole body response to the lateral force over time is shown in Fig. 18b. For comparison purposes, the response to identical conditions except for the lack of musculature is given in Fig. 18a. Although the musculature does not completely prevent the lateral deflection of the body the response is significantly delayed with the head and neck maintaining the upright position for a longer period of time. This result is better observed in Fig. 19 which plots the angular displacement of the upper trunk for both conditions. At the end of 256 msec the angular displacement is reduced by 12° with the use of musculature. Based on the time history, the response with the musculature lags up to 30 msec behind the control response.

VI. RECOMMENDATIONS:

These two series of simulations validate the use of a simple muscle function to model an active neuromuscular response to dynamic mechanical stresses. However, for a more accurate simulation three modifications are recommended:

1) To satisfactorily describe the anatomical placement of muscles, more than 5 harness (muscle) systems need to be permitted by the current version of the ATB. A minimum number required for the torso and neck would be 20, with an additional 20 needed for the limbs.

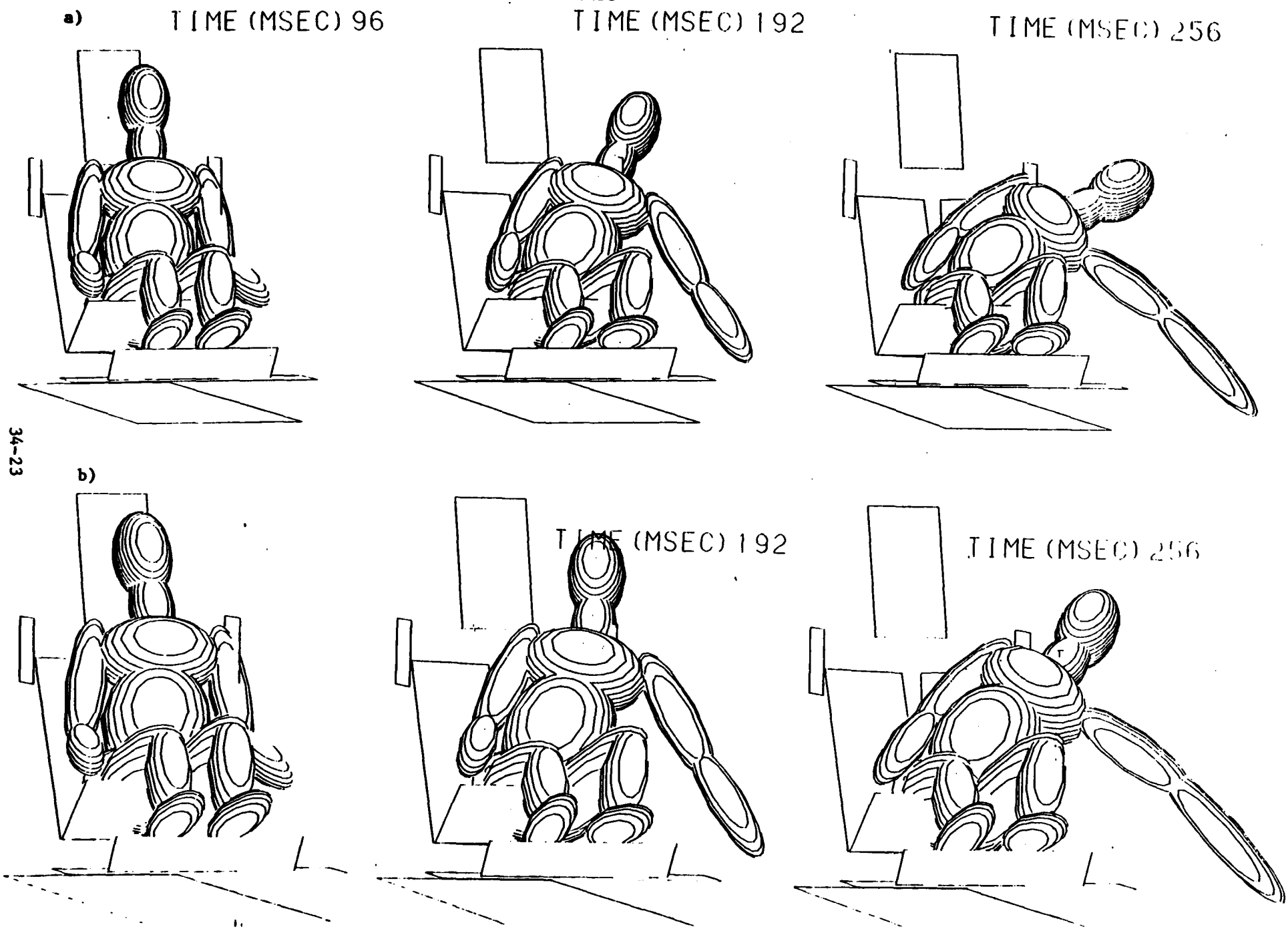
TABLE 2

SUMMARY OF MUSCLES BENDING TRUNK LATERALLY

Muscle	Origin (in.)	Insertion (in.)	Resting Length (in.)	Slack (in.)
1) Interior Obliques Exterior Obliques	Top of pelvis 4.7 in. laterally from midline	Bottom of 12th rib, 5.12 in. laterally from midline	4.35	-1.244
2) Psoas Erector Spinae Quadratus Lumborum Others	3.14 in. from midline laterally at hip level	1 in. laterally from center of upper trunk	17.24	-4.926
3) Trapezius	3.64 in. from midline laterally on clavicle	.4 in. laterally on occipital bone	7.85	-2.24
4) Scalenus Levator Scapulae Sternocleidomastoid	1.82 in. from midline laterally on clavicle	.4 in. laterally from center of neck segment	4.05	-1.16

	Cross-sectional Area cm^2	%	Max Bending Force (lbs)	Max Force Per lbs/cm^2 Area	Max Isometric Tension (lbs)
1) Interior Obliques		26	225		128.3
Exterior Obliques		31 } 57			
2) Psoas		14			
Erector Spinae		12			96.8
Quadratus Lumborum		9 } 43			
Others		8			
3) Trapezius	10			22	220
4) Scalenus	4			22	231
Levator Scapulae	3.5 } 10.5				
Sternocleidomastoid	3.0				

Fig. 18 - Graphical Display of Whole Body Response to Lateral G-Forces
a) Control b) Neuromusculature



2) To more accurately describe the muscle performance, features such as the active state function, force build-up time, delineation of slow and fast twitch fibers, orderly recruitment patterns, fatigue effects and reflexes could be eventually included into the muscle model.

3) To account for the irregularities of the human body, a more detailed modeling of joint biomechanics, range of motion of limbs, multiple muscle insertions and the effects of ligaments should be included into the ATB Model.

A very important application for a completely muscularized ATB Model, besides the Air Force pilot simulations, is the simulation of manual material handling tasks in industrial jobs. The prediction of work strengths during dynamic job activities is a very desirable employee placement technique and has been strongly recommended by the National Institute of Occupational Safety and Health (Chaffin, et.al., 1977). Present results indicate the muscularized ATB Model to be a very feasible approach with good future potential.

REFERENCES

An, K. N., F. C. Hui, B. F. Morrey, R. L. Linscheid, and E. Y. Chao, "Muscles Across the Elbow Joint: A Biomechanical Analysis," J. Biom., 14:659-669, 1981.

Bawa, P., A. Mannard, and R. B. Stein, "Predictions and Experimental Tests of a Viscoelastic Muscle Model Using Elastic and Inertial Loads," Biol. Cybernetics, 22:139-145, 1976.

Butler, F. E. and J. T. Fleck, Advanced Restraint System Modeling, AFAMRL-TR-80-14, Wright-Patterson AFB, OH, 1980.

Chaffin, D. B., G. D. Herrin, W. M. Keyserling and J. A. Foulke, Preemployment Strength Testing, U.S. Dept. of HEW, NIOSH, Pub. #77-163, 1977.

Close, R. I. Dynamic Properties of Mammalian Skeletal Muscles. Physiol. Rev., 52:129-196, 1972.

Dempster, W. T. Space Requirements of the Seated Operator, WADC Technical Report 55-159, Wright-Patterson AFB, OH, 1955.

Fleck, J. T., F. E. Butler, and S. L. Vogel, "An Improved Three Dimensional Computer Simulation of Motor Vehicle Crash Victims," Final Technical Report No. ZQ-5180-L-1, Calspan Corp., 1974, 4 Vols.

Fleck, J. T. "Calspan Three-Dimensional Crash Victim Simulation Program", Aircraft Crashworthiness, University Press of Virginia, 1975.

Fleck, J. T. and F. E. Butler, Development of an Improved Computer Model of the Human Body and Extremity Dynamics, AFAMRL-TR-75-14, Wright-Patterson AFB, OH, 1975.

Fleck, J. T. and F. E. Butler, "Validation of the Crash Victim Simulator, Vol. 3, User's Manual, Final Report, ZS-5881,V-3, Calspan Corp., 1982.

Fung, Y. C., Biomechanics, Mechanical Properties of Living Tissues, Springer-Verlag, NY, 1981.

Gordon, A. M., A. F. Huxley and F. J. Julian, "The Variation in Isometric Tension with Sarcomere Length in Vertebrate Muscle Fibers," J. Physiol., 225:237-253, 1972.

Hatze, H. Myocybernetic Control Models of Skeletal Muscle, University of South Africa, Pretoria, 1981.

Huxley, H. E., "Electron Microscope Studies of the Organization of the Filaments in Striated Muscle," Biochem. Biophys. Acta, 12:387, 1953.

McMinn, R. M. H. and Hutchings, R. T., Color Atlas of Human Anatomy, Yearbook Medical Publisher, Chicago, 1977.

McNeill, T. D. Warwick, G. Anderson and A. Schultz, "Trunk Strengths in Attempted Flexion, Extension and Lateral Bending in Healthy Subjects and Patients with Low-Back Disorders, Spine, 5:529-538, 1980.

Rab, G. T., "Muscle Forces in the Posterior Thoracic Spine," Clin. Orthoped., 139:28-32, 1979.

Rab, G. T., E. Y. S. Chao and R. N. Stauffer, "Muscle Force Analysis of the Lumbar Spine," Orthoped. Clinics of North Amer., 8:193-199, 1977.

Takashima, S. T., S. P. Singh, K. A. Harderspeck and A. B. Schultz, "A Model for Semi-Quantitative Studies of Muscle Actions," J. Biom., 12:929-939, 1979.

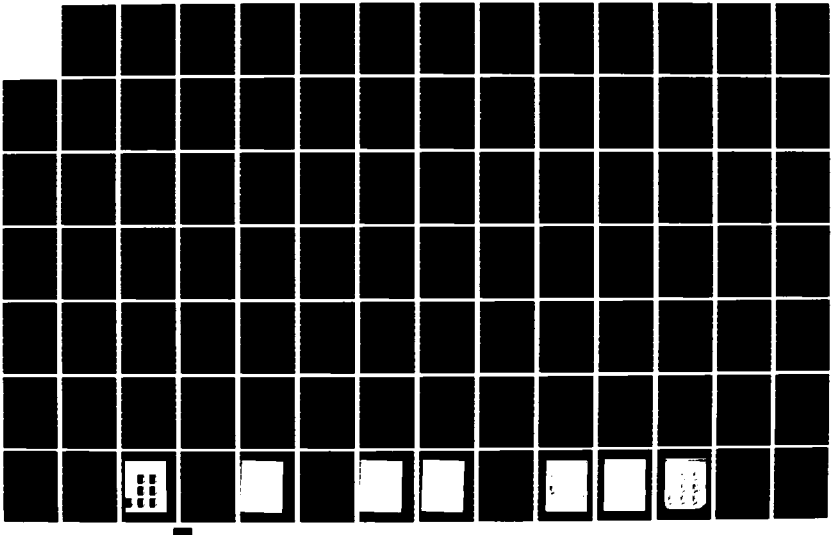
Wilkie, D. R., "The Relation Between Force and Velocity in Human Muscle," J. Physiol., 110:249-280, 1950.

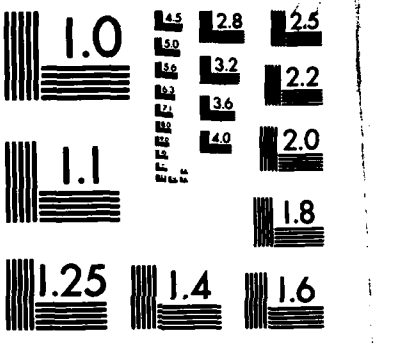
Williams, J. and T. Belytschko, A Dynamic Model of the Cervical Spine and Head, AFAMRL-TR-81-5, Wright-Patterson AFB, OH, 1981.

Yamada, H., Strength of Biological Materials, Baltimore: Williams & Wilkins, 1970.

AD-A130 769 USAF/SCEEE SUMMER FACULTY RESEARCH PROGRAM RESEARCH REPORTS VOLUME 1.. (U) SOUTHEASTERN CENTER FOR ELECTRICAL ENGINEERING EDUCATION INC S.. 9/11

UNCLASSIFIED W D PEELE ET AL. OCT 82 AFOSR-TR-83-0613 F/G 5/1 NL





MICROCOPY RESOLUTION TEST CHART
NATIONAL BUREAU OF STANDARDS-1963-A

1982 USAF-SCEEE GRADUATE STUDENT SUMMER SUPPORT PROGRAM

Sponsored by the

AIR FORCE OFFICE OF SCIENTIFIC RESEARCH

Conducted by the

SOUTHEASTERN CENTER FOR ELECTRICAL ENGINEERING EDUCATION

FINAL REPORT

THE MANUFACTURING CONTROL LANGUAGE FOR ROBOTIC WORK CELLS

Prepared by:	Brian O. Wood
Academic Department:	Industrial Engineering
University:	Penn State
Research Location:	Air Force Wright Aeronautical Laboratories Materials Laboratory Wright-Patterson AFB, Ohio
USAF Research Contact:	Lt. Gordon Mayer
SFRP Supervising Faculty Member:	Dr. Mark A. Fugelso, Assistant Professor
Date:	August 10, 1982
Contract No:	F49620-82-C-0035

THE MANUFACTURING CONTROL LANGUAGE FOR ROBOTIC WORK CELLS

by

Mark A. Fugelso and Brian O. Wood

ABSTRACT

Under contract F33615-78-C-5189 within the United States Air Force ICAM program, the McDonnell Douglas Corporation has developed the Manufacturing Control Language (MCL) for use with robotic work cells. An extension of the numerical control language APT, MCL contains control words for real time decision making and vision processing. These facilities, along with several other features, make this language a versatile off-line programming tool. This paper gives a basic overview of MCL's capabilities. Suggestions for further research in this area are offered.

ACKNOWLEDGEMENTS

The authors would like to thank the Air Force Systems Command, the Air Force Office of Scientific Research, and the Southeastern Center for Electrical Engineering Education for providing us the opportunity to spend a worthwhile and interesting summer at the Air Force Wright Aeronautical Laboratories, Wright-Patterson AFB, Ohio. In particular, we would like to thank Lt. Gordon Mayer and everyone else at the Materials Laboratory for their hospitality.

Additionally, we would like to extend a special thank you to Glenn Houston and David Clare of the McDonnell Douglas Corporation in St. Louis for information they have provided during the course of our research period.

1982 USAF-SCEEE SUMMER FACULTY RESEARCH PROGRAM

Sponsored by the

AIR FORCE OFFICE OF SCIENTIFIC RESEARCH

Conducted by the

SOUTHEAST CENTER FOR ELECTRICAL ENGINEERING EDUCATION

FINAL REPORT

PARAFOVEAL VISUAL INFORMATION PROCESSING AS A SECONDARY TASK LOAD

Prepared by:	Eugene H. Galluscio
Academic Rank:	Professor and Head
Department and University:	Psychology Department Clemson University
Research Location:	USAF Human Resources Laboratory/ Operations Training Division
USAF Research Colleague:	Robert Woodruff
Date:	August 25, 1982
Contract No:	F49620-82-C-0035

PARAFOVEAL VISUAL INFORMATION PROCESSING AS A SECONDARY TASK LOAD

by

Eugene H. Galluscio

ABSTRACT

Thirteen Air Force pilots were presented with a parafoveal visuospatial task while "flying" the A-10 version of the Advanced Simulator for Pilot Training (ASPT). The subjects' primary task was to maintain optimum bank and pitch control while attempting, as a secondary task, a figure matching task in the visual periphery. The results showed a left-visual field (right-brain) advantage for the visuospatial task. The results are discussed in terms of lateralized differences in brain function and the potential application of parafoveal displays for future instrument arrays. Suggestions for further research in this area are offered.

I. INTRODUCTION:

In an increasingly technical Air Force, man is becoming the "weak link" in the man/machine interface problem. Many jobs require heavy visual task loads in increasingly restricted work space. This is particularly true in fighter aircraft where the primary cockpit space (space in front of the pilot) is critically small and the need for visually displayed information is great. Visual displays for flight control, navigation, aircraft support systems, weapons control, radar warning and communications all require their share of the visual work space so as to insure rapid and accurate detection and interpretation.

Presenting usable information in the periphery of the visual work space to be processed parafoveally (without requiring direct foveation) presents an attractive alternative for providing additional visual displays without taxing the primary visual work space. There are, however, two problems associated with parafoveal information processing. The peripheral retinae are specialized for motion detection and therefore, have an extremely high convergence ratio between receptor cells and ganglion (output) cells. The convergence ratio increases rapidly with deviation from the fovea resulting in a precepitous loss in visual acuity beyond a few degrees from the foveal center. Secondly, the number of cones decrease rapidly with divergence from the fovea resulting in the loss of color vision (see Haber, 1980 and Ogle, 1962 for a review of these visual

characteristics). Additionally, the visual neuroanatomy in man is such that the visual pathways for each eye hemidecussate at the optic chiasma. This results in complete lateralization of the visual fields for each eye. That is, the optic fibers for the temporal retina of the left eye and the nasal retina of the right eye (both of which receive light from the right visual field) project to the left hemisphere of the brain. The reverse condition is true for the complimentary half retinae which receive light from the left visual field and project to the right hemisphere (Risse, et al., 1978). Following projection to the primary visual cortex of one hemisphere the information from a visual field can be shared with homologous areas of the contralateral visual cortex via the neo-cortical commissures (Meyers, 1956; Meyers and Sperry, 1958; Risse, et al., 1978).

The lateralization of visual pathways is an important consideration in parafoveal information processing. Recent studies have demonstrated that the two sides of the brain do not share identical functions (see Bogen, 1969a; Bogen, 1969b; Dimond and Blizard 1977 for extensive reviews). Generally, it appears that the left brain is more analytical and superior for the interpretation and production of language while the right brain is more intuitive and is superior for the perception of space and form. There is some evidence, however, (Bagnara, et al., 1980) that these relationships are less clearly defined in females and in familial left-handers. The partially separated visual pathways have in

fact, been used as a means to help define differences in brain function. By presenting stimuli tachistoscopically in either the left or right visual field while the individual attends to a central fixation point, the information is received exclusively by one hemisphere and can be shared with the contralateral hemisphere only via transcallosal transmission. Using reaction times and error scores as dependent variables, it may be assumed that increased latencies and errors reflect the additional neuronal processing required when the visual information is received by the "incorrect" hemisphere first and must be transferred to the contralateral hemisphere for processing (Moscovitch, 1976). Using this technique it has been demonstrated, for example, that the left brain is able to process verbal material better than the right and that the right brain can process spatial material better than the left (Moscovitch, 1976; White, 1969).

II. OBJECTIVES:

The research which has been done to evaluate parafoveal information processing has taken place in rigorously controlled laboratory conditions where the lateralized input task was the only task load for the subjects. If parafoveal vision is to be useful in real world environments it must be demonstrated that the relationships which have been found in the laboratory persist under more applied conditions. It is reasonable to question

whether or not parafoveal stimuli can be usefully interpreted when attention must be divided between two or more tasks when one of the tasks requires processing stimuli in the visual periphery. Additionally, it is reasonable to question whether or not the lateralized differences in brain function observed under controlled laboratory conditions remain constant under additional task loading.

The objective of this study was to evaluate a spatial task that has demonstrated a clear left field advantage as a primary task (Cohen, 1973; Galluscio, 1980; Geffen, et al., 1972) under secondary task load conditions. The primary task selected was a visuospatial tracking task to provide maximum task loading on spatial information processing (Wickens, Mountford and Schreiner, 1981).

III. METHODOLOGY:

Equipment: The A-10 version of the Advanced Simulator for Pilot Training (ASPT) was used as the flight simulation platform. A detailed description of the ASPT computer image generation (CIG), visual display characteristics and operator console may be found in Gum, Albery and Basinger (1975). The CIG provided a dynamic display of the terrain features of the Davis-Monthan airfield area and the peripheral test stimuli. The stimuli were computer generated, simple geometric figures; squares, triangles and circles (the circles were composed of 16 outside edges) 2^{o} of arc in height and width with central edges displaced 2^{o}

of arc to the left or right of a dot in the center of the attitude indicator on the A-10 heads-up display (HUD). In addition to the attitude indicator the HUD provided digital displays for aircraft heading, G load and vertical ladder scales for airspeed and altitude.

Subjects: Thirteen male T-37 and T-38 pilots served as subjects for this study. They had a mean of 864 hrs. total flying time with a mean of 291 hrs. in the last six months. The mean age of the pilots was 25.6 yrs. with a range of 23 to 30 yrs. The subjects were given a modified handedness questionnaire (Swiercinsky, 1978) and determined to be strongly dextral with no significant familial sinistrality. None of the subjects had previous experience with the A-10 aircraft or the ASPT.

Approach: The subjects were brought to the simulator facility briefed on the purpose of the study, and were told that the primary task in the study was to control aircraft bank and pitch using the attitude indicator on the A-10 HUD. The secondary task was to respond to figures presented in their visual periphery by depressing the cannon trigger on the control stick. Emphasis was placed on sacrificing the secondary task for aircraft attitude control.

The figures were presented in pairs with each pair preceded by a .5 sec. 2030 hz. tone. The stimuli were presented tachistoscopically at 66 msec. duration with a 1 sec. delay between the figures of each pair and a 5 sec. delay separated each stimulus

pair. The subject held the control stick with both hands and responded by depressing the cannon trigger with the left or right index finger only when the second figure of each pair was the same as the first. The subjects were given 5 practice trials in each visual field followed by 60 test trials in each field for a total of 130 figure pairs. Half of the pairs in each field were matches. The order of presentation by visual field and hand response was counterbalanced.

IV. RESULTS:

The mean correct reaction times for each subject and the combined subject means are shown in Table 1. The error scores were too small to permit meaningful analyses. Analyses of the reaction times for left- and right-hand responses showed that there was a right-hand advantage in both the left-field condition ($\underline{t}_{12} = 3.854$, $\underline{p} < .005$) and for the right-field condition ($\underline{t}_{12} = 3.704$, $\underline{p} < .005$). A comparison of left- and right-field reaction times with left-hand responses indicated a left-field (right-brain) advantage ($\underline{t}_{12} = 2.367$, $\underline{p} < .025$). The field effect for right-handed responses also evidenced a right hemisphere superiority ($\underline{t}_{12} = 2.543$, $\underline{p} < .025$).

V. DISCUSSION:

The results of this study show that the reaction times for responses made with the right hand were faster than those made with

Table 1. Mean Correct Reaction Times (in msec.) as a Function of Visual Field and Response Hand

	Left Field		Right Field	
	Left Hand	Right Hand	Left Hand	Right Hand
SUBJECT				
1	561	502	626	528
2	795	743	815	700
3	470	410	601	514
4	496	471	533	487
5	444	476	473	485
6	551	530	645	575
7	481	486	556	527
8	519	462	456	457
9	502	491	507	504
10	759	672	744	651
11	820	706	874	765
12	516	478	567	555
13	460	431	430	515
$\bar{X}$	567.2	527.5	602.0	558.7

the left. A preferred hand advantage has not been reported in other brain laterality studies (Cohen, 1972; Galluscio, 1980; Geffen, et al., 1972; Moscovitch, 1976) and probably reflects the previous experience of the subjects for making flight control input with the right hand. The left-field (right-brain) advantage found with both left- and right-hand responses is consistant with earlier studies that have shown a right-hemisphere advantage for spatial matching tasks.

Moscovitch (1976) noted that the reaction time delays resulting from lateralized stimulus input varied depending on the complexity of the stimuli and the nature of the task. Delays for the recognition of simple stimuli were in the range of 2 to 20 msec. while delays for more complex stimuli which required same-different judgements ranged from 20 to 50 msec. Moscovitch hypothesized that the shorter delays reflected transcallosal transmission from the receiving, inferior hemisphere to the processing hemisphere while the longer delays reflected the additional encoding and analyses required by the dominant hemisphere following transmission across the cerebral commissures (Moscovitch, 1976, pp 61-62).

The delays resulting from right-field presentations in this study averaged 33 msec. (34.8 msec. for left-hand responses and 31.2 msec. for right-hand responses) suggesting that independent of which hand was used to make the responses, the actual processing of the visuospatial task was accomplished by the right cerebral

hemisphere. Of importance to the key issue of this study, the right-brain advantage for the visuospatial task, which has been frequently reported under highly controlled laboratory conditions persisted even as a secondary task in a more applied setting. These results suggest that visual information presented in the peripheral work space may be of potential utility in the design of instrument displays and may be an important consideration in the design of future display systems.

VI. RECOMMENDATIONS:

This study should be viewed as a preliminary investigation for a systematic program to evaluate parafoveal information processing. Specifically, research efforts should be considered along the following lines:

1. This study demonstrated that right-brain functions hold up as a secondary task. A logical follow-on study could evaluate the persistance of the lateralized verbal functions of the left brain under secondary task load conditions. This could be done at the Human Resources Laboratory as a close replication of the present study or at the Clemson University Laboratories using a bench type tachistoscope modified to present a tracking task through one channel.

2. A second area of study should evaluate parafoveal information processing as a means of improving performance in complex multitask environments while not sacrificing mission

requirements. If the central processing operations for verbal and spatial material draw upon separate neuronal resources (Moscovitch, 1977) it may be possible to increase visual information processing by simultaneous hemifield presentations of verbal and spatial information to the appropriate hemispheres of the brain while using contralateral manual responses to maintain "hemispheric-task integrity" (see Wickens et al., 1981, pp 211-212).

Acknowledgment

The author would like to express his appreciation to the Air Force Systems Command, the Air Force Office of Scientific Research, and the Southeastern Center for Electrical Engineering Education for providing him with the opportunity to work on parafoveal visual display research at the Human Resources Laboratory, Operations Training Division, Williams AFB, AZ. Additionally, he would like to thank the administrative and research staff of the laboratory for providing him with timely and effective support. Finally, the author would like to thank Robert Woodruff for his many hours of colleagial support and guidance, and he would like to acknowledge the extraordinary technical assistance of Alex Shaw and Tom Farnan.

REFERENCES

Bagnara, S., Roncato, S., Simion, F., & Umilta, C. Sex-related differences in hemispheric asymmetries in processing simple geometric figures. Perceptual and Motor Skills, 1980, 51, 223-229.

Bogen, J. E. The other side of the brain. I. Dysgraphia and dyscopia following cerebral commissurotomy. Bulletin of the Los Angeles Neurological Societies, 1969a, 34, 73-105.

Bogen, J. E. The other side of the brain: II. An oppositional mind. Bulletin of the Los Angeles Neurological Societies, 1969b, 34, 135-162.

Cohen, G. Hemispheric differences in a letter classification task. Perceptual and Motor Skills, 1972, 11, 137-142.

Cohen, G. Hemispheric differences in serial versus parallel processing. Journal of Experimental Psychology, 1973, 97, 349-356.

Dimond, S. J., and Blizard, D.A. (Eds.), Evolution and Lateralization of the Brain. New York: New York Academy of Sciences, 1977.

Galluscio, E. H., Deras, D. A. and Plavney, D. Processing of sequential and holistic stimuli in left and right visual fields. USAFA-TR-80-19, United States Air Force Academy, CO: Department of Behavioral Sciences and Leadership, October, 1980.

Geffen, G., Bradshaw, J. L., and Nettleton, N. C. Hemispheric asymmetry: Verbal and spatial encoding of visual stimuli. Journal of Experimental Psychology, 1972, 93, 25-31.

Gum, D. R., Albery, W. B., and Basinger, J. D. Advanced simulation in undergraduate pilot training; an overview. AFHRL-TR-75-59 (I), AD-AD30224. Wright-Patterson AFB, OH: Advanced Systems Division, Air Force Human Resources Laboratory, December 1975.

Haber, R. N., and Hershenson, M. The psychology of visual perception. (2nd Ed.). New York: Holt, Rinehart, and Winston, 1980.

Meyers, R. E. Function of the corpus callosum in interocular transfer. Brain, 1956, 79, 358-363.

Meyers, R. E. and Sperry, R. W. Interhemispheric communication through the corpus callosum. Archives of Neurology and Psychiatry. 1958, 80, 298-303.

Moscovitch, M. On the representation of language in the right hemisphere of right-handed people. Brain and Language, 1976, 3, 47-71.

Moscovitch, M. Information processing and the cerebral hemispheres. In M. S. Gazzanaga (Ed.), The Handbook of Behavioral Neurobiology, Vol 1. New York: Plenum Press, 1978.

Ogle, K. N. Spatial localization through binocular vision. In The Eye. New York: Academic Press, 1962.

Risse, G. L., Le Doux, J., Springer, S. P., Wilson, D. P., and Gazzaniga, M. S. The anterior commissure in man: Functional variation in a multisensory system. Neuropsychologia, 1978, 16, 23-31.

Swiercincky, D. Manual for the adult neuropsychological evaluation. Springfield IL: Thomas, 1978.

White, M. J. Laterality differences in perception: A review. Psychological Bulletin, 1969, 72, 387-405.

Wickens, C. D., Mountford, S. J., and Schreiner, W. Multiple resources, task-hemispheric integrity, and individual differences in time-sharing. Human Factors, 1981, 23, 211-229.

1982 USAF-SCEEE SUMMER FACULTY RESEARCH PROGRAM

Sponsored by the

AIR FORCE OFFICE OF SCIENTIFIC RESEARCH

Conducted by the

SOUTHEASTERN CENTER FOR ELECTRICAL ENGINEERING EDUCATION

FINAL REPORT

THREE-DIMENSIONAL VISUAL INFORMATION PROCESSING WITH BINOCULAR HELMET-MOUNTED DISPLAYS

Prepared by:	Eugene H. Galluscio
Academic Rank:	Professor and Head
Department and University:	Psychology Department Clemson University
Research Location:	Human Resources Laboratory/Operations Training Division
USAF Research Colleague:	Robert Woodruff
Date:	August 15, 1982
Contract No:	F49620-82-C-0035

THREE-DIMENSIONAL VISUAL INFORMATION PROCESSING WITH BINOCULAR HELMET-MOUNTED DISPLAYS

by

Eugene H. Galluscio

ABSTRACT

The efficacy of a binocular helmet-mounted display (HMD) to provide usable stereopsis in a dynamic, simulated aerial refueling environment was examined. Twelve pilots made distance judgments from a computer image-generated (CIG) model of a KC-135 tanker in the A-10 version of the Advanced Simulator for Pilot Training (ASPT). Half of the subjects viewed the tanker with a biocular display and half viewed the tanker with a binocular display that provided the perception of depth by stereopsis. Retinal image disparity in the binocular viewing condition was provided by presenting two independent CIG displays separated 76.9 mm in perspective. The results show that pilots in the binocular condition were able to judge distance more accurately. The results are discussed in terms of the additive effect of pictorial, kinetic, and stereoscopic depth cues. Suggestions for further research in this area are offered.

Acknowledgment

The author would like to express his appreciation to the Air Force Systems Command, the Air Force Office of Scientific Research, and the Southeastern Center for Electrical Engineering Education for providing him with the opportunity to work on helmet-mounted display research at the Human Resources Laboratory, Operations Training Division, Williams AFB, AZ. Additionally, he would like to thank the administrative and research staff of the laboratory for providing him with timely and effective support. Finally, the author would like to thank Robert Woodruff for his many hours of collegial support and guidance, and he would like to acknowledge the extraordinary technical assistance of Alex Shaw and Tien-Fu Sun.

I. INTRODUCTION:

A major Air Force need for existing and future operational and training systems is to present visual information in a manner that provides operators with accurate data about three-dimensional space. This is especially true in flight operations and flying training environments where the perception of depth is particularly critical. Existing aircraft visual systems such as head-up displays (HUDs), helmet-mounted displays (HMDs), and the visual displays of flight simulation training devices are totally dependent on the use of pictorial cues to present the perception of depth (Harker, 1980).

Pictorial cues are those attributes of depth in a visual scene that may be presented in a two-dimensional drawing or still photograph. An extensive review of these monocular depth cues may be found in Haber (1980) and in Ogle (1962). The ability to use these two-dimensional representations of depth is apparently not innate and requires experience with the environment.

A special class of pictorial depth cues is the kinetic cues of motion parallax and streaming. The kinetic depth cues reflect changes in the perspective of objects in the visual scene as the observer moves in relation to the scene. These cues obviously require dynamic computer image generation (CIG) or motion pictures. As is true with static pictorial depth cues, the kinetic cues seem to require experience with the environment, may be represented on a two-dimensional surface, and may effectively present the perception of depth when viewed with just one eye.

There are two categories of depth cues which are not used effectively in existing visual display systems. These are: the intrinsic and extrinsic oculomotor cues for accommodation of the lens and convergence of the eyes and the binocular depth cues. Most displays use either a projected or cathode ray tube (CRT) real image or a collimated, virtual image. In either case, the actual points of focus and vergence are always at the plane of the image (the CRT faceplate or infinity for collimated images) and may not be in concert with the pictorial depth cues presented on the display. In a mix of visual depth cues where the physiological cues are contraindicative to the pictorial cues, the pictorial cues appear to be dominant in the interpretation of depth (Ittelson, 1960). Additionally, these displays present identical images to each eye. Since the eyes are displaced laterally by approximately 65 mm, they do not share identical points of reference. In normal binocular viewing of three-dimensional space, objects located in front or behind the point of vergence are displaced laterally on the retinae in relation to objects on the horopter (Tyler, 1979). The resultant retinal image disparity provides an exceptionally sensitive form of depth information. Lateral displacements on the retina of each eye of just 5-10 arc sec are sufficient for the detection of depth (Tyler & Scott, 1979; Tyler, 1977; Ogle, 1952).

It has been known since Wheatstone's early experiments with stereoscopic images (1852) that the fusion of two slightly disparate figures presented independently to each eye can produce the illusion

of depth. It is now known that this phenomenon is under the control of hypercomplex cells in the visual cortex which require simultaneous input from homologous visual fields of each eye (see Tyler and Scott, 1979, for a review). These cells appear to be "tuned" to detect very small, horizontal retinal image disparities (5 to 10 arc sec) and are clearly functional in processing stereoscopic depth information (Mitchell, 1972). Therefore, when two complex images presented from binocular perspective are fused through the vergence mechanism, the resultant retinal image disparities simulate the disparities which normally result from viewing objects in three-dimensional space. This activates the hypercomplex cells in the visual cortex which are responsible for detecting and interpreting disparate images on the retinae and presumably produces the illusion of depth. Whether or not this illusion of depth can be effectively used to aid in making accurate depth judgments is still in question.

II. OBJECTIVES:

New technological developments have made it feasible to utilize retinal image disparity to present usable depth information in dynamic visual displays (Roark and French, 1982). These displays can provide integrated pictorial, kinetic, and binocular depth cues. The Human Resources Laboratory/Operations Training Division has developed an HMD system which is capable of presenting CIG video independently to each eye through two Honeywell 40^{o} field of view (FOV) displays.
The helmet is equipped with a magnetic sensor developed by Polhemus

Navigation Sciences which continuously detects head position. The output from the magnetic sensor is used to align the CIG so as to correspond with head position.

The purpose of this study was to evaluate the effectiveness of this HMD in providing usable binocular depth information. A simulated aerial refueling task was selected for the study. Harker (1980) determined that this type task would be likely to benefit from stereoscopic displays because binocular depth cues become effective at distances under 580 m and because the mid-line point of reference of the tanker aircraft would tend to emphasize stereopsis in a mix of pictorial, kinetic, and binocular depth cues. Thus, although the FOV is only 40^{o}, the wearer is able to look at almost any point by moving his head.

III. METHODOLOGY:

Equipment: The A-10 version of the Advanced Simulator for Pilot Training (ASPT) was used as the simulator platform. A detailed description of ASPT may be found in Gum, Albery, and Basinger (1975). The KC-135 imagery for ASPT was modified to permit either identical perspectives for each eye (biocular condition) or imagery presented from two points of reference separated by 76.9 mm (binocular condition). The two viewing conditions were presented through the Honeywell 40^{o} FOV HMD, and the Polhemus magnetic sensor was used to align the CIG with head position. For a detailed description of the tanker model, see Woodruff, Longridge, Irish, and Jeffreys (1979).

A dynamic program was prerecorded depicting closure on the tanker at a constant rate and at a fixed vertical separation that was level with the end of the extended boom. Points were established at 25, 50, 100, and 200 ft from the end of the boom, to be used as target distances for the study. (Metric displays were not available at the experimenter console.)

Subjects: Twelve pilots (five F-16 student pilots, four T-37, and three T-38 instructor pilots) served as subjects for this study. They had a mean of 795 hours total flying time and a mean of 150 hours in the last six months. Only two of the subjects had previous experience with aerial refueling - one in the back seat of F-4s, the second in the back seat of F-16s.

Approach: The subjects were assigned to either the binocular or biocular group but were not informed of their viewing condition. Some attempt was made to balance the two groups by type of aircraft and aerial refueling experience. Each subject was tested for his ability to fuse independent images using a stereoscope. The subject was first shown a stereoscopic view of a natural scene and then a random dot stereogram which, when fused, produced a central square surface in depth (Julesz, 1971). The subjects were then briefed on the alignment procedures for the HMD and were fitted to the helmet.

Subjects were shown static displays of the tanker model at 200, 100, 50, and 25 ft. The simulator was then placed at an initial point 440 ft from the tanker. For each trial, the CIG closed on the tanker and the subject reported verbally at one of the four test distances.

No control inputs to the simulator were required of the subject. After each trial, the subject was informed of the actual distance at which he responded and was shown the static display of the correct distance. Each subject received seven such trials with feedback, at each test distance. The order of trials was randomized within each group and counterbalanced between groups. After all 28 trials were completed, the subject completed a brief questionnaire dealing with the comfort of the helmet, the usability of the display, and his subjective assessment of the depth cues used at each test distance.

IV. RESULTS:

The mean absolute error scores of the biocular group for each of the test distances are plotted by trials in Figure 1. The equivalent data points for the binocular group are shown in Figure 2. These data show that for both viewing conditions, the absolute error scores drop off rapidly over the first three trials and the performance of both groups becomes relatively stable over the last three trials. The mean absolute error for the last three trials for each distance was computed. The overall means for each group are shown in Table 1.

Table 1. Comparison of Mean Absolute Error for the Last Three Trials for Each Distance from the Tanker

Distance in Feet	Biocular Group	Direction of Difference	Binocular Group
200	17.1	>	13.8
100	11.0	>	9.8
50	7.2	>	5.7
25	5.4	>	1.5

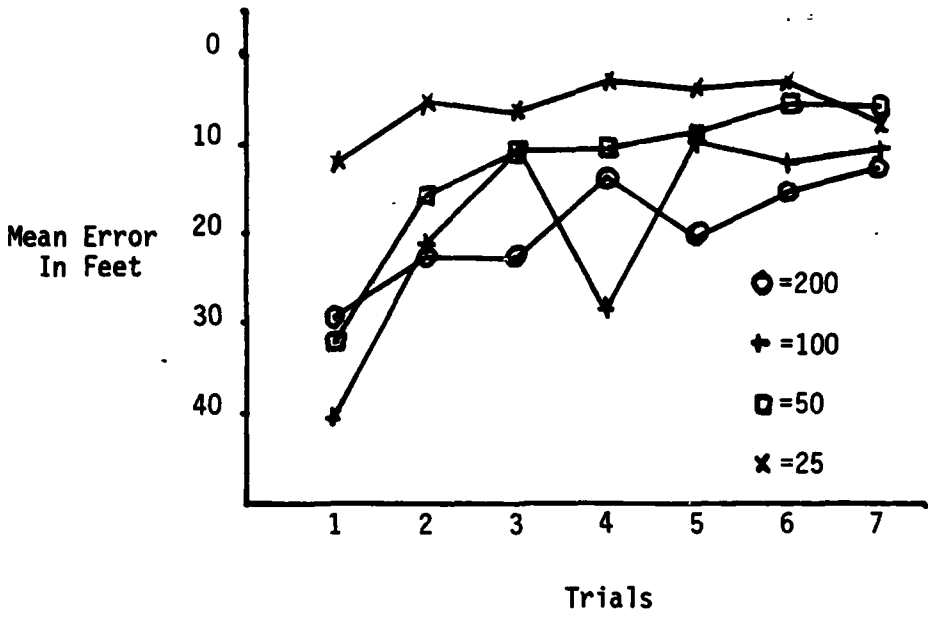


Figure 1. Biocular Group Mean Absolute Error for Each Trial.

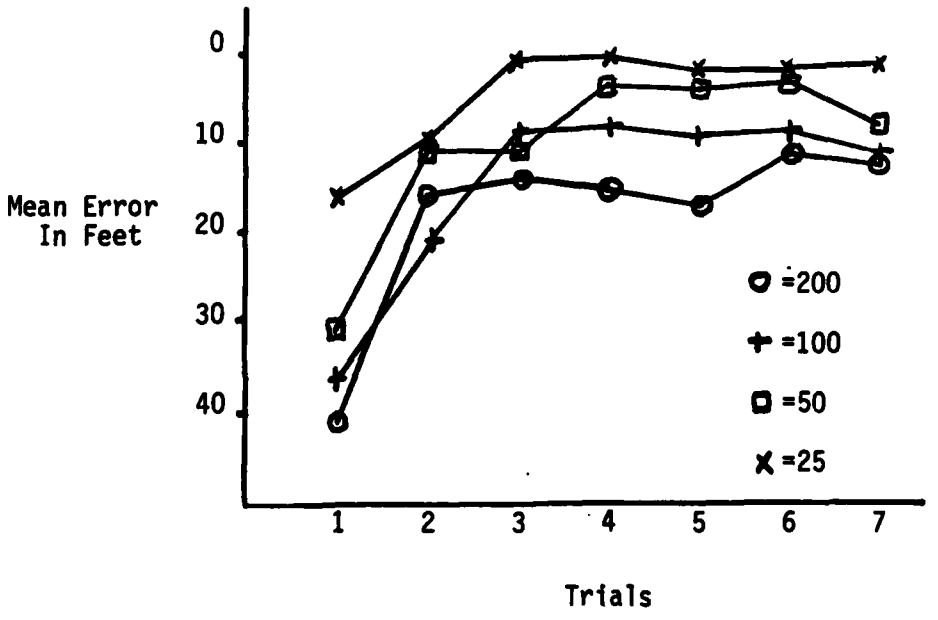


Figure 2. Binocular Group Mean Absolute Error for Each Trial.

A two-factor mixed design ANOVA with repeated measures across distances was performed on these data (Bruning and Kintz, 1968). Examination of Table 1 shows that the error scores for the binocular viewing condition were smaller than those of the biocular condition for each test distance. The between-subjects test for significance, however, failed to reach significance at the .05 level ($F_{1, 10}$ = 1.348; $\underline{p}$ = .2723). The within-subjects F test was significant ($F_{3, 30}$ = 5.258; $\underline{p}$ = .0052), indicating, as would be expected, that accuracy of distance judgments varied with distance from the tanker. The interaction between viewing condition and distance was not significant ($F_{3, 30}$ = .078; p = .971). Tuckey pair-wise comparisons were made at the .05 significance level. These show that the combined group mean absolute scores at the 25 ft distance were significantly smaller than the 100 and 200 ft distances. None of the other pair-wise comparisons were significant.

Since observation of the data showed that all binocular mean error scores were smaller than the biocular group scores, post-hoc Mann-Whitney U tests were performed between groups at each distance. The comparison at the 25 ft point was significant (U = 0; $\underline{p} < .001$). The U test is a conservative test as compared to the $\underline{t}$ test, especially with a small sample. Nonetheless, the α of this comparison should be dealt with cautiously, since the overall between-groups F test was not significant.

V. DISCUSSION:

The data clearly show that the subjects were able to learn to make accurate judgments about depth in a simulated aerial refueling task using both biocular and binocular viewing conditions. This can be attributed to the pictorial and kinetic depth cues provided by the dynamic tanker model. Harker (1980) found that pilots who had aerial refueling experience tended to use pictorial cues such as the size of the tanker, details on the tanker aircraft, relative position of the tanker, and kinetic cues related to the relative motion of the tanker to make distance judgments. The responses of the subjects in this study on the questionnaire clearly indicate that pictorial and kinetic cues were primary, independent of viewing condition. Additionally, the edge of the 40^{o} FOV display provided another reference for judging size and motion cues. This cue was reported as the best distance cue more often than any other by both groups. Only two subjects in the binocular group indicated that the stereopsis provided by the display was useful.

The smaller absolute errors attained by the binocular group suggests that the perception of depth provided by stereopsis adds to the pictorial and kinetic depth cues which were available in both viewing conditions. That the differences between the two viewing conditions were significant only at the 25 ft point is not surprising. The tanker model was presented against a homogeneous background; therefore, the only available disparate images were from points on the tanker itself. Harker (1980) has suggested that in a

mix of monocular and binocular depth cues, the binocular cues may not be useful much beyond 20 ft, as subjects tend to rely more on the monocular pictorial and kinetic cues at greater distances. Finally, although the subjects in the binocular group were informed of the stereoscopic nature of their display, they were not alerted to attend to the depth cues provided by stereopsis. It seems quite possible that with directed training in the use of binocular displays, performance could be improved.

VI. RECOMMENDATIONS:

This study demonstrated that stereoscopic displays can provide usable depth information in a simulated aerial refueling task. This should be viewed as the first step in the systematic investigation of the potential application of three-dimensional imaging for future operational and training display systems. The prototype HMD used in this study had some severe limitations. Physically, the HMD was heavy and cumbersome, and the housing restricted peripheral vision. The HMD had a virtual, collimated image; therefore, the effective horopter was a plane at infinite distance and thus did not necessarily correspond to the pictorial depth cues displayed. Even with these limitations, this HMD did provide useful depth information and in that respect may be a harbinger of more effective three-dimensional displays.

Continued research along the following lines appears to be warranted:

1. The 40^{o} FOV display should be used to evaluate the effect of stereopsis in aiding pilots to control airspeed and maintain

contact during aerial refueling. Woodruff, Longridge, Irish, and Jeffreys (1979) found that experienced pilots had great difficulty controlling airspeed during simulated aerial refueling in ASPT. Their findings may well be attributed to problems in judging depth. Accurate feedback concerning distance is critical for throttle control in this task.

2. The edge of the 40^{0} FOV HMD in this study served as a powerful pictorial depth cue. HRL has contracted for the development of a wide angle binocular HMD which should be used to evaluate stereoscopic imaging. The 135^{0} horizontal FOV of this display would provide a more accurate assessment of the effectiveness of binocular stereo displays.

3. Other techniques of providing stereopsis should be investigated, particularly lenticular screens and pulse synchronized lead lanthanum zirconate tetante (PLZT) wafer lenses (see Roark and French, 1982). The latter have the advantages of providing color and high luminance, and they can present both CIG and video displays. The PLZT system holds much promise, but there are some perceptual questions relevant to this system which require investigation; specifically, the effect of pulsed images on retinal image rivalry (Tyler and Scott, 1979; Hershberger and Guerin, 1975) and the effect of horizontal raster alignment on stereoacuity (Mitchell, 1970).

REFERENCES

Bruning, J. L., Kintz, B. L. Computational handbook of statistics. Glenview: Scott, Foresman, 1968.

Gum, D. R., Albery, W. B., & Basinger, J. D. Advanced simulation in undergraduate pilot training; an overview. AFHRL-TR-75-59(I), AD-A030 224. Wright-Patterson AFB, OH: Advanced Systems Division, Air Force Human Resources Laboratory, December 1975.

Haber, R. N., and Hershenson, M. The psychology of visual perception (2nd Ed.). New York: Holt, Rinehart, and Winston, 1980.

Harker, G. S., and Jones, P. D. Depth perception in visual simulation. AFHRL-TR-80-19, Williams AFB, AZ: Operations Training Division, Air Force Human Resources Laboratory, August 1980.

Hershberger, M. L., and Guerin, D. F. Binocular rivalry in helmet-mounted display applications. AMRL-TR-75-48, Wright-Patterson AFB, OH: Aerospace Medical Research Laboratory, June 1975.

Ittelson, W. H. Visual space perception. New York: Springer, 1960.

Julesz, B. Foundation of cyclopean perception. Chicago: University of Chicago Press, 1971.

Mitchell, D. E. Properties of stimuli eliciting vergence eye movements and stereopsis. Vision Research, 1970, 10, 145-162.

Ogle, K. N. Spatial localization through binocular vision. In The Eye. New York: Academic Press, 1962.

Ogle. K. N. On the limits of stereoscopic vision. Journal of Experimental Psychology, 1952, 44, 253-259.

Roark, D., and French, H. Bringing true 3D imagery to color raster graphics. Mini-micro Systems, 1982, 6, 164-168.

Tyler, C. W. Spatial limitations of stereoscopic vision. Proceedings of the Society of Photo-optical Instrumentation Engineers, 1977, 120.

Tyler, C. W., and Scott, A. B. Binocular vision. In R. E. Records (Ed.), Physiology of the human eye and visual system. Hagerstown: Harper and Row, 1979.

Woodruff, R. R., Longridge, T. M., Irish, P. A., and Jeffreys, R. T. Pilot performance in simulated aerial refueling as a function of tanker model complexity and visual display field of view. AFHRL-TR-78-98, Williams AFB, AZ: Flying Training Division, Air Force Human Resources Laboratory, May 1979.

Wheatstone, C. On some remarkable and hitherto unobserved phenomena of binocular vision: Part 2. Philosophical Magazine, 1852, Series 4, 504-523.

1982 USAF-SCEEE SUMMER FACULTY RESEARCH PROGRAM

Sponsored by the

AIR FORCE OFFICE OF SCIENTIFIC RESEARCH

Conducted by the

SOUTHEASTERN CENTER FOR ELECTRICAL ENGINEERING EDUCATION

FINAL REPORT

Shallow Donor and Exciton Binding Energies in Quantum Wells

Prepared by:	Dr. Ronald L. Greene
Academic Rank:	Assistant Professor
Department and University:	Department of Physics University of New Orleans
Research Location:	Air Force Avionics Laboratory Electronic Research Branch
USAF Research Colleague:	Dr. Krishan K. Bajaj
Date:	August 5, 1982
Contract No:	F49620-82-C-0035

ACKNOWLEDGMENTS

I am particularly grateful to Dr. K. K. Bajaj of the University Research Center of Wright State University for suggesting the research problems considered in this report and for many helpful discussions concerning them. I am also indebted to Captains Dwight Phelps and George Norris for aid in using the computer at Wright-Patterson AFB, and to Dr. Bill Theiss for the use of his personal computer terminal during my stay.

Finally, I would like to thank the Air Force Systems Command, the Air Force Office of Scientific Research, the Air Force Avionics Laboratory (particularly the Electronic Research Branch), and the Southeastern Center for Electrical engineering Education for the opportunity for working on the research summarized in this report.

Shallow Donor and Exciton Binding Energies in Quantum Wells

by

Ronald L. Greene

ABSTRACT

We examine the theory of shallow donors and excitons trapped in quantum wells formed by sandwiching one semiconductor between layers of another with a larger band gap (e.g., GaAs between $Al_xGa_{1-x}As$). The anisotropy of the valence bands is taken into account for the exciton. Using a variational calculation, we investigate the dependence of the ground state binding energy of the shallow donor and exciton upon the width and height of the quantum well, and compare with results obtained using an infinitely deep well. We also consider the behavior of the n=2 states (in the hydrogenic limit) as a function of the width of the quantum well.

I. Introduction

Recent advances in crystal growth techniques such as molecular beam epitaxy have made it possible to grow materials consisting of alternate layers of two different semiconductors. The thicknesses of these layers and the sharpness of the interfaces can be controlled sufficiently well that these "superlattices" show quantum behavior due to one-dimensional periodicity.[1]

One of the most common superlattices consists of alternating layers of GaAs and $Al_xGa_{1-x}As$, with the GaAs widths in the range of about 40-500 Å. For small to moderate Al fractions ($x \lesssim 0.4$), $Al_xGa_{1-x}As$ is a direct gap semiconductor with a band gap larger than that of GaAs. Thus, at the interfaces between the two semiconductors, band discontinuities of order several hundred meV occur, depending on x. The conduction band discontinuity is about 85%, and the valence band discontinuity about 15%, of the total band gap difference between the two materials.[2] Because of the band discontinuity, conduction electrons preferentially move from the $Al_xGa_{1-x}As$ layers to the GaAs. (The holes behave in a similar way.) This fact has been used with "modulation doping"[3,4] to produce very high mobilities in GaAs which hold promise of high speed devices.[5]

Because of the conduction and valence band discontinuities at the GaAs-$Al_xGa_{1-x}As$ interfaces, the electrons and holes move in quantum wells with barrier heights determined by the band discontinuities. For good quality superlattices these wells can be described within experimental accuracy by one-dimensional square well potentials, resulting in the breaking of the normal bulk band structure into sub-bands.[1]

The study of atomic-like systems such as shallow donors and excitons, which play an important role in bulk semiconductors, is just beginning in superlattices. Bastard[6] has recently calculated the binding energy of a shallow donor associated with the lowest conduction sub-band. This calculation assumed the electron to be totally confined to the GaAs layer by an infinite square well potential. The binding energy of a donor in the well was found to increase monotonically with decreasing well size, L, from the three-dimensional (bulk) hydrogenic limit for large L to the two-dimensional limit at L=0. A similar kind of calculation has been made for an exciton trapped in an infinite well by Miller, et al.,[7] although their calculation is limited to small well sizes because of the choice of variational wave function.

II. Objectives of the Research

The primary objective of this research was to study the dependence of the binding energy of shallow donors and excitons confined by quantum wells such as are formed in superlattices. We were particularly interested in determining the sensitivity of the binding energies to the height of the potential barriers, and to calculate binding energies as a function of well size for realistic barrier heights. Additionally, we wished to study the behaviour of some of the excited states of such systems.

III. The Shallow Donor in a Quantum Well

A. Theoretical Approach

For simplicity the donor impurity is assumed to be at the center of the well. The effective mass Hamiltonian is then given by

$$H = -\frac{\hbar^2}{2m_e^*}\nabla^2 - \frac{e^2}{\epsilon_0 r} + V_w(z) \,. \tag{1}$$

The potential $V_w(z)$ is taken to be a square well of height V_o and width L:

$$V_w(z) = \begin{cases} 0 & |z| < \frac{L}{2} \\ V_0 & |z| > \frac{L}{2} \end{cases} \,. \tag{2}$$

The electron effective mass, m_e^*, and the dielectric constant, ϵ_0, vary across the interfaces between the two semiconductors. However, since the barrier height is generally much larger than the donor binding energy, the bound electron is largely confined to the GaAs layer. Thus it should be a reasonably good approximation to use the GaAs values for m_e^* and ϵ_0.

It is convenient to recast the Hamiltonian in a dimensionless form. For this purpose we use the effective Bohr radius

$$a_0^* = \frac{\hbar^2 \epsilon_0}{m_e^* e^2} \tag{3}$$

as our unit of length, and effective Rydberg

$$R^* = \frac{e^2}{2\epsilon_0 a_0^*} \tag{4}$$

as our unit of energy. For GaAs ($\epsilon_0 = 12.5$, $m_e^* = .067\ m_e$) these quantities are $a_o^* = 98.7$ Å and $R^* = 5.83$ meV.

We calculate the total energy variationally, approximating the electron wave function in terms of cylindrical coordinates by the following:

$$\Psi = f(z) \sum_{ij} b_{ij}\, g_{ij}(\rho, z, \phi) \,. \tag{5}$$

The function

$$f(z) = \sum_k a_k e^{-\alpha_k z^2} \tag{6}$$

is an approximate solution to the ground state of an electron in the one-dimensional square-well potential $V_w(z)$. The parameters a_k and α_k are determined by minimizing the square-well energy

$$\langle E_w \rangle = \int_{-\infty}^{\infty} dz\ f(z)\left[-\frac{d^2}{dz^2} + V_w(z)\right] f(z) . \tag{7}$$

The basis functions g_{ij} are of the form

$$g_{ij}(\rho,z,\phi) = z^q \rho^{|m|} e^{im\phi} e^{-\beta_i(\rho^2+\gamma_j z^2)} , \tag{8}$$

where m is the usual azimuthal quantum number, and m+q (q=0,1) determines the parity of the function. Since we consider the case of the donor impurity in the center of the well, parity is conserved. For a general location a linear combination of q=0 and q=1 functions would be required. The variational parameters β_i, γ_j, and b_{ij} are obtained from minimization of the total energy,

$$\langle E \rangle = \int_0^{\infty} \rho\, d\rho \int_{-\infty}^{\infty} dz \int_0^{2\pi} d\phi\ \Psi^* H \Psi . \tag{9}$$

The basis functions of Eq. (8) are slight modification of the set used by Aldrich and Greene[8] to calculate the binding energy of hydrogenic systems in a magnetic field. In that work the basis set was shown to give good results for the ground state and a number of excited states over the complete range from spherical symmetry (zero field) to the quasi-one-dimensional case (large field). Our investigations show that this basis set also has the versatility to handle the quasi-two-dimensional case which occurs in the present problem for large V_o and small L. Consequently, the hydrogenic part of the problem should be adequately handled by the functions $g_{ij}(\rho,z,\phi)$. We tried various numbers of β and γ parameters, and finally settled on seven values of β_i (geometrically spaced) and two

values of γ_j as a reasonable compromise between accuracy and computer time. Seven values of β_i are sufficient to give results for the two and three dimensional hydrogenic limits (with $\gamma_j=0$ and $\gamma_1=1$, $\gamma_{j\neq1}=0$ respectively) accurate to a few ten-thousandths of an effective Rydberg.

The major limitation in the accuracy of our energies is set by the function f(z). However, since the exact solution to the one-dimensional square-well problem is known,[9] it is easy to determine how well Eq. (6) approximates the correct result. We have chosen the number of terms in the right side of Eq. (6) by requiring our variational solution to the one-dimensional square-well problem to be accurate to within 0.005 effective Rydbergs. For the cases considered this requires ten or fewer Gaussians for f(z).

Once the eigenvalues of H are determined, the binding energy of the electron to the donor is obtained by subtracting the ground state energy of the electron in the well. This energy is determined by numerically solving the transendental equation[9]

$$\sqrt{\frac{E}{V_o}} = \cos\left(\frac{\sqrt{E}\,L}{2}\right) \tag{10}$$

for E. This procedure results in our variational binding energies being rigorous upper bounds for the true binding energies.

B. Results and Discussion

We have calculated the binding energies of the ground state and the first four excited states of the shallow donor at the center of the quantum well. The dependence of the ground state binding energy upon the width of the well, L, is shown in Fig. 1. Two barrier heights, V_o=25 and V_o=50 effective Rydbergs are shown. For large L the binding energy approaches

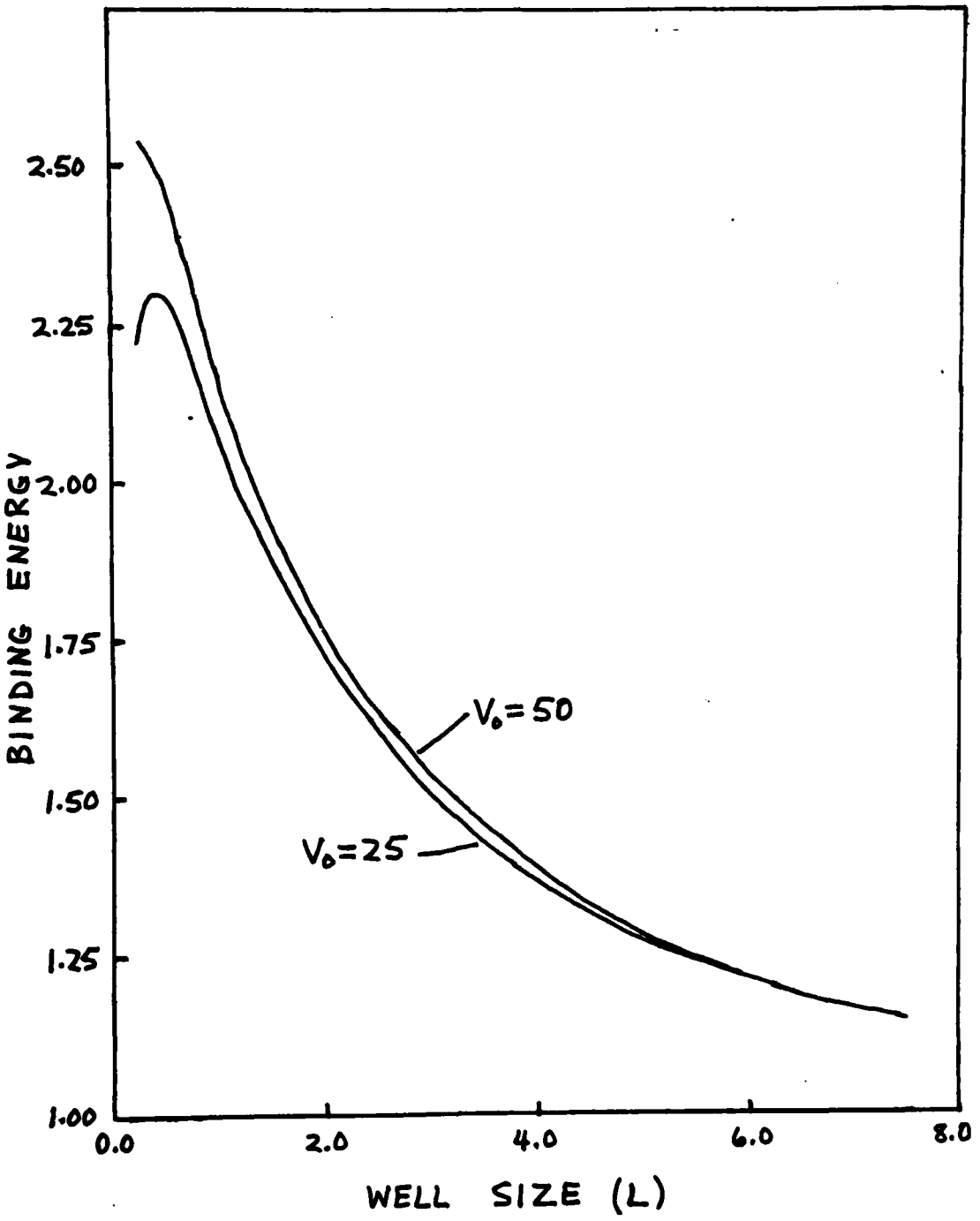


Fig. 1. Donor Ground State Binding Energy as a Function of the Well Size. All Energies are in terms of the effective Rydberg, and L is in units of the effective Bohr radius.

that of the isolated donor in GaAs. For small L, the binding energy reaches a peak and then begins to drop again. This is a result of the finite potential barrier and thus was not seen in Bastard's calculation. In our model the binding energy should drop back to one effective Rydberg at L=0; however, this is not physically correct because for very small L the effective mass and dielectric constant of $Al_xGa_{1-x}As$ would be more appropriate than the GaAs values that we have used.

Figure 2 shows the dependence of the ground state binding energy upon the well height, V_o, for a width of one effective Bohr radius. The binding energy varies linearly with $V_o^{-1/2}$. Extrapolating to infinite V_o yields a result of about 2.36 effective Rydbergs for the binding energy of the donor in the infinite well. This is larger than that found by Bastard which indicates that our basis is better suited to the donor problem than his simple one-parameter function. The figure also shows that for typical well heights, $V_o \sim 25\text{-}50\ R^*$, the binding energy of the donor in the finite well is significantly lower than that in the infinite well.

The behavior of the n=2 (hydrogenic limit) excited states as a function of the size of the well is shown in Fig. 3. For this figure the well height is 50 R^*. Notice that the degeneracy of the level is split by the quantum well (except for m=±1). The "2s" and "$2p_\pm$" states become more strongly bound with decreasing L, while the binding energy of the "$2p_o$" state decreases, and actually vanishes near 6.5 a_o^*. This behaviour occurs because the "$2p_o$" state has lobes along the z-axis (normal to the layers) and so is most strongly affected by the barriers at the interfaces. This state, in fact, has no two-dimensional analog, whereas the "2s" and "$2p_\pm$" states do. For very small L ($\lesssim .25\ a_o^*$) the binding energy of the

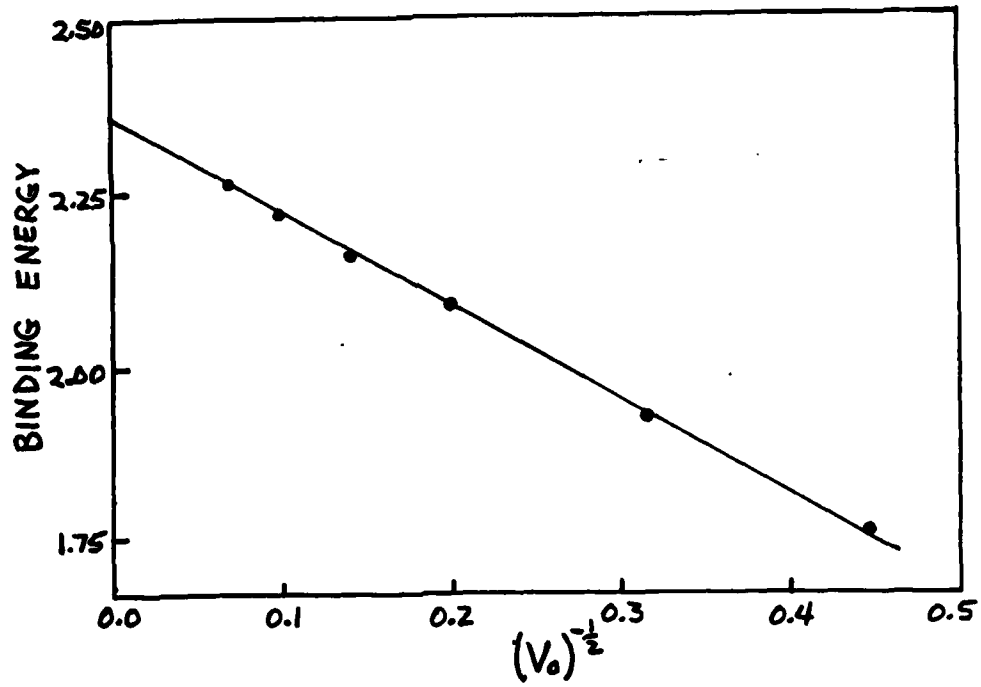


Fig. 2. Donor Ground State Binding Energy as a Function of the Well Height. Units are the same as in Fig. 1. L = 1.0 a_o^* for these data.

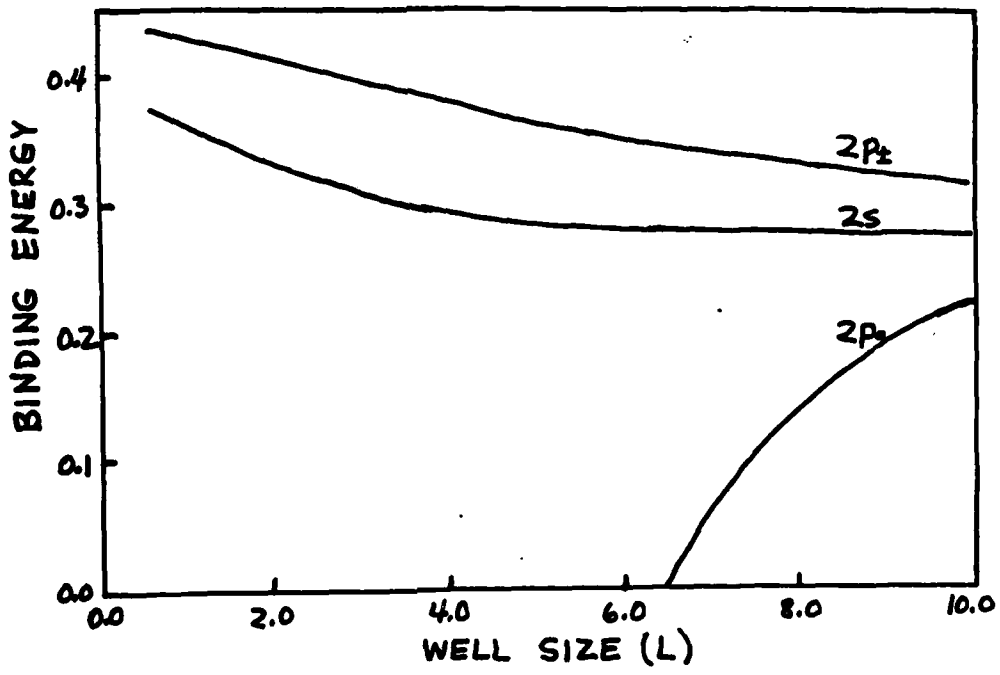


Fig. 3. Dependence of the Excited State Binding Energies upon the Well Size. The well height V_o = 50 R^*, and L is in units of effective Bohr radii.

"2s" and "$2p_{\pm}$" states begin to decrease as L decreases, and at still smaller L ($\sim .01\ a_o^*$) the "$2p_o$" state again becomes bound. These effects are due to significant spillover into the $Al_xGa_{1-x}As$ layers. However, for these small values of L our approximation of the GaAs values for m_e^* and ϵ_o are no longer valid. Moreover, the effective mass theory itself should probably be modified. Consequently, we do not show binding energies for $L < 0.5\ a_o^*$ (~ 50 Å) in Fig. 3.

IV. Exciton in a Quantum Well

A. Theoretical Approach

Because of the complex nature of the degenerate valence bands of GaAs and $Al_xGa_{1-x}As$, the correct Hamiltonian must be written in terms of 4 x 4 matrix operators.[10] It may be simplified in our case with some reasonable assumptions. First, since GaAs-$Al_xGa_{1-x}As$ superlattices are most commonly grown on (100) GaAs substrates,[1,2] our z-axis is along a [100] axis. The electron-hole reduced effective masses of the diagonal terms of the Hamiltonian are then cylindrically symmetric. In terms of the Luttinger parameters γ_1 and γ_2 and the free electron mass, m_o, they are given by[10]

$$\frac{1}{\mu_\perp^*} = \frac{1}{m_e^*} + \frac{1}{m_o}(\gamma_1 \pm \gamma_2) \tag{11}$$

and

$$\frac{1}{\mu_z^*} = \frac{1}{m_e^*} + \frac{1}{m_o}(\gamma_1 \mp 2\gamma_2) \quad . \tag{12}$$

The upper sign in these equations refers to the $J_z = \pm 3/2$ (heavy hole) band, and the lower sign to the $J_z = \pm 1/2$ (light hole) band. The off-diagonal elements of the Hamiltonian involve p_x^2 and p_y^2 operators which for typical

well sizes are significantly smaller than p_z^2 because of the relatively large kinetic energy of the hole in the quantum well. We will henceforth neglect the off-diagonal terms. Physically this corresponds to the assumption that the superlattice potential splits the valence band degeneracy enough that they may be treated as isolated bands with respect to the exciton binding energy. This seems to be empirically justified.[1,7]

With this approximation the exciton effective mass Hamiltonian (in cylindrical coordiates) is given by

$$H = -\frac{\hbar^2}{2\mu_\perp^*}\left[\frac{1}{\rho}\frac{\partial}{\partial\rho}\rho\frac{\partial}{\partial\rho} + \frac{1}{\rho^2}\frac{\partial^2}{\partial\phi^2}\right] - \frac{\hbar^2}{2m_e^*}\frac{\partial^2}{\partial z_e^2} - \frac{\hbar^2}{2m_{hz}^*}\frac{\partial^2}{\partial z_h^2} - \frac{e^2}{\epsilon_0|\vec{r}_e - \vec{r}_h|} + V_{ew}(z_e) + V_{hw}(z_h) \,. \tag{13}$$

In writing this expression we have not included the center-of-mass energy in the ρ-direction since it forms a continuum. The reduced mass $\mu_\perp^*$ is given in Eq. (11), and the effective hole mass along the z-axis is obtained from Eq. (12),

$$\frac{1}{m_{hz}^*} = \frac{1}{m_0}(\gamma_1 \mp 2\gamma_2) \,. \tag{14}$$

The well potentials V_{ew} and V_{hw} are the same as used in the donor problem, Eq. (2), except that the well heights are V_e and V_h for the electron and hole, respectively. They are determined by the Al fraction in $Al_xGa_{1-x}As$. Typically, the conduction band discontinuity (V_e) is about 85%, and the valence band discontinuity (V_h) about 15%, of the total band discontinuity between the two semiconductors.

To solve this problem variationally, we assume that the wave function can be written as a product of $f(z_e,z_h)$, the solution to the electron and

hole one-dimensional square-well problem, and a function of the relative coordinates between the electron and hole. As seen earlier, this approach gives good results for the donor. We first attempted to approximate $f(z_e,z_h)$ by a series of Gaussians, as for the donor; however, since about ten Gaussians are required for each square-well solution, $f(z_e,z_h)$ requires about 100 Gaussians. This results in 10^4 terms in each matrix element evaluation. The advantage of being able to perform all the integrals analytically with Gaussians is lost because of the very large number of terms. In addition, this large number of terms tends to cause numerical round-off problems.

To avoid the above problems, we took the following form for the variational ground state:

$$\Psi = f(z_e,z_h)\, g(\rho,z,\phi) = f_e(z_e) f_h(z_h)\, g(\rho,z,\phi) \tag{15}$$

where ρ, z, and ϕ are relative cylindrical coordinates. The functions $f_e(z_e)$ and $f_h(z_h)$ are the exact (unnormalized) solutions to the finite square-well problem. For example,[9]

$$f_e(z_e) = \begin{cases} \cos k_e z_e & |z_e| < \frac{L}{2} \\ B_e e^{-\kappa|z_e|} & |z_e| > \frac{L}{2} \end{cases} . \tag{16}$$

The parameter k_e is determined by the energy, and B_e and κ_e are obtained from k_e by requiring continuity of f_e and its derivative at the interface. A similar result is obtained for f_h. With the trial function given in Eq. (15) the variational energy is found to be

$$\langle E \rangle = \int_{-\infty}^{\infty} dz_e\, f_e(z_e)^2 \int_{-\infty}^{\infty} dz_h\, f_h(z_h)^2 \left\{ -\frac{\hbar^2}{2\mu_z^*} \left|\frac{\partial g}{\partial z}\right|^2 - \frac{e^2|g|^2}{\epsilon_0(\rho^2+z^2)^{1/2}} \right.$$
$$\left. -\frac{\hbar^2}{2\mu_\perp^*}\left[g^* \frac{1}{\rho}\frac{\partial}{\partial\rho}\rho\frac{\partial g}{\partial\rho} + g^*\frac{1}{\rho^2}\frac{\partial^2 g}{\partial\phi^2}\right]\right\} . \tag{17}$$

The use of the exact functions for f_e and f_h means that the z_e and z_h integrals can no longer be performed analytically for realistic functions $g(\rho, z, \phi)$. However, this weakness is overcome by the fact that a good choice for $g(\rho, z, \phi)$ needs many fewer terms and fewer matrix elements than would be required with Gaussians. To find the binding energy of the ground state we choose

$$g(\rho, z, \phi) = [1 + az^2]\, e^{-\alpha(\rho^2 + z^2)^{1/2}} \quad . \tag{18}$$

The parameters a and α are determined by minimizing the variational energy as for the donor. The addition of a z^4 term to Eq. (18) results in an insignificant improvement in the energy. In order to obtain good excited state energies $g(\rho, z, \phi)$ would have to be modified slightly. For example, the addition of a term proportional to ρ and a factor $z^q \rho^{|m|} e^{im\phi}$ as in Eq. (8) should significantly improve its ability to handle excited states. Thus far, however, we have calculated only the ground state energies.

B. Results and Discussion

For our calculation of the ground state binding energy of the exciton we selected the Luttinger parameters γ_1 and γ_2 to give .45 m_o and .08 m_o for the heavy and light holes along the [100] direction.[1] [See Eq. (14).] This choice gives $\gamma_1 = 7.36$ and $\gamma_2 = 2.57$. We calculated both the heavy- and light-hole binding energies for three cases: x=0.15, x=0.30, and an infinite well. The total band discontinuity between GaAs and $Al_xGa_{1-x}As$ was obtained from[11]

$$\Delta = 1.155x + .37x^2 \quad . \tag{19}$$

The conduction and valence band discontinuities were assumed to be 85%

and 15% of Δ, respectively.

Our results are shown in Figs. 4 and 5. Probably the most important result that can be seen in these figures is that the assumption of an infinite well gives much too large values for the binding energy for small to moderate well sizes ($L \lesssim 300$ A). As for the the donor, the infinite-well binding energy increases monotonically to the two-dimensional limit as L decreases, while all the finite-well results reach a peak and then begin to decrease.

There is another qualitative difference between the infinite-well and finite-well results. For all values of L the infinite-well calculation predicts the light-hole exciton to be more strongly bound than the heavy-hole exciton. This is also seen in the calculation of Miller, et al.[7] However, for small well sizes (i.e., for $L \lesssim 100$ A, depending on x) the finite-well results suggest that , in fact, the heavy-hole binding is larger. This is what is expected physically because the light hole is much more difficult to confine in a small quantum well.

Again we note that our results become less accurate at very small L where the wave function has a large probability of being in the $Al_xGa_{1-x}As$. These errors should not be large, however, because the parameters of the two semiconductors are fairly close, particularly for small x. More serious is the possible breakdown of effective mass theory for small L and large well heights.

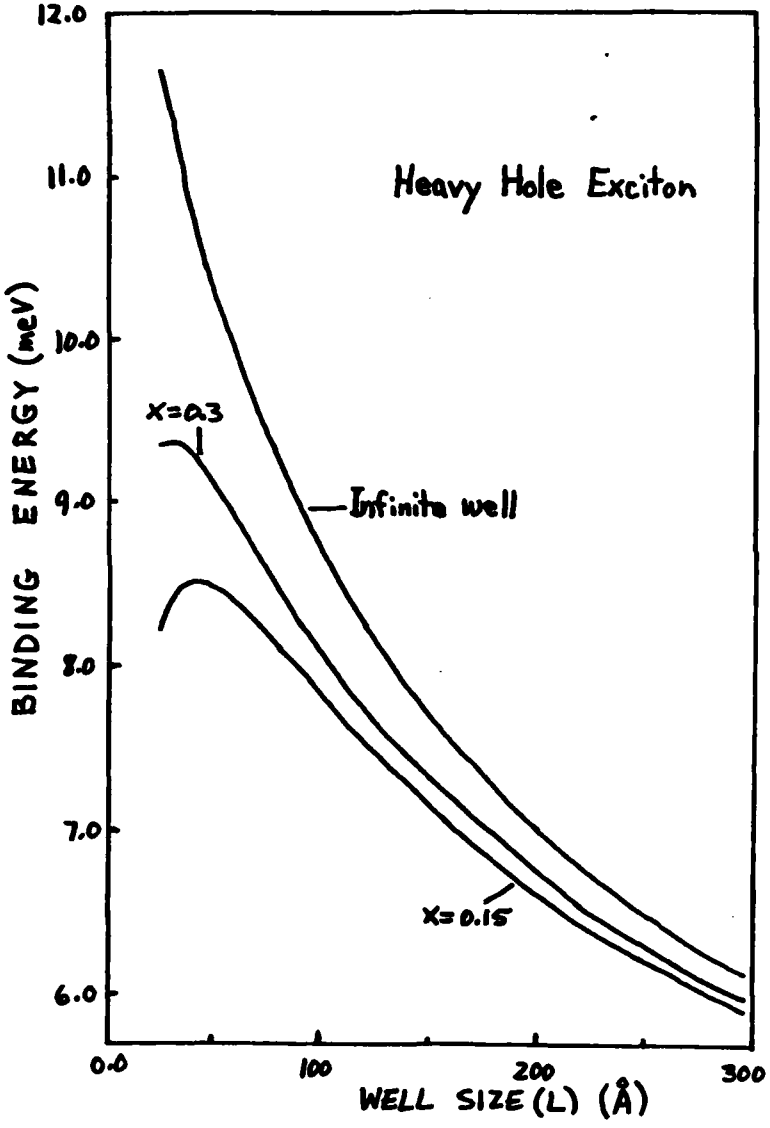


Fig. 4. Binding Energy of the Heavy-Hole Exciton as a Function of L.

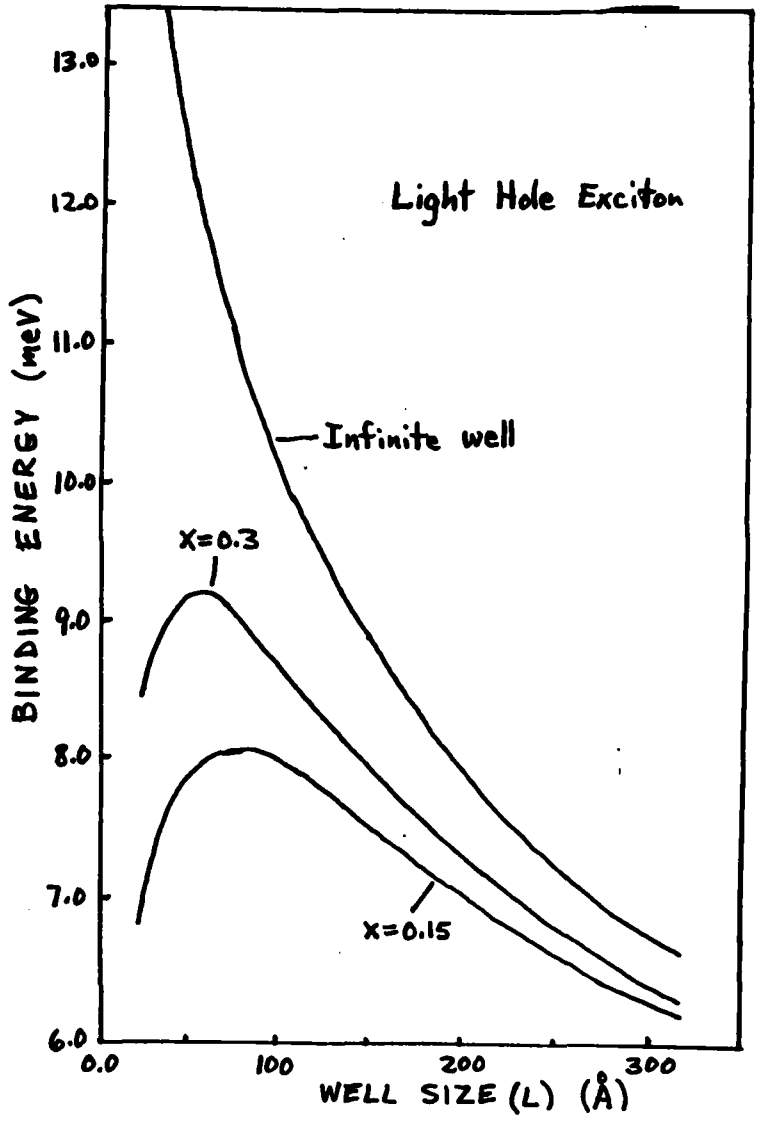


Fig. 5. Binding Energy of the Light-Hole Exciton as a Function of L.

V. Recommendations

Thus far there are very few experimental checks of the atomic-like systems studied in this report. Superlattices are relatively new systems because only in recent years has the technology been developed for producing sharp interfaces between semiconductors. If the theoretical results of this work are verified by experimental investigations of shallow states in quantum wells, the calculations could then be used as an aid in characterization of the quality of superlattice materials.

Some of our theoretical results will be very difficult to verify experimentally. In particular, it is very difficult to measure properties of excited states of hydrogenic systems except in the presence of a magnetic field. Because of this the logical follow-up to this work is the calculation of the energy and line strengths of these same systems in the presence of a magnetic field. Experiments capable of measuring properties of the ground and excited states of hydrogenic systems in a magnetic field can be performed at the Avionics Laboratory, among other places.

Further down the road is a more careful investigation of the effective mass approximation in the region near the interfaces of the two semiconductors. Also, the problem of screening by a quasi-two-dimensional electron gas needs to be solved if systems in modulation-doped superlattices are to be studied with success. Such studies are important in understanding the behavior of any device produced using superlattice technology.

REFERENCES

1. R. Dingle, W. Wiegmann, and C. H. Henry, "Quantum States of Confined Carriers in Very Thin $Al_xGa_{1-x}As$-GaAs-$Al_xGa_{1-x}As$ Heterostructures," Phys. Rev. Lett., Vol. 33, pp. 827-830 (1974).

2. Raymond Dingle, "Optical Properties of Semiconductor Superlattices," Proc. 13th Int. Conf. Phys. Semicond., ed. by F. G. Fumi (Rome, Tipografia Marver, 1976), pp. 1013-1020.

3. H. L. Stormer, R. Dingle, A. C. Gossard, W. Wiegmann, and R. A. Logan, "Electronic Properties of Modulation-Doped GaAs-$Al_xGa_{1-x}As$ Superlattices," Physics of Semiconductors, 1978, ed. by B. L. H. Wilson (London, The Institute of Physics, 1979), pp. 557-560.

4. H. L. Stormer, "Modulation Doping of Semiconductor Superlattices and Interfaces," Proc. 15th Int. Conf. Physics of Semiconductors, J. Phys. Soc. Japan, Vol. 49, Suppl. A, pp. 1013-1020 (1980).

5. Takashi Mimura, Satoshi Hiyamizu, Kazakiyo Joshin, and Kohki Hikosaka, "Enhancement-Mode High Electron Mobility Transistors for Logic Applications," Jpn. J. Appl. Phys., Vol. 20, pp. L317-319 (1981).

6. G. Bastard, "Hydrogenic Impurity States in a Quantum Well: A Simple Model," Phys. Rev. B, Vol. 24, pp. 4714-4722 (1981).

7. R. C. Miller, D. A. Kleinman, W. T. Tsang, and A. C. Gossard, "Observation of the Excited Level of Excitons in GaAs Quantum Wells," Phys. Rev. B, Vol. 24, pp. 1134-1136 (1981).

8. C. H. Aldrich and Ronald L. Greene, "Hydrogen-Like Systems in Arbitrary Magnetic Fields," Phys. Stat. Solidi (b), Vol. 93, pp. 343-350 (1979).

9. Albert Messiah, Quantum Mechanics, Vol. I (Amsterdam, North-Holland Publishing Company, 1961), pp. 88-91.

10. M. Altarelli and Nunzio O. Lipari, "Exciton States of Semiconductors in a High Magnetic Field," Phys. Rev. B, Vol. 9, pp. 1733-1750 (1974).

11. H. J. Lee, L. Y. Juravel, and J. C. Woolley, "Electron Transport and Band Structure of $Ga_{1-x}Al_xAs$ Alloys," Phys. Rev. B, Vol. 21, pp. 659-669 (1980).

1982 USAF-SCEEE SUMMER FACULTY RESEARCH PROGRAM

Sponsored by the

AIR FORCE OFFICE OF SCIENTIFIC RESEARCH

Conducted by the

SOUTHEASTERN CENTER FOR ELECTRICAL ENGINEERING EDUCATION

FINAL REPORT

NITRO ORGANIC COMPOUNDS: A SYNTHETIC STUDY

Prepared by:	Keith C. Hansen
Academic Rank:	Professor of Chemistry
Department and University	Department of Chemistry Lamar University
Research Location:	Frank J. Seiler Research Laboratory Directorate of Chemical Sciences
USAF Research Colleague	Dr. John S. Wilkes
Date:	August 20, 1982
Contract No:	F49620-82-C-0035

NITRO ORGANIC COMPOUNDS: A SYNTHETIC STUDY

by

Keith C. Hansen

ABSTRACT

Laboratory investigations directed toward the synthesis of hexanitrotolane (HNT) and trinitrophenylacetylene (TNPA) are described. Several intermediate compounds, including hexanitrostilbene (HNS), hexanitrobibenzyl (HNBB), trinitroethylbenzene, and trinitroacetophenone, were synthesized, and attempts to convert these into the desired compound are described. All attempts were unsuccessful.

The synthesis of three nitro butenes are described. These compounds are of interest as model compounds in the study of the mechanism of the thermal decomposition of trinitrotoluene (TNT). (E)-2-nitro-2-butene was prepared by the addition of nitryl iodide (from $AgNO_2$ and I_2) to cis-2-butene followed by the elimination of HI with base. Both 1-nitro-2-methylpropene and 3-nitro-2-methylpropene were synthesized by a base catalyzed condensation of nitromethane and acetone to give a nitro alcohol, conversion of the alcohol into its acetate, and then elimination of acetic acid with base. The isomeric nitro isobutenes were separated by fractional distillation.

Acknowledgement

The author would like to thank the Air Force Systems Command, the Air Force Office of Scientific Research and the Southeastern Center for Electrical Engineering Education for providing him with the opportunity to spend a very worthwhile and interesting summer at the Frank J. Seiler Research Laboratory, USAF Academy, CO.

He would like to thank all of the laboratory personnel for their hospitality, assistance, and cooperation in making the research effort successful. Particular thanks go to Lt. Colonel A. A. Fannin, Dr. John S. Wilkes, Mr. Lloyd Pflug, and Mr. Fred Kibler.

I. INTRODUCTION

The Energetic Materials Division of the Frank J. Seiler Research Laboratory is interested in the synthesis and properties of new, potentially explosive materials, and in the study of the properties of known explosive materials. Many polynitro organic compounds are used as explosive materials, and of these, polynitro aromatic compounds are some of the more commonly used. These include trinitrotoluene (TNT), hexanitrostilbene (HNS) and hexanitrobibenzl (HNBB). Several potentially explosive compounds of structure analogous to the above mentioned materials have never been prepared. The synthesis of these new compounds and the investigation of their properties is of interest.

Thermal stability is one of several properties of energetic materials which is important in determining the potential of materials as an explosive. An investigation into the mechanism of the thermal decomposition of TNT will possibly help determine the relationship between structure and thermal stability of explosive material. This study will include both theoretical calculations and experimental laboratory work, and small nitroalkenes of specific geometry are needed to serve as model compounds for laboratory work that is to be correlated with theoretically calculated data.

II. OBJECTIVES

The objectives of this project were to initiate laboratory studies directed toward the synthesis of two types compounds of interest to the Energetic Materials Division of the FJSRL. In the first area of interest,

the goal was to synthesize two nitroaryl acetylenic compounds which have not been previously prepared. These compounds are hexanitrotolane (HNT) and trinitrophenylacetylene (TNPA). These compounds are analogous in structure to several other known explosive materials, and would be expected to have properties which would make them useful as explosives.

As support for ongoing investigations into the mechanism of the thermal decomposition of TNT, the synthesis of some nitrobutenes of specific geometry was also an objective of this project. These nitrobutenes, which are of relatively low molecules weight, are needed to serve as model compounds for experimental work to be correlated with theoretical calculations.

III. Synthesis of Nitro Aryl Acetylenic Compounds

The synthesis of hexanitrotolane, (PiC≡CPi where Pi = 2,4,6-trinitrophenyl) is of interest in that it would complete the homologous series consisting of hexanitrobibenzyl ($PiCH_2$-CH_2Pi), hexanitrostilbene (PiCH=CHPi), and hexanitrotolane (HNT). Both of the first two compounds are known[1], and their thermal stability increases from HNBB to HNS. It is possible then that HNT would have both good explosive properties as well as good thermal stability. The synthesis of trinitrophenylacetylene (PiC≡CH) is of interest both as a potentially explosive material, and also as a possible intermediate in the synthesis of HNT.

The synthesis of HNT can be approached in two basic ways. One would be to start with known compounds in which the basic carbon structure of 14 atoms is already in place, and to effect transformations in those

molecules to generate the proper functionality of HNT. Hexanitrobibenzyl and hexanitrostilbene, both easily prepared from TNT[1], could serve as the desired starting compounds. Both of these compounds are relatively unreactive in the aliphatic portion of the molecule. HNBB has been shown not to react with NaOCl[2] and HNS was unreactive toward Br_2 under several sets of conditions[2]. Due to the greater reactivity of chlorine over that of bromine, it was deemed worthwhile to attempt the addition of of chlorine to HNS to give a vicinal dichloride (1) which could be transformed into HNT by dehydrochlorination. No reaction was observed. The reaction was repeated (2) with the addition of a

$$PiCH{=}CHPi + Cl_2 \xrightarrow[40°]{DMF} PiCHCl\text{-}CHClPi \qquad (1)$$

catalytic amount of the Lewis acid, ferric chloride. Again the starting

$$PiCH{=}CHPi + Cl_2 + FeCl_3 \xrightarrow[DMF]{100°} PiCHCl\text{-}CHClPi \qquad (2)$$

compound was recovered unchanged.

Another approach to the synthesis of HNT would be to join two compounds together giving the proper carbon structure and functionality of HNT simultaneously. The reaction of cuprous acetylides with aryl iodides has been shown to be a good route to diaryl acetylenes[3].

$$ArC{\equiv}C\text{-}Cu + Ar\text{-}I \longrightarrow ArC{\equiv}CAr \qquad (3)$$

To apply this method to the synthesis of HNT, trinitrophenylacetylene and picryl iodide are required (4). Picryl iodide is readily prepared[4],

$$PiC{\equiv}CH + PiI \xrightarrow{Cu^+} PiC{\equiv}CPi \qquad (4)$$

but trinitrophenylacetylene (TNPA) has not been reported. Synthetic work was therefore directed toward the synthesis of this compound.

The first approach considered for the preparation of TNPA was the reaction of a picryl halide with a metal acetylide (5). This

$$PiX + MC{\equiv}CH \longrightarrow PiC{\equiv}CH \qquad (5)$$

reaction required the use of a non-basic solvent and also consideration of the possibility that the metal acetylide would react with the nitro groups in the picryl halide. Three reactions were attempted (6) using tetrahydrofuran (THF) as the solvent and employing low temperature to

$$PiX + MC{\equiv}CH \xrightarrow[-78°]{THF} \qquad (6)$$

X = Cl, I M = Li, Na

attempt to minimize reaction with the nitro group. In all cases, the reaction mixture immediately turned very dark and no characterizable material could be obtained. It is assumed that even at -78°, the nitro groups are interacting with the organometallic.

Two other methods [5,6] to prepare monoaryl acetylenes were considered as possible routes to the synthesis of trinitrophenylacetylene. In order to apply either of these reaction paths to the synthesis of

$$ArCOCH_3 + PCl_5 \longrightarrow ArCCl{=}CH_2 \xrightarrow{-HCl} ArC{\equiv}CH \qquad (7)$$

$$ArC(=NNHCONH_2)CH_3 + SeO_2 \longrightarrow \text{1,2,3-selenadiazole} \xrightarrow{\Delta} ArC{\equiv}CH \qquad (8)$$

trinitrophenylacetylene, 2,4,6-trinitroacetophenone must be prepared as an intermediate. Equations 9 and 10 outline the sequence by which trinitroacetophenone was prepared. All attempts to convert the

$$PhCH_2CH_3 + H_2SO_4 + HNO_3 \longrightarrow (NO_2)_3PhCH_2CH_3 \qquad (9)$$

$$(NO_2)_3PhCH_2CH_3 + Na_2Cr_2O_7 \xrightarrow[HNO_3]{H_2SO_4} (NO_2)_3PhCOCH_3 \qquad (10)$$

trinitroacetophenone into trinitrophenylacetylene by either of the routes shown in equations 8 or 9 were unsuccessful. Trinitroacetophenone was recovered unchanged when heated to 140° for 3.5 hrs. with PCl_5. All attempts to convert the ketone into its semicarbazone derivative were unsuccessful. Solvent, temperature, reaction time, and catalyst were all varied in many attempts to produce the semicarbazone, but no reaction was ever observed.

IV. Synthesis of Nitrobutenes

Studies of the mechanism of the thermal decomposition of TNT have resulted in the postulate that the loss of OH as a result of interaction between a methyl hydrogen and an ortho nitro group may be an important step. In order to compare theoretical calculations with experimental data, small compounds which contain the components of TNT involved in the loss of OH are needed. This would be an alkene with a cis arrangement of a methyl group and NO_2 group. The smallest molecule with these features would be cis-1-propene. Work in this laboratory has not as yet resulted in the synthesis of a pure sample compound since it is thermodynamically less stable than the corresponding trans isomer.

The synthesis of (Z)-2-nitro-2-butene was contemplated in that the additional methyl group may result in increased stability of the desired geometric isomer. 2-Nitro-2-butene was synthesized according to the scheme in eq. 11. The addition of NO_2I to an alkene has been shown to

$$CH_3CH{=}CHCH_3 \xrightarrow{AgNO_2} CH_3CH(NO_2)CH(I)CH_3 \xrightarrow{\text{pyridine}} CH_3CH{=}C(NO_2)CH_3 \quad (11)$$

be an <u>anti</u> addition[7] and the reaction of the nitro iodide should proceed by an E2 mechanism in which an anti-periplanar elimination[5] is favored. If the sterochemistry of reactions described above is applicable, the desired (Z)-2-nitro-2-butene would be obtained by starting with <u>cis</u>-2-butene. Reaction of <u>cis</u>-2-butene with $AgNO_2$ and I_2 followed by treatment with pyridine, however, resulted in the formation of the other geometric isomer, (E)-2-nitro-2-butene, in low yield along with the nitro iodide and higher molecular weight material. Analysis of the material by pmr, gas chromatography, and mass spectrometry showed no evidence that any of the (Z) isomer has been produced. Again the desired isomer is less thermodynamically stable and the more stable (E) isomer is formed by a less favored syn-periplanar E2 reaction[8]. This is analogous to results reported in the formation of nitroalkenes by nitro mercuration[8].

The nitrobutene, 1-nitro-2-methylpropene, would have the desired orientation of the methyl and nitro group with no geometric isomers. This compound was synthesized as shown in eq. 12, 13, 14.

$$CH_3C(O)CH_3 + CH_3NO_2 + CH_3ONa \longrightarrow (CH_3)_2C(OH)CH_2NO_2 \quad (12)$$

$$(CH_3)_2C(OH)CH_2NO_2 + (CH_3\overset{O}{\overset{\|}{C}})_2O \longrightarrow (CH_3)_2C(O\overset{O}{\overset{\|}{C}}CH_3)CH_2NO_2 \quad (13)$$

$$(CH_3)_2C(O\overset{O}{\overset{\|}{C}}CH_3)CH_2NO_2 + NaOCCH_3 \longrightarrow (CH_3)_2C{=}CH(NO_2) + CH_2{=}C(CH_3)CH_2NO_2 \quad (14)$$

The desired compound, 1-nitro-2-methylpropene was contaminated with 20% of its non-conjugated isomer, 3-nitro-2-methylpropene. A pure sample of the 1-nitro-2-methylpropene was obtained by repeated fractionation under reduced pressure.

Some support for the postulated loss of OH in TNT as part of the mechanism of the thermal decomposition of TNT is obtained from the mass spectra of the nitroalkenes synthesized. 1-Nitro-2-methylpropene, which has a cis orientation of the methyl and the nitro group, shows the loss of OH as a major fragmentation pathway in its mass spectrum as does TNT[2]. The compounds trans-1-nitropropene and (E)-2-nitro-2-butene, which do not have a cis alignment of a methyl and a nitro group, do not show loss of OH as a fragmentation pattern in the mass spectra.

V. EXPERIMENTAL DETAILS

2,4,6-Trinitrotoluene - 40.8 g of 90% nitric acid was added to 152 g of 15% fuming sulfuric acid. When the addition was complete, 35.3 g (0.2 mole) of 2,4-dinitrotoluene (MCB) was added. The reaction mixture was heated slowly with stirring to 90°C, at which point an exothermic reaction ensued. The reaction was controlled with an ice bath and, after the reaction had subsided, the reaction mixture was maintained at 90-100° with stirring for 2 hrs. The mixture was cooled

and allowed to stand overnight at room temperature. The reaction mixture was extracted with three 200 mL portion of CH_2Cl_2, and the combined CH_2Cl_2 extracts were washed with $NaHCO_3$ solution and water. The CH_2Cl_2 extract was then dried with anhydrous Na_2SO_4, stripped of CH_2Cl_2 under vacuum and the residue recrystalized from ethanol yielding 32.2 g (73%), m.p. 83-84°C, lit.[9] m.p. 82-83°C.

Hexanitrostilbene - TNT (10 g, 0.044 mole) was dissolved in 100 mL of THF and 50 mL of CH_3OH and the solution cooled to 0°C. This solution was then poured rapidly with stirring into 100 mL of 5% NaOCl (chlorox) which was also at 0°C. The solution turned immediately dark red. The reaction mixture was stirred and cooled for 1 min, then allowed to stand at room temperature for 2 hrs. during which time a solid precipitated. The solid was collected by filtration, washed with CH_3OH, and recrystalized from DMF to yield 4.2 g (42%), m.p. 315-317°C, lit.[1] m.p. 316°C.

2,4,6-Trinitroethylbenzene - Fuming HNO_3 (108 mL) was added slowly with stirring and cooling to 500 mL of 15% fuming H_2SO_4. This mixture was cooled to below 20°C and 40 g (0.38 mole) of ethylbenzene was added dropwise with stirring. The reaction mixture was heated at 45°C for 3 hrs., at 85°C for 4 hrs, and then allowed to stand at room temperature overnight. The mixture was poured onto ice and the crude product collected by filtration, washed with $NaHCO_3$ solution and H_2O, and recrystallized from CH_3OH yielding 40.3 g (44%), m.p. 38-40°C, lit.[10] 38.5°C.

2,4,6-Trinitroacetophenone - 2,4,6-Trinitroethylbenzene (30.3 g, 0.13 mole) was mixed with 128.8 g $Na_2Cr_2O_7 \cdot 2H_2O$ and 322 mL of 90% HNO_3. The mixture was cooled with an ice bath and 62 mL of 15% fuming H_2SO_4

was added dropwise with stirring. The reaction mixture was then stirred at room temperature for 5 hrs. and then poured onto crushed ice. The crude product was collected by filtration, washed with $NaHCO_3$ solution and water, then air dried. Recrystallization from $CHCl_3$ gave 14.3 g (43%), m.p. 134-136°C, lit.[11] m.p. 135-136°C.

Picryl iodide (1-iodo-2,4,6-trinitrobenzene) - Sodium iodide (12.0 g, 0.08 mole) was dissolved in 50 mL dry acetone and added to a mixture of 10 g (0.04 mole) picryl chloride (MCB), 5 mL glacial acetic acid, and 25 mL dry acetone. Reaction mixture turned dark red immediately and was stirred at room temperature for 30 min. The mixture was then poured into 350 mL of H_2O containing 0.3 g of $NaHSO_3$. Crude product was collected by filtration and recrystallized from $CHCl_3$ yielding 7.1 g (52%), m.p. 159-162°C, lit.[4] m.p. 161-163°C.

Reaction of Hexanitrostilbene with Chlorine - Hexanitrostilbene (1.0 g) was dissolved in 50 mL of DMF at 60°C and Cl_2 was passed through the solution for 3 hrs. Upon cooling, a solid crystallized which was identified by m.p. (315-318°C) and pmr to be hexanitrostilbene (starting compound). The reaction was repeated at 100° with a small amount of anhydrous $FeCl_3$ added. 80% of starting compound was recovered unchanged.

Reaction of picryl chloride with lithium acetylide - Lithium acetylide was prepared at -78°C in THF according to the method of Midland[12]. Picryl chloride (2.0 g) in 25 mL dry THF was added to the lithium acetylide at -78° over a period of 30 min. The reaction mixture immediately turned dark upon addition of first portion of picryl chloride. Mixture allowed to warm to room temperature and to

stand overnight. The dark mixture was stripped of solvent under vacuum and poured into 2N HCl. This mixture was extracted with ether, ether extracts dried, and solvent removed under vacuum to give a dark reddish-brown amorphous solid which could not be recrystallized. IR did not indicate any acetylenic bond in the solid. The reaction was repeated with the mode of addition reversed (lithium acetylide added to picryl chloride). This reaction resulted in the same brown amorphous solid.

Reaction of picryl iodide with sodium acetylide - Picryl iodide (2.0 g.) dissolved in 50 mL THF (dried over CaH_2) was cooled to 0°C with an ice bath. To this solution was added 0.46 g. sodium acetylide (mineral oil suspension, Alfa) with stirring. Solution immediately turned very dark. Reaction mixture was allowed to warm to room temperature and stirred for 1 hr. Mixture was poured into dilute HCl resulting in the separation of black intracable tar.

Reaction of trinitroacetophenone with PCl_5 - 2,4,6-Trinitroacetophenone (5.0 g.), 6.25 g. PCl_5, and 2 mL of $POCl_3$ were mixed under N_2 and heated with stirring to 140°C for 3.5 hrs. Mixture turned progressively darker with time. The reaction mixture was poured onto ice, and the resulting mixture was stirred for 2 hrs. The crude product was collected by filtration and recrystallized from ethanol yielding 3.8 g of material melting at 134-135°C. Mixed m.p. and pmr identified the material as unreacted trinitroacetophenone.

Reaction of trinitroacetophenone with semicarbazide - 2,4-trinitro-acetophenone (0.5 g.) was reacted with 0.8 g. of semicarbazide hydrochloride

in refluxing ethanol - H_2O with a small amount of sodium acetate. The solution became a wine-red color. After 1 hr. the mixture was allowed to cool resulting in the crystallization of a solid which was identified by m.p. and pmr to be unreacted trinitroacetophenone. The reaction was repeated several times varying reaction time (up to 6 hrs.), solvent THF/H_2O, and base (pyridine). In all cases the starting compound was recovered unchanged.

Reaction of cis-2-butene with silver nitrite - iodine - Silver nitrite (5.9 g.) and 19.5 g. of iodine were stirred together in 75 mL of anhydrous ether under nitrogen for 30 min. The flask was fitted with a dry ice-acetone condenser and the flask cooled with an ice bath. 2.2 g. of cis-2-butene was added and the mixture stirred for 4 hrs. and then warmed to room temperature and allowed to stand overnight. The mixture was filtered, the ether filtrate was washed with $NaHSO_3$ solution and NaCl solution, and dried with anhydrous Na_2SO_4. 10 mL of pyridine was added resulting in an exothermic reaction and the formation of a solid. The mixture was stirred for 2 hrs. The mixture was extracted with pentane and water, the pentane extracts were washed with $NaHSO_3$ solution, dried, and vacuum distilled yielding a dark fraction, b.p. 50-60°C @ 18 mm Hg. Proton magnetic resonance spectrum showed material to be a mixture, but the presence of (E)-2-nitro-2-butene was confirmed (absence of vinyl absorption at δ = 6.2 ppm ruled out possibility of presence of (Z)-2-nitro-2-butene)[13]. Analysis of the fraction by gas chromatography - mass spectrometry revealed at least five components

including pyridine (13%), 2-nitro-2-butene (19%), 2-iodo-3-nitro-butane (58%), and two higher molecular weight iodine containing compounds.

1-Nitro-2-methyl-2-propanol - Sodium methoxide (4.5 g.) dissolved in 30 mL. of methanol was added to 53.5 mLs (1 mole) nitromethane and 300 mL of acetone. The mixture was stirred for 3 days at room temperature. The mixture was neutralized with concentrated HCl, dried with $MgSO_4$, filtered, and vacuum distilled yielding 27.8 g. (23.4%), b.p. 72-74°C at 8 torr, lit.[14] b.p. 76-77°C at 10 torr.

Nitro-t-butyl acetate - Acetic anhydride (28.3 g, 0.28 mole) was added dropwise with stirring to a mixture of 27.6 g. (0.23 mole) 1-nitro-2-methyl-2-propanol and 4 drops concentrated H_2SO_4 at such a rate as to keep the temperature at 60°C. After the addition, the mixture was heated at 80° for 0.5 hr. and then vacuum distilled yielding 35.7 g. (97%), b.p. 87-90° at 10 torr, lit.[14] b.p. 86-88 at 13 torr.

1-Nitro-2-methylpropene - Anhydrous sodium acetate (1.8 g, 0.002 mole) was mixed with 35.7 g. (0.22 mole) of nitro-t-butyl acetate and heated to 110°C for 30 min. The reaction mixture was the vacuum distilled collecting material boiling between 35° and 50° at 11 torr. The distillate was diluted with ether, washed with $NaHCO_3$ solution and NaCl solution, dried over $MgSO_4$, and vacuum distilled to give 16.4 g. (74%) of nitroisobutene, b.p. 50-58°C and 10 torr. Analysis by pmr, and gas chromatography - mass spectrometry showed the material to be a mixture of 3-nitro-2-methyl-propene (20%) and 1-nitro-2-methylpropene. Fractionation three times through a 24 cm vacuum-jacketed vigreaux column yielded about 5 g. (b.p. 74° at 28 torr.) of 1-nitro-2-methylpropene which pmr and GC-MS showed to contain less than 1% of the 3-nitro-2-methyl-propene.

VI. RECOMMENDATIONS

It is recommended that work be continued in both of the synthetic areas in which investigations were initiated. Attempts to synthesize hexanitrotolane and trinitrophenylacetylene should be pursued. Due to time constraints, several promising synthetic routes were not attempted and should be investigated. Also, several of the reactions found to be unsuccessful for the preparation of the desired compounds should be more fully investigated in that they may be useful under different reaction conditions.

Additional synthetic work is also needed in the area of nitroalkenes. The model compound, 1-nitro-2-methylpropene, was prepared, and is available for a laboratory investigation of its thermal decomposition. As part of this project, isotopically labeled samples of 1-nitro-2-methylpropene are needed to complete the study. The synthetic route developed to synthesize 1-nitro-2-methylpropene can be utilized to prepare deuterium labeled samples and ^{15}N labeled samples.

REFERENCES

1. Shipps, K. G. and L. A. Kaplan, "Reactions of α-Substituted Polynitrotoluenes," J. Org. Chem., 31, 857 (1966).

2. Dr. John S. Wilkes, personal communication.

3. Stephens, R. D. and C. E. Castro, "The Substitution of Aryl Halides with Cuprous Acetylides," J. Org. Chem., 28, 3313 (1963).

4. Blatt, A. H. and N. Grass, "Replacement of Halogen by Hydrogen in Nitro Aryl Halides," J. Org. Chem., 22, 1046 (1957).

5. March, Jerry, Advanced Organic Chemistry, (McGraw-Hill, New York, 1977), p. 935

6. Lalezari, I., A. Shafice, and M. Yalpani, "A Simple New Synthesis of Arylalkynes," Angew. Chem. internat. Edit., 9, 464 (1970).

7. Hassner, A., J. E. Kropp, and G. J. Kent, "Addition of Nitryl Iodide to Olefins," J. Org. Chem., 34, 2628 (1969).

8. Corey, E. J. and H. Estreicher," A New Synthesis of Conjugated Nitro Cyclic Olefins," J. Am. Chem. Soc , 100, 6294 (1978).

9. Dennis, W. H. D. H. Rosenblatt, W. G. Blucher, and C. L. Coon, "Improved Synthesis of TNT Isomers," J. Chem. Egr. Data, 20, 202 (1975).

10. Gay-Lussac, A. and H. Ficheroulle, "Preparation of 2,4,6-Trinitro-ethylbenzene", Mem. poudres, 36, 71 (1954).

11. Adolph, H. G., J. C. Dacons, and M. J. Kamlet, "Polynitroaromatics," Tetrahedron, 19, 801 (1963).

12. Midland, M. M., "Preparation of Monolithium Acetylide in Tetra-hydrofuran," J. Org. Chem., 40, 2250 (1975).

13. Descotes, G., Y. Bahurel, M. Baurillot, G. Pingeon, and R. Rostaing, "Nitroolefins. Etude Spectrale des Configurations et Conformations," Bull. Soc. Chim. Fr., 282 (1970).

14. Lambert, A. and A. Lowe, "Aliphatic Nitro-compounds", J. Chem. Soc., 1517 (1947).

1982 USAF-SCEEE SUMMER FACULTY RESEARCH PROGRAM

Sponsored by the

AIR FORCE OFFICE OF SCIENTIFIC RESEARCH

Conducted by the

SOUTHEASTERN CENTER FOR ELECTRICAL ENGINEERING EDUCATION

FINAL REPORT

THE EFFECT OF CERTAIN IMAGE DATA REDUCTION TECHNIQUES ON EDGE QUALITY

Prepared by:	Dr Donald J Healy
Academic Rank:	Assistant Professor
Department and University:	School of Electrical Engineering Georgia Institute of Technology
Research Location:	Air Force Armament Laboratory Guided Weapons Division Electro-Optical Terminal Guidance Branch
USAF Research Colleague:	Lt Col Lawrence A Ankeney
Date:	August 18, 1982
Contract No:	F49620-82-C-0035

THE EFFECT OF CERTAIN IMAGE DATA REDUCTION TECHNIQUES ON EDGE QUALITY

BY

DONALD J. HEALY

ABSTRACT

The purpose of this research is to ascertain ways in which preliminary feature extracting calculations can be reduced and evaluate the effect of these reductions on pertinent feature information. Techniques are implemented which map an original intensity image into a smaller image before applying edge detecting (e.g. Kirsch) operators. The effect on edge content is quantitatively evaluated. It is shown that straightforward application of standard edge detectors to reduced images does not fully extract the edge information that is available. Suggested areas for further research include:

1. Design of edge detectors which incorporate knowledge of the image reducing technique used; and

2. Implementation of feature extracting algorithms using table look-up of pre-calculated output feature information.

I. INTRODUCTION:

The development of algorithms to extract informational features from imagery is an area of active research. These algorithms enable computerized devices to automatically identify objects in the field of view of a sensor. The Air Force Armament Laboratory (AFATL) is interested in automatic target identification and weapon guidance. An important commercial application is controlling robot arms on assembly lines.

Practical implementation of feature extracting algorithms is constrained by size, weight, power, and data throughput requirements imposed by the particular application. These constraints limit the amount of computation that can be accomplished on the input image data. In order to allow more of the available computational time and hardware to be devoted to sophisticated and computationally intensive feature classification routines, it is desirable to minimize the preliminary feature extracting calculations. The purpose of this research is to ascertain ways in which these preliminary calculations can be reduced and evaluate the effect of these reductions on pertinent feature information.

The approach to the problem of reducing calculations considered here would map the original image into a smaller image before applying feature extracting algorithms. Since edges in an image contain much of the information necessary to classify objects, edge detectability and edge quality are used in this work as measures of feature information loss.

II. OBJECTIVES:

1. To develop techniques for reducing the computational load required to implement feature extracting algorithms; and

2. To implement quantitative methods for evaluating spatial degredation caused by these image reducing techniques.

III. IMAGE REDUCTION TECHNIQUES IMPLEMENTED:

Several algorithms were implemented to reduce the number of image pixels (picture elements) on which feature extracting algorithms (specifically, edge detectors) might operate. In this work the techniques used achieve a 4:1 reduction in image data by effectively mapping each 4x4 block into a 2x2 block as depicted in Figure 1 and described below:

Method 1:

Sample odd-numbered columns in odd-numbered rows.

$A=X_{11}$; $B=X_{13}$; $C=X_{31}$; $D=X_{33}$

Method 2:

Sample the four corners of each 4x4 block.

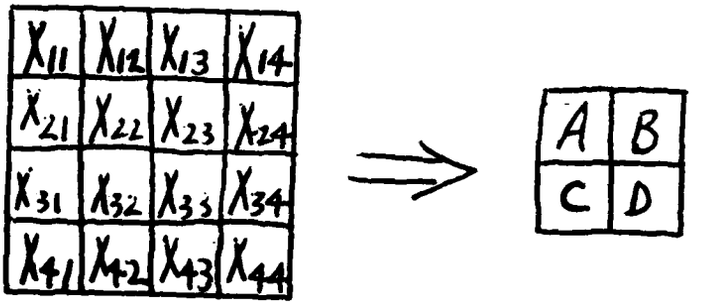


Figure 1: Blocks for Defining Image Reducing Methods

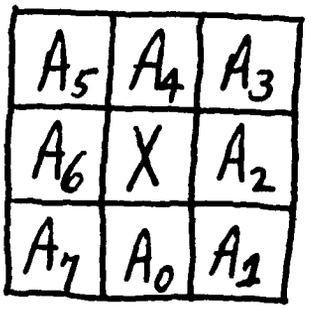


Figure 2: Neighborhood for Defining Kirsch

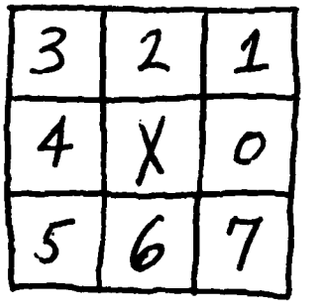


Figure 3: Neighborhood for Defining Local Edge Coherence Evaluator

$A=X_{11}$; $B=X_{14}$; $C=X_{41}$; $D=X_{44}$

Method 3:

Average non-overlapping 2x2 subblocks to get a single pixel for each.

$A=.25(X_{11}+X_{12}+X_{21}+X_{22})$

$B=.25(X_{13}+X_{14}+X_{23}+X_{24})$

etc.

Method 4:

Replace each 4x4 block with 1 of 9 overlapping contiguous 2x2 subblocks. For example, three possibilities are:

$A=X_{12}$; $B=X_{13}$; $C=X_{22}$; $D=X_{23}$

or

$A=X_{23}$; $B=X_{24}$; $C=X_{33}$; $D=X_{34}$

or

$A=X_{33}$; $B=X_{34}$; $C=X_{43}$; $D=X_{44}$.

The 2x2 subblock is chosen which maximizes the sum of gradient magnitudes defined by

$$\text{SUMGRAD} = |A-B| + |C-D| + |A-C| + |B-D| + |A-D| + |B-C|.$$

Method 5:

Replace each 4x4 block by the corners of 1 of 4 overlapping contiguous 3x3 subblocks. For example, two possibilities are:

$A=X_{11}$; $B=X_{13}$; $C=X_{31}$; $D=X_{33}$

or

$A=X_{22}$; $B=X_{24}$; $C=X_{42}$; $D=X_{44}$.

The 3x3 subblock is chosen whose corners maximize the resulting sum of gradient magnitudes as defined for Method 4.

Method 6:

Represent each of the four 2x2 quadrants of a 4x4 block by a single pixel. For each quadrant the representative pixel value is obtained by selectively averaging only those pixels in the quadrant that are on the same side of the dominant detected edge (passing through the 4x4 block) as the corner pixel in that quadrant. Here the dominant edge is traced and defined as follows:

The edge enters the 4x4 block along the boundary between 2 of the 12 outer pixels which has the largest gradient magnitude. For example, if $|X_{24}-X_{34}|$ is larger than $|X_{34}-X_{44}|$ $|X_{44}-X_{43}|$ etc, then the edge enters horizontally going from right to left between pixels X_{24} and X_{34}. The edge then continues to grow along a path which crosses the largest gradient magnitudes at each intersection, excluding growth in a direction which would cross itself. Continuing the above example, the edge might be traced downward between X_{33} and X_{34}, then left between X_{33} and X_{43}, then upward between X_{32} and X_{33}. At that point the edge would be forced to continue upward or left, excluding the direction right which would cross itself, and excluding the downward direction which retrace itself. Eventually the edge exits the 4x4 block and the dominant edge is completely defined.

Methods 1-3 contain no overt effort to retain edge information while Methods 4-6 are intended to do so. Methods 1 and 2 simply sample 1 out of 4 of the available pixels, ignoring the information contained in the other 3/4 of the pixels. Methods 4 and 5 selectively smaple pixels so as to preserve the dominant gradient information in a 4x4 block. Method 3 partially incorporates the information from all pixels by systematically averaging 2x2 blocks of pixels; this tends to blur and weaken edges that run through a 2x2 averaged block. Method 6 tries to prevent averaging across dominant edges.

IV. THE EDGE DETECTORS:

Two edge detectors were implemented for this study:

1. Kirsch operator: Determines a pixel's edge value based on a 3x3 neighborhood [1, 2]. The specific implementation used here is defined using Figure 2 as

$$X = \frac{1}{15} \max_{i=0}^{7} \left| 3(A_i+A_{i+1}+A_{i+2}+A_{i+3}+A_{i+4}) - 5(A_{i+5}+A_{i+6}+A_{i+7}) \right|$$

Where the subscripts are evaluated modulo 8. For each pixel this operator calculates gradients in 8 different directions and sets the pixel equal to the largest gradient magnitude. For an ideal edge this implementation results in a Kirsch output magnitude equal to the edge height.

2. Robert's operator: Determines a pixel's edge value based on a 2x2 neighborhood [1-3]. The specific implementation used here is defined using the notation of Figure 1 as

$$A = \max(|A-D|, |B-C|)$$

For each pixel this operator estimates the maximum diagonal gradient magnitude at a point a half unit to the right and a half unit down.

The Kirsch operator is generally considered superior to the Robert's operator. For this reason most of the work contained herein is based on the Kirsch edge detector using 3x3 neighborhoods.

V. EDGE EVALUATION METHODS:

It is difficult to find edge evaluation techniques applicable to real-world imagery. This is due in part to the inability to clearly define the actual location of edges in an image and thus form a reliable basis for comparison. However, a recent paper by Kitchen and Rosenfeld [4] proposes an edge quality evaluation based on edge coherence incorporating connectedness, thinness, and gradient directions as seen by 3x3 neighborhoods. Their edge evaluation technique is used here in two ways:

1. To evaluate the coherence of edges detected using the Kirsch edge detector; and

2. As a basis for thresholding of an edge image to estimate edge locations.

The local edge coherence evaluation technique described in (4) requires two types of input data:

1. A binary edge image obtained by globally thresholding an edge image such that pixels below the threshold are set to zero and the others are set to some convenient positive value (in this case the Kirsch operator generates the edge image); and

2. The gradient direction resulting in the Kirsch output value for each pixel.

Each non-zero pixel in the binary image is considered to be an edge pixel, and the corresponding 3x3 neighborhood surrounding an edge pixel is called an edge neighborhood. The edge evaluating calculations for an edge pixel will be illustrated by the following example using Figure 3.

Let d_x be the gradient direction resulting in the Kirsch output value for the edge pixel being evaluated. Similarly let d_0, d_1, ... , d_7 be the gradient directions for the 8 neighbors of X. For this example assume d_x = PI/2 radians (i.e. the gradient is positive going upward). To evaluate edge connectedness, the best continuations to the left and right of the gradient are sought from neighbors 3,4,5 and 1,0,7, respectively. The quality of the left and right continuations for neighbor K are defined by

$$L(K) = \begin{cases} a(d_x, d_k) \cdot a\left(\frac{k\pi}{4}, d_x + \frac{\pi}{2}\right) & \text{if neighbor K is an edge pixel,} \\ 0 & \text{otherwise} \end{cases}$$

$$R(K) = \begin{cases} a(d_x, d_k) \cdot a\left(\frac{k\pi}{4}, d_x - \frac{\pi}{2}\right) & \text{if neighbor K is an edge pixel,} \\ 0 & \text{otherwise} \end{cases}$$

where

$$a(s, t) = \frac{\pi - |s-t|}{\pi}$$

with angles s and t defined such that $|s-t| \leq$ PI.

The above definitions result in values for L(K) and R(K) in the range $[0,1]$. Of the three neighbors (3,4,5) left of the gradient, the one with the highest value of L is chosen as the left edge continuation. Similarly the best right continuation is chosen from neighbors 1, 0, and 7. Ideally, in this example, neighbors 4 and 0 would be chosen and would have Kirsch output directions $d_4=d_0=d_x$, resulting in $L(4) = L(0) = 1$. A continuation measure C for the neighborhood is then defined as the average of the highest values of L and R.

From (4): "The thinness measure T for the neighborhood is computed as that fraction of the remaining six pixels of the neighborhood which are non-edge pixels. This will range from one for a perfectly thin edge, down to zero for a very blurred edge."

The overall edge coherence value for the edge pixel being evaluated is defined as

$$E = wC + (1-w)T$$

where w is a weighting factor in the interval $[0,1]$. In [4] w=0.8 was selected as the best compromise between thinness and continuity. In this implementation the above definition of E is modified slightly by setting E=0 if C=0. This forces E to be zero for isolated edge pixels. For an ideal edge pixel on an edge one pixel wide with good left and right continuity and consistent gradient directions E=1.

In addition to providing an edge quality measure, the edge coherence value E for each pixel in an edge image can itself be thresholded to give a binary image. Pixels with value E greater than the threshold are considered edge pixels. This global thresholding of the "E image" is equivalent to locally thresholding the edge detector output image to estimate edge locations. Having thus extracted edge locations allows edge output comparisons which separately treat edge and non-edge pixels.

One such technique used here is a selective mean-square error comparison which calculates the mean-square difference between a reference and test edge image averaged only over those edge pixels identified by thresholding E in the reference image. Global mean-square error comparisons based on all output pixels generated by the edge detectors are also used.

The last edge comparison technique implemented uses an approach from signal theory which calculates the probabilities of edge detection P_D and false-alarm P_F. These calculations use binary reference and test images generated by globally thresholding the edge detector output images. The resulting edge pixels are compared to give P_D and P_F where:

P_D is the fraction of edge pixels in the reference image that are correctly classified as edge pixels in the test image:

and

P_F is the fraction of non-edge pixels in the reference image that are incorrectly classified as edge pixels in the test image.

VI. EVALUATION OF IMAGE REDUCING TECHNIQUES:

The techniques described in Section III were evaluated using passive forward-looking infrared (FLIR) image data. The original image size is 112 lines with 120 pixels per line. Intensity resolution is 6-bit (0-63).

Figure 4 was obtained by implementing image reducing Methods 1-6 and duplicating each reduced image pixel (each pixel becomes a 2x2 block) to expand the reduced image to its original size for comparison with the original image. Table 1 shows the result of a simple mean-square error (MSE) comparison. The minimum MSE in the intensity domain is achieved using Method 3. This result is theoretically guaranteed since Method 3 represents each 2x2 block by its local (conditional) mean [5, p. 216]. However, as shown below, there is no theoretical guarantee that lower MSE in the intensity domain guarantees lower MSE or better edges in the edge output domain.

Figure 5 was obtained by performing Kirsch edge detection on the reduced images and expanding the result. Alternatively, Figure 6 was obtained by performing Kirsch edge detection on the expanded images of Figure 4. Figure 5 is representative of the loss of resolution that occurs by simply applying the Kirsch edge detector to a reduced image. Since the number of pixels operated on by the Kirsch operator is reduced, this technique has the desired quality of reducing the number of calculations used to extract edges. However, since the resolution in Figure 6 seems generally superior to that in Figure 5 (especially in areas where edges are close together), the edge information available in

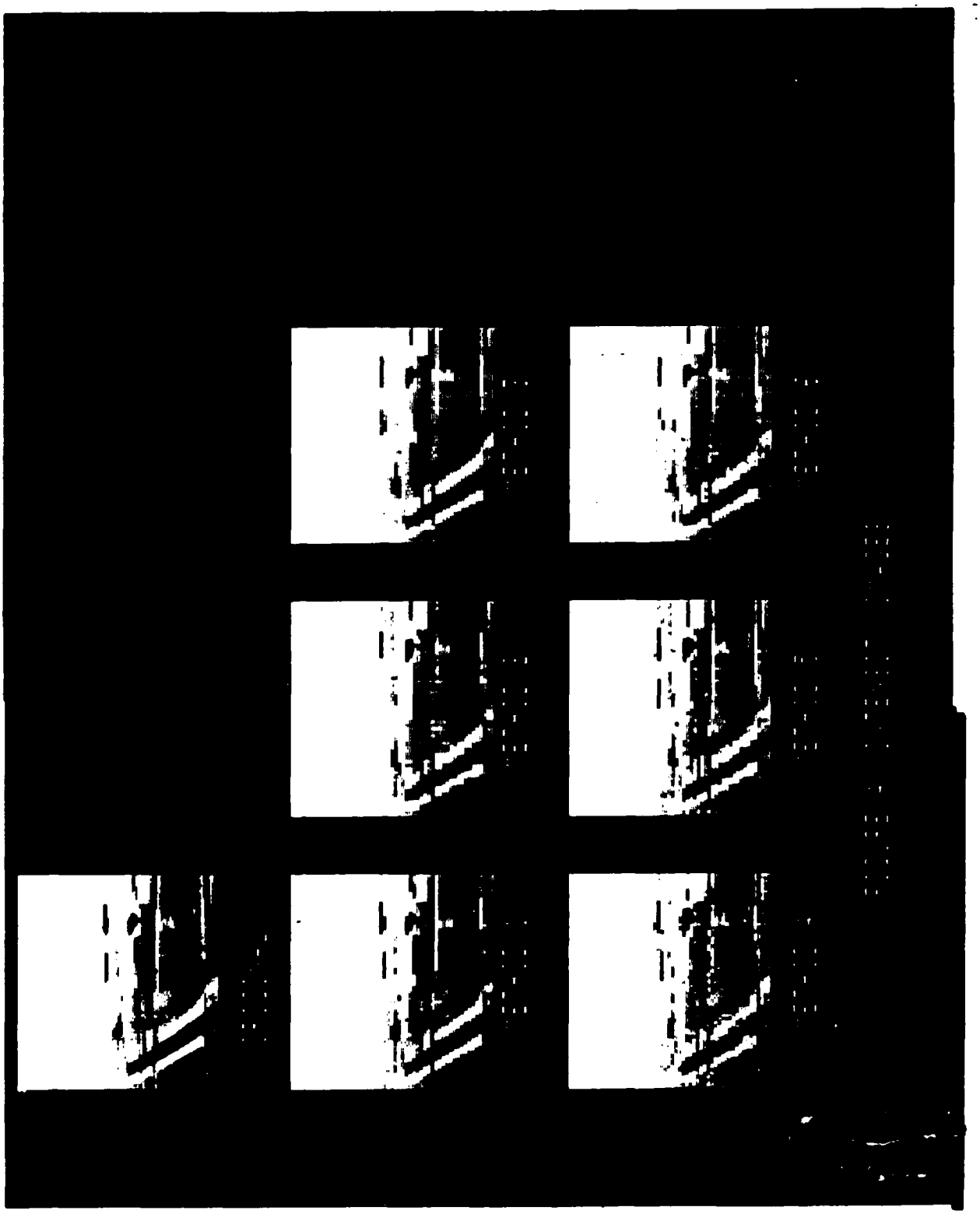


TABLE 1

QUANTITY CALCULATED	METHOD NUMBER 1	2	3	4	5	6
Intensity MSE:	1.23	1.36	0.78	2.03	1.54	1.11
Global Edge MSE:						
Figure 5:	1.90	2.10	1.38	1.95	2.43	1.79
Figure 6:	1.03	1.28	0.75	1.42	1.47	0.99
Figure 7:	2.41	2.76	1.81	3.27	3.53	2.40
Selective Edge MSE:						
Figure 5:	3.65	4.91	2.91	3.21	4.45	4.02
Figure 6:	2.78	4.21	2.12	3.73	3.62	3.00
P_D:						
Figure 5:	.800	.793	.777	.820	.888	.804
Figure 6:	.762	.657	.700	.719	.812	.706
P_F:						
Figure 5:	.165	.162	.139	.177	.214	.154
Figure 6:	.074	.070	.038	.106	.124	.055

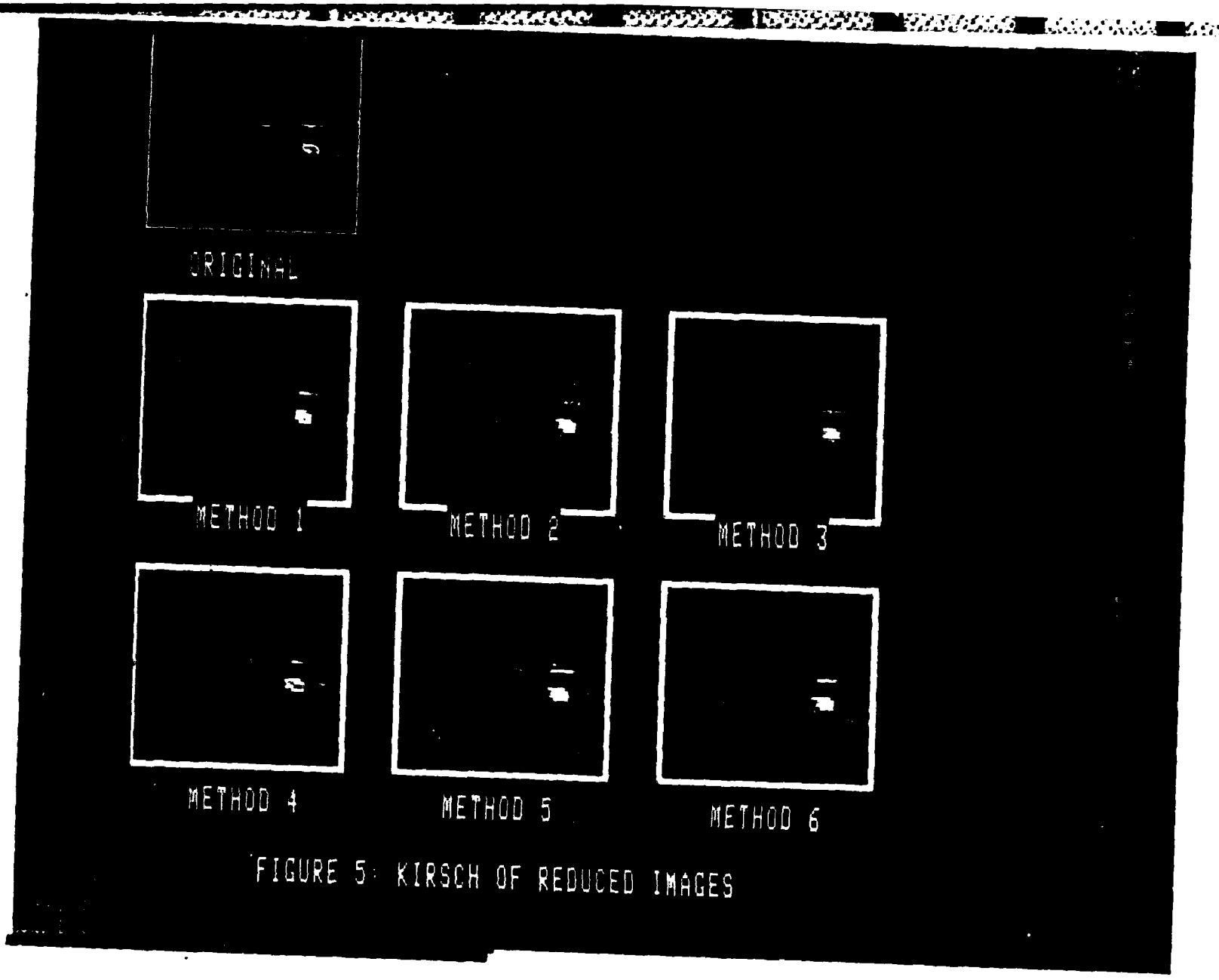


FIGURE 5: KIRSCH OF REDUCED IMAGES

the reduced image does not seem to be fully extracted by applying the Kirsch operator to the reduced image. One reason for this is that the Kirsch operator generates edge outputs that are two pixels wide, yielding edge outputs that are four pixels wide after expanding the Kirsch output. This tends to smear close edges so they are indistinguishable. The superiority of Figure 6 is especially evident using Methods 1 and 3. One possible explanation is that the technique of duplicating pixels to obtain Figure 4 may be a nearly optimal inverse to Methods 1 and 3 for reconstructing the original intensity image so as to preserve edges. If so, then the results for Methods 1 and 3 in Figure 6 in effect incorporate knowledge of the reducing technique which the results in Figure 5 do not. These subjective comparisons of edge quality will be quantitatively supported later in this section.

Because of the wide edge outputs generated using the Kirsch operator, the Robert's operator was applied to the reduced images. The expanded edge outputs are shown in Figure 7. The thinner Robert's edge outputs of Figure 7 are visually more pleasing than the Kirsch outputs of Figure 5. The reported superiority of the Kirsch versus the Robert's detector is not evident in the original edge output images.

Global MSE calculations for the edge images in Figures 5-7 are also given in Table 1. Comparisons for Figures 5 and 6 are based on the Kirsch output for the original image in those figures. Similarly the Robert's output is the reference used in Figure 7. The non-representative high valued border edge output pixels are excluded from all comparisons. As seen in Table 1, the best global edge MSE results are obtained by Methods 3 and 6 which tend to reduce noise since they

FIGURE 6: KIRSCH OF EXPANDED IMAGES

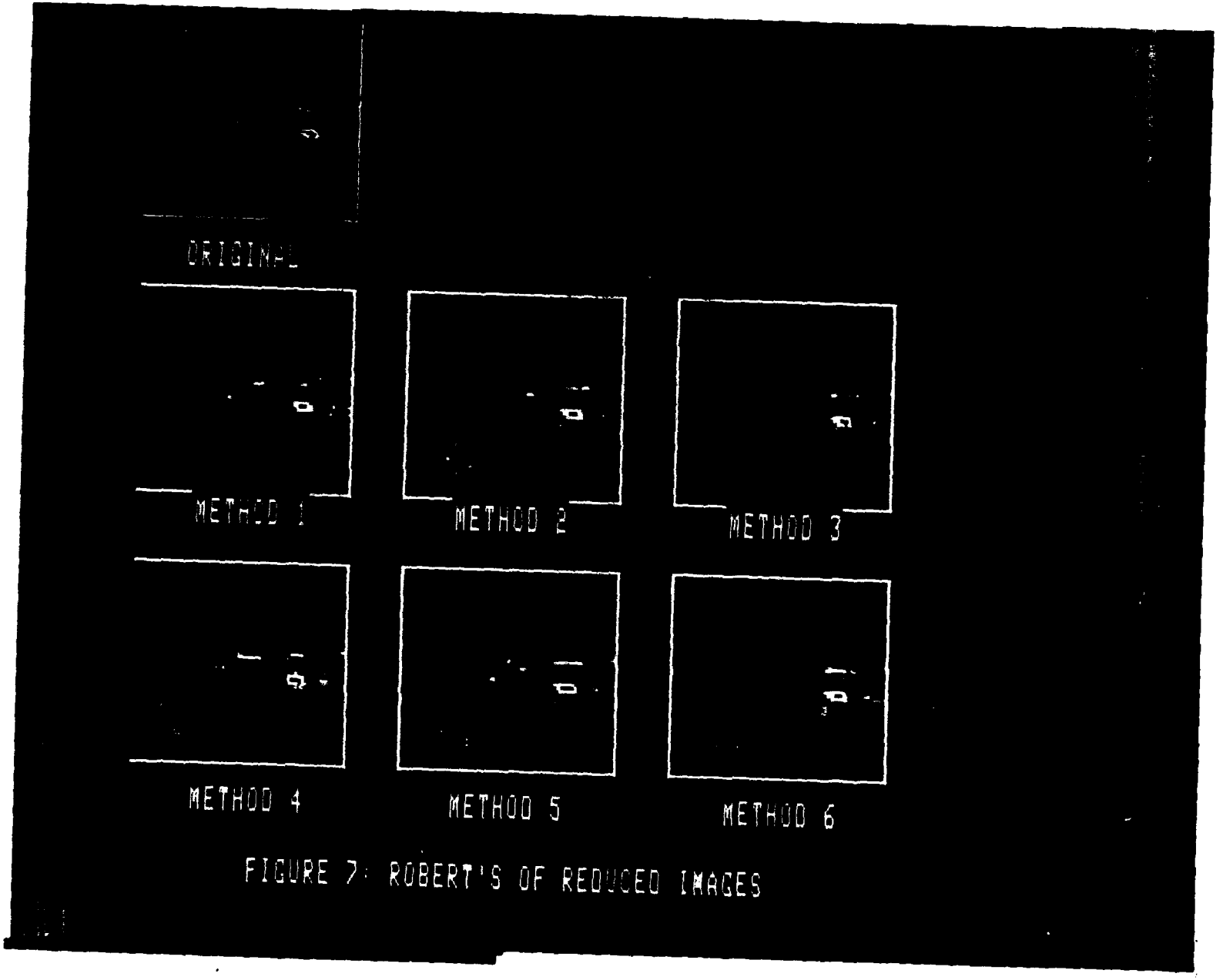


FIGURE 7: ROBERT'S OF REDUCED IMAGES

are averaging techniques. The worst results are obtained by the more computationally complex Methods 2, 4, and 5. Methods 4 and 5 tend to emphasize noise since they preserve the largest gradients. Methods 1 and 2 are simply periodic sampling techniques.

Selective MSE comparisons for the Kirsch outputs in Figures 5 and 6 are also accomplished as described in Section V. However, rather than generate a single edge coherence value E for each pixel based on a single thresholded Kirsch output image, visually better results were obtained by calculating E for Kirsch images using global thresholds from 3 through 9, and retaining the largest value of E achieved for each edge pixel. This "maximum E image" was then globally thresholded at 0.47 to yield an edge location mask. This maximum E image mask along with E image masks based on single Kirsch thresholds are shown in Figure 9 for w=0.4. Figure 8 shows the thresholded Kirsch images upon which E values are based. The thresholded maximum E image (shown in Figure 9) based on Kirsch thresholds 3-9 appears superior to any individual Kirsch thresholded mask in Figure 8. Selective edge MSE calculations based on this mask are given in Table 1.

Figure 10 shows the result of thresholding the Kirsch outputs (thresh = 3) shown in Figure 6. These binary images were used to calculate P_D and P_F as described in Section V. Similar calculations were done on the Kirsch outputs shown in Figure 5. Results are included in Table 1.

As described in Section V, the edge coherence criterion of Kitchen and Rosenfeld [4] was used to evaluate the quality of Kirsch edge

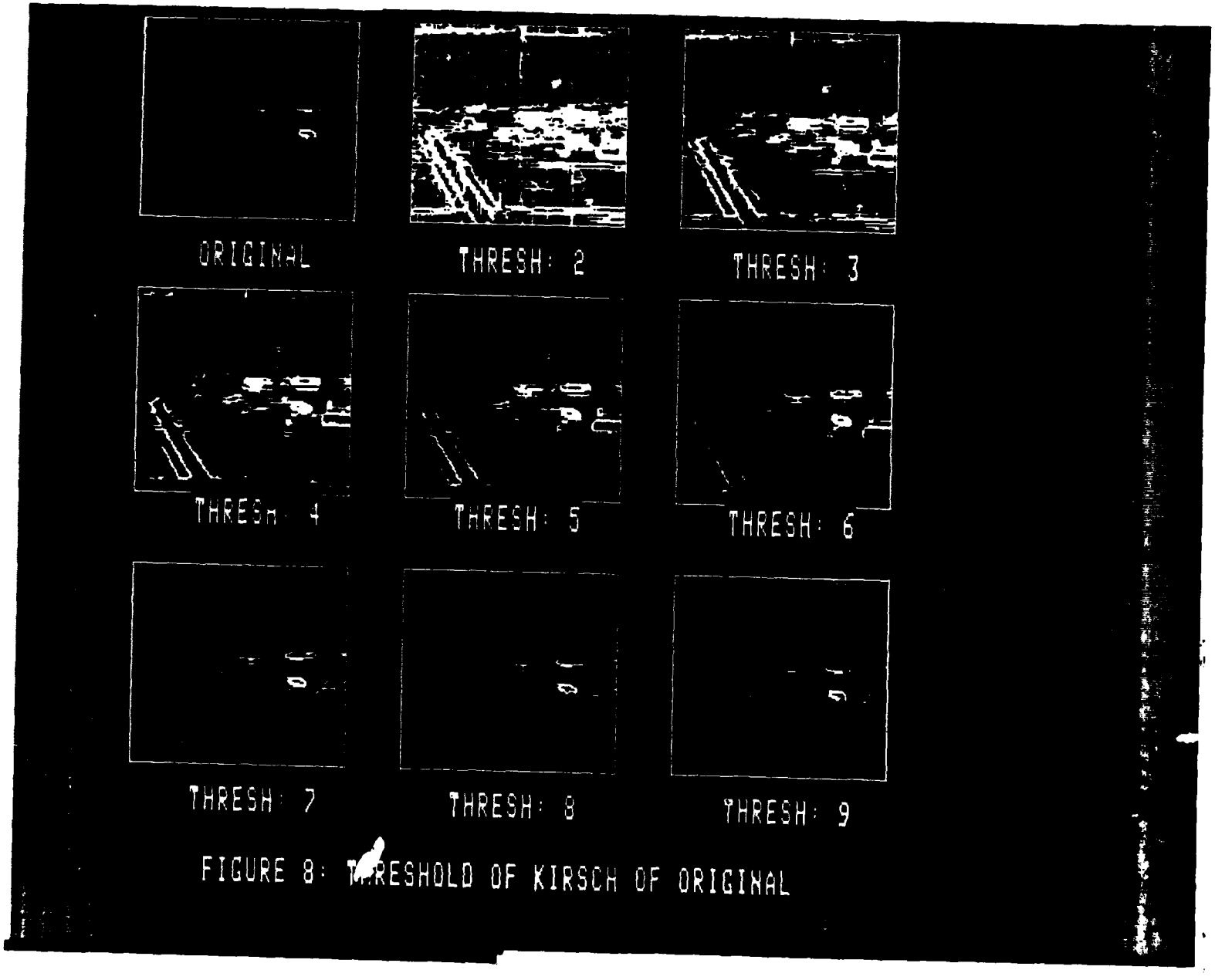
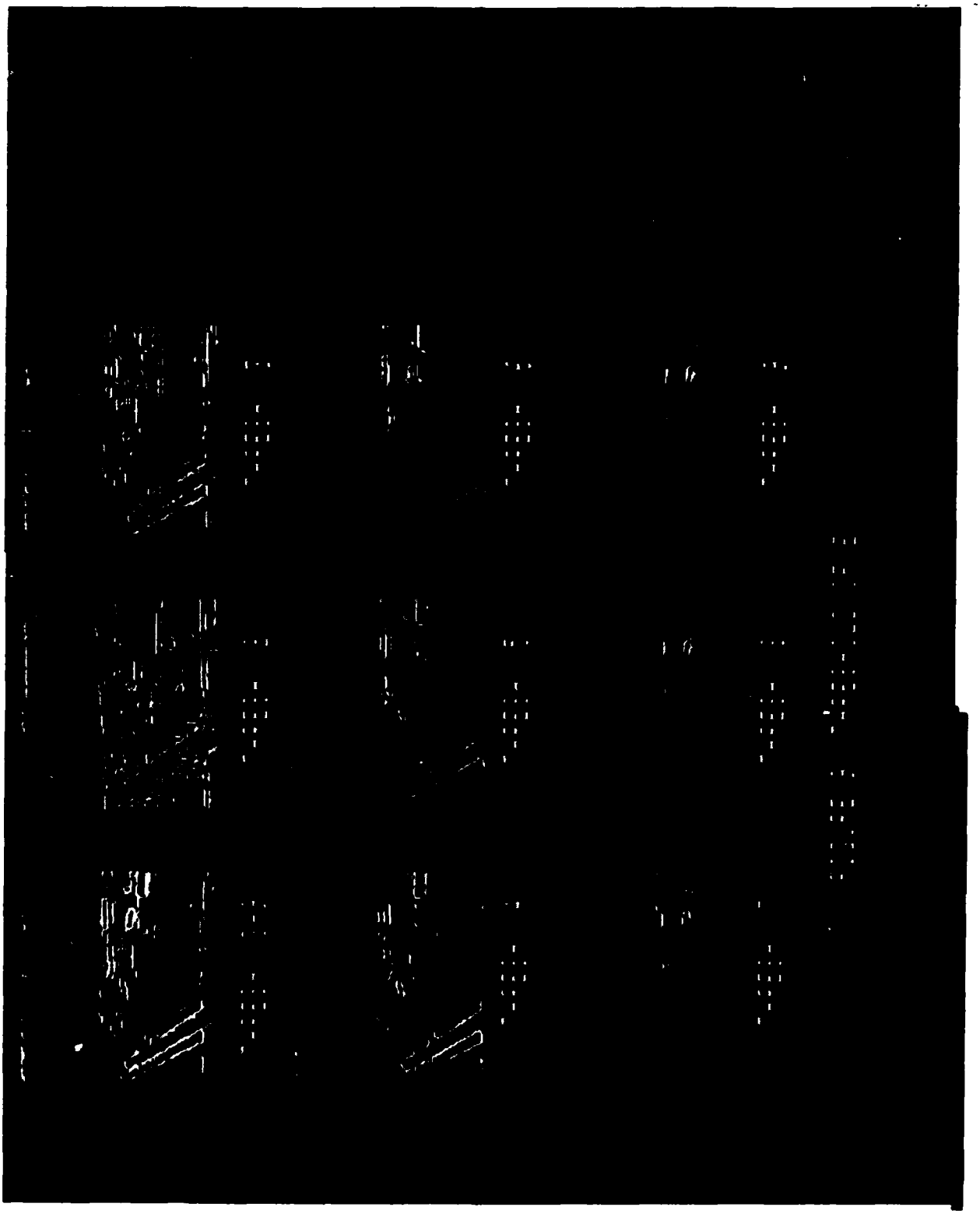


FIGURE 8: THRESHOLD OF KIRSCH OF ORIGINAL



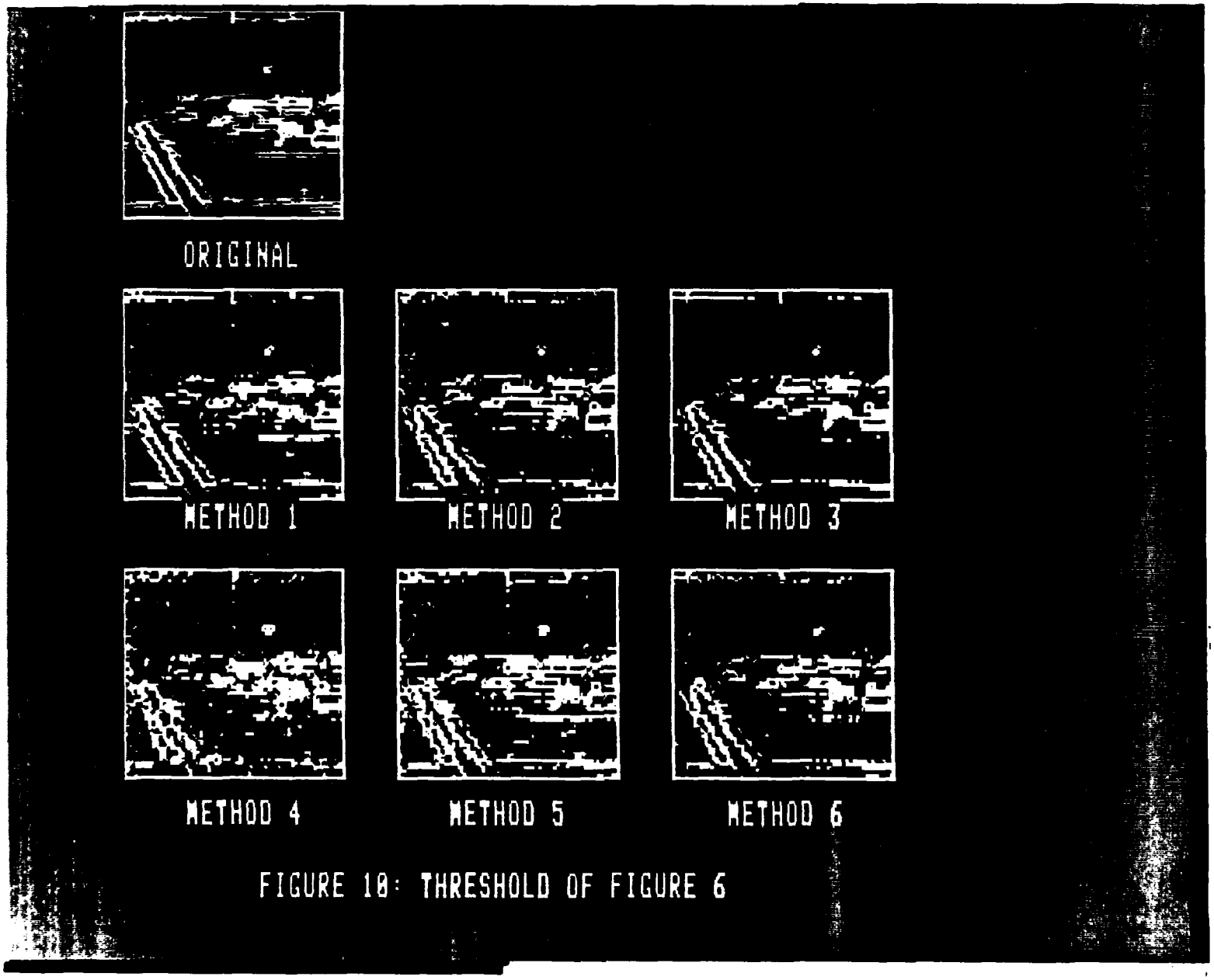


FIGURE 10: THRESHOLD OF FIGURE 6

outputs. The quality of the Kirsch output for a given image is calculated as the average value of E averaged over all edge pixels in the image. The number of edge pixels depends on the threshold used on the Kirsch output (See Section V). From Figure 8, Kirsch thresholds of 3 and 4 were selected as reasonably good. The resulting average edge quality values are given in Table 2 for w=0.4 and w=0.8. The edge quality of the original exceeds that of the processed images, lending creedence to this evaluation technique.

Overall, the best results were obtained using the simple averaging of Method 3. As mentioned in Section III, this does tend to weaken edges which run through averaged blocks. This effect can be seen in Figure 10 by comparing Methods 1, 3, and 6 at the rightmost edge of the runway portion of the image. Selective averaging (Method 6) has a stronger edge response than Method 3, while Method 1 (which does not average) has the strongest response.

Method 3, which minimizes MSE in the intensity domain, achieved the best overall performance. However, lower MSE in the intensity domain does not guarantee better edges. For example, Method 4 has a much higher MSE than Method 5 in the intensity domain, but overall Method 4 performed better than Method 5 in the edge domain.

VII. CONCLUSIONS AND RECOMMENDATIONS:

The primary emphasis of this work has been to implement techniques for reducing 4x4 blocks of image pixels to 2x2 blocks, and to quantitatively evaluate the effect on edge content. It is evident that

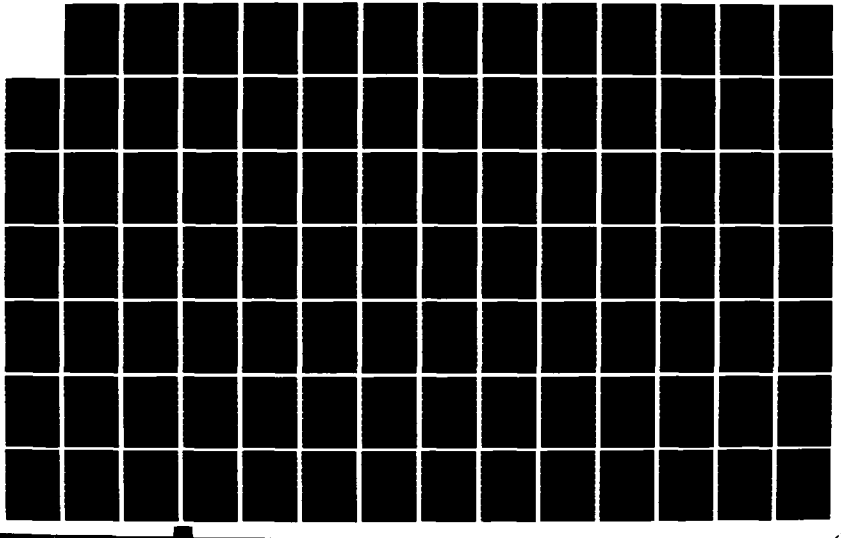
TABLE 2

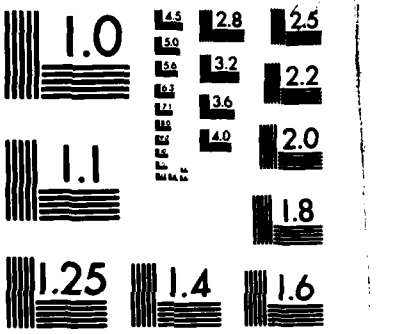
Average Edge Coherence Value (E)

	Kirsch Threshold - w value			
	3-.4	4-.4	3-.8	4-.8
Original:	.617	.642	.762	.768
Kirsch of Reduced Images:				
Method 1:	.590	.609	.741	.727
Method 2:	.563	.594	.731	.718
Method 3:	.607	.641	.755	.746
Method 4:	.558	.604	.692	.700
Method 5:	.559	.603	.728	.725
Method 6:	.594	.628	.747	.736
Kirsch of Expanded Images:				
Method 1:	.550	.573	.730	.730
Method 2:	.563	.590	.719	.736
Method 3:	.565	.574	.749	.732
Method 4:	.524	.555	.690	.681
Method 5:	.544	.577	.731	.736
Method 6:	.560	.599	.722	.741

AD-A130 769 USAF/SCEEE SUMMER FACULTY RESEARCH PROGRAM RESEARCH REPORTS VOLUME 1.. (U) SOUTHEASTERN CENTER FOR ELECTRICAL ENGINEERING EDUCATION INC S.. 10/1

UNCLASSIFIED W D PEELE ET AL. OCT 82 AFOSR-TR-83-0613 F/G 5/1 NL





MICROCOPY RESOLUTION TEST CHART
NATIONAL BUREAU OF STANDARDS-1963-A

the straightforward application of standard edge detectors to the reduced images does not fully extract the edge information that is available. This is demonstrated by the substantially better results achieved by applying the Kirsch operator to re-expanded versions of reduced images. Therefore it would seem appropriate to expand the scope of image reducing research efforts to include the design of edge detectors which incorporate knowledge of the image reducing technique used. The crux of this design problem will be to design such edge detectors without increasing the number of calculations per pixel (compared to standard edge detectors) to the point where the advantage of reducing the image is lost.

A second research area worth pursuing is the implementation of feature extracting algorithms using table look-up of pre-calculated output feature (e.g. edge) information. The idea is to reduce the number of calculations done in real time by fitting the pixel values used to calculate feature output values to one of a manageable number of patterns, and simply looking up the stored output for that pattern. Mapping a set of pixel values into a pattern could be accomplished as in [6] by normalizing each set to yield values from 0 to 1, and choosing the pattern with the least normalized mean-square difference. Some preliminary work on this idea has been accomplished in this research effort. The indications are that more patterns would be required to achieve good edge detection than were needed for the vehicle guidance work in [6]. Two possible implementations are:

1. Look up Kirsch outputs for each individual pixel based on the pattern of its 8 neighbors; or

2. Look up the Kirsch output for a 3x3 block of pixels based on the pattern formed by a 5x5 block of pixels surrounding it.

More generally, the Kirsch output for an NxN block of pixels could be based on a pattern of (N+2)x(N+2) pixels.

ACKNOWLEDGEMENTS

I thank the Air Force Systems Command, Air Force Office of Scientific Research, and the Southeastern Center for Electrical Engineering Education for providing this opportunity to do full-time research for a 10-week period. My thanks also to the personnel at the Air Force Armament Laboratory (Eglin AFB, Florida) for their hospitality and participation in the Summer Faculty Research Program, especially the supportive individuals in the Image Processing Laboratory, whose guidance helped to minimize the time necessary to become conversant with the operating system and peripherals. I also gratefully acknowledge the financial support of the Georgia Tech Foundation.

I especially thank Lt Col Larry Ankeney for suggesting this area of research and for his collaboration and guidance, and Mr Neal Urquhart for his hospitality.

REFERENCES

1. William K. Pratt, Digital Image Processing, John Wiley and Sons, New York, 1978.

2. Ikram E. Abdou and William K. Pratt, "Quantitative Design and Evalution of Enhancement/Thresholding Edge Detectors," Proc. IEEE, Vol 67, May 1979.

3. Azriel Rosenfeld and Avinaxh C. Kak, Digital Picture Processing, Academic Press, New York, 1976.

4. Les Kitchen and Azriel Rosenfeld, "Edge Evaluation Using Local Edge Coherence," IEEE Trans. Sys. Man and Cyb., vol, SMC-11, Sept 1981.

5. Athanasios Papoulis, Probability, Random Variables, and Stochastic Processes, McGraw-Hill, New York, 1965.

6. Bruce J. Berger and Rafael M. Inigo, "Block Stored Pattern Coding of Video Signals."

1982 USAF-SCEEE SUMMER FACULTY RESEARCH PROGRAM

Sponsored by the

AIR FORCE OFFICE OF SCIENTIFIC RESEARCH

Conducted by the

SOUTHEASTERN CENTER FOR ELECTRICAL ENGINEERING EDUCATION

FINAL REPORT

EVALUATION OF GAS CHROMATOGRAPHIC METHODS FOR DETERMINING TRACE LEVELS OF TRICHLOROETHYLENE IN WATER

Prepared by	Ervin Hindin
Academic Rank	Professor
Department and University	Department of Civil and Environmental Engineering Washington State University
Research Location	Environmental Chemistry Laboratory, Environmental Chemistry Branch, Environics Division, Air Force Engineering and Services Center
USAF Research	Major R. Channell
Date	August 20, 1982
Contract No.	F 49620-82-C-0035

EVALUATION OF GAS CHROMATOGRAPHIC METHODS FOR DETERMINING TRACE LEVELS OF TRICHLOROETHYLENE IN WATER

by

Ervin Hindin

ABSTRACT

An evaluation is made of gas chromatographic methods for the analysis of trichloroethylene in water. It is shown that electron capture detection is more sensitive than flame ionization detection. Either method of detection requires prior sample enrichment and cleanup. Static head space and purge and trap techniques can be used for enrichment and cleanup. A gas-liquid chromatographic phase of 1% SP-1000 on Carbopack-B shows excellent partitioning characteristics for trichloroethylene in the presence of other volatile organic compounds. Based on the evaluation, sample enrichment, cleanup, and gas-liquid chromatographic systems are recommended. Aqueous trichloroethylene standards and a stock solution of trichloroethylene dissolved in methanol at 4°C showed no change in concentration for up to 20 days of storage. An automated gas chromatograph with semiautomated purge and trap sampler and microprocessor data system is recommended for use by operators with limited training.

ACKNOWLEDGEMENT

The author wishes to thank the Air Force Engineering and Services Center, the Air Force Office of Scientific Research, and the Southeastern Center for Electrical Engineering Education for providing him with the opportunity to spend a worthwhile and interesting summer at the laboratory of the Environmental Chemistry Branch of the Environics Division. He would like to acknowledge the laboratory for its hospitality and for providing excellent working conditions.

The author also acknowledges the valuable assistance of Mr. T. Stauffer and Dr. D. Stone in executing this study. Finally, he wishes to thank Major R. Channell and Major S. Termaath for suggesting this area of study.

INTRODUCTION

Volatile synthetic organic compounds, termed VOC, of which 1, 1, 2-trichloroethylene is a member, do not occur naturally. The organic compound cited, more commonly referred to as trichloroethylene, has been used as an industrial and commercial metal degreaser, dry cleaning agent, and as a cleaner and dryer for electronic parts. Being a synthetic organic compound, it is not found naturally in surface and groundwaters. Rather it is one of the spent products of anthropogenic activities. All sites where trichloroethylene is used or stored become potential sources of ground and surface water contamination. Contamination of the water resource occurs through the accidential spill or intentional release of solutions containing trichloroethylene. Petura[1] cites five states where trichloroethylene has created serious problems in the groundwater resource. One of the states mentioned is Michigan. At Wurtsmith Air Force Base, located in northeastern Michigan, contamination of an aquifer occurred when a solution leaked from a waste storage tank, from landfills, from seepage lagoons, and from the wastewater treatment plant effluent according to an administrative report prepared by the U.S. Geological Survey[2]. In order to prevent the contaminant from reaching other aquifers and bodies of surface water, water was pumped out of the affected aquifer and treated by removal of the trichloroethylene.

Trichloroethylene is classified as a contaminant because of its carcinogenic nature. The U.S. Environmental Protection Agency, in a recent issue of an advance notice of proposed rule making of the National Revised Primary Drinking Water Regulation[3], cites volatile synthetic

organic chemicals in drinking water as biohazardous substances. It is proposed in the revised regulation that the potential maximum contaminant level for trichloroethylene be between 5-500 ug/L.

In order to remove trichloroethylene from water and to meet the maximum contaminant level concentration, some type of water treatment process is required. In the course of the water treatment process it becomes necessary to evaluate the efficiency of the process by determining the trichloroethylene level in the treated water. Thus, an analytical method is required in order to quantitatively determine the trichloroethylene content in the presence of other substances dissolved or suspended in the water. If other organic compounds are present in the water, sophisticated analytical instrumental methods must be used and the analysis performed by skilled personnel. The personnel must not only be able to correctly operate the instrument and provide routine maintenance, but also be able to interpret the generated information. The most commonly used chemical analytical method for determining volatile organic compounds is gas-liquid chromatography. When the organic compounds, such as trichloroethylene, are present in the water in the parts per billion range, the chromatographic method must be preceeded by cleanup and enrichment steps. Several cleanup and enrichment approaches can be used for volatile organics in water. A survey of a half dozen of the more commonly used techniques for low level multicomponent cleanup and enrichment techniques is presented by Mieure[4]. The nature of the water, estimated level of components of interest, the magnititude and type of interfering substances, and personal preference of one method over another enter in selecting the procedures to be used.

II OBJECTIVES

The principal goals of this study are to recommend cost-effective sample enrichment and cleanup methods and gas-liquid chromatographic systems for the analysis of trichloroethylene in aqueous systems by personnel having a minimal amount of training and technical knowledge of chromatography. These goals are to be reached by evaluating current sample enrichment and cleanup techniques and gas chromatographic systems. The specific objectives are the evaluation of:

a. Detector types and detector response.

b. Enrichment and sample cleanup by static head space and by purge and trap methods.

c. Stability of stock and standard trichloroethylene solutions stored at 4°C.

III APPARATUS AND MATERIALS

a. Perkin-Elmer model 900 Gas Chromatograph with flame ionization and electron capture detectors.

b. Tracor model 222 Gas Chromatograph with a flame ionization detector.

c. Tekmar Liquid Sample Concentrator, Model LSC-2.

d. One percent SP-1000 on Carbopack B 60/80 mesh.

e. Ten percent SP-1000 on Supelcoport 100/120 mesh.

f. Sodium sulfate, anhydrous ACS grade.

g. Methanol, HPLC grade.

h. Pentane, HPLC grade.

i. Trichloroethylene, ACS grade.

j. Microsyringes, 5, 10, 50 and 100 uL.

k. Syringes, one and 5 mL.

l. Vials, 32 mL capacity with caps and teflon liners.

m. Volumetric flasks, ground glass stoppered, 50, 200 and 1000 mL.

n. Volumetric pipets, 5, 10 and 50 mL.

IV STANDARD SOLUTIONS

Stock and standard trichloroethylene solutions were prepared using a modification of the method found in the EPA Guidelines Establishing Test Procedures for the Analysis of Pollutants[5]. The method was modified in step 5.5.2.1 of the aforementioned procedure by dispensing a weighed amount of trichloroethylene, weighed to the nearest 0.1mg, into a ground glass stoppered volumetric flask containing an appropriate solvent. The solvents used were pentane and methanol.

a. Strong stock solution, 1000 mg/L trichloroethylene in pentane.

b. Moderate stock solution, 100 mg/L trichloroethylene in pentane.

c. Weak stock solution, 10 mg/L trichloroethylene in pentane.

d. Strong stock solution, 1000 mg/L trichoroethylene in methanol.

e. Weak stock solution, 100 mg/L trichloroethylene in methanol.

f. Strong standard solution, 100 ug/L trichloroethylene in water.

g. Weak standard solution, 10 ug/L trichloroethylene in water

V EXPERIMENTAL PLAN

a. Detector Response. A Perkin-Elmer model 900 Gas Chromatograph equipped with a flame ionization detector (FID) and an electron capture detector (ECD) was used to evaluate the sensitivity of each detector for trichloroethylene. Table 1 lists the operating conditions used to determine trichloroethylene by each detector.

Table 1. Trichloroethylene Analysis by FID and ECD Gas Chromatography Perkin-Elmer Model 900

GC Conditions

Column: 10% SP-1000 coated on 100/120 mesh Supelcoport packed in a 10 ft. X 1/8 in. stainless steel column.

Detector - FID

Carrier Gas Nitrogen at a flow rate of 55 mL/min
Temperatures: Injector 150°C. Column isothermal at 95°C. Detector 225°C. Attenuation 16x10 and 1x1.

Detector ECD -

Source: Tritium
Carrier Gas: Agron-Methane (5%)
Temperature: Injector 140°C, Column isothermal at 95°C. Attenuation 16x10.

In determining the FID and ECD response, one uL of a trichloroethylene in pentane stock was injected into the chromatograph.

A comparison was made of the trichloroethylene response between flame ionization detectors installed in a Perkin-Elmer Model 900 and in a Tracor 222 gas chromatograph. The operating conditions used for the Perkin-Elmer model 900 are the same as those found in Table 1. Table 2 lists the parameters used in operating the Tracor model 222 gas chromatograph.

Table 2. Trichloroethylene Analysis by FID Gas Chromatography-Tracor Model 222

Column: 10% SP-1000 coated on 100/120 mesh Supelcoport packed in a 10 ft x 1/8 in. stainless steel column.

Carrier Gas: Nitrogen at a flow rate of 40 mL/min

Temperature: Injector 150°C. Column 90°C. Detector 210°C

Attenuation: 1 x 10 and 2 x 1

In the comparison study, one ml samples of a solution containing 100mg/L of trichloroethylene in a pentane stock solution were injected into each gas chromatograph.

b. Column Comparison. In studying the chromatographic separation of trichloroethylene, two different solid phase supports coated with SP-1000 were investigated. One such support was Supelcoport, a fluxed calcined diatomaceous earth material. The other support was Carbopack-B, a graphitized carbon having a surface area of appoximately 100 m^2/g. The percent of SP-1000 coated on 100/120 mesh Supelcoport and on 60/80 mesh Carbopack-B was 10% and 1% respectively. EPA method 601, found in the EPA Guidelines Establishing Test Procedures for the Analysis of Pollutants[5], uses the 1% SP-1000 on 60/80 mesh Carbopack-B for the analysis of purgable hydrocarbons such as trichloroethylene. The 10% SP-1000 on 100/120 mesh Supelcoport is suggested by Supelco Inc[6] for use in separating components in complex solvent mixtures. The packed columns were individually installed in a Tracor model 222 gas chromatograph. The operational parameters used for isothermal temperature operation of the Tracor instrument for both columns were the same as those found in Table 2. Table 3 lists the conditions used for temperature program operation for both columns.

Table 3. Operational Parameters for Tracor Model 222 G.C. Using Temperature Programming

Columns:	1% SP-1000 on 60/80 mesh Carbopack-B packed in a 6 ft. x 1/8 in. stainless steel column.
	10% SP-1000 on 100/120 mesh Supelcoport packed in a 10 ft. 1/8 in. stainless steel column.
Carrier Gas:	Nitrogen at a flow rate of 40 mL/min.
Column Temperature:	3 min. isothermal at 80°C then programmed to 160°C at 8°C/min. Cooldown to 80°C in 8 minutes.
Attenuation:	1 x 10

One uL of a 1.0 mL = 100 mg trichloroethylene in methanol solution was injected into the gas chromatograph.

c. Static Head Space. Headspace sampling is one of the two most commonly used methods for the cleanup and enrichment of trichloroethylene from aqueous solution. Temperature, electrolyte content, and liquid/gas volume ratio are among the factors which seriously affect the trichloroethylene content of the gas phase. Electrolyte and temperature effects were studied simultaneously, while the liquid/gas volume ratio was investigated independently. The electrolyte-temperature study was carried out with duplicate samples. Twelve pairs of solutions were used. After placing the liquid into the 32 mL vials, the vials were sealed with teflon faced septa and capped. The contents of the vials were shaken for 5 minutes and allowed to equilibrate for one hour. Three pairs of vials filled with 15 mg of glass distilled water constituted the blank. One pair was refrigerated at 4°C, another pair held at ambient temperature (approximately 25°C), and the final pair incubated at 70°C. To another three pairs of vials, 10 grams of sodium sulfate were added followed by 15 grams of water. One pair was held at 4°C, another pair at

25°C, and the final pair at 70°C. The final set of six vials contained 10 grams sodium sulfate and 15 grams of an aqueous trichloroethylene solution. One pair of each set of vials was held at 4°C, 25°C, and 70°C respectively.

The liquid/gas volume ratio effect was studied using the same basic approach as that used to study the temperature-electrolyte relationship. Ten grams of sodium sulfate were added to a 32 mL vial followed by either a weighed amount of trichloroethylene standard or glass distilled water. The vials were then sealed with teflon lined septa and capped. The blanks and standard vial solutions were shaken for 5 minutes and allowed to equilibrate for one hour. All vials were kept at ambient temperature, approximately 25°C. Twelve sets of duplicates were analyzed. One set contained 10 grams of glass distilled water plus 10 grams of sodium sulfate, another set contained 15 grams of water plus 10 grams of sodium sulfate, and the third set contained 20 grams of glass distilled water and 10 grams of sodium sulfate. The same sequence was repeated except that a 10 ug/L aqueous trichloroethylene solution was substituted for the glass distilled water.

One mL of headspace gas was injected into a Tracor model 222 gas chromatograph containing a column of 1% SP-1000 coated on 60/80 mesh Carbopack-B. The same operating conditions as appear in Table 3 were used except that the column temperature was maintained isothermally at 125°C.

d. Purge and Trap. The purge and trap technique is another method commonly used for the removal and enrichment of volatile organic compounds from water. The purge and trap procedure involves the stripping of the volatile organics from the water phase with an inert gas.

The partitioned organics are continously trapped from the gas stream on a short chromatographic column consisting mainly of Tenax. Purging is essentially a dynamic sampling process requiring the control of more instrumental operating steps than simple static headspace sampling. Desorption of the adsorbed volatile organic compounds from the Tenax adsorbent requires the determination of optimum operating conditions. Thus, the purge time and temperature and the desorption time and temperature will vary depending on the nature of the volatile organic compounds being analyzed. The previously mentioned operational variables were investigated in order to optimize the gas stripping of trichloroethylene from water and the subsequent desorption of the chloro-organic from the Tenax adsorbent. The sampling procedures used are the same as those found on page 69470 of the EPA publication, Guidelines Establishing Test-Procedures for the Analysis of Pollutants[5]. A Tracor model 222 gas chromatograph operating under the same conditions as those described in the headspace analysis study was used. In the purge and trap method, five mL samples of an aqueous 10 ug/L trichloroethylene standard solution were introduced in the purge unit of a Tekmar Liquid Sample Concentrator LSC-2. Two purge temperatures, 50°C and 40°C, and purge times ranging from two to eleven minutes were investigated. In addition, the temperature for desorbing trichloroethylene from the Tenax adsorbent was studied.

A comparison between the sensitivity of trichloroethylene detection using the static headspace and the purge and trap methods was made.

e. Stock/standard stability. In order for any analytical method to be applicable for field use, preparation of solutions in the field must

be held to a minimum, if not totally eliminated. This restriction prompted a study to determine the stability of a methanolic stock and aqueous standard trichloroethylene solutions. Stock and standard solutions were dispensed into 10 mL ampules and sealed. The following solutions were used: 100 mg/L of trichloroethylene in methanol stock and a 10 ug/L aqueous trichloroethylene standard. One set of stock and two sets of aqueous standard solutions were prepared. The sequence at which the solutions were sampled was: initially, 1, 3, 5, 7, 10, and 20 days. All ampules were stored at 4°C. A Tracor model 222 gas chromatograph was used. The operational parameters used were the same as previously described for the static headspace and purge and trap studies. Two one mL quantities of the stock solution were randomly selected from the ampules and injected into the gas chromatograph. One set of aqueous standards was subjected to purge and trap sampling, while the other was analyzed using the static headspace method. Duplicate analyses were performed using the aqueous standards.

VI RESULTS AND DISCUSSION

a. Detector response. The response of a gas chromatographic detector towards a specific organic compound is dependent on the detector type, its age and condition, as well as the condition of its amplifier. The two types of detectors employed in this phase of the study were a flame ionization detector and an electron capture detector. The electron capture detector is capable of sensing electronegative organic compounds. The stronger the electronegativity, the greater the relative response. Electroneutral compounds show very little response. The flame ionization detector, a universal detector for most organic compounds, does not possess the sensitivity equal to that of an electron capture detector.

The Perkin-Elmer model 900 gas chromatograph used in this study was about 14 years old and in fair condition. The tritium source of the electron capture detector had been replaced once. Using the Perkin-Elmer chromatograph with the column packing material and operating conditions specified in section V part A, the electron capture detector had an absolute sensitivity of two picograms of trichloroethylene. This amount, translated in terms of concentration, would be equivalent to a one uL injection of a solution containing 2 ug/L of trichloroethylene. The amplifier attentuation for determining the absolute amount and relative concentration was 16 x 10. A lower attenuation is theoretically obtainable, however, the noise level would be too great for an accurate evaluation. Work by Kolb and Auer[7] with trichloromethane showed that packed columns, including those containing SP-1000, had a relatively high bleed rate. The high bleed rate required that the electron capture detector be operated at a sensitivity which did not achieve the theoretical detection limit.

The flame ionization detector amplifier was capable of operating at a much lower attenuation, 160 times lower, than that used for the electron capture detector. The sensitivity of the flame ionization detector for trichloroethylene was one ng or 1000 pg of trichloroethylene. In terms of concentration, this would be equivalent to a one uL injection of 1000 ug/L of trichloroethylene.

The Perkin-Elmer model 900 gas chromatograph using electron capture detection showed a sensitivity 500 times greater than that of the same instrument using flame ionization detection. This value is less than that anticipated by the author. The rule of thumb is that a properly

operating electron capture detector using a Ni-63 source should be 1000 times more sensitive to trichloro compounds than a flame detector. The age and condition of the detectors is probably the reason for the discrepancy.

Detector response can vary substantially between flame ionization detectors in two different gas chromatographs. The Tracor model 222 gas chromatograph using the same column and operating conditions as found in Table 3 had an absolute sensitivity of 800 pg of trichloroethylene. The Tracor instrument gave a 12 percent greater response than the Perkin-Elmer gas chromatograph.

b. Column comparison. The separation characteristics of a gas liquid chromatographic (GLC) stationary phase is dependent on the partition of a specific organic compound between the carrier gas and the stationary phase-liquid coated solid support. Where the same liquid portion of the stationary phase is used, the nature of the solid support and the percent of liquid on the solid support will influence the separation characteristics of the column packing. Other external conditions such as temperature of the column, type and flow rate of the carrier gas, and length and diameter of the packed column are also important.

The liquid coating SP-1000 is a moderately polar polyglycolester resin, according to Supelco Inc[8]. The Supelcoport solid support is a fluxed calcined diatomaceous earth material of 100/120 mesh. The surface area and the surface characteristics of Supelcoport would require a greater percent coating to cover the surface area than would a 60/80 mesh Carbopack-B support. In addition, Carbopack-B by itself has certain separation properties according to Supelco Inc. Bulletin 747[6].

In the isothermal temperature operation of the Tracor model 222 gas chromatograph under identical operating conditions, the retention time for trichloroethylene using the 1% SP-1000 column was 6.2 minutes; when using the 10% SP-1000 column it was 3.5 minutes. The column temperature for both was 90°C. The difference in retention time indicates that solid support, Carbopack-B, takes an active part in the separation. The role of solid support, Carbopack-B, is further reinforced by the fact that the sequence of elution for trichloroethylene benzene mixtures is reversed from that obtained using a Supelcoport solid support.

In order to decrease the retention time for trichloroethylene eluting from the 1% SP-1000 column, the temperature was increased to 125°C, giving a retention time to 5.3 minutes. A retention time of 5.3 minutes has certain advantages in multicomponent systems as a better separation of the components can be achieved.

In order to achieve a better separation of the constituents of a multicomponent system, temperature programming can be used. Various temperature schemes were investigated. The scheme which gave the best separation of trichloroethylene from a multicomponent system containing methanol, benzene and pentane was: initial temperature of 80°C for 3 minutes followed by programming at 8°C/min to a temperature of 160°C. Under these conditions methanol, trichloroethylene, benzene, and pentane had retention times of 2.0, 9.6, 10.2, and 14.5 minutes respectively.

c. Static Headspace. It is recognized that the water solubility of most gases and volatile organic compounds having high to moderate vapor pressure decreases with an increase in electrolyte concentration. Also, as the temperature increases, the solubility of the gases and volatile

organics decrease. Thus, an investigation was undertaken to determine the effect of temperature and electrolyte content on trichloroethylene concentration in the head space of a sealed container. Tables 4 and 5 are a compliation of the data obtained at ambient temperature, 25°C, and at 70°C.

Table 4. Effect of Electrolyte Addition on TCE Levels at 25°C

Sample Composition	H_2O	H_2O	10 ugTCE/L	10 ugTCE/L
Sodium Sulfate added	0	10	0	10
Absolute Amt. of TCE in the headspace, ng	0	0	75.3	200

Table 5. Effect of Electrolyte Addition on TCE Levels at 70°C

Sample Composition	H_2O	H_2O	10 ugTCF/L	10 ugTCE/L
Sodium Sulfate Added	0	10	0	10
Absolute Amt. of TCE in the headspace, ng	0	0	163	192

Studies carried out at 4°C gave inconclusive results due to the precipitation of sodium sulfate from solution.

A comparison of the data showed no significant difference in the amount of trichloroethylene in the headspace with added electrolyte at ambient 25°C and at 70°C. About 80% of the amount of trichloroethylene found in the headspace when electrolyte was added at 25°C or 70°C was found in the headspace of samples containing no electrolyte stored at 70°C.

The last phase of the study was to determine the effect of the volume occupied by the sample to that occupied by the headspace. Ratios of headspace volume to sample volume of 2:1, 1:1 and 1:2 gave, after volume normalization, absolute amounts of 55.6, 60.7 and 56.5 ng of trichloroethylene. This experiment shows that a 1:1 ratio gave the greatest response for a trichloroethylene concentration at 10 ug/L .

d. Purge and trap (Dynamic headspace). The optimum conditions for purging trichloroethylene from an aqueous solution and trapping it on a column of Tenax housed in a Tekmar liquid sample concentrator were: purge at 40°C for 5 minutes, desorb at 180°C for 4 minutes and bake the Tenax at 200°C for 7 minutes. Aqueous solutions of trichloroethylene purged at a temperature of 50°C for greater than four minutes gave a lower recovery than those purged for three to four minutes. Purge time at 40°C had no effect on the recovery. The purge and trap conditions used were different than those used in the EPA Guidelines Establishing Test Procedures for the Analysis of Pollutants.[5]

A series of 5 mL volumes of aqueous trichloroethylene standards were purged under the optimum conditions with isothermal gas chromatographic separation. The results of the experiments showed the purge and trap method to have a sensitivity of 1.0 ug/L or an absolute amount of 5 ng of trichloroethylene. However, when the gas chromatograph was temperature programmed a sensitivity of 0.7 ug/L of trichloroethylene or an absolute value of 3.5 ng was observed.

e. Stock/standard stability. In examining the sealed vials of trichloroethylene stock and standard solutions over a period of 20 days, no significant changes in the trichloroethylene concentration were observed, as shown in Table 6.

Table 6. Concentration of Trichloroethylene at Various Times

Stock/Std.	DAY						
	0	1	3	5	7	10	20
Conc. of TCE in Stock Solution, mg/L	102	105	109	102	102	103	103
Conc. of TCE in Standard Solution ug/L by purge and trap method	3.4	3.3	3.3	3.2	3.2	3.3	3.4

An attempt was made to directly sample the headspace of the vials containing an aqueous trichloroethylene standard solution. Headspace sampling was not found feasible as the integrity of the headspace volume was lost once the stem of the vial was broken.

f. Gas chromatographic systems-background. The research work described thus far was undertaken to justify the approach to be used in recommending an analytical instrumental system for the volatile organics. In presenting the several gas chromatographic systems, the following assumptions and conditions are made:

(1) The organic compounds of interest are the volatile synthetic organics, trihalomethanes, and certain volatile aromatic organic compounds.

(2) Gas chromatography is the analytical approach to be used.

(3) The gas chromatographic detector must be responsive to all organic compounds regardless of electronegativity.

(4) The techniques used for the analysis of specific organic compounds must be a method recognized by federal and state agencies.

(5) A permanent record must be kept of the operational parameters and the resulting data.

(6) The analysis should require as little operator interaction with the gas chromatographic system as possible. The operator should not be required to know either the theory of chromatography or the principles and detailed operation of each component of the system. The operator will have had minimal training in use of the gas chromatographic system.

Thus, the ideal analytical system would be one where the operator introduces a sample or standard into the chromatographic system, activates the system, and reads the results as finished data which includes the concentration of specific compounds of interest. In order to accomplish this goal and control the capital cost of such a system, several instrumental options are presented.

g. Gas chromatographic systems-options. The three basic parts of a gas chromatographic system are the enrichment-sample cleanup unit, the gas chromatograph, and the data readout system. By applying the above mentioned restrictions and assumptions to each part of the system, the instrumental component can be defined in greater detail. The enrichment-sample cleanup unit can be either a static headspace or a purge and trap (dynamic headspace) apparatus. Because purge and trap and liquid-liquid extraction are the only methods recognized by EPA[5], the only automated method to be considered is the purge and trap. However, the automated and semi-automated static headspace systems have been shown to have comparable or, in certain instances, better accuracy than the purge and trap method. A variance can be obtained from federal and most state agencies for use of this method as a substitute for purge and trap. Therefore, this method will be considered in several of the options.

The liquid-liquid extraction method is a manual procedure and is effort intensive. Therefore, this approach is not an acceptable option. The gas chromatograph should have temperature programming capabilities. This capability is essential in separating individual compounds in multicomponent mixtures. The more complex the mixture, the greater the need for temperature programming. Chromatographic separation can be accomplished through the use of a 1% SP-1000 liquid phase coated on a Carbopack-B solid support. A column packing having equivalent or similar chromatographic separating capability could be substituted.

The gas chromatograph detector signal output can be processed in either of two ways: by a strip chart recorder or by a microcomputerized data system. The recorder is a relatively simple instrument which graphically shows the detector output signal. Manual interpretation of the graphical information is required. The data system is essentially a microcomputer which will accept the detector signal and process the data. The information can appear in the form of a complete report of the analysis or it may be stored in the memory of the data system. Some data systems have the capability of serving as the controller for the gas chromatograph. The controller can be capable not only of setting the operating conditions, but also monitoring these conditions.

Prior to considering the costs of various gas chromatographic systems it should be recognized that as the degree of automation increases, so does the complexity and capital equipment costs. In manual operation, human error is always a possibility. With automation, once the system is corrected for any inaccuracy, errors will not occur.

h. Gas chromatographic systems-cost evaluation. The information which appears in Table 7 are costs of components of a gas chromatographic analytical system based on June 1982 prices. All prices are rounded off to the nearest $100 and do not include shipping or installation charges.

Table 7. Estimated Cost of Components for Gas Chromatographic System

Type of Unit	Code	Costs (Dollars)
Automated gas chromatograph with automatic flow rate control	1	12,700
Automated gas chromatograph with manual flow rate control	2	10,300
Manual gas chromatograph	3	8,000
Automated purge and trap sampler	4	7,000
Semi automated purge and trap sampler	5	5,000
*Semi automated headspace sampler	6	1,000
Microprocessor data system	7	9,000
**One way data system	8	6,000
Recorder	9	900

* Accessory to a Perkin-Elmer gas chromatograph.

** Can not be used as a gas chromatograph controller

A variety of possible gas chromatographic systems are possible. Only eight are presented in the following figure. Other combinations area possible.

Table 8. Possible Gas Chromatographic Systems

Type of System	Item Nos.	Cost (Dollars)
Totally automated	4,1,7	28,700
Automated except for manual flow rate	4,2,7	26,300
Semi automated	5,2,7	24,300
Automated with semi automated headspace	5,2,7	27,700
Automated with semi automated purge and trap	5,1,7	20,300
Semi automated with one way microprocessor	6,2,8	26,700
Manual system with one way microprocessor	5,3,8	17,000
Manual system with recorder	5,3,9	11,000

VII CONCLUSIONS

a. Gas chromatography using electron capture detection is capable of detecting 2 pg of trichloroethylene, while flame ionization detection has a sensitivity of 800-1000 pg towards the chloro-organic compound.

b. Response by the same type of gas chromatographic detector is dependent on the condition and make of the detector.

c. A gas chromatographic stationary phase of 1% SP-1000 on 60/80 mesh Carbopack-B gave good separation of trichloroethylene from other volatile organic compounds when temperature programming was utilized.

d. The addition of a strong inert electrolyte and an elevated temperature causes higher trichloroethylene concentration in the headspace.

e. The purge and trap method is essentially a cleanup and enrichment method capable of causing a gas chromatographic response for one ug/L of trichloroethylene.

f. In sealed vials, methanolic stock and aqueous standard solutions are stable for at least 20 days.

g. An automated gas chromatographic system consisting of a semi-automated purge and trap unit, computerized operated gas chromatograph with flame ionization detector, and an automated input/output information system is recommend for use by personnel with a minimal amount of training in gas chromatography for use in trichloroethylene and other volatile synthetic organic compound analyses.

VIII RECOMMENDATIONS

a. A gas chromatograph utilizing a stationary phase of 1% SP-1000 coated onto a Carbopack-B solid support for separation and equipped with a flame ionization detector should be used for the analysis of volatile organic compounds such as trichloroethylene.

b. The purge and trap, also known as dynamic headspace, should be the method used for enrichment and cleanup of aqueous samples containing volatile organic compounds such as trichloroethylene.

c. A microprocessor data system should be used for raw data input, interpretation, and reporting of the analytical information.

d. An automated gas chromatographic system consisting of a semi-automated purge and trap sampling apparatus, automated gas chromatograph with an automated flow rate controller, and a microprocessor data system should be used when operators with a limited knowledge of the practice of chromatography and a minimal amount of training are employed. Other gas chromatographic systems are available but should be considered only after due evaluation of the operator and instrumental limitations.

e. If a program of monitoring volatile organic compounds is instituted at various Air Force bases, a well managed quality control program should be instituted.

REFERENCES

1. John C. Petura "Trichloroethylene and Methyl Chloroform in Groundwaters: A Problem Assessment," Journal of the American Water Works Association 73, pp 458-463, 1981.

2. J. R. Stark, T. R. Cumings and F. R. Twenter, "Ground Water Contamination at Wurtsmith Air Force Base, Michigan", An Administrative Report to the Air Force, U.S. Geological Survey, Jan 1981.

3. Environmental Protection Agency, "National Revised Primary Drinking Water Regulations, Volatile Synthetic Organic Chemicals in Drinking Water; Advanced Notice of Proposed Rulemaking", Federal Register, Part IV, 47, 43 pp 9350-9358, Thursday March 4, 1982.

4. James P. Mieure, "Determining Volatile Organics in Water," Environmental Science and Technology 14 pp 930-935, 1980.

5. Environmental Protection Agency, "Guidelines Establishing Test Procedures for the Analysis of Pollutants; Proposed Regulation, "Federal Register, 44, 233 Part III pp 69468-69469, December 3, 1976.

6. Supelco Inc. "G.C. Separations of Alcohols, Acetates, Cellosolves, Chloroalkanes, Formates and Ketones." Bulletin 747, Supelco Inc. Bellefonte, PA.

7. B. Kolb and M. Auer. "Application of Gas Chromatographic Headspace Analysis", Bodenseewerk Perkin-Elmer Co. Report 17 Uberlinger, Germany 1978.

8. Supelco Inc. Chromatography Catalog 20 p 32 and p 74. Supelco Inc. Bellefonte, PA (1982).

1982 USAF-SCEE SUMMER FACULTY RESEARCH PROGRAM

Sponsored by the
Air Force Office of Scientific Research

Conducted by the
Southeastern Center for Electrical Engineering Education

FINAL REPORT

BASIC RESEARCH ISSUES IN ELECTROMAGNETIC RAIL LAUNCHERS WITH PLASMA DRIVEN PROJECTILES

Prepared by: Dr. Manuel A. Huerta

Academic Rank: Associate Professor

Department and University: Department of Physics
University of Miami
Coral Gables, Florida 33124

Research Location: Air Force Armament Laboratory (AFSC)
AFATL/DLDL
Eglin AFB, Florida 32542

USAF Research Collegue: Mr. Kenneth K. Cobb

Date: July 9, 1982

Contract No: F49620-82-C-0035

BASIC RESEARCH ISSUES IN ELECTROMAGNETIC RAIL LAUNCHERS WITH PLASMA DRIVEN PROJECTILES

By

Dr. Manuel A. Huerta

ABSTRACT

A one dimensional steady model of the arc plasma is extended to include time varying currents. The breech voltage-current relation for the rail gun as a circuit element is obtained. The muzzle voltage measures the resistive drop at the plasma arc. The plasma is subject to the flute instability which is analogous to the Rayleigh-Taylor instability in fluids. Recommendations for future theoretical and experimental research are given.

I. INTRODUCTION

The successful demonstration of an inductively driven electromagnetic rail gun by S.C. Rashleigh and R.A. Marshall, Ref. 1, at the Australian National University in Canberra has spurred a great deal of interest in these devices. During the period from 1968 to 1977 the above authors, together with Marshall's student, John Barber, launched Lexan cubes with masses of about 3 grams to speeds of about 6 km/sec. Their best results were obtained using an arc plasma as an armature to push the projectile. Westinghouse Corp. has built a gun using a solid armature that has launched a 317 gm. projectile with a speed of 4.2 km/sec. General descriptions of the history and recent work on rail launchers and related devices have been given by B.M. Schwarzschild, Ref. 2, and by H. Kolm and P. Morgenau, Ref. 3.

The ANU gun used the largest homopolar generator in the world to generate the current required (in the order of 500,000 amps). This was a large and very heavy device. The possibility of developing a rail gun that might be a weapon of interest to the USAF has been strongly put forward by J. Barber et al, Ref. 4. Their system concept is based on a fast-start turbine combined with a small DC homopolar generator and inductive energy storage. Important mass savings are achieved with this concept leading to a total system mass around 4,000 kg. for a gun capable of launching 50 gm. projectiles, with a speed of 3 km/sec, with a 20 Hz. firing frequency, in bursts with a duration of 5 sec.

There are various primary energy sources and switching schemes; these will not be discussed here. We concentrate on how the projectile is accelerated down the gun barrel. A schematic of the barrel is shown in Fig. 1.

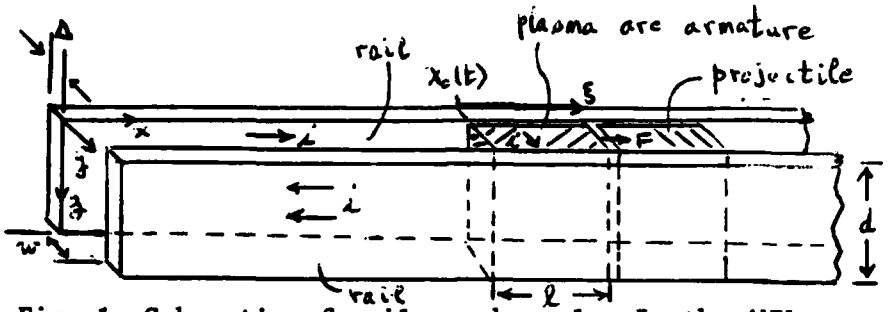


Fig. 1 Schematic of rail gun barrel. In the ANU gun d=19.1 mm, w=12.7 mm, and Δ=3.2 mm

The current goes in one rail, across a plasma (ionized gas) arc or a solid armature, and out the other rail. Before the ANU work, it was thought that the melting of the armature would be the limiting factor in rail guns. The ANU researchers established that plasma arc armatures work well. The properties of this plasma are the main subject of this study.

The plasma is generated by providing the rear of the nonconducting projectiles with a metallic foil that makes the initial contact between the rails. The heat produced by the enormous current vaporizes the foil and ionizes the vapor producing a conducting plasma. The rail currents produce a magnetic field B_r at the plasma. This field acts on the current through the plasma to produce a driving force F given by

$$F = i w B_r \quad . \tag{1}$$

This equation may be rewritten in terms of the rail inductance per unit length L' as

$$F = \frac{1}{2} L' i^2 \quad . \tag{2}$$

For the ANU gun $L' = 0.42 \times 10^{-6}$ henry/meter. With their current of about 300 kA the force is 1.9×10^4 Newton. This force imparts an acceleration of 6×10^6 m/s^2 to a 3 gm projectile . For their projectile with a rear area of 161 mm^2 this corresponds to a plasma pressure of 1.1×10^8 N/m^2 or 1,095 atmospheres.

II. OBJECTIVES OF THE RESEARCH EFFORT

1. To study and improve the models for the properties of the arc plasma produced in the rail gun.

2. To identify the basic research issues associated with the plasma.

III. GENERAL PLASMA EQUATIONS

The principal theoretical studies of the plasma properties have been done by J. McNab, Ref. 5, and by J.D. Powell and J.H. Batteh, Ref. 6. Their model uses the Euler equations of magnetohydrodynamics for a fluid of density ρ, velocity $\vec{u}$, pressure p, energy per unit mass ϵ, current density $\vec{J}$, magnetic field $\vec{B}$, electric field $\vec{E}$, conductivity σ, and no viscosity. Since the mass of the electrons is negligible, the density ρ is

$$\rho = m_o n_a \quad , \tag{3}$$

where m_o and n_a are the mass and the density respectively of the atoms. The density n_a is given by

$$n_a = n_o + n_1 + n_2 + \cdots \quad , \tag{4}$$

where n_o is the density of neutral atoms, n_1 is the density of once ionized atoms, n_2 is the density of twice ionized atoms, etc. The electron density n is given by

$$n = n_1 + 2n_2 + 3n_3 + \cdots \quad . \tag{5}$$

The pressure is given by

$$p = (n_a + n) k T \quad . \tag{6}$$

At equilibrium the densities are related by the Saha equations

$$\frac{n_{j+1}\, n}{n_j} = 2 \left(\frac{2\pi m k T}{h^2} \right)^{3/2} \frac{Z_{j+1}}{Z_j} e^{-I_{j+1}/kT} \quad , \tag{7}$$

where Z_j is the electronic partition function of the jth ion (often Z_j is merely a number of order one), I_1 is the energy to ionize a neutral atom, I_2 is the energy to produce a twice ionized atom by removing an electron from a once ionized atom, etc., m is the mass of the electron, and h and k are Planck's and Boltzmann's constants.

The energy per unit mass ϵ is given by

$$\rho\epsilon = \frac{3}{2}(n_a+n)kT + \sum_{m=1} Q_m n_m + \sum_{m=0} W_m n_m \approx \frac{3}{2}(n_a+n)kT, \quad (8)$$

where $Q_m = I_1 + I_2 + \ldots + I_m$ (m=1,2,...) is the energy required to remove m electrons from an atom and W_m (m=0,1,2,...) is the electronic excitation energy of an m-atom. The radiation energy and pressure have been neglected at these relatively low temperatures.

The governing equations are Maxwell's equations in a good conductor (where the charge density and the displacement current are neglected)

$$\vec{\nabla}\times\vec{E} = -\frac{\partial\vec{B}}{\partial t} \quad \text{and} \quad \vec{\nabla}\times\vec{B} = \mu_0\vec{J} \quad . \quad (9)$$

In the gun plasma the electron density $n\approx 10^{26}/m^3$. The plasma frequency ω_p is then around 10^{14}/sec. All frequencies of interest in the gun are well below ω_p. We then take $\vec{J}$ as given by Ohm's Law in a moving medium,

$$\vec{J} = \sigma\,(\vec{E} + \vec{u}\times\vec{B}) \quad . \quad (10)$$

The conductivity of the plasma is taken to be the Spitzer conductivity, given in Ref. 7, as

$$\sigma = 2.63\times10^{-2}\gamma_E \frac{(n_1+2n_2)}{(n_1+4n_2)} T^{3/2}\left[\ln\left(\frac{1.23\times10^7\, T^{3/2}(n_1+2n_2)}{\sqrt{n}\,(n_1+4n_2)}\right)\right]^{-1}, \quad (11)$$

where all quantities are in MKS units. The factor is given by $\gamma_E \approx 0.6833$.

The fluid properties are governed by the equation of mass conservation

$$\frac{\partial\rho}{\partial t} + \vec{\nabla}\cdot(\rho\vec{u}) = 0 \quad , \quad (12)$$

the momentum equation

$$\rho\left[\frac{\partial\vec{u}}{\partial t} + (\vec{u}\cdot\vec{\nabla})\vec{u}\right] = -\vec{\nabla}p + \vec{J}\times\vec{B} \quad , \quad (13)$$

and the energy equation

$$\rho\left[\frac{\partial\epsilon}{\partial t} + (\vec{u}\cdot\vec{\nabla})\epsilon\right] + p\vec{\nabla}\cdot\vec{u} = -\vec{\nabla}\cdot\vec{q} + \frac{J^2}{\sigma} \quad . \quad (14)$$

The second term in the right hand side of Eq. (14) is the Joule heat while the heat flux vector $\vec{q}$ is given by

$$\vec{q} = -(K_T + K_R)\,\vec{\nabla} T \quad . \tag{15}$$

Here K_T is the coefficient of heat conduction, given in Ref. 7 as

$$K_T = 1.96\times10^{-4}\,\frac{(n_1+n_2)}{(n_1+4n_2)}\,T^{5/2}\left[\ln\left(\frac{1.23\times10^{7}\,T^{3/2}(n_1+2n_2)}{\sqrt{n}\;(n_1+4n_2)}\right)\right]^{-1}\ \frac{\text{Joule}}{\text{m.sec.}^{\circ}\text{K}} \quad . \tag{16}$$

K_R is the coefficient of heat conduction by radiation. It is given by

$$K_R = \frac{16}{3}\,\sigma_s\,\lambda\,T^3 \quad , \tag{17}$$

where σ_s =5.67x10^{-8} Joule/m^{2}deg^{4}sec. is the Stefan-Boltzmann constant, and λ is the radiation mean free path which is given in Ref. 6, Eq. (3.17). The expression for q given in Eq. (15) is valid provided the plasma is optically thick. That is, provided λ is much smaller than the dimensions of the plasma. In the gun plasma this is well satisfied because λ is of the order of 10^{-4} m. Typical gun conditions calculated in Ref. 6 give $T \approx 5.6\times10^4$deg K. Then $K_R/K_T \approx 15$ so radiation heat transport dominates.

IV. CONSTANT CURRENT, ONE DIMENSIONAL MODEL

The authors of Ref. 6 apply the equations of Section III to a one dimensional model of a plasma arc undergoing constant acceleration, in which all quantities are steady in the frame of the plasma. The rear edge of the plasma is located at $x_0(t)$ where

$$v_0 = \frac{dx_0}{dt} \text{ , and } \quad a = \frac{dv_0}{dt} \text{ , } \qquad (18)$$

with a constant. They change variable from x to ξ where

$$\xi = \frac{x - x_0(t)}{\ell}$$

where ℓ is the length of the plasma.

For any function f(x,t), one has

$$df = \left(\frac{\partial f}{\partial x}\right)_t dx + \left(\frac{\partial f}{\partial t}\right)_x dt \text{ . } \qquad (19)$$

Dividing by $d\xi$ and keeping t constant (dt=0), one has

$$\left(\frac{df}{d\xi}\right)_t \equiv \left(\frac{\partial f}{\partial \xi}\right)_t = \left(\frac{\partial f}{\partial x}\right)_t \left(\frac{dx}{d\xi}\right)_t + 0 \text{ , }$$

so

$$\left(\frac{\partial f}{\partial \xi}\right)_t = \ell \left(\frac{\partial f}{\partial x}\right)_t \text{ . } \qquad (21)$$

Dividing Eq. (20) by dt and keeping ξ constant, one has

$$\left(\frac{df}{dt}\right)_\xi = \left(\frac{\partial f}{\partial x}\right)_t \left(\frac{dx}{dt}\right)_\xi + \left(\frac{\partial f}{\partial t}\right)_x \left(\frac{dt}{dt}\right)_\xi$$

but

$$\left(\frac{dx}{dt}\right)_\xi = \frac{dx_0}{dt} = v_0 \text{ , and } \left(\frac{dt}{dt}\right)_\xi = 1 \text{ , so}$$

$$\left(\frac{\partial f}{\partial t}\right)_\xi = v_0 \left(\frac{\partial f}{\partial x}\right)_t + \left(\frac{\partial f}{\partial t}\right)_x \text{ . } \qquad (22)$$

Introducing a velocity

$$\vec{u}' = \vec{u} - v_0(t)\,\hat{x} \quad , \tag{23}$$

the main equations are rewritten in terms of the ξ variable as

$$\left(\frac{\partial \rho}{\partial t}\right)_\xi + \frac{1}{\ell}\,\vec{\nabla}_\xi \cdot (\rho \vec{u}') = 0 \quad , \tag{24}$$

$$\rho\left[\left(\frac{\partial \vec{u}'}{\partial t}\right)_\xi + \frac{1}{\ell}(\vec{u}'\cdot\vec{\nabla}_\xi)\vec{u}'\right] = -\frac{1}{\ell}\vec{\nabla}_\xi p + \vec{J}\times\vec{B} - \rho\,\frac{dv_0}{dt}\hat{x}, \tag{25}$$

$$\rho\left[\left(\frac{\partial \epsilon}{\partial t}\right)_\xi + \frac{1}{\ell}(\vec{u}'\cdot\vec{\nabla}_\xi)\epsilon\right] + p\,\frac{1}{\ell}\vec{\nabla}_\xi\cdot\vec{u}' = -\frac{1}{\ell}\vec{\nabla}_\xi\cdot\vec{q} + \frac{J^2}{\sigma} \quad , \tag{26}$$

$$\frac{1}{\ell}\,\vec{\nabla}_\xi \times \vec{B} = \mu_0 \vec{J} \quad , \quad \frac{1}{\ell}\,\vec{\nabla}_\xi \times \vec{E} = -\left(\frac{\partial \vec{B}}{\partial t}\right)_\xi + \frac{v_0}{\ell}\left(\frac{\partial \vec{B}}{\partial \xi}\right)_t \quad , \tag{27}$$

and $$\vec{J} = \sigma\,(\vec{E} + \vec{u}' \times \vec{B} + v_0 \hat{x} \times \vec{B}) \quad , \tag{28}$$

where $\vec{E}$ and $\vec{B}$ are the fields measured in the laboratory frame of reference. The authors of Ref. 6 found a solution where the acceleration $a = \frac{dv_0}{dt}$ and the externally controlled current i are constant. Furthermore, their quantities are steady in the frame of the accelerating plasma and depend only on the variable ξ, so $\vec{u}'=0$, $\rho = \rho(\xi)$, $p=p(\xi)$, $\vec{B} = B(\xi)\hat{z}$, $\vec{J} = J(\xi)\hat{y}$ and $E = E_y(\xi,t)\,\hat{y}$. For the current density J and the field B they found

$$J(\xi)=0 \ , \ \xi<0 \ ; \ J(\xi) = \frac{J(0)}{\sigma(0)}\sigma(\xi) \ , \ 0\le\xi\le 1 \ ; \ J(\xi)=0 \ , \ \xi>1 \ , \tag{29}$$

with

$$i = d\ell \int_0^1 J\, d\xi \quad , \tag{30}$$

while

$$B(\xi) = \frac{\mu_0 i}{d} \equiv B_0 \quad , \ \xi<0 \quad , \tag{31}$$

and

$$B(\xi) = B_0 - \mu_0 \ell \int_0^\xi J\, d\xi \ , \ 0\le\xi\le 1 \ ; \ B(\xi)=0 \ , \ \xi>1 . \tag{32}$$

$B(\xi)$ decreases from its maximum at the left of the plasma to zero at the back of the projectile. The electric field in the plasma was found to be

$$E_y(\xi,t) = \frac{J(0)}{\sigma(0)} + \bar{l}_c B(\xi) \quad , \quad 0 \le \xi \le 1 \qquad (33)$$

with no field given in the space to the left of the plasma. To the right of the plasma the field $E_y = J(0)/\sigma(0)$. The voltage at the muzzle V_0 is then simply given by the resistive drop at the plasma. The pressure in the plasma is found to be

$$p(\xi) = \frac{B_0^2 - B^2(\xi)}{2\mu_0} - a\ell \int_0^\xi \rho \, d\xi \quad . \qquad (34)$$

This pressure rises from zero at $\xi=0$ to large values near the back of the projectile at $\xi=1$. At the back of the projectile, $p(\xi=1)wd = Ma$, where M is the mass of the projectile. Combining this with Eq. (34) one gets

$$a = \frac{wd \, \frac{1}{2}\mu_0 (i/d)^2}{M + m_p} = wd \, \frac{B_0^2/2\mu_0}{M + m_p} \approx \frac{wd}{M} \, B_0^2/2\mu_0 \quad , \qquad (35)$$

where m_p is the mass of the plasma given by

$$m_p = wd\ell \int_0^1 \rho \, d\xi \quad . \qquad (36)$$

The interpretation of Eq. (35) is that the mass of the plasma and the projectile is accelerated by a magnetic pressure $B_0^2/2\mu_0$ acting over the rear area wd. The approximate equality in Eq. (35) is obtained by neglecting the mass of the plasma compared to the mass of the projectile. Eq. (35) shows that the detailed properties of the plasma do not matter very much in determining the acceleration. This is as it should be. So long as the plasma is not disrupted and is able to carry the current across the rails, the acceleration will be given by Eq. (35).

The temperature is found by solving Eq. (26), which reduces to

$$\frac{1}{\chi} \vec{\nabla}_\xi \cdot \vec{q} = \frac{J^2}{\sigma} \quad , \qquad (37)$$

in combination with the equations for $\vec{q}$, σ, p, n_i, and Eq. (29). The boundary conditions are that

$$q(\zeta=0) = -2\sigma_s T_c^4 \quad \text{and} \quad q(\zeta=1) = 2\sigma_s T_1^4 \,. \qquad (38)$$

Due to the T dependence of λ and σ this equation is solved numerically. In Ref. 6, an analytic solution is found under the approximation that σ is constant and λ is independent of T and inversely proportional to the pressure p. Valuable results are then obtained for the scaling of the important quantities in terms of the current per unit rail height j=i/d. Some of these are $\ell \sim j^{-16/11}$, $a \sim j^2$, $p \sim j^2$, $\rho \sim j^{16/11}$, $T \sim j^{6/11}$. The work of Ref. 6 gives interesting values for the quantities in the Rashleigh-Marshall experiments of Ref. 1. Some of these are $a=1.48\times10^7$ m/s^2, $\ell=9.2$cm, $V_o=47$ volts, $T=5.61\times10^4$ deg K, $n=9.8\times10^{25}/m^3$.

V. VARYING CURRENT MODEL

The previous model has the strong restriction that the current is constant. The operation of the gun can be made much more efficient if the current is allowed to drop to a low value as the projectile exits the muzzle. The rails are connected to a storage inductor and/or other driving components. To understand the behavior of the rails as a circuit element, the problem of time varying fields has been attacked. To the left of the plasma Maxwell's equations neglecting displacement currents are applied to the rails and to the nonconducting space between them. The fields in the rails are $\vec{E}_r = E_{rx}(y,t)\hat{x}$ and $\vec{B}_r = B_{rz}(y,t)\hat{z}$, with

$$\frac{\partial^2 E_{rx}}{\partial y^2} - \frac{1}{c^2}\frac{\partial^2 E_{rx}}{\partial t^2} - \mu_0 \sigma_r \frac{\partial E_{rx}}{\partial t} = 0 \quad , \quad (39)$$

and similarly for B_{rz}. The solutions are found in terms of the Fourier components of the current

$$i(t) = \int I(\omega)\, e^{-i\omega t}\, d\omega \quad , \quad (40)$$

as

$$E_{rx}(y,t) = \int E_{rx}(\omega)\, e^{-(1-i)y/\delta}\, e^{-i\omega t}\, d\omega \quad , y \geq w,$$

and

$$B_{rz}(y,t) = \int B_{rz}(\omega)\, e^{-(1-i)y/\delta}\, e^{-i\omega t}\, d\omega \quad , y \geq w, \quad (41)$$

where

$$E_{rx}(\omega) = -\frac{I(\omega)(1-i)}{\sigma_r d\delta}\, e^{(1-i)w/\delta} \quad ,$$

and

$$B_{rz}(\omega) = \frac{\mu_0 I(\omega)}{d}\, e^{(1-i)w/\delta} \quad . \quad (42)$$

Similar expressions hold for the field in the other rail at $y \leq 0$. Here δ is the skin depth given by

$$\delta = \sqrt{\frac{2}{\mu_0 \sigma_r \omega}} \quad . \quad (43)$$

In the space between the rails for $x < x_0$ there is an E_{xv},

$$E_{xv}(y,t) = \left(1 - \frac{2y}{w}\right) \int e^{-i\omega t} I(\omega) \left[\frac{l'(\omega)}{2} - \frac{i\omega l(\omega)}{2}\right] d\omega \quad ,$$

where

$$r'(\omega) = \frac{2}{\sigma_r d \delta} \quad \text{and} \quad l'(\omega) = \frac{\mu_0 \delta}{d} \quad . (44)$$

There is also an E_{yv},

$$E_{yv}(x,y,t) = \frac{(x_0 - x)}{w} \int e^{-i\omega t} I(\omega)\left[r'(\omega) - i\omega L'(\omega)\right] d\omega + E_{yv}(x_0, t) ,$$

where

$$L'(\omega) = \frac{\mu_0 w}{d} + l'(\omega) = \frac{\mu_0}{d}(w + \delta(\omega)) \quad , \quad (45)$$

and there is a constant magnetic field

$$B_v = B_0 = \frac{\mu_0 i(t)}{d} \hat{z} \quad . \quad (46)$$

The voltage V_b at the breech (x=0) is found from $E_{yv}(0,y,t)$ to be

$$V_b(t) = x_0 \int e^{-i\omega t} I(\omega)[r'(\omega) - i\omega L'(\omega)] d\omega + V(x_0, t) , \quad (47)$$

where $V(x_0,t)$ is the voltage at the left edge of the plasma. In the general case we cannot express $V_b(t)$ in terms of i(t) because of the ω dependence of δ. However, if the rail thickness Δ is much smaller than the rail separation a simplification is possible. There is a frequency ω_1 for which $\delta(\omega_1) = \sqrt{2/\mu_0 \sigma_r \omega_1} = \Delta$. Then $\delta(\omega) = \sqrt{2/\mu_0 \sigma_r \omega}$ for $\omega > \omega_1$ and $\delta(\omega) = \Delta$ for $\omega < \omega_1$. Because of this the rail resistance per unit length $r'(\omega)$ is $r'(\omega) = \frac{2}{\sigma_r d \Delta}\sqrt{\frac{\omega}{\omega_1}}$ for $\omega > \omega_1$ and $r'(\omega) = \frac{2}{\sigma_r d \Delta}$ for $\omega < \omega_1$. We note that the skin reactance $\omega l' = r'(\omega)$ for $\omega > \omega_1$. Since $w \gg \Delta$, we have $\omega L' \gg r'$. We can then take $r' = \frac{2}{\sigma_r d \Delta}$ for all ω because this is true for $\omega < \omega_1$, while for $\omega > \omega_1$, $r'(\omega)$ is negligible anyway even though it is greater than $\frac{2}{\sigma_r d \Delta}$. We also see that $l'(\omega)$ is negligible at all ω. We are then able to simplify the breech voltage V_b to get

$$V_b(t) = x_0\left[r' i(t) + L' \frac{di}{dt}\right] + V(x_0, t) \quad , \quad (48)$$

with

$$r' = \frac{2}{\sigma_r d \Delta} \quad \text{and} \quad L' = \frac{\mu_0 w}{d} \quad . \quad (49)$$

We may neglect skin effects to compute voltages and currents. After calculating the current i(t), one could take the skin depth into account as a function of ω in order to compute the power dissipated in the rails.

To obtain the breech voltage, we still need to calculate $V(x_o,t)$ which is the voltage at the left side of the plasma. So far we have not made any assumptions about the state of the plasma. We will take $\vec{J}=J(\xi,t)\hat{y}$ and $\vec{B}=B(\xi,t)\hat{z}$ with

$$\frac{\partial B}{\partial \xi} = -\mu_o J(\xi,t) \quad . \tag{50}$$

For the electric field we have

$$\vec{E} = \frac{J}{\sigma}\hat{y} - \vec{u}\times\vec{B} = \frac{J}{\sigma}\hat{y} - B\,\vec{u}'\times\hat{z} + v_o B\hat{y} \quad . \tag{51}$$

The plasma surely obeys $u' \ll v_o$. Then Faraday's law gives

$$\frac{\partial}{\partial \xi}\left[\frac{1}{\mu_o\sigma}\frac{\partial B}{\partial \xi}\right] - \left.\frac{\partial B}{\partial t}\right|_{\xi} \approx 0 \quad . \tag{52}$$

The plasma satisfies the condition that the skin depth in the plasma $\delta = \sqrt{\frac{2}{\mu_o\sigma\omega}}$ is much greater than the plasma thickness ℓ. Then Eq. (52) can be approximated as

$$\frac{\partial}{\partial \xi}\left[\frac{1}{\mu_o\sigma}\frac{\partial B}{\partial \xi}\right] \approx 0 \quad .$$

This gives the same solutions as Eqs. (29) - (32) but now i is a function of time. Therefore

$$E(\xi,t) = \frac{J(o,t)}{\sigma(o,t)} + v_o B(\xi,t) \quad . \tag{53}$$

We then get for the voltage at the breech side of the plasma

$$V(x_o,t) = i R_p + L' i \frac{dx_o}{dt} \quad , \tag{54}$$

where the plasma resistance R_p is

$$R_p = \frac{w}{\ell d \int_o^1 \sigma d\xi} \quad , \tag{55}$$

and L' is given in Eq. (49). Combining Eq. (54) with Eq. (48) we obtain for the breech voltage

$$V_b(t) = i(t) R + \frac{d}{dt}(L i) \quad , \tag{56}$$

where

$$R = r' x_o + R_p \quad ,$$

and

$$L = L' x_o \quad , \tag{57}$$

with r' and L' given in Eq. (49).

Eq. (56) is combined with

$$(m_p + M)\frac{d^2 x_c}{dt^2} = \frac{1}{2} L' i^2(t) \qquad (58)$$

to define the rail gun as a circuit element. The electric field to the right of the plasma has the constant value $J(c,t)/\sigma(0,t)$ so the muzzle voltage is again $V_0 = J(0,t)w/\sigma(0,t)$ as in Sec. IV.

The above discussion shows that the time dependent fields in the plasma obey the same equations as the static ones in Sec. IV. Furthermore, provided that the time variations of i(t) are slow, as they are in the rail gun, the plasma pressure, density and temperature obey the same equations as in Sec. IV neglecting $\partial/\partial t|_s$ and u'. In effect the plasma constantly adjusts its "static" state to follow the current variations. This section justifies applying the work of Ref. 6 even when there is a variable current.

VI. PLASMA STABILITY

It is well known, Refs. 8 and 9, that when the direction of B is everywhere the same, a static plasma as in Sec. IV, accelerated by a B field, as in our case, or a plasma supported against gravity by a B field, is unstable. The instability leads to a corrugation or fluting of the plasma surface, hence the name flute instability. It is analogous to the Rayleigh-Taylor instability of a heavy fluid supported against gravity by a light fluid. For the case where the plasma density is constant, surface waves of the form $e^{iky}\, e^{\alpha t}$ grow with

$$\alpha = \sqrt{ak} \qquad (51)$$

as shown in Refs. 8 and 9. In the gun case, the instability is more complicated because of the density variation. I have obtained the required eigenvalue equation that must be solved to study the instability. The equation is too long to write here. The state of the plasma after the development of the instability is unknown. There are three possibilities. The first is that the growth of the instability is so slow that it has little effect by the time the projectile exits the gun. In this case the solution of Secs. IV and V would be very accurate. The second is that the instability is not terribly disruptive. Rather it merely establishes a steady flow in the plasma. Most likely this flow would involve a vortex near each rail. The third possibility is that the instability completely disrupts the plasma. Since the gun is known to work, it would then have to be true that the plasma constantly replenishes itself by working against the rails and the back of the projectile. I believe the second possibility is the most likely. As the plasma edge breaks up due to the instability, pieces of current free plasma are left behind. These plasma blobs would expand and touch the rails. A large current would then flow that would slam the plasma blob

back against the rear of the projectile. This indicates that a new, more complicated steady state, one with flow, is reached by the arc plasma. This state is not well described by the model of Sec. IV. Yet, the scaling laws found in Ref. 4, given at the end of Sec. IV, remain as an important guide on the variation of plasma parameters with rail current.

VII. RECOMMENDATIONS ON RESEARCH ISSUES

A good amount of theoretical and experimental work needs to be done to understand the properties of the plasma arc and its effect on the operation of the rail gun.

Theoretical Work

1. Study the behavior of the plasma as a circuit element using Eqs. (56) - (58). This work is not too complicated since it only involves a couple of nonlinear o.d.e.'s. It can be of significance in improving the efficiency of the gun.

2. Study the influence of the plasma sheaths at the plasma-solid interfaces upon the operation of the gun.

3. Study the effect on the plasma of propellant gases that may be used to inject the projectile into the rails.

4. Study the initial stages of vaporization and ionization of the metallic foil.

5. Do the stability calculation discussed in Sec. VI.

6. Find a stable solution that better describes the plasma state.

7. There are a variety of practical questions that should be addressed. For example, whether one could impart spin to the projectile by magnetic means in rails with round bores.

Experimental Work

1. The ANU gun design is wasteful of energy. As the projectile leaves the gun, the barrel is filled with a strong B field. This represents a magnetic energy about equal to the kinetic energy imparted to the projectile. This magnetic energy is wastefully dissipated by an arc at the muzzle with attendant heat dissipation problems. A capacitor cut into the rail circuit as the projectile leaves the muzzle is an elementary way to recover this energy. This or other energy recovery schemes should be studied.

2. Up to now the only properties that have been measured are the projectile velocity and various voltages and currents. The plasma temperature, size ℓ, composition, and other properties are only inferred. These quantities can be measured optically and used to verify the theoretical plasma models. A barrel with several transparent slits can be used. The duration of the light flash through a slit gives ℓ. Since the plasma is optically thick, its spectrum will be a continuous background close to that of a black body with absorption lines. The temperature and composition can be obtained from the spectrum.

ACKNOWLEDGMENTS

I would like to thank the Air Force Systems Command, the Air Force Office of Scientific Research, and the Southeastern Center for Electrical Engineering Education for providing me with the opportunity to spend the summer of 1982 at Eglin Air Force Base working on interesting problems in the theory of electromagnetic rail launchers. More specifically, I would like to thank Dr. Donald C. Daniel and Lt. Col. James R. Crowder for providing me with the working atmosphere at the DLDL branch that enabled me to carry out this work. I would especially like to thank Mr. Kenneth K. Cobb and Mr. Billy F. Lucas. I had many valuable discussions with them. They also provided me with copies of the main references on electromagnetic launchers. Finally, I would like to thank Dr. Warren D. Peele for a very well run 1982 USAF-SCEEE Summer Faculty Research Program.

REFERENCES

1. S.C. Rashleigh and R.A. Marshall, J. Appl. Phys. 49, 2540 (1978).

2. B.M. Schwarzschild, Physics Today, 33, 19 (Dec 1980).

3. H. Kolm and P. Morgenau, IEEE Spectrum, page 30, April 1982.

4. J.P. Barber, T.J. McCormick, and D.P. Bauer, "Electromagnetic Gun Study", AFATL Report No. AFATL-TR-81-82, Contract No. F08635-81-C-0048, Final Report for period March 1981 - September 1981.

5. I.R. McNab, J. Appl. Phys. 51, 2549 (1980).

6. J.D. Powell and J.H. Batteh, J. Appl. Phys. 52, 2717 (1981).

7. L. Spitzer, Physics of Fully Ionized Gases (Interscience, New York, 1965), Chap. 5.

8. L. Spitzer, ibid, Chap. 4.

9. S. Chandrasekhar, Hydrodynamic and Hydromagnetic Stability (Oxford University Press, 1961), Chap. 10.

1982 USAF-SCEEE SUMMER FACULTY RESEARCH PROGRAM

Sponsored by the

AIR FORCE OFFICE OF SCIENTIFIC RESEARCH

Conducted by the

SOUTHEASTERN CENTER FOR ELECTRICAL ENGINEERING EDUCATION

FINAL REPORT

OPERATIONAL SAFETY REVIEW METHODOLOGY

Prepared by:	Dr. Francis J. Jankowski, P.E.
Academic Rank:	Professor
Department and University:	Department of Engineering Wright State University
Research Location:	Air Force Weapons Laboratory, Nuclear Systems Division, Nuclear Surety Branch
USAF Research Colleague:	Andrew J. Smith
Date:	September 16, 1982
Contract No.:	F49620-82-C-0035

OPERATIONAL SAFETY REVIEW METHODOLOGY

Dr. Francis J. Jankowski, P.E.

ABSTRACT

Methods of making safety reviews of hazardous operations, with an emphasis on human factors, were reviewed. Several methods exist. A comprehensive review procedure was not found. For a human factors review of tasks, Swain's Man-Machine System Analysis (MMSA) is recommended. For human error analysis, his Technique for Human Error Rate Prediction (THERP) is good; this subject is being actively worked on by others. Safety is strongly dependent on the organization, on attitudes, and on the system in which the operation is performed. Factors important in the review of each of these areas are discussed; specific review procedures are to be developed.

A study of safety records of several countries shows a number better than that of the USA. The safer countries also have a high Quality of Life Index, suggesting that safety may be improved through selection of individuals for high risk tasks.

The biorhythm based on birthdate has been shown not valid. Biological cycles determined on other basis may provide a means of making task assignments to minimize risk of human error.

ACKNOWLEDGEMENTS

The author wishes to thank the Air Force Systems Command, the Air Force Office of Scientific Research and the Southeastern Center for Electrical Engineering Education for the opportunity to spend a worthwhile and interesting summer at the Air Force Weapons Laboratory, Kirtland Air Force Base, NM. He would like to thank Andrew J. Smith for many helpful discussions and for suggestions on areas of investigation.

PREFACE

This is a short summary report based on the report prepared for the Air Force Weapons Laboratory. The original report consists of 44 pages of text, 21 pages of appendices and 6 pages of references, abstract, title page and acknowledgements. This summary report retains the reference numbering of the original report, but omits those not referred to directly.

I. INTRODUCTION

A planned, coordinated effort is required to maintain and improve safety in a hazardous operation. A first step is a design review of equipment and facilities. A further step is to include human factors and human engineering principles in the design review. However, as important as these steps are, they only represent about half of the safety problem. The operations themselves, the planning of the procedures, the job aids, the performance of individuals and organizations, and the control of operations represent the other half of the safety problem. In the past, most efforts have been directed toward safety review of hardware and toward selection and training of personnel. More recently, methods have been developed[7,8,9] to expand these safety reviews to include all phases of operations. A human factors-system approach is needed. That is what this report attempts.

Safety should be considered another component of engineering design and of operations planning, along with energy balance, stability, control and other factors. Since most practicing engineers and administrators have not been formally educated into the importance, principles, and implementation of safety, other means of promoting safety have evolved. One such means is the safety review. Several excellent review techniques have been developed. Some good examples are Swain[11] (NRC), and System Safety Development Center[10,12] efforts. All of these point out the necessity of applying human factors or human engineering principles.

Safety efforts have progressed from making machines safe to making the machines safe and operable (application of human factors). Future gains

in safety of operations are likely to be made by giving attention to the management of the operation, the system in which the operations are performed, and the attitude and support toward safety.

II. OBJECTIVES

A heirarchy of objectives governs this investigation. These are:

1. Improve the safety in hazardous Air Force operations.

2. To produce a method for reviewing and evaluating operations in regard to human factors.

3. To continue exploration of other possible factors which may produce greater safety in hazardous operations.

III. FACTORS IN DESIGN AND MANAGEMENT TO PROMOTE SAFETY

In operations, methods of minimizing hazards can generally be categorized as engineering design or as management control. Engineering design methods include: 1) redundancy, 2) coincidence, requiring two or more independent signals to initiate an action, 3) variety to minimize common cause/common mode failures, 4) interlocks, to insure necessary steps are satisfactorily completed before proceeding, 5) failsafe, which may not be possible in complex systems, 6) perfection in design, to uncover and correct all potential accident causes, 7) fault-tolerant design, so that component failure or human error will not cause an accident, and 8) cultural consistent design, which meets the expectation of the operator.

To the extent that the safety of operations depends on the human operators following specific instructions, one has management control of safety. Maximum safety is attained by a combination of engineered and managed safety systems.

Some management control principles are: 1) redundancy of personnel, 2) control of over-rides, such as control of keys to switches and tagging procedures, 3) check lists and other job aids, 4) internal inspections and audits, and 5) selection, training and retraining programs.

IV. THE SAFETY REVIEW OF OPERATIONS

The method outlined here for the safety review of operations is presented as a comprehensive review. An attempt has been made to outline a method which

will have logic and will be workable at many levels.

A. The Method. This section outlines the approach and the steps involved in a safety review of operations. Further discussion and details are given in other sections below.

1. Assumptions and Limits. The safety review method presented here is developed around principles and concepts. Detailed procedures may be obtained by:

   a. Reference to review methods now in use.
   b. Developed by the review team.
   c. Developed through further research into methods of review.

2. Application. As a comprehensive review, this is likely to be performed on an infrequent basis, possibly biennially. The principles also may be applied to more limited reviews.

3. Organization of the Review Method. To make this review method comprehensive and workable, the effort has been divided into phases. Each phase represents an area of professional expertise. The areas are common to most operations. The areas are separable. To prevent overlooking deficiencies which may be present in the overall system but not detectable on limited reviews, coordination and integration of the phase reviews are required.

4. Steps in the Safety Review Process. The steps are:

   a. Plan the overall review. Specify what is to be included, excluded, identify sources of information, and set a schedule.
   b. Select and assign personnel to do the safety review.
   c. Develop specific plans, involving the people who will do the review.
   d. Perform the review.
   e. Coordinate and integrate the results; specify additional steps or data needed.
   f. Document the review and the recommendations.
   g. Provide feedback to those who can use the review recommendations.

B. Principles of Safety Reviews. There are a number of techniques and ideas applicable to performing safety reviews. A few of these are:

1. Operations Diagrams. Block diagrams, flow diagrams, PERT charts and similar devices.

2. Tree Diagrams, including fault trees[12,16] event trees, probability trees[13], information trees[17], risk trees[12], and cause/consequence diagrams[13].

3. Forward - Reverse Analysis. It will be noted that event trees start with an initiating event and move forward in time. Fault trees start with a result and work backward in time, identifying various possible causes. Conditional events are included in both.

4. Field Techniques, include audit, observation, interview, walk-through inspections, and investigations.

C. Concepts Important to Operational Reviews. Certain concepts and principles are applicable to all phases of the review. These will be well known to human factors engineers, and are covered in various texts[18,19,20] and handbooks[13]. Some of these human factors concepts and some engineering concepts will be outlined briefly here.

1. Stimulus - Organism - Response (S-O-R). Stimulus represents the cues; Organism is the individuals who are supposed to act; Response is the action, or inaction, taken as a result of the stimulus and the mental processes generated.

   The S-O-R analysis is central to the review of operations and to human factors engineering.

2. Work Load Levels and Task Enrichment. The demands on the operator in respect to skills and speed of performance should be within the capabilities of the individual, and must be great enough to gain his attention and interest.

3. Performance Shaping Factors (PSF), include the psychological and physiological characteristics of the operator, the organizational and physical environment, and the design of the task and of the equipment. These have been summarized neatly by Swain[8,13].

4. Human Error Probabilities (HEP). Quantitative probabilities of errors permit estimates of consequences and costs of accidents.

5. Man-Machine Interface Design is the province of the human factors engineer.

6. Value Engineering emphasizes function rather than hardware, to produce optimum value/cost ratios. These concepts may be applied to operations evaluations.

7. Systems Engineering (or Systems Analysis). The central principle in the systems approach to a problem is the unitary concept. The objective is to optimize the satisfying of specified criteria within the constraints imposed on the system.

D. Planning the Safety Review. The plan will include:

1. Defining the operation to be reviewed.
2. Identifying the professional areas of expertise needed.
3. Establishing a time schedule.
4. Organizing for the review.
5. Formulating detailed plans, with input from the reviewers.

E. Review Personnel. The review process, as proposed here, has two major dimensional axes. These are the professional areas covered in the operations and the phases into which the operation is divided. Review personnel need to include experts in the professional areas covered who have experience in the type of operations.

V. PHASES OF THE REVIEW

The phases of the review represent areas of the operation which can be separated and examined independently; these phases might be looked upon as tasks for the review team to complete. The suggested phases are:

A. History, Experience, Documentation. If the operation is one which has been in existence for some period of time, the records of past performances should be examined. Note should be made of the completeness of the records. From the records it should be possible to analyze and reconstruct accidents, incidents and events that may have a safety implication.

B. Written Instructions. All written instructions should be identified and evaluated. These will include Operation Manuals, Operating Instructions, Tech Orders, Maintenance Manuals, Job Guides, Job Aids, Check Lists, and others.

A first step is to verify the technical accuracy of the written instructions.

Next, the instructions are reviewed in relation to application of human factors and engineering principles. In this process, the instructions can be evaluated on the basis of many of the concepts presented above. A check list has been developed by Brune and Weinstein[7]. Swain and Guttmann[13] point out the importance of well prepared written instructions. They cite results by Haney[23] which found that columnar instructions produce one-third fewer errors relative to narrative instructions.

A further evaluation of written instructions is that of readability. There are many indexes for readability. One of the more common Readability Indexes is the Fog Index. A similar one is in use by the military[25].

C. Task Analysis. Many methods have been developed for industrial, office, and other tasks. Only a few give instructions for applying human factors in the review of and analysis of tasks.

Possibly the best technique for task analysis including human factors is the Man-Machine Systems Analysis (MMSA) developed and described by Swain[8,13]. The steps are:

1. Describe the system goals and functions of interest.
2. Describe the situational characteristics.
3. Describe the characteristics of the personnel.
4. Describe the jobs and tasks performed by the personnel.
5. Analyze the jobs and tasks to identify error-likely situations.
6. Estimate the likelihood of each potential error.
7. Estimate the likelihood that each error will be undetected (or uncorrected).
8. Estimate the consequences of each detected (or uncorrected) error.

9. Suggest changes to the system.
10. Evaluate the suggested changes (repeat Steps 1 through 9).

In addition to MMSA and THERP[8,13] (which uses probability trees), fault trees, and other techniques can be applied to task analysis.

D. Inspection, Audits and Reviews. A safety review of an operation will include an evaluation of internal inspections, audits and reviews.

E. Organization and Management. Review of organizational structure and functioning in regard to safety of operations is a field that has not received much attention. However, the Kemeny Report[15] calls deficiencies in the organization of the utility and of the NRC a major contributor to the TMI nuclear accident. Clearly, the organization can be a positive factor, or a neutral, or even a negative factor in promoting safety.

A procedure for a safety review of the organization involved in the operation was not found in the literature. Some of the factors which should be evaluated include:

1. Technical Understanding of the operation by upper levels of management.
2. Communication Channels, vertically and horizontally.
3. A Safety Group or Office within the organization.
4. Communication Links, external, for emergencies.
5. Standards, Procedures, and Policies of the company, established and available to those having need.
6. A Method for Learning from experiences of other groups.
7. Responsibility and Decision-Making Authority defined.
8. Adequacy of Staff for the operation as a whole and for safety.
9. Procedures should exist for modifying operating and maintenance instructions, updating drawings, and controlling the distribution of instructions and drawings (so that outdated ones are not in use).

F. Attitude and Support of Safety. Safety must be important to the individuals in an organization. It must be supported by upper management; if not important to upper management it is not likely to be given high

priority at lower level and by the workers.

Likewise, safety must have the support of the working crew. If procedures are not workable or reasonable, or if instructions are obscure or not readily available, workers will give low priority to safety. Even when threatened with severe penalties workers can find ways to evade or give nominal attention to safety.

This is an area that has not received much attention in safety reviews. Swain[8,13] includes "attitude" as one of 62 Performance Shaping Factors. However, no procedure was found for measuring attitude or for correcting deficiencies. Some factors which measure attitude include:

1. Safety budgets.
2. Recognition of good safety records.
3. Availability and currency of written procedures and standards.
4. Use of written procedures and standards.
5. Priority of safety in decision making.

G. Systems Engineering Analysis. Methods for reviewing safety of an operation generally concentrated on task analysis. A method for evaluating the effects of system design and functioning on operational safety does not appear to be available.

Some measures of system safety effectiveness are:

1. Goals should be consistent throughout all units.
2. The Performance of equipment should optimize safety and system goal attainment, not to optimize limited local goals.
3. Communication between human units, between machine elements, and between humans and machines should be adequate in content, timing, clarity, recall and the other factors which are essential to safe operations.
4. Support with information and materials in sufficient quantity, type, and timing would be a measure of the functioning of a system.

VI. CONCLUDING THE SAFETY REVIEW

A. Integration. Some of the likely causes of safety degradation are deficiencies in attitudes, organization, procedures, instructions, and

systems iteratives. To maximize the probability of detecting deficiencies, the team members making the safety review should meet periodically to discuss their findings. They should examine the possible implications to safety in their phase from the results in the other phases. This integration process is a continuing one. It is also an interactive process.

B. Documentation. Documentation should start with the plan of review and its objectives. During the review, discoveries, data, analysis, and results should be documented. A final report can include: 1) organization and objectives of the review, 2) description of review process (brief), 3) findings as to safety of the operations, and 4) recommendations for improving safety.

C. Implementation. A final safety review report usually goes to the manager of the operation reviewed, and to one or more management levels above the operation. The recommendations may be compulsary or may be optional. If optional, the operating crew and management may have to explain any action of not adopting a recommendation.

If recommendations are made and implemented, continuing observations and evaluations will determine whether the changes are effective.

VII. SOME FACTORS AFFECTING OPERATIONAL SAFETY

In large, complex, hazardous operations, the cost of an accident can be great. It is worthwhile investigating all possible means of reducing errors and accidents. Some thoughts on two factors which might lead to better safety are discussed briefly below.

A. Cultural and Nationalistic Factors. Looking at accident statistics from various countries, one notes that the USA is frequently in fourth or fifth place, rarely in first or second, in safety ratings. Comparing industrial accident rates in Japan and the USA, Japan had a better safety record than the USA in nine of ten areas of activity, with an average of 40 percent fewer loss time accidents per million worker-hours.

Japan's superior performance in industrial production and safety records can be partially explained by several factors in their culture:

1. Quality Circles provide worker participation.
2. The worker is a company's most important asset.

3. Primary goals of industry are continuity and service.

Explaining why countries other than Japan have better safety records than the USA is not as easily done. One possible explanation emerges from a comparison of the ranking of countries by Quality of Life[37] with their rankings on safety. It is noted that Holland, the Scandinavian countries, and Australia often rank above the USA in safety. These countries also rank above the USA in Quality of Life, as does Japan.

Possibly peoples enjoying a higher Quality of Life may be less aggressive and less prone to risk-taking. This line of reasoning could lead to new measures for selecting individuals for responsible positions in hazardous operations.

B. Biological Cycles and Safety. Individuals have their ups and downs, their good days and their bad days. Many safety engineers and managers have reasoned that if the bad days could be predicted, then either by cautioning the individual or assigning the person to a less risky task, accidents could be reduced.

The biorhythm based on date of birth theory has not been supported by any careful test[40,41,42].

An interesting study would be to observe the nature and stability of physical, emotional, and intellectual cycles, and try to correlate those with variations in physiological parameters. If results were positive, this could lead to a factor in making work assignments which could reduce the risks of human error and accidents.

VIII. SUMMARY AND CONCLUSIONS

From a study of safety review methods it is concluded that good methods exist for:

1. Review of tasks and jobs, with application of human factors.
2. Review of machine and facility design, including human factors applications.
3. Review of written instructions.

Methods and quantitative probability values for the occurrence of human error are available for a limited number of cases. Efforts are

continuing to expand these data, and to determine effective ways to apply them.

Methods of safety review and standards are being developed for computer control of operations. Both hardware and software reliability and safety are being studied. There are no generally accepted methods or standards at this time.

Methods are generally lacking for the safety review of operations in regard to:

1. Organization and management.
2. Attitudes and support.
3. Systems operations

These are areas that strongly impact the safety of large, complex operations. They are also areas which are difficult to measure quantitatively.

Certain other countries frequently have better safety records than the USA. These include Japan, Holland, Australia and the Scandinavian countries. These countries also have a higher Quality of Life Index. This leads to a hypothesis that the nature of a society may be the ultimate determinant of the degree of safety which might be expected.

Biological cycles may provide a means for making task assignments in hazardous operations. The simple biorhythm based on date of birth has been shown not to be valid.

IX. RECOMMENDATIONS

The following recommendations are the author's recommendations for the continuation of this study. Recommendations on the needs for the general field of safety reviews would be broader.

The recommendations are:

1. Choose an Air Force Operation; to it apply the review method in Sections IV, V, and VI above.
2. Proceed to develop techniques for safety review of the three following phases of an operation:
   a. Attitudes and support
   b. Organization and management
   c. System safety

This study would have to identify elements within each phase that would affect safety, quantities which could be observed or measured, means of relating these measures to the safety of the operation. The emphasis would be to detect situations which if modified or corrected, would reduce the probability of error or accident.

3. Continue the study of international safety records. Attempt to explain differences in the records of various countries. Seek to identify cultural practices or other factors which might be adapted to USA practices to improve safety.
4. Study biological cycles. Look for correlations between biological states of physical, emotional or intellectual levels with the physiological measures of quantities such as heart beat, blood pressure, skin electro-potential, or brain waves potential. If any correlations are found beyond the one-day cycles, a combination measurement-analysis device might be developed to aid in task assignment with reduced accident risk.

REFERENCES

7. Brune, R.L., and Weinstein, M., Development of a Checklist for Evaluating Maintenance Test, and Calibration Procedures Used in Nuclear Power Plants, NUREG/CR-1368 SAND80-7053, HPT Inc., Thousand Oaks, CA, 1980.

8. Swain, A.D., Sandia Human Factors Program for Weapon Development, SAND 76-0326, June 1976.

9. Malone, T.B.; Kirkpatrick, M.; Mallory, K.; Eike, D.; Johnson, J.H.; and Walker, R.W. Human Factors Evaluation of Control Room Design and Operator Performance at Three Mile Island-2, Vols. I, II, III, NUREG/CR-1270, Three Mile Island Special Inquiry Group, US NRC, Washington, D.C., January, 1980.

10. Nertney, R.J. and Bullock, M.G., Human Factors in Design, ERDA-76-45-2, February 1976.

11. Division of Human Factors Safety, Office of Nuclear Reactor Regulation, US NRC, Guide for Control Room Design Reviews, NUREG-0700, September 1981.

12. Knox, N.W. and Eicher, R.W., MORT User's Manual, ERDA-76-45-4, March 1976.

13. Swain, A.D. and Guttmann, H.E., Handbook of Human Reliability Analysis with Emphasis on Nuclear Power, NUREG-CR-1278, October, 1980.

15. Report of the President's Commission on the Accident at Three Mile Island, The Need for Change: The Legacy of TMI, U.S. Government Printing Office, October, 1979 (often referred to as the Kemeny Report).

16. Malasky, S.W., System Safety, Hayden Book Company, 1974, and Briscoe, G.J., Risk Management Guide, ERDA 76-45-11, 1977.

17. Bullock, M.G., Safety Information System Guide, ERDA 76-45-9, 1977.

18. McCormick, E.J., Human Factors Engineering and Design, 4th Edition, McGraw Hill, 1976.

19. Huchingson, R.D., New Horizons For Human Factors in Design, McGraw Hill, 1981.

20. McCormick, E.J., and D.R. Illgen, Industrial Psychology, 7th Edition, Prentice Hall, 1980.

23. Haney, R.W., "The Effects on Instructions Format on Functional Testing Performance", Human Factors, Vol. 11, pp. 181-187 (1969).

25. Military Specifications MIL-M-38784A(5), "Manual, Technical, General Style and Format Requirements," 24 July 1978.

37. "U.S. Ranks 41st in Quality of Life", Albuquerque Journal, p. A-12, Column 1, August 18, 1982.

40. Wolcott, J.H.; R.R. McMeekin, R.E. Burgin, and R.E. Yonowitch, "Correlation of General Aviation Accidents with Biorhythm Theory", Human Factors, Vol. 19, No. 3, pp. 283-293, 1977.

41. Berry, J.R., and S.L. DeLoach, A Statistical Analysis of Selected Human Factors Involved in Aviation Safety, LSSR 6-78A, Air Force Institute of Technology, 1978.

42. Englund, C.E., and P. Naitoh, "An Attempted Validation Study of the *Birthdate-Based Biorhythm (BBB) Hypothesis*", Aviation, Space, and Environmental Medicine, Vol. 51, No. 6, pp. 583-590, 1980.

1982 USAF-SCEE SUMMER FACULTY RESEARCH PROGRAM

Sponsored by the

AIR FORCE OFFICE OF SCIENTIFIC RESEARCH

Conducted by the

SOUTHEASTERN CENTER FOR ELECTRICAL ENGINEERING EDUCAT ON

FINAL REPORT

MODELING LOCALIZED STRESS FIELDS IN COMPOSITE LAMINA S

Prepared by:	Eric Raymond Johnson
Academic Rank:	Assistant Professor
Department and University:	Aerospace and Ocean Engineering Virginia Polytechnic Institute and St e University
Research Location:	Flight Dynamics Laboratory Analysis and Optimization Branch Wright-Patterson Air Force Base, Ohio
USAF Research Colleague:	Dr. V. B. Venkayya
Date:	September 16, 1982
Contract No:	F49620-82-C-0035

Modeling Localized Stress Fields in Composite Laminates

by

Eric Raymond Johnson

An approximate theory is developed to analyze stress concentration and stress gradient problems in composite laminates. It includes interlaminar stresses. The theory features a global-local modeling scheme, similar to the one developed by Pagano, which results in a more tractable mathematical model for thicker laminates. The global region is modeled by classical lamination theory. In the local region the field equations are obtained from the variational method using Reissner's functional with assumed stresses.

Acknowledgement

The author thanks the Air Force Systems Command, the Air Force Office of Scientific Research, and the Southeastern Center for Electrical Engineering Education in providing the opportunity for resident research at the Flight Dynamics Laboratory, Wright-Patterson AFB, Ohio. The laboratory, and in particular the Analysis and Optimization Branch, provided a hospitable and stimulating working environment.

Special acknowledgement must be extended to Dr. V. B. Venkayya, Dr. N. S. Khot, and Dr. N. J. Pagano for their valuable comments on my research.

I. Introduction:

Classical lamination theory[1,2] ignores the thickness stress components with respect to the in-plane stress components, and models a laminate as an equivalent single layer with the familiar A, B, and D stiffness matrices. It is a direct extension of classical plate theory based on the Kirchhoff hypothesis. This theory is adequate for many engineering problems. However, there are problems where thickness effects are important and, consequently, classical lamination theory is inadequate.

Laminated plates manufactured from advanced filamentary composite materials, like graphite-epoxy, are susceptible to thickness effects because their effective transverse shear moduli are significantly smaller than the effective elastic modulus along the fiber direction. The concept of a "thin" plate, based solely on geometric parameters obtained from analyses of homogeneous metallic plates, must be carefully considered for these materials. The higher order plate theory of Whitney and Sun,[3] for example, is based on accounting for thickness shear and thickness normal deformations, although the laminate is treated as an equivalent single layer.

Refined plate theories which integrate the lamina properties through the plate thickness into an equivalent single layer theory provide improved global response estimates for deflections, vibration frequencies, and buckling loads in this class of materials. However, thickness stress response in localized regions of geometric, load, and material discontinuity require more detailed analysis. For example, interlaminar stresses which are significant near the straight free edge of tensile coupons,[4] near cutouts,[5] and near supported edges,[6] are neglected in the formulation of equivalent single layer theories. Although interlaminar stresses may be small with respect to in-plane stress components, so is the thickness strength of advanced composite laminates significantly smaller than their in-plane fiber direction strength. Hence, a theory which incorporates interlaminar stress response is necessary to implement a rational delamination failure criteria. A minimum requirement of such a theory would be a ply-by-ply analysis. Such theories have been developed by Seide,[7] Srinivas,[8] and

Pagano.[9] Of course, the more detailed the theory the more difficult and/or cumbersone it is to obtain solutions to specific problems. Elasticity solutions, which model each ply as a homogeneous anisotropic material with effective moduli, are intractable for practical laminates, and are fraught with difficult issues such as the existence of stress singularities and, if they exist, how to effectively incorporate them into the analysis. The approximate ply-by-ply structural theories are more tractable with respect to elasticity, but obliterate singularities. Nevertheless, such approximate theories should provide improved estimates of interlaminar stresses for delamination studies. Finally, the level of detail which a ply-by-ply theory contains is not needed for the entire domain of the laminate, but is needed only in regions of stress concentration or where large stress gradients exist. Outside of these localized regions an equivalent single layer theory is sufficient.

II. OBJECTIVES OF RESEARCH EFFORT:

The objective of this research effort is to examine a practical means of determining improved estimates of laminate stress response in localized regions of stress concentration and/or large stress gradients. It will be necessary to account for all six stress components on a layer-by-layer basis in the vicinity of the discontinuity. Away from the discontinuity, an equivalent single layer theory is sufficient. Thus, matching a localized theory to a simpler far field theory is an essential element of the objective to achieve a tractable overall mathematical model.

III. PAGANO'S GLOBAL-LOCAL MODEL:

Pagano[9] established three criteria required of a new theory to realistically model stress concentrations and large stress gradient regions in composite laminates. These are: (1) All six stress components are nonzero in general. (2) Traction and displacement continuity conditions at interfaces between adjacent layers are to be satisfied. (3) "Layer equilibrium" for each layer is to be satisfied; i.e., internally computed stresses acting on the layer and any externally prescribed

boundary tractions acting on it satisfy the conditions of vanishing resultant force and moment. In addition, Pagano discusses the deficiencies of various refined plate theories with respect to modeling stress concentrations in composite laminates. He develops a new theory satisfying the three criteria using Reissner's functional in the variational principle. The theory results in a mathematical model of 23N partial differential equations in the laminate's midsurface coordinates x and y and 7N edge boundary conditions, where N is number layers in the laminate or number of mathematical subdivisions through the thickness. Pagano[10] applies this theory to predict the interlaminar stress components near the straight free edge of a symmetric balanced laminate subject to uniform extension (tensile coupon). The mechanics of this classic free edge problem permit a mathematical reduction of the general theory equations to ordinary differential equations applicable in a cross section perpendicular to the load axis. Hence, because of the symmetry in this problem, only two of the four layers are modeled. For this simplified example, Pagano obtains very good agreement between his theory and existing solutions for N = 6. Numerical difficulties were encountered for larger values of N, leaving open the question of the tractability of the theory for thicker laminates.

Subsequently Pagano and Soni[11] developed a global-local model to provoide a more manageable theory for thicker laminates. This model incorporates the detail of Pagano's previous theory in an arbitrarily selected number of parallel layers (local model). The remaining portions of the laminate are modeled using a simpler theory[3] smeared over many lamina thicknesses (global model). The variational principle is employed using Reissner's functional with assumed stress fields in the local region, and using the strain energy with assumed displacement fields in the global region. Proper matching conditions between the global and local regions are a consequence of the variational principle. It should be noted that the local regions are confined to being parallel with the layers in the laminate. The efficacy of the model is examined using the previous test problem of a symmetric laminate subject to uniform extension. The stress fields obtained from the global-local formu-

lation compared well with those obtained by other approaches.

Soni and Pagano[12] further examined the global-local model for the free-edge boundary value problem. It is concluded that a local layer should be retained on each side of the interface to be examined, and that small values of the interlaminar normal stress are sensitive to the mode of the global-local modeling. In addition, the model is used in combination with the average stress failure criterion of Whitney and Nuismer[13] to define the range where the interlaminar normal stress exerts a significant influence on the free-edge failure for a class of T300-5208 laminates. At the delamination failure load for these particular laminates, this criterion predicted a reasonably consistent value of the average interlaminar normal stress. This result lends support to using integrated stress values, rather than point stresses, as a criterion. Apparently it justifies a ply-by-ply approximate model for stress field computations in composite laminates, as opposed to an elasticity approach.

IV. DEVELOPMENT OF THEORY:

A variant of the global-local theory formulated by Pagano, which was discussed in the previous section, is developed in this section. The theory is simpler than Pagano's in two respects: (1) The local region requirs one, versus three, displacement quantities in the thickness direction within each layer, while retaining the independence of the interlaminar stress components. (2) The global region is modeled with classical lamination theory as opposed to the more sophisticated theory of Whitney and Sun.[3] In addition the local region is defined perpendicular to the laminae rather than parallel to them. This latter feature is attractive for stress boundary layers confined to narrow edge zones through the laminate thickness; i.e., at holes and near supported edges.

The field equations for the theory are developed for a specific class of boundary value problems to illustrate the methodology. The extension to a wider class of problems is evident. The boundary value problems considered are symmetric bidirectional laminates subject to uniform extension along the load axis, or x-axis. The boundary condi-

tions on the lateral surfaces are assumed spatially uniform along the load axis, symmetric across the width, but otherwise are arbitrary. The situation is depicted in Fig. 1. The rectangular coordinate system (x,y,z) is also shown. The laminate occupies the region $|x| \leq a$, $|y| \leq b$, and $|z| \leq h$, where 2a is the length, 2b the width, and 2h is the thickness of the laminate.

The laminae are parallel to the x-y midplane, have thickness t, and are assumed to be filamentary composite materials with the fiber direction indicated by the 1-axis in Fig. 1. The angle between the x-axis and 1-axis is θ. For symmetric laminate $\theta(z) = \theta(-z)$, and for a bidirectional laminate θ is limited to either 0° or 90°. The lamina are numbered sequentially from one at the bottom ($z = -h$) of the laminate to N at the top ($z = h$). Fig. 2 shows further notation for the kth lamina. A local thickness coordinate z_k, $|z_k| \leq t/2$, is defined as $z_k = z - \bar{h}_k$, where $\bar{h}_k = (h_k + h_{k-1})/2$, and h_k designates the z-coordinate of the interface between the k and k + 1 laminae. Each lamina is treated as a homogeneous, linear elastic orthotropic material with principal axes parallel to the laminate coordinate axes. Consequently, the constitutive equations can be written as

$$\begin{Bmatrix} \varepsilon_x \\ \varepsilon_y \\ \varepsilon_z \\ \gamma_{yz} \\ \gamma_{xz} \\ \gamma_{xy} \end{Bmatrix}^{(k)} = \begin{bmatrix} s_{11} & s_{12} & s_{13} & 0 & 0 & 0 \\ s_{12} & s_{22} & s_{23} & 0 & 0 & 0 \\ s_{13} & s_{23} & s_{33} & 0 & 0 & 0 \\ 0 & 0 & 0 & s_{44} & 0 & 0 \\ 0 & 0 & 0 & 0 & s_{55} & 0 \\ 0 & 0 & 0 & 0 & 0 & s_{66} \end{bmatrix}^{(k)} \begin{Bmatrix} \sigma_x \\ \sigma_y \\ \sigma_z \\ \tau_{yz} \\ \tau_{xz} \\ \tau_{xy} \end{Bmatrix}^{(k)} \tag{1}$$

in which $\varepsilon_x^{(k)}, \varepsilon_y^{(k)}, \ldots, \gamma_{xy}^{(k)}$ are the engineering strains in the kth lamina, $\sigma_x^{(k)}, \ldots, \tau_{xy}^{(k)}$ are the corresponding stress components, and the $S_{ij}^{(k)}$ i,j = 1,2,..,6 are the compliances of the kth lamina.

For the boundary value problems under consideration the displacement fields have the special form[4]

$$u = \varepsilon_x x, \quad v = v(y,z), \quad w = w(y,z), \tag{2}$$

where u, v, and w are the displacements of a material point originally located at (x,y,z) in the directions of the x-, y-, and z-coordinate axes, respectively, and ε_x is the spatially constant applied strain. Mathematically the problem reduces to a two-dimensional one, and from the strain-displacement relations of linear elasticity we have $\gamma_{xz} = \gamma_{xy} = 0$. Hence, from Eq. 1 $\tau_{xz} = \tau_{xy} = 0$.

Fig. 3 shows the global-local scheme in a half of the laminate cross-section. The z-axis is an axis of symmetry. The local region is confined to $c < y < b$ and $|z| < h$, and the individual lamina areas are designated $A_l^{(k)}$, $k = 1,2,\ldots,N$. (In Fig. 3, N equals four only for convenience of illustration.) The global region occupies $0 < y < c$ and $|z| < h$, and its area is designated Ag. Individual laminae are not identified in Ag since a smeared theory is assumed to apply here. If the edge $y = b$ is traction-free, then very large interlaminar stress gradients are known to exist within a distance of one laminate thickness of the edge.[4] This is the motivation for putting the local region at the edge.

Following Pagano and Soni,[11] we use the same variational approach, but applied to the section shown in Fig. 3. Consider the functional

$$\pi = (1/2) \int_{A_g} (\sigma_x \varepsilon_x + \sigma_y \varepsilon_y + \sigma_z \varepsilon_z + \tau_{yz} \gamma_{yz}) dA_g$$
$$+ \sum_{k=1}^{N} \int_{A_l^{(k)}} [u_{,x}\sigma_x + v_{,y}\sigma_y + w_{,z}\sigma_z + (v_{,z} + w_{,y})\tau_{yz} - w_c(\sigma)] dA_l^{(k)} \qquad (3)$$
$$- \int_{L'} (\tilde{T}_y v + \tilde{T}_z w) ds$$

in which partial differentiation with respect to a coordinate is indicated by a comma followed by the coordinate as a subscript, and $W_c(\sigma)$ is the complementary strain energy density. The external surface traction components prescribed on portion L' of the lateral edge are

$$\tilde{T}_y = \tilde{\sigma}_y n_y + \tilde{\tau}_{zy} n_z, \quad \tilde{T}_z = \tilde{\tau}_{yz} n_y + \tilde{\sigma}_z n_z . \qquad (4),(5)$$

The tilde designates a prescribed quantity, and (n_y, n_z) are the components of the unit outward normal to the lateral edge line in the $x = 0$

cross-section. It is assumed $\tilde{T}_x$ is zero. The integral in Eq. 3 over the global region Ag is the strain energy per unit x-direction length. The integrals over the local region $A_1^{(k)}$ laminae are the Reissner functionals per unit x-direction length. The field equations and boundary conditions governing equilibrium are obtained from the vanishing of the first variation of π; i.e., $\delta\pi = 0$. In the global region only the displacements are varied. In the local region both the stresses and displacements are permitted to vary in the Reissner functionals. After using Green's theorem and some manipulations the first variation of π is

$$
\begin{aligned}
\delta\pi = \; & \int_{A_g} [-(\sigma_{y,y} + \tau_{zy,z})\delta v - (\tau_{yz,y} + \sigma_{z,z})\delta w]\, dA_g \\
& + \sum_{k=1}^{N} \int_{A_1^{(k)}} \{[\varepsilon_x - (s_{11}\sigma_x + s_{12}\sigma_y + s_{13}\sigma_z)]^{(k)} \delta\sigma_x^{(k)} \\
& + [v_{,y} - (s_{12}\sigma_x + s_{22}\sigma_y + s_{23}\sigma_z)]^{(k)} \delta\sigma_y^{(k)} \\
& + [w_{,z} - (s_{13}\sigma_x + s_{23}\sigma_y + s_{33}\sigma_z)]^{(k)} \delta\sigma_z^{(k)} \\
& + [v_{,z} + w_{,y} - s_{44}\tau_{yz}]^{(k)} \delta\tau_{yz}^{(k)} \\
& - [\sigma_{y,y} + \tau_{zy,z}]^{(k)} \delta v^{(k)} - [\tau_{yz,y} + \sigma_{z,z}]^{(k)} \delta w^{(k)}\} dA_1^{(k)} \\
& + \int_o^c [(\sigma_z - \tilde{\sigma}_z)\delta w + (\tau_{zy} - \tilde{\tau}_{zy})\delta v]_{z=-h}^{z=+h} dy \\
& + \int_{-h}^{+h} [\sigma_y \delta v + \tau_{yz}\delta w]_{y=c} dz - \int_{-h}^{+h} [(\sigma_y - \tilde{\sigma_y})\delta v + (\tau_{yz} - \tilde{\tau}_{yz})\delta w]_{y=0} dz \\
& + \int_c^b [(\sigma_z^{(N)} - \tilde{\sigma}_z)\delta w^{(N)} + (\tau_{zy}^{(N)} - \tilde{\tau}_{yz})\delta v^{(N)}]_{z=h} dy \\
& - \int_c^b [(\sigma_z^{(1)} - \tilde{\sigma}_z)\delta w^{(1)} + (\tau_{zy}^{(1)} - \tilde{\tau}_{yz})\delta v^{(1)}]_{z=-h} dy \\
& + \sum_{k=1}^{N-1} \int_c^b \{[\sigma_z \delta w + \tau_{zy}\delta v]_{z_k=t/2}^{(k)} - [\sigma_z \delta w + \tau_{zy}\delta v]_{z_{k+1}=-t/2}^{(k+1)}\} dy \\
& + \sum_{k=1}^{N} \int_{-t/2}^{+t/2} [\sigma_y^{(k)} \delta v^{(k)} + \tau_{yz}^{(k)} \delta w^{(k)}]_{y=c}^{y=b} dz_k - \int_{-h}^{+h} [\tilde{\sigma}_y \delta v + \tilde{\tau}_{yz}\delta w]_{y=b} dz
\end{aligned}
\tag{6}
$$

Recall that ε_x is a prescribd strain so that in the process of obtaining Eq. 6 $\delta\varepsilon_x = 0$. Also in Eq. 6 the difference in a quantity between two coordinate values is described symbolically by

$$[\cdot]_{z=-h}^{z=h} = [\cdot]_{z=h} - [\cdot]_{z=-h}.$$

We are now in a position to introduce the approximate theories in each region. Following the usual procedure in structure theories, explicit assumptions on the dependence of the field variables in the thickness coordinate z are made. The displacement fields are assumed to have the form

$$v(y,z) = \begin{cases} V(y) - z\,W_{,y}(y), & 0 < y < c \\ V(y) - z\,W_{,y}(y) + v^{(k)}(y,z_k) & c < y < b \end{cases} \tag{7}$$

$$w(y,z) = \begin{cases} W(y), & 0 < y < c \\ W(y) + w^{(k)}(y,z_k), & c < y < b \end{cases} \tag{8}$$

In the global region the displacement fields have the form consistent with Kirchhoff's hypothesis. In the local region the additional displacements $v^{(k)}$ and $w^{(k)}$ with respect to the global displacements are left arbitrary. This rationale is adopted from Pagano's[9] discussion about the objectional features of assuming displacement fields for laminate stress concentration problems. Instead, we assume the in-plane stresses in the local region are of the form

$$\sigma_x^{(k)} = N_x^{(k)}/t - (12M_x^{(k)}/t^3)z_k \tag{9}$$

$$\sigma_y^{(k)} = N_y^{(k)}/t - (12M_y^{(k)}/t^3)z_k \tag{10}$$

where

$$(N_\alpha^{(k)}, M_\alpha^{(k)}) = \int_{-t/2}^{+t/2} \sigma_\alpha^{(k)} \cdot (1, -z_k)\,dz_k \;;\; \alpha = x,y\,. \tag{11}$$

Eq. 10 is substituted into the equilibrium equations of linear elasticity. These are integrated to determine the explicit functional dependence in z_k of the stress components $\tau_{yz}^{(k)}$ and $\sigma_z^{(k)}$. This process intro-

duces an arbitrary function of y in each stress component. These two functions are determined in terms of the interlaminar stress components at the top and bottom of the layer using the definitions

$$\sigma_z^{(k)}(y,\pm t/2) = \begin{Bmatrix} p_2^{(k)} \\ p_1^{(k)} \end{Bmatrix}, \quad \tau_{zy}^{(k)}(y,\pm t/2) = \begin{Bmatrix} s_2^{(k)} \\ s_1^{(k)} \end{Bmatrix}. \tag{12}$$

In addition equilibrium of an element in the kth layer, as shown in Fig. 4, is used to eliminate derivatives of the resultants in terms of interlaminar stress components. In the limit as $\Delta y \to 0$, equilibrium of the element in Fig. 4 requires

$$N_{y,y}^{(k)} + s_2^{(k)} - s_1^{(k)} = 0 \tag{13}$$

$$V_{y,y}^{(k)} + p_2^{(k)} - p_1^{(k)} = 0 \tag{14}$$

$$M_{y,y}^{(k)} + V_y^{(k)} - (t/2)(s_1^{(k)} + s_2^{(k)}) = 0 \tag{15}$$

in which

$$V_y^{(k)} = \int_{-t/2}^{+t/2} \tau_{yz}^{(k)} dz_k. \tag{16}$$

As anticipated, Eqs. 13 to 15 will be recovered at the completion of the variational procedure. Finally, the explicit form of the stress components are

$$\begin{aligned} \tau_{yz}^{(k)} &= (s_2 - s_1)^{(k)}(z_{k/t}) + (s_1 + s_2)^{(k)}/4 \cdot (12\, z_k^2/t^2 - 1) \\ &\quad + (3/2)V_y^{(k)}/t(1 - 4z_k^2/t^2), \qquad c < y < b \end{aligned} \tag{17}$$

$$\begin{aligned} \sigma_z^{(k)} &= (p_1 + p_2)^{(k)}/2 + (3/2)(p_2 - p_1)^{(k)}(z_k/t - (4/3)z_k^3/t^3) \\ &\quad + (t/8)(s_2 - s_1)_{,y}^{(k)}(1 - 4z_k^2/t^2) \\ &\quad - (t/8)(s_2 + s_1)_{,y}^{(k)}(2z_k^2/t^2 - 8z_k^3/t^3), \quad c < y < b \end{aligned} \tag{18}$$

It should be noted that the assumed shear stress, Eq. 17, is the same as in Pagano's[9] work, but that the normal stress component, Eq. 18, is not.

The displacement field assumptions, Eqs. 7 and 8, and the stress

field assumptions, Eqs. 9, 10, 17, and 18, are substituted into the variational principle Eq. 6. Integration with respect to the z-coordinate is performed. In this process weighted displacement components defined by

$$(f, f^*, \hat{f}) = \int_{-1/2}^{+1/2} f \cdot (1, z_k/t, z_k^2/t^2) d(z_k/t) \qquad (19)$$

occur naturally in the local region. Also, in the local region the displacement components at the top of the kth layer are denoted by $v_2^{(k)}$ and $w_2^{(k)}$, and at the bottom by $v_1^{(k)}$ and $w_1^{(k)}$. The steps described are lengthy, and involve many integrations by parts. Upon completion the first variation is

$$\begin{aligned}
\delta\pi = & \int_o^c \{-[N_{y,y} + \tilde{s}_2 - \tilde{s}_1]\delta V - [-M_{y,yy} + h(\tilde{s}_2 + \tilde{s}_1)_{,y} + p_2 - p_1]\delta W\} dy \\
& + \int_b^c \{-[\sum_{k=1}^{N} N_{y,y}^{(k)} + \tilde{s}_2 - \tilde{s}_1]\delta V - [-\sum_{k=1}^{N} (M_{y,yy} - \bar{h}_k N_{y,y})^{(k)} \\
& \qquad + h(\tilde{s}_2 + \tilde{s}_1)_{,y} + \tilde{p}_2 - \tilde{p}_1]\delta W\} d_y \\
& + \sum_{k=1}^{N} \int_c^b \{\delta N_x^{(k)} [\varepsilon_x - s_{11} N_x/t - s_{12} N_y/t - s_{13}[(p_1 + p_2)/2 \\
& \qquad + (t/12)(s_2 - s_1)_{,y}]]^{(k)} \\
& - \frac{12}{t} \delta M_x^{(k)} [s_{11} M_x/t^2 + s_{12} M_y/t^2 - s_{13}[(p_2 - p_1)/10 \\
& \qquad - (t/120)(s_1 + s_2)_{,y}]]^{(k)} \\
& + \delta N_y^{(k)} [V_{,y} - \bar{h}_k W_{,yy} + \bar{v}_{,y} - s_{12} N_x/t - s_{22} N_y/t - \\
& \qquad s_{23}[(p_1 + p_2)/2 + (t/12)(s_2 - s_1)_{,y}]]^{(k)} \\
& - \frac{12}{t} \delta M_y^{(k)} [-W_{,yy} t/12 + v^*_{,y} + s_{12} M_x/t^2 + s_{22} M_y/t^2 - \\
& \qquad s_{23}[(p_2 - p_1)/10 - (t/120)(s_1 + s_2)_{,y}]]^{(k)} \\
& + \frac{3}{2} \delta V_y^{(k)} [8v^*/t + (\bar{w} - 4\hat{w})_{,y} - s_{44}[-(s_1 + s_2)/15 + (12/15) V_y/t]]^{(k)} \\
& + \frac{1}{2} \delta p_2^{(k)} [2w_2 - 3(\bar{w} - 4\hat{w}) - s_{13} \bar{x}_2 t - s_{23} \bar{y}_2 t - s_{33} t R_2]^{(k)}
\end{aligned}$$

$$+\frac{1}{2}\,\delta p_1^{(k)}[-2w_1+3(\bar{w}-4\hat{w})-s_{13}\bar{X}_1 t-s_{23}\bar{Y}_1 t-s_{33}t\,R_1]^{(k)}$$

$$+t\delta s_{2,y}^{(k)}[+w^*+(\bar{w}-12\hat{w})/4-s_{13}X_2 t/12-s_{23}Y_2 t/12-s_{33}\frac{t}{8}U_2]^{(k)}$$

$$+t\delta s_{1,y}^{(k)}[-w^*+(\bar{w}-12\hat{w})/4+s_{13}X_1 t/12+s_{23}Y_1 t/12+s_{33}\frac{t}{8}U_1]^{(k)}$$

$$+t\delta s_2^{(k)}[v_2/t-\bar{v}/t-6v^*/t+w^*_{,y}-(\bar{w}_{,y}-12\hat{w}_{,y})/4-s_{44}T_4]^{(k)}$$

$$+t\delta s_1^{(k)}[-v_1/t+\bar{v}/t-6v^*/t-w^*_{,y}-(\bar{w}_{,y}-12\hat{w}_{,y})/4-s_{44}Q_4]^{(k)}$$

$$-\delta\bar{v}^{(k)}[N_{y,y}+s_2-s_1]^{(k)}-\frac{12}{t}\,\delta v^{*(k)}[-M_{y,y}+V_y-\frac{t}{2}(s_1+s_2)]^{(k)}$$

$$-(3/2)(\delta\bar{w}-4\delta\hat{w})^{(k)}[V_{y,y}+p_2-p_1]^{(k)}\}dy$$

$$+\int_c^b[(p_2^{(N)}-\tilde{p}_2)\delta w_2^{(N)}+(s_2^{(N)}-\tilde{s}_2)\delta v_2^{(N)}-(p_1^{(1)}-\tilde{p}_1)\delta w_1^{(1)}-(s_1^{(1)}-\tilde{s}_1)\delta v_1^{(1)}]dy$$

$$-[(M_{y,y}+V_y-h(\tilde{s}_2+\tilde{s}_1))\delta w]_{y=0}^{y=c}$$

$$-[[\sum_{k=1}^{N}(M_{y,y}-\bar{h}_k N_{y,y}+V_y)^{(k)}-h(\tilde{s}_2+\tilde{s}_1)\delta w]_{y=c}^{y=b}$$

$$-[(N_y-\tilde{N}_y)\delta V+(M_y-\tilde{M}_y)\delta w_{,y}+(V_y-\tilde{V}_y)\delta w]_{y=0}$$

$$+\{[N_y-\sum_{k=1}^{N}N_y^{(k)}]\delta V+[M_y-\sum_{k=1}^{N}(M_y^{(k)}-\bar{h}_k N_y^{(k)})\delta w_{,y}+[V_y-\sum_{k=1}^{N}V_y^{(k)}]\delta w\}_{y=c}$$

$$+\{[\sum_{k=1}^{N}N_y^{(k)}-\tilde{N}_y]\delta V+[\sum_{k=1}^{N}(M_y-\bar{h}_k N_y)^{(k)}-\tilde{M}_y]\delta w_{,y}+[\sum_{k=1}^{N}V_y^{(k)}-\tilde{V}_y]\delta w\}_{y=b}$$

$$-\sum_{k=1}^{N}\{N_y\delta\bar{v}-[12M_y/t]\delta v^*+[-(s_1+s_2)+3V_y/t](\delta\bar{w}-4\delta\hat{w})t$$

$$+\sum_{k=1}^{N}\{[N_y-\tilde{N}_y]\delta\bar{v}-12[M_y/t-\tilde{M}_y/t]\delta v^*+(s_2-s_1)t\delta w^*\}_{y=c}^{(k)}$$

$$+[-(s_1+s_2)+3V_y/t+(\tilde{s}_1+\tilde{s}_2)-3\tilde{V}_y/t](\delta\bar{w}-4\delta\hat{w})\cdot t$$

$$+[(s_2-s_1)-(\tilde{s}_2-\tilde{s}_1)]\delta w^* t\}^{(k)} \qquad (20)$$

In Eq. 20 we defined (The superscript (k) is omitted, but is implied.)

$$\left.\begin{matrix} R_2 \\ R_1 \end{matrix}\right\} = (p_1 + p_2)/2 \pm 17(p_2 - p_1)/70 + \frac{t}{12}(s_2 - s_1)_{,y} \mp \frac{3t}{140}(s_1 + s_2)_{,y} \tag{21}$$

$$\left.\begin{matrix} U_2 \\ U_1 \end{matrix}\right\} = (p_1 + p_2)/3 \mp 4(p_2 - p_1)/105 + \frac{t}{15}(s_2 - s_1)_{,y} \pm \frac{t}{105}(s_1 + s_2)_{,y} \tag{22}$$

$$T_4 = (4s_2 - s_1)/30 - V_{y}/(10t) \tag{23}$$

$$Q_4 = (4s_1 - s_2)/30 - V_{y}/(10t) \tag{24}$$

$$\left.\begin{matrix} X_2 \\ X_1 \end{matrix}\right\} = \frac{N_x}{t} \pm \frac{6}{5}\frac{M_x}{t^2} \quad , \quad \left.\begin{matrix} Y_2 \\ Y_1 \end{matrix}\right\} = \frac{N_y}{t} \pm \frac{6}{5}\frac{M_y}{t^2} \tag{25}$$

(26)

$$\left.\begin{matrix} \bar{X}_2 \\ \bar{X}_1 \end{matrix}\right\} = \frac{N_x}{t} \mp \frac{12}{5}\frac{M_x}{t^2} \quad , \quad \left.\begin{matrix} \bar{Y}_2 \\ \bar{Y}_1 \end{matrix}\right\} = \frac{N_y}{t} \mp \frac{12}{5}\frac{M_y}{t^2} \tag{27}$$

(28)

For consistency, the prescribed edge tractions at y = b for each layer are assumed to have the form of Eqs. 10 and 17. To obtain Eq. 20, it was assumed that interlaminar continuity is satisfied. These conditions are

$$p_2^{(k)} = p_1^{(k+1)}, \; s_2^{(k)} = s_1^{(k+1)}, \; v_2^{(k)} = v_1^{(k+1)}, \; w_2^{(k)} = w_1^{(k+1)}; \; k=1,2,..,N=1. \tag{29}$$

Therefore the interlaminar stress components in Eq. 20 cannot be varied independently. Taking Eq. 29 into account reduces the number of independent interlaminar stress components per interface from four to two. Also, it is necessary to integrate by parts the terms in Eq. 20 involving derivatives of the interlaminar shear stress. Examination of Eq. 20 reveals that independent equilibrium equations do not result for $\delta w^{*(k)}$ and $\delta \hat{w}^{(k)}$ with respect to the equations associated with $\delta \bar{w}^{(k)}$. Hence, $w^{*(k)}$ and $\hat{w}^{(k)}$, k=1,2...N, are specified to be zero for all y. This insures an equal number of unknown variables and field equations.

If the first variation as expressed in Eq. 20 is modified to account for the considerations detailed above, and then set equal to zero, the following theory results:

$$0 < y < c$$

Constitutive law

$$N_y = A_{12}\varepsilon_x + A_{22}V,_y \tag{30}$$

$$M_y = D_{22}W,_{yy} \tag{31}$$

Equilibrium equations

$$N_{y,y} + \tilde{s}_2 - \tilde{s}_1 = 0 \tag{32}$$

$$-M_{y,yy} + h(\tilde{s}_1 + \tilde{s}_2),_y + \tilde{p}_2 - \tilde{p}_1 = 0 \tag{33}$$

$$c < y < b$$

Constitutive law

$$\varepsilon_x = \{s_{11}N_x/t + s_{12}N_y/t + s_{13}[(p_1 + p_2)/12 + (t/12)(s_2 - s_1),_y]\}^{(k)} \tag{34}$$

$$0 = \{s_{11}Mx/t^2 + s_{12}My/t^2 - s_{13}[(p_1 + p_2)/10 - (t/120)(s_1 + s_2),_y]\}^{(k)} \tag{35}$$

$$V,_y - \bar{h}_k W,_{yy} + \bar{v}^{(k)},_y = \{s_{12}N_x/t + s_{22}N_y/t + s_{23}[(p_1 + p_2)/2 + (t/12)(s_2 - s_1),_y]\}^{(k)} \tag{36}$$

$$\frac{t}{12} W,_{yy} - v^{*(k)},_y = \{s_{12}Mx/t^2 + s_{22}M_y/t^2 - s_{23}[(p_2 - p_1)/10 - (t/120)(s_1 + s_2),_y]\}^{(k)} \tag{37}$$

$$\frac{8}{t} v^{*(k)} + \bar{w}^{(k)},_y = s_{44}^{(k)}[-(s_1 + s_2)/15 + (12/15)(V_y/t)]^{(k)}, \quad k=1,2,\ldots,N \tag{38}$$

Equilibrium equations

$$N_{y,y}^{(k)} + s_2^{(k)} - s_1^{(k)} = 0 \tag{39}$$

$$M_{y,y}^{(k)} + V_y^{(k)} - (t/2)(s_1 + s_2)^{(k)} = 0 \tag{40}$$

$$V_{y,y}^{(k)} + p_2^{(k)} - p_1^{(k)} = 0 \quad , \; k = 1,2,\ldots,N \tag{41}$$

$$\sum_{k=1}^{N} N_{y,y}^{(k)} + \tilde{s}_2 - \tilde{s}_1 = 0 \tag{42}$$

$$\sum_{k=1}^{N} (M_y^{(k)} - \bar{h}_k N_y^{(k)}),_{yy} + h(\tilde{s}_1 + \tilde{s}_2),_y + \tilde{p}_2 - \tilde{p}_1 = 0 \tag{43}$$

Interlaminar continuity

$$p_2^{(k)} = p_1^{(k+1)} \quad , \quad s_2^{(k)} = s_1^{(k+1)} \qquad (44),(45)$$

$$\{3\bar{w}/t + s_{13}\bar{X}_2 + s_{23}\bar{Y}_2 + s_{33}R_2\}^{(k)} - \{3\bar{w}/t - s_{13}\bar{X}_1 - s_{23}\bar{Y}_1 - s_{33}R_1\}^{(k+1)} \qquad (46)$$

$$\{\tfrac{1}{2}\bar{w}_{,y}/t + \bar{v}/t^2 + 6v^*/t^2 - s_{13}X_{2,y}/12 - s_{23}Y_{2,y}/12 + s_{33}U_{2,y}/8 + s_{44}T_4/t\}^{(k)}$$

$$+ \{(1/2t)\bar{w}_{,y} - \bar{v}/t^2 + 6v^*/t^2 + s_{13}X_{1,y}/12 + s_{23}Y_{1,y}/12 + s_{33}U_{1,y}/8 + s_{44}Q_4/t\}^{(k+1)} = 0 \qquad (47)$$

At the top surface of the Nth layer there are two conditions.

Either

$$p_2^{(N)} = \tilde{p}_2 \text{ or } \{3\bar{w}/t + s_{13}\bar{X}_2 + s_{23}\bar{Y}_2 + s_{33}R_2\}^{(N)} = 2\tilde{w}_2/t. \qquad (48)$$

Either

$$s_2^{(N)} = \tilde{s}_2 \text{ or } \{\bar{w}_{,y}/2t + \bar{v}/t^2 + 6v^*/t^2 - s_{13}X_{2,y}/12 - s_{23}Y_{2,y}/12 - s_{33}U_{2,y}/8 + s_{44}T_4/t\}^{(N)} = \tilde{v}_{2/t^2} \qquad (49)$$

At the bottom surface of the first layer there are two conditions.

Either

$$p_1^{(1)} = \tilde{p}_1 \text{ or } \{\tfrac{3}{t}\bar{w} - s_{13}\bar{X}_1 - s_{23}\bar{Y}_1 - s_{33}R_1\}^{(1)} = 2\tilde{w}_1/t \qquad (50)$$

Either

$$s_1^{(1)} = \tilde{s}_1 \text{ or } \{-\bar{w}_{,y}/2t + \bar{v}/t^2 - 6v^*/t^2 - \tfrac{1}{12}s_{13}X_{1,y} - \tfrac{1}{12}s_{23}Y_{1,y} - \tfrac{1}{8}s_{33}U_{1,y} - \tfrac{1}{t}s_{44}Q_4\}^{(1)} = \tilde{v}_{1/t} \qquad (51)$$

Edge Conditions

At y = 0 and y = b:

Either $V = \tilde{V}$. or $Ny = \tilde{N}y$ (52)

Either $W = \tilde{W}$ or $M_{y,y} = -\tilde{V}_y + h[\tilde{s}_2 + \tilde{s}_1]$ (53)

Either $w_{,y} = \tilde{w}_{,y}$ or $M_y = \tilde{M}_y$ (54)

Continuity at y = c:

$$N_y = \sum_{k=1}^{N} N_y^{(k)} \quad , \quad M_y = \sum_{k=1}^{N} [M_y - \bar{h}_k N_y]^{(k)} \quad , \quad M_{y,y} = \sum_{k=1}^{N} (M_y - \bar{h}_k N_y)_{,y}^{(k)} \qquad (55),(56),(57)$$

$$\bar{v}^{(k)} = 0 \quad , \quad v^{*(k)} = 0 \quad , \quad \bar{w}^{(k)} = 0 \qquad (58),(59),(60)$$

At y = c and y = b:
Either $s_2^{(k)}$ is prescribed or

$$\{\bar{w}/(4t) - \frac{1}{12} s_{13} X_2 - \frac{1}{12} s_{23} Y_2 - \frac{1}{8} s_{33} U_2\}^{(k)}$$

$$+ \{\bar{w}/(4t) + \frac{1}{12} s_{13} X_1 + \frac{1}{12} s_{23} Y_1 + \frac{1}{8} s_{33} U_1\}^{(k+1)} = 0$$

k = 1, 2,..., N-1

Either $s_2^{(N)} = \tilde{s}_2$ or $\{\bar{w}/(4t) - \frac{1}{12} s_{13} X_2 - \frac{1}{12} s_{23} Y_2 - \frac{1}{8} s_{33} U_2\}^{(N)} = 0$

Either $s_1^{(1)} = \tilde{s}_1$ or $\{\bar{w}/(4t) + \frac{1}{12} s_{13} X_1 + \frac{1}{12} s_{23} Y_1 + \frac{1}{8} s_{33} U_1\}^{(1)} = 0$

At y = b one term in each of the following three products is prescribed for each layer.

$$(\bar{v}^{(k)}, N_y^{(k)}), \quad (v^{*(k)}, M_y^{(k)}), \quad (\bar{w}^{(k)}, (s_1 + s_2)^{(k)}/4 - 3/2 \; Vy^{(k)}/t) \qquad (62),(63),(64)$$

The constitutive Eqs. (30) and 31 do not result directly from the variational principle, but are clearly classical lamination theory results obtained in a straightforward manner.

The theory summarized above consists of four dependent variables in the global region and 12N + 2 in the local region. An equal number of equations are provided. There are three edge conditions at y = 0, and 4N + 4 at c and b. The choice of c is arbitrary, and would have to be selected by engineering judgement to solve a problem. Finally, Pagano's local theory would have 2N more variables and equations than the present one.

V. RECOMMENDATIONS:

The merit of the present theory is its relative simplicity for analyzing stress concentrations and stress gradients in composite laminates including the interlaminar stress components. Clearly, as an approximate theory, it must be examined with respect to previous results on pertinent problems. Therefore, it is recommended to solve the problem of uniform extension of a symmetric bidirectional laminate with stress-free edges using the field equations summarized in Sec. IV.

It is recognized that the plausibility of this approximate theory depends upon the initial assumptions for the stress fields. Other choices are possible since we are free to choose the stresses in Reissner's functional. The question of what to select is a difficult one. It should be examined in the light of experiences gained from previous results, and the results obtained by exercising the present theory. As a long term recommendation, then, the choice on the form of the assumed stress fields should be scrutinized.

References

1. E. Reissner and Y. Stavsky, "Bending and Stretching of Certain Types of Heterogeneous Aeolotropic Elastic Plates," J. of Appl. Mech., Vol. 28, p. 402, (1961).

2. S. B. Dong, K. S. Pister, and R. L. Taylor, "On the Theory of Laminated Anisotropic Shells and Plates," J. Aero. Sci., Vol. 28, p. 969, (1962).

3. J. M. Whitney, and C. T. Sun, "A Higher Order Theory for Extensional Motion of Laminated Composites," J. Sound and Vibration, Vol. 30, pp. 85-97, (1973).

4. R. B. Pipes, and N. J. Pagano, "Interlaminar Stresses in Composite Laminates Under Uniform Axial Extension," J. Composite Materials, Vol. 4, pp. 538-548, (1970).

5. J. B. Whiteside, I. M. Daniel, and R. E. Rowlands, "The Behavior of Advanced Filamentary Composite Plates with Cutouts," Air Force Flight Dynamics Laboratory Technical Report AFFDL-TR-73-48, Wright-Patterson Air Force Base, Ohio, (1973).

6. T. L. Waltz, and J. R. Vinson," Interlaminar Stresses in Laminated Cylindrical Shells of Composite Materials," AIAA Paper No. 75-755,

presented at the 16th Structures, Structural Dynamics, and Materials Conference, Denver, CO, May 27-29, 1975.

7. Paul Seide, "An Improved Approximate Theory for the Bending of Laminated Plates," in proc. of symposium honoring E. Reissner, University of California San Diego, La Jolla, CA, June 23, 1978.

8. S. Srinivas, "A Refined Analysis of Composite Laminates," J. Sound and Vibration, Vol. 30., pp. 495-507, (1973).

9. N. J. Pagano, "Stress Fields in Composite Laminates," Int. J. Solids and Structures, Vol. 14, pp. 385-400, (1978).

10. N. J. Pagano, "Free Edge Stress Fields in Composite Laminates," Int. J. Solids and Structures, Vol. 14, pp. 401-406, (1978).

11. N. J. Pagano, and S. R. Soni, "Global-Local Laminate Variational Model," to appear in the Int. J. of Solids and Structures.

12. S. R. Soni, and N. J. Pagano, "On the Applicability of the Global-Local Model in the Stress Analysis of Composite Laminates," presented at the IUTAM Symposium on Mechanics of Composite Materials, August 16-19, 1982, Virginia Polytechnic Institute and State University, Blacksburg, VA.

13. J. M. Whitney, and R. J. Nusimer, "Stress Fracture Criteria for Laminated Composites Containing Stress Concentrations," J. Composite Materials, Vol. 8, pp. 254-265, (1974).

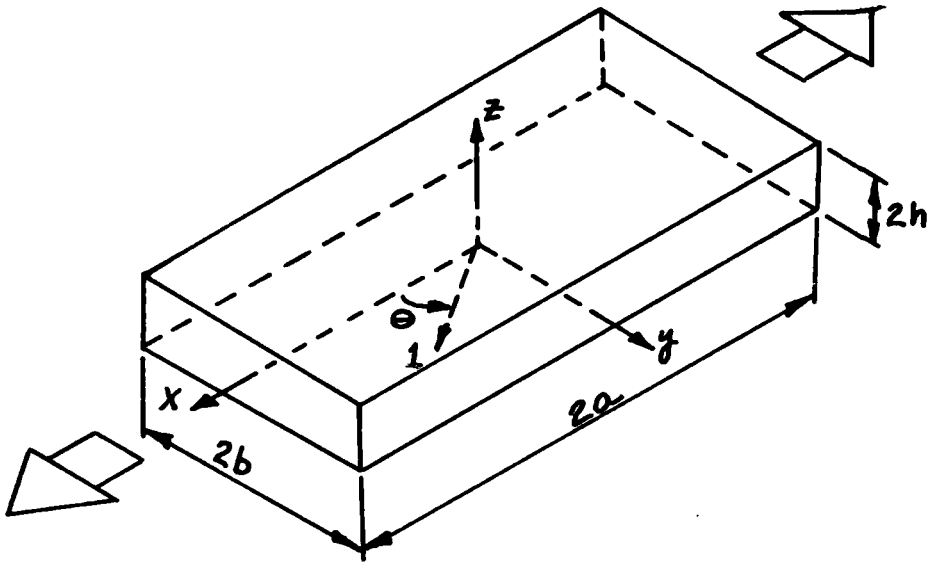


FIG. 1 LAMINATE CONFIGURATION

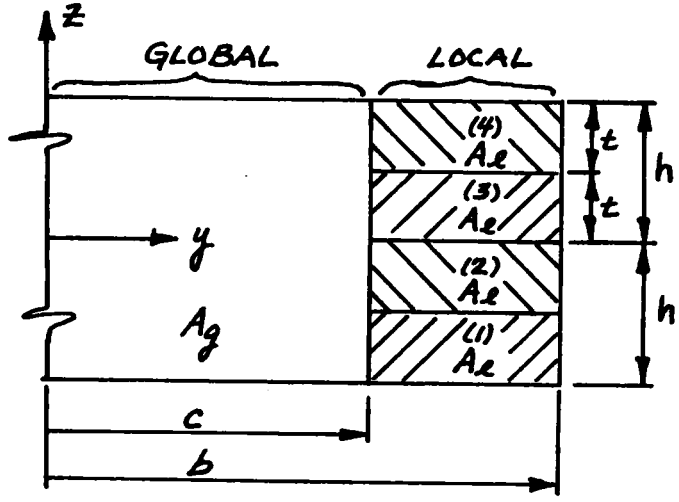


FIG. 3 GLOBAL-LOCAL REGIONS

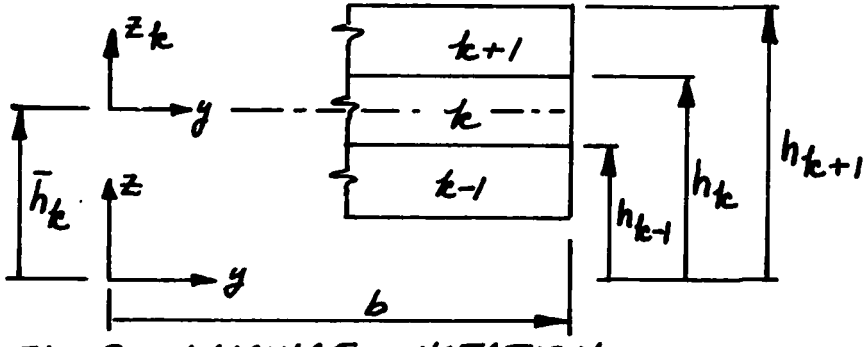


FIG. 2 LAMINAE NOTATION

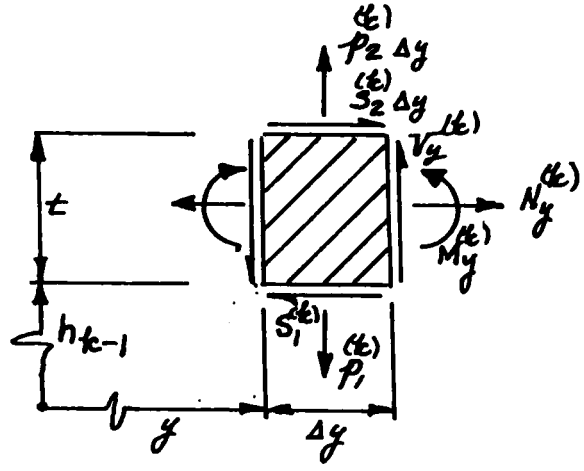


FIG. 4 FREE BODY ELEMENT

1982 USAF-SCEEE SUMMER FACULTY RESEARCH PROGRAM

Sponsored by the

AIR FORCE OFFICE OF SCIENTIFIC RESEARCH

Conducted by the

SOUTHEASTERN CENTER FOR ELECTRICAL ENGINEERING EDUCATION

FINAL REPORT

SYNTHESIS OF ACETYLENE TERMINATED SULFONE (ATS) CANDIDATES

Prepared by:	James J. Kane
Academic Rank:	Associate Professor
Department and University:	Department of Chemistry Wright State University
Research Location:	Air Force Wright Aeronautical Laboratories Materials Laboratory, Polymer Branch Wright Patterson Air Force Base, Ohio
USAF Research Colleague:	Dr. Fred E. Arnold
Date:	August 20, 1982
Contract No:	F49620-82-C-0035

SYNTHESIS OF ACETYLENE TERMINATED SULFONE (ATS) CANDIDATES

by

James J. Kane

and

Brenda G. Evans

ABSTRACT

Certain acetylene terminated sulfone (ATS) systems are of interest as possible replacements for epoxy resins. The beneficial feature which the ATS systems are expected to offer is their insensitivity to moisture. Reaction schemes for their synthesis are outlined and discussed. Finally, the synthesis of certain of the intermediates required for the ATS candidates are reported and discussed and recommendations for future work in this area are presented.

Acknowledgement

The authors would like to express their sincere appreciation to the Air Force Systems Command, the Air Force Office of Scientific Research and the Southeastern Center for Electrical Engineering Education for their support and for the opportunity to spend a rewarding and interesting summer at the Air Force Materials Laboratory, Wright Patterson Air Force Base, Ohio. We would like to thank the people of the Polymer Branch in particular for their friendliness and their generosity in sharing their space, equipment, facilities and ideas so openly.

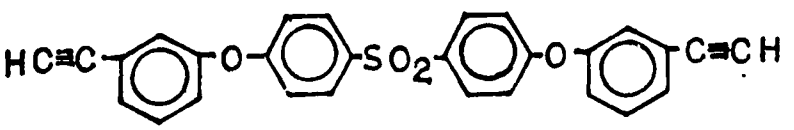
Finally, we would like to thank Dr. Fred E. Arnold for suggesting this area of research and for his helpful collaboration and guidance, and we would like to acknowledge the helpful discussions with Dr. Fred Hedberg, Lt. Patricia Lindley and Mr. Bruce Reinhardt.

I. INTRODUCTION

Previous workers[1,2,3] in the Materials Laboratory synthesized and characterized acetylene terminated (AT) oligomers for use as addition curable, moisture resistant, thermoset systems. The cure process of the tetrafunctional AT system has been shown by kinetic studies[4] to involve a thermally induced free-radical chain mechanism resulting in a cross-linked conjugated polyene network. Subsequent higher temperature reactions are believed to occur by cyclization reactions which convert the polyene system to a variety of aromatic structures.

Early workers[1,2] demonstrated that acetylene terminated phenylquinoxaline (ATQ) oligomers exhibit excellent properties for application as adhesives[5] and fiber reinforced composites.[6]

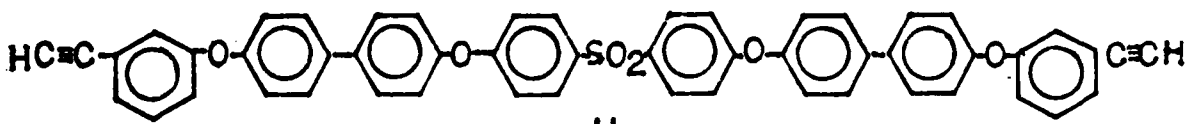
More recent[3] work was directed toward application of the AT chemistry to overcome the problem of moisture sensitivity common to epoxy matrix systems. Thus it was expected that certain AT resins would provide an epoxy substitute having all of the processing, handling and performance characteristics of epoxies combined with the characteristic moisture insensitivity of AT systems. This work resulted in the synthesis of the first AT system which incorporates a phenylsulfone. This compound, 4,4'-di-(3-ethynylphenoxy)-diphenylsulfone (ATS) (I) has



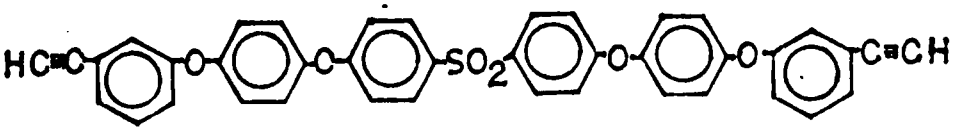
I

thermal properties (after cure) described as quite good. Further, it met all the processing criteria for a 350°F matrix material. Composites retained their strength properties after being saturated with moisture at 165°F.[7] However, the values for elongation to break and energy to fracture were marginal.[8] Thus it was considered desirable to introduce structural modifications into the ATS system which would be expected to improve these marginal properties and provide a more flexible material.

Cross-link density is one of the structural features in a cured material which contributes to brittleness. Thus the decision was made to synthesize ATS systems expected to have modified or decreased cross-link densities after cure. A straightforward route to this end is to synthesize ATS oligomers with greater distance between the reactive end groups than in the original ATS (I). Two compounds chosen for evaluation of this approach are the ATS systems II and III which incorporate in their backbone the rigid 4,4'-diphenyl and 1,4-phenylene segments respectively.



II



III

II. OBJECTIVES

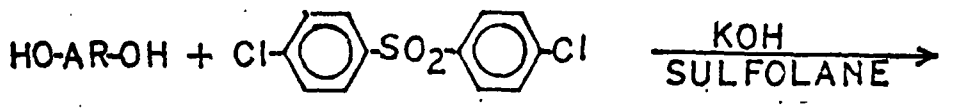
The objective of this project was to synthesize compounds II and III. The general synthetic routes are based on the bis-phenols (hydroquinone and p,p'-biphenol), m-dibromobenzene and 4,4'-dichlorodiphenylsulfone, all readily available materials.

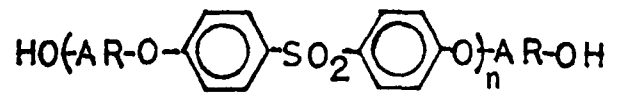
A series of reaction schemes are outlined below (Reactions 1-12). It is appropriate at this point to comment on some specific aspects of certain of these reactions.

III. DISCUSSION OF REACTIONS

Three reaction types are proposed in these syntheses. All involve displacement of aromatic halides. In those reactions where nucleophilic aromatic substitution is involved, (Reactions 1, 6, 10) it is first necessary to convert the bisphenol to its potassium salt with KOH. The resulting water is then removed by azeotropic distillation with benzene before reaction of the phenoxide with dichlorodiphenylsulfone in sulfolane. The other ether forming reactions (Reactions 2, 5, 7, 8, 12) are of the classical Ullman ether synthesis type. The mechanism of this reaction is still the subject of study.[9] The active catalyst appears to be Cu^{+1} and it is necessary to do the reaction in inert atmosphere to avoid oxidation to Cu^{++}. However, it has been reported[10] that aryl halides react with cuprous ion to reduce the halide and form cupric ion.

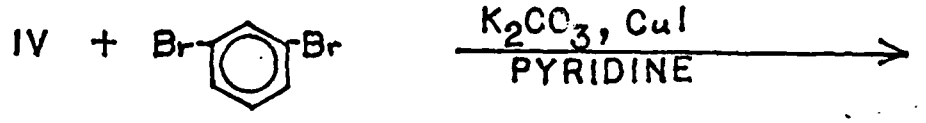
The final displacement reaction was recently developed[11] and is effective for displacement of aromatic and vinylic bromides and iodides with an acetylene using the catalyst combination of cuprous iodide and bis-triphenylphosphine palladium dichloride in a tertiary amine solvent (Reaction 3). In a final step, the protective group is removed from the



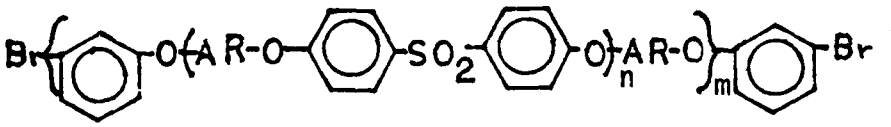


IV

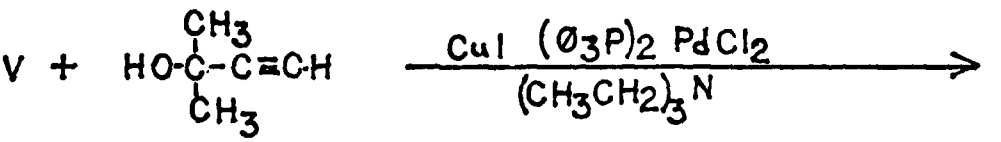
REACTION 1



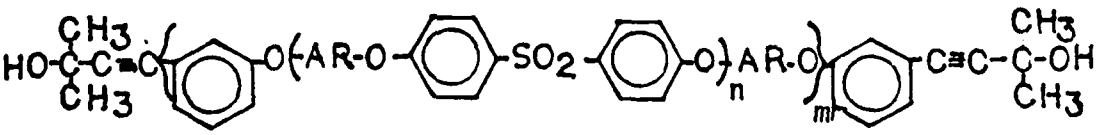
REACTION 2



V



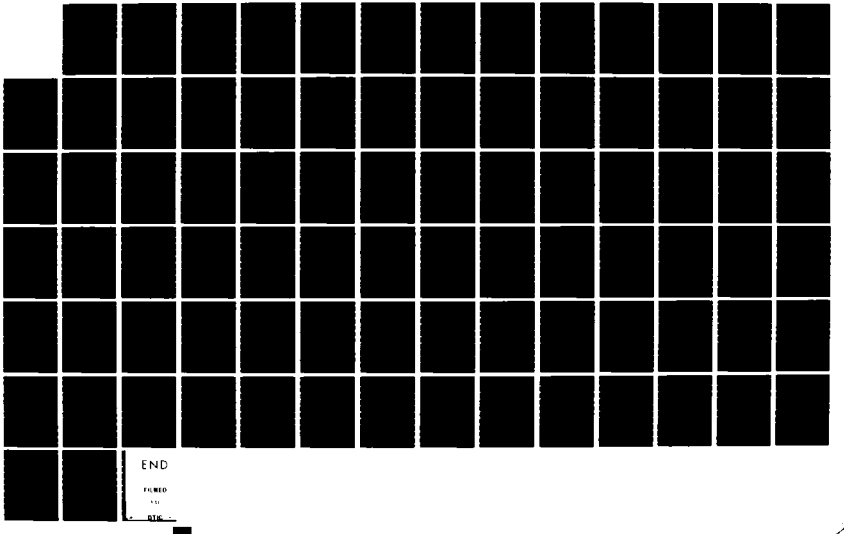
REACTION 3



VI

AD-A130 769 USAF/SCEEE SUMMER FACULTY RESEARCH PROGRAM RESEARCH REPORTS VOLUME 1. (U) SOUTHEASTERN CENTER FOR ELECTRICAL ENGINEERING EDUCATION INC S.. 11/11

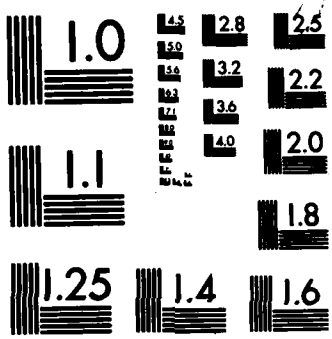
UNCLASSIFIED W D PEELE ET AL. OCT 82 AFOSR-TR-83-0613 F/G 5/1 NL



END

FILMED

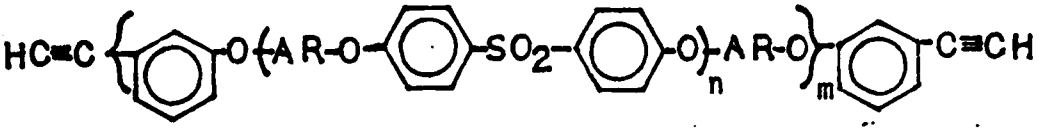
DTIC



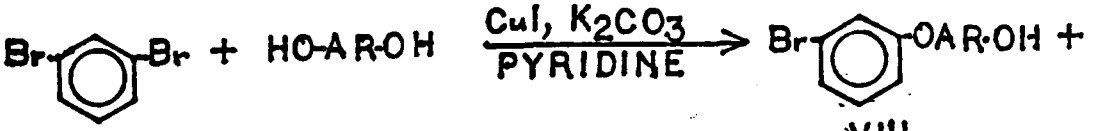
MICROCOPY RESOLUTION TEST CHART
NATIONAL BUREAU OF STANDARDS-1963-A

VI + KOH ⟶

REACTION 4

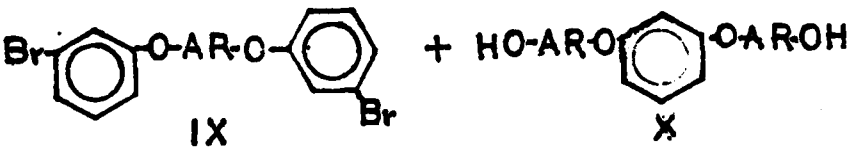


VII

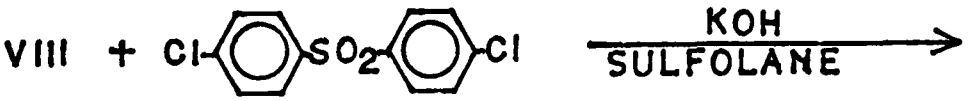


VIII

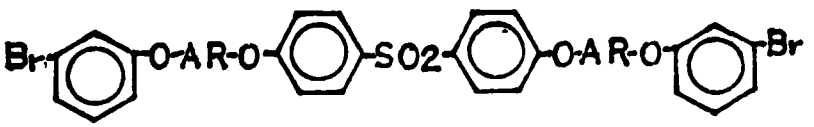
REACTION 5



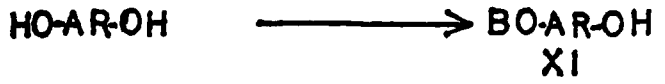
IX X



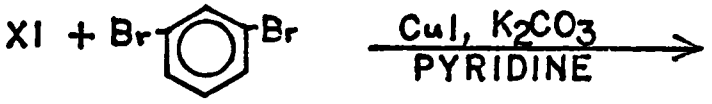
REACTION 6



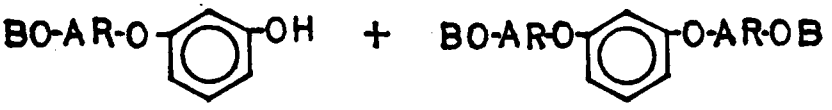
V(n=1)



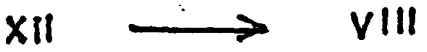
REACTION 7



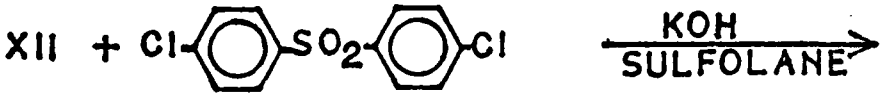
REACTION 8



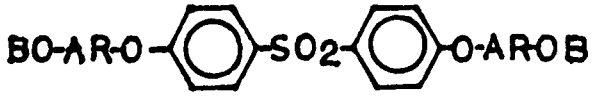
XII XIII



REACTION 9



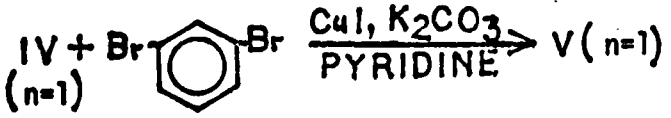
REACTION 10



XIV



REACTION 11



REACTION 12

terminal butynol functions by base catalyzed reversed addition to produce the AT product (Reaction 4).

Those condensation reactions in which the reactants are difunctional can lead to an array of oligomeric products. Use of an excess of bisphenol in Reaction I assures hydroxyl end-capping. However, the distribution of oligomers (Compound IV, values of n) is related to the relative rates of the competing reactions. Similarly Reaction 2 produces oligomers. In this case an excess of m-dibromobenzene assures m-bromophenyl end-caps and, as above, the distribution of oligomers (Compound V, values of m) is related to competing reaction rates.

Production of higher molecular weight oligomers may be useful to the overall goal of this project since values of n and/or m greater than one puts even greater distance between functional end groups. Alternatively, a reaction scheme assuring formation of oligomer in which the values of n and m are one is shown in Reaction 5. This reaction yields, among other products, the "half-product," VIII which when reacted with dichlorodiphenylsulfone yields V. Carrying V through the sequence of Reactions 3 and 4 yields compounds II and III as the lowest molecular weight oligomers (n=1, m=1).

Reaction 5 is complicated since the desired product, VIII, will react with starting materials to yield IX and X. IX and X can then go on to higher molecular weight products. Consideration of the various competing reactions suggests that an excess of m-dibromobenzene should suppress formation of X and higher molecular weight products while favoring formation of "half-product" VIII and "di-product" IX. It would be necessary to do an optimization study to determine the factors which favor

production of "half-product" VIII over "di-product," IX.

An alternate approach which might be expected to provide over-all high yields of "half-product" VIII involves blocking or protection of one of the phenol functions (Reaction 7) before its condensation with an excess of m-dibromobenzene to yield XII (Reaction 8) which after removal of the protecting groups provides "half-product" VIII.

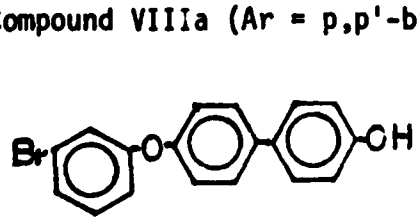
Examples of protecting groups are methyl ether, dihydropyran and esters. All of these groups are relatively easily removed. However, of the three, an ester function would be least likely to survive the basic conditions of the Ullman ether synthesis.

IV. RESULTS

The synthetic sequences outlined in Section II represent a long range synthetic undertaking. During the term of this project a relatively small number of the reactions were accomplished. In some cases a sufficient quantity of a desired intermediate was prepared for future workers to carry on to the next step. In other cases, only small quantities were isolated and the reaction was evaluated and described for future workers to repeat and prepare sufficient quantities for subsequent synthetic steps.

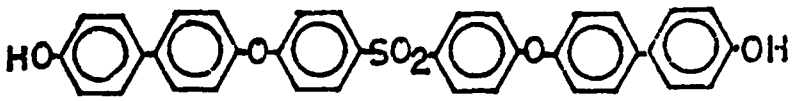
In the following paragraphs the results of these synthetic experiments are reported.

A. Compound VIIIa (Ar = p,p'-biphenylene)



This compound was prepared in 26 percent yield by the Ullman ether synthesis (Reaction 5) using 4,4'-dihydroxybiphenyl and m-dibromobenzene. The reaction was repeated a number of times and the yields were found to be not reproducible although a total of 10 grams was prepared.

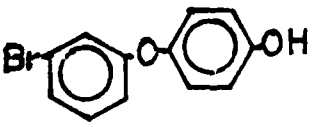
B. Compound IVa (Ar = p,p'-biphenylene)



This oligomeric material was prepared in 88 percent yield by reaction of 4,4'-dihydroxybiphenyl with 4,4'-dichlorodiphenylsulfone (Reaction 1).

The lower molecular weight oligomers were separated from the mixture by base extraction.

C. Compound VIIIb (Ar = p-phenylene)



This "half-product" was prepared in very poor yield (traces only) by reaction of hydroquinone and m-dibromobenzene (Reaction 5). The appearance of the reaction mixture suggested extensive oxidation of the hydroquinone occurred despite the inert reaction atmosphere. Presumably the oxidizing agent is cupric ion which results from interaction of m-dibromobenzene and cuprous ion.[10]

Compound VIIIb was more successfully prepared by a two step sequence involving first the preparation of Compound XIIb (Ar = p-phenylene; B= CH_3), 4-methoxy-4'-bromodiphenylether. XIIb was made in 43 percent yield by Reaction 8 with hydroquinone monomethyl ether and m-dibromobenzene. Cleavage of the methyl group with refluxing aqueous HBr gave the desired product, 4-hydroxy-4'bromodiphenylether (VIIIb). Although the yield of this step was under 10 percent, it was observed that a large amount of the methyl ether (XIIb) was unreacted. This observation suggests that another reagent (e.g. pyridine hydrochloride see paragraph D below) would be expected to cleave the ether more efficiently.

D. Compound IVb (Ar = p-phenylene, n=1)

Compound IVb was prepared by a two-step synthesis involving first the reaction of hydroquinone monomethyl ether with 4,4-dichlorodiphenylsulfone (Reaction 10). The resulting dimethyl ether, XIVb (Ar = p-phenylene; B=CH_3) was obtained in 68 percent yield. Cleavage of the methyl-ether functions was done with pyridine hydrochloride and gave the desired bisphenol, IVb, in 46 percent yield.

E. Compound Vb (Ar = p-phenylene; n=1)

Compound Vb was prepared in 80 percent yield by reaction of the bisphenol IVb with m-dibromobenzene. The product obtained was a viscous clear material which is probably oligomeric (m>1).

V. RECOMMENDATIONS

The synthetic sequences outlined in Section II offer several areas for concentration of effort. These may be classified into two categories. The one leads to ATS products which are monomeric (n=1, m=1) and the other leads to ATS products which are oligomeric.

On the basis of initial experimental work carried out in the term of this project, it appears that synthetic yields obtained with the Ullman ether synthesis are not reproducible. When applied to reactions which form oligomeric products, it will be extremely difficult to obtain product with similar molecular weight distribution from batch to batch. Thus post cure properties of such oligomeric products will be difficult to evaluate and to reproduce. It would probably be necessary to determine the factors necessary for better control of the Ullman ether synthesis before this problem could be simplified.

On the other hand, synthesis of the monomeric products II and III would provide, after cure, materials which would be of use in evaluating the effect of decreasing cross-link density by curing ATS materials of known structure. It is recommended that initial effort go into synthesis of the monomeric compounds.

The "half-product" VIIIa, 4-hydroxy-4'-(3-bromophenoxy)biphenyl was prepared in a sufficient quantity to take on through the next steps (Reactions 6, 3 and 4) to provide the required amount of the desired compound II. It is suggested that this be the first synthesis to be carried out. However, for future synthesis of this compound, it is strongly suggested that "half-product" be synthesized by first protecting one of the hydroxyl functions of the bis-phenol with either a methyl or a tetrahydropyranyl group (Reaction 7, Compound XI, Ar = p,p'-biphenylene; B=CH_3[1,2] or THP) as discussed in Section III.

The synthesis of the ATS III should be approached in the same general way using the reactions reported in this project for synthesis of 4-methoxy-4'-bromodiphenyl ether, and its subsequent cleavage with

pyridine-hydrochloride to form the "half-product" 4-hydrooxy-4'-bromo-diphenyl ether.

REFERENCES

1. R. F. Kovar, G. F. L. Ehlers and F. E. Arnold, J. of Polymer Sci., Poly. Chem. Ed., 15, 1081 (1977).

2. F. L. Hedberg and F. E. Arnold, J. of Appl. Poly. Sci., 24 (3), 763 (1979).

3. G. A. Laughran and F. E. Arnold, Polymer Preprints, 21 (1), 199 (1980).

4. J. M. Pickard, E. G. Jones and I. J. Goldfarb, Macromolecules, 12 (5), 895 (1979).

5. M. G. Maximovitch, S. C. Lockerby, R. F. Kovar and F. E. Arnold, Adhesive Age, 40 (1977).

6. M. G. Maximovitch, S. C. Lockergy, R. F. Kovar and F. E. Arnold, Soc. Adv. Mat'rs. and Process Eng., 22, 713 (1977)

7. M. G. Maximovitch, S. C. Lockerby, G. A. Laughran and F. E. Arnold, Soc. Adv. Mat'rs. and Process Eng., 23, 490 (1978)

8. F. E. Arnold, Non-Metallic Materials Division, Air Force Materials Laboratory, Wright Patterson Air Force Base, Ohio 45433. Private Communication.

9. A. A. Moroz and M. S. Shvartsberg, Russ. Chem. Rev., 43, 679 (1974).

10. R. G. R. Bacon and O. J. Stewart, J. Chem. Soc., 4953 (1965).

11. E. T. Sabourin, Petroleum Chem. Preprints, 20 (1), 233 (1979).

12. O. T. Schmidt, E. Komarek, and H. Rentel, Ann 602, 50 (1957). Chem. Abstr. 51, 12041i.

1982 USAF-SCEEE SUMMER FACULTY

RESEARCH PROGRAM

Sponsored by the

SOUTHEASTERN CENTER FOR ELECTRICAL

ENGINEERING EDUCATION

FINAL REPORT

MATHEMATICAL FORMULATION OF THE SHEAR LAYER OVER AN OPEN CAVITY

Prepared by:

Dr. Samuel G. Kelly, III

Academic Rank: Assistant Professor

Department and University: Department of Mechanical Engineering
University of Akron

Research Location: Air Force Wright Aeronautics Lab
Wright Patterson Air Force Base, Ohio

USAF Research: Howard Wolfe

Date: September 13, 1982

Contract No.: F49620-82-C-0035

Acknowledgements

The author would like to thank the Air Force Systems Command, the Air Force Office of Scientific Research, and the Flight Dynamics Lab at Wright Patterson Air Force Base, Ohio for providing him with an opportunity to work on such a worthwhile and interesting project.

The author would like to thank, in particular, Mr. Howard Wolfe for his helpful suggestions and conversations, Mr. Leonard Shaw for providing a helpful reading list and for discussions on the topic, and all other members of the Acoustics and Sonic Fatigue Group of the Structural Integrity Branch for their hospitality.

MATHEMATICAL FORMULATION OF THE SHEAR LAYER OVER AN OPEN CAVITY

By

Samuel G. Kelly, III

ABSTRACT

The problem of shear layer oscillations over an open cavity is investigated including the effects of shear layer thickness. The Navier-Stokes equations are used to derive governing equations for the unsteady pressure distributions in the cavity, the shear layer, and the external flow. Boundary conditions are written for these equations with a discussion of the boundary condition at the trailing edge included. The problem results in a set of partial differential equations with boundary conditions applied over an oscillating boundary. Possible solution techniques are discussed as well as suggestions for future work.

I. Introduction

The analysis of the shear layer over an open cavity is a problem of great practical importance. An example of beneficial use of this analysis to the Air Force is in analyzing the acoustic environment inside weapons bays on aircraft. Bartel and McAvoy (1) note that sound pressure levels can reach as high as 170 d B inside weapons bay like cavities. Effects of high sound pressure levels include structural failure and extreme personnel discomfort. Other applications of the present work include aircraft wheel wells and instrumentation crevices on aircraft.

There have been many experimental investigations of the problem including those by Karamcheti (2), Bartel, and McAvoy (1), and Heller and Bliss (3). There have also been many analytical attempts at the solution of the problem. These will be reviewed here.

The first strong analytical work on cavity oscillations was performed by Plumble , Gibson, and Lassiter (4). Their model was based upon the assumption that pressure distributions inside the cavity were caused by boundary layer turbulence. It was later discovered that their model works best for cavities with

length to depth ratios less than unity $(L/D < 1)$.

Rossiter (5) proposed a feedback mechanism to explain the physical phenomena observed in his experiments. He postulated that vortices are shed periodically from the leading edge of the cavity and are convected downstream until they reach the trailing edge. The interaction of the shed vortices with the trailing edge generates acoustic waves inside the cavity which then propagate upstream affecting the shear layer at the leading edge. Rossiter's model works best for Mach numbers in the range $0.4 < M < 1.2$.

Bilanin and Covert (6) modeled the shear layer as a thin vortex sheet. They modeled the phenomenon at the trailing edge by an acoustic monopole. Their model agrees well with experimental data only for Mach numbers, $M > 2.0$.

Heller and Bliss (3) suggested that the appropriate model at the trailing edge should be based upon an entrainment concept. Hence they used a pseudo piston analogy to model the behavior of the trailing edge. They then analyzed the problem assuming an infinitesimally thin shear layer. They obtained good correlation with experimental data, but note that their results do not agree well for low Mach number external

flows. Heller and Bliss attribute this to the model overestimating the amplification of a wave propagating downstream in the absence of shear layer thickness effects.

Tam and Block (7) also performed both experimental and mathematical studies of the shear layer problem. They analyzed the problem both by including thickness effects in the shear layer and by not including it. To include thickness effects they assumed that the shear layer can be characterized by a mean momentum thickness, which was determined in the course of the analysis. They modeled the behavior at the trailing edge with a feedback mechanism. Their model compares favorably with their own data for Mach numbers in the range $0.2 < M < 0.4$. Tam and Block note that inclusion of shear layer thickness is an important effect and should be considered to yield favorable results.

Rockwell and Naudscher (8) present an excellent review of related work on self-sustaining oscillations on flow part cavities. They present the results of some of the investigators mentioned as well as showing extensions of the work to nonrectangular cavities.

II. Objectives

The main objective of this project was to analytically investigate shear layer oscillations over an open cavity. In particular it was desired to arrive at a mathematical formulation of the shear layer that can be used in finite element programs to completely describe the flow field in an open cavity. The specific objectives were:

(1) To survey the literature on shear layer oscillations over an open cavity focusing an analytical techniques and to classify these attempts.

(2) To use the literature survey to identify research areas in cavity oscillations which, when pursued, would add significantly to current knowledge in the field.

(3) To mathematically formulate such a problem involving shear layer oscillations and to attempt its solution.

(4) To access the feasibility of using a mathematical formulation of the shear layer over an open cavity as input in a general finite element analysis of the overall cavity problem.

III. Shear Layer Modeling

A survey of the literature revealed that many analytical studies by reputable investigators have been performed on a free shear layer over an open cavity. The author noted that:

(1) Most models are valid only for some limited range of the Mach number. Tam and Block (7) obtained results that are good for $M < 0.4$, which is well within their range of interest as they were studying landing gear wheel well noise. The model of Heller and Bliss (6), on the other hand works best for $M > 2.0$.

(2) Most investigators acknowledge that the inclusion of thickness effects in their shear layer model would increase its usefulness. However, only Tam and Block (7) include thickness effects of any kind in their model.

(3) There is some question as to the handling of the boundary condition at the trailing edge of the cavity. Heller and Bliss (3) proposed an entrainment mechanism to model the physical phenomenon while Rossiter (5) and Bilanin and Covert (6) proposed a feedback mechanism.

(4) Many investigators used empirical data to build a semi-empirical analytical model. This seems to be necessary in many cases due to the complex nature of the problem and the complete lack of understanding of physical mechanisms.

In view of the above, the author decided that the state of the art of shear layer oscillation over an open cavity could best be advanced by a comprehensive study of thickness effects on shear layer oscillations. It was hoped that such a study could be conducted to yield results valid for all ranges of Mach numbers and all L/D ratios. This proved to be a formidable challenge. The preliminary work toward this goal will be summarized here. The author intends to continue the work started at the Flight Dynamics Lab to meet this goal.

There are three regions which must be considered when modeling flow over an open cavity. These are the region above the shear layer, the shear layer itself, and the region below the shear layer, as shown in Figure 1. The fluid mechanics must be adequately modeled based upon a consistent set of assumptions in each layer. Each layer should be analyzed independently with boundary conditions providing the coupling between the regions. The Navier-Stokes equations, White (10), were

used as a starting point for the derivation of the equations of motion in each region. They are

$$\rho \frac{D\vec{v}}{Dt} = \rho\vec{g} - \vec{\nabla}p + \frac{\partial}{\partial x_j}\left[\mu\left(\frac{\partial v_i}{\partial x_j} + \frac{\partial v_j}{\partial x_i}\right) + \delta_{ij}\lambda\, div\, \vec{v}\right] \quad (1)$$

$$\frac{D\rho}{Dt} + \rho\, div\, \vec{v} = 0 \quad (2)$$

where ρ is the fluid density, $\vec{v}$ is the velocity vector, p is the fluid pressure, $\vec{g}$ is the body force vector, and μ and λ are the first and second coefficients of viscosity respectively. A repeated subscript indicates summation over that particular index in equation (1). Equation (1) is a statement of momentum conservation while equation (2) states mass conservation.

To analyze the flow inside the cavity the following assumptions are made:

(a) The cavity is free of any mean flow. A cavity mean flow could be added later as a second order effect.

(b) The fluid is inviscid.

(c) The flow is two-dimensional with only a volocity component in the x direction.

(d) The body forces can be neglected. The above

assumptions can be used to simplify equations (1) and (2). Indeed after algebraic manipulation one obtains

$$\frac{\partial^2 p_1}{\partial t^2} - a_1^2\left(\frac{\partial^2 p_1}{\partial x^2} + \frac{\partial^2 p_1}{\partial y^2}\right) = 0 \quad ; \quad a_1^2 = \frac{d\rho_1}{d p_1} \tag{3}$$

$$\rho_1 \frac{\partial v_1}{\partial t} + \frac{\partial p_1}{\partial y} = 0 \tag{4}$$

where a subscript 1 denotes fluid quantities inside the cavity.

To analyze the flow above the shear layer it is assumed that a mean flow of velocity U_∞ and Mach number M exists. Assumptions (b)-(d) are also used in this region. Flow quantities are then written in terms of pertulation quantities.

$$u_2 = U_\infty + \hat{u} \tag{5}$$

$$p_2 = p_\infty + \hat{p} \tag{6}$$

$$v_2 = \hat{v} \tag{7}$$

where a subscript ∞ refers to a mean flow quantity and a subscript 2 refers to a quantity above the shear layer. Equations (5) - (7) are then substituted into equations (1) and (2) to yield

$$\frac{\partial^2 p_2}{\partial t^2} + 2 U_\infty \frac{\partial^2 p_2}{\partial x \partial t} + U_\infty^2 \frac{\partial^2 p_2}{\partial x^2} - a_1^2 \left(\frac{\partial^2 p_2}{\partial x^2} + \frac{\partial^2 p_2}{\partial y^2} \right) = 0 \tag{8}$$

$$\rho_2 \left(\frac{\partial v_2}{\partial t} + U_\infty \frac{\partial v_2}{\partial x} \right) = - \frac{\partial p_2}{\partial y} \tag{9}$$

In obtaining (8) and (9) nonlinear convective terms have been neglected. These terms are products of the perturbation quantities and will be small in comparison to other terms in the equation. Their effect could be included in a later analysis of the problem.

Finally the shear layer is considered. The shear layer is bounded by an upper surface and a lower surface defined by $\eta_u(x,t)$ and $\eta_\ell(x,t)$ respectively. The values of $\eta_u(x,t)$ and $\eta_\ell(x,t)$ are initially unknown and must be solved for as part of the solution process. The thickness of the shear layer is given as

$$\delta(x,t) = \eta_u(x,t) - \eta_\ell(x,t) \tag{10}$$

To analyze the shear layer it is best to define a new set of coordinates. The shear layer thickness δ should be small in comparison to other dimensions in the problem. Thus to adequately describe the variation of fluid quantities in the vertical direction it is convenient of stretch the vertical variable. To this end, define

$$y^* = y/\delta \tag{11}$$

The vertical component of velocity v will also be small within the shear layer. Thus one defines

$$v^* = v/\delta \tag{12}$$

The fluid in the shear layer is assumed to have a mean velocity profile $\bar{U}(y)$. As noted by Tam and Block (7) the mean profile of a shear layer has not been adequately measured. Thus following Tam and Block (7) it is perhaps best to use the profile of a two dimensional frec turbulent mixing layer at the trailing edge of a thin flat plate. This is given by

$$\bar{U}(y) = \frac{U_\infty}{2}\left(1 + \tanh\left(\frac{y}{2\delta}\right)\right) \tag{13}$$

Perturbation quantities for the variable in the shar layer are introduced by

$$\bar{u}(x,y^*,t) = \bar{U}(y^*) + \tilde{u}(x,y^*,t) \tag{14}$$

$$\bar{p}(x,y^*,t) = \bar{p}(y^*) + \tilde{p}(x,y^*,t) \tag{15}$$

Equations (11)-(15) are introduced in equations (1) and (2). An asynptotic analysis is also used to yield the following equation for the shear layer varialbes.

$$\rho\left(\frac{\partial\tilde{u}}{\partial t} + \bar{U}\frac{\partial\tilde{u}}{\partial x} + v^*\frac{d\bar{U}}{dy^*}\right) = -\frac{\partial\tilde{p}}{\partial x} + \frac{\mu}{\delta^2}\left(\frac{d^2\bar{U}}{dy^{*2}} + \frac{\partial^2\tilde{u}}{\partial y^{*2}}\right)$$

$$\frac{\partial\tilde{\rho}}{\partial t} + (\bar{U}+\tilde{u})\frac{\partial\tilde{\rho}}{\partial x} + v^*\frac{\partial\tilde{\rho}}{\partial y^*} + \tilde{\rho}\frac{\partial\tilde{u}}{\partial x} + \rho\frac{\partial v^*}{\partial y^*} = 0 \tag{16}$$

The boundary conditions are next formulated. These are

(a) The fluid velocity is zero on the walls of the cavity. Thus

$$u_1(0,y,t) = v_1(0,y,t) = 0 \tag{17}$$

$$u_1(L,y,t) = v_1(L,y,t) = 0 \tag{18}$$

$$u_1(x,-D,t) = v_1(x,-D,t) = 0 \tag{19}$$

(b) The flow must approach that of the free stream away from the cavity.

$$\hat{u}(x,y,t) \rightarrow 0 \quad \text{as} \quad y \rightarrow \infty \tag{20}$$

$$\hat{v}(x,y,t) \rightarrow 0 \quad \text{as} \quad y \rightarrow \infty \tag{21}$$

$$\hat{\rho}(x,y,t) \rightarrow 0 \quad \text{as} \quad y \rightarrow \infty \tag{22}$$

(c) The pressure and velocity components must remain continuous across the surfaces of the shear layer.

$$\frac{\vec{v}_1 \cdot \vec{\nabla}\eta_l}{|\vec{\nabla}\eta_l|} = \frac{\vec{v}_s \cdot \vec{\nabla}\eta_l}{|\vec{\nabla}\eta_l|} \quad \text{at} \quad y = \eta_l(x,t) \tag{23}$$

$$\frac{\vec{v}_2 \cdot \vec{\nabla}\eta_u}{|\vec{\nabla}\eta_u|} = \frac{\vec{v}_s \cdot \vec{\nabla}\eta_u}{|\vec{\nabla}\eta_u|} \quad \text{at} \quad y = \eta_u(x,t) \tag{24}$$

(d) Finally, a condition must be applied at the trailing edge of the cavity to model the observed physical phenomenon. It has not been decided the correct method to model the trailing edge phenomenon when shear layer thickness effects are included. Tam and Bloch (7) model the trailing edge phenomenon by a line vartex. Research is continuing into this area.

A successful solution has not yet been obtained for the equations and boundary conditions presented above. Work is continuing toward this goal.

IV. Recommendations

Due to time limitations and prior lack of experience of the principal investigator in this research area, not as much progress was made on the project as originally projected. Thus, there are obvious follow up projects to the work already performed. It is the opinion of the principal investigator that a major contribution to the area of cavity flows would be a comprehensive analytical study of shear layer oscillations over open cavities including the effects of shear layer thickness. Indeed most of the good analytical work in the area has assumed infinitessimally thin vartex sheets modeling the shear layer (7) or an average shear layer thickness across the length of the cavity (7). In fact, Heller and Bliss (3) state that their model can best be improved upon by adding shear layer thickness effects to it. Inclusion of thickness effects presents a formidable research problem. The problem is one of solving for unsteady pressure distributions in three regions with the exact location of the boundaries of the middle region to be solved for as part of the solution process. Classical solutions were attempted as part of this project but,

as expected, did not work. It is recommended that asymptotic techniques next be employed in an attempt to yield an approximate analytical solution. An appropriate small parameter in the problem should first be identified with which a perturbation expansion can be performed. The problem would first be examined for a wave of a single frequency followed by the analysis of a group of waves of different frequencies. It is hoped that this technique would predict the acoustic resonances of the cavity for all L/D ratios and Mach numbers.

If analytical solutions are unsuccessful, then it is proposed that numerical solutions be employed. Perhaps a finite difference procedure or a numerical form of the method of characteristics would work best.

A second recommendation is to analytically examine the method of appliction of applying a boundary condition at the trailing edge of the cavity. There has been significant discussion in the literature concerning the dominant physical mechanism at the trailing edge. Bilanin and Covert (6) modeled the process at the trailing edge by an acoustic monopole. Their results seem valid only for $M > 1.0$. Heller and Bliss (3) used a pseudo-piston analogy to model the mass addition

and subtraction process at the trailing edge. Their model, however, did not include shear layer thickness effects which would complicate the solution procedure. It appears that the method of application of the boundary conditions at the trailing edge significantly limits the application of the results of the study. Thus, it is recommended that a detailed analysis of this phenomenon be performed.

Finite element techniques are powerful numerical techniques that can be used to solve a wide variety of problems. These techniques are now in vogue for solving fluid mechanics problems. Indeed finite element techniques have been used in the cavity oscillation problem (i.e. Hankey and Shang (9). However, a complete finite element analysis of the cavity problem seems extremely involved. Instead it has been suggested, Wolfe (10), that a mathematical formulation of the shear layer be used as input for a general finite element cavity model. The author feels that while this idea has a great deal of merit, it is extremely optimistic at this time: There are several reasons for this; (1) The equations governing the shear layer are coupled by the boundary conditions with those governing the fluid motion inside the cavity and outside of the cavity.

Experimental studies have shown that the shear layer is involved in a feedback process. The anlysis of this feedback process is crucial in modeling the shear layer. (2) The exact location of the shear layer is dependent upon the external flow. Thus placement of elements in the flow field would be very difficult. In short the author feels that at this time it is not possible to simply substitute a mathematical formulation of the shear layer in a finite element code. However the idea is a good one and research should continue toward its development.

In summary, the author recommends a comprehensive study of the problem of an oscillating shear layer over an open cavity including thickness effects. The authors feel that such a study is viable analytically and will yield favorable comparisons with experimental data. It is felt that an analysis can be developed that will be valid for all L/D ratios as well as all Mach numbers. It is also hoped that valid solutions can be obtained for both laminar and turbulent external flows.

The author intends to continue this study and work towards such a theory.

REFERENCES

1. Bartel, H.W., and McAvoy, J.M., "Cavity Oscillation In Cruise Missile Carrier Aircraft," AFWAL-TR-81-3035, 1981.
2. Karamcheti, K., "Acoustical Radiation From Two-Dimensional Rectangular Cutouts in Aerodynamic Surfaces," NACA TN 3487, 1955.
3. Heller, H.H., and Bliss, D.B., "Aerodynamically Induced Pressure Oscillations in Cavities - Physical Mechnisms and Suppression Concepts.," AFFDL-TR-74-133, 1975.
4. Plumblee, H.E., Gibson, J.S. and Lassiter, L.W., "A Theoretical and Experimental Investigation of the Acoustical Response of Cavities in an Aerodynamic Flow," WADD-TR-61-75, 1962.
5. Rossiter, J.E., "Wind Tunnel Experiments on the Flow Over Rectangular Cavities at Subsonic and Transonic Speeds," ARCR & MNO.3438, 1964.
6. Bilanin, A.J., and Covert, E.E., "Estimation Of Possible Excitation Frequencies For Shallow Rectangular Cavities," AIAA Journal, Vol. II, No. 3, pp. 347-351, 1973.
7. Tam, C.K.W., and Block, P.J.W., "On the Tones

and Pressure Oscillations Induced by Flow Over Rectangular Cavities, " J. Fluid Mech., Vol. 89, Part 2, pp. 373-399.

8. White, F.M., Viscous Fluid Flow, (McGraw Hill, New York, NY), 1974.

9. Wolfe, H.., Private Communication, 1982.

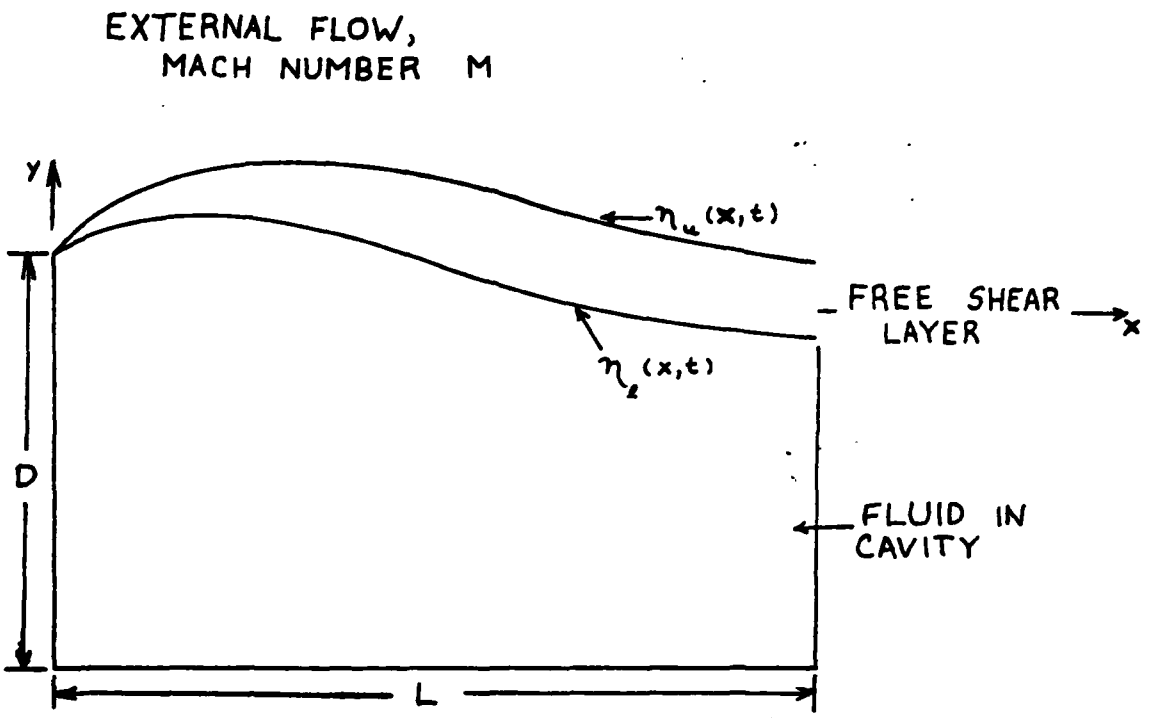

EXTERNAL FLOW,
MACH NUMBER M
y
$\eta_u(x,t)$
FREE SHEAR LAYER
x
$\eta_\ell(x,t)$
D
FLUID IN CAVITY
L

FIGURE 1

1982 USAF-SCEEE SUMMER FACULTY RESEARCH PROGRAM

Sponsored by the

AIR FORCE OFFICE OF SCIENTIFIC RESEARCH

Conducted by the

SOUTHEASTERN CENTER FOR ELECTRICAL ENGINEERING EDUCATION

FINAL REPORT

AUTOMATING THE NUMERICAL STEREO CAMERA

Prepared by:	Dr. Dennis M. Kern
Academic Rank:	Assistant Professor
Department and University:	Statistics and Computer Science Department University of Georgia
Research Location:	United States Air Force School of Aerospace Medicine Dental Investigation Service
USAF Research Colleague:	Dr. Bruce R. Altschuler
Date:	September 8, 1982
Contract No:	F49620-82-C-0035

AUTOMATING THE NUMERICAL STEREO CAMERA

by

Dennis M. Kern

ABSTRACT

A Numerical Stereo Camera (NSC) has been set up in the lab. The image acquisition portion of the NSC has been automated and takes approximately 4 seconds. Several sets of points have been collected using different objects. This data has been checked for reasonableness, but a complete evaluation of the output remains to be done.

Acknowledgement

The author would like to thank the Air Force Systems Command, the Air Force Office of Scientific Research and the Southeastern Center for Electrical Engineering Education for providing him with the opportunity to spend a very worthwhile and interesting summer at the School of Aerospace Medicine, Brooks AFB, TX. He would like to acknowledge the school, in particular the Dental Investigation Service, for its hospitality and excellent working conditions.

Finally, he would like to thank Dr. Bruce R. Altschuler for his collaboration and guidance and he would like to acknowledge many helpful discussions with Dr. Walter Kuklinski.

I. INTRODUCTION:

The concept of computer or robotic vision[1] has potential application in many areas from medicine[2,3,4] to manufacturing.[5] Before "vision" can be achieved, however, an "eye" must be built. To be compatible with a digital computer such an "eye" would need to output digital data which the computer could then manipulate to produce vision.

It is the problem of building such an "eye" that we address here. The technique chosen here is the Numerical Stereo Camera (NSC). This technique uses a laser beam array generator as the active camera and a standard TV camera as the passive camera in a stereo pair. With the relative positions of the two cameras known and fixed, a sequence of TV images are acquired. A sequence is required so that each of the beams in the array that is striking the object and that is visible to the TV camera can be identified.

In order to minimize the number of images required to identify the beams striking the object, binary coding is used on the rows and columns of the beam array. Binary coding requires $1 + \log_2 M + \log_2 N$ images for an MxN array where M and N are both powers of two. Thus for the 128 x 128 array we will be using, $1 + 7 + 7 = 15$ images will be required. A shutter placed between the beam array generator and the object can control which beams are allowed to strike the object in each image. The shutters we will be using are of the electro-optical type.[5,6]

The TV images are digitized and, from the sequence of images, we can obtain, corresponding to the beams, a set of points (x^*, y^*, n) where x^* and y^* are the location in the sequence of images of the beam and n is the numeric label of the beam. From the geometry of the

cameras, the points (x^*, y^*, n) can be transformed to (x, y, z), a set of points in three-dimensional space which lie on the surface of the object. A more detailed discussion of the transformation is available in the literature.[5,7]

II. OBJECTIVE

The NSC has previously been set up and exercised manually, but no real digitized data has been acquired. The current research effort is the development of an automated NSC. Thus, our research objective is to develop the appropriate computer controls and interfaces necessary to obtain the images automatically and to create a computer file containing the set of points.

III. HARDWARE SETUP

The master controller for the system is a Digital Equipment Corporation PDP 11 model 23. Using the DRV11J interface board, the 11/23 was programmed to control the shutter or programmable spatial light modulator (PSLM). This allows us to control, at any time, which of the laser beams in the array are projected onto the object.

Two different types of shutters were available for use in the lab. The first or slow shutter takes approximately 500 miliseconds to change patterns. The slow shutter also produces only rows or columns of beams. Thus two of these shutters must be placed in front of the generator to provide horizontal and vertical control. The second or fast shutter takes approximately 30 microseconds to change patterns and allows control of both the horizontal and vertical simultaneously.

The video digitization and image storage are handled by a Gould de Anza 8500 Image Processor (IP) which is fed by a Cohu low-light (surveilance type) video camera. Additional processing power is available through the Floating Point Systems Array Processor (AP). Both the IP and AP are connected to the 11/23 unibus for high-speed data transfer and control by the 11/23.

To operate the NSC we first acquire the space coded data using the IP. Second, we use the all on image to create a mask or template for determining the beams in the image. Third, we use this mask to obtain the regions of the image which contain valid data. Fourth, we compute, display and store to disk the x^*, y^* and space code of each of the beams found in the image.

IV. ACQUIRING THE DATA

The IP and shutter are first programmed to obtain the image with all the laser beams on. The IP and shutter are next programmed to obtain the image in which alternating columns of beams are on and off, respectively. Next the IP and shutter are programmed to average the previous (on-off) image with the image where the columns are alternately off and on respectively. This average image is called the threshold image and is used to determine the presence or absence of a beam in the following images.

The concept of the threshold is to set a value on a pixel by pixel basis against which we could compare succeeding images to determine if a beam is striking the object. The average mentioned above is a straight arithmetic average on a pixel by pixel basis with a small

constant, currently 3, being added. The constant is added so that in areas where no beams are visible in either image the threshold will be higher than the image value. For other areas of the image the threshold is slightly above the average of the value when a beam is providing illumination and when a beam is not providing illumination.

The all on and threshold images each require one whole 512 x 512 x 8 bit IP memory channel to store. The information for our binary coding, however, requires only knowledge of presence or absence of a beam, i.e. 1 bit, for each of the 15 images. Thus we next program the IP and shutter to cycle through the 15 patterns for our 128 x 128 shutter and store the data in 2 IP memory channels (16 bits) one bit at a time.

The images for coding are first all on then 1/2 of the columns (64) on and 1/2 off. The next image has 1/4 of the columns (32) on, 1/4 off, 1/4 on and 1/4 off. This continues until we have alternating 1/128's or one column on and one column off. This sequence of fractions is then repeated for the rows. The choice of doing columns first and using them for the threshold is completely arbitrary.

Thus, the data acquired consists of four images or IP channels. These are all beams on, the threshold image, the horizontal coding and the vertical coding. Using the fast shutter this entire phase of the process runs automatically and currently takes approximately 4 seconds. This speed does not represent what is capable with state of the art, but only what we are currently obtaining with present equipment.

V. OBTAINING THE POINTS

Once the image data is acquired, the problem of obtaining the

centers and codes for the visible beams remains. The signal to noise ratio is small, however, and so a fair amount of post-acquisition processing is required. Problems with the AP also make the current processing time quite lengthy.

The first step is to use the all on image to establish where beams can occur. This is done by sliding a weighting function in the form of an array across the entire image. The output of this operation is an image containing the number 255 (8 ones) where recognizable beams can occur and zero elsewhere.

The size of the weighting function is dependent on the size of a typical beam. It is designed to find values that are greater than those surrounding it. Thus it is designed to find the peak values or beam centers.

Once this mask has been created the IP is used to AND the mask with the coded images. This process delineates the beams and allows us to proceed with the determination of the points. The reported values x^* and y^* are the average of all the horizontal and vertical locations of the pixels comprising the beam. The other item output for each beam is its code value or label.

VI. RECOMMENDATIONS

Acquiring the images has now been automated and sets of points (x^*, y^*, n) have been collected for several objects. The sets of points have been checked for reasonableness and consistency. The output has not, however, been evaluated in detail for its accuracy. This evaluation, then, must be the next effort undertaken. The results of this

evaluation will determine where following efforts will need to be directed.

Once it has been verified that the output has an acceptable accuracy, the data can be transformed to standard three-dimensional points. From these sample points a mathematical description or model of the surface can be obtained. Other efforts that can then also proceed are the automation and speed up of the entire NSC, and the correlation of multiple views obtained with multiple NSC's.

REFERENCES

1. Moravec, H. P., "Obstacle Avoidance and Navigation in the Real World by a Seeing Robot Rover," CMU-RI-TR-3, Robotics Institute, Carnegie-Mellon University, 1980.

2. Altschuler, M. D., Posdamer, J. L., Frieder, G., Manthey, M. J., Altschuler, B. R., and Taboada, J., "A Medium-Range Vision Aid for the Blind," Proc. Int. Conf. on Cybemetics and Society, Boston, Massachusetts, 1980, p. 1000.

3. Wedendal, P. R. and Bjelkhagen, H. I., "Dental Holographic Interferometry In-Vivo Utilizing a Ruby Laser System, I and II," Acta Odont. Scand., Vol. 32, 1974, pp. 131-145 and pp. 345-356.

4. Young, J. M. and Altschuler, B. R., "Topographic mapping of oral structures, problems and applications in Prosthodontics," Proc. SPIE, Vol. 283, 1981, pp. 70-77.

5. Altschuler, M. D., Posdamer, J. L., Frieder, G., Altschuler, B. R., and Taboada, J., "The Numerical Stereo Camera," Proc. SPIE, Vol. 283, 1981, pp. 15-24.

6. Cutchen, J. T., Harris, J. O., Jr., and Laguna, G. R., "PLZT Electro-Optic Shutters: Applications," Appl. Optics, Vol. 14, 1975, p. 1866.

7. Altschuler, M. D., Altschuler, B. R., and Taboada, J., "Laser electro-optic system for rapid three-dimensional (3-D) topographic mapping of surfaces," Opt. Eng., Vol. 20, No. 6, November/December 1981, pp. 953-961.

1982 USAF-SCEEE SUMMER FACULTY RESEARCH PROGRAM

Sponsored by the

AIR FORCE OFFICE OF SCIENTIFIC RESEARCH

Conducted by the

SOUTHEASTERN CENTER FOR ELECTRICAL ENGINEERING EDUCATION

FINAL REPORT

MEMORY AND PROCESSING LIMITS IN DECISION MAKING

Prepared by:	Dr. Stuart T. Klapp
Academic Rank:	Professor
Department and University:	Department of Psychology, California State University, Hayward
Research Location:	Air Force Human Resources Laboratory Logistics and Technical Training Division Logistics Research Branch Ground Operations Section
USAF Research Colleague:	Dr. Lawrence E. Reed
Date:	September 3, 1982
Contract No:	F49620-82-C-0035

MEMORY AND PROCESSING LIMITS IN DECISION MAKING

by

Stuart T. Klapp

ABSTRACT

The demands of command and control decision making seem to approach and often exceed the limits of human information processing. A literature review indicated that much of the potentially relevant research may not generalize from the laboratory to decision making. However, transfer appropriate learning and a multiple store view of short-term memory and resource limits are ideas worth exploring from the standpoint of decision making. A model task was developed to permit efficient study of these and other issues within a decision making context. This task, involving trucking and transportation, appears to be suitable for use with a large subject population because it involves only general knowledge. Several optional auxillary features were built into the model task in order to address specific research issues. Experiments are suggested which address principles raised by the literature review and other relevant issues.

ACKNOWLEDGEMENT

The author would like to thank the Air Force Systems Command, the Air Force Office of Scientific Research and the Southeastern Center for Electrical Engineering Education for providing him with the opportunity to spend a very worthwhile summer at the Air Force Human Resources Laboratory at Wright Patterson Air Force Base, Ohio. He would like especially to thank Dr. Larry Reed for suggestions, advice, collaboration and encouragement throughout this project and to express his appreciation to Mr. Bert Cream and Dr. George Frekany for helpful discussions and encouragement.

I. INTRODUCTION

The study of tactical decision making has been undertaken by AFHRL/LRLG based on the need to measure, assess, and possibly improve, decision making performance in command and control (C^2). In particular, interest has centered on the generation of the Air Tasking Order for "tomorrow's" war. To handle this problem, the C^2 decision maker must allocate scarce resources including aircraft, ordnance, fuel, etc. against specified targets [1].

The generation of these decisions requires that the decision maker keep track of and process an enormous amount of information. Psychologists have long been interested in the theoretical analysis of problems of information overload including how people cope with the overload and how overload reduces performance. The problem addressed in this investigation is to review the previous literature on the theory of information overload from the perspective of its applicability to C^2 decision making. Emphasis was to be on gaining an understanding of what is known and how it might be applied, and on identifying ways in which additional research might focus on applications to C^2 decision making.

My interest in this problem is an outgrowth of previous work in the study of limits in human information processing [2,3].

II. OBJECTIVES OF THE RESEARCH EFFORT

The following specific subgoals were established in conjuction with the above problem statement:

A. Become familiar with C^2 decision making.

B. Conduct a theoretical analysis and literature search on limits in human information processing and memory from the perspective of C^2 decision making.

C. Develop a simplified model task to facilitate future research in areas identified by the literature review.

D. Prepare a report including the above and suggestions for follow-on research as appropriate.

Section III to follow presents the theoretical analysis and literature review from the C^2 perspective (subgoals A and B above).

Section IV outlines the model task (subgoal C) which is detailed in a supplement available from the Air Force Human Resources Laboratory at WPAFB. Section V describes recommended research with the model task and is based, in part, on insights from the literature review. Section VI summarizes the recommendations from the research effort.

III. LITERATURE REVIEW AND THEORETICAL ANALYSIS

A. ORIENTATION

This review considers the following potential limits in human information processing from the perspective of C^2 decision making:

1. Memory limits
    a. Retrieval problems involving long-term memory
    b. Capacity problems involving short-term (working) memory
2. Processing resource limits

B. RETRIEVAL FROM LONG-TERM MEMORY

Long-term memory is generally assumed to be unlimited in capacity, but subject to forgetting. An important viewpoint, attributed to Craik and Lockhart [4], holds that material which is processed more "deeply" in the sense that it is made more meaningful will be remembered for a longer time. Although the concept of "depth" is only vaguely defined [5], this perspective on memory research has become the dominant viewpoint in current textbooks. Recently, however, a modification known as transfer appropriate learning [6] and the related but older notion of encoding specificity [7] have tended to replace the original "depth" formulation. In this view, the probability of retrieving an item from long-term memory depends upon the match between input processing and output requirements. Usually, but not always, that match will be better when input processing is deeper. Thus, depth of processing is a special case within the more general framework of transfer appropriate learning.

The several illustrative experiments all tend to seem rather artificial. For example, words to be remembered were presented together with questions which ask about the meaning (does it play music?), or about which letter is capitalized out of context (raDio, does it have a capital D?). According to depth of processing, the first question should

lead to better memory than the second. However, the results are that the first question at input leads to better recognition of the target "raDio" from a context of other words, but (and this is critical) the second question leads to better recognition in a context of raDio, rAdio, etc. This is clearly contrary to depth of processing which predicts better memory when the input processing is "deeper" i.e., more meaningful. The result is consistent with the transfer appropriate learning viewpoint.

The experimental situations used to demonstrate transfer appropriate learning have tended to employ rather "wierd" tasks such as rhyme acquisition or capital letters out of context. For these cases, subjects recall more if they are induced to concentrate upon the sounds, appearance, etc. of the words rather than upon the meaning. One wonders, therefore, if the concept of transfer appropriate learning really applies to more relevant situations. In particular, is it possible to present material to decision makers in such a way as to maximize performance by making the input processing more "appropriate" to this form of output? One approach to a more realistic assessment of the applicability of the notion of transfer appropriate learning appears in Section V-B below.

If transfer appropriate learning is found to hold for decision making, two recommendations would follow:

1. Display of information should be "appropriate" to decision making. Unfortunately, the notion of "appropriate" is not defined in a way that would permit application of this principle in other than general terms.

2. A clearer implication is that experiments conducted to assess the merits of various modalities of information presentation to decision makers should use decision making performance rather than performance on tests of memory in standard recall and recognition contexts as the criterion measure. This is because the most appropriate input for one context may not be the most appropriate for another.

C. SHORT-TERM (WORKING) MEMORY LIMITS

1. Working Memory Concept. Whereas long-term memory is assumed to be unlimited in capacity, short-term memory is assumed to be limited to about 7 "chunks" [8]. A recent survey [3] indicates that most

textbooks in cognitive psychology proclaim that this limit reflects the limit in capacity of the working space for all mental operations. This view appears to have its origins in the classical notions of William James [9] who distinguished "primary" or short-term memory from secondary or long-term memory on the grounds that primary memory is the current contents of awareness. (Secondary memory is that memory which has left awareness, but which can be recalled into awareness). A little leap of logic leads to the standard proclamation that we have a working memory (awareness?) which is limited to 7 chunks. This is the limit of our thinking space which, when filled, cannot accept any new information without loss of the old.

2. Problems With This View. Several problems with the working memory viewpoint can be identified:

a. People with very poor short-term span memory often have normal capability for processing information [10,11].

b. Rather than a unitary short-term memory, we actually seem to have several unrelated systems for immediate memory. The following evidence is relevant:

(1) The missing digit task [12], in which subjects report which digit did not appear in a random string of 8 digits, exhibits properties which are quite unlike the properties of ordered recall. Missing digit does not show carry-over between trials with identical sequences like is the case for ordered recall [13]. It is also insensitive to irrelevant articulation at input and to grouping of items at input [3].

(2) Whereas holding a load of letters for ordered recall interferes with an imbedded task involving ordered recall of digits, a load of letters for ordered recall does not interfere with an imbedded Sternberg scanning task. Therefore, ordered recall and Sternberg scanning must involve different memory systems.

c. The interference often attributed to overfilling memory load actually can best be attributed to interference between rehearsal and subsequent action rather than between retention and subsequent action, as proposed by the working memory formulation.

3. Detailed Findings. Elaboration of the evidence relevant to points b-2 and c above is considered in this section. The experimental paradigm [3] involved presentation of a variable number of letters for subsequent ordered recall, with an intervening task between presentation and recall of these letters. The two critical conditions differ with respect to the presence or absence of a delay between presentation of the memory letters and presentation of the intervening task.

According to the working memory viewpoint, filling up working memory with letters should interfere with the intervening task regardless of the presence or absence of this delay. In this view, there is but one working memory system, and that system would be filled by the letters and hence unavailable for the intervening task. Contrary to this prediction of the working memory viewpoint, interference occured only when there was no delay between memory letter input and intervening task. No interference occurred when the delay was present.

This result can be interpreted by considering that rehearsal is needed only early but not late in the retention interval of ordered recall. The relevant evidence is discussed in detail in the formal report of this work [3]. When the delay is present, the obligatory rehearsal can be completed during the delay. When no delay is present, rehearsal must be done either before the intervening task (causing an increase in the reaction time for the intervening task), or during that task (causing interference).

The above pattern of results (no interference with delay, interference with no delay) was obtained for numerical reasoning and Sternberg scanning as intervening tasks. Presumably these tasks involve memory systems distinct from that used for ordered recall so that retention (without rehearsal) of a memory load for ordered recall does not interfere with these intervening tasks. By contrast, when ordered recall of digits was used as an intervening task, mutual interference occurred either with or without a delay. This result shows that a short-term memory system for ordered recall can be filled up (by the initial memory letters) and then rendered unavailable for processing the intervening task (ordered recall of numbers) even with a delay. Thus,

the data support the multiple store view of short-term memory. Interference (other than that involving rehearsal) between memory retention and intervening memory tasks occurs if and only if the two memory tasks involve the same system of memory (ordered recall in this example).

The findings are consistent with most of the previous literature. Studies with no delay show interference [14,15,16,17,18,19,20,21(Exp3)]. A study with delay shows no interference [22]. There are exceptions to this principle, however.

One study [23] was similar in concept to ours [3] in that the presence of a delay prior to the intervening task was systematically manipulated. Contrary to our results, this study showed no interaction between the delay and memory load variables. Memory loads of 3, 6, or 9 letters were used, but recall was worse with a 9 letter input than with a 6 letter input. Therefore, we cannot assume (as the authors did) that the effective memory load was greater when 9 letters were presented than when 6 letters were presented. If we look at the reported data for 3 and 6 letter inputs only, an interaction consistent with our results appears, i.e., increasing memory load reduced performance on the intervening task more when there was no delay between memory input and task presentation.

Another contrary study [24] showed only a trend for the interference to become less with increasing delay, but interference occurred even at the longest (6 sec.) delay. Perhaps the interference would vanish at even longer delays, but 6 sec. was enough delay to eliminate interference in other studies. This experiment remains as a possible exception.

All of the above studies used ordered recall as the memory load. Ordered recall is not representative of memory requirements in C^2 decision making because decision makers must remember facts, but normally not the order in which the facts were presented. Possibly, the above conclusions are particular to ordered recall and will not generalize. Some reason to suppose that the situation is different for other forms of memory load comes from an unpublished dissertation [21(Exp1)] in which interference was observed even with a delay using an associative memory load. In this experiment, pairs of the form "A=3" were presented and

tested with question of the form "A=?". After the subject responded to a test item, the fact was changed, e.g., "A=7." This new pair was presented for 3 sec. and on 75% of the trials a probe appeared during presentation of the changed fact. The probe was a visual pattern to which any key was to be pressed. The probe appeared at delays up to 1.5 sec. after the pair first appeared. Reaction time (RT) to respond to the probe stimulus increased as a function of the number of pairs being retained even at the longest (1.5 sec.) delay.

Before we conclude that this study shows a pattern of results which differs from that found for ordered recall, several points should be considered:

(a) Perhaps the delay (1.5 sec.) was not long enough to permit sufficient rehearsal to be completed.

(b) There has been a failure to replicate [25].

(c) The simple RT task may be sensitive to effects that would not be a problem in decision making. Thus, even if the effect of memory load on probe RT is real, it may be of no practical significance.

These possibilities could be tested in an experiment involving memory loads and decision making (see Section V-B). Perhaps decision making requires the same system of short-term memory as does the associative memory load so that the capacity overloads will occur even with a delay for rehearsal. Or perhaps when the experiment is repeated with sufficient delay and with a realisitic intervening task, interference will occur only when no rehearsal delay is provided.

4. Conclusion. As things now stand, the following conclusions appear to be correct:

a. Rather than a unitary working memory, people have several immediate memory systems. Any of these can be filled to capacity, but filling one leaves the others available. Thus, in looking for limits in short-term memory which are applicable to C^2 decision making, one should look in detail for overfilling of some particular type of memory.

b. Rehearsal (and possibly other processes of memory consolidation) can interfere with tasks unless a time interval is available for memory consolidation prior to starting the next event. This effect has often been incorrectly interpreted as reflecting capacity limits in a unitary working memory. It suggests the possibility of interference if events occur in rapid succession in C^2 decision making.

D. PROCESSING LIMITS

According to theories such as that of Kahneman [26], all cognitive tasks draw from the limited pool of attentional "resources," the precise nature of which remains vague. This framework has lead to a great deal of research, which I will not venture to summarize. Rather, I shall inject a note of caution.

One paradigm within this tradition uses a "secondary task" to measure the resource demands of some "primary task." For example, reaction time (RT) to some "probe" stimulus is used to assess the resources demanded by a letter recognition task as a function of time or of some experimental variable. The same pattern of results (resources demanded as a function of time or other factors) should be obtained regardless of what task happens to be used as the probe. Unfortunately, reality is considerably different from this simplified view. The pattern of probe RT differs depending on whether a visual or auditory signal is used [27] and depending on whether a vocal or manual response is used [28]. We conclude that any inferences about the resources demanded by a primary task apply only with respect to a particular secondary task.

These studies show that small changes in the secondary (probe) task can alter the pattern of results for a given primary task. The converse is also true. A given probe task can "pick up" processing demands of one primary task but not another. For example, performance on holding a constant position against a constant pressure as a secondary task changes as a function of the primary task of solving Raven matrices, but not upon a primary task of reading perception [25].

In conclusion, the notion of a single limited pool of resources which is tapped by all tasks does not fit the data. Rather it appears that people have multiple pools of resources, just as we have multiple systems

of short-term memory [29,30]. Therefore, understanding of limited resources in C^2 decision making requires detailed analysis of decision making itself. Generalizations from unrelated laboratory situations are questionable.

IV MODEL TASK

One salient point in the literature review is the inherent difficulty of generalizing from simple laboratory tasks involving recall, reaction time, etc., to decision making. The concept of transfer appropriate learning suggests that conclusions regarding optimum methods of information input will be highly dependent upon the way that information is subsequently used, so that conclusions from memory experiments are likely not to generalize to decision making. The notions of multiple short-term memory stores and multiple resource pools indicate the need for detailed analysis of the forms of memory and resources in particular situations.

This conclusion indicates the appropriateness of current efforts by AFHRL to study C^2 decision making in a realistic simulation [1]. A realistic simulation is by nature complex, and only those very few persons who are familiar with the decision task are able to serve as subjects. Therefore, I recommend that this effort be paralleled with research using a simplified model task which would tap the same sort of decision making processes as are present in C^2 decision making, but which would permit testing of a wide subject population and a wider range of hypotheses at relatively lower cost and with less elapsed time. Relaxation of stringent requirements for realism to the C^2 situation, would also permit the introduction of features to permit simplified control and outcome interpretation.

The essential features of C^2 decision making to be captured in the model task are allocation of scarce resources among competing missions in a situation involving risks of unexpected events. Both initial planning of "tomorrow's" action, and in-course corrections in the plan are to be simulated. The recommended simplified model task involves scheduling of trucking transportation mission in order to place the situations within

the common knowledge of a wide population of subjects who do not have expertise concerning aircraft mission requirements.

Although I have discussed trucking operations with the president of a local trucking firm in order to increase my understanding of how things are done, the model task developed does not follow actual practice in the trucking industry. Rather, the emphasis was on duplicating the cognitive processes required in C^2 decision making in a context which permits experimental manipulations. Different modalities of information presentation and plan decision output are provided and "probe" events are available to permit specialized experimental tests. These "probe" events are unrelated to the decision task itself, and are used for measurement purposes only.

A detailed description of the model task and specifications for an implementing computer program have been generated as part of this research effort, and can be obtained from the Technical Documents Center of the Air Force Human Resources Laboratory at Wright-Patterson Air Force Base. Only the general outline of the model task is presented here.

The goal of the task game, from the subject's viewpoint, is to schedule "missions" involving the delivery of loads from point A to point B. He must allocate a trailer, a tractor and a driver to each mission and plan the routes to take. The subject attempts to maximize the profit, i.e., payments for deliveries less costs. The costs include hourly fees for tractors and drivers and overtime pay for drivers stranded away from "home base." Often it may be necessary to get a trailer, driver or tractor from another location in order to carry out a mission. "Enemy" activity (road repair crews, police) introduce an element of risk.

The three modes for display of information to the subject are:

1. Serial interactive, in which the subject makes keyboard entries to call for the information.

2. Serial noninteractive, in which information is displayed in fixed sequence without the necessity of entries on the keyboard.

3. Parallel noninteractive, in which the information is presented in one unitary table rather than one piece at a time as in the other options.

The two modes of plan input are:

1. Serial, in which the decisions are entered one unit at a time.

2. Parallel in which the overall plan outline remains visible as a table in which the blank spaces are to be filled in.

Auxiliary or probe events include introduction of memory loads (ordered and associative) and tests of memory concerning resources currently available at each "location."

V. REPRESENTATIVE RESEARCH EMPLOYING THE MODEL TASK

This section sketches some research problems which could be addressed using the model task. The problems are organized into phases which could overlap to some extent, although some of the information developed in early phases would be useful in detailing subsequent phases.

A. PILOT AND OBSERVATIONAL

1. The model task would be tried, its parameters adjusted and other changes made as needed.

2. Acquisition of skill would be observed informally and the subjects interviewed to generate and refine hypotheses for subsequent formal investigation. Some specific behaviors which would be considered include:

a. "Opportunity solution" [31] in which subjects set up small portions of the solution without regard for overall implications.

b. Generation of tentative plan fragments which are later changed.

c. Note taking.

d. Order of input in serial command mode. Do any strategies develop?

B. FOLLOW-UP OF ISSUES RAISED IN THE LITERATURE REVIEW

1. Transfer appropriate learning. Transfer appropriate learning holds that memory performance is best when the input to memory is in a format which is appropriate for the demands of output from memory. Laboratory demonstrations of this prinicipal have involved artificial situations. The model task would permit two tests of the applicability of this view to decision making:

a. In two by two factorial design, two types of stimulus input (serial vs. parallel) would be crossed with two types of response output (serial vs. parallel). Transfer appropriate learning predicts that serial input leads to better performance than parallel with serial output but parallel input is better than serial with parallel output. A weaker prediction of transfer appropriate learning would be an interaction of input and output formats of the sense described, but without the "cross over."

b. The probe feature of the model task permits a test of a more radical prediction of transfer appropriate learning. If probes occur infrequently (and do not pay-off in the reward system), memory storage strategies should favor the problem solution task. It is predicted that information would be missing in probed recall which appears in the problem solution (as assessed from lack of a second retrieval of the information). Similarly, if probes are frequent (and rewarded) information should appear in probed recall which is not used in decision making.

2. Short-Term Memory Capacity Limits. The literature review concluded that the commonly held notion of a unitary short-term working memory should be replaced with a multi-store model. In this view, interference between memory load and intervening memory tasks should occur only if either: (a) all items enter the same memory sub-system, or (b) rehearsal or other information processing associated with memory consolidation interferes with another task.

The model task would permit a test of the applicability of this conclusion to decision making. Ordered memory span, as measured in the laboratory, does not seem to be needed in decision making because order information is irrelevant to the task. Therefore, we predict that an auxiliary span memory load will not interfere with decision making if a memory consolidation delay is provided between memory load input and subsequent decision task demands. This experiment is a more ecologically relevant version of the paradigm used previously by the author [3].

In contrast to the lack of loading predicted for the ordered span auxiliary memory load, an associative load (A=3, B=7, etc.) would seem to

tap the same type of memory used to keep track of information such as "how may trailers are available at location B?" In this case, the auxiliary memory load should interfere with decision making even when a consolidation interval is provided.

A further issue related to short-term memory limits could be investigated by use of two "covers" for the presentation of probes in which the probe is presented as irrelevant or relevant to the decision making task. For example, digits could be presented as an extraneous memory task, or as part of the problem (as a telephone number to be called). Similar covers could be developed with regard to the associative memory probe. The question to be addressed concerns the difference in memory loading and overloading when the probe material is presented within the decision making context, and outside of that context.

C. COMPUTER AIDS

It has been observed by members of AFHRL that the initial version of computer aids have been unpopular among C^2 decision makers during exercises. The model task would provide an opportunity to explore the following possible interpretations of this observation:

1. Perhaps these aids are unpopular because the decision makers have more experience with the "grease board" display than with the newly-introduced menu-based computer retrieval system. To test this with the model task independent groups of subjects would receive training with either a simulated computer retrieval system (serial interactive mode) or with a simulated grease board system (parallel noninteractive mode). Then subjects would be shifted to the other condition after training is complete. According to the experience hypothesis, all subjects would prefer the display modality under which they had been trained initially.

2. If the experience hypothesis (#1 above) is not supported, the model task could next be used to assess a hypothesis from the working memory viewpoint. Brainerd [32] has suggested that implicit in the working memory viewpoint is the idea that rules (such as those for operating the menu-based retrieval system) compete with other information in the limited-capacity working memory. A test of this notion would compare performance in the serial interactive versus serial

noninteractive modes of information input. First, we would need to know the order in which trained subjects retrieve information in the serial interactive modality. Each subject would be run in this modality until a pattern of retrieval order had been obtained. Then half of the subjects would be shifted to serial noninteractive input using their individualized order of presentation. The remaining subjects would continue with serial interactive input. After post-shift performance stabilizes, performance of the two groups could be compared. If retrieval rules produce interference, then performance should be lower in the serial interactive mode (which requires rule based action from the subject).

If neither of the above hypotheses receive support, it would appear that the parallel and continuous display of the grease board is essentially preferable to sequential displays such as are involved in current computer aids. Therefore, it may be desirable to explore developing multiple display computer aids which would make a large amount of data available continuously.

D. TRAINING

Insights from previous phases could be applied to training issues during this phase. In addition to these yet-to-be-developed hypotheses, some other issues are:

1. Is it best to train with simplified tasks involving few resources and missions, and then to progress to the more complex situation? Or is it best to start out with the fully complex situation so that strategies which are not appropriate to complex situations do not develop during training?

2. If subjects develop consistent strategies for the order in which information is retrieved from the serial-interactive mode of information input, then one could ask whether these strategies can be trained. Are there better strategies than those developed by the subjects? Is training more efficient than allowing subjects to discover the appropriate strategy on their own, or does the discovery process have benefits worth the cost in extra learning time?

3. A question similar to #2 above can be asked about the output of the plan. Do subjects develop strategies of withholding tentative solutions until the "big picture" is formulated? Do they learn increased willingness to change tentative plans as they gain more understanding of the particular situation? Can strategies of withholding or changing tentative solutions be trained?

VI. RECOMMENDATIONS

This section briefly summarizes some of the recommendations presented in detail in the body of this report.

A. The literature review documents a recommendation that memory and human resource limitations should be investigated within a decision making context because of inherent problems in generalizing from existing laboratory data to decision making.

B. A simplified decision making task was developed and is recommended as a supplement to investigating of actual C^2 decision making. This model task was designed to permit efficient experimental manipulation and control, and to be accessible to experimental subjects who are not technically qualified to deal with actual C^2 problems.

C. Some issues to be addressed with this model task are recommended in Section V. These include:

1. Observation of partial solutions, solution shifts, note taking, input order strategies, etc.

2. Study of transfer appropriate learning and short-term memory limits within a decision making context.

3. Investigation of why computer aids have not been popular.

4. Study at alternative approaches to training.

REFERENCES

[1] Frekany, G.A. Research plan for studies of tactical decision-making (Draft). AFHRL White paper, 1982.

[2] Klapp, S.T. Temporal Compatibilty in dual motor tasks II: Simultaneous articulation and hand movements. Memory & Cognition, 1981, 9, 398-401.

[3] Klapp, S.T., Marshburn, E.A., & Lester, P.T. Short-Term memory does not involve the "working memory" of information processing: The demise of a common assumption. Submitted for publication.

[4] Craik, F.I.M., & Lockhart, R.S. Levels of processing: A framework for memory research. Journal of Verbal Learning and Verbal Behavior, 1972, 11, 671-684.

[5] Baddeley, A.D. The trouble with levels: A re-examination of Craik and Lockhart's framework for memory research. Psychological Review, 1978, 85, 139-152.

[6] Morris, C.D., Bransford, J.D., & Franks, J.J. Levels of processing versus transfer appropriate processing. Journal of Verbal Learning and Verbal Behavior, 1977, 16, 519-533.

[7] Tulving, E., & Thompson. Encoding specificity and retrieval processes in episodic memory. Psychological Review, 1973, 80, 352-272.

[8] Miller, G.A. The magical number seven, plus or minus two: Some limits on our capacity for processing information. Psychological Review, 1956, 63, 81-97.

[9] James, W. Principles of Psychology. New York: Holt, 1890.

[10] Shallice, T. & Warrington, E.K. Independent functioning of verbal memory stores: A neurpsychological study. Quarterly Journal of Experimental Psychology, 1970, 22, 261-273.

[11] Martin, M. Memory span as a measure of individual differences in memory capacity. Memory & Cognition, 1978, 6, 194-198.

[12] Buschke, H. Relative retention in immediate memory determined by the missing span method. Nature, 1963, 1129-1130.

[13] Bower, G.A. Commentary. In D. Kimble (Ed.), The organization of recall. New York: The New York Academy of Sciences, 1967, 42-44.

[14] Crowder, R.G. Short-term memory for words with a perceptual-motor interpolated activity. Journal of Verbal Learning and Verbal Behavior, 1967, 6, 753-761.

[15] Johnston, W.A., Greenberg, S.N., Fisher, R.P., & Martin, D.W. Divided Attention: A vehicle for monitoring memory processes. Journal of Experimental Psychology, 1979, 83, 164-171.

[16] Hitch, G.J., & Baddeley, A.D. Verbal reasoning and working memory. Quarterly Journal of Experimental Psychology, 1976, 28, 603-621.

[17] Logan, G.D. Short-term memory demands of reaction-time tasks that differ in complexity. Journal of Experimental Psychology: Human Perception and Performance, 1980, 6, 375-389.

[18] Posner, M.I., & Rossman, E. Effects of size and location of informational transforms upon short-term retention. Journal of Experimental Psychology, 1965, 79, 496-503.

[19] Shulman, H.G., & Greenberg, S. Perceptual deficit due to division of attention between memory and perception. Journal of Experimental Psychology, 1971, 88, 171-176.

[20] Wanner, E., & Shiner, S. Measuring transient memory load. Journal of Verbal Learning and Verbal Behavior, 1976, 15, 159-167.

[21] Lansman, M. An attentional approach to individual differences in immediate memory (Tech. Rep. for grant W00014-77-C-0225, Office of Naval Research). Wright-Patterson Air Force Base, Ohio: AF Human Resources Laboratory, HQ/AFHRL. (10433TR)

[22] Roediger, H.L., Knight, F.L., & Kantowitz, B.H. Inferring decay in short-term memory: The issue of capacity. Memory & Cognition, 1977, 5, 167-176.

[23] Shulman, H.G., Greenberg, S.N., & Mating, J. Intertask delay as a parameter of perceptual deficit in divided attention. Journal of Experimental Psychology, 1971, 88, 439-440.

[24] Stanners, R.F., Meunier, G.F., & Headley, D.B. Reaction time as an index of rehearsal in short-term memory. Journal of Experimental Psychology, 1969, 82, 566-570.

[25] Hunt, E., Lansman, M., & Wright, J. Some remarks on doing two things at once (Tech. Rep. for grant N00014-77-C-0225, Office of Naval Research). Wright-Patterson Air Force Base, Ohio: AF Human Resources Laboratory, HQ/AFHRL. (10652TR)

[26] Kahneman, D. Attention and Effort. Englewood Cliffs, N.J.: Prentice-Hall, 1973.

[27] Schwartz, S.P. Capacity limitations in human information processing. Memory & Cognition, 1976, 4, 763-768.

[28] McLeod, P. Does probe RT measure central processing demand? Quarterly Journal of Experimental Psychology, 1978, 30, 83-89.

[29] Naven, D. & Gopher, D. On the economy of the human processing system. Psychological Review, 1979, 86, 214-255.

[30] Wickens, C.D., Mountford, S.J. & Schreiner, W. Multiple resources, task-hemispheric integrity and individual differences in time-sharing. Human Factors, 1981, 23 211-229.

[31] Hayes-Roth, B. & Hayes-Roth, F. Cognitive Processes in Planning (TR-R-2366-ONR). Santa Monica, California: Rand Corporation.

[32] Brainerd, C.J. Working memory and the developmental analysis of probability judgement. Psychological Review, 1981, 88, 463-151.

1982 USAF-SCEEE SUMMER FACULTY RESEARCH PROGRAM

Sponsored by the

AIR FORCE OFFICE OF SCIENTIFIC RESEARCH

Conducted by the

SOUTHEASTERN CENTER FOR ELECTRICAL ENGINEERING EDUCATION

FINAL REPORT

ANALYSIS AND MODELING OF A REAL-TIME HOLOGRAPHY SYSTEM

Prepared by:	Dr. Jerome Knopp
Academic Rank:	Assistant Professor
Department and University:	Department of Electrical Engineering University of Missouri-Rolla
Research Location:	Rome Air Development Center, Surveillance Division, Strategic Surveillance Branch, Electro-Optics Section
USAF Research:	Dr. Donald W. Hanson
Date:	August 13, 1982
Contract No:	F49620-82-C-0035

ANALYSIS AND MODELING OF A REAL-TIME HOLOGRAPHY SYSTEM

by

Jerome Knopp

and

Jeffrey M. Swindle

ABSTRACT

The real-time holography system was studied in some detail using a generic model. It is shown that aberrations are introduced by wavelength rescaling. Further errors are generated by the very nature of phase recording a hologram plus the non-linearities in the recording media. Resolution requirements and MTF limitations show that present day phase recording devices are just barely adequate to correct low level turbulence.

A study of the system using dimensional analysis showed that the Fresnel approximation may be used to construct a scale model based on Arkadiew's Law.

ACKNOWLEDGEMENT

The authors would like to thank the Air Force Systems Command, the Air Force Office of Scientific Research and the Southeastern Center for Electrical Engineering Education for providing them with the opportunity to spend a very worthwhile and interesting summer at Rome Air Development Center, Griffiss AFB, NY. They would like to acknowledge Dr. Don Hanson and the Electro-Optics Section for their hospitality and excellent working conditions.

I. INTRODUCTION

At the present, DARPA has considerable interest in the application of optical phase conjugation techniques to visible laser communication. In principle, phase conjugation can be used to compensate for most of the optical phase distortions along the beam path of a propagating laser. In cases of practical interest, the aberrations are due primarily to the atmosphere; however, phase conjugation can be used to correct other aberrations such as those due to errors in optical components or within a laser cavity.

At the present there are several different methods of phase conjugation which are being considered including adaptive mirrors, nonlinear optics and real-time holography.

Adaptive mirrors represent conventional technology and have been under active development for more than 14 years. In order to employ mirrors for phase conjugation, a wavefront sensor is required that can determine the aberrated wave profile and then apply a best estimate of the profile conjugate to the adaptive mirror surface by distorting the surface with an array of actuators. The practical problems of constructing such systems are considerable. In order to apply these mirrors to total atmospheric compensation would require mirrors better than those presently available off the shelf. Atmospheric compensation requires a fast time response (i.e., in the millisecond range) and large numbers of actuators (on the order of 10^3 to 10^4). While it is possible to build adaptive mirrors meeting the required performance criteria, the costs are high. For this reason, other approaches to phase conjugation are being investigated.

Nonlinear optics refers to a collection of methods that use wavefront reversal (i.e., phase conjugation) caused by elastic photon scattering or stimulated interactions of inelastic photon scattering. Both three wave and four wave mixing techniques are described in the literature.[1,2] It appears that these techniques are the leading technologies for future work in phase conjugation; however, they are not

available in the near term because most mixing schemes are very inefficient. In most practical schemes that implement phase conjugation, the conjugate must be produced from a very weak aberration sensing beacon that is not strong enough to produce a clean conjugate wave.

The most promising near term prospect for phase conjugation is real-time holography. A hologram is made of the aberrated wavefront from which a conjugate wavefront is produced. Real-time holography requires a fast recording medium in which to form the phase correcting holograms. Devices, such as the Ediphor, Ruticons, photo-TITUS and the PROM which employ fast (real-time) media, are possible candidates for real-time holography.[3] The cost versus risks for developing a workable phase conjugation system based on real-time holography appear reasonable; it is this particular approach which is the subject of this report.

The fundamental propagation problem to be analyzed is shown in Fig 1. It is desired to direct the energy from a laser source of wavelength λ_1 to a target aperture of diameter D_T from a telescope with a diameter D_S. It is assumed that a pointing and tracking system keeps the beam boresighted on the target aperture. Mounted at the center of the target aperture is a beacon source of wavelength λ_2. The beacon propagates a wave from the target. The wave travels through the aberrated atmosphere and is used to form a hologram of an aberrated wavefront at the source. The hologram is used to produce a conjugate wavefront that is propagated back through the atmosphere. In principle, this conjugate would precisely cancel the wavefront aberrations of the atmosphere. This corrected wavefront could deliver energy very efficiently from the source to the target provided the target aperture was large enough to collect the energy from an ideal diffraction limited spot. In practice, the implementation of a real-time holography system presents many problems that will prevent ideal correction of a wavefront. An attempt will be made here to analyze some of these problems and to examine the possibility of studying a real-time

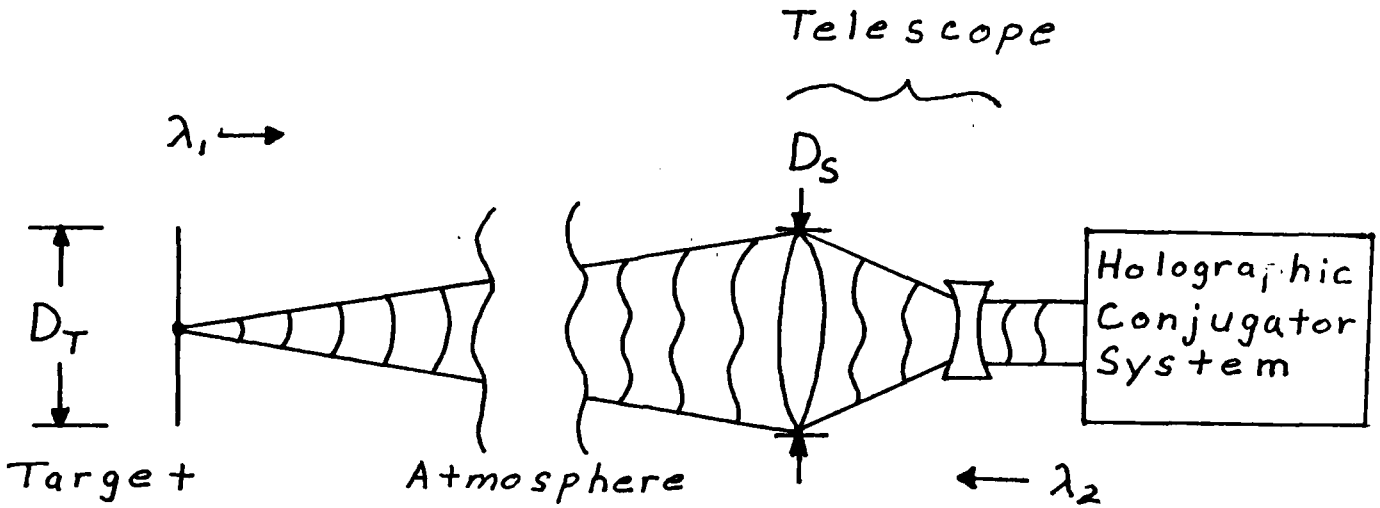


Figure 1 The Problem to be Analyzed

holography system using a scale model.

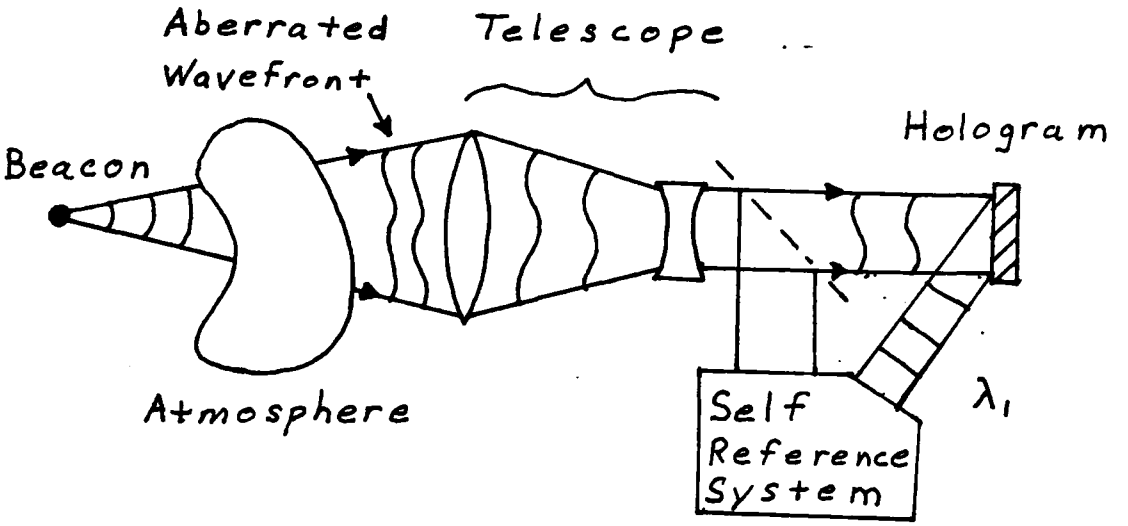
II. OBJECTIVES AND OUTLINE OF THE APPROACH

The objectives of this report are to conduct a systems level study of the real-time holographic approach and to discuss the possibility of constructing scale model experiments. The systems study will be conducted by defining a generic model and applying scalar diffraction theory to examine certain problems associated with a working system. Scale modeling will be discussed using dimensional analysis to construct a group of dimensionless parameters to model a working system. Using this group, certain scaling effects will be examined.

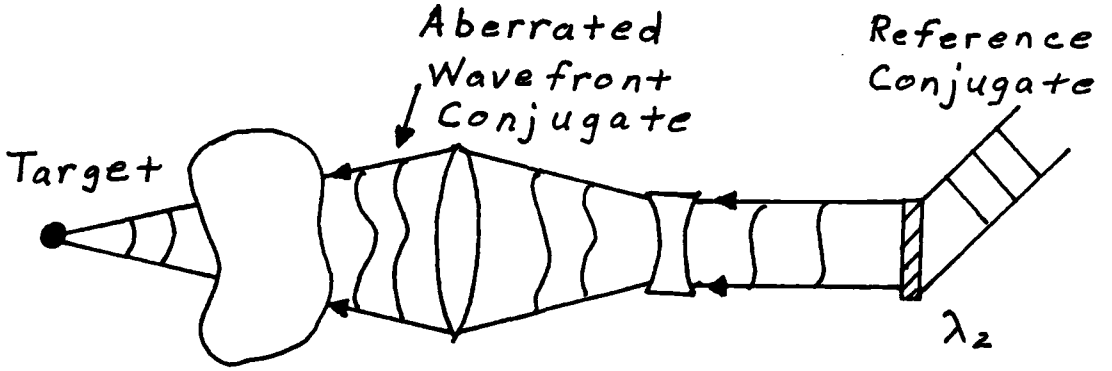
III. GENERIC MODEL OF A REAL-TIME HOLOGRAPHY SYSTEM

The system model for real-time holography will be broken into two parts: hologram formation as shown in Fig 2(a) and conjugate playback as shown in Fig 2(b). In Fig 2(a) a hologram is formed of an aberrating atmosphere using a beacon wavefront at wavelength λ_1. The beacon is received by the pointer telescope and the received beam cross section is reduced by the telescope expansion ratio M. The reduced beam is directed to a beam splitter from which a reference wave is derived. In general, the reference may be formed in one of several ways; no generally accepted scheme is available yet. (Some comments on this issue are included in the conclusions.) For the purpose of the model, it will be assumed that a spherical or plane reference wave is produced. The interference of the reference wave with the aberrated beam produces a hologram of the aberration. The hologram will be assumed to be a phase hologram, since most of the materials being considered at present for real-time holography depend on index changes, surface relief or birefringence to encode the wavefront. In the model, the material is assumed non-linear, with a band limited modulation transfer function.

The playback system used in Fig 2(b) produces a conjugate wavefront that would in principle be perfect; however, in most practical systems the conjugate would be reconstructed at a different wavelength, λ_2,



(a) Hologram Formation



(b) Conjugate Playback

Figure 2 Generic Model

than the beacon wavelength. (This is done in part to assure good separation between outgoing scatter and the weaker beacon.) The "laser power amplifier" is used to strengthen the reconstructed conjugate. Strictly speaking, the power amplifier may in practice upshift or downshift the conjugate wavelength; however, this model will not include that effect. It will also ignore atmospheric effects due to wavelength differences between the beacon and the conjugate wave as well as the pointing and stationkeeping problems of a beacon in geosynchronous orbit. These issues are addressed elsewhere.[4]

IV. ANALYSIS OF THE GENERIC MODEL

In the analysis that follows, the generic model will be used to examine the following issues:

i) Aberrations introduced by the rescaling of wavelengths between the beacon and conjugate waves.

ii) Reconstruction errors in phase recording the aberrated wavefront.

iii) The effects of non-linearities in the recording media.

iv) Resolution requirements and MTF limitations.

A. Wavelength Rescaling

The problem of reconstructing holograms with a reference wave different from the reference used in forming the hologram has been studied extensively in the past; however, most of these studies are concerned primarily with image aberrations rather than wavefront reconstruction. The concern here is with reproduction of an exact conjugate.[5] Consider the most general situation, a beacon wavefront $\underline{U}_B(x,y,z)$ to be recorded with a reference $\underline{U}_R(x,y,z)$. Note that underlined quantities represent clockwise phasors. Assume that a hologram is formed with an exposure range that is in a linear region of

the field amplitude transmittance-exposure curve for the recording media that encodes the hologram. Then the following field amplitude transmittance will result:

$$\tau(x,y) = C_o\,(\underline{U}_B + \underline{U}_R)(\underline{U}_B + \underline{U}_R)^* \qquad (1)$$

where C_o is a constant and the asterick indicates conjugation.

Expanding Eq. (1)

$$\tau(x,y) = C_o\,(U_B^2 + U_R^2 + \underline{U}_B\,\underline{U}_R^* + \underline{U}_B^*\,\underline{U}_R). \qquad (2)$$

Rewriting the phasor quantities explicitly gives

$$\underline{U}_B = U_B\; e^{-j\,\phi_B(x,y)}$$

and

$$\underline{U}_R = U_R\; e^{-j\,\phi_R(x,y)}.$$

Substituting into Eq. (2) and using Euler's identity gives

$$\tau = C_o\,(U_B^2 + U_R^2 + 2\,U_R\,U_B\,\cos(\phi_B - \phi_R)). \qquad (3)$$

In equation (3) the first two terms represents the intensities of the waves used to record the hologram while the last term encodes the phase difference in a fringe structure. From a communication viewpoint the last term represents encoding of the beacon information on a reference carrier. In order to retrieve the information the carrier must be known. In order to accurately retrieve the conjugate wave, the conjugate of the reference must be used to reconstruct the hologram. If the reconstructed field is designated as $\underline{U}_H$, then

$$\underline{U}_H = \tau\,\underline{U}_R^*$$

or from (2)

$$\underline{U}_H = C_o\,(\underline{U}_R^*\,U_B^2 + \underline{U}_R^*\,U_R^2 + \underline{U}_R^{*2}\,\underline{U}_B + U_R^2\,\underline{U}_B^*). \qquad (4)$$

The last term in equation (4) represents the reconstructed conjugate provided that U_R^2 is relatively uniform in amplitude. This term is of special interest and will be designated as $\underline{U}_c$, therefore

$$\underline{U}_c = U_R^2 \, \underline{U}_B^* . \tag{5}$$

The first two terms represent low frequency bias terms due to the intensities associated with $\underline{U}_B$ and $\underline{U}_R$. They are a source of noise in the reconstruction. The third term in general, $\underline{U}_R^{*2} \underline{U}_B$ represents a distorted version of $\underline{U}_B$ since $\underline{U}_R^{*2}$ is not necessarily a constant phasor. Usually $\underline{U}_R$ is chosen as an easily reproducible wavefront. Failure to accurately reproduce $\underline{U}_R$ results in errors.

For the applications of interest here, a plane wave or a spherical reference wave is of interest. For the case of a plane wave the reference can be defined as:

$$\underline{U}_R = C_p \, e^{-jk_1(\alpha x + \beta y + \gamma z)}$$

where α, β, γ are direction cosines with respect to the x, y and z axes, respectively. If a wavelength of λ_1 is used in recording the hologram then $k_1 = 2\pi/\lambda_1$. The only term of interest in reconstruction is $\underline{U}_c$. Assuming the conjugate is used in reconstruction, then, substituting the plane wave conjugate into (5) gives $\underline{U}_c = C_p^2 \, \underline{U}_B^*$ and an exact duplicate of the beacon is produced; however, if a different wavelength, λ_2, is used in the reconstruction then

$$\underline{U}_c = C_p^2 \, e^{-j(k_1 - k_2)(\alpha x + \beta y + \gamma z)} \underline{U}_B^* \tag{6}$$

where $k_2 = 2\pi/\lambda_2$. Equation (6) shows two types of error; one is a tilt term represented by the exponential, the second error is an error in the optical path. The tilt term is not a problem since it is a fixed pointing error. The path error is more of a problem. The $\underline{U}_B^*$ term is the correct phase at the wrong wavelength. Therefore, a path error of $(1 - \lambda_2/\lambda_1)\phi_B$ is produced. The path error can not be eliminated easily. It could be approximately corrected using an Arnulf lens,[6] a device that approximately multiplies the phase at each point by a

constant without changing the lateral dimensions of the beam. Since the resolution requirements for atmospheric correction are quite low (to be discussed later) such a lens is workable if the wavelength ratio between λ_1, and λ_2 becomes a significant problem.

If a spherical reference is used and a change in wavelength is involved, then for an off-axis reference point located at (x_c, y_c, z_c) then

$$\underline{U}_R = C_s \frac{e^{-j k_1 r}}{r}$$

where C_s is a constant and

$$r = \sqrt{(z - z_c)^2 + (x - x_c)^2 + (y - y_c)^2} \; .$$

Reconstructing the conjugate at a different wavelength gives

$$\underline{U}_c = C_s^2 \frac{e^{-j(k_1 - k_2) r}}{r} \underline{U}_B^* . \qquad (7)$$

Equation (7) shows that a spherical error is introduced that presents no problems since it can be corrected with a fixed lens and the path length error is identical to the one previously discussed.

Therefore provided a plane or spherical reference is used, reconstruction phase errors should be determined by $(1 - \lambda_2/\lambda_1)\, \phi_B$.

B. Reconstruction Error in Phase Holograms

As previously mentioned, real-time holography is based primarily on phase holograms. Phase holograms encode the holographic fringe structure as a phase change that is directly proportional to exposure. Unfortunately, they are inherently more noisy than amplitude transmission holograms. This can be seen by rewriting the exposure, E, directly in terms of a phase shift and using a second order approximation to the phasor exponential to describe the field amplitude transmittance $\underline{T}$. In phasor form

$$\underline{T} = T_0 \, e^{-j \mu E(x, y)} \qquad (8)$$

where μ is a constant. Now expanding the exponential term gives

$$\underline{\tau} = T_o \left(1 + j\mu E - \frac{\mu^2}{2} E^2 + \cdots\right). \qquad (9)$$

If

$$E(x,y) = U_R^2 + U_B^2 + \underline{U}_R \underline{U}_B^* + \underline{U}_R^* \underline{U}_B$$

Then equation (9) describes a phase hologram for the beacon. The only terms of interest in reconstructing the phase hologram are the ones containing $\underline{U}_B^*$, all other terms are ignored. It will be assumed that the angle between the beacon wave and the reference wave is large enough to provide adequate angular separation between these other terms and $\underline{U}_B^*$. Therefore

$$\underline{\tau} = T_o \left[1 - (\mu^2 U_R^2 - j\mu)\underline{U}_R \underline{U}_B^* - (\mu^2 U_B^2)\underline{U}_R \underline{U}_B^* + \text{other terms}\right] \qquad (10)$$

Since U_R^2 is assumed uniform, the first set of parentheses in Eq (10) yields only a quadrature component. The second set of parentheses contains U_B^2 which is not uniform and is in fact highly speckled in the case of atmospheric recordings. This term is intermodulation noise and is referred to as "flare light" or "halo". This halo, in general, may not be easily removed. Therefore, by its very nature a phase hologram will have noise. The only way to reduce the noise is to keep μ small and accept very low diffraction efficiencies.

It should be pointed out that in devices used for real-time holography, the intermodulation will be worse than that normally observed in bleached photographic emulsions. In emulsions, both relief and index changes occur at low frequencies and they tend to cancel out and compensate for the low frequency speckle.

C. The Effects of Non-Linearities in the Recording Media

In the previous section, only linear phase recording was considered. The recording media in general will not record the phase in a linear fashion. Therefore, this section will concern itself to the effect of a quadratic approximation to the non-linear recording. The previous hologram transmittance Eq (8) now becomes:

$$\underline{\tau} = T_0 \, e^{-j(\mu E + \Delta E^2)} \tag{11}$$

where μ and Δ are constants and E(x,y) is as previously described. Expanding the exponential yields:

$$\underline{\tau} = T_0 [1 + j\mu E - (\tfrac{1}{2}\mu^2 - j\Delta) E^2 - \mu\Delta E^3 - \tfrac{\Delta^2}{2} E^4 + \cdots] . \tag{12}$$

Considering, as before, only terms containing $\underline{U}_B^*$:

$$\begin{aligned} \tau = T_0 \{ 1 - [& \mu^2 U_R^2 + 6\mu\Delta U_R^4 + 2\Delta^2 U_R^6 \\ & - j(\mu - 2\Delta U_R^2)] \underline{U}_R \underline{U}_B^* - U_B^2 [\mu^2 \\ & + 6\mu\Delta (U_B^2 + U_R^2) + 2\Delta^2 (U_B^4 + 6U_B^2 U_R^2 + 6U_R^4) \\ & - j2\Delta] \underline{U}_R \underline{U}_B^* + \text{other terms} \} . \end{aligned} \tag{13}$$

Comparing Eq. (13) to Eq. (10), it is seen that the non-linear recording makes matters worse; it increases the number of intermodulation terms. These terms cannot be filtered out by angular separation like the terms that are not shown. Therefore, maintaining linearity is very important since there is no way to compensate for the non-linearities. It might be hoped that nonlinearities in the media could be played against the inherent non-linearity of phase recording; unfortunately, if equation (13) is examined closely, it will be observed these non-linearities terms are at quadrature with respect to one another.

D. Resolution Requirements and MTF Limitations

The best of the present devices being considered for real-time holography use a crystalline material that have modulation transfer functions that roll off at spatial frequencies on the order of the crystal thickness. Typically, these devices depend on materials that are difficult to fabricate much thinner than about 100 microns. This suggests that, at present, spatial frequencies are limited to about 10 lines/mm. For correction of atmospheric disturbances in "good" seeing the angular spectrum extends to about 10 μrads. Under the best turbulence conditions, given a receiving telescope with a beam expansion ratio of M, the received angular spectrum at the hologram will extend to about 10M μrads. Since the angular spectrum interprets the aberrated wavefront in terms of plane waves, it is only necessary to determine the highest spatial frequency needed for an off-axis recording of the plane wave making the largest angle with respect to the reference. For two plane waves at angles θ_1 and θ_2 on either side of a normal to a thin hologram, the spatial frequency S of the recording is given by

$$S = \frac{\sin\theta_1 + \sin\theta_2}{\lambda} \qquad (14)$$

where λ is the recording wavelength. For small angles

$$S \simeq \frac{\theta_1 + \theta_2}{\lambda} .$$

Since the minimum reference angle for adequate separation of the conjugate must be at least three times the atmospheric bandwidth[7] then the minimum spatial frequency S_{min} is given by

$$S_{min} = \frac{40 \times 10^{-6} M}{\lambda} \quad \text{cycles/meter.}$$

For an expected demagnification on the order of 100 this means resolution requirements of about $S_{min} = 8$ lines/mm which is just about the state-of-the-art. Therefore, we may expect that there is

adequate resolution in presently available materials to make turbulence corrections in good seeing. For extreme levels of high turbulence, it will be necessary to reduce M and increase the hologram surface. This would require growing fairly large crystals to record the holograms, it is not clear what the limitations are here, but such devices are not off-the-shelf.

V. SCALE MODELING OF THE REAL-TIME HOLOGRAPHY SYSTEM

The only exact way to evaluate any real system is to construct a prototype to make measurements on; however, for system development it is often reasonable to consider building a scale model in cases where the model is economical. Unfortunately, it is not always possible to fabricate a scale model in such a way that useful information can be extracted from it. In order to be of value, a direct relationship must be established between measurements made on the model and measurements made on the prototype. If a scale model is possible, a set of linear scales can be used to establish a correspondence or "similarity" between the systems. In what follows, the theoretical question of a scale model will be examined using techniques from dimensional analysis. From this analysis certain dimensionless groups will be established. These groups will define a set of dimensionless variables and parameters through which model and prototype measurements can be related. It will also provide a complete system description using a minimum number of variables and parameters. This is useful in reducing the amount of data and the number of experiments needed by a considerable amount.

Consider rescaling the generic model. In practice the beacon will be essentially at infinity. Therefore, the fundamental problem is that of a plane wave on an atmospheric "slab" that has an index of refraction, $n(x,y,z,t)$, that varies randomly from point to point. For the purposes of this analysis, the atmosphere will be examined at a specific instant of time; all of the index variations will be frozen in place. If index variations are small then it can be rewritten as

$$n(x,y,z) = n_0 + \tilde{n}(x,y,z)$$

where n_o is an average value and $\tilde{n}(x,y,z)$ is a perturbation about the average. If the perturbation is small, then the diffracted field from the slab can be approximated by examining only first order diffraction.

Consider a plane wave <u>propagating</u> in the z direction impinging normally on the atmospheric slab at z=0 and through the randomly varying index until it reaches a receiving aperture at $z = z_o$. The problem is to model accurately the field in the $z = z_o$ plane using a three dimensional scale model of the atmosphere. This can be done for the first order diffracted part of the field. The first order effects are estimated by dividing the slab into a thin stack of lamina; each thick, then the field from a single lamina at z is given approximately by

$$A e^{jk n_o z} e^{jk \tilde{n} \Delta z} \simeq A e^{jk n_o z} (1 - jk \tilde{n} \Delta z) .$$

Here A represents the amplitude of a plane wave that passes through the slab with negligible loss. The diffracted field from each lamina is assumed to reach z without further diffraction by other laminae. This represents first order effects only and ignores the "diffraction of the diffraction". Using the Fresnel approximation[7] and ignoring the undiffracted part of the field, the diffracted field $\underline{U}_D$ at z_o is given by integrating over all laminae:

$$\underline{U}_D = \frac{A e^{jk n_o z_o}}{\lambda n_o} \int_0^{z_o} \int_{-\infty}^{\infty} \frac{\tilde{n}}{z_o - z} e^{j \frac{k n_o}{2(z_o - z)} [(x_o - x)^2 + (y_o - y)^2]} dx\, dy\, dz \quad (15)$$

By defining a set of dimensionless variables equation (15) can be redefined in dimensionless form.[8] One particularly useful set is:

$$\overline{\underline{U}}_D = \frac{\lambda n_o}{kA} e^{-jk n_o z_o} \underline{U}_D \quad (16)$$

$$\bar{x} = \frac{x}{\sqrt{\lambda z_o}} \quad (17)$$

$$\bar{y} = \frac{y}{\sqrt{\lambda z_o}} \quad (18)$$

$$\bar{x}_o = \frac{x_o}{\sqrt{\lambda z_o}} \qquad (19)$$

$$\bar{y}_o = \frac{y_o}{\sqrt{\lambda z_o}} \qquad (20)$$

$$\bar{z} = z/z_o \; . \qquad (21)$$

Rewriting (15) gives the normalized diffracted field at = 1 as

$$\underline{U}_D = \int_o^1 \iint_{-\infty}^{\infty} \frac{\tilde{n}}{n_o(1-\bar{z})} e^{j\frac{\pi n_o}{(1-\bar{z})}[(\bar{x}_o-\bar{x})^2+(\bar{y}_o-\bar{y})^2]} d\bar{x}\, d\bar{y}\, d\bar{z} \; . \qquad (22)$$

The normalized equation represents a generalized form through which a relationship can be established between model and prototype variables since this equation represents both systems. Letting primed and double primed variables represent model and prototype systems respectively the scale relations between the model and prototype can be derived directly from equations (16) through (21). They are

$$\bar{U}_D = \frac{U_D' \lambda' n_o}{k' A_p'} e^{-jk' n_o z_o'} = \frac{U_D'' \lambda'' n_o}{k'' A_p''} e^{-jk'' n_o z_o''} \qquad (23)$$

$$\bar{x} = \frac{x'}{\sqrt{\lambda' z_o'}} = \frac{x''}{\sqrt{\lambda'' z_o''}} \qquad (24)$$

$$\bar{y} = \frac{y'}{\sqrt{\lambda' z_o'}} = \frac{y''}{\sqrt{\lambda'' z_o''}} \qquad (25)$$

$$\bar{x}_o = \frac{x_o'}{\sqrt{\lambda' z_o'}} = \frac{x_o''}{\sqrt{\lambda'' z_o''}} \qquad (26)$$

$$\bar{y}_o = \frac{y_o'}{\sqrt{\lambda' z_o'}} = \frac{y_o''}{\sqrt{\lambda'' z_o''}} \qquad (27)$$

$$\bar{z} = \frac{z'}{z_o'} = \frac{z''}{z_o''} \qquad (28)$$

These relations establish a linear scale between the diffracted fields in the model and prototype systems, hence, measurements of the diffracted field from the model can be directly related to those in the prototype. Therefore a scale model is possible at least as far as first order diffraction effects.

These equations also determine how the scale model is to be constructed in order to keep a linear relation between the diffracted fields in the model and prototype systems. The scaling of refractive index coordinates is a key point in the modeling. The index coordinates in equation (22) must be scaled in normalized coordinates. Index coordinates will follow the scale relations given by equation (23) through (28). This means that if the thickness z_o is reduced by a factor p in the model, then the lateral index variations in x and y are scaled by the $\sqrt{p}$ provided the wavelength remains unchanged. This scale relation is not new, it was discussed by Arkadiew[9] in 1913; however, his presentation was highly intuitive, based on Fresnel zone construction, while the results given are rigorous. It should also be pointed out that only the diffracted field was discussed here. In general, it is not possible to scale the total field including the undiffracted part. It can be shown that the ratio of the diffracted to the undiffracted part of the field does not scale linearly. Fortunately, the effect is not critical since the net effect is to lower the contrast in the intensity variations. This effect is easy to account for since the undiffracted part is an additive constant.

It should be pointed out that the non-dimensional parameters given in equations (16) through (21) are the most compact representation of the atmospheric slab possible. They are ideal for minimizing parameters needed for either experimental or computer simulation. If two particular parameters such (e.g., wavelength and thickness) are in the same dimensionless group, then varying one is equivalent to varying the other as far as making measurements are concerned. Therefore, using non-dimensional variables and parameters reduces the number of parameter changes needed for investigation. This often means orders of magnitude

reduction in the amount of effort needed in experimental or computer simulation.

VI. CONCLUSIONS

From the results of the analysis using the generic model the following conclusions have been reached:

1. Phase aberrations introduced by rescaling the wavelengths will depend only on the ratio of the wavelengths used in forming and playing back the hologram if spherical aberration and tilt are accounted for. This assumes that a perfectly plane or spherical reference can be derived from a beam split off from the beacon wave. This is highly debateable. Since adequate filtering of the reference means that a small portion of the angular spectrum from the derived beam is used and therefore a small portion of the energy from it. This means a weak reference beam and requires a weak or attenuated object wave to form a proper hologram. This represents a great waste of photons. Furthermore, some suggested schemes for deriving a reference, filter out the reference using a pinhole filter in conjunction with a lens to carry out optical Fourier transform filtering. Considering the very speckled nature of the return wave impulse repsonse, the pinhole filter will be a very hit and miss operation that will provide a reference with large dynamic variations. This issue definitely needs more thought.

2. The problems of phase reconstruction errors in phase holograms are two fold,

   i. Inherent errors due to the non-linearities in phase recording
   ii. Additional errors due to non-linearities in the mapping of intensity into phase.

These problems are inescapable and lead to intermodulation noise in the reconstructed wave. The first is avoided by accepting low diffraction efficiency, the second by making sure the phase recording have adequate

dynamic range, this may be a difficult problem considering the intensity variations inherent in the speckled beacon return.

3. The resolution requirements of present materials appears adequate for correction in loss turbulence. Correction in high turbulence may require devices with larger surface areas than are presently available off-the-shelf to accomodate the higher space bandwidth product required.

4. Modeling the effects of the atmosphere appears to be practical. It is possible in principle to construct a small model atmosphere, if the index variations can be properly scaled using Arkadiew's scaling laws for the diffracted field.

VII. RECOMMENDATIONS

In order to further reduce risks in developing a working real-time holography system it is recommended that in future work the following issues be examined:

1. The effects of speckle on a reference wave derived from the incoming beam.
2. Alternate techniques for deriving a reference wave to avoid wasting photons.
3. Dynamic range effects of present real-time media and trade-offs that can be made between dynamic range and signal-to-noise ratios.
4. Applications of scale modeling to reducing development cost and improving laboratory simulations, presently being considered.

REFERENCES

1. Pepper, D. M., "Nonlinear Optical Phase Conjugation," Optical Engineering, Vol. 21, No. 2, p156, March-April, 1982.

2. White, J. O. and Amnon Yariv, "Spatial Information Processing and Distortion Correction Via Four-Wave Mixing," Optical Engineering, Vol. 21, No. 2, p224, March-April, 1982.

3. Lipson, G. G., "Recyclable Incoherent-to-Coherent Image Converters," in Advances in Holography, Vol. 2, ed. by N. H. Farhat, p69, Marcel-Dekker Inc., NY, 1976.

4. Strategic Laser Communications Uplink Analysis, (Volumes 1 and 2), RADC-TR-341 V. 1, RADC-TR-81-186 V. 2, Rome Air Development Center, Griffiss AFB, NY, Dec and July, 1981.

5. Smith, H. M., Principles of Holography, Wiley Interscience, NY, 1975.

6. Gabor, D., "Summary and Directions for Future Progress," in Acoustical Holography V 1, ed. by Methrell, A. F., H. M. A. El-Sum and L. Larmore, p267, Plenum Press, NY, 1969.

7. Goodman, J. W., Introduction to Fourier Optics, McGraw-Hill, NY, 1968.

8. Kline, S. J., Similitude and Approximation Theory, McGraw-Hill, NY, 1965

9. Sommerfield, A., Optics, Academic Press, NY, 1954.

END

FILMED

9-83

DTIC